City Research Online

City, University of London Institutional Repository

Citation: Zavliaris, K.D. (1990). Mechanical behaviour of adhesive anchors installed in concrete. (Unpublished Doctoral thesis, City University London)

This is the accepted version of the paper.

This version of the publication may differ from the final published version.

Permanent repository link: https://openaccess.city.ac.uk/id/eprint/7534/

Link to published version:

Copyright: City Research Online aims to make research outputs of City, University of London available to a wider audience. Copyright and Moral Rights remain with the author(s) and/or copyright holders. URLs from City Research Online may be freely distributed and linked to.

Reuse: Copies of full items can be used for personal research or study, educational, or not-for-profit purposes without prior permission or charge. Provided that the authors, title and full bibliographic details are credited, a hyperlink and/or URL is given for the original metadata page and the content is not changed in any way.

City Research Online: http://openaccess.city.ac.uk/ publications@city.ac.uk

MECHANICAL BEHAVIOUR OF ADHESIVE ANCHORS INSTALLED IN CONCRETE

KONSTANTINOS D. ZAVLIARIS

VOLUME 2

Figures, Plates and Appendices

A thesis submitted for the degree of Doctor of Philosophy

Department of Civil Engineering
City University London
June 1990

C O N T E N T S

VOLUME 2

Page

1.FIGURES

Fig.1.1. Types of chemical anchors..... 19

Fig.1.2. Failure mechanisms of adhesive anchors..... 19

Fig.1.3. Interrelations of the ways chosen to approach the mechanical behaviour of adhesive anchors... 20

Fig.1.4. Progressive failure of an adhesive anchor..... 21

Fig.1.5. Effect of distributed shear and radial stresses induced in concrete by pulling out of an adhesive anchor..... 21

Fig.1.6. Splitting mode of failure..... 22

Fig.1.7. Force interaction between a threaded bolt and surrounding concrete..... 22

Fig.2.1. P=P(δ) law after Biviridge /2/..... 23

Fig.2.2. P=P(δ) relationship after Sell /4/..... 23

Fig.2.3. Experimental setup used by Eibl et al /5/..... 24

Fig.2.4. Local bond-local slip relationship after Eibl et al. /5/..... 24

Fig.2.5. Influence of elevated temperatures on the local bond-local slip relationship after Eibl et al /5/..... 24

Fig.2.6. Stresses in an adhesive anchor after Farmer /6/..... 24

Fig.2.7. Distribution of shear stresses along an anchor after Farmer /6/..... 25

Fig.2.8. Distribution of steel strains along the anchor

Page

axis after Farmer /6/..... 25

Fig.2.9. Local bond-local slip law after Rehm and Franke /7/..... 25

Fig.2.10. Influence of load duration and ambient temperature on slip, after Rehm and Franke /7/. 25

Fig.2.11. Determination of anchorage length after Rehm et al /7/ in relation to expected values of slip 26

Fig.2.12. Concrete cone failure after Daws /8/..... 26

Fig.2.13. Time dependent characteristics for 75mm bond length after Daws /8/..... 26

Fig.2.14. Double coned concrete failure after Lee Mayfield et al /9/..... 26

Fig.2.15. Creep performance of adhesive anchors after Lee et al /9/..... 27

Fig.2.16. Ductile load deflection behaviour after Canon et al /10/..... 27

Fig.2.17. Dependence of the pull-out load on ambient temperature after P.P. Wachtsmuth and Eligehausen /11/..... 27

Fig.2.18. Dependence of anchor slip on the duration of loading and ambient temperature, after P.P. Wachtsmuth and R. Eligehausen /11/..... 28

Fig.2.19. Concrete block used by Kobarg /12/..... 28

Fig.2.20. Dependence of the development length on concrete strength after Kobarg /12/..... 28

Fig.2.21. Assumed law $\varepsilon_b = \varepsilon_b$ (x) for concrete after Kobarg /12/..... 29

Fig.2.22. Strain and displacement distribution along the

Page

anchor after Kobarg /12/..... 29

Fig.2.23. $\tau=\tau(\delta)$ diagram after Kobarg /12/..... 30

Fig.2.24. Dependence of embedment length on hole and anchor diameter, particles size and concrete strength after Kobarg /12/..... 30

Fig.2.25. Bond stress distribution along the anchor, after Kobarg /12/..... 31

Fig.2.26. Steel stress distribution along the axis after Kobarg /12/..... 31

Fig.2.27. Crack zone of an adhesive anchor under tensile loading after Peier /13/..... 32

Fig.2.28. Calculated pull-out ultimate load curve and 5% and 95% fraction curves from experimental results according to Eligehausen et al /14/.... 32

Fig.2.29. Dependence of anchor slip on the duration of loading and ambient temperature, after Eligehausen et al /14/..... 33

Fig.2.30. Reduction of ultimate pull-out load as a function of crack width after Eligehausen et al /14/..... 33

Fig.2.31. Mohr-Coulomb failure contours, after James et al /1/..... 33

Fig.2.32. Predicted non-linear stress-displacement relationship after James et al /1/..... 33

Fig.2.33. P-δ relationship as reported by different authors..... 34

Fig.2.34. Local bond-local slip law as reported by different authors..... 34

Fig.3.1. Complete and incomplete wetting of the

Page

substrate..... 35

Fig.3.2. Microtopography of a system of adherent - adhesive after Fiebrig /17/..... 35

Fig.3.3. Schematic illustration of covalent, ionic and metallic bond, after Fiebrig /17/..... 36

Fig.3.4. Secondary forces:a)Keesom forces b)Debye forces c)London forces d)Hydrogen bond..... 36

Fig.3.5. Energy potential as function of the distance between centres of loads, after Fiebrig /17/.. 37

Fig.3.6. Types of failure..... 37

Fig.3.7. Low and great contact angle of an adhesive with a solid, after Fiebrig /17/..... 38

Fig.3.8. A realistic model of contact between the substrate and adhesive with air bubbles in the interface..... 38

Fig.3.9. Intermolecular forces in the interior and surface molecules of a liquid, Fiebrig /17/.... 38

Fig.3.10. Conditions across a liquid-solid interface. Schematic illustration by Fiebrig /17/..... 39

Fig.3.11. Equilibrium conditions of a 3 phase system (Solid-Liquid-Vapour)..... 39

Fig.3.12. Zisman's plot..... 40

Fig.3.13. Capillary height..... 40

Fig.3.14. Losses of bond strength after Allen /35/..... 40

Fig.3.15. Elliptical crack in a uniformly stressed, infinite lamina..... 40

Fig.3.16. G and K values for different adhesive joints, after Kinloch /15/..... 41

Fig.3.17. Induction of stresses in an adhesive anchor due to shrinkage of the adhesive, after Gent /40/.. 42

Page

Fig.3.18. Butt joints (under tension)..... 42

Fig.3.19. Single lap joint analysed by Volkersen /18/ ... 43

Fig.3.20. Shear loaded joints with (a) thin and (b) thick adhesive layer, analysed by Gent /40/..... 43

Fig.4.1. a)Schematic configuration of thermoplastics long chain molecules in space. b)Schematic configuration of a cross-linked polymer molecule, after Arridge /41/..... 44

Fig.4.2. Curing of epoxy resin after Schutz /43/..... 44

Fig.4.3. Schematic configuration of EP resin and hardener after Shaw /44/..... 44

Fig.4.4. Possibilities of formation of polymer composites after Charnecki and Puterman /32/..... 45

Fig.4.5. Chemical structure of epichlorohydrin - - bisphenol A epoxy resin reported by Furr /45/..... 45

Fig.4.6. Chemical bond between quartz aggregate and epoxy resin, reported by Fiebrig /27/..... 46

Fig.4.7. Schematic configuration of Polyester resin, after Shaw /44/..... 46

Fig.4.8. Effect of aromatic diluent addition on tensile properties of epoxy resin, after Furr /45/.... 46

Fig.4.9. Change of viscosity of EPR by isothermic increase of ambient temperature, after Fiebrig /50/..... 47

Fig.4.10. Physical and chemical changes during the curing process, after Furr /45/..... 47

Fig.4.11. Stress-strain diagrams for cured EP resin (a):after Conrad /54/ (b):after Fiebrig /50/... 47

Page

Fig.4.12. Effect of ratio "aggregates to resin" on the strength, after Seidler /48/..... 48

Fig.4.13. Effect of aggregates on the thermal coefficient, after Furr /45/..... 48

Fig.4.14. Rate of strength gain of an epoxy mortar, after Furr /45/..... 48

Fig.4.15. Effect of time under load on: a)strain (constant load) and b)stress relaxation (constant strain), of epoxy systems, after Furr /45/..... 48

Fig.4.16. Effect of temperature on "σ-ε" relationship of epoxy system under compression, after Hertig /53/..... 49

Fig.4.17. Effect of temperature on tensile strength and elongation and on the modulus of elasticity of a resin after Furr /45/..... 49

Fig.5.1. The components of an adhesive anchor system.... 50

Fig.5.2. Internal axial forces and displacements of the components of an adhesive anchor slice..... 50

Fig.5.3. Envelopes of shear interfacial bond $\tau_{c,r}(z)$, steel tension $P_s(z)$ and resin tensile strain $\varepsilon_r(z)$..... 51

Fig.5.4. System of coordinates used by Mindlin /55/ and simulation of the forces acting on the concrete by pulling out the anchor..... 51

Fig.5.5. Distribution of steel, resin and concrete strains and of interfacial concrete-resin shear stresses derived from theoretical analysis of a particular system..... 52

Page

Fig.6.1. The model analysed by finite element elastic analysis..... 53

Fig.6.2. The slip elements used in the finite element elastic analysis..... 54

Fig.6.3. Results obtained from the linearly elastic finite element analysis (steel and resin strain distribution due to an axial pull-out load P=10 kN)..... 55

Fig.6.4. Results obtained from the linearly elastic finite element analysis (interfacial shear stress and concrete strain distribution due to an axial pull-out load P=10kN)..... 56

Fig.6.5. Results obtained from the linearly elastic finite element analysis (steel and resin strain distribution due to an axial pull-out load P=10 kN)..... 57

Fig.6.6. Results obtained from the linearly elastic finite element analysis (interfacial shear stress and concrete strain distribution due to an axial pull-out load P=10 kN)..... 58

Fig.7.1. Outline sketch of the specimen..... 59

Fig.7.2. Precast mortar cube and prism for carrying the concrete strain gauges. Test series No1..... 60

Fig.7.3. Load - slip relationship obtained from tests series No 2..... 61

Fig.7.4. Experimental set up..... 62

Fig.7.5. Experimental set up - Elevation I-I..... 63

Fig.7.6. Experimental set up - Detail D3 of the coupling device and the LDT for the measurement of the

Page

slip 64

Fig.7.7. Experimental set up - Detail D1 (steel and resin strain gauges)..... 65

Fig.7.8. Experimental set up - Detail D2 of the concrete block with the precast cubes carrying the strain gauges..... 66

Fig.7.9. Experimental set up - Detail D4. Fixing of specimen to loading machine..... 67

Fig.7.10. Loading frame converting the upward movement of the piston of the machine to tension..... 68

Fig.7.11. Experimental set up for pull-out of group of anchors (specimen 3.30)..... 69

Fig.7.12. Experimental set up for the pull-out of the anchor placed near the edge (specimen 3.31).... 70

Fig.7.13. Formwork for casting the concrete specimens and fixing the precast mortar cubes..... 71

Fig.7.14. Direct shear tests..... 72

Fig.7.15. Direct shear specimens used..... 73

Fig.7.16. Resin tensile tests..... 74

Fig.7.17. Resin tensile set up. Detail D6..... 75

Fig.7.18. Effect of a)anchor free length and deflection of concrete specimen, and b)eccentricity of the needle of LDT..... 76

Fig.7.19. Configuration of the data acquisition and recording system..... 77

Fig.7.20. Test series No.2. Details of tests..... 78

Fig.7.21. Test series No.2. Details of tests..... 79

Fig.7.22. Grading of the aggregates used..... 80

Fig.7.23. Initial specimens for the direct shear test.... 81

Fig.7.24. Calibration of the tension transfer system..... 82

Page

Fig.7.25-7.57.P=P(δ) curves for each test..... 83

Fig.7.58-7.91.Summary of the most important data for each test (anchor details, plan and sections of failure surfaces, P-δ results, fit curve to P-δ results).....116

Fig.7.92. Tests 4.01, 4.02 (partially bonded anchors)....150

Fig.7.93. Tests 4.03-4.04 (partially bonded anchors).....151

Fig.7.94. Tests 4.05-4.07 (partially bonded anchors).....152

Fig.7.95. Comparison of the fundamental law P=P(δ) for different types of adhesives.....153

Fig.7.96. Comparison of the fundamental law for different values of embedment lengths.....153

Fig.7.97. Comparison of the fundamental law P=P(δ) for different types of anchor.....154

Fig.7.98. Comparison of the fundamental law for different anchor diameters.....154

Fig.7.99. The effect of concrete strength on the fundamental law P=P(δ).....155

Fig.7.100.The effect of the method of insertion of resin on the P=P(δ) relationship.....155

Fig.7.101.The influence of the thickness of resin, on the P=P(δ) relationship.....156

Fig.7.102.The influence of the eccentricity of the anchor on the P=P(δ) curve.....156

Fig.7.103.The influence of the method of drilling.....157

Fig.7.104.The effect of the size of specimen on the relationship P=P(δ).....157

Fig.7.105.The effect of the amount of reinforcement.....158

Fig.7.106.The relationship P=P(δ) for different modes of failure.....158

Page

Fig.7.107.The group and edge effect on the P=P(δ) relationship.....159
Fig.7.108.Dependence of ultimate pull-out load on concrete strength.....160
Fig.7.109.Effect of concrete strength on anchor displacement.....160
Fig.7.110.Effect of embedment length on the ultimate pull-out load.....161
Fig.7.111.Effect of embedment length on the anchor displacement.....161
Fig.7.112.Effect of the diameter of the anchor on ultimate pull-out load and the anchor displacement.....162
Fig.7.113.Effect of the thickness of resin on the pull-out load and on the anchor displacement.....163
Fig.7.114.Effect of the type of anchor.....164
Fig.7.115.Effect of the type of adhesive.....165
Fig.7.116.Effect of the size of specimen.....166
Fig.7.117.Effect of the amount of reinforcement.....167
Fig.7.118.Effect of the method of drilling, the injection of resin and the eccentricity of the anchor.....168
Fig.7.119.Specimen 3.01. Point C1. Concrete strains.....169
Fig.7.120.Specimen 3.01. Point C3. Concrete strains.....169
Fig.7.121.Specimen 3.01. Resin strains.....170
Fig.7.122.Specimen 3.01. Steel strains.....170
Fig.7.123.Specimen 3.02 (l=7.0d). Point C1. Concrete strains.....171
Fig.7.124.Specimen 3.02 (l=7.0d). Point C2. Concrete strains.....171

Page

Fig.7.125.Specimen 3.02 (l=7.0d). Point C3. Concrete strains.....172

Fig.7.126.Specimen 3.02 (l=7.0d). Resin strains.....172

Fig.7.127.Specimen 3.02 (l=7.0d). Steel strains.....173

Fig.7.128.Specimen 3.03 (l=5d). Point C3. Concrete strains.....173

Fig.7.129.Specimen 3.03 (l=5d). Resin strains.....174

Fig.7.130.Specimen 3.03 (l=5d). Steel strains.....174

Fig.7.131.Specimen 3.04 (plain bar). Point C1. Concrete strains.....175

Fig.7.132.Specimen 3.04 (plain bar). Point C3. Concrete strains.....175

Fig.7.133.Specimen 3.04 (plain bar). Point C3. Concrete strains.....176

Fig.7.134.Specimen 3.04 (plain bar). Resin strains.....176

Fig.7.135.Specimen 3.04 (pain bar). Steel strains.....177

Fig.7.136.Specimen 3.14 (C50). Point C1. Concrete strains.....177

Fig.7.137.Specimen 3.14 (C50). Point C2. Concrete strains.....178

Fig.7.138.Specimen 3.14 (C50). Point C3. Concrete strains.....178

Fig.7.139.Specimen 3.05 (ribbed bar). Resin strains.....179

Fig.7.140.Specimen 3.05 (injection of resin). Steel strains.....179

Fig.7.141.Specimen 3.15 (injection of resin). Resin strains.....180

Fig.7.142.Specimen 3.15 (splitting mode). Steel strains..181

Fig.7.143.Specimen 3.17 (non shrink grout). Point C1. Concrete strains.....182

Page

Fig.7.144.Specimen 3.17 (non shrink grout). Point C2. Concrete strains.....182

Fig.7.145.Specimen 3.17 (non shrink grout). Point C3. Concrete strains.....183

Fig.7.146.Partially bonded anchors. $P=P(\delta)$ and $\tau=\tau(\delta)$ relationships obtained experimentally.....184

Fig.7.147.Local bond - local slip law for concrete to concrete adhesive joints.....185

Fig.7.148.Local bond - local slip in concrete to steel adhesive joints.....185

Fig.7.149.Local bond - local slip for steel to steel adhesive joints.....186

Fig.7.150.Resin tensile test for C1380 type of resin.....187

Fig.7.151.Resin tensile test for LV type of resin.....188

Fig.8.1. Comparison of the steel strains and displacement and the resin strains derived from theoretical and finite element analyses with those obtained experimentally....189

Fig.8.2. Comparison of interfacial concrete-resin shear stresses calculated by theoretical analysis with those computed by finite element analysis, and of concrete strains derived from both analyses with those obtained experimentally.....190

Page

2. PLATES

Plate 1 :The experimental set up 191

Plate 2 :The experimental set up.....191

Plate 3 :Fixing of concrete specimen on the testing machine.....192

Plate 4 :Details of the experimental set up.....193

Plate 5 :Detail of the slip measuring device (LDT).....194

Plate 6 :Failure surface with the precast mortar cube carrying the concrete strain gauges.....195

Plate 7 :Failure surface with the precast mortar cube carrying the concrete strain gauges. Close-up...195

Plate 8 :Typical combined mode of failure.....196

Plate 9 :Typical combined mode of failure. Close-up.....196

Plate 10:Typical combined mode of failure.....197

Plate 11:Typical combined mode of failure.....198

Plate 12:Split specimen.....199

Plate 13:Failure surface of split specimen.....200

Plate 14:Failure surface of split specimen. Close-up.....200

Plate 15:Details of split specimen.....201

Plate 16:Details of split specimen.....202

Plate 17:Split specimen.....203

Plate 18:Typical bond failure.....204

Plate 19:Typical bond failure.....205

Plate 20:Typical combined mode of failure.....206

Plate 21:Double cone of concrete failure.....207

Plate 22:Detail of the double cone of failure.....208

Plate 23:Double cone of concrete failure.....209

Plate 24:Double cone of concrete failure. Close-up.....210

Plate 25:Concrete failure cone profiles.....211

Plate 26:Resin failure at the bottom.....212

Page

Plate 27:Resin failure at the bottom.....212

Plate 28:Detail of resin failure at the bottom.....213

Plate 29:Detail of resin failure at the bottom.....214

Plate 30:Detail of resin failure at the bottom of split specimen.....215

Plate 31:Detail of bond failure at the bottom of anchor..216

Plate 32:Resin failure at the bottom.....217

Plate 33:Details of the ribbed bar-resin interface.....217

Plate 34:Details of the ribbed bar-resin interface. Close-up.....217

Plate 35:Failure of resin in the case of threaded anchor.218

Plate 36:Detail of the threaded anchor-resin interface...218

Plate 37:Details of the threaded anchor-resin interface..218

Plate 38:Pull-out test of partially bonded anchor.....219

Plate 39:Pull-out test of partially bonded anchor.....220

Plate 40:Pull-out test of partially bonded anchor.....221

Plate 41:Pull-out test of partially bonded anchor.....222

Page

3. APPENDICES

APPENDIX A: CALCULATION OF ULTIMATE STRENGTH OF DIFFERENT CONCRETE-RESIN JOINTS

A.1.: Ultimate tensile strength of a concrete-resin butt joint..... A.1

A.2.: Ultimate shear strength of a concrete-resin single lap joint..... A.2

A.3.: Strength of a concrete-resin double shear joint..... A.3

A.4.: Calculation of stress and strain of each component of the standard model according to theoretical analysis..... A.4

A.4.1.: Interfacial shear stress τ A.5

A.4.2.: Steel force A.5

A.4.3.: Resin strain A.5

A.4.4.: Distribution of stresses and strains at P=10 kN A.6

A.4.5.: Steel displacement at P=10 kN A.7

A.4.6.: Concrete strains

A.4.6.1.:Contribution of shear forces A.8

A.4.6.2.:Contribution of radial pressure..... A.9

A.4.6.3.:Calculation of values of lateral forces A.10

A.4.6.4.:Mindlin solution for interfacial shear forces (S_A)..... A.12

A.4.6.5.: Mindlin solution for lateral pressure

A.4.6.5.1: Forces $(H_{1.1})+(H_{1.2})+(H_{1.3})$, $(S_{b.1})$..A.13

A.4.6.5.2: Forces $(H_{2.1})+(H_{2.2})+(H_{2.3})$, $(S_{b.2})$..A.14

A.4.6.5.3: Forces $(H_{3.1})+(H_{3.2})+(H_{3.3})$, $(S_{b.3})$..A.15

A.4.6.5.4: Forces $(H_{4.1})+(H_{4.2})+(H_{4.3})$, $(S_{b.4})$..A.16

Page

A.4.6.5.5: Stresses due to $(S_{b.1})+(S_{b.2})+(S_{b.3})$ $+(S_{b.3})$.....A.17

A.4.6.5.6: Overall stresses and strains.....A.17

A.4.6.5.7: Calculation of the first crack load.A.17

APPENDIX B: MINIMUM SIZE OF PULL-OUT SPECIMENS ACCORDING TO BS 5080 PART 1-1974, AND ASTM 488.81..... B.1

Appendix C: FINITE ELEMENT ELASTIC PARAMETRIC ANALYSIS

C.1: Data..... C.1

C.2: Correction of the resin values obtained..... C.4

C.3: Calculation of the first crack load..... C.5

C.4: Some of the results of the finite element analysis..... C.6

APPENDIX D: CHARACTERISTICS OF THE MATERIALS USED. SUPERPLASTICIZERS - C.1380 - LV - GEL-PMMA GROUT - NON SHRINK GROUT..... D.1

APPENDIX E: CALIBRATION OF TESTING EQUIPMENT..... E.1

APPENDIX F: CALCULATIONS OF DEFLECTION OF THE CONCRETE SPECIMENS UNDER CONCENTRATED LOAD OF P=10 kN AT THE CENTRE..... F.1

APPENDIX G: AUGMENTATION FACTOR OF THE LATERAL SURFACE OF OF A THREADED BAR IN RELATION TO THAT OF PLAIN CYLINDER..... G.1

Page

APPENDIX H: CALCULATIONS FOR NORMALIZATION WITH RESPECT TO CONCRETE STRENGTH OF DIFFERENT TEST RESULTS IN ORDER TO OBTAIN COMPARABLE VALUES. H.1

APPENDIX I: CALCULATIONS TO CORRECT THE VALUES OBTAINED FROM TESTS 4.01, 4.03..... I.1

APPENDIX J: CALCULATED DESIGN EXAMPLE OF A PARTICULAR ADHESIVE ANCHOR..... J.1

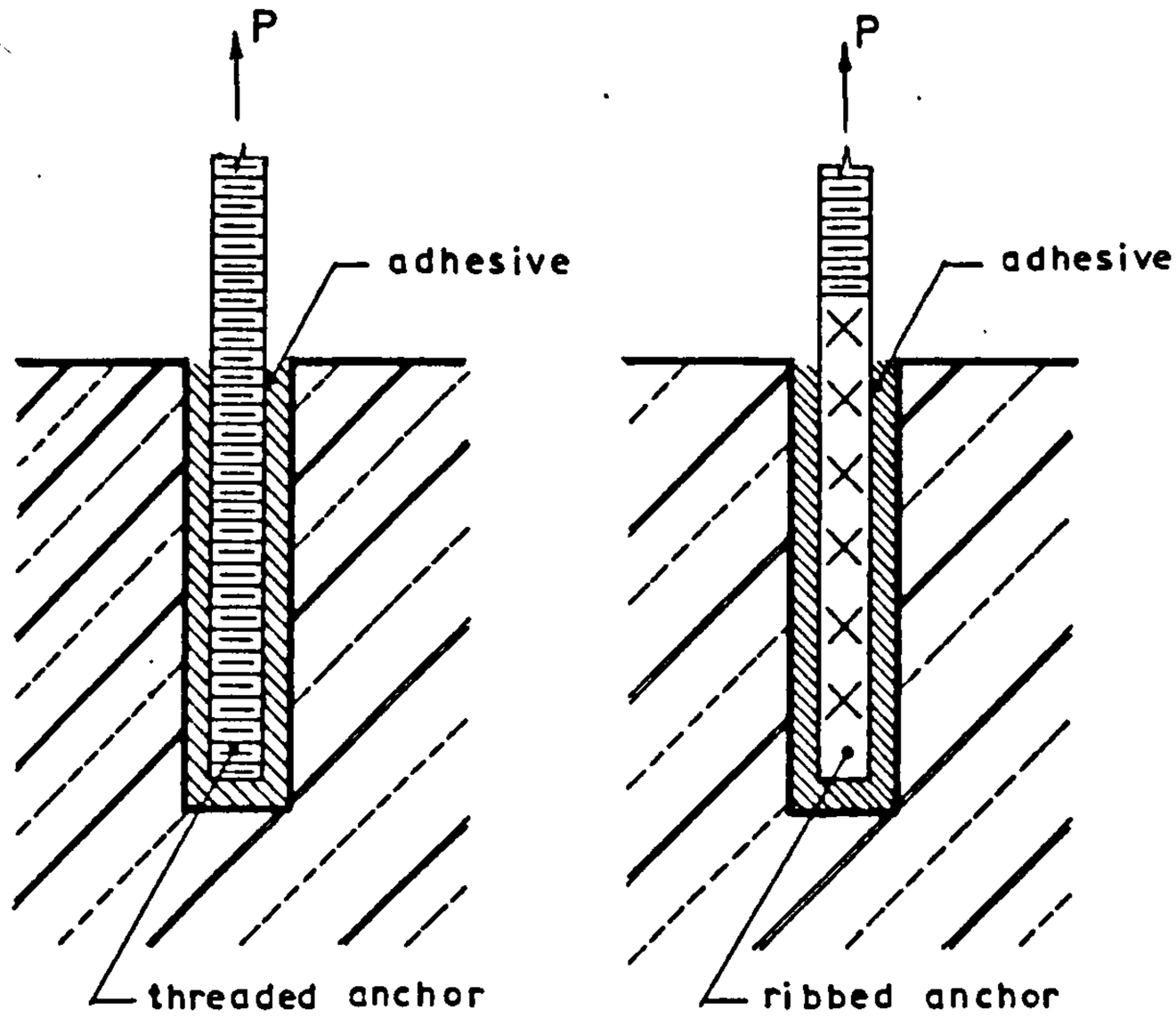

Fig.1.1. Types of chemical anchors

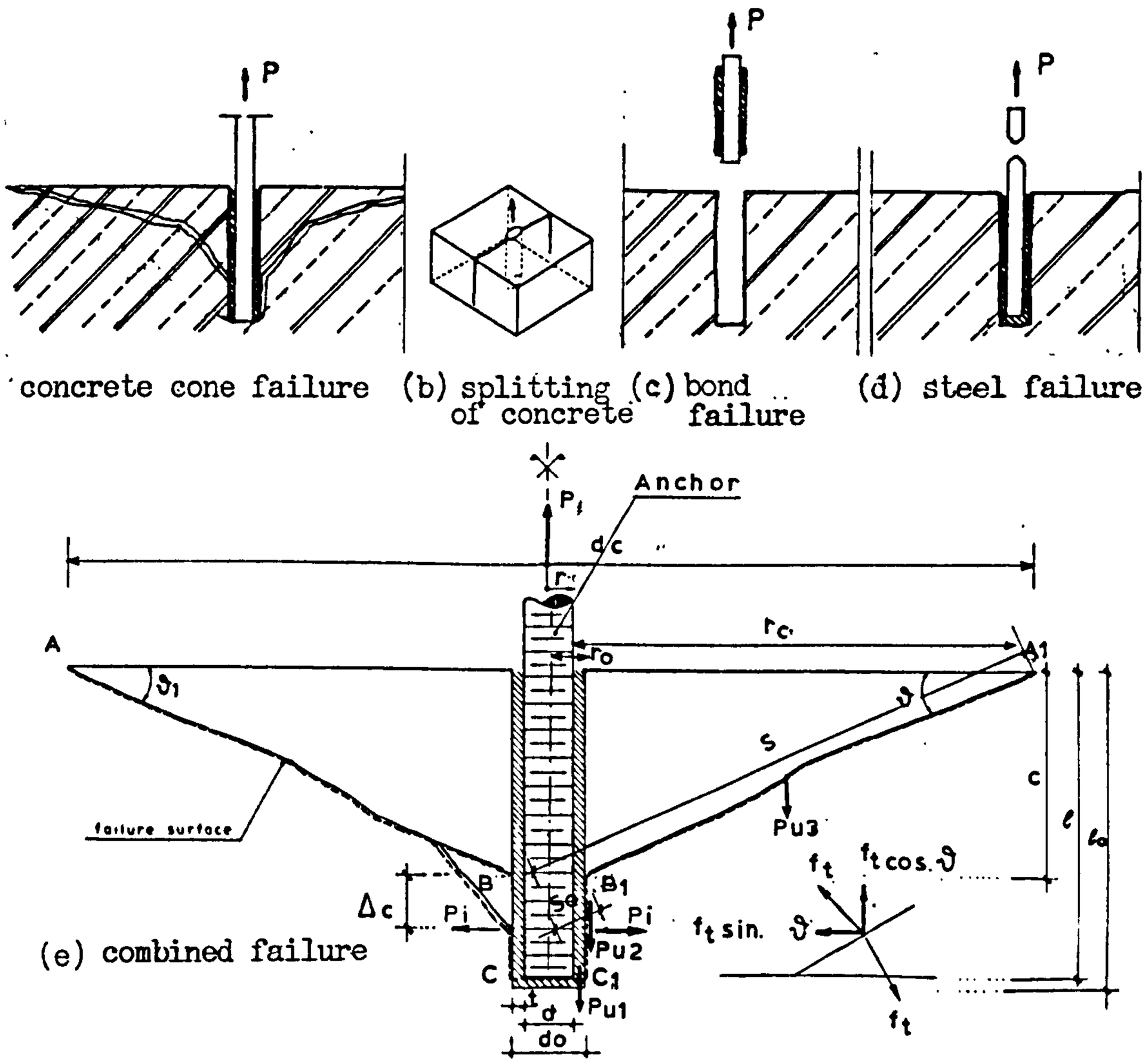

Fig.1.2. Failure mechanisms of adhesive anchors

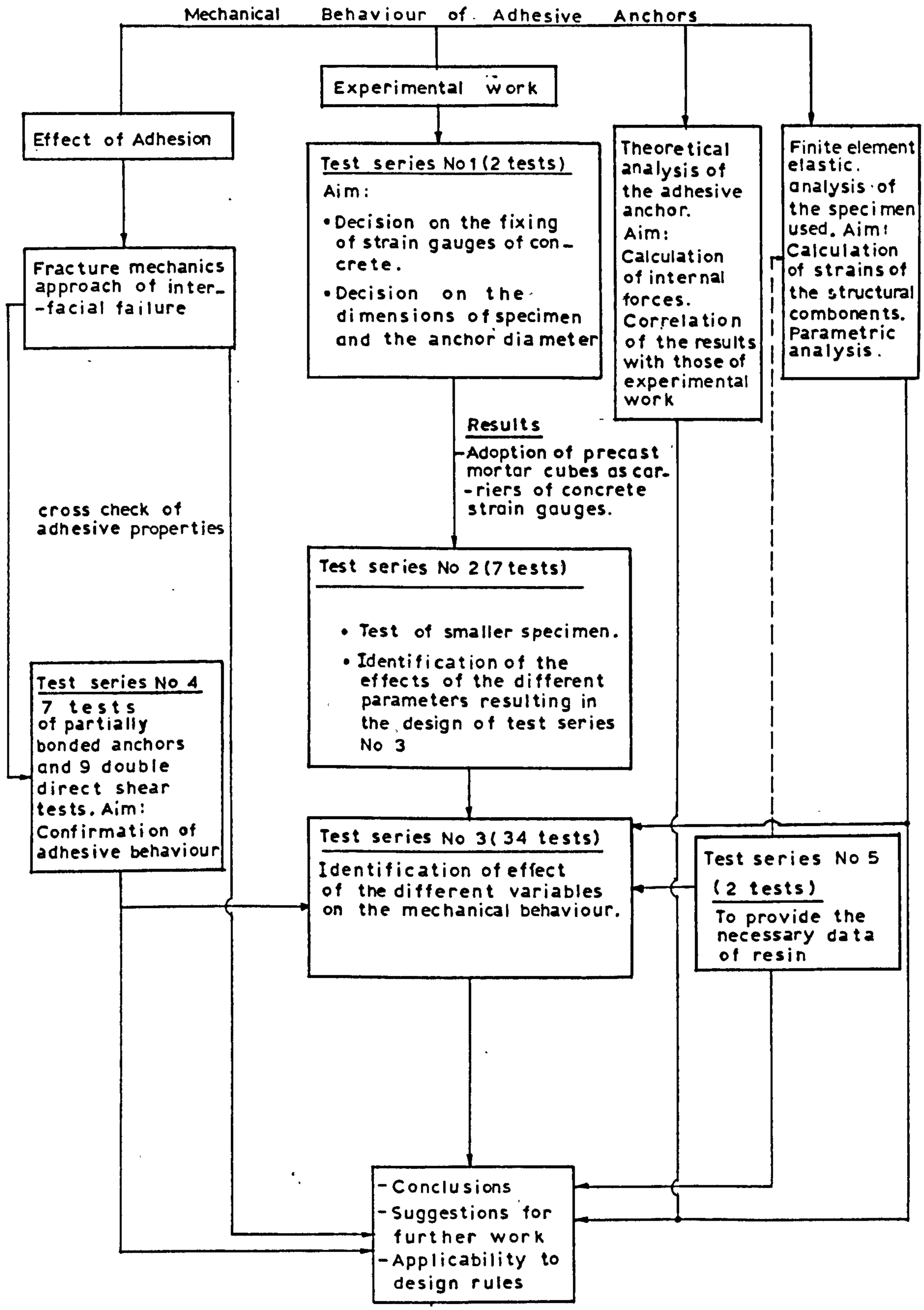

Fig.1.3. Interrelations of the ways chosen to approach the mechanical behaviour of adhesive anchors.

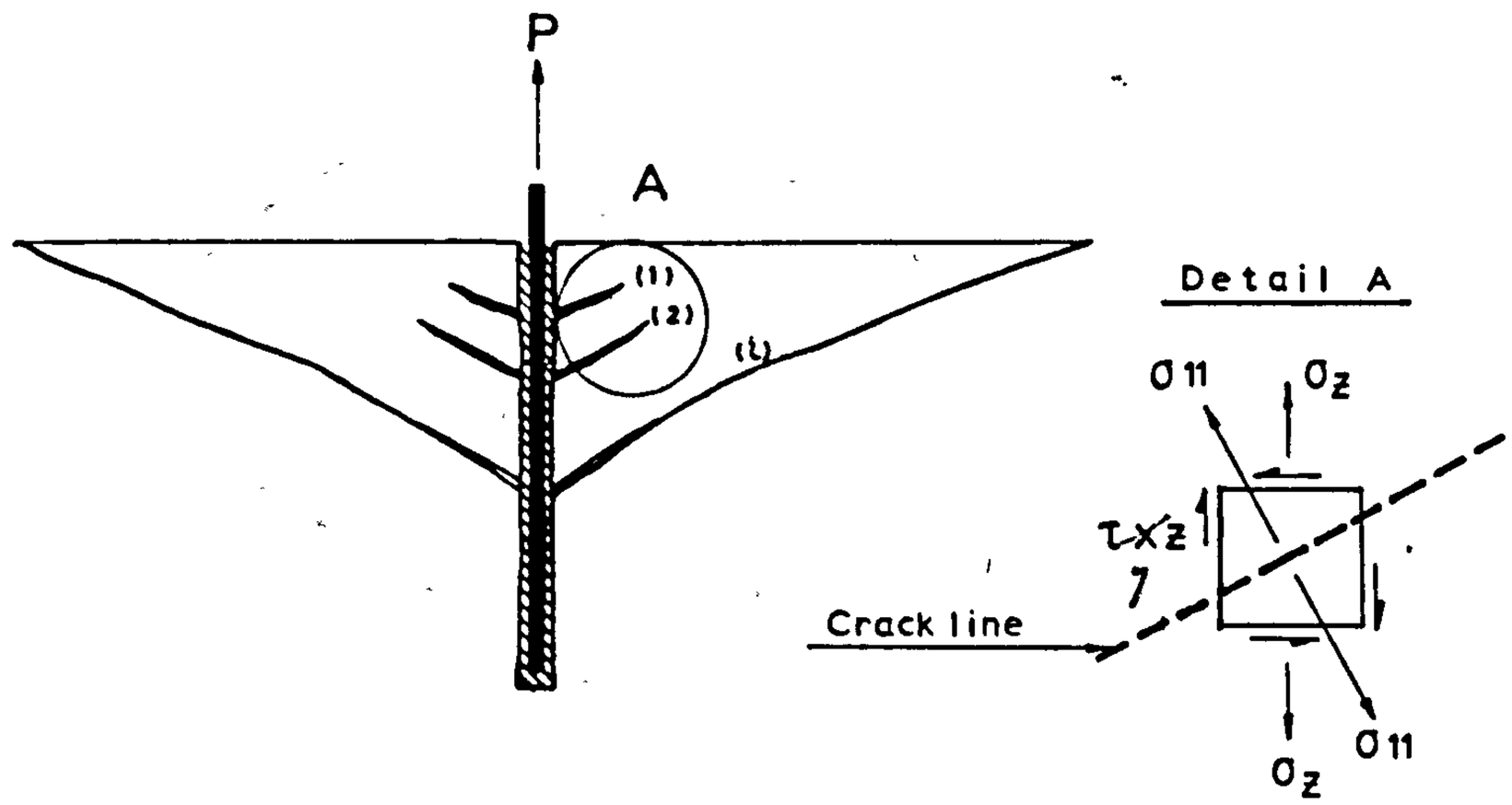

Fig.1.4. Progressive failure of an adhesive anchor

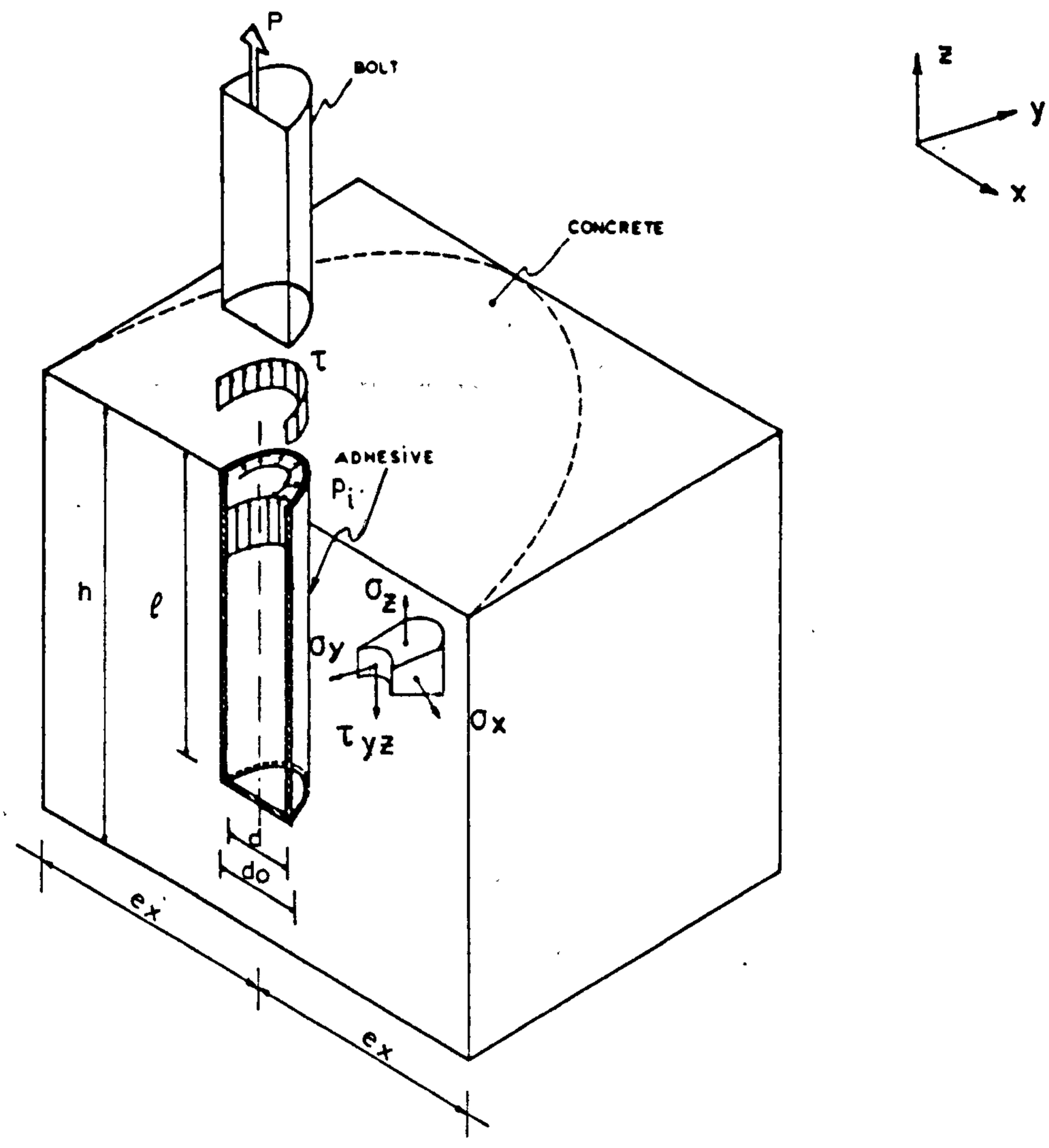

Fig.1.5. Effect of distributed shear and radial stresses induced in concrete by pulling out of an adhesive anchor.

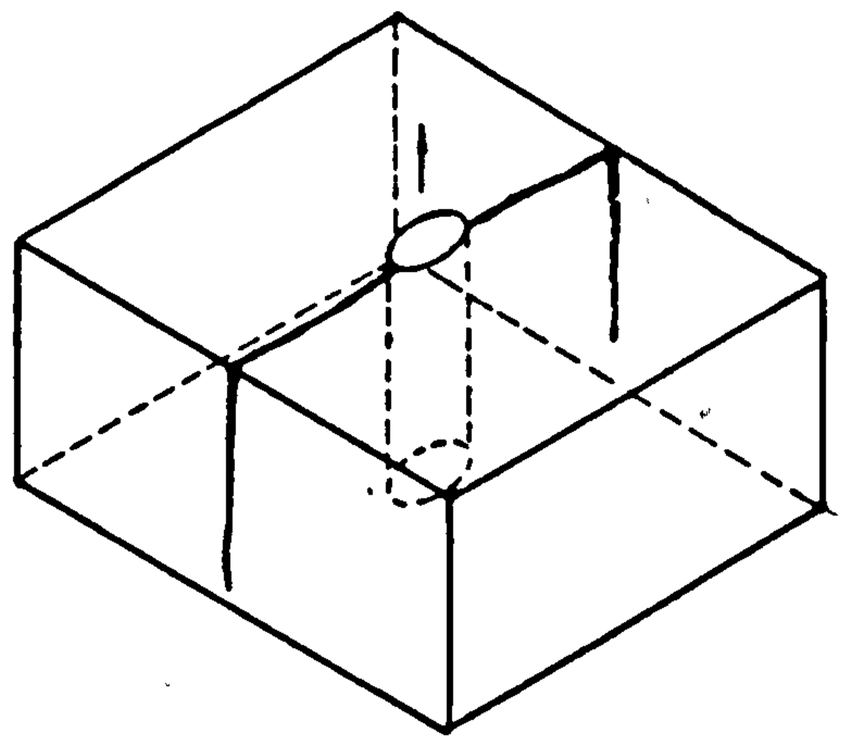

Fig.1.6. Splitting mode of failure

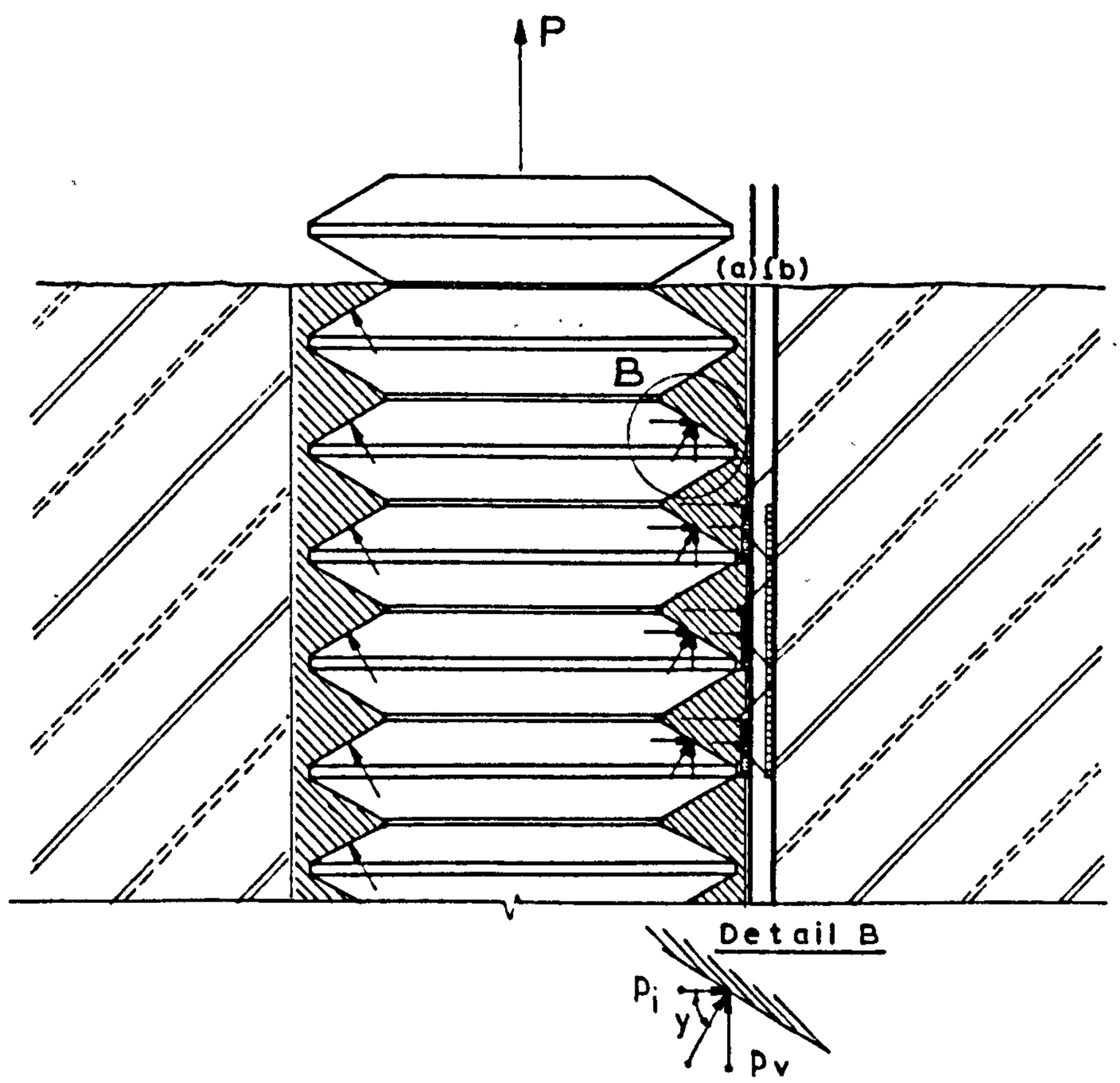

Fig.1.7. Force interaction between a threaded bolt and surrounding concrete.

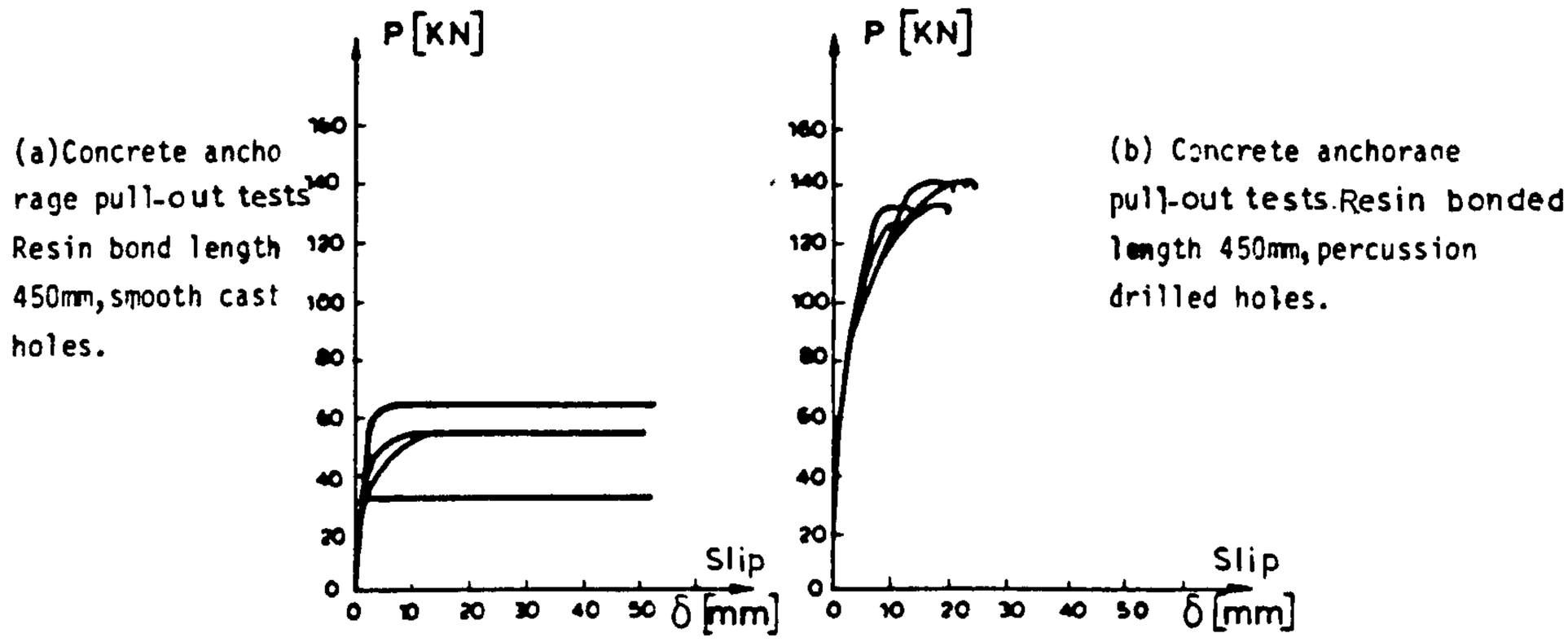

Fig.2.1 P=P(δ) law after Biviridge /2/

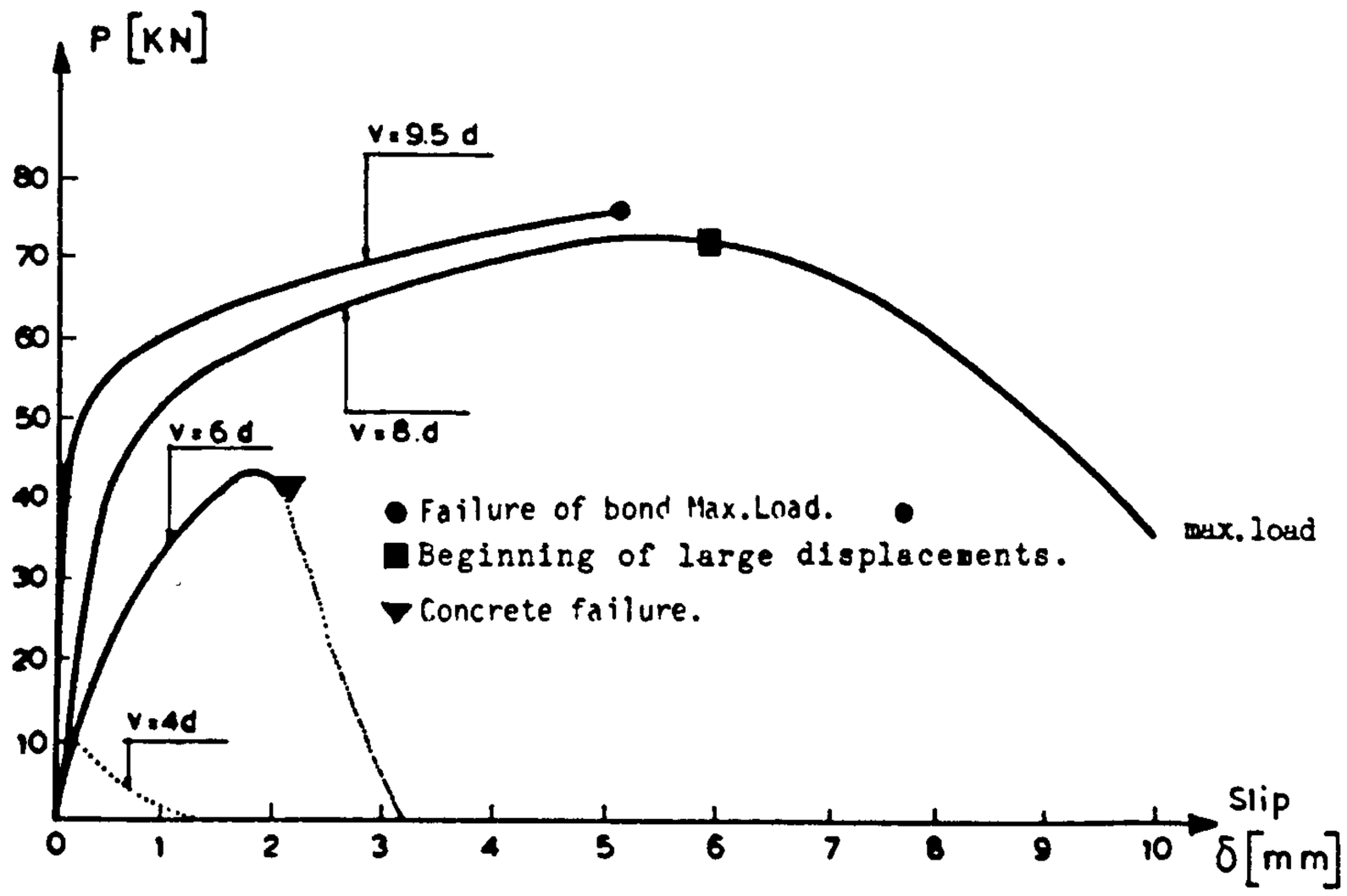

Fig.2.2. P=P (δ) relationship after Sell. /4/

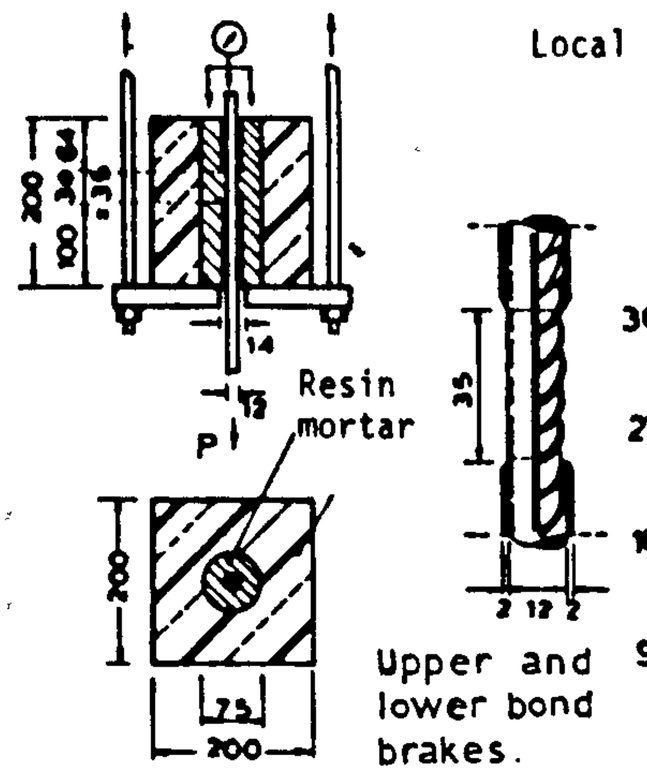

Fig.2.3 Experimental set up used by Eibl, et al./5/

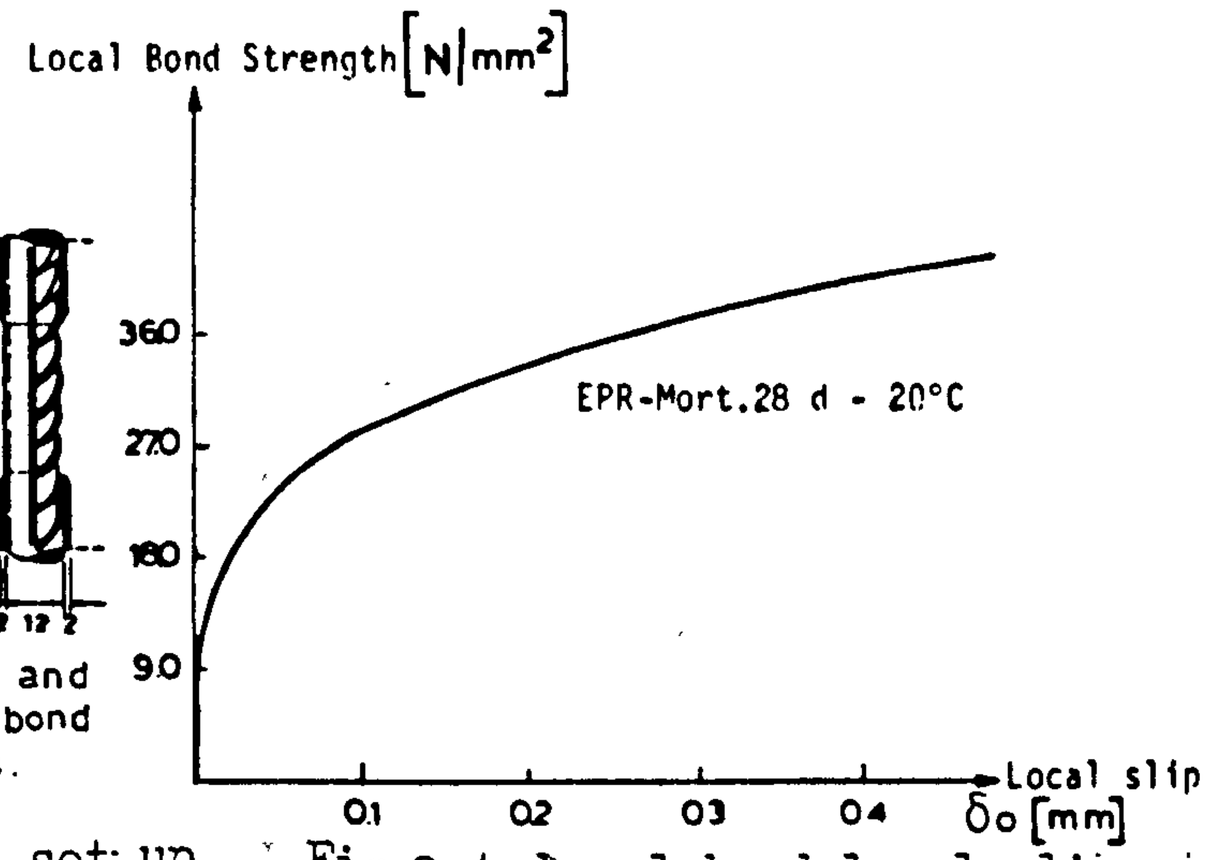

Fig.2.4. Local bond-local slip relationship after Eibl et al /5/

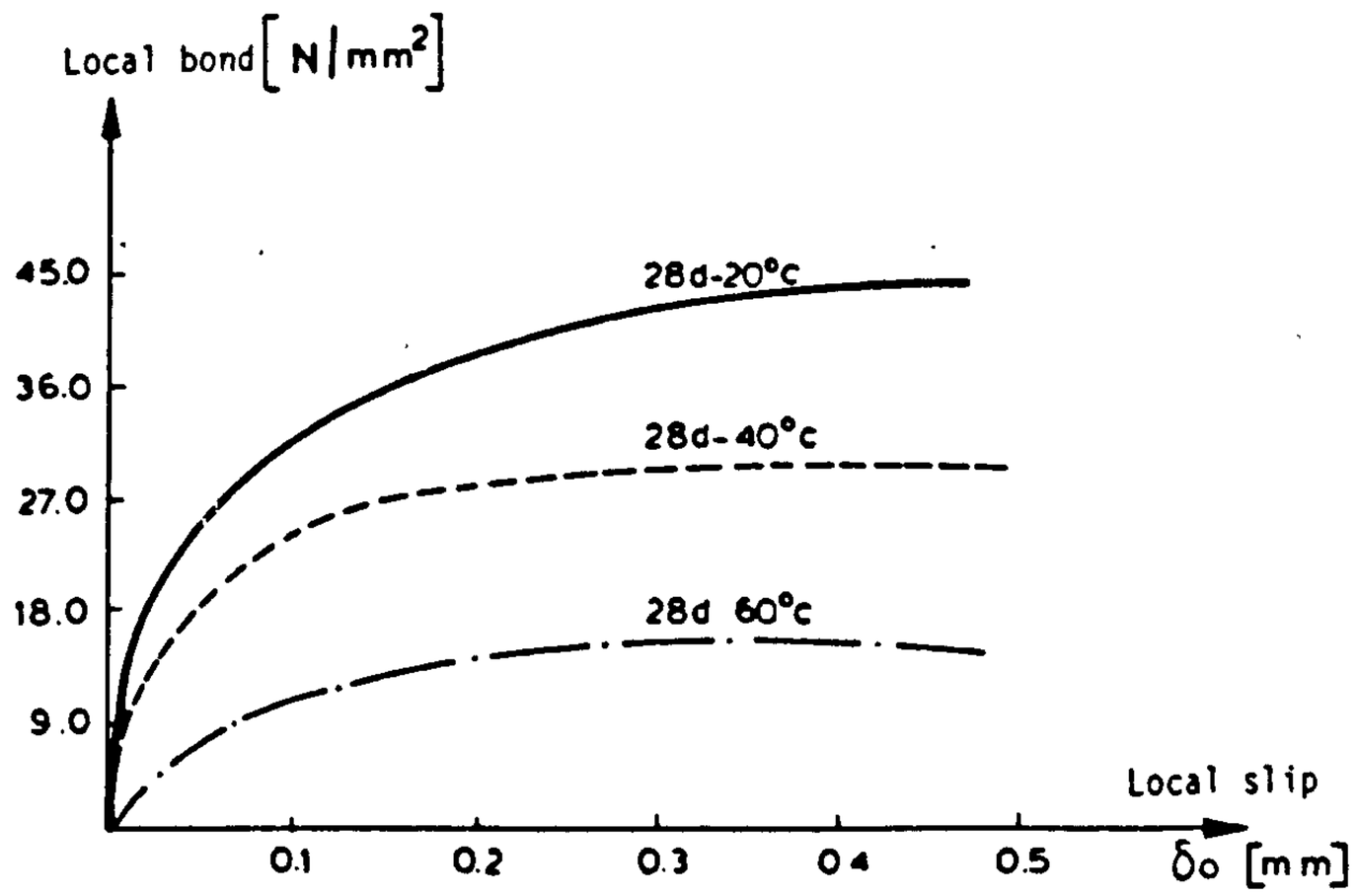

Fig.2.5. Influence of elevated temperatures on the "local bond-local slip" relationship after Eibl et al. /5/

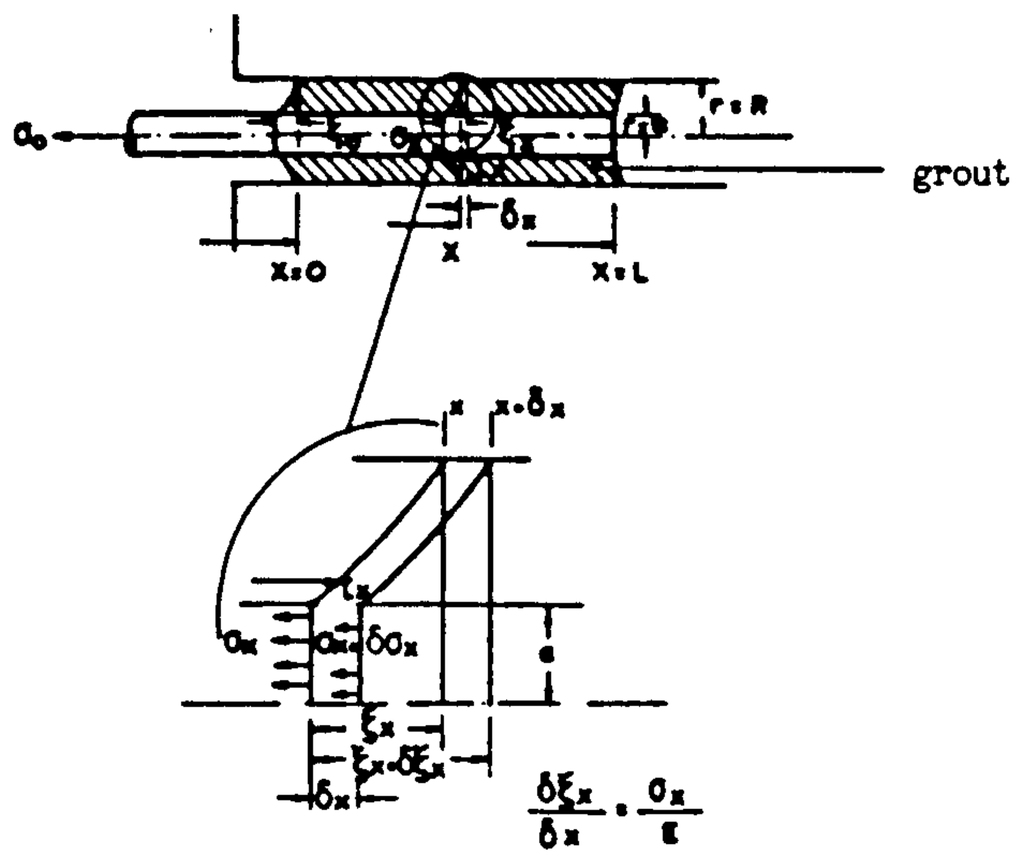

Fig.2.6 Stresses in an adhesive anchor after Farmer. /6/

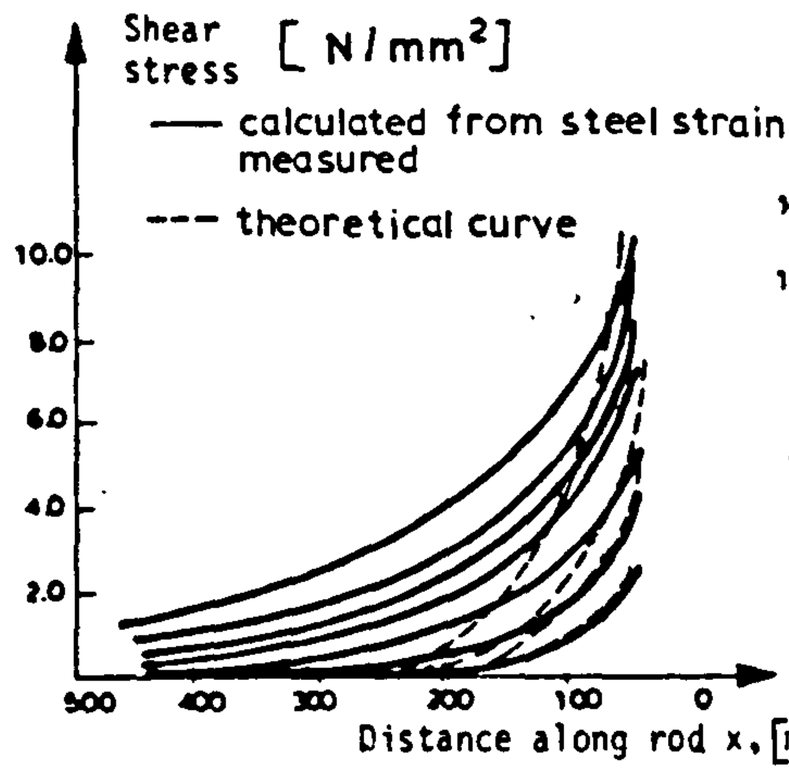

Fig.2.7. Distribution of shear stresses along the anchor after Farmer. /6/

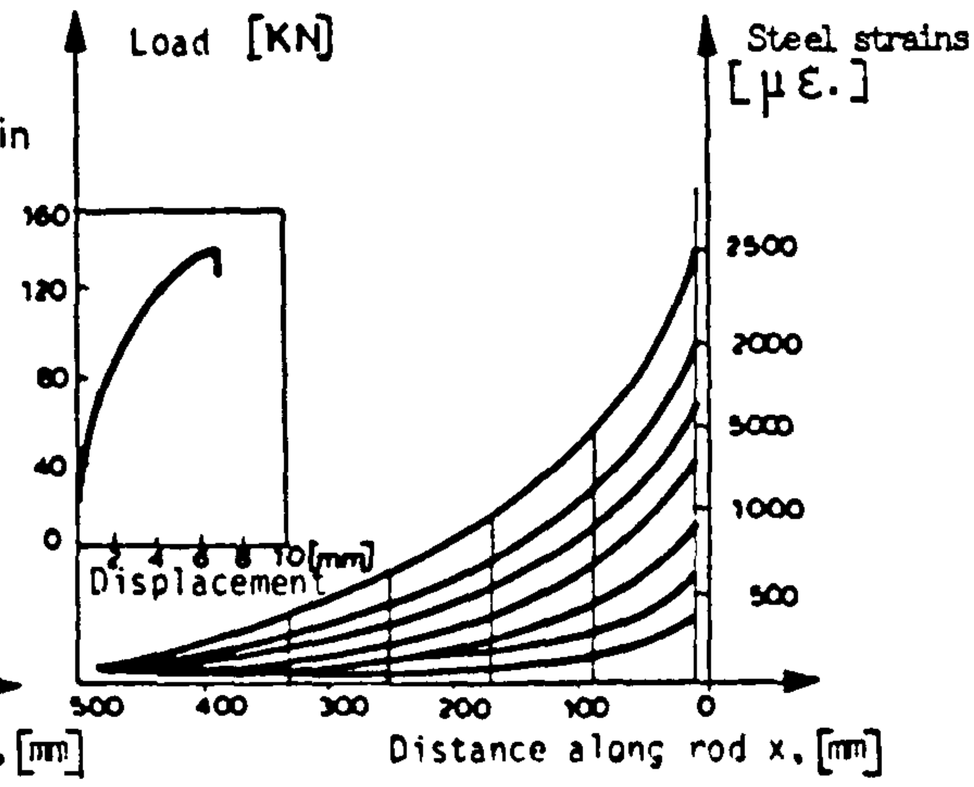

Fig.2.8. Distribution of steel strains along the anchor axis after Farmer. /6/

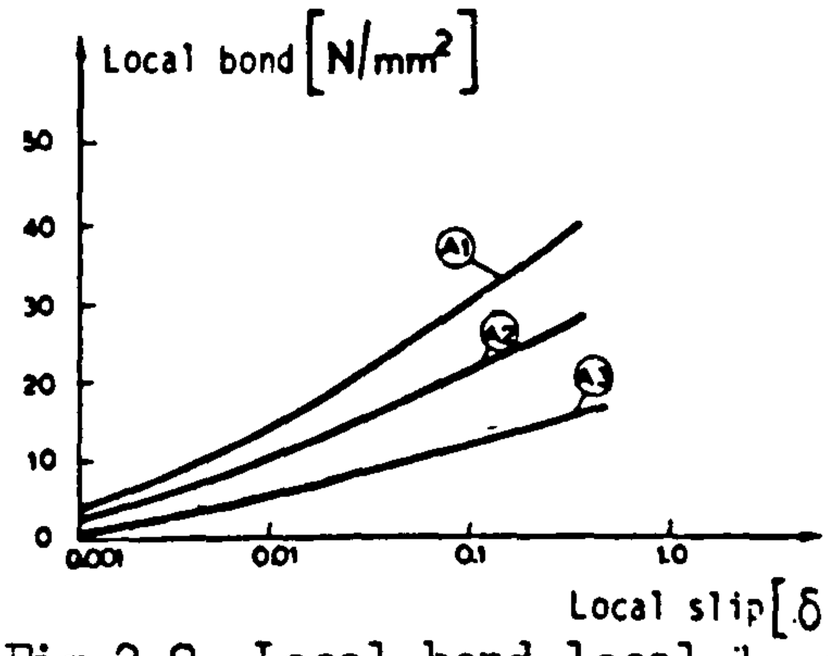

A1,2,3: Local bond-local slip curves for 20° C, with local bond calculated as an average of a ℓ=3d embedment length for commercially available types of ribbed bars.
A1, A2 : St 42|50, A3: St 50|55

Fig.2.9. Local bond local-local slip law after Rehm and Franke/7/

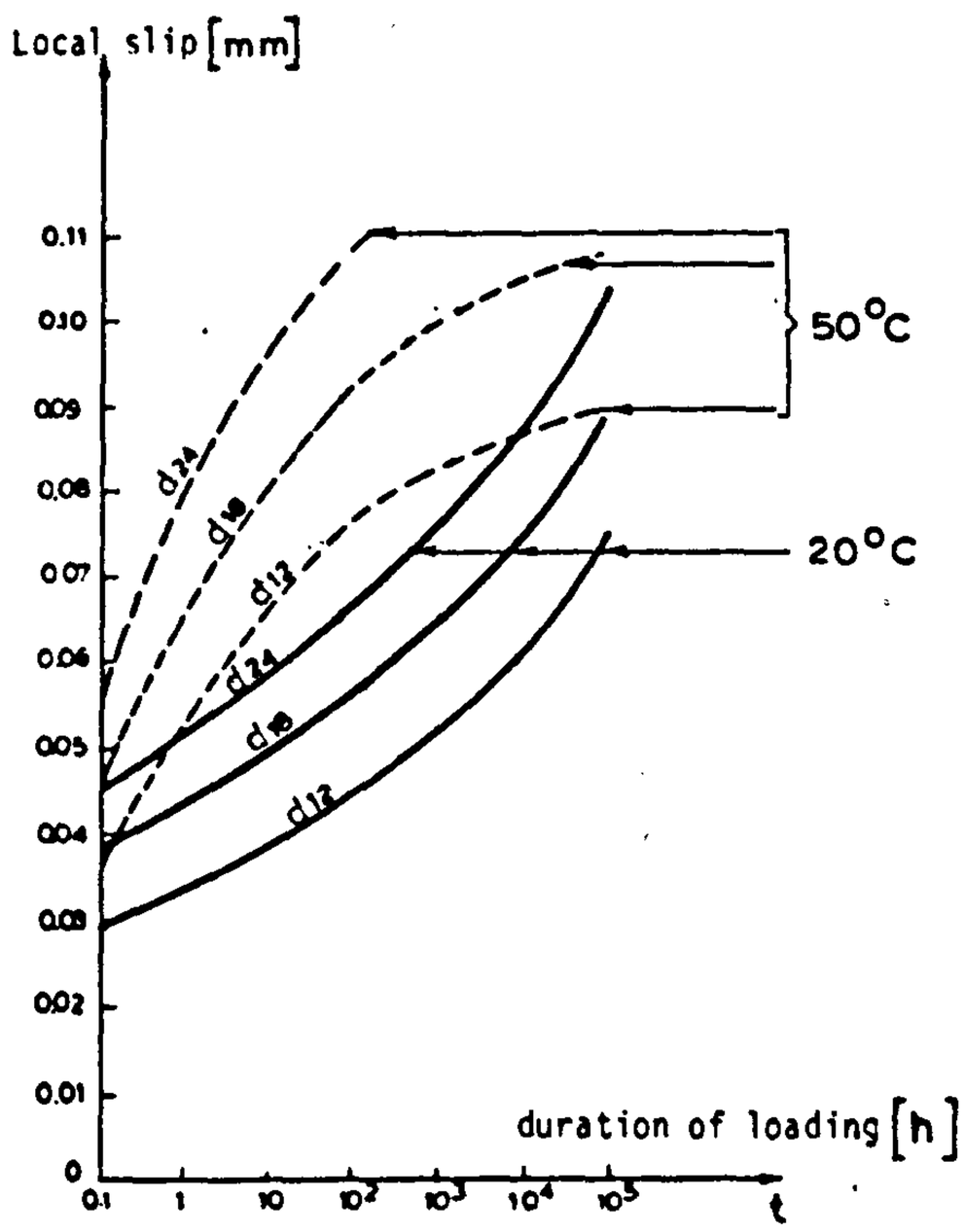

Fig.2.10. Influence of load duration and ambient temperature on slip, after Rehm and Franke. /7/

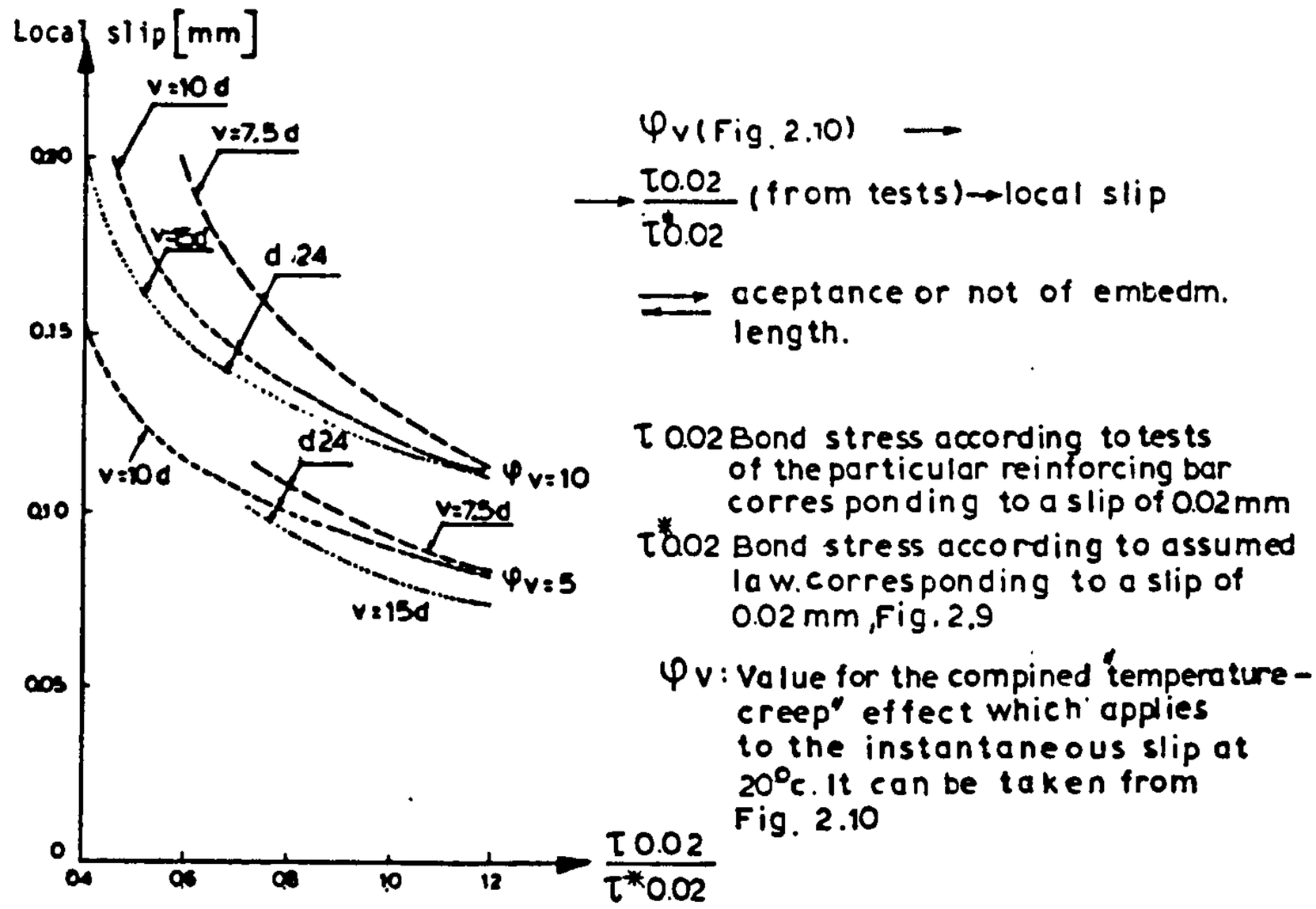

Fig.2.11. Determination of ancnorage length after Rehm et al /7/ in relation to the expected value of slip.

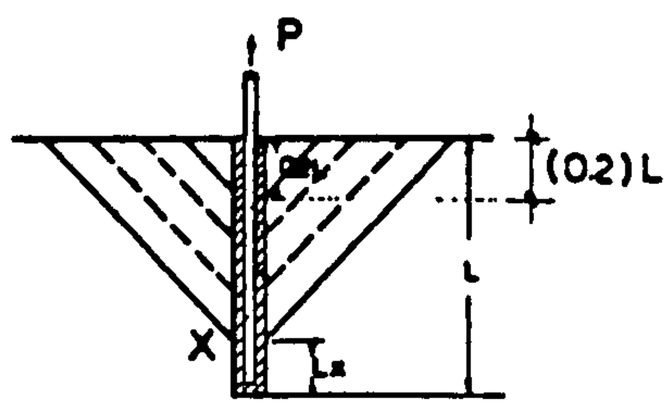

Fig.2.12. Concrete cone failure after Daws. /8/

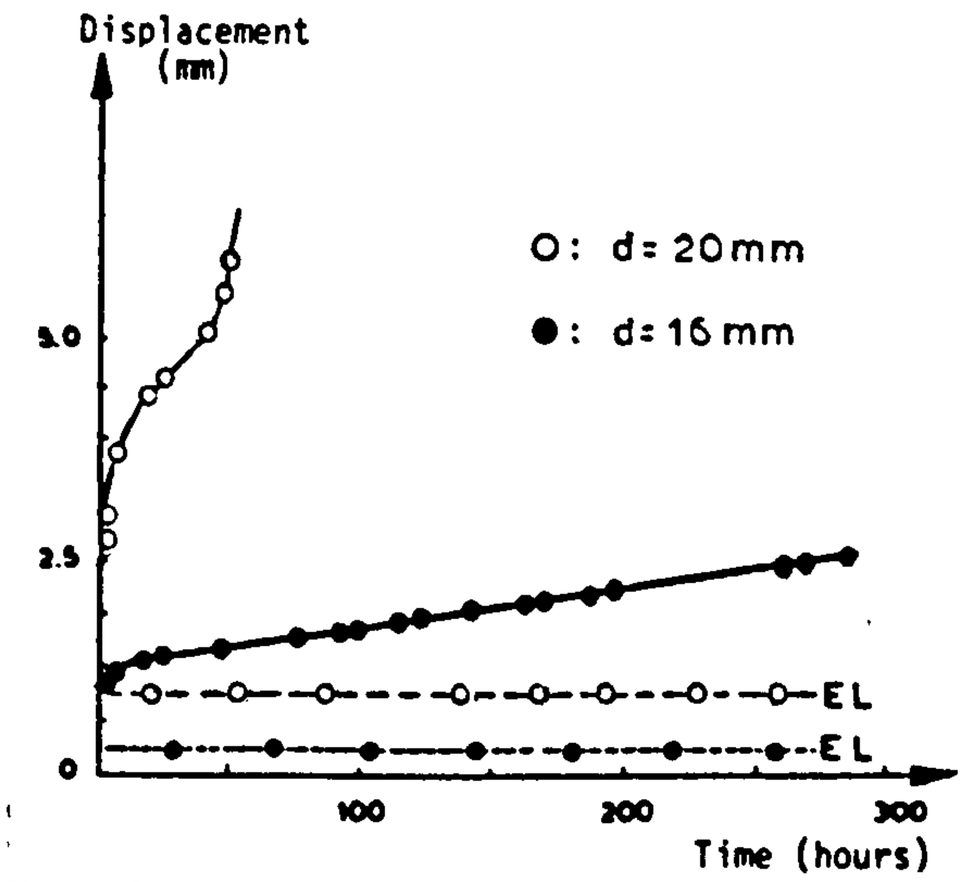

Fig.2.13. Time dependent characteristics for 75mm bond length after Daws. /8/

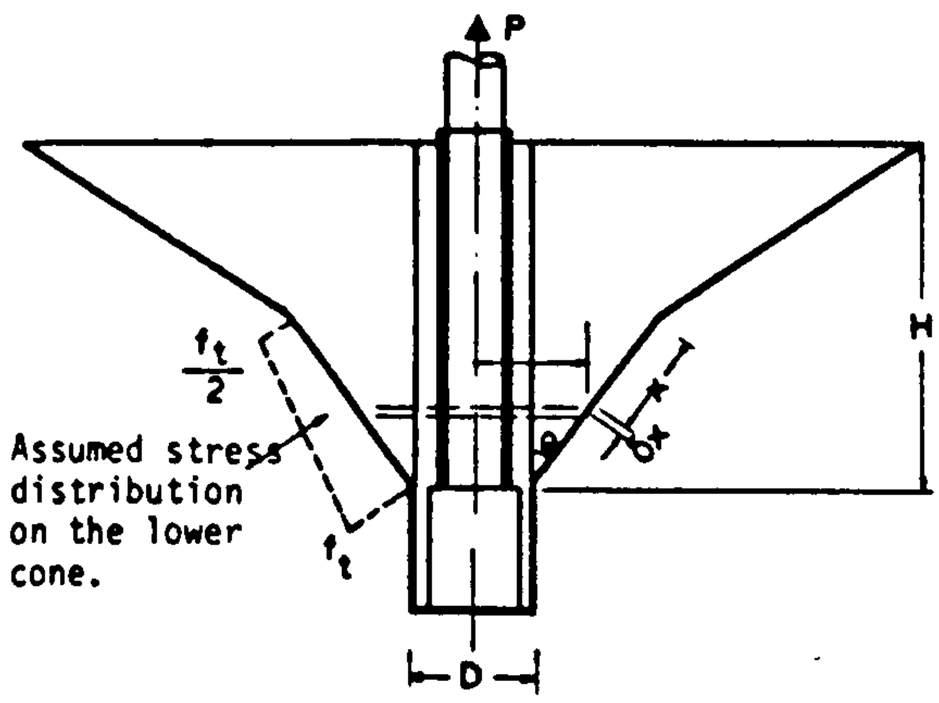

Nonimal Hole Depths (mm)	Rebars NLB2		NLB6	
75	29.2 / 5.7	28.1 / 8.8		
	31.4 / 15.6	38.0 / 5.2		
	27.1 / 8.8	31.8 / 18.2		
	31.8 / 8.8	35.9 / 15.6		
100			48.9 / 13.0	46.9 / 15.6
			49.9 / 10.4	54.7 / 21.9
125			74.9 / 26.0	63.0 / 20.8
			80.1 / 13.0	70.8 / 20.8

Ultimate load (kN) / Load at 0.1 mm slip (kN)

Fig.2.14. Double coned concrete failure after Lee, Mayfield et al/9/

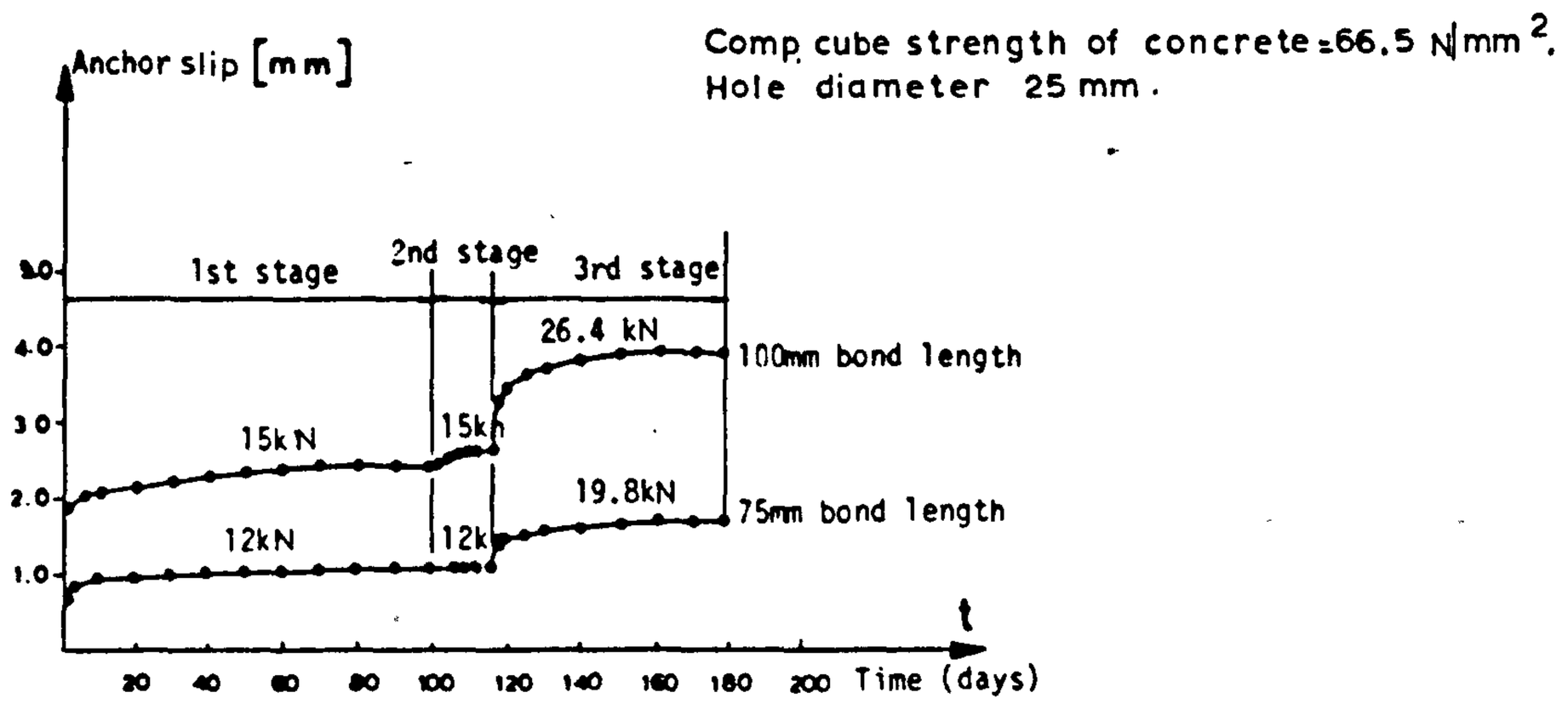

Fig.2.15. Creep performance of adhesive anchors after Lee et al /9/

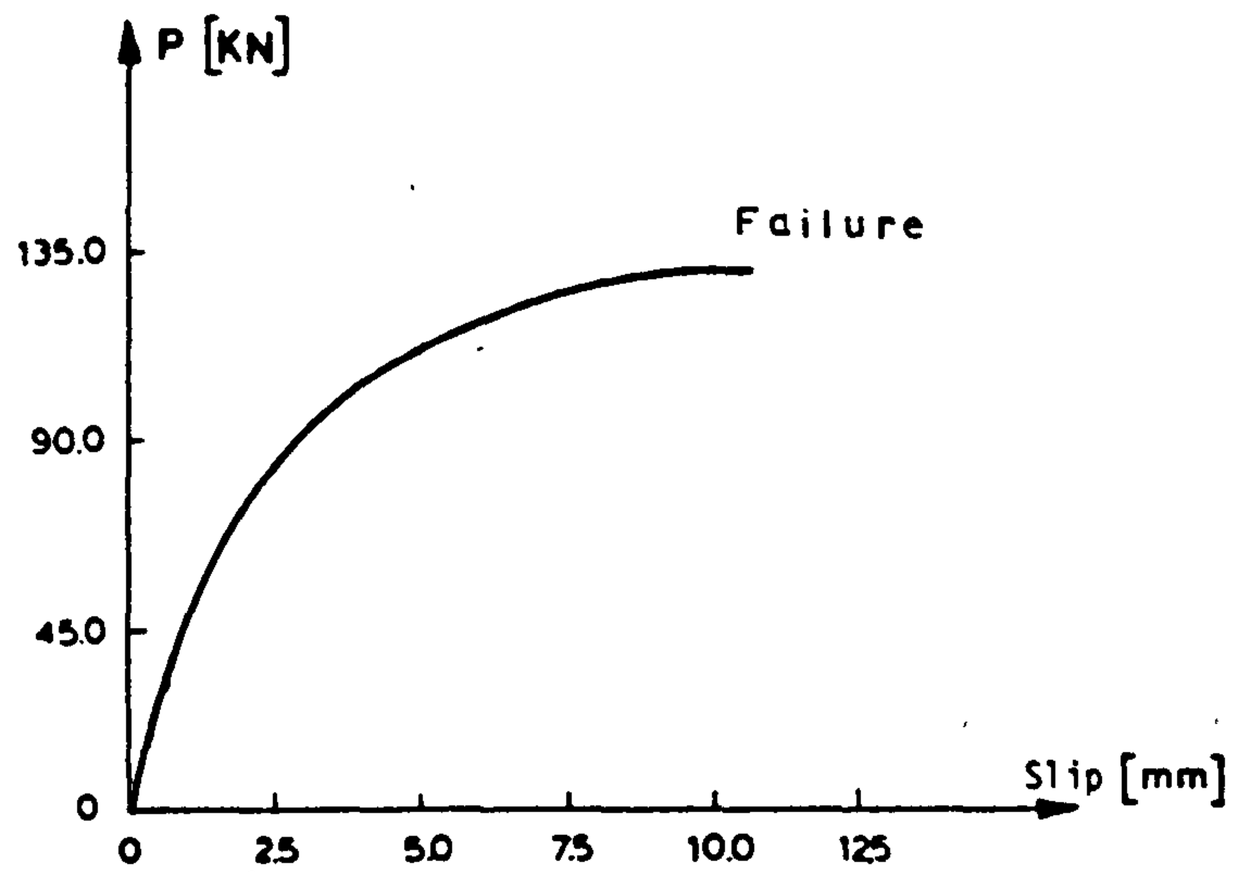

Fig.2.16. Ductile load deflection behaviour after Canon et al /10/

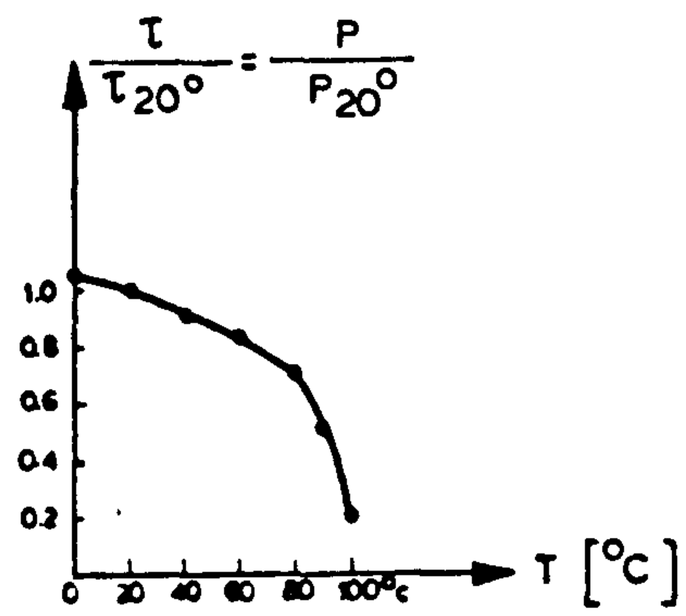

Fig.2.17. Dependence of the pull-out load on ambient temperature after P. P. Wachtsmuth and R. Eligehausen. /11/

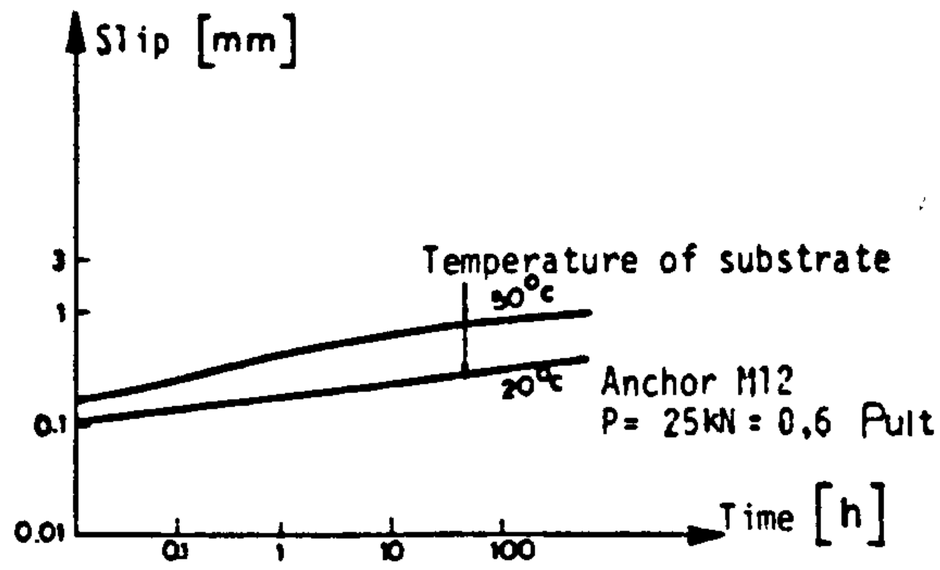

Fig.2.18. Dependence of anchor slip on the duration of loading and ambient temperature, after P.P. Wachtsmuth and R. Eligehausen. /11/

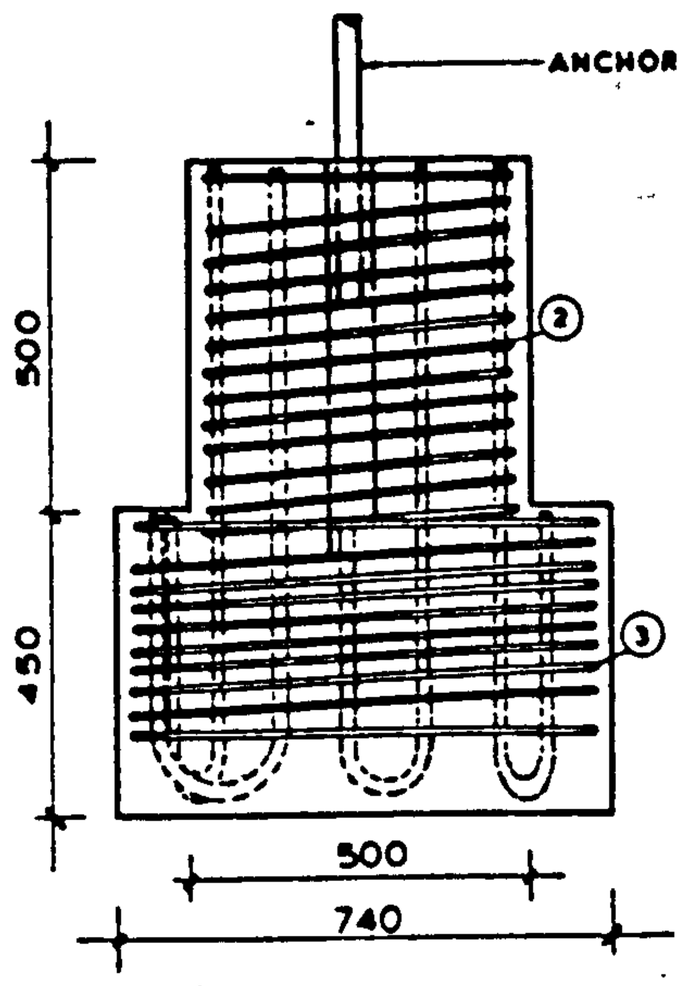

Fig.2.19. Concrete block used by Kobarg. /12/

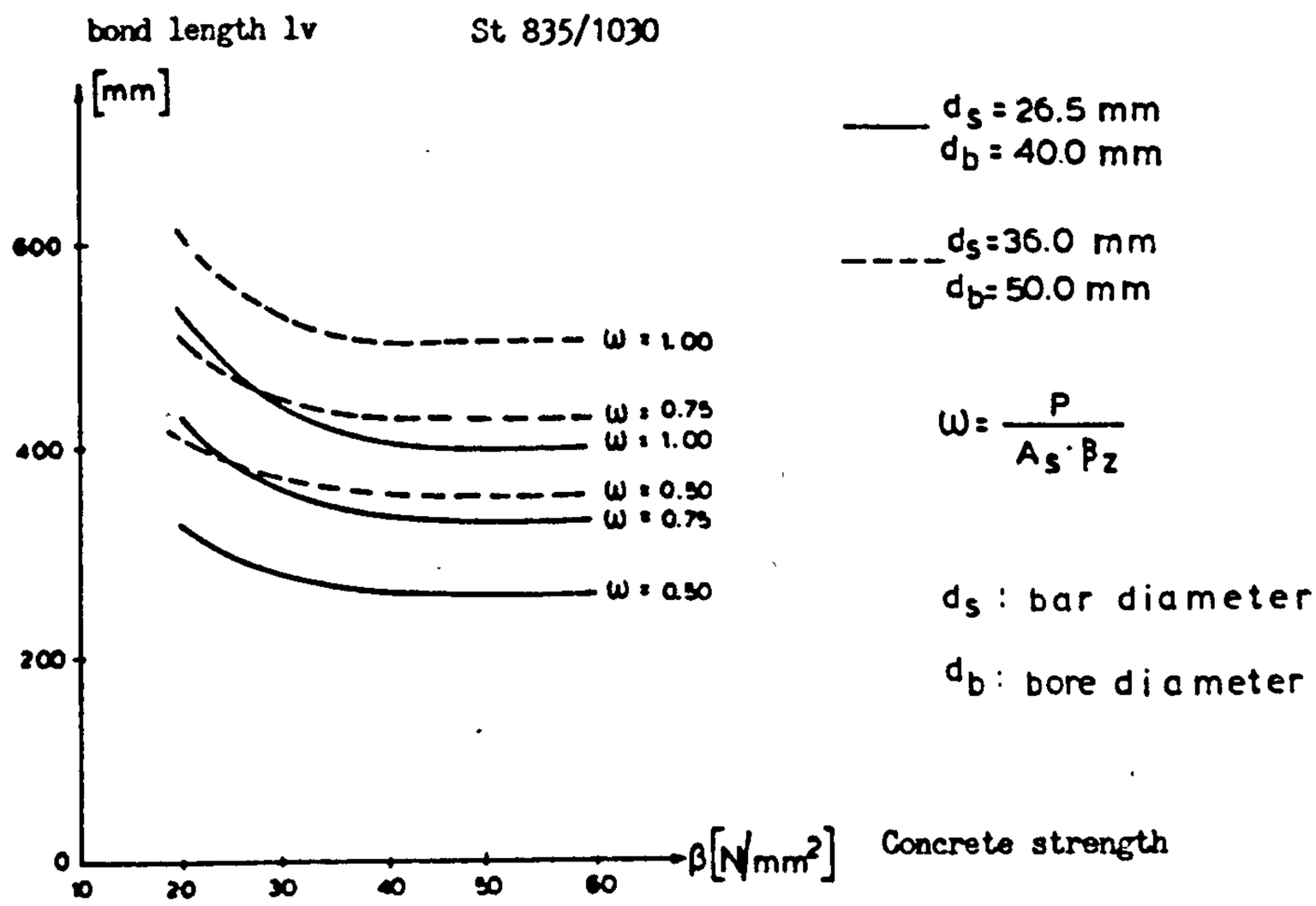

Fig.2.20. Dependence of the development length on concrete strength after Kobarg. /12/

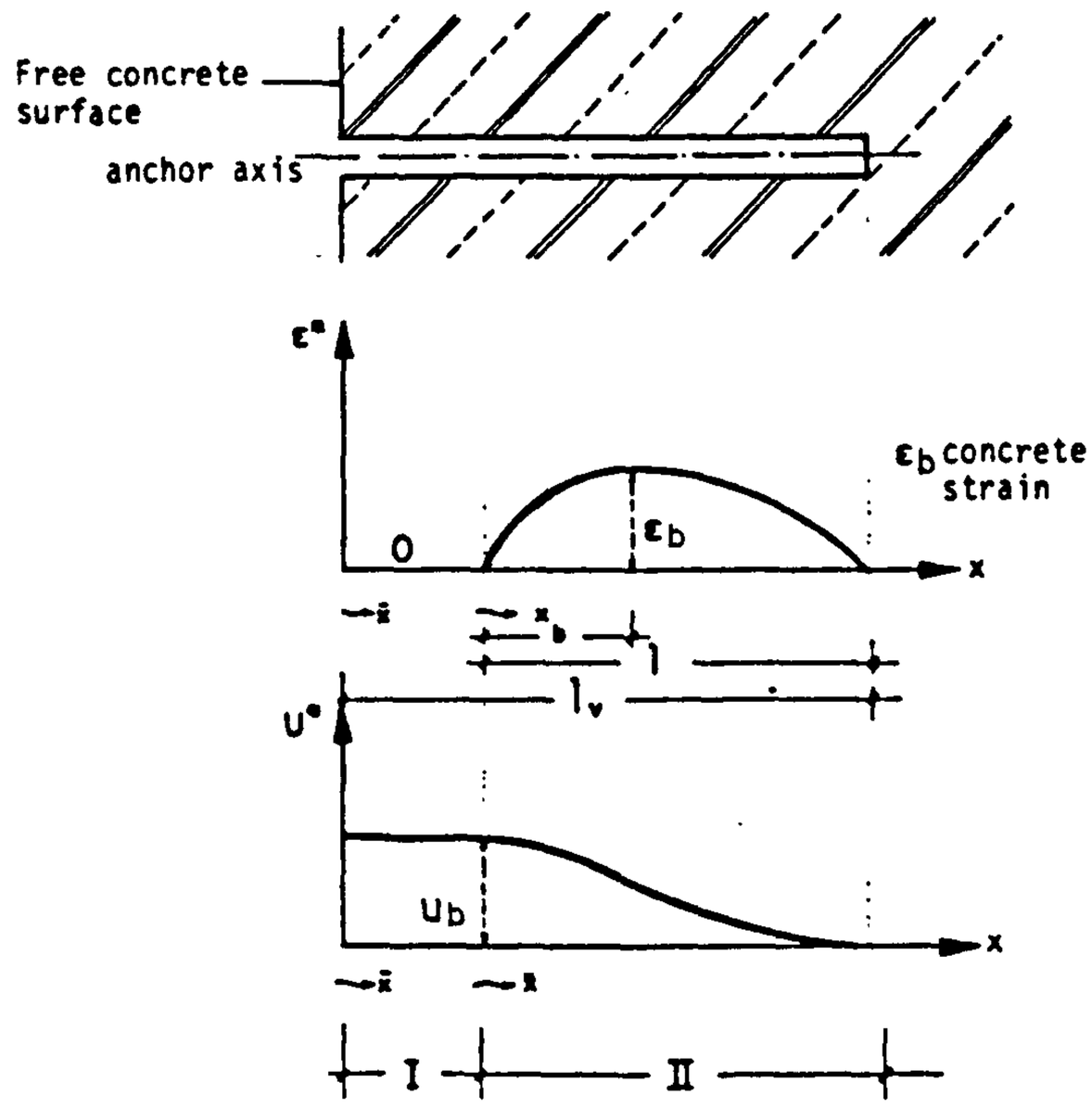

Fig.2.21. Assumed law $\varepsilon_b = \varepsilon_b$ (x) for concrete after Kobarg /12/

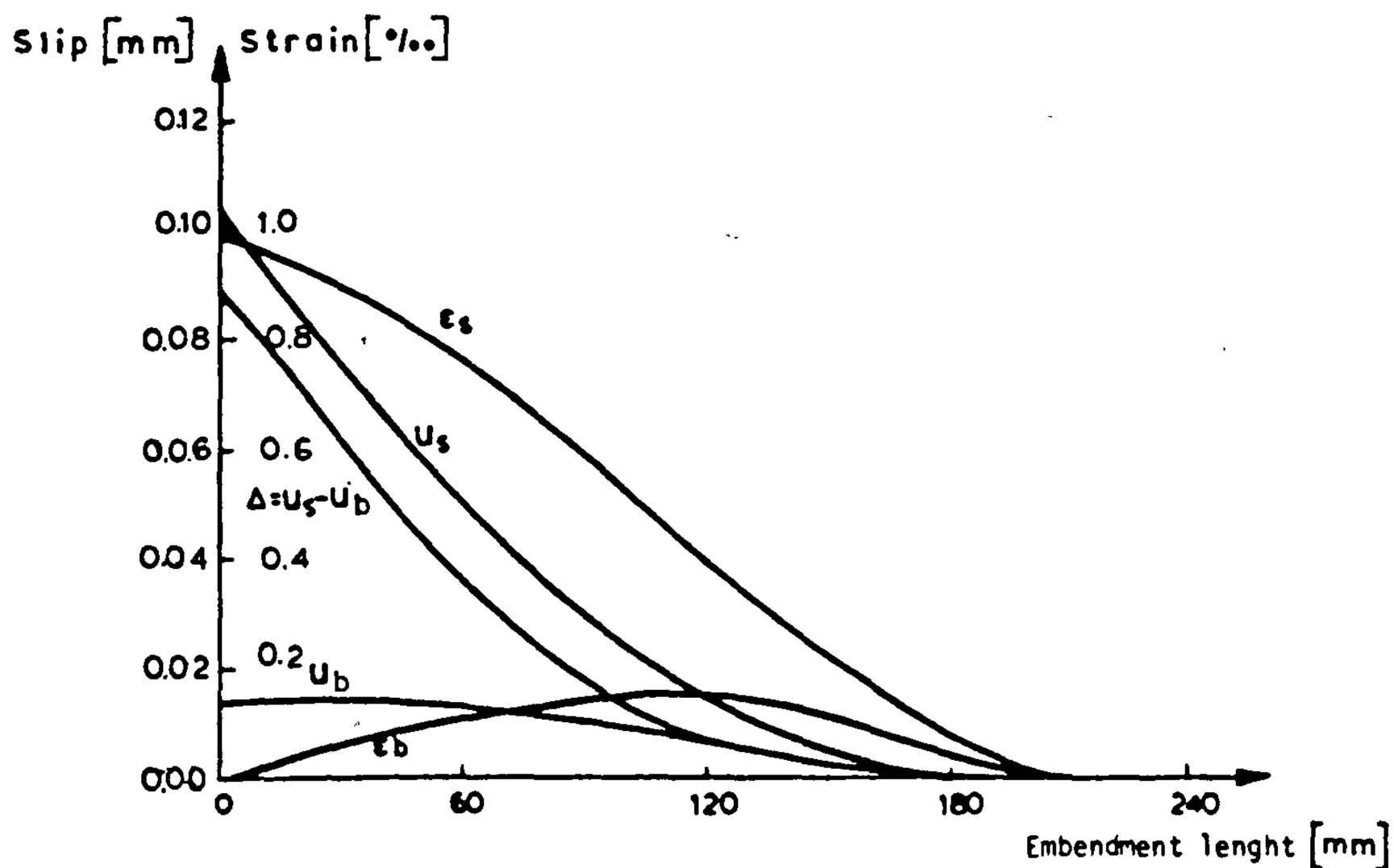

Fig.2.22. Strain and displacement distribution along the anchor, after Kobarg /12/

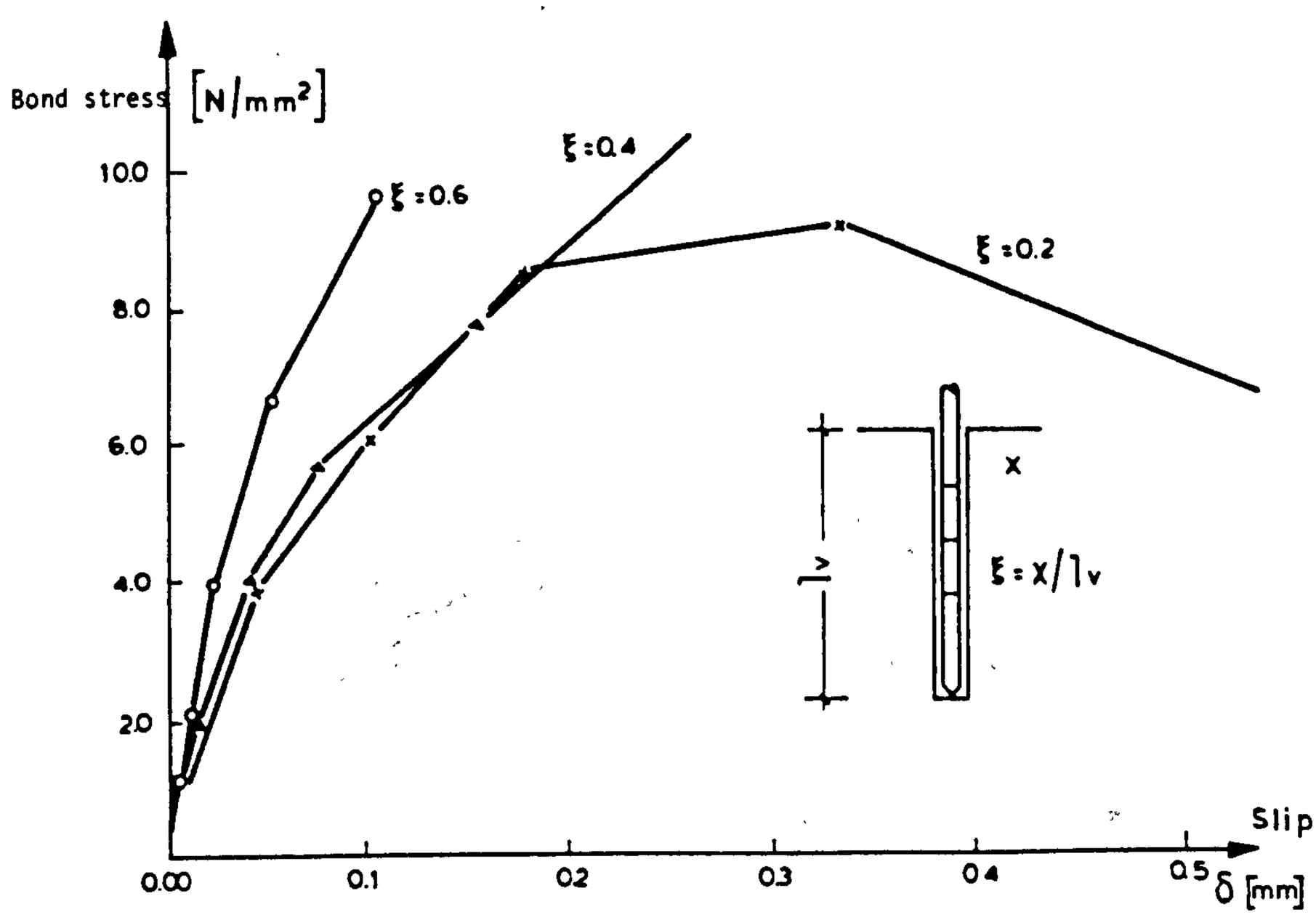

Fig.2.23 τ=τ (δ) diagram after Kobarg /12/

$$\lambda = \frac{l_v}{d_b} = \frac{\beta_z(n/\varphi^2 - 4k)}{2\left[1 - 2c_1 . c_2 . n\, 0255 (\beta_w)^{\frac{2}{3}} \left(1 + \sqrt[4]{\frac{m}{m^*}}\right)\right]}$$

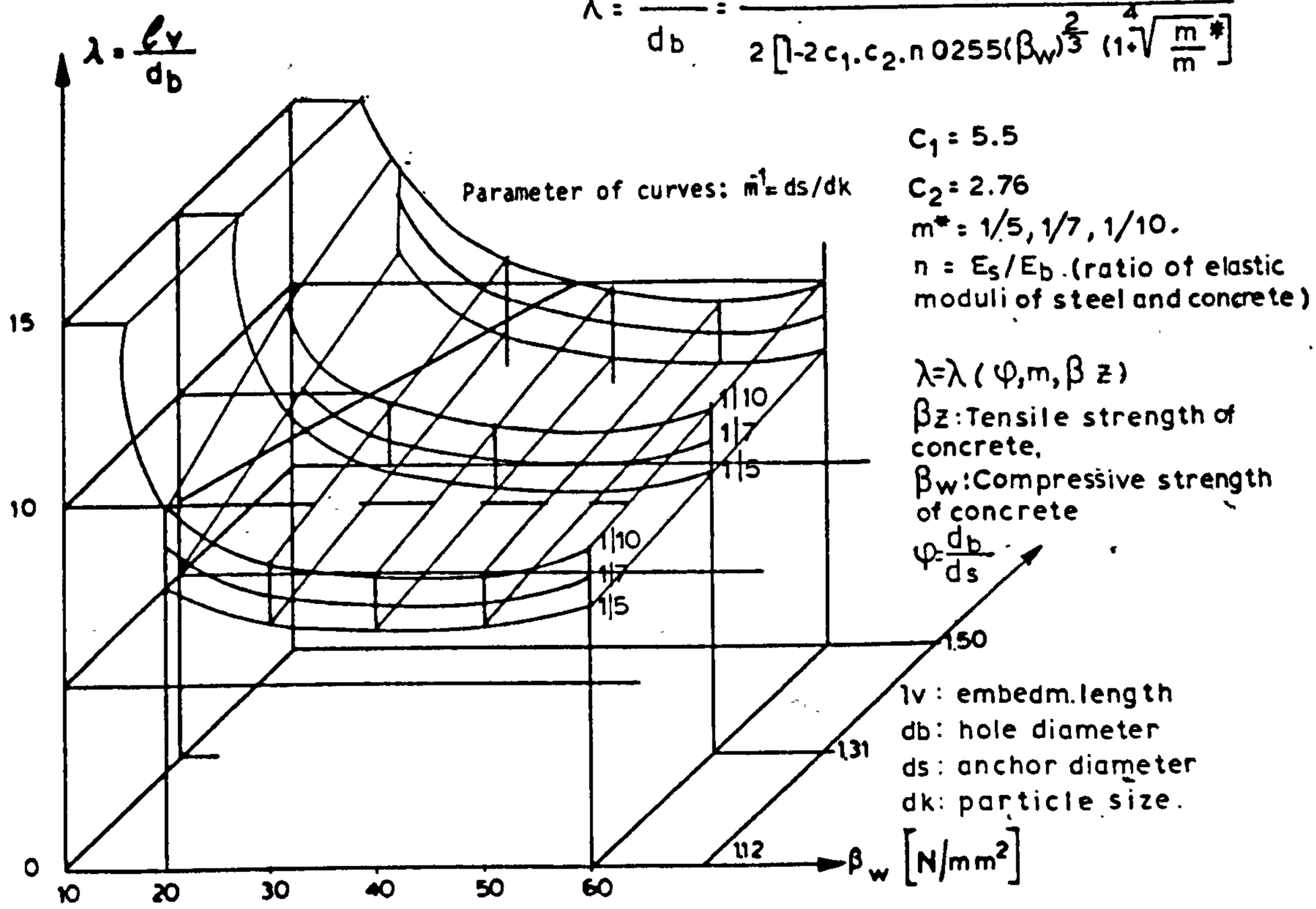

Fig.2.24. Dependence of embedment length on hole and anchor diameter, particle size and concrete strength after Kobarg /12/

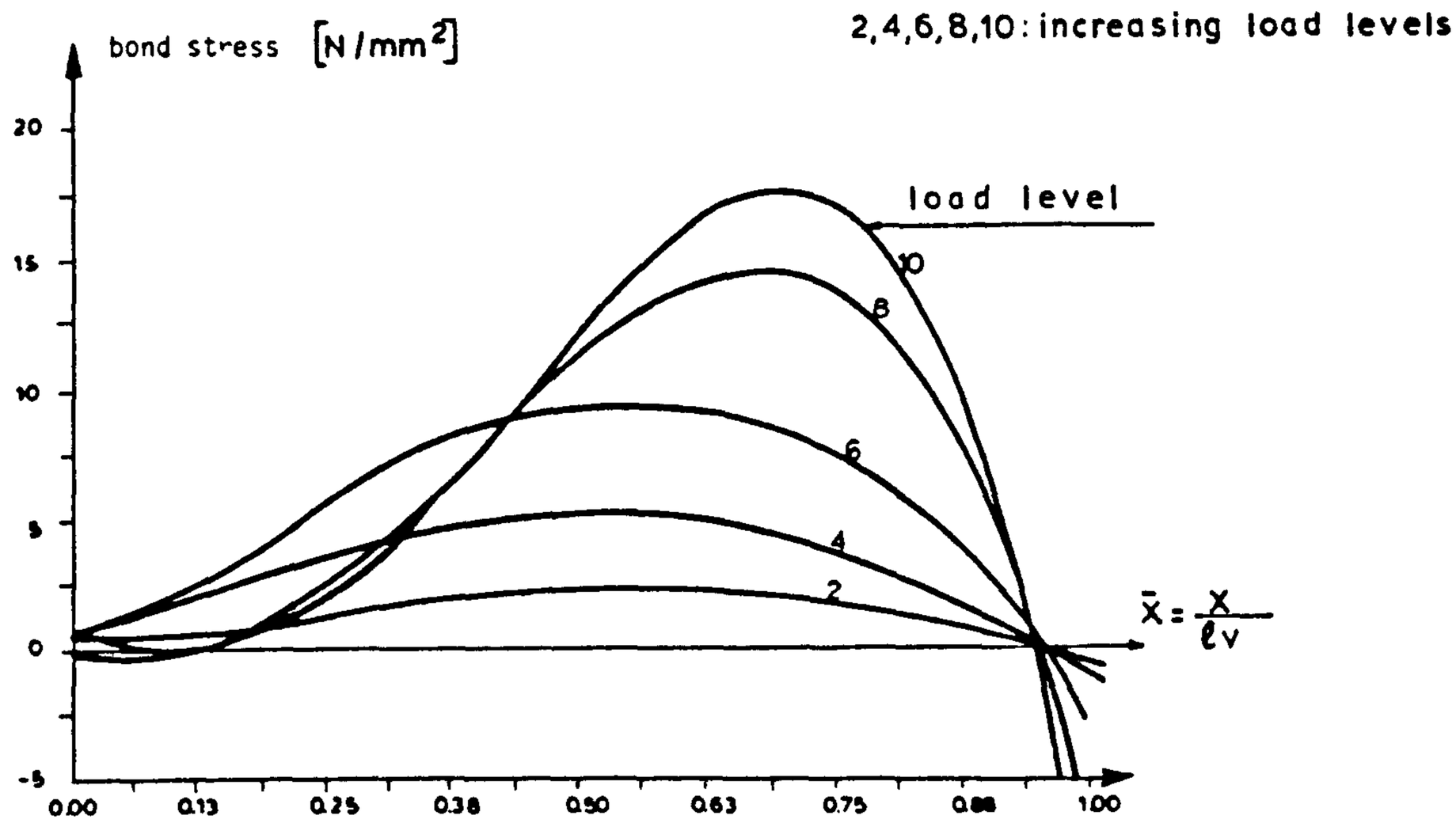

Fig.2.25. Bond stress distribution along the anchor, after Kobarg /12/

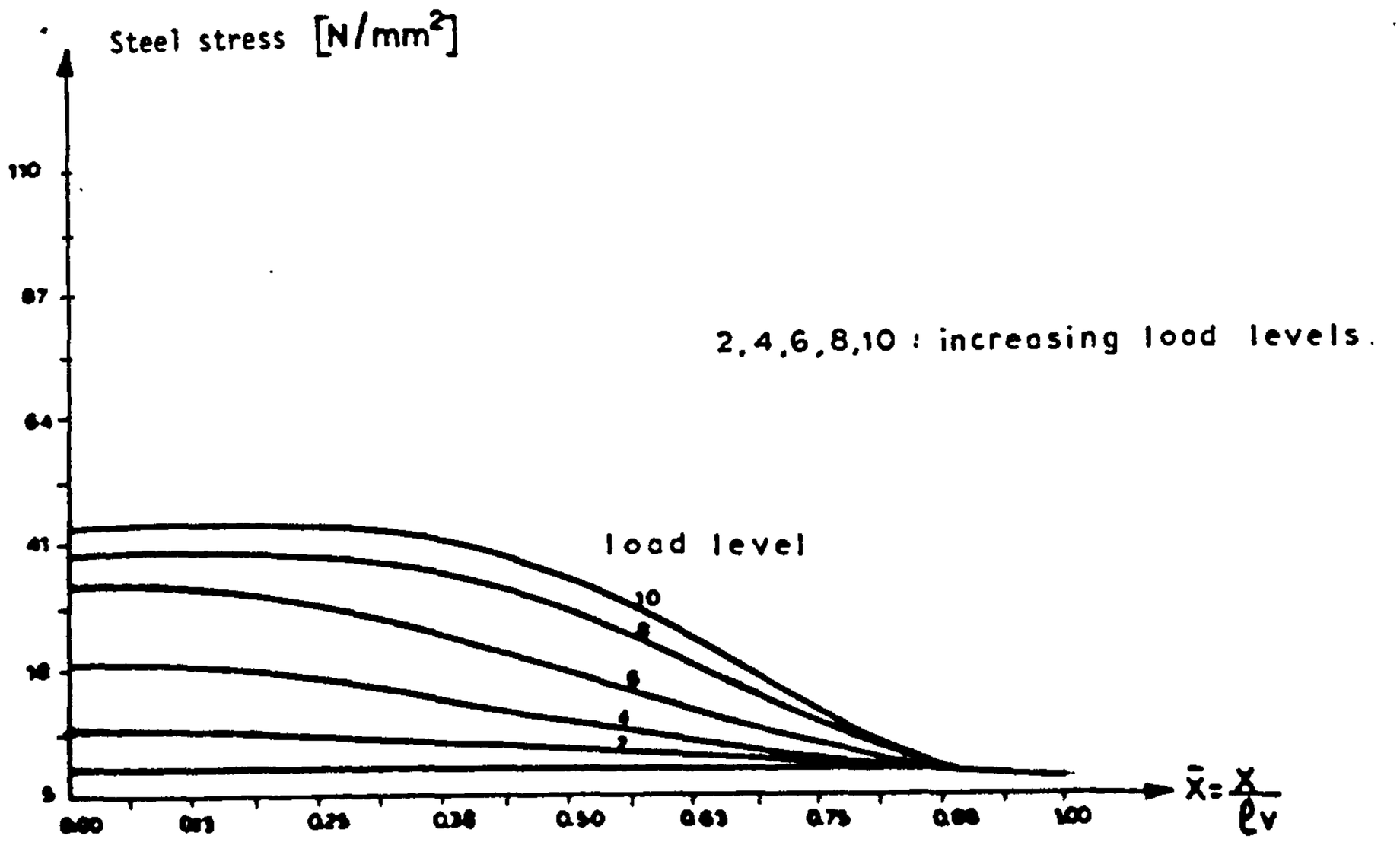

Fig.2.26. Steel stress distribution along the axis after Kobarg. /12/

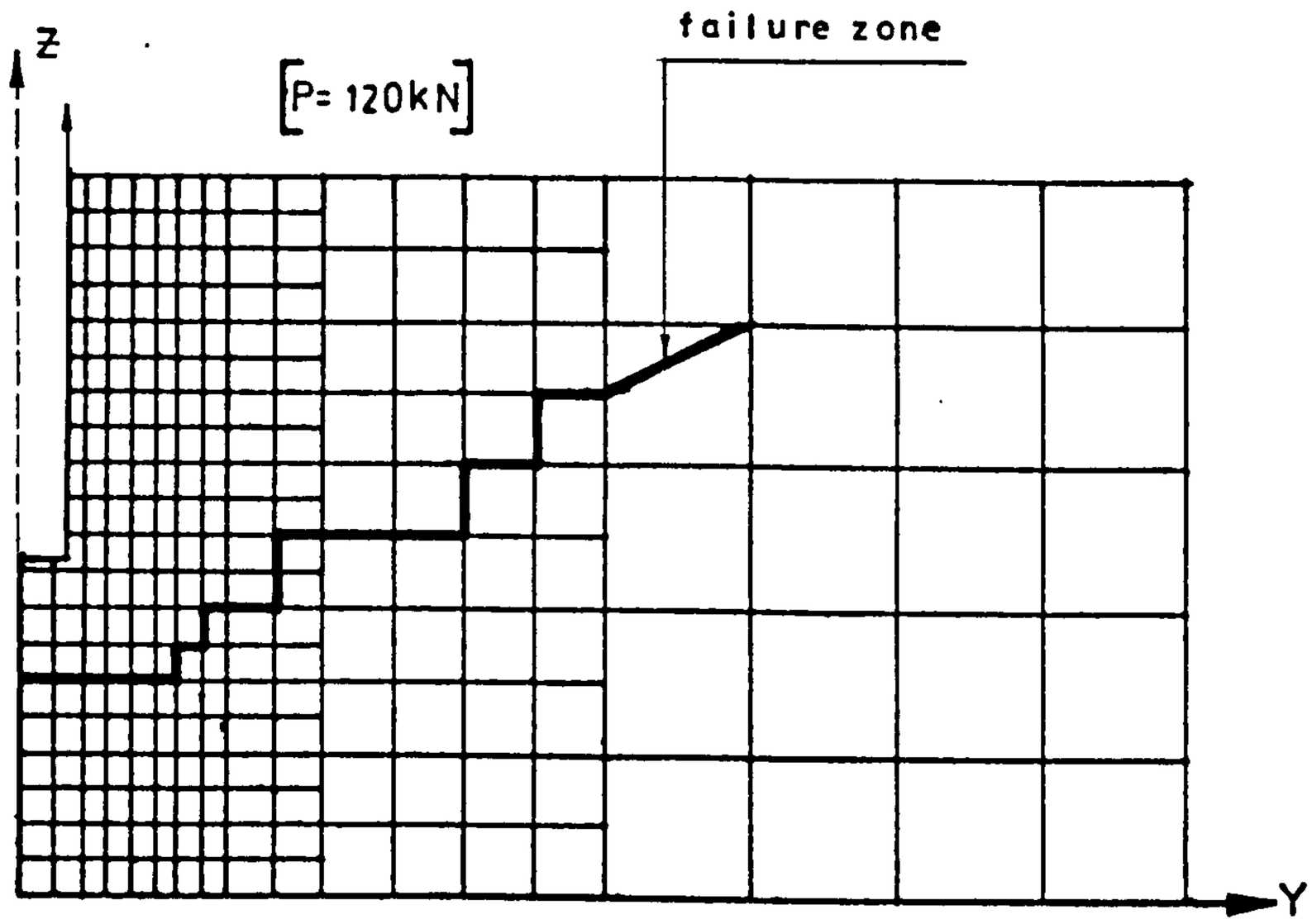

Fig.2.27. Crack zone of an adhesive anchor under tensile loading, after Peier /13/

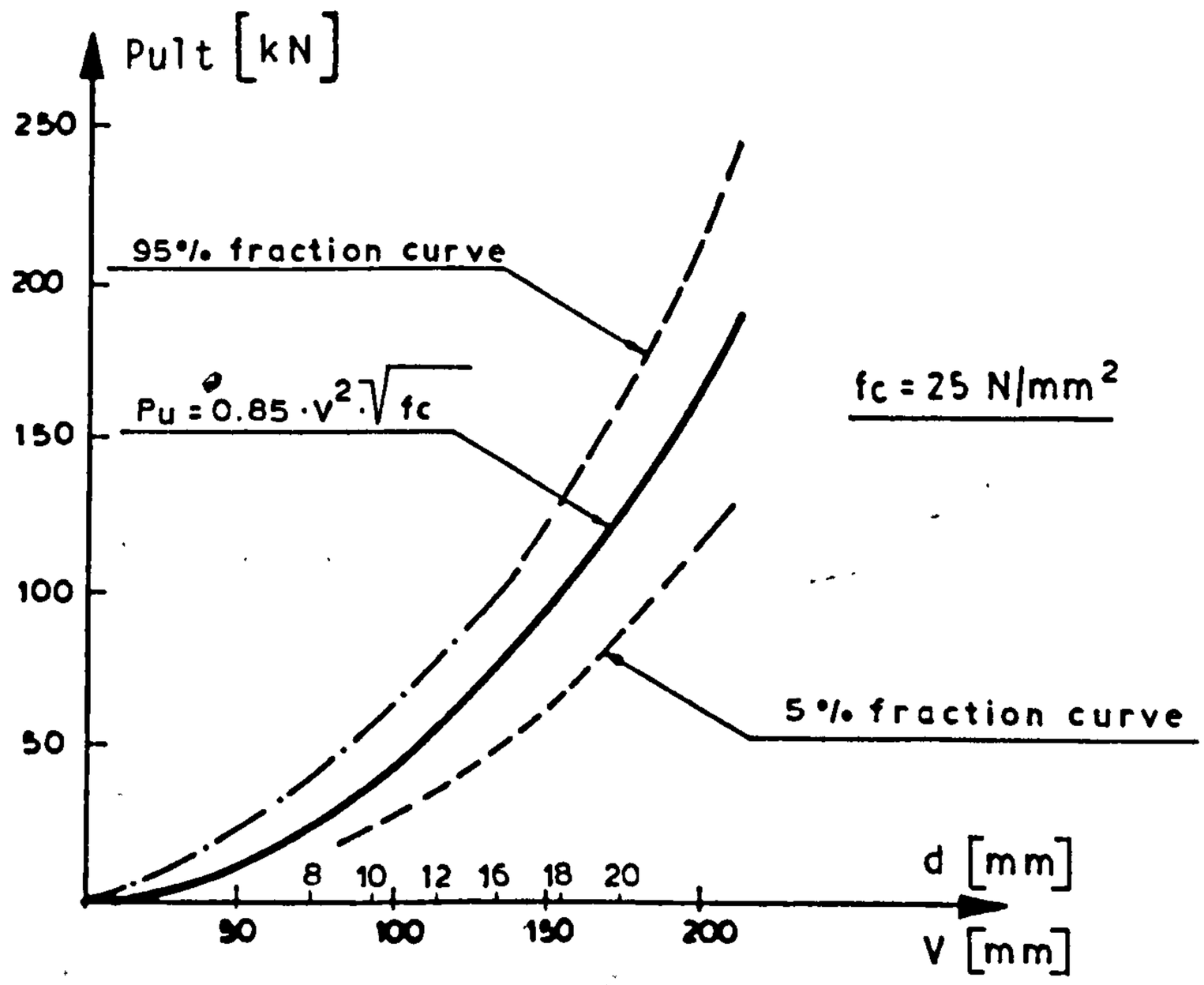

Fig.2.28. Calculated pull-out ultimate load curve and 5% and 95% fraction curves from experimental results according to Eligehausen et al. /14/

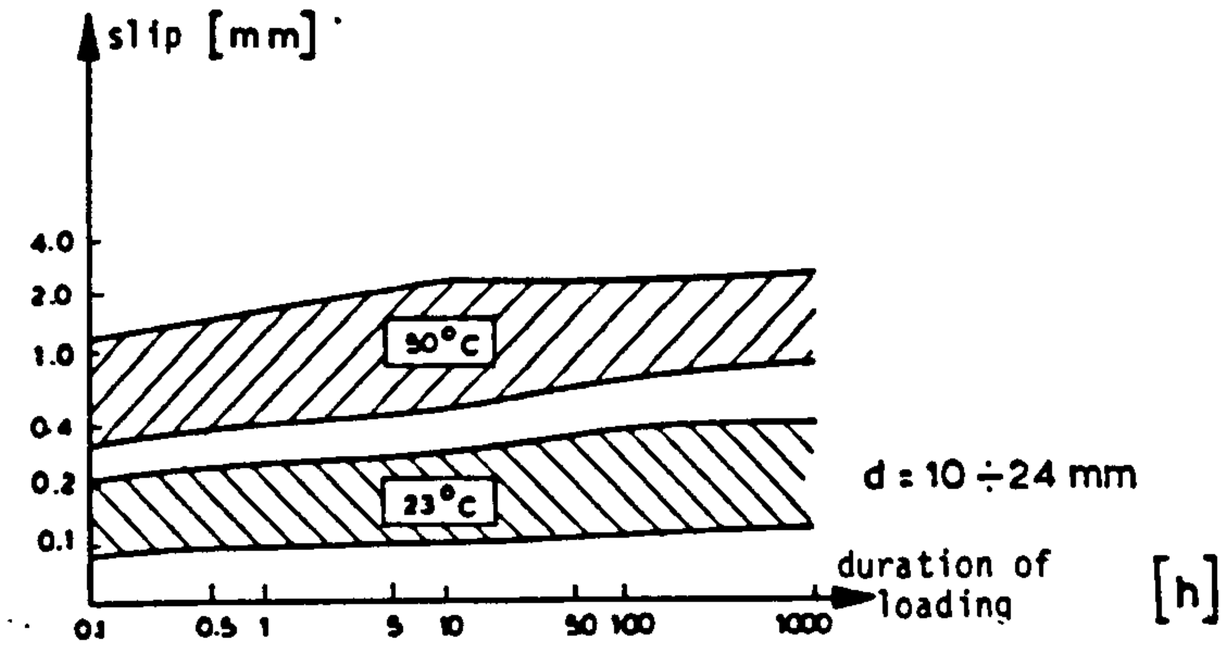

Fig.2.29. Dependence of anchor slip on the duration of loading and ambient temperature, after Eligehausen and al /14/

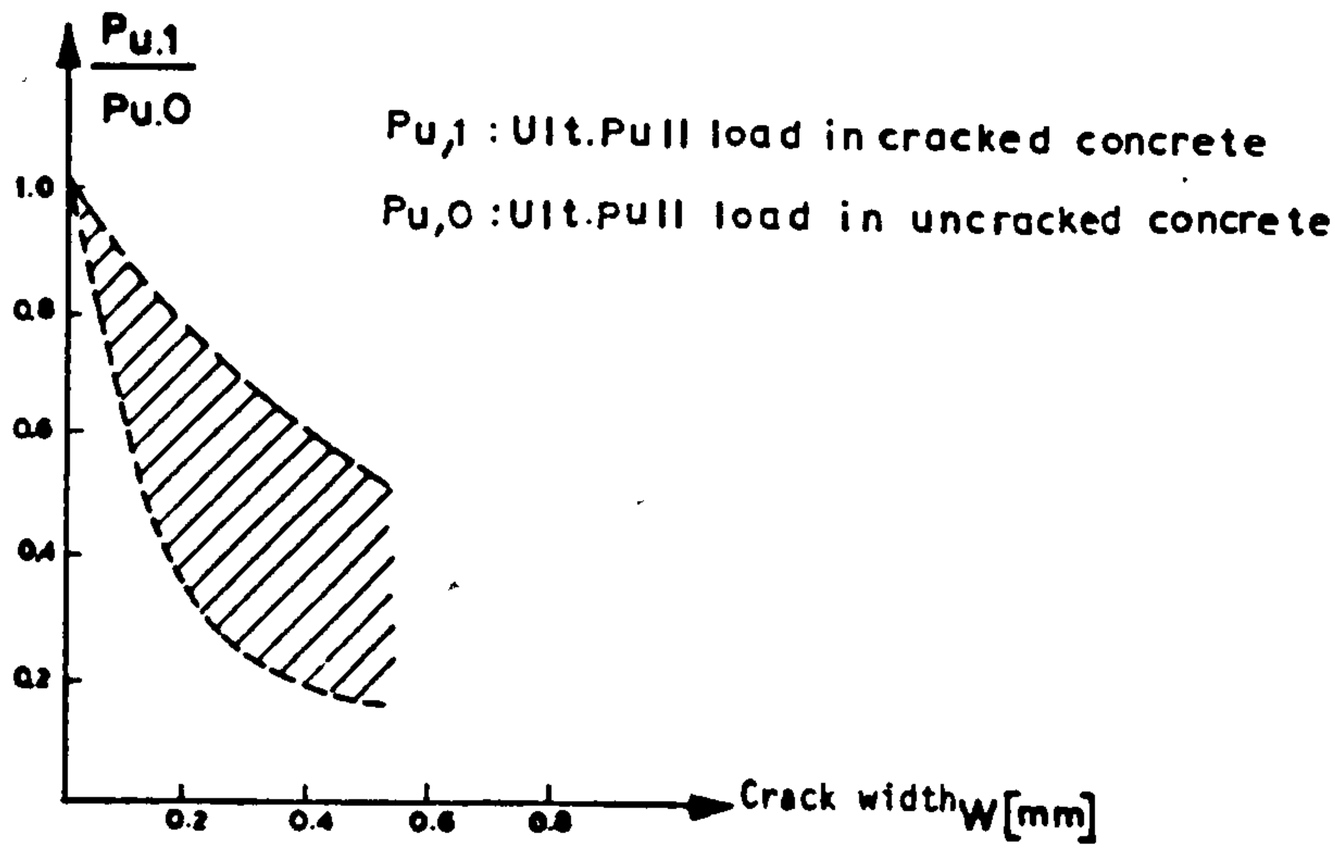

Fig.2.30. Reduction of ult.pull-out load as a function of crack width, after Eligehausen et al /14/

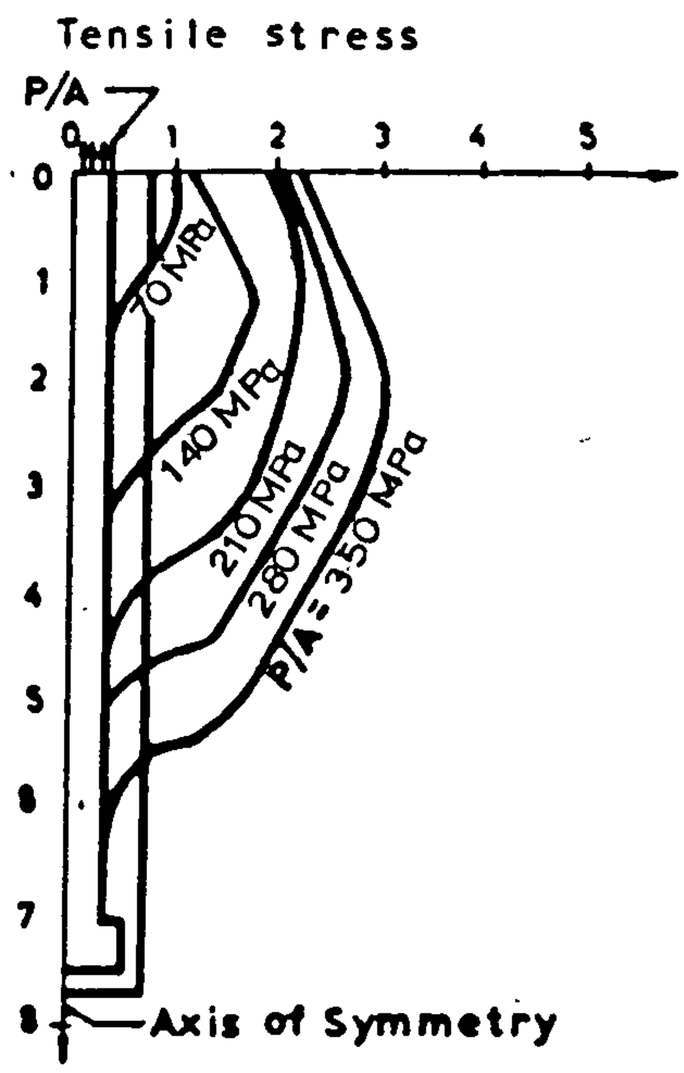

Fig.2.31. Mohr-Coulomb failure contours, after James et al /1/

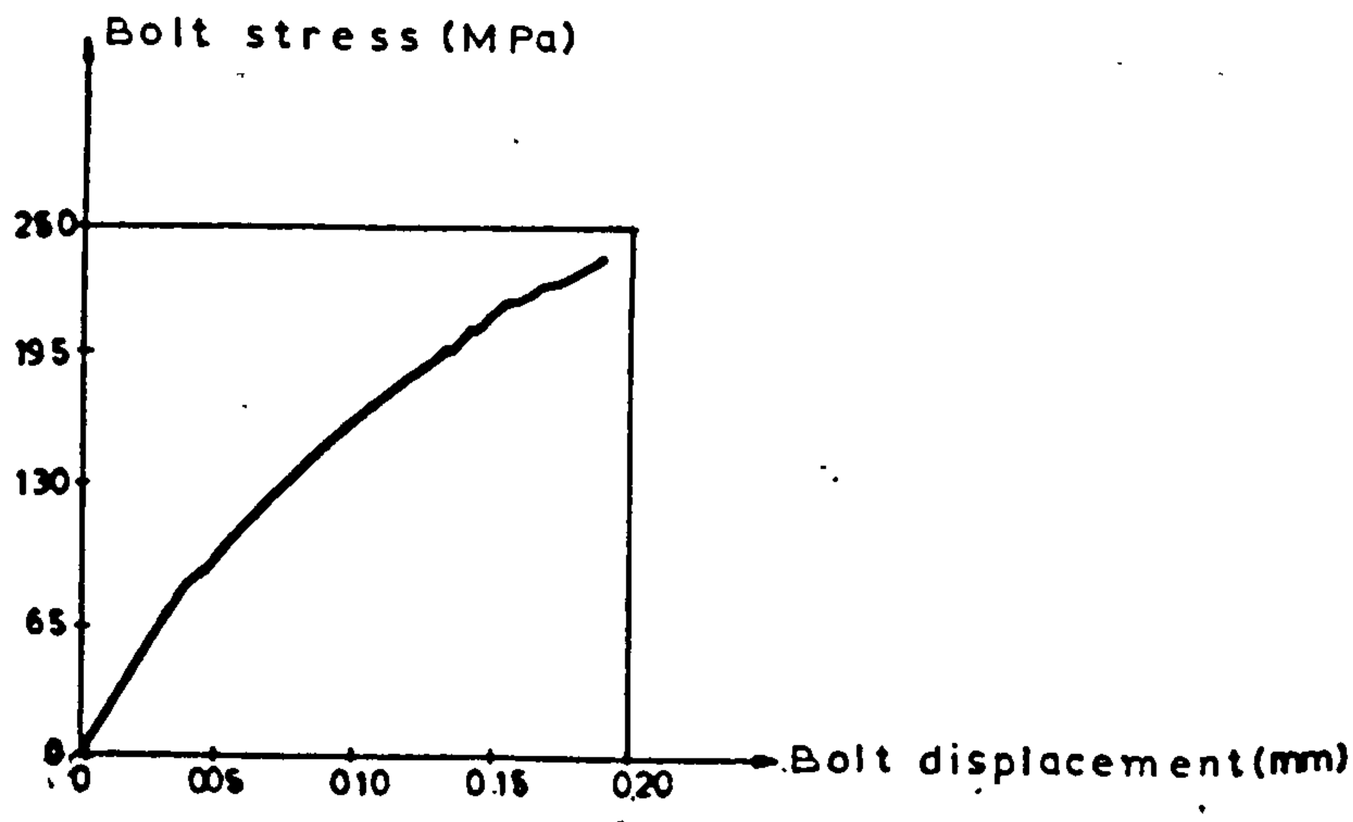

Fig.2.32. Predicted nonlinear stress-displacement relationship after James et al. /1/

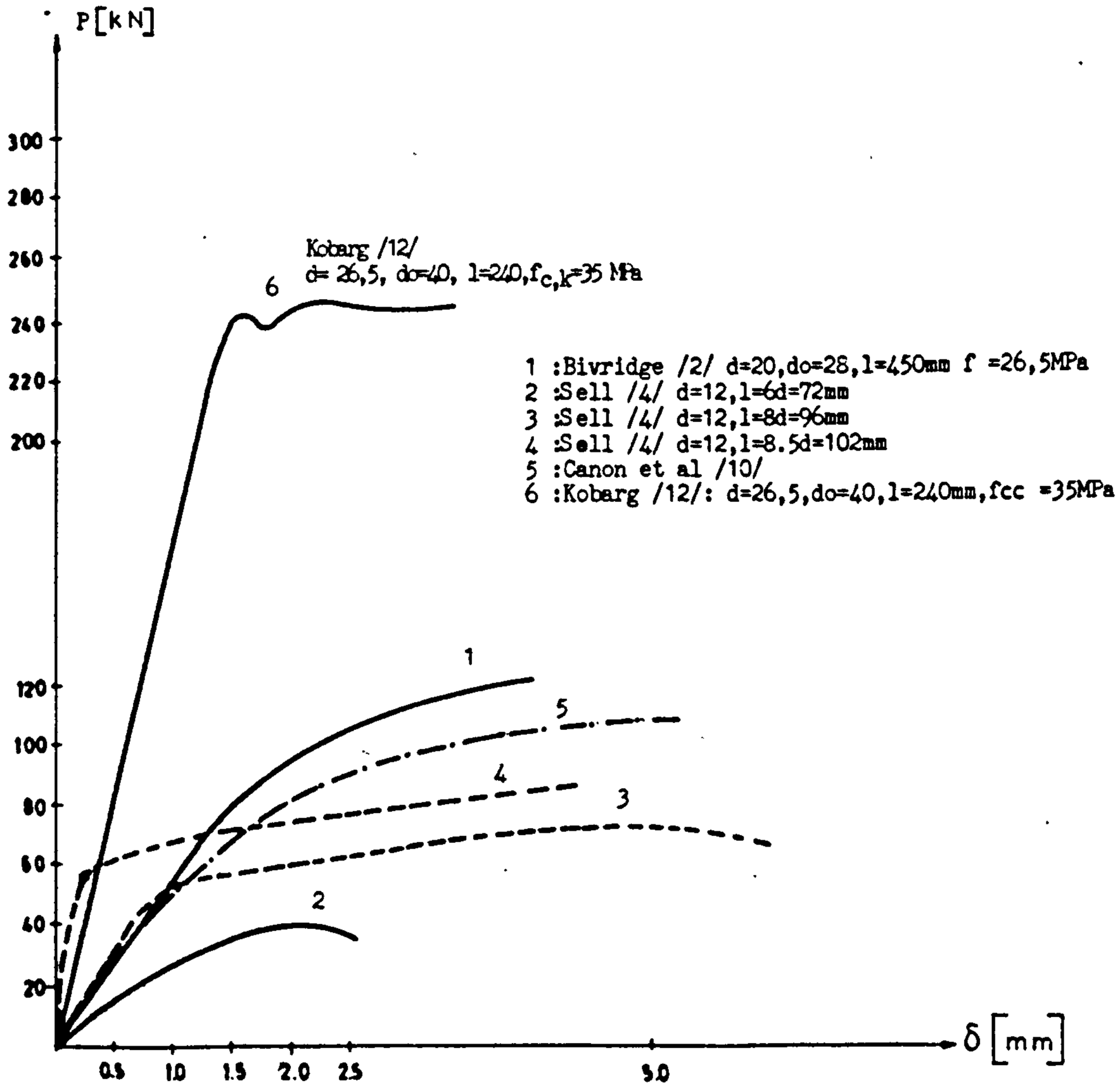

Fig.2.33. P-δ relationship as reported by different authors

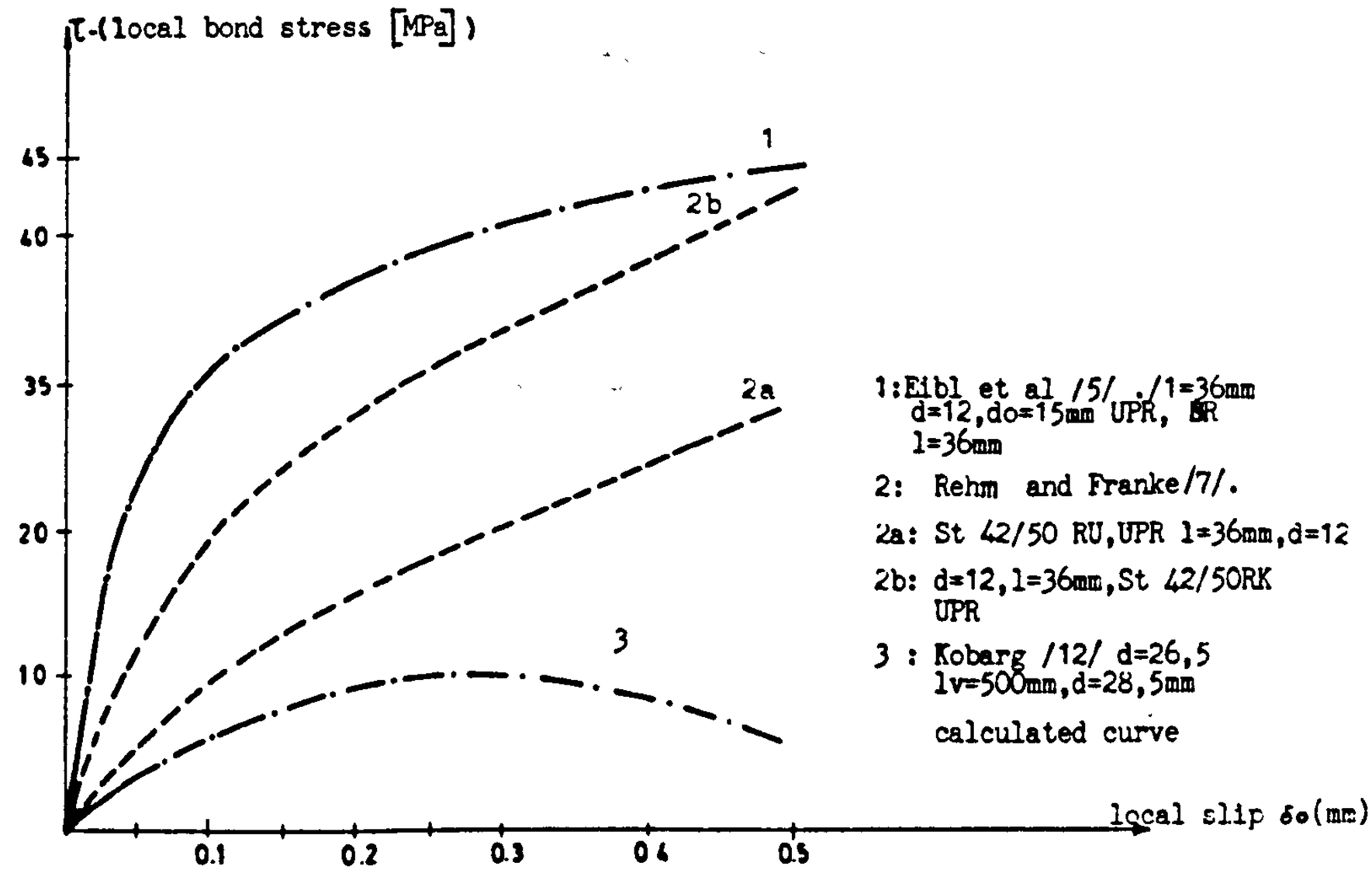

Fig.2.34 Local bond-local slip law as reported by different authors.

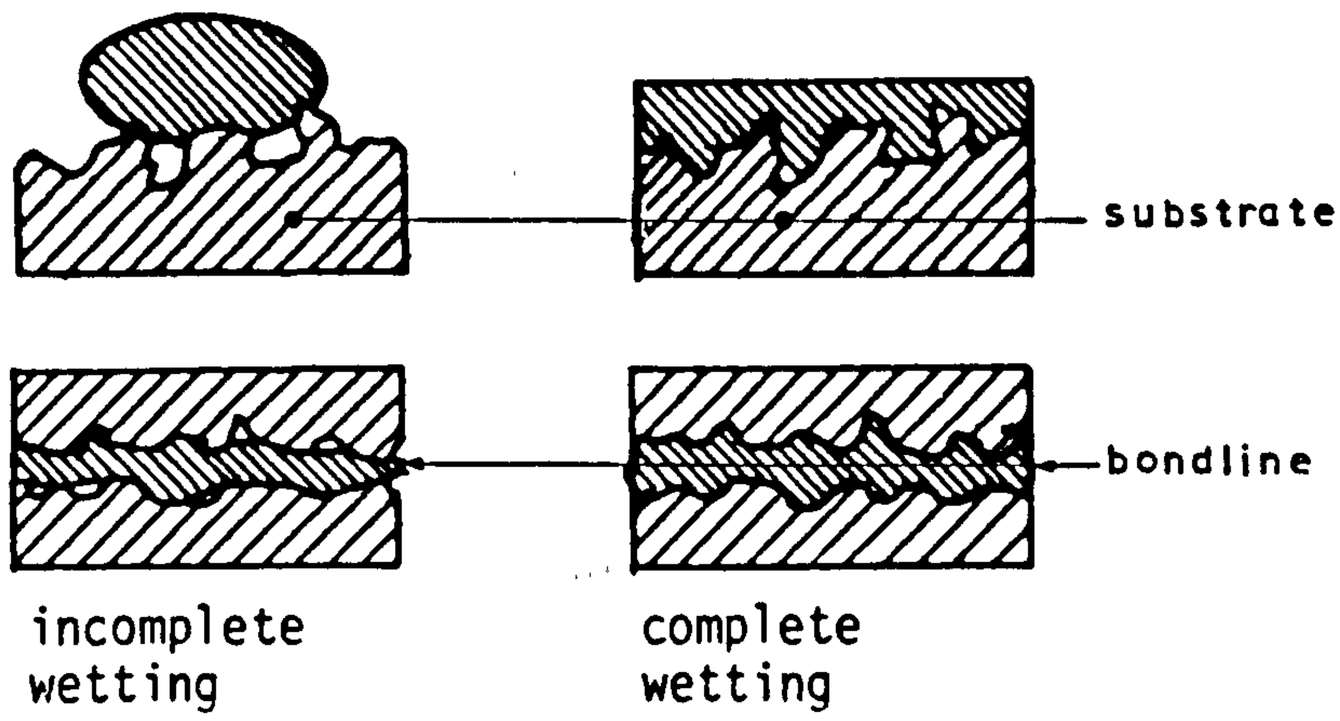

Fig.3.1 Complete and incomplete wetting of the substrate

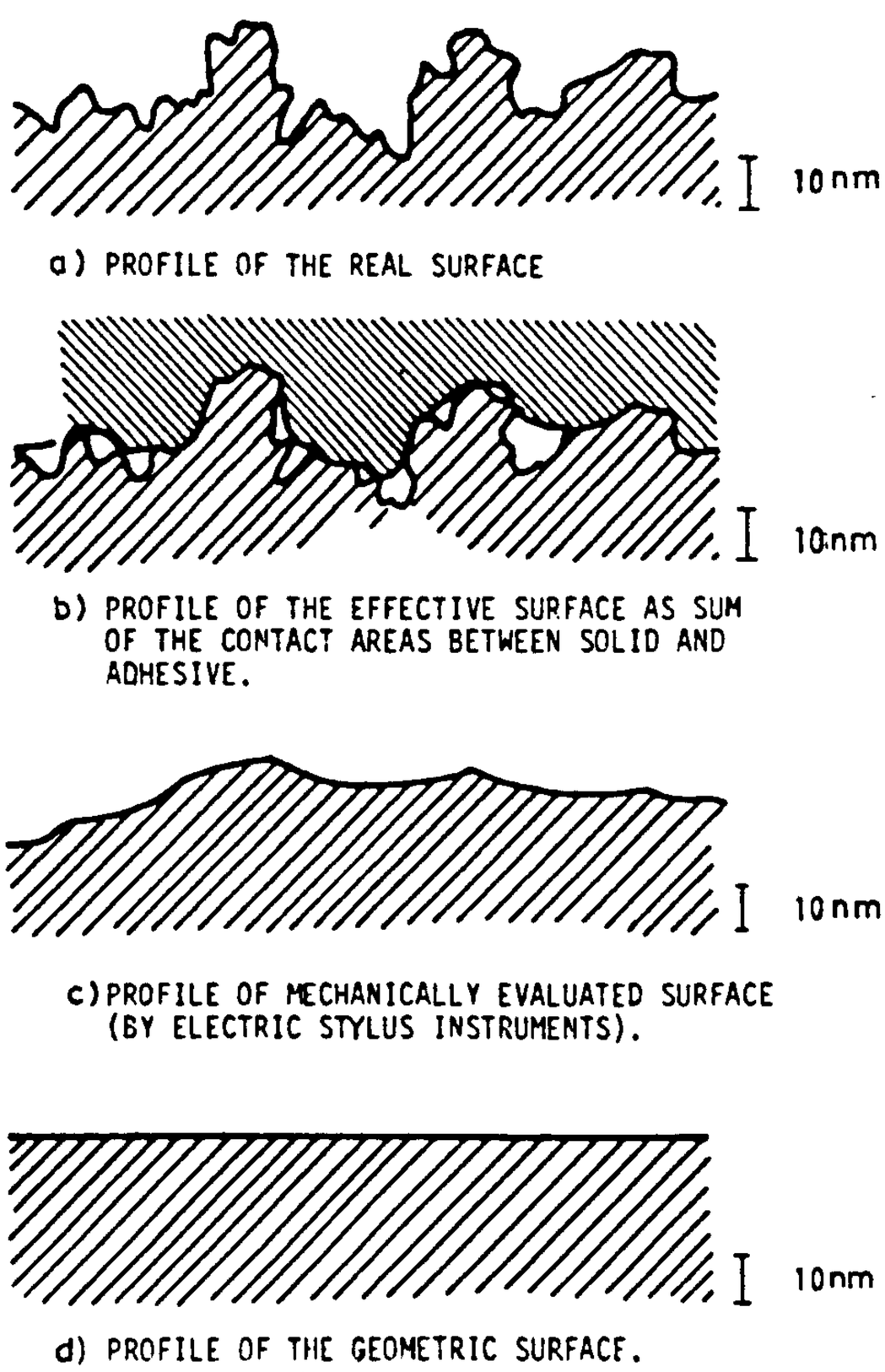

Fig.3.2. Microtopogragpy of a system of adherend-adhesive, after Fiebrig. /17/

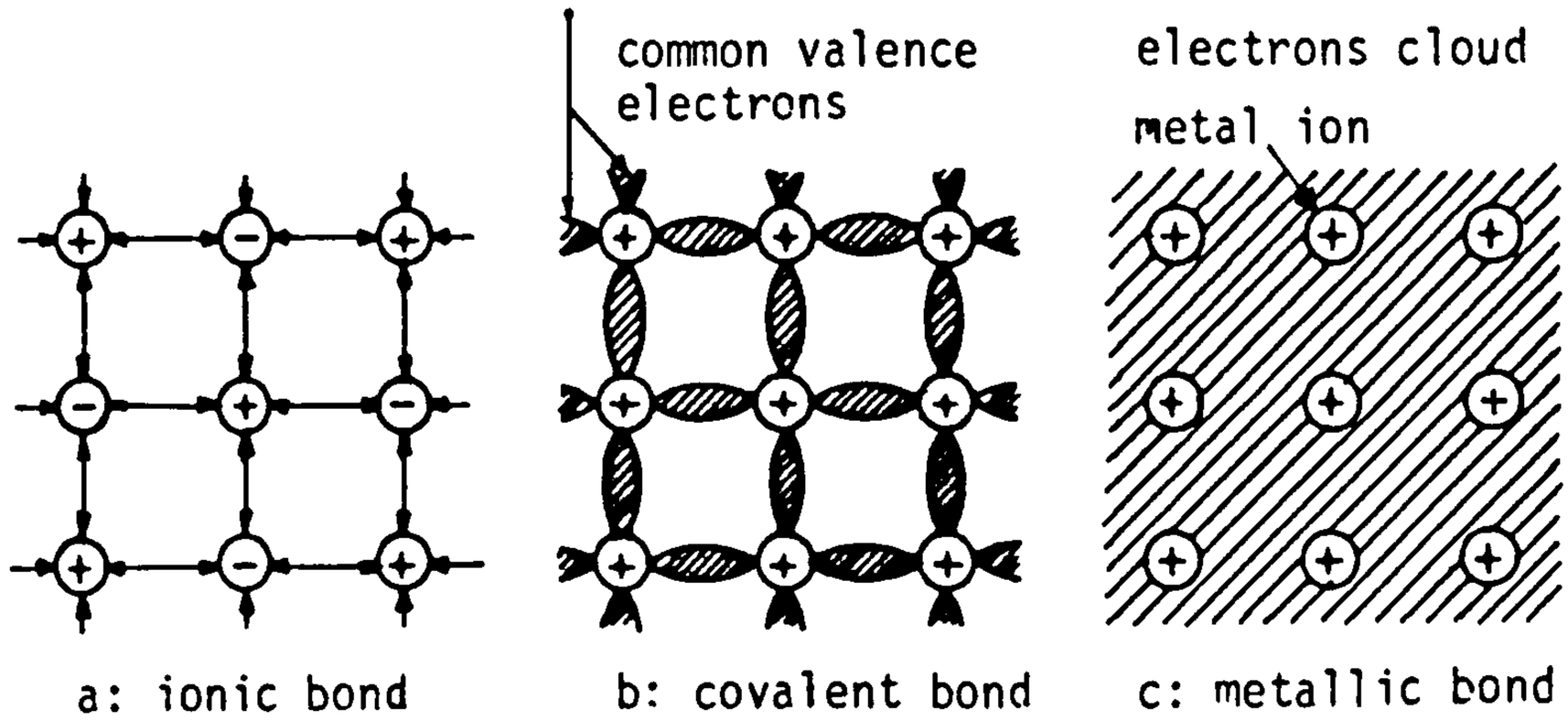

Fig.3.3. Schematic illustration of covalent, ionic and metallic bond, after Fiebrig /17/

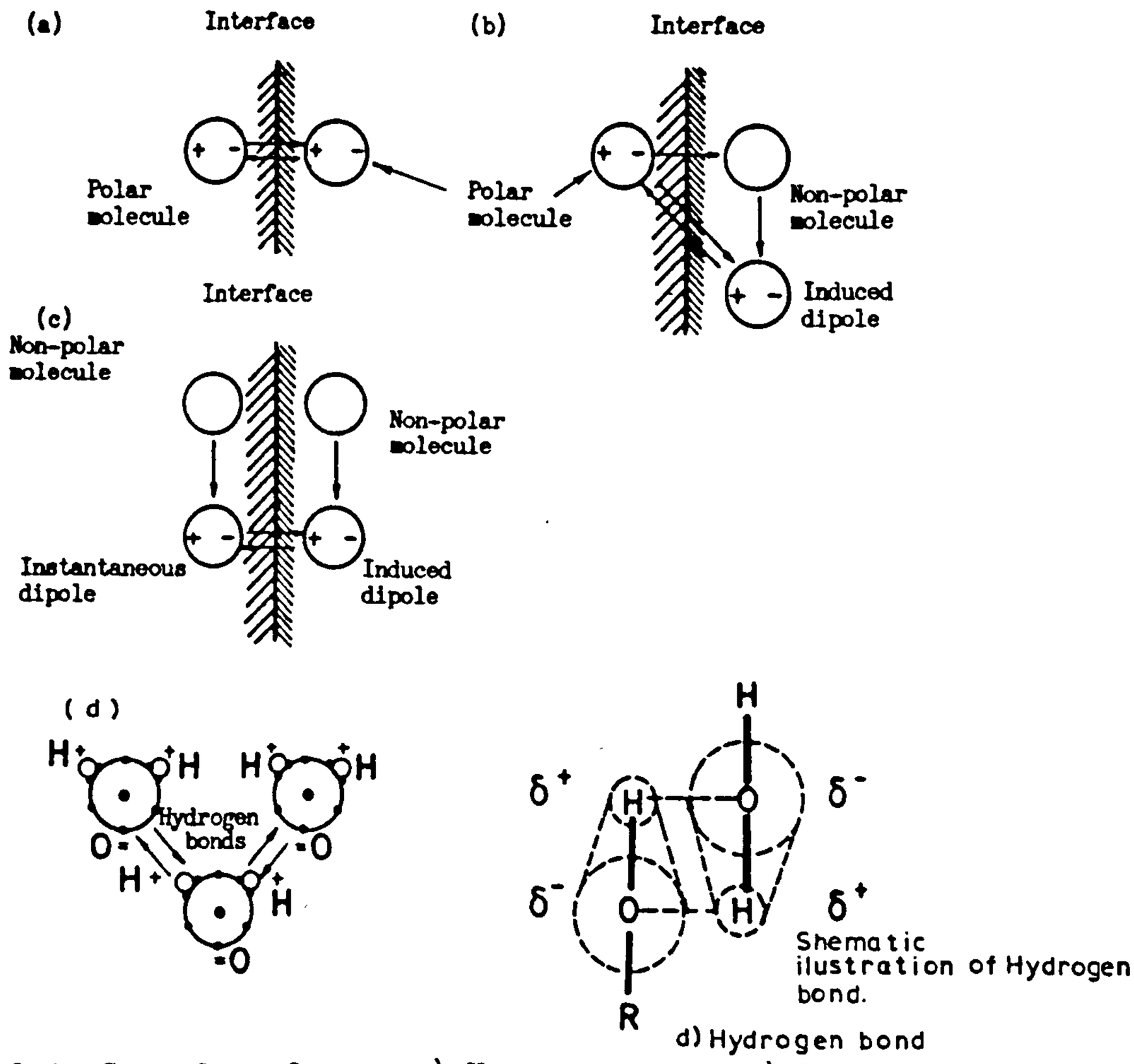

Fig.3.4. Secondary forces.a) Keesom forces. b) Debye forces c) London forces d) Hydrogen bond.

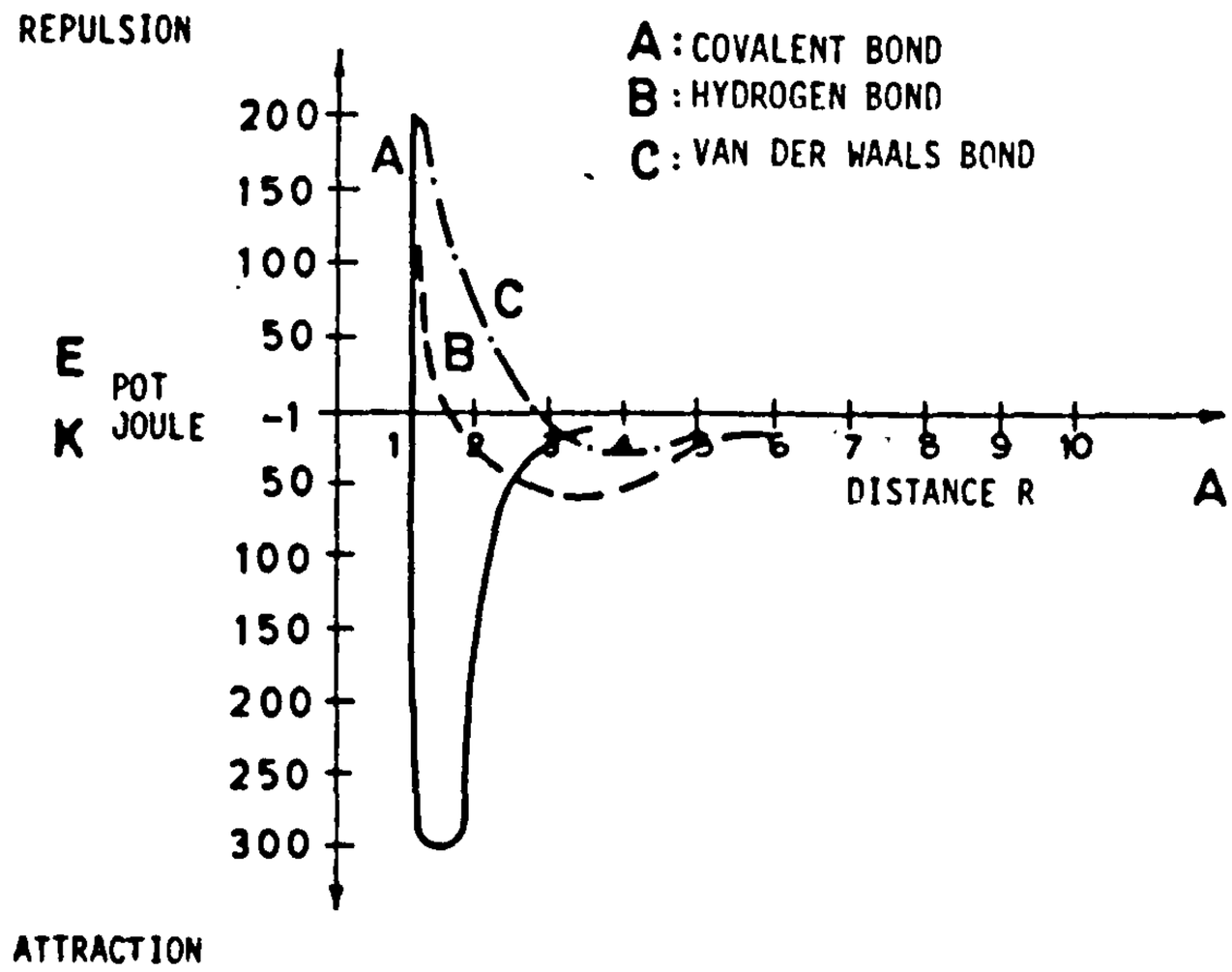

Fig.3.5. Energy potential as function of the distance between centres of loads, after Fiebrig /17/

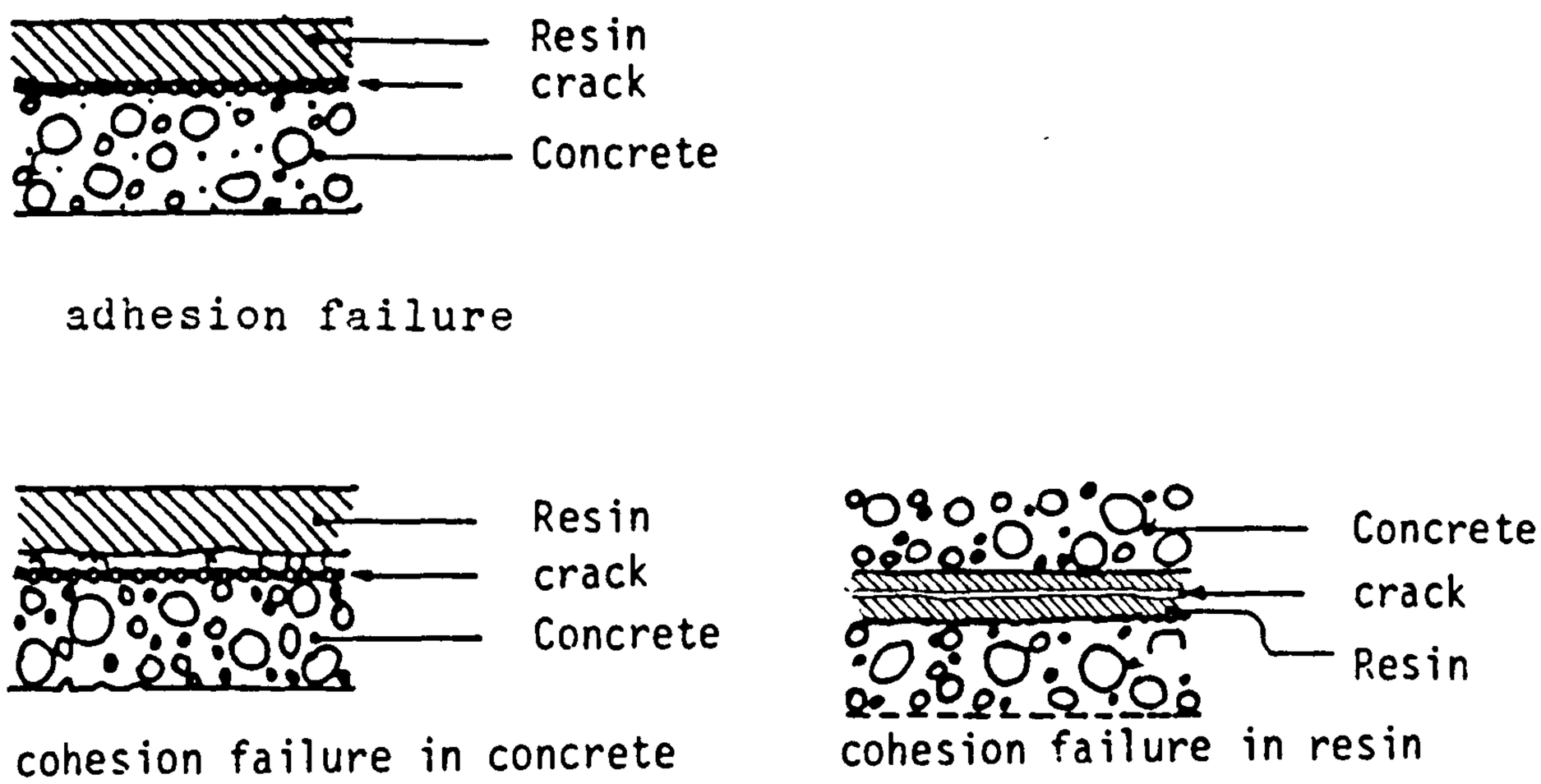

Fig.3.6. Types of failure.

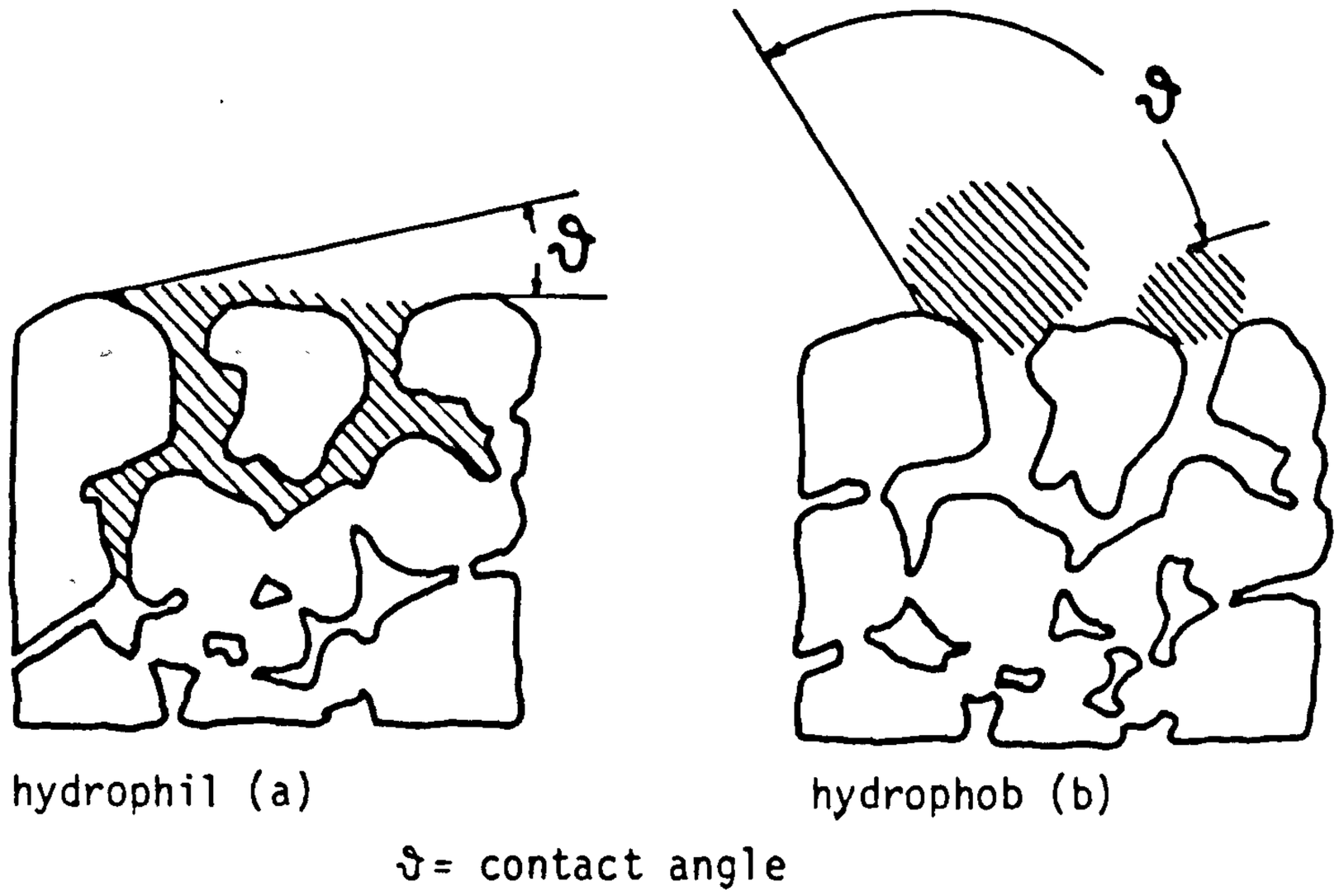

Fig.3.7. Low and great contact angle of an adhesive with a solid, after Fiebrig /17/

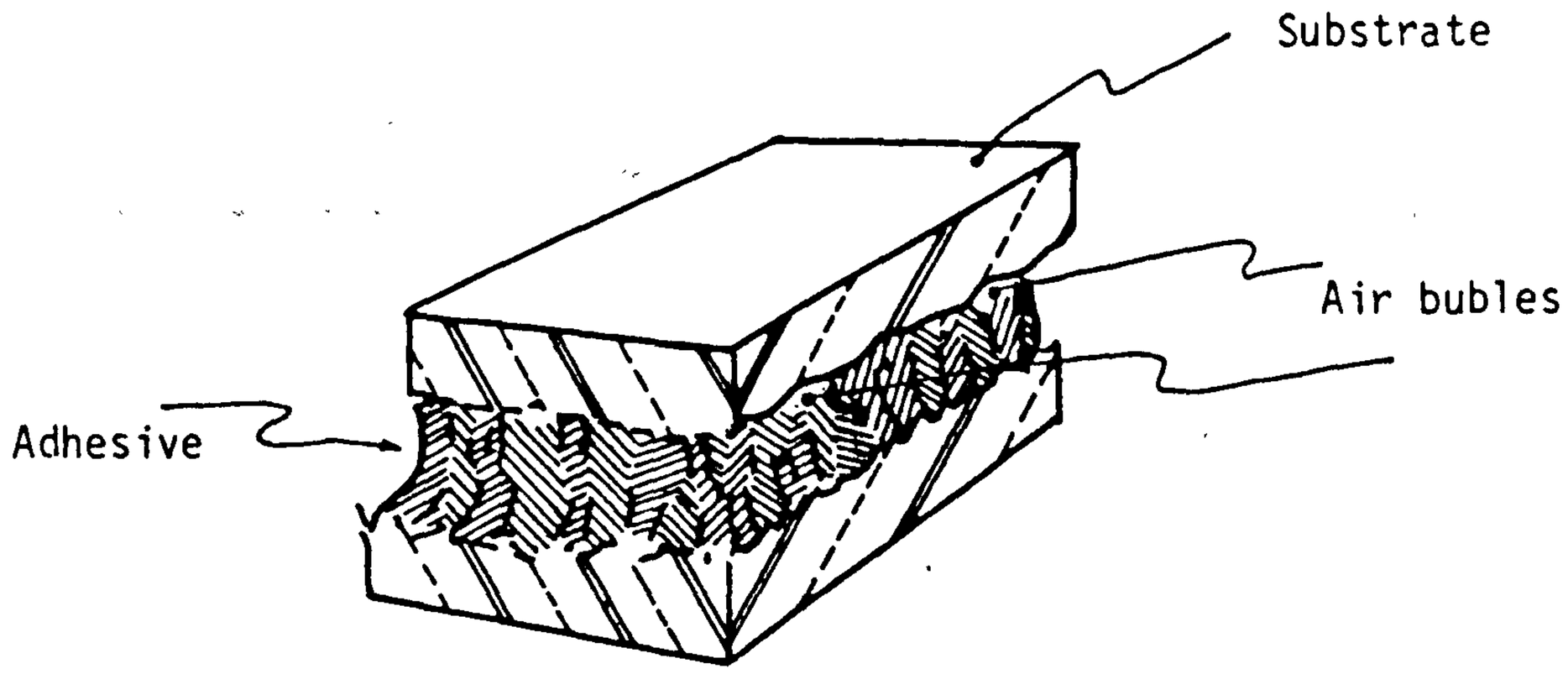

Fig.3.8. A realistic model of the contact between substrate and adhesive with air bubbles in the interface.

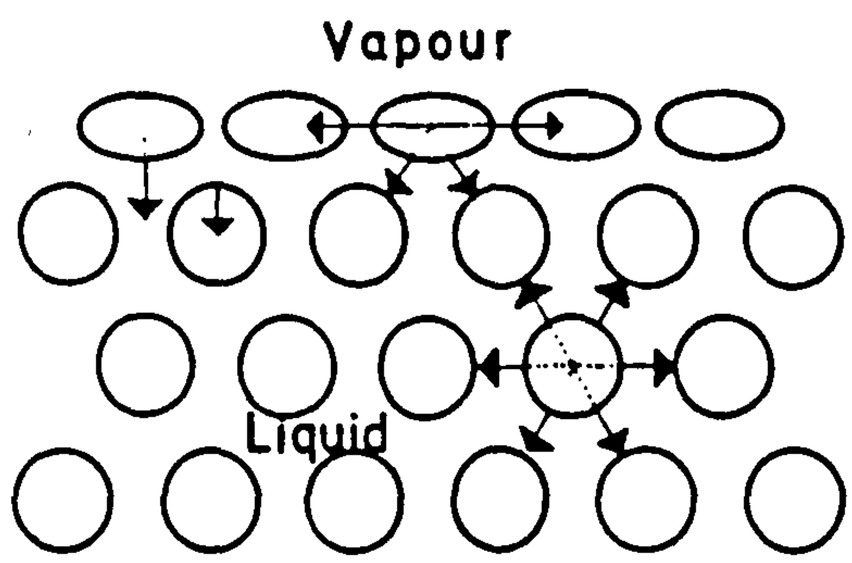

Fig.3.9. Intermolecular forces in the interior and surface molecules of a liquid, Fiebrig /17/

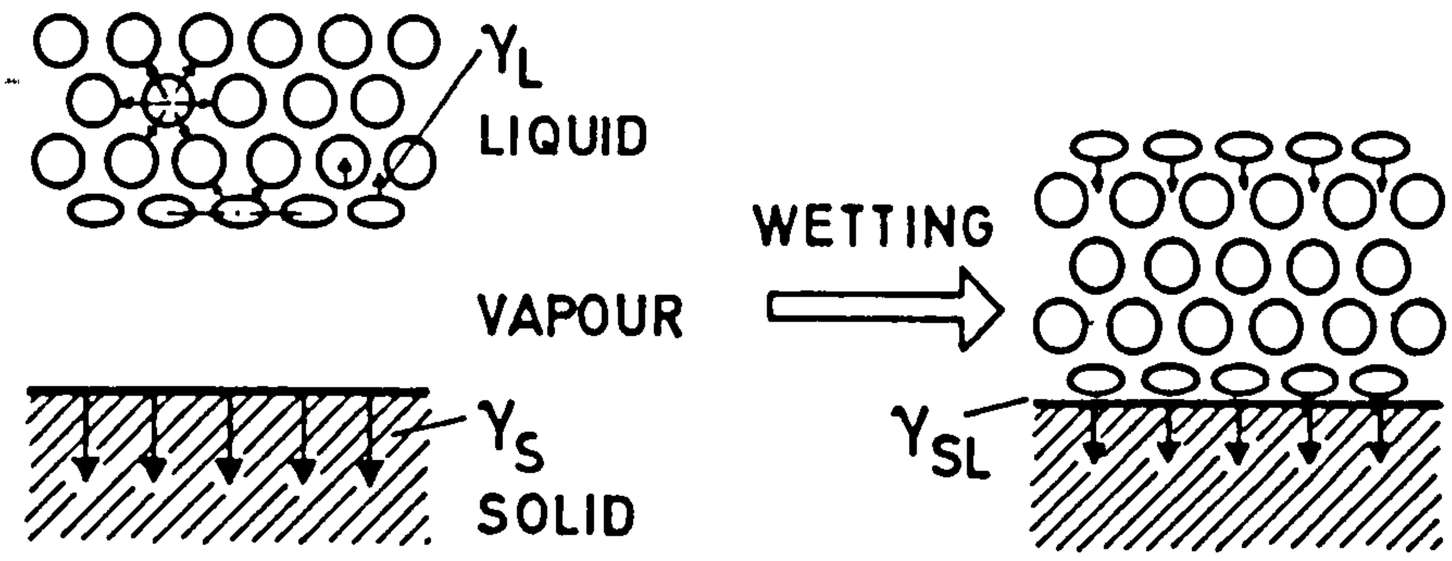

WETTING PROCEDURE

Fig.3.10. Conditions across a liquid-solid interface. Schematic illustration by Fiebrig /17/

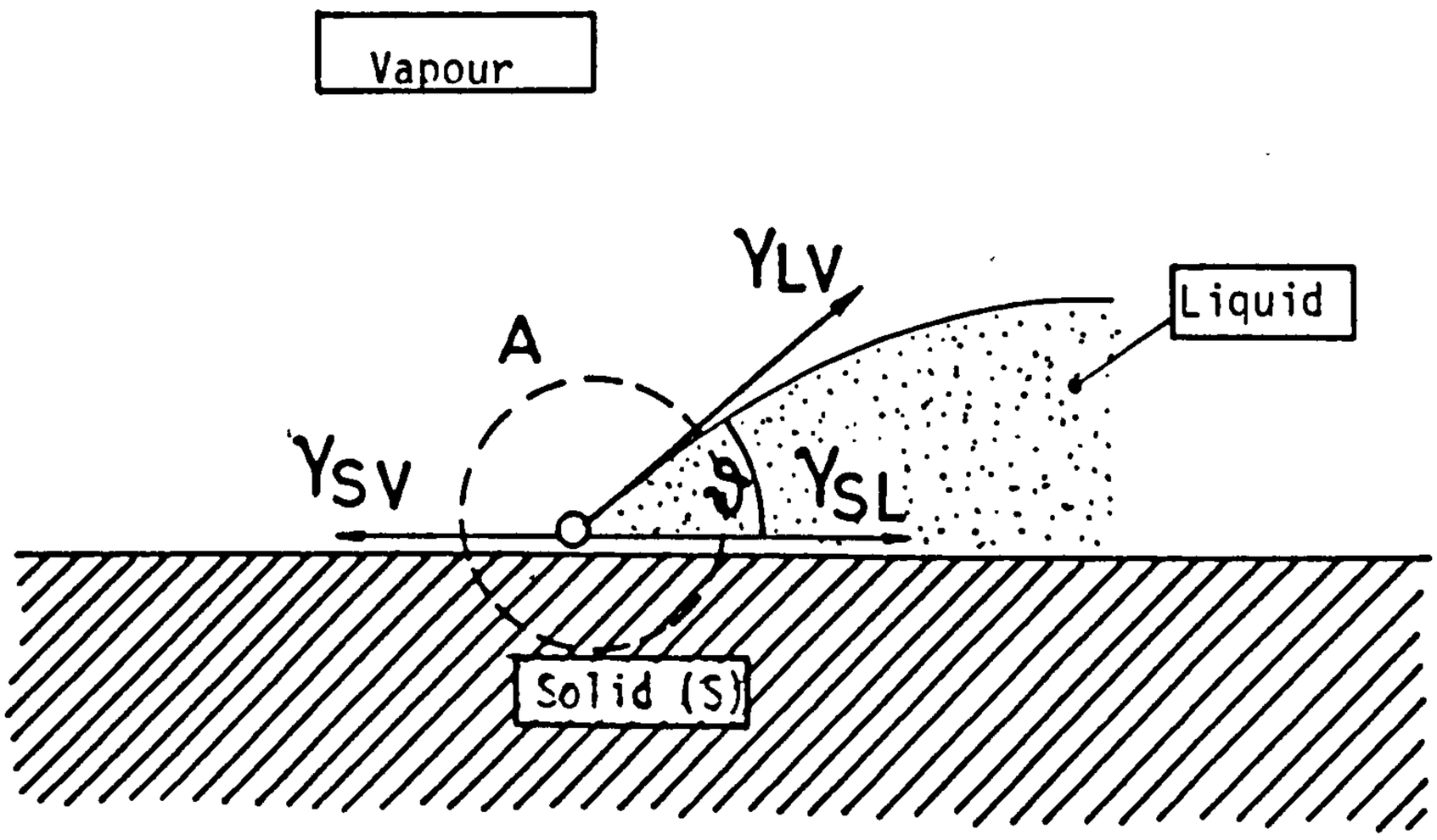

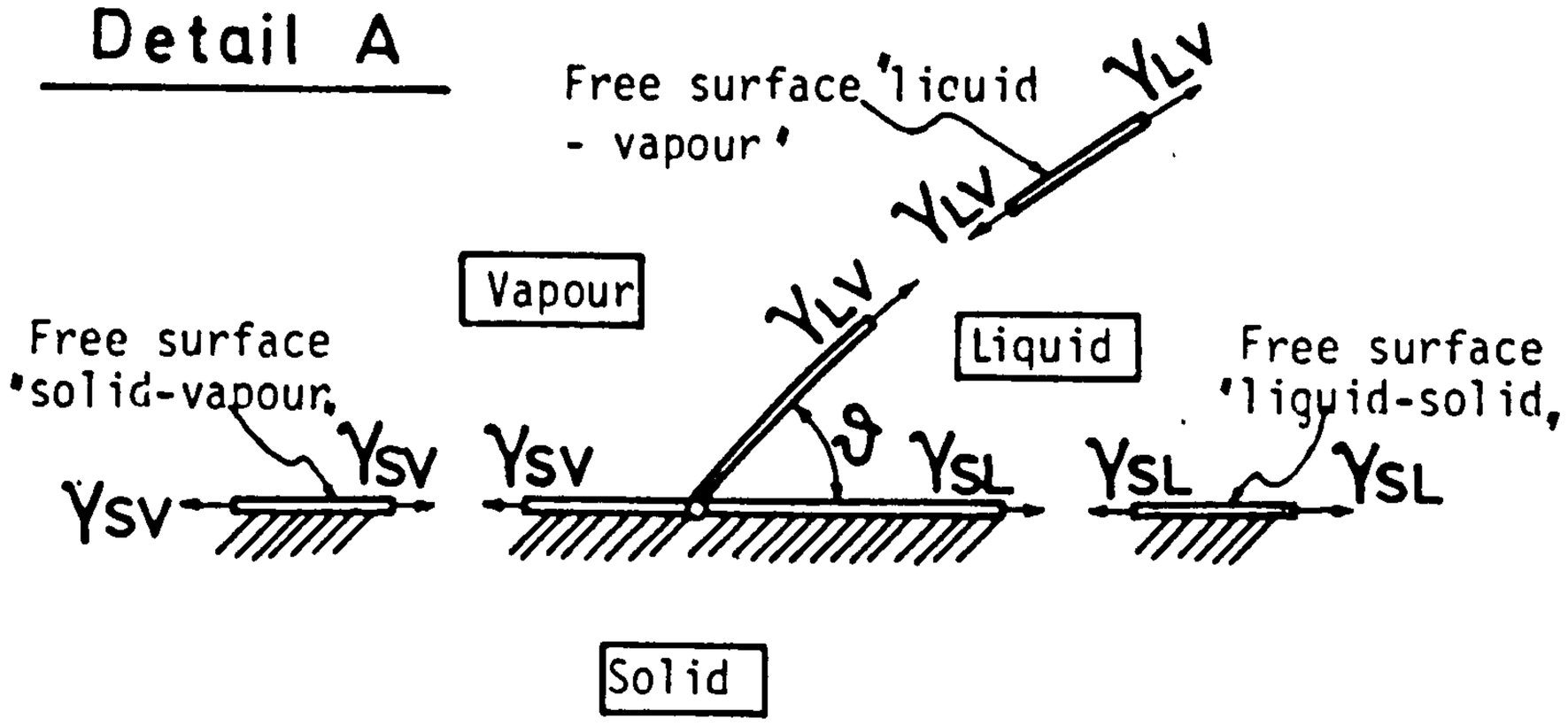

Fig.3.11. Equilibrium conditions of a 3 phase system. (Solid-Liquid-Vapour).

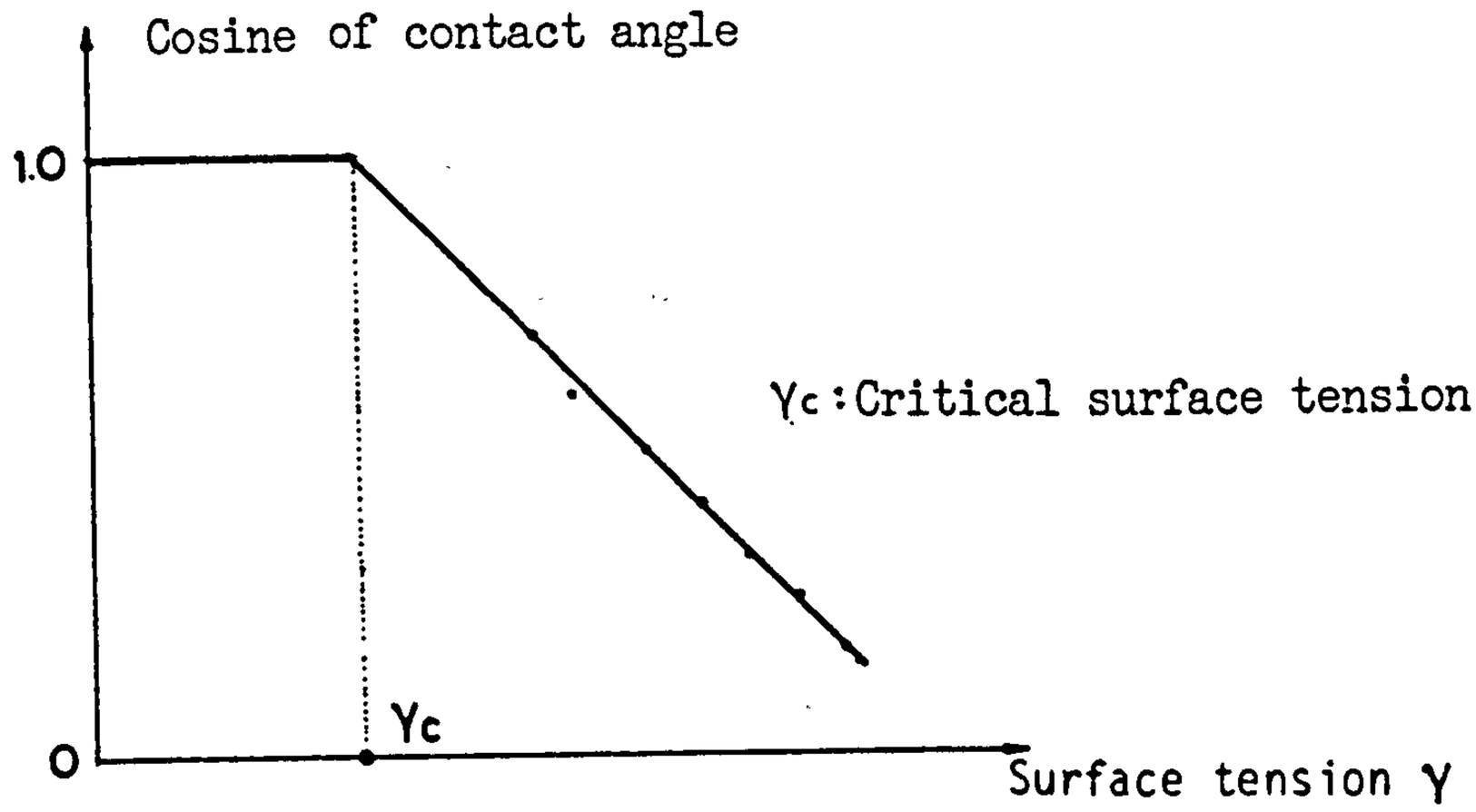

Fig.3.12. Zisman's plot

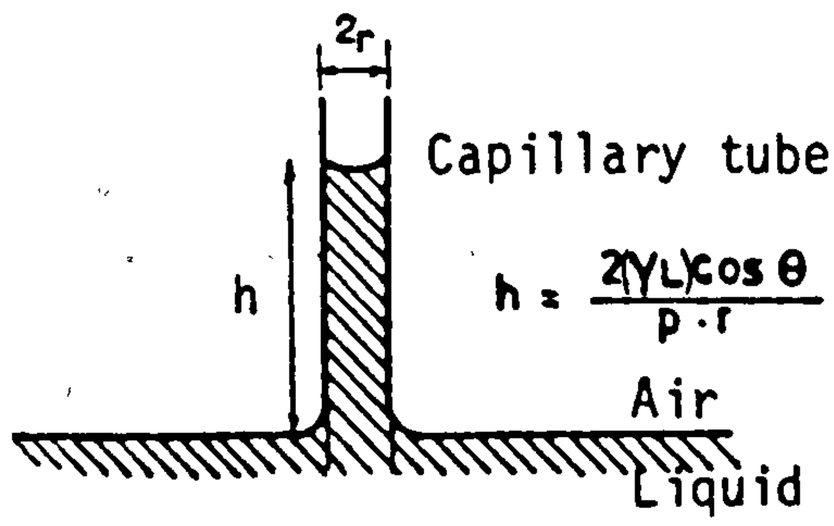

Fig.3.13. Capillary height.

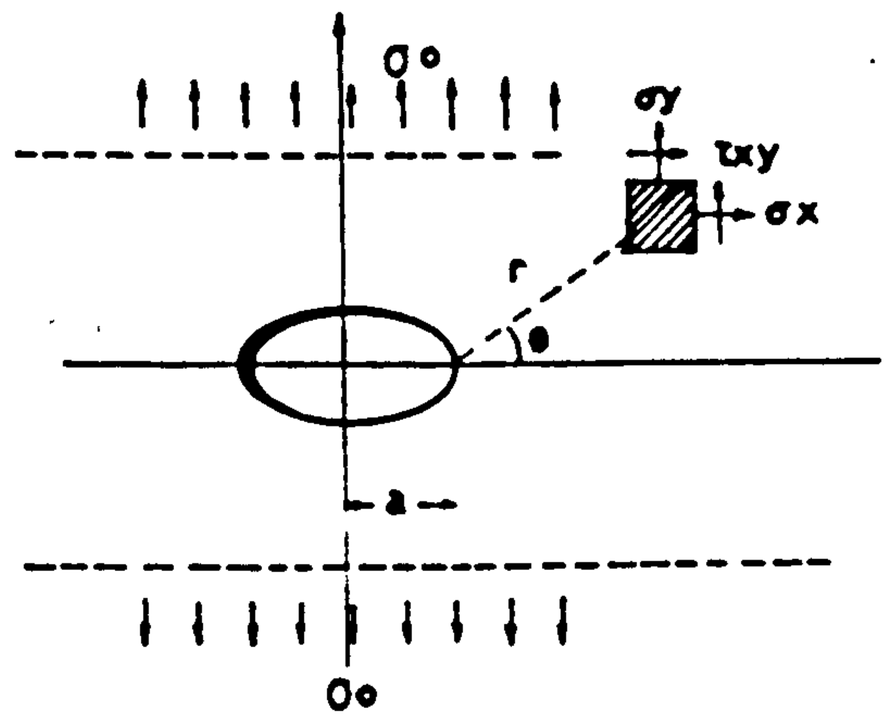

Fig.3.15. Elliptical crack in a uniformly stressed lamina, analysed by Irwin /38/

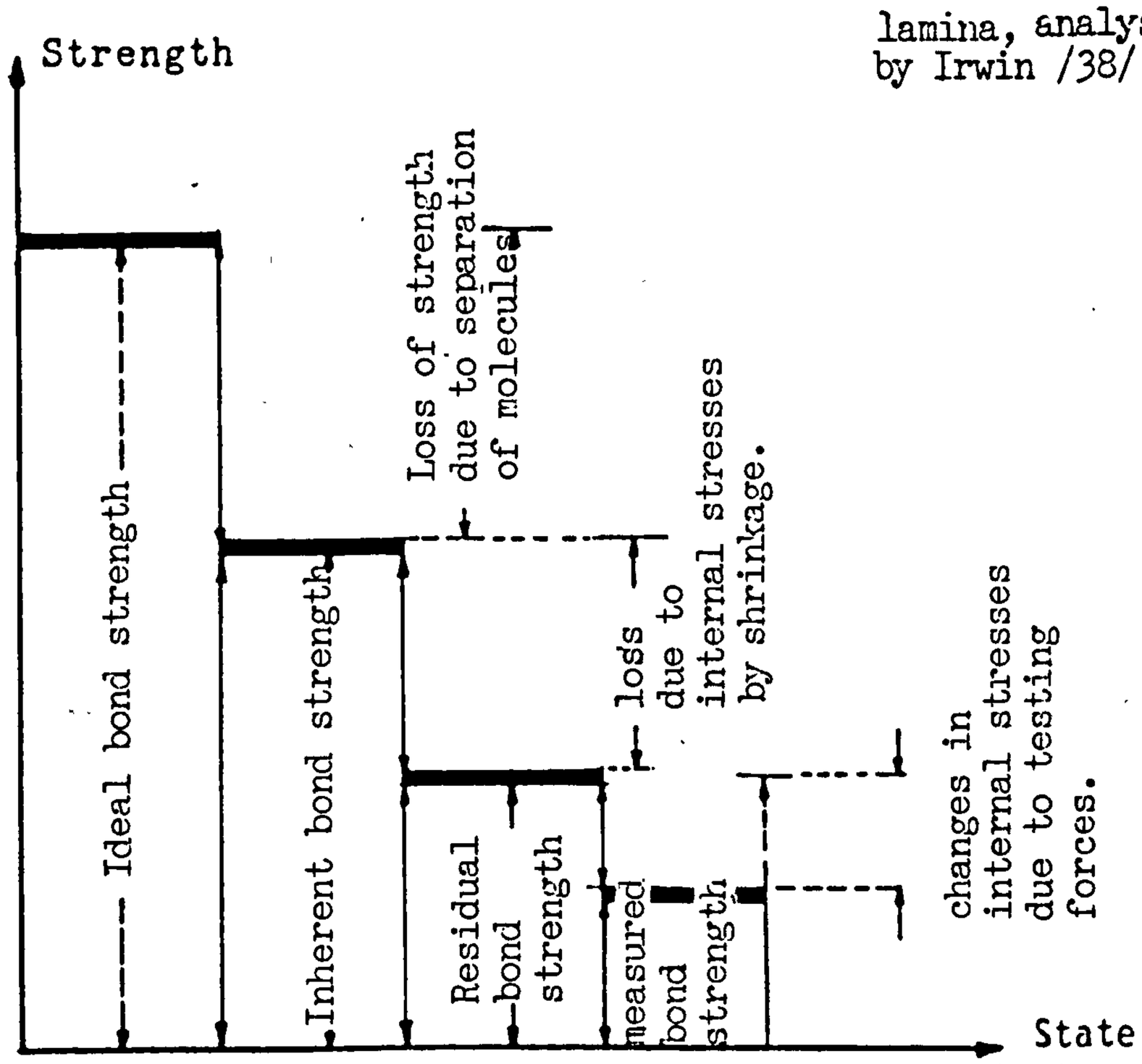

Fig.3.14. Losses of bond strength after Allen /35/

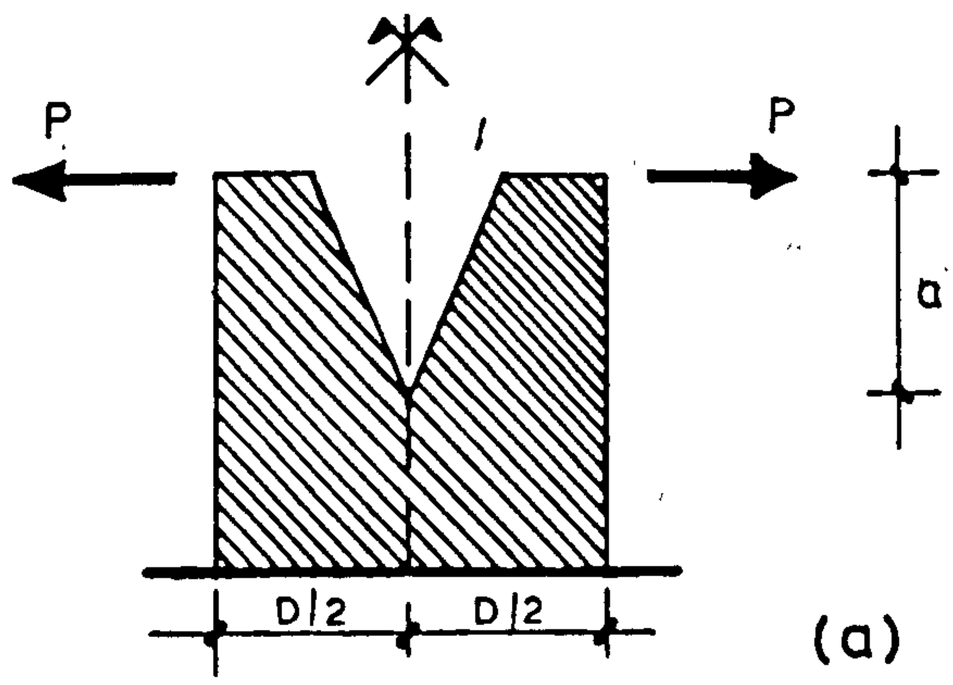

(a)

$$u = \frac{8a^3 \cdot P}{E\,t\,D^3}$$

$$C = \frac{u}{P} = \frac{8\,a^3}{E.\,t.D^3}$$

$$\frac{dC}{da} = \frac{24\,a^2}{E.t.D^3}$$

$$G = \frac{12\,P^2 a^2}{E.t^2.D^3} = \frac{3}{16}\,\frac{E\,D^3 u^2}{a^2}$$

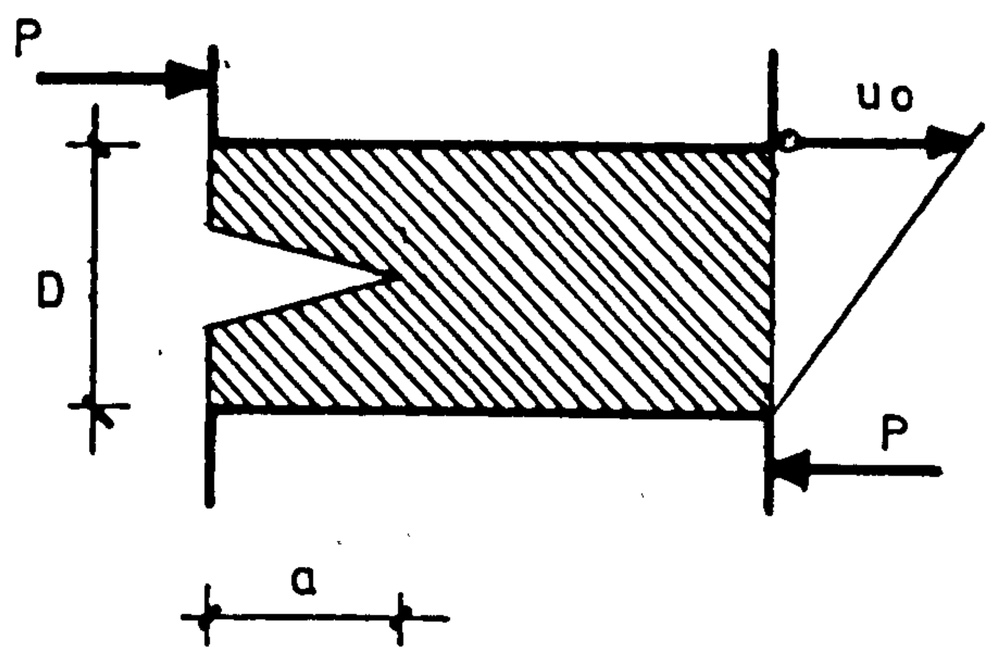

$$G = \frac{E}{4}\,\frac{u_o^2}{D}$$

(b)

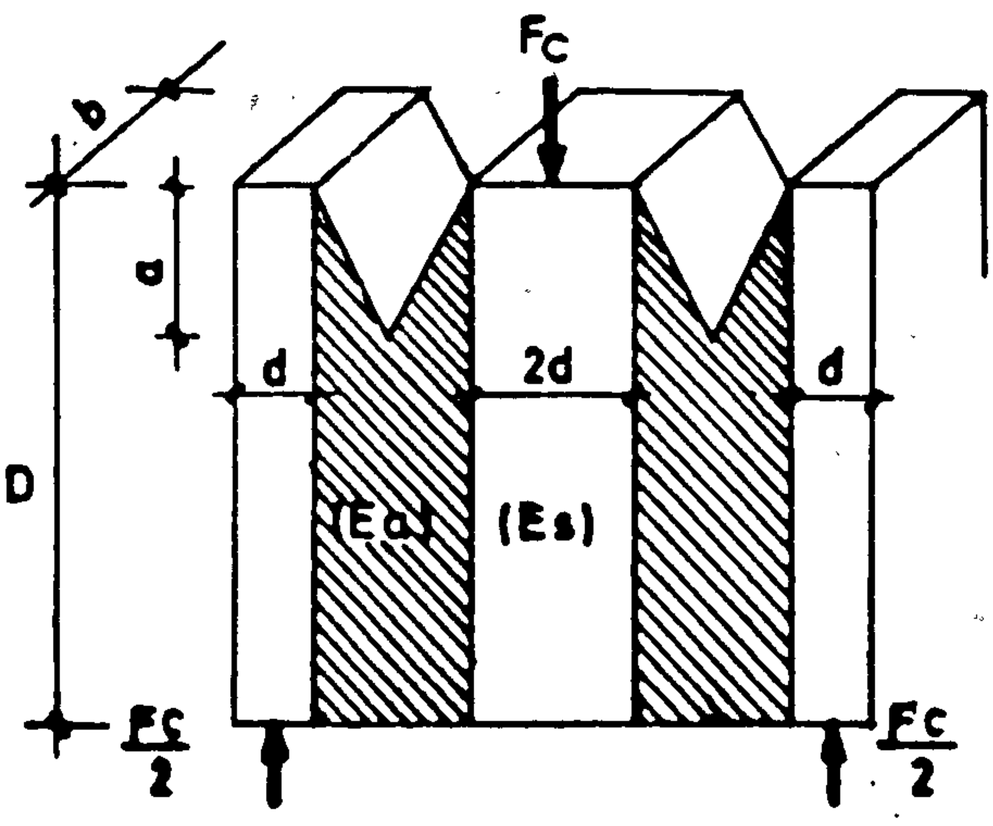

$$K_c = \tau_c \cdot Q \cdot \sqrt{a} \qquad (6)$$

$$\tau_c = \frac{F_c}{2\,b \cdot d} \qquad (7)$$

$$Q = Q_h \sqrt{\frac{E_a}{E_s}} \qquad (8)$$

$$Q_h = \frac{d}{D} \cdot \left[0.0325 + 14.63\left(\frac{a}{D}\right) - 46.07\left(\frac{a}{D}\right)^2 + 61.03\left(\frac{a}{D}\right)^3 - 28.86\left(\frac{a}{D}\right)^4\right] \qquad (9)$$

(c)

Fig.3.16. G and K values for different adhesive joints, after Kinloch /15/ and Williams /37/.

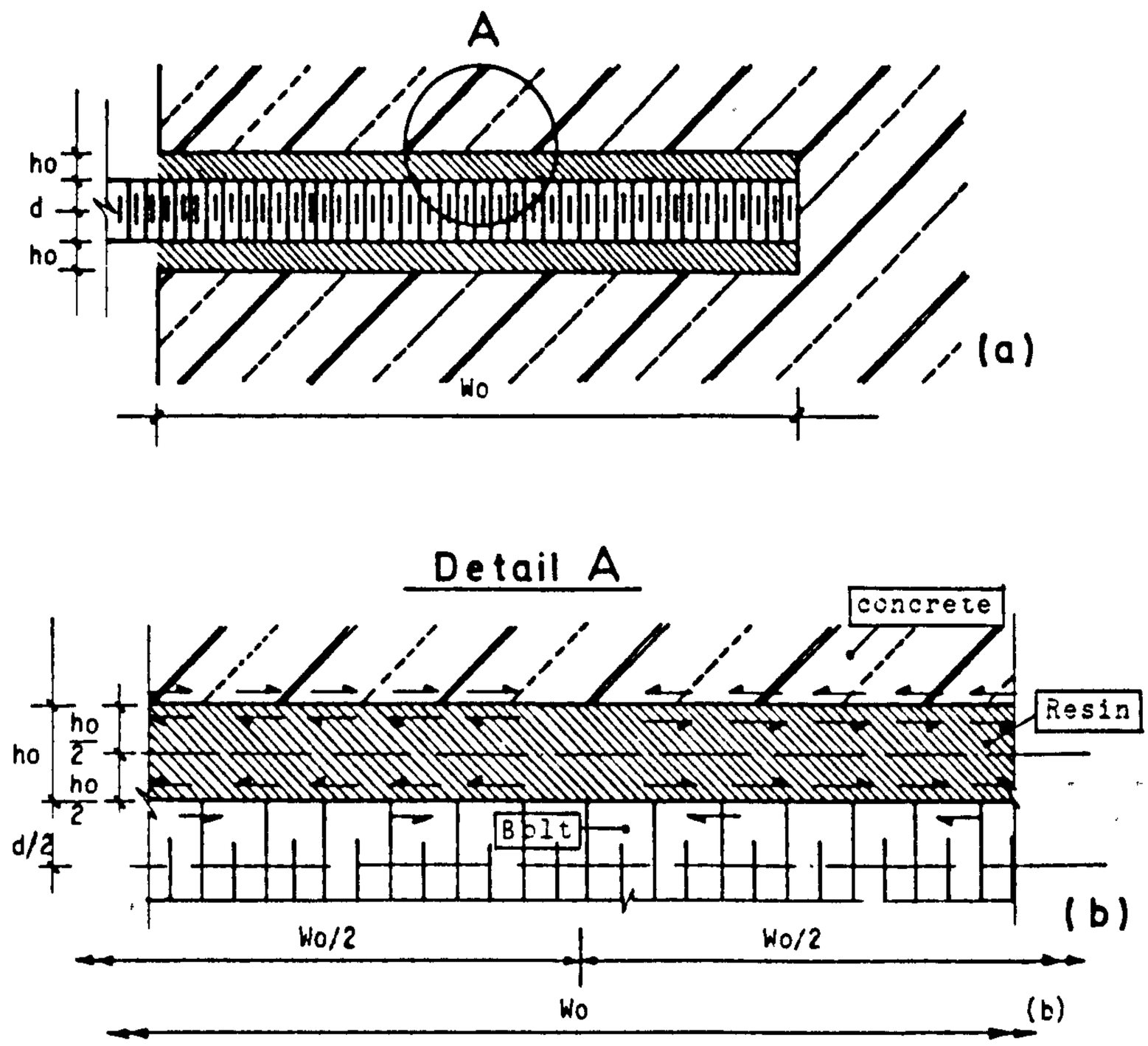

$$\sigma = E.\varepsilon.\left[2 + \frac{6}{h_o^2}\left(\frac{w_o^2}{4} - x^2\right)\right]$$

$$\tau = 3.E.\varepsilon\ \frac{w_o}{h_o}$$

Fig.3.17. Induction of stresses in an adhesive anchor due to shrinkage of the adhesive after Gent /40/

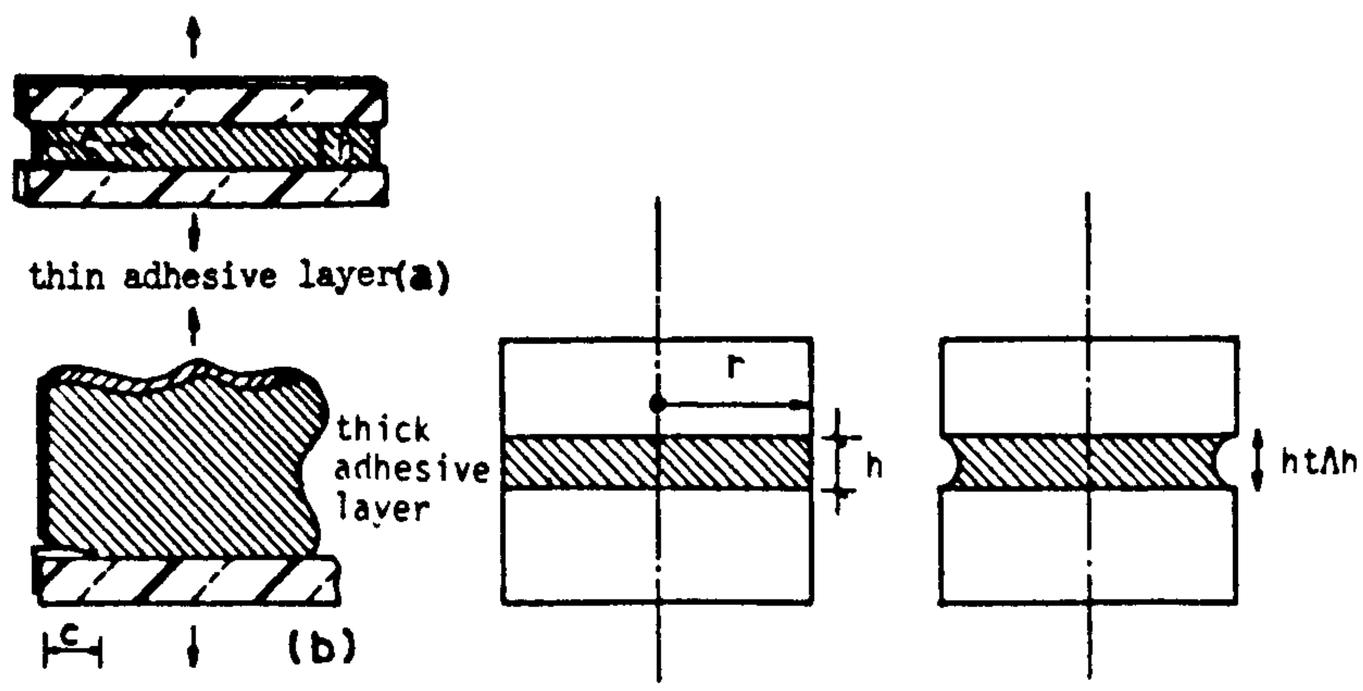

Fig.3.18. Butt joints (under tension)

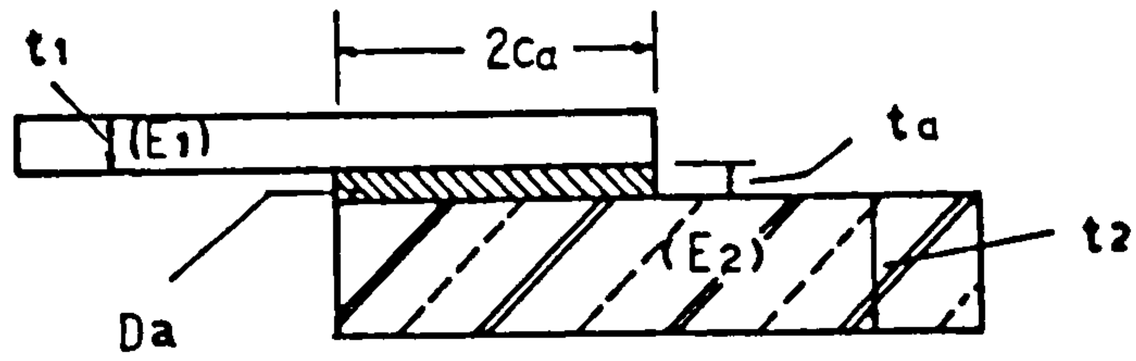

Fig.3.19. Single lap joint analyzed by Volkersen /18/

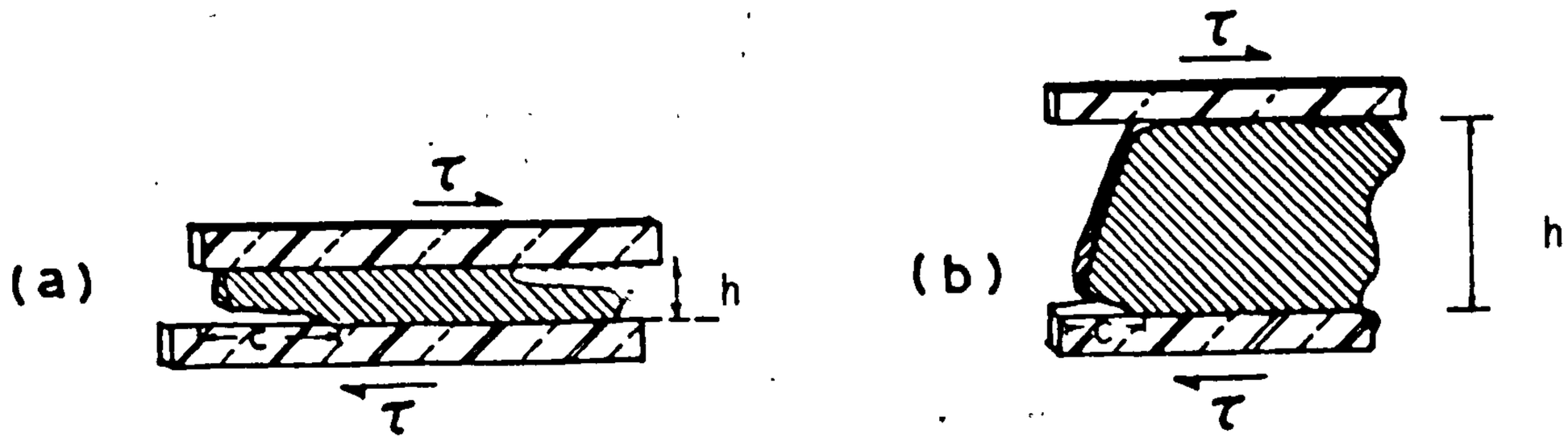

Fig.3.20. Shear loaded joints with (a) thin and (b) thick adhesive layer, analyzed by Gent /40/.

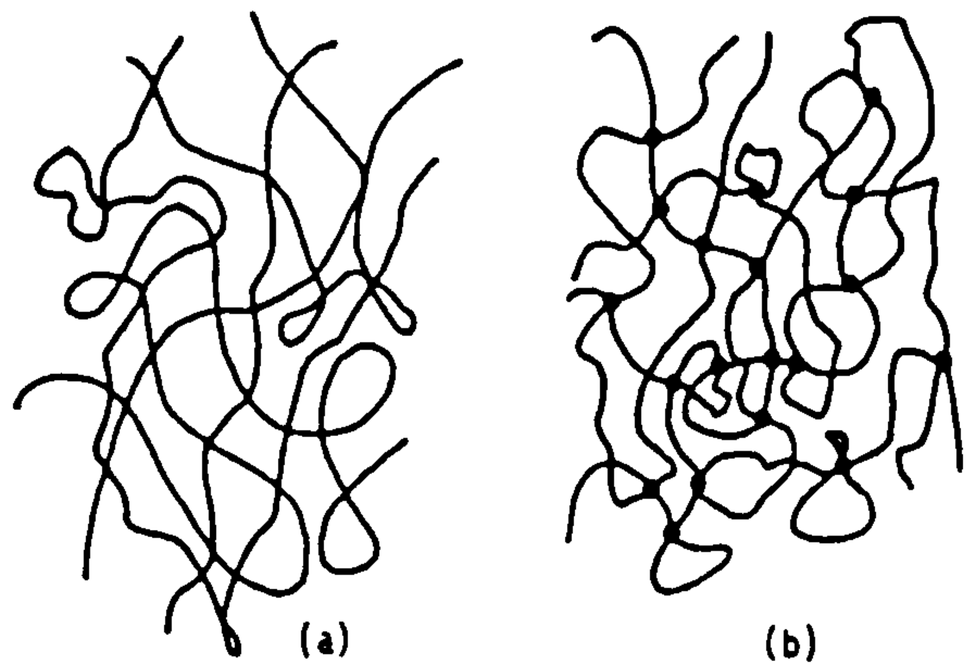

Fig.4.1. a) Schematic configuration of thermoplastics long chain molecules in space. b) Schhematic configuration of a cross-linked polymer molecule, after Arridge /41/

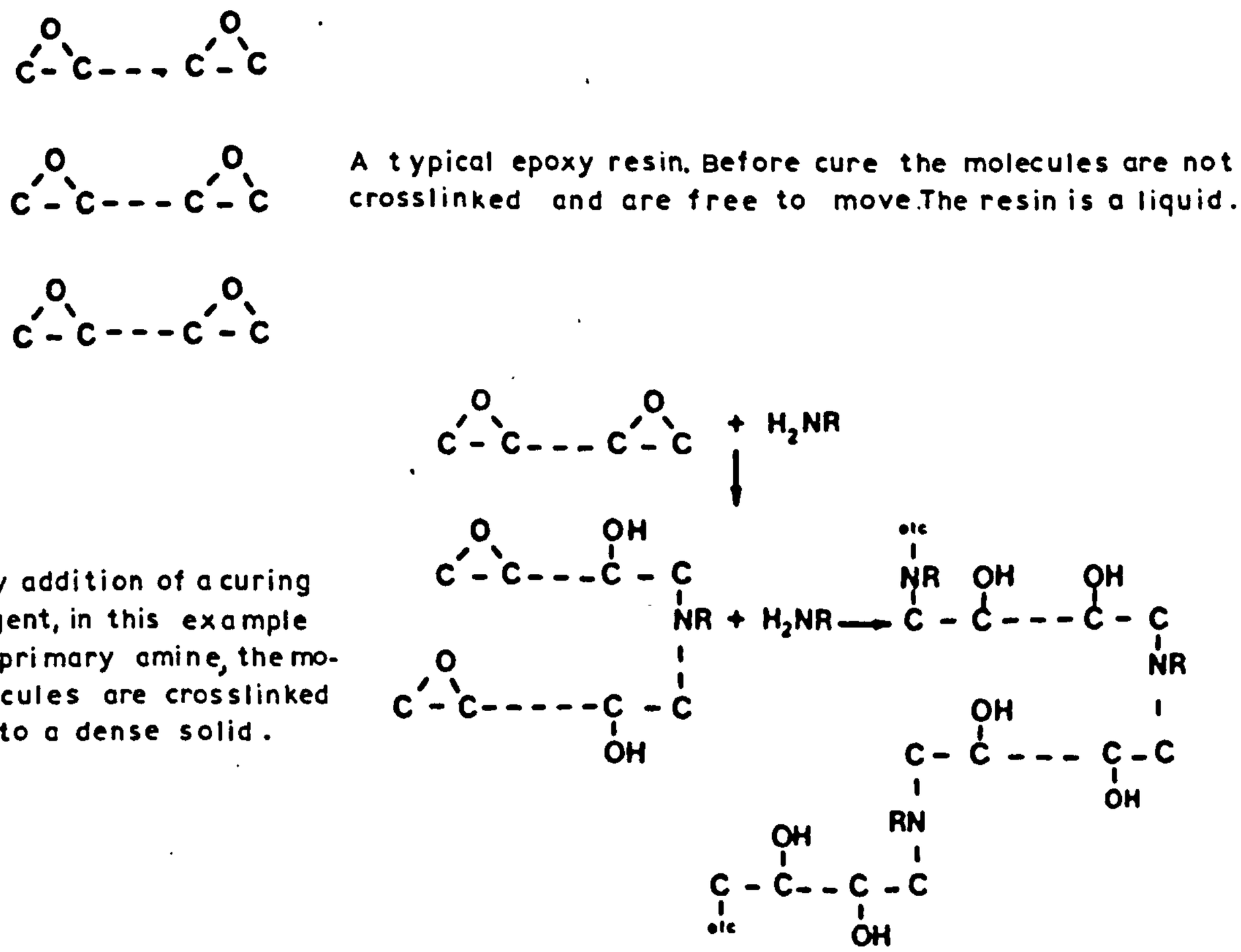

Fig.4.2. Curing of epoxy resin after Schutz /43/

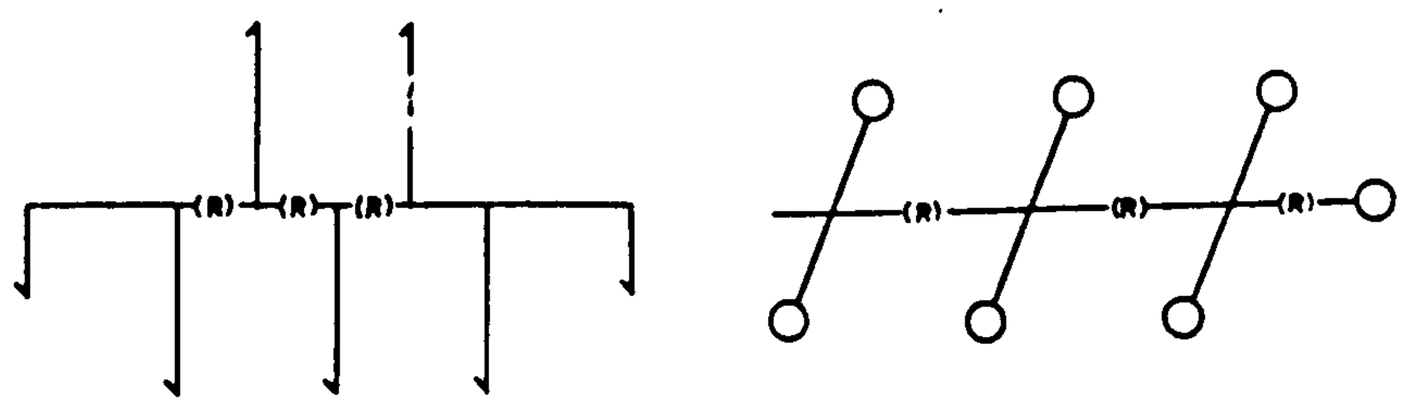

Fig.4.3. Schematic configuration of E P-resin and hardener after Shaw. /44/

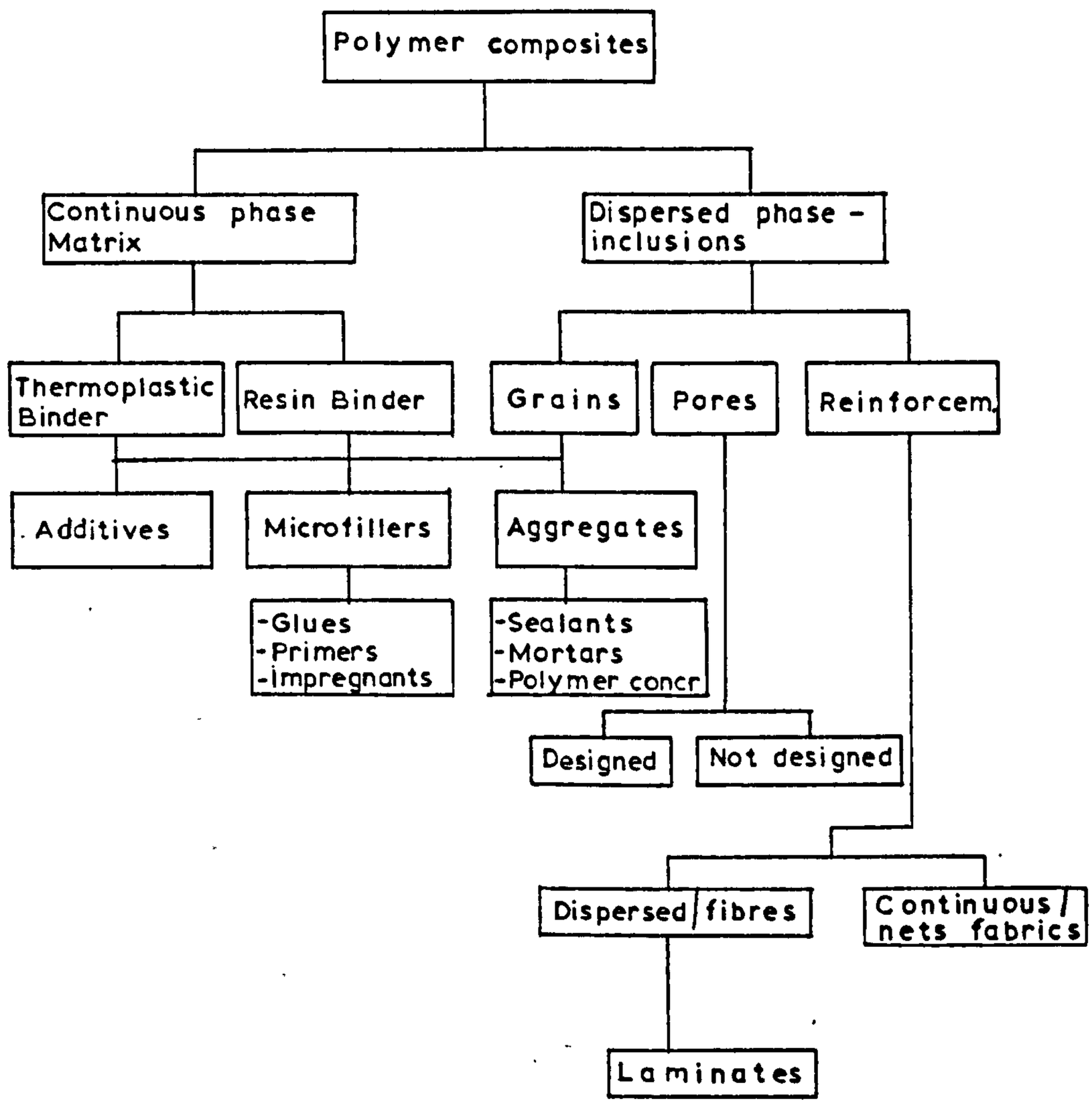

Fig.4.4. Possibilities of formation of polymer composites after Charnecki and Puterman. /32/

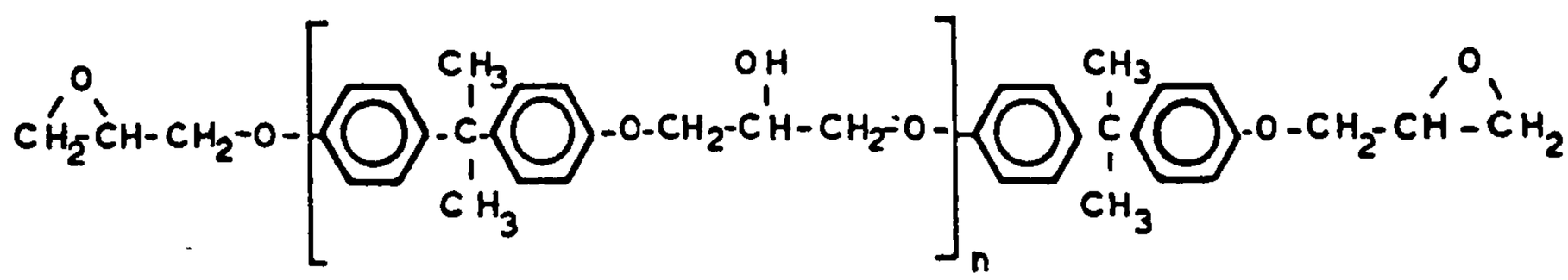

Fig.4.5. Chemical structure of epichlorohydrin-bisphenol A epoxy resin reported by Furr. /45/

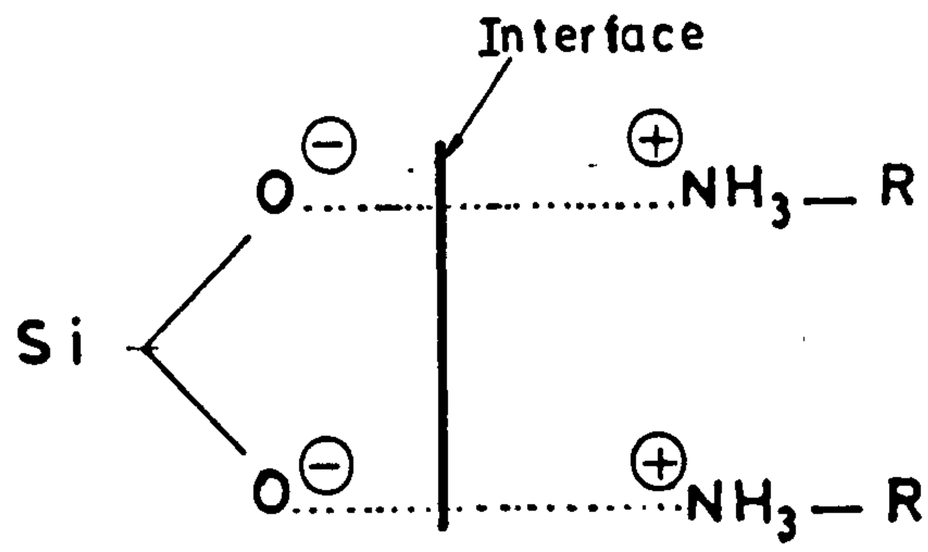

Fig.4.6. Chemical bond between quartz aggregate and epoxy resin, reported by Fiebrig /27/

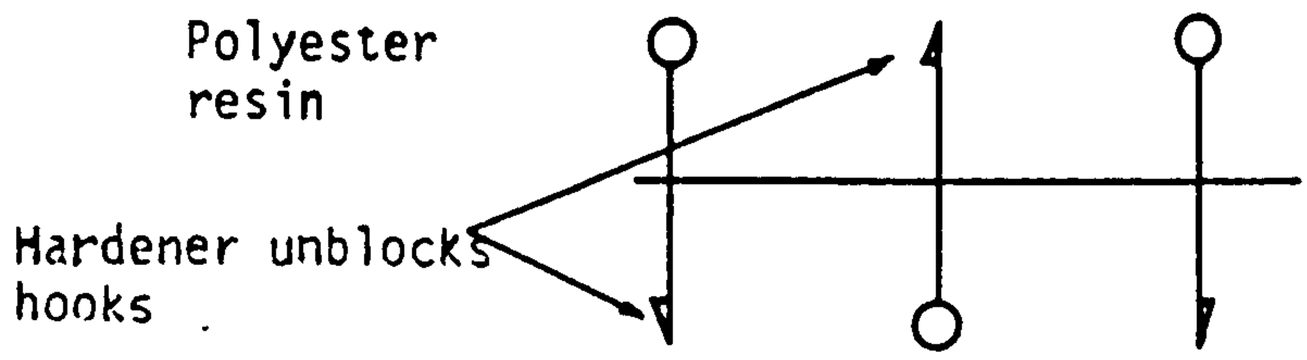

Fig.4.7. Schematic configuration of Polyester resin, after Shaw. /44/

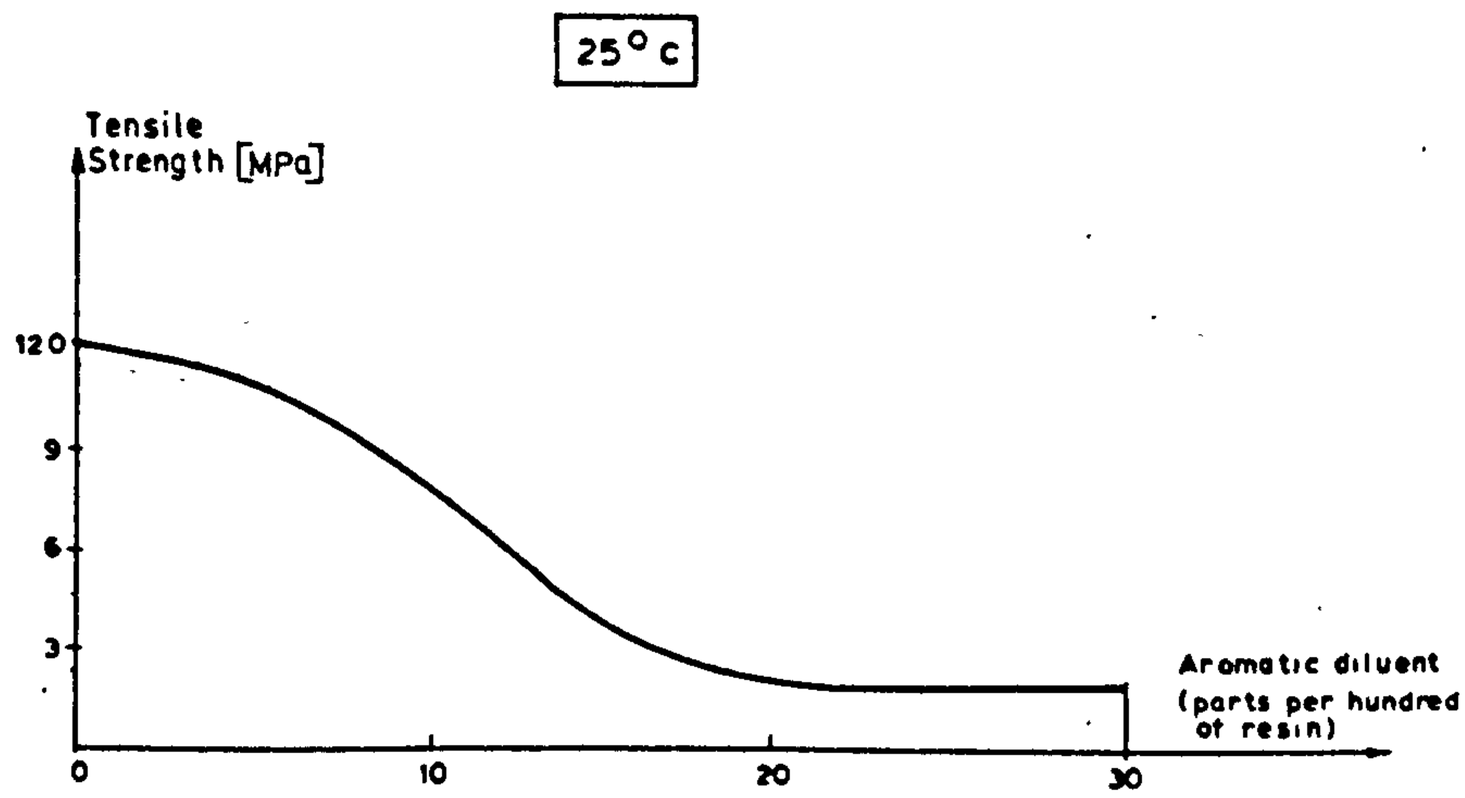

Fig.4.8. Effect of aromatic diluent addition on tensile properties, of epoxy resin, after Furr /45/

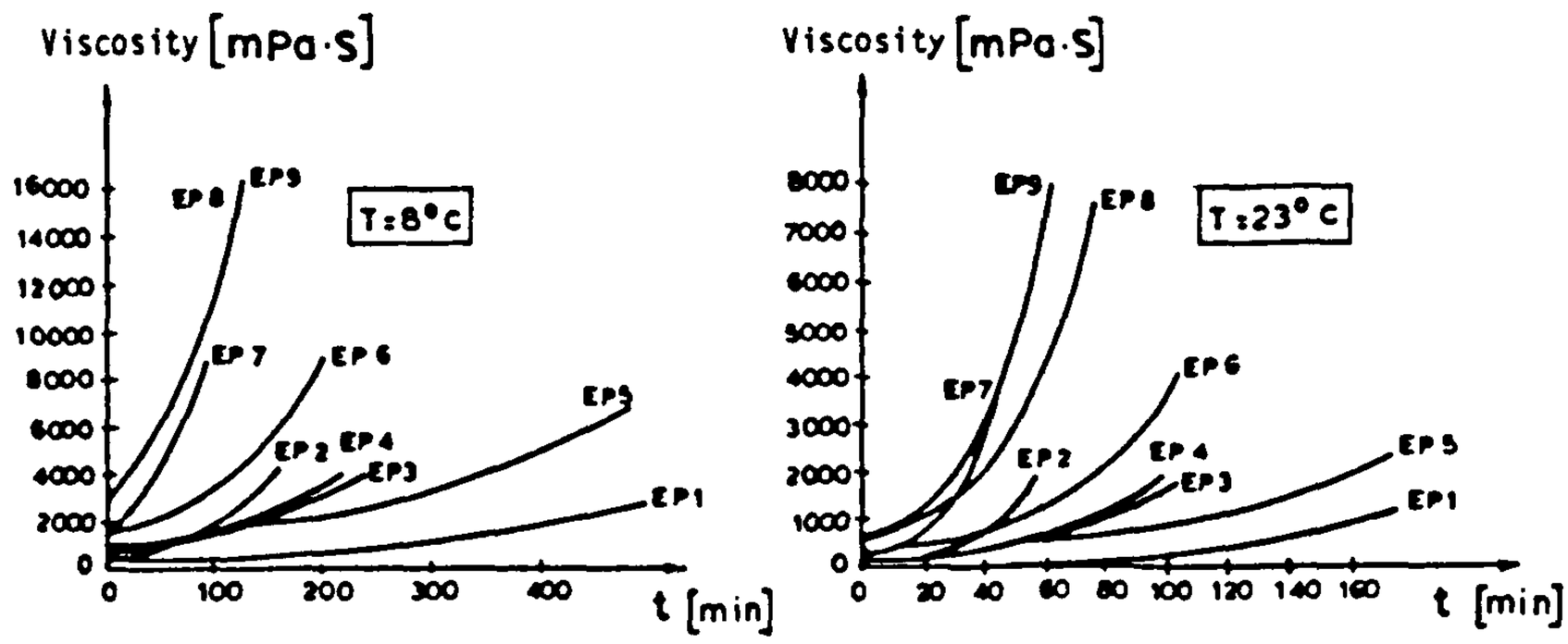

Fig.4.9. Change of viscosity of EPR by isothermic increase of ambient temperature, after Fiebrig /50/

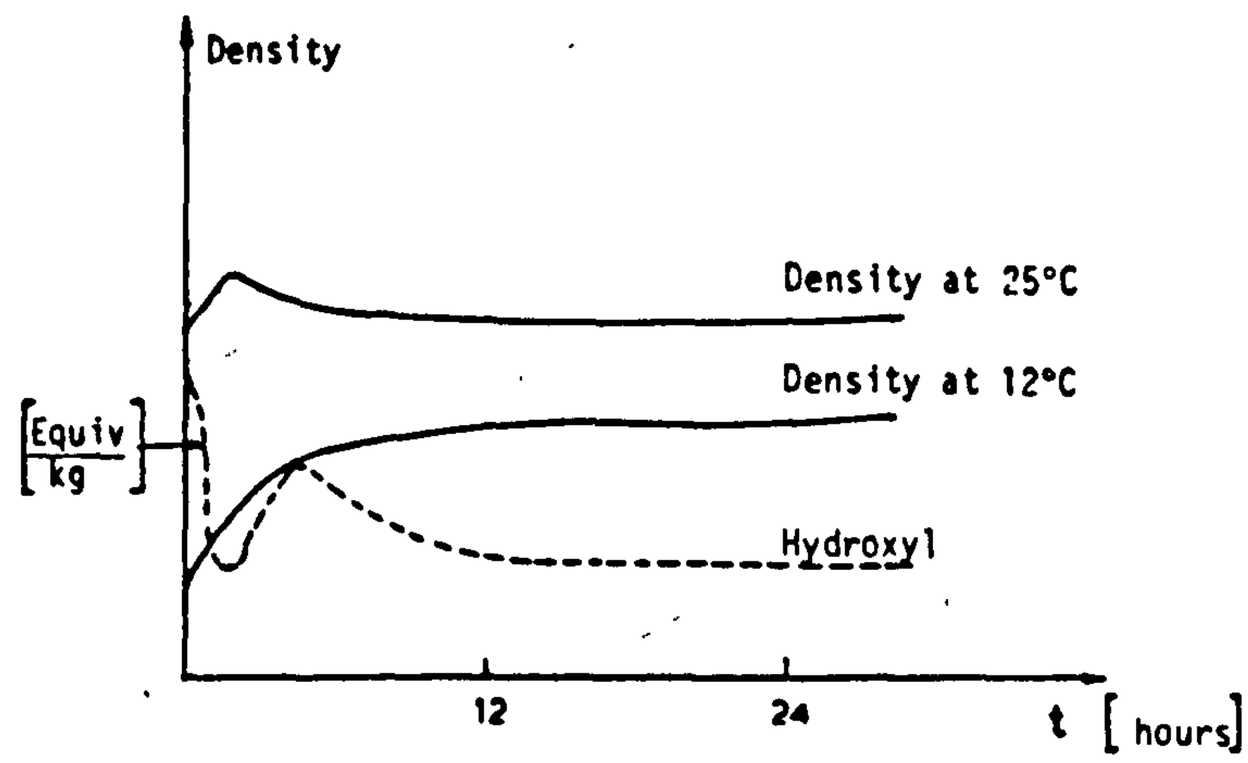

Fig.4.10. Physical and chemical changes during the curing process, after Furr /45/

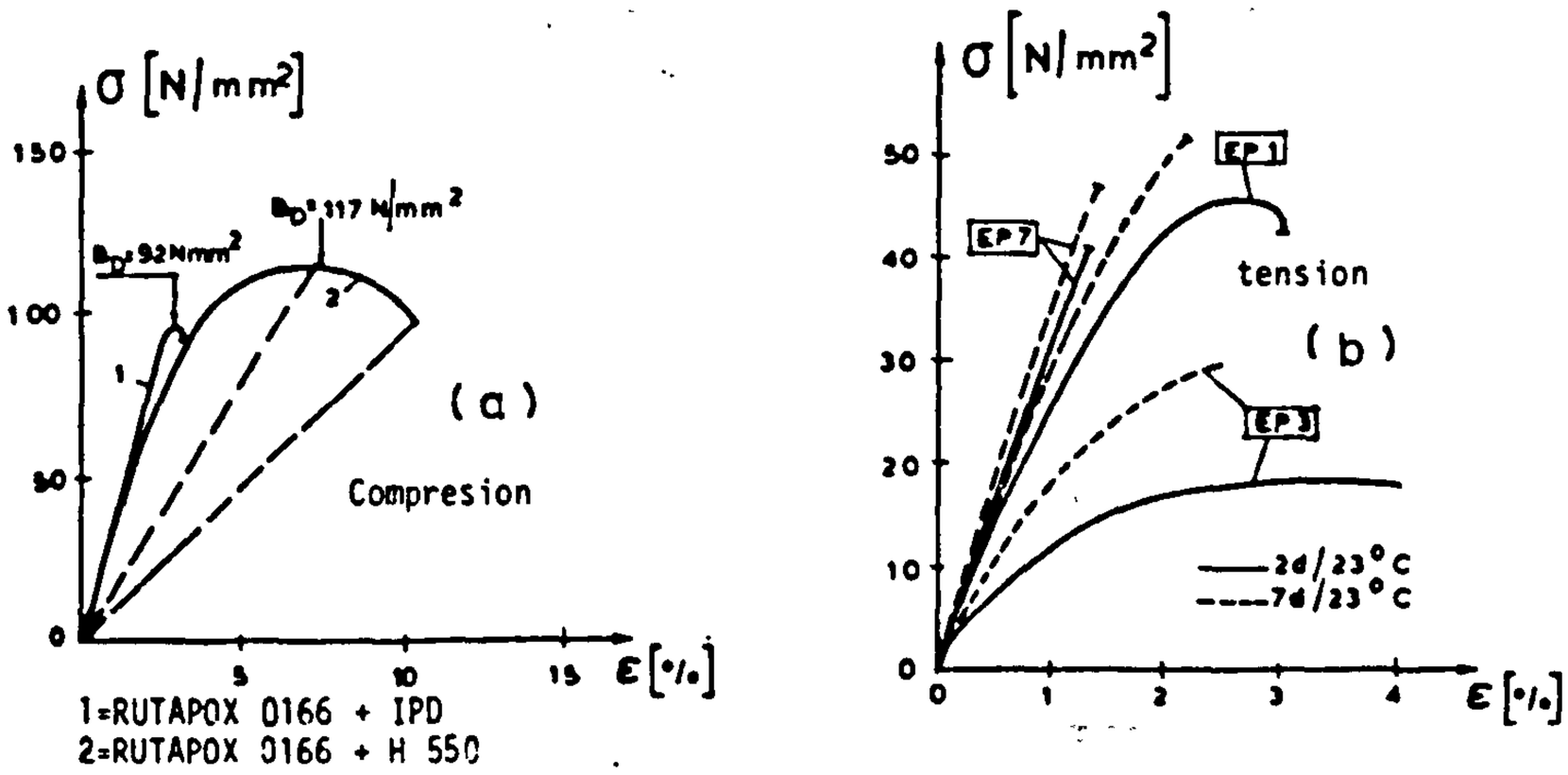

Fig.4.11. Stress-strain diagrams for cured EP resins
a) after Conrad. /51/
b) after Fiebrig. /50/

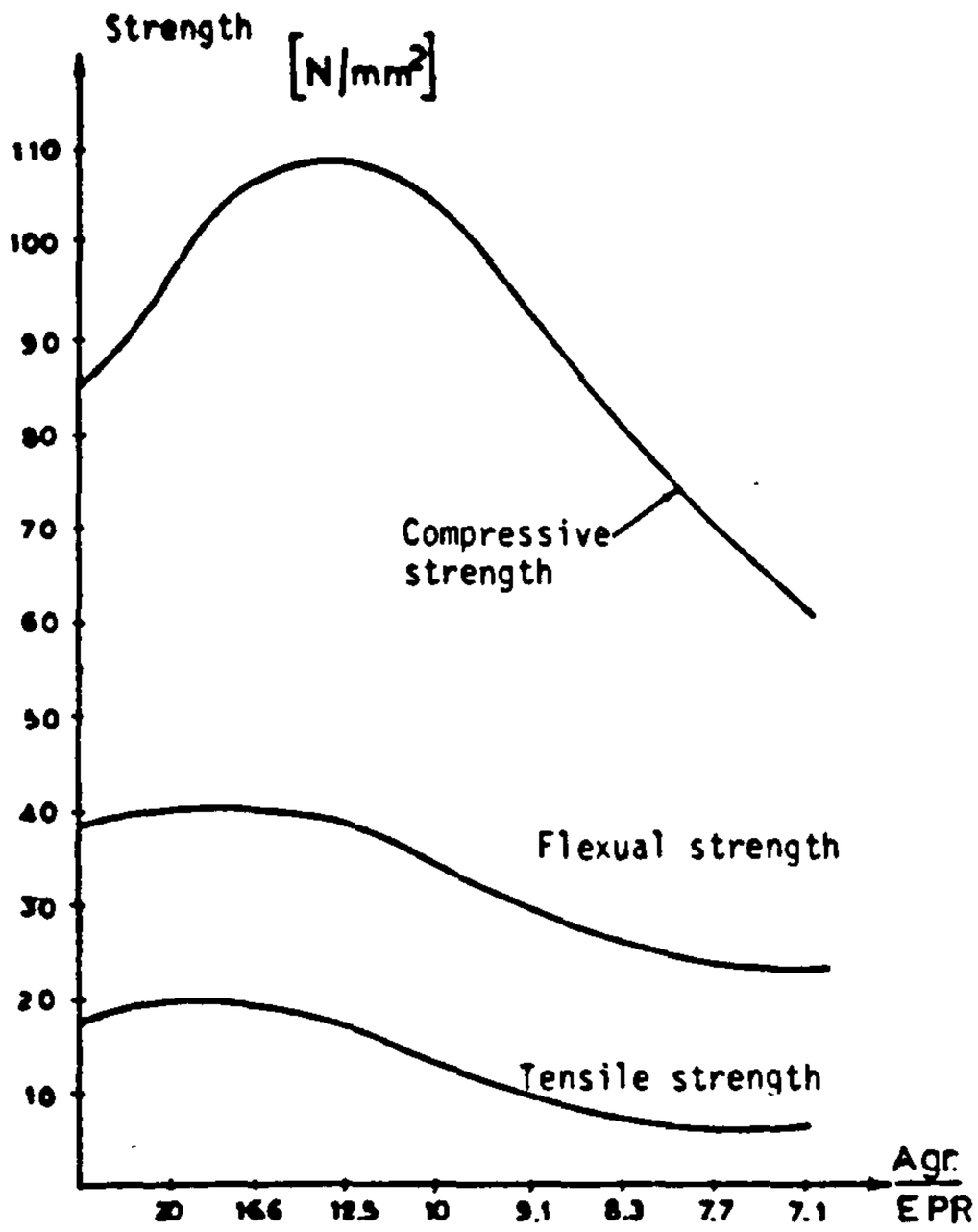

Fig.4.12. Effect of ratio of aggregates to resin on the strength, after Seidler. /48/

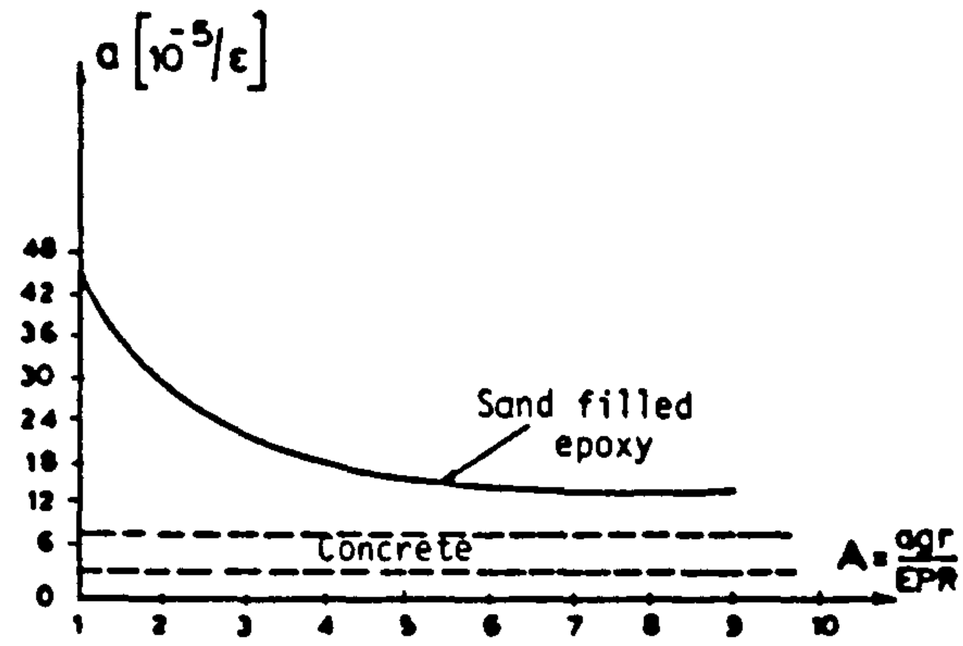

Fig.4.13. Effect of aggregates on the thermal expansion coefficient, after Lorman /52/

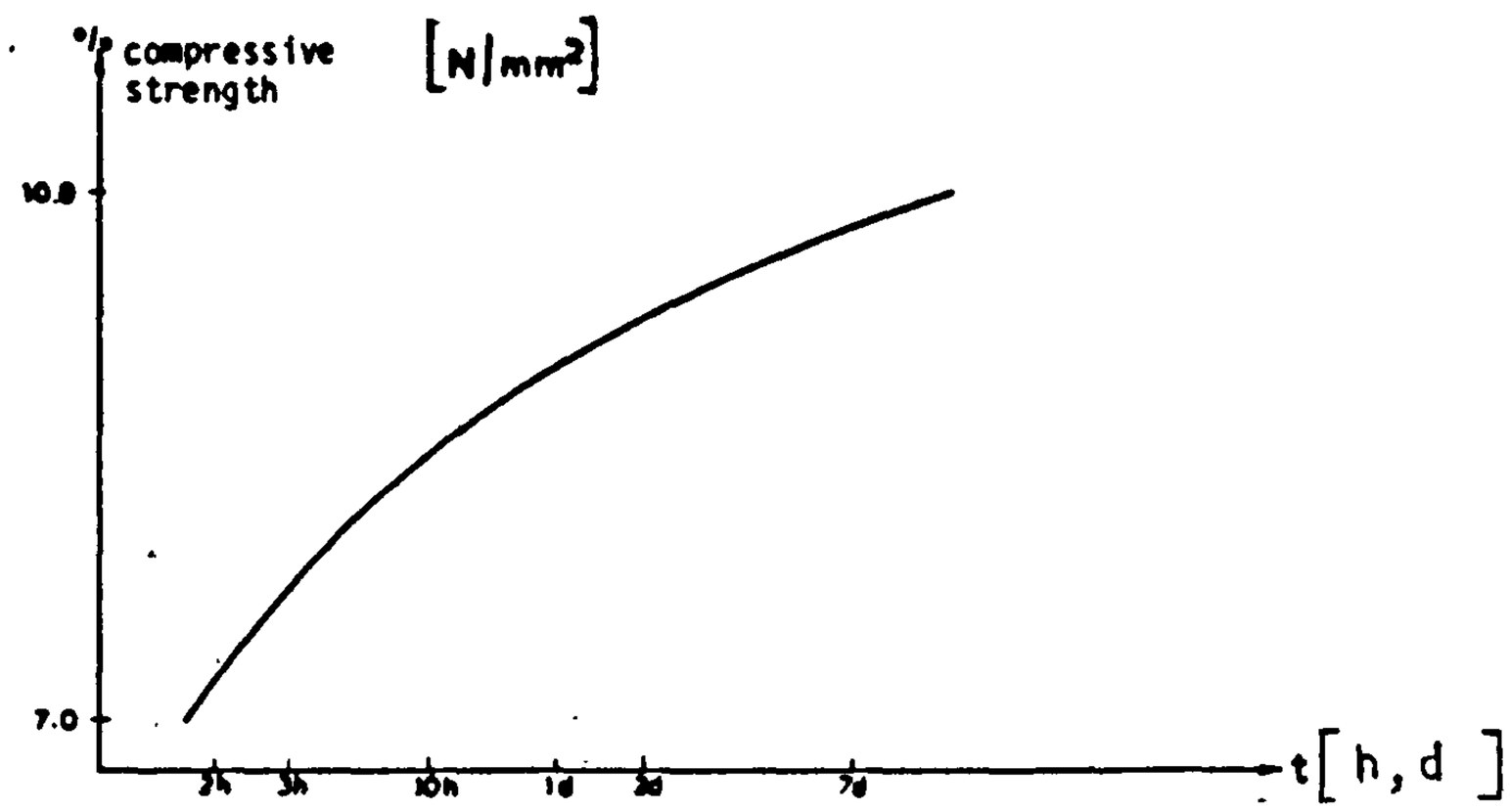

Fig.4.14. Rate of strength gain of an epoxy mortar, after Furr /45/

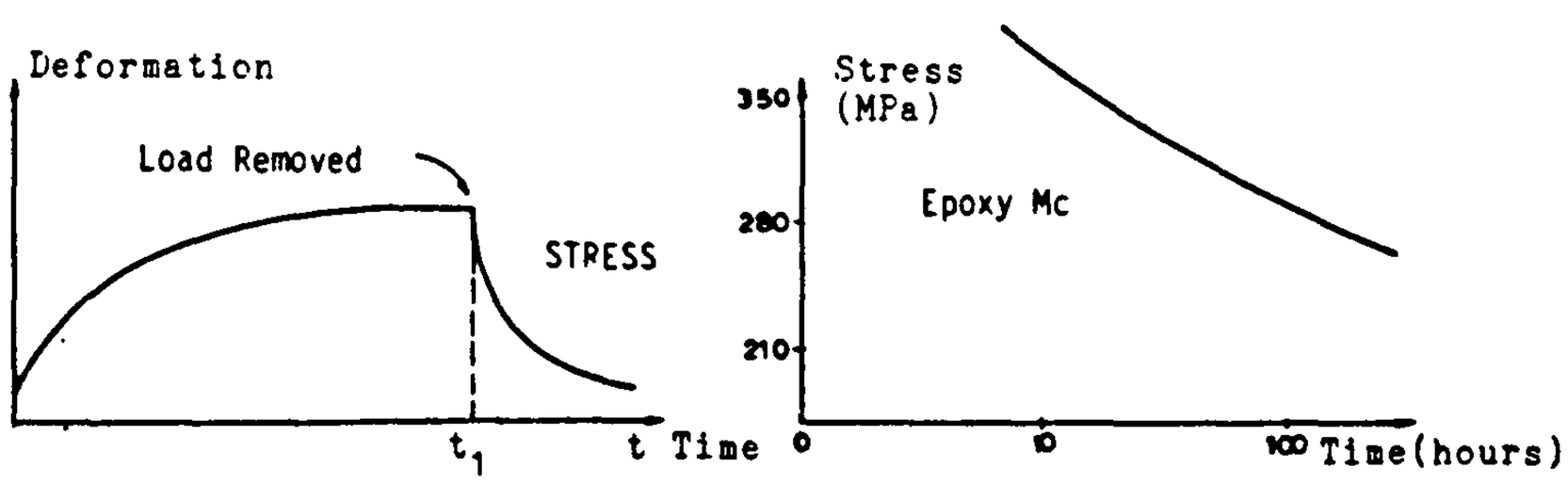

Fig.4.15. Effect of time under load on: a) strain (constant load and b) stress relaxation (constant strain), of epoxy systems, after Furr /45/.

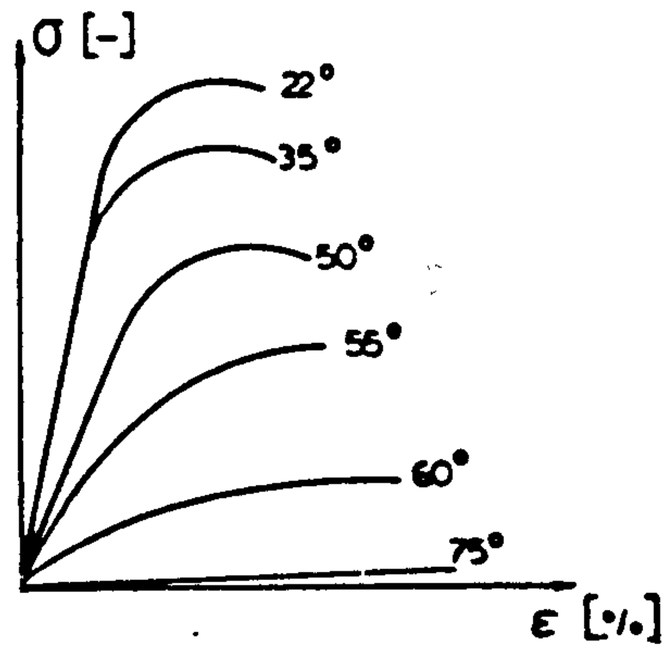

Fig.4.16. Effect of temperature on "σ-ε" relationship of epoxy systems under compression, after Hertig /53/.

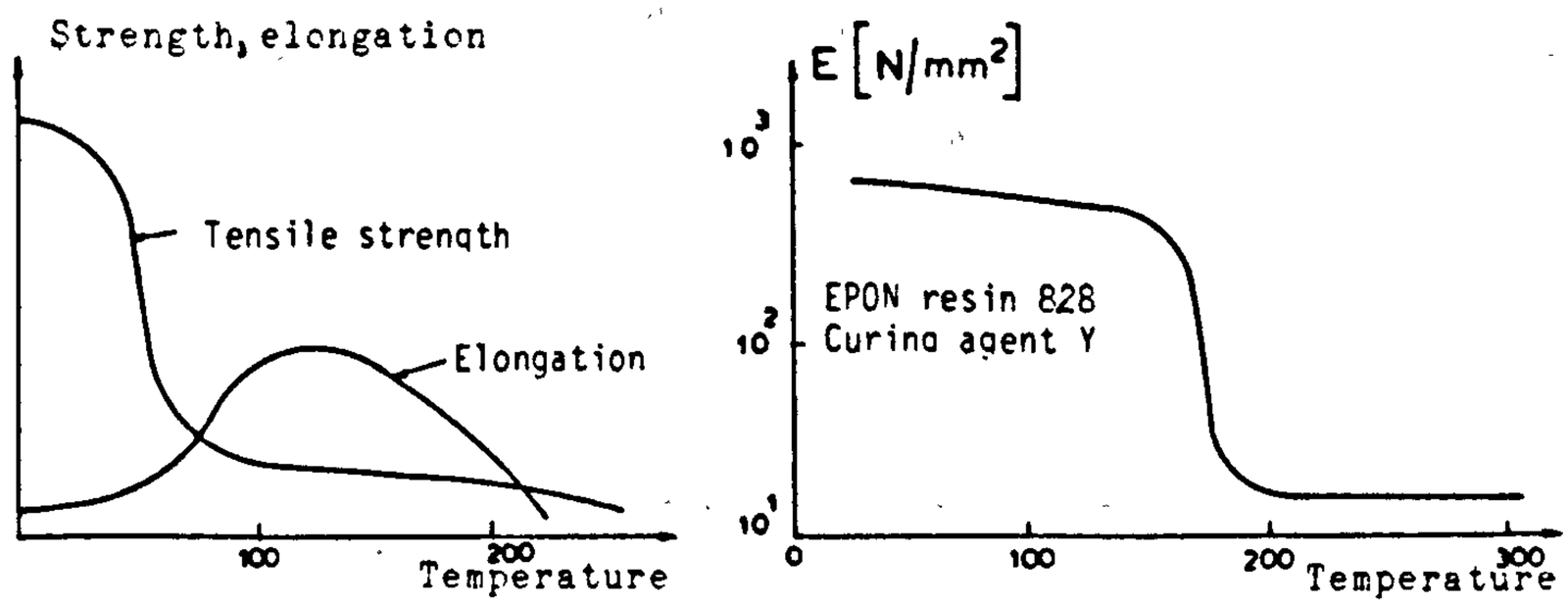

Fig.4.17. Effect of temperature on tensile strength and elongation and on the modulus of elasticity of a resin, after Furr/45/

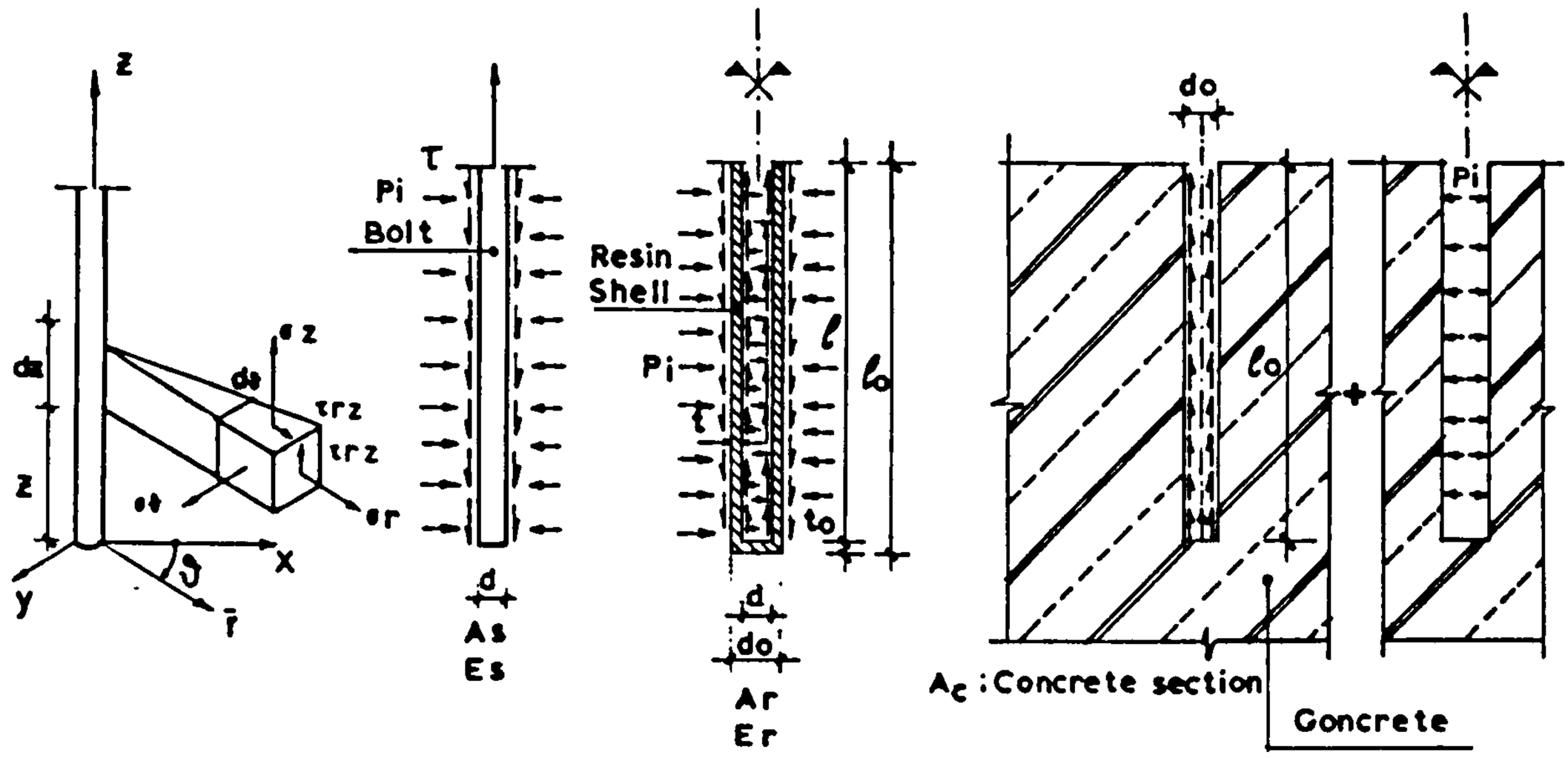

Fig.5.1. The components of an adhesive anchor system.

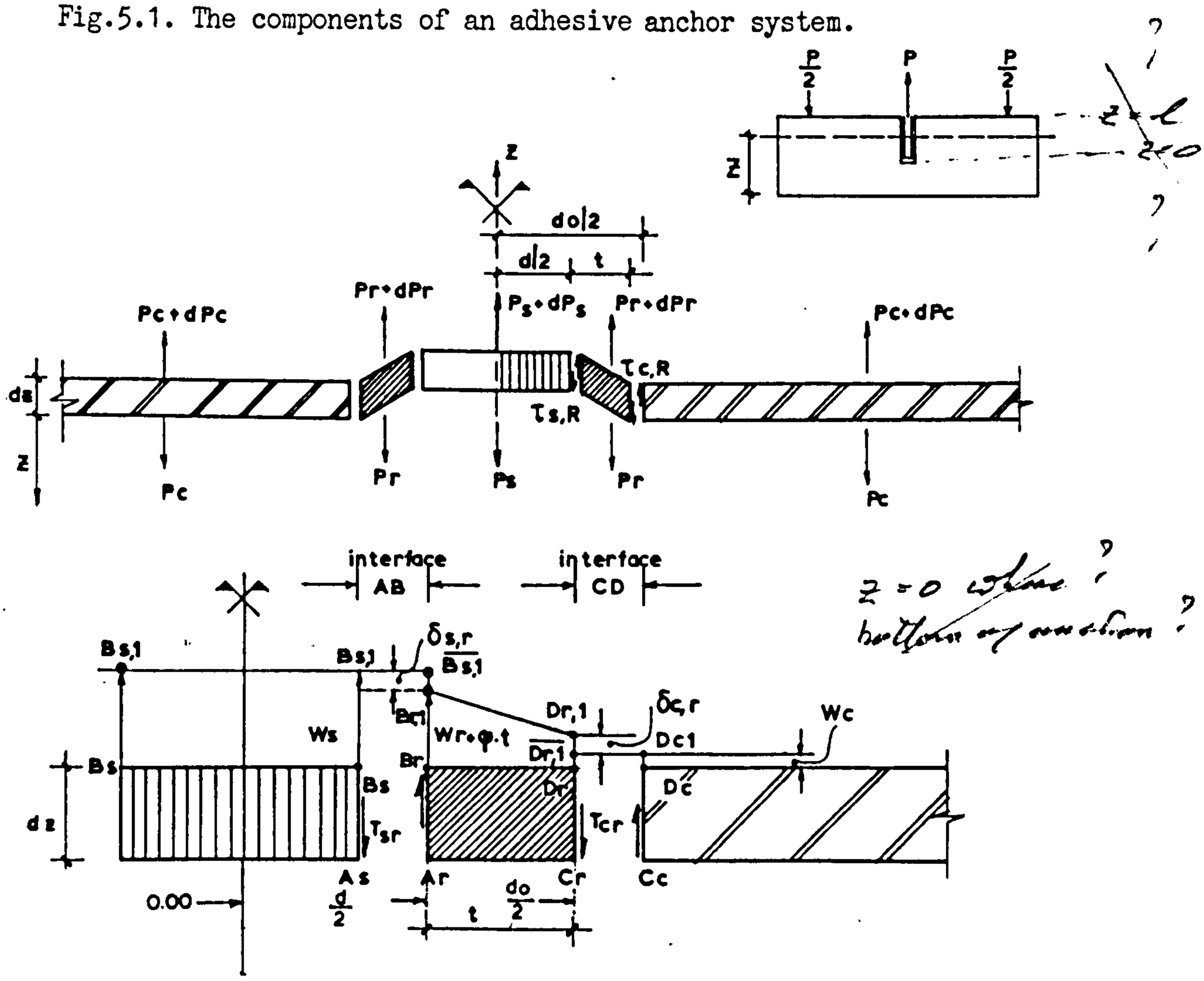

Line "Bs - Bs - Br - Dr1 - Dc1". will be removed to: "Bs1 - Bs1 - $\overline{Bs1}$ - Br1 - Dr1 - $\overline{Dr1}$ - Dc1 - Dc."

Fig.5.2. Internal axial forces and displacements of the components of an adhesive anchor slice.

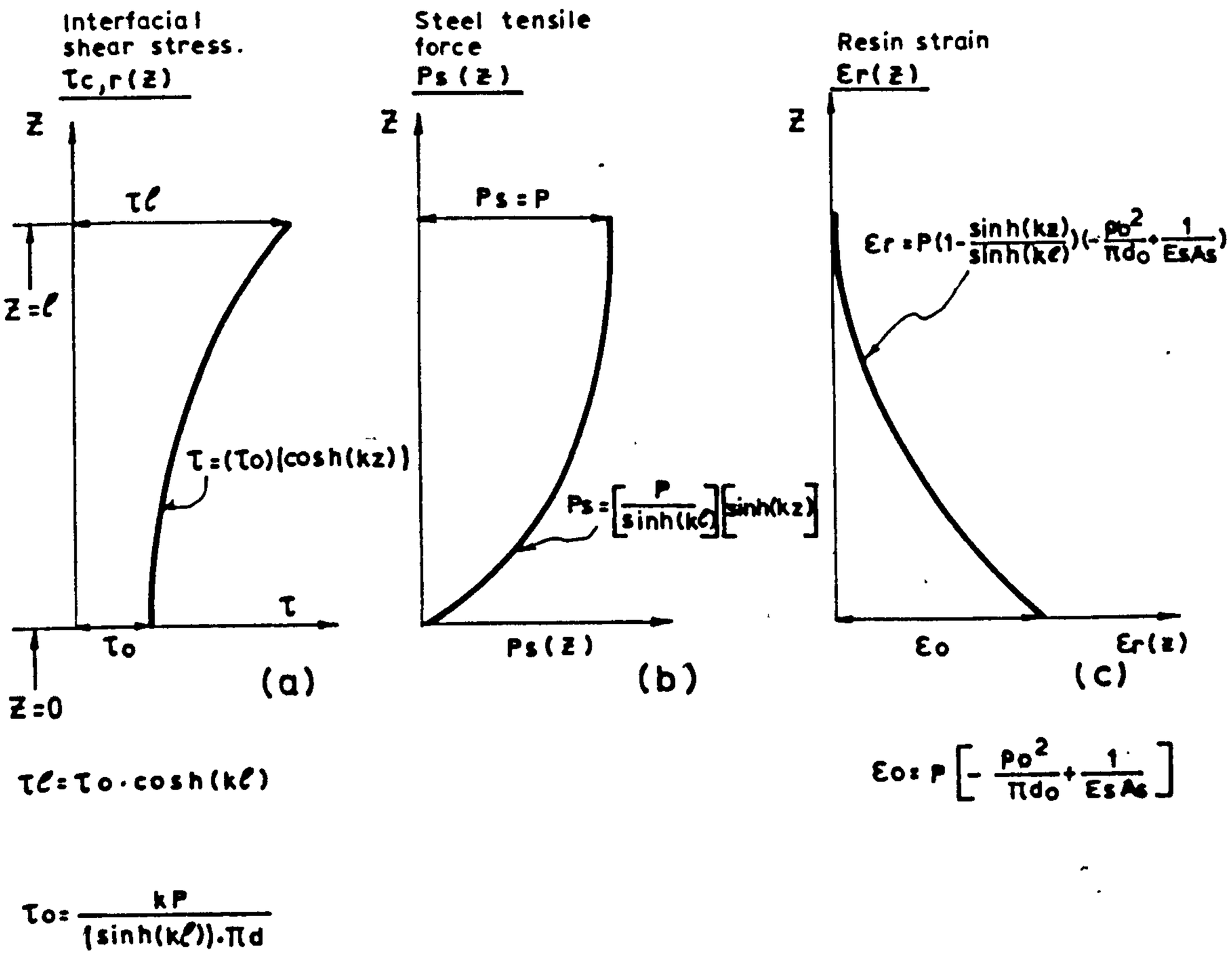

Fig. 5.3. Envelopes of shear interfacial bond $\tau_{c,r}(z)$, steel tension Ps (z) and resin tensile strain $\varepsilon_r(z)$.

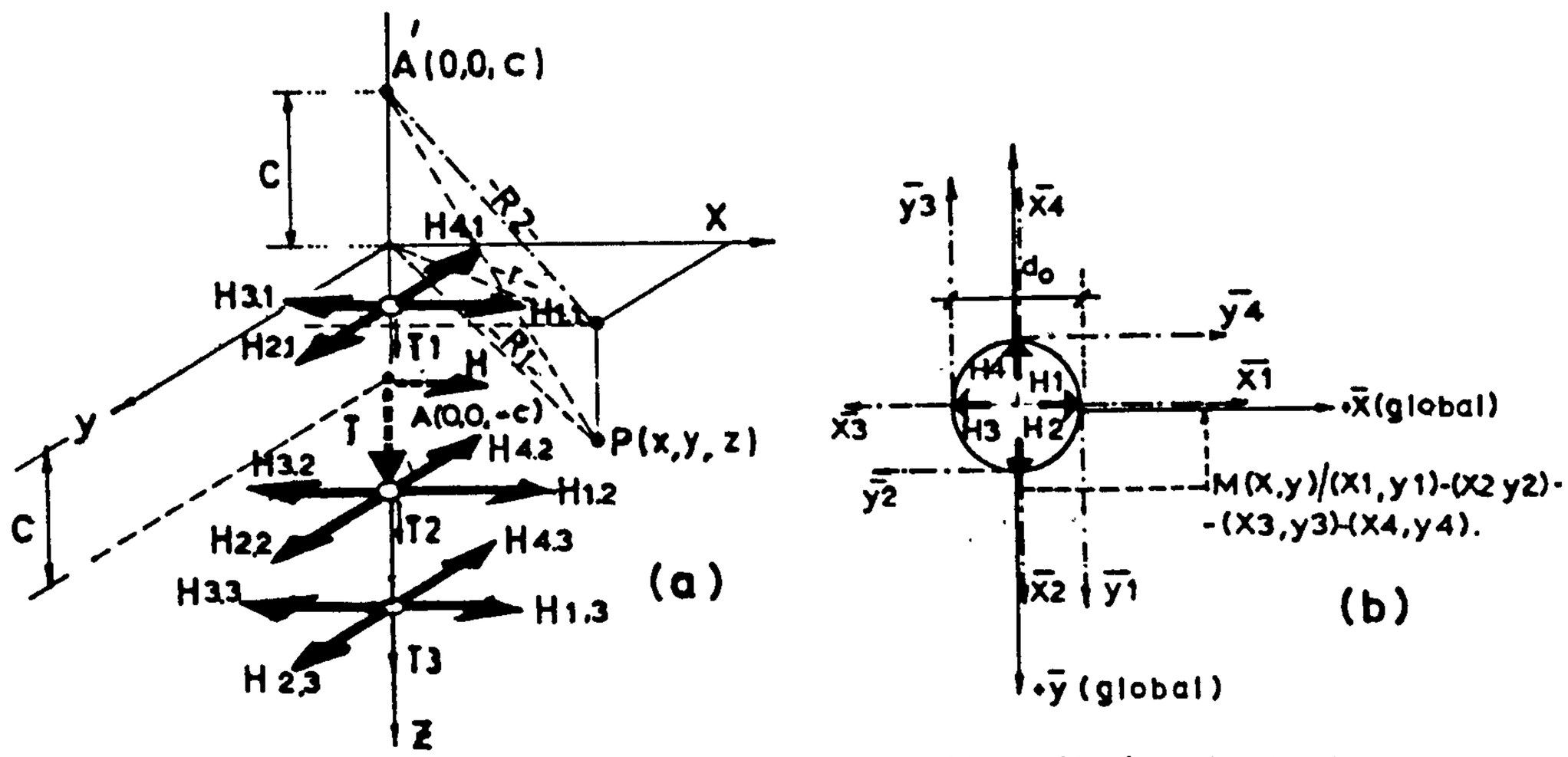

Fig.5.4. System of coordinates used by Mindlin /58/ and simulation of the forces acting on the concrete by pulling out the anchor.

Steel strain $\varepsilon_s(\mu\varepsilon)$ distribution.

Z (mm)	ε_s ($\mu\varepsilon$)
0	771
10	685
20	600
30	520
40	440
50	364
60	285
70	216
80	143
90	71
100	0

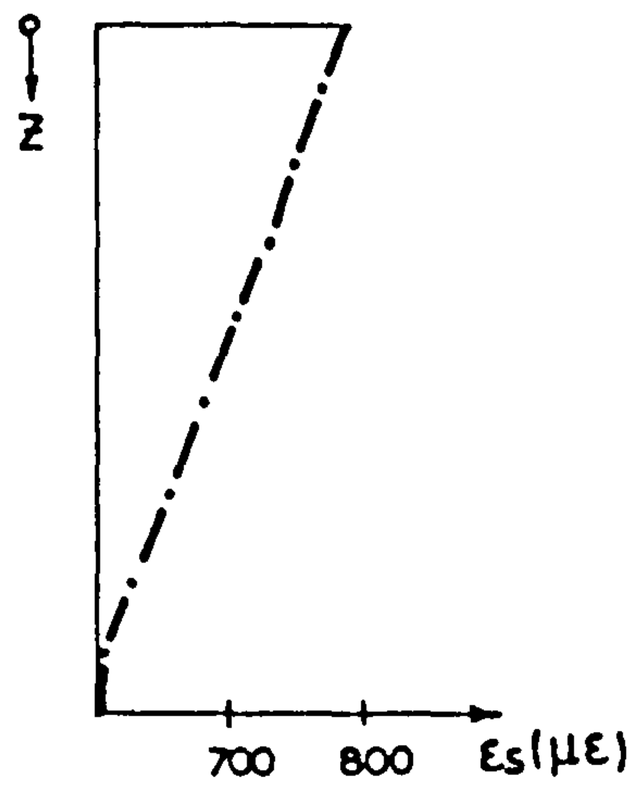

Resin strain $\varepsilon_r(\mu\varepsilon)$ distribution

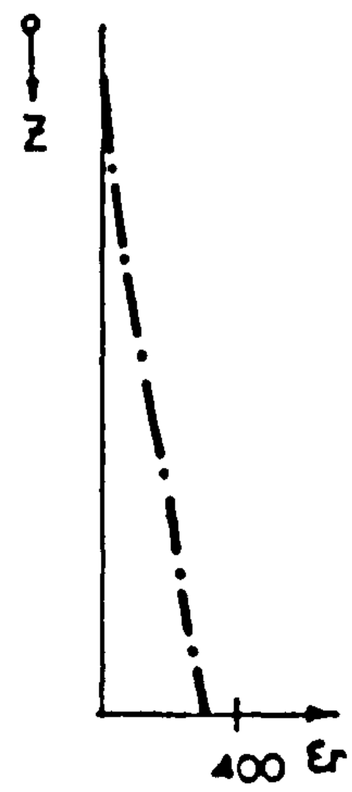

Z (mm)	ε_r ($\mu\varepsilon$)
0	0
10	8
20	44
30	84
40	113
50	146
60	177
70	208
80	238
90	298
100	300

Interfacial shear stress τ_{cr} (N/mm^2) distribution

Z (mm)	τ_{cr} (N/mm^2)
0	2.24
10	2.21
20	2.13
30	2.06
40	2.00
50	1.95
60	1.91
70	1.88
80	1.86
90	1.84
100	1.84

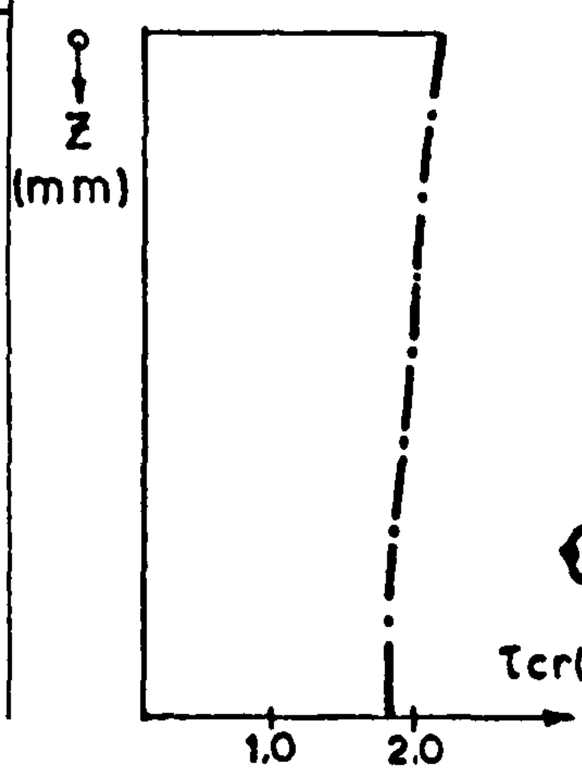

Section $\overline{x_4}=0$ $\overline{y_4}=18$mm. Distribution of concrete radial strain $\varepsilon_{yy}(\mu\varepsilon)$

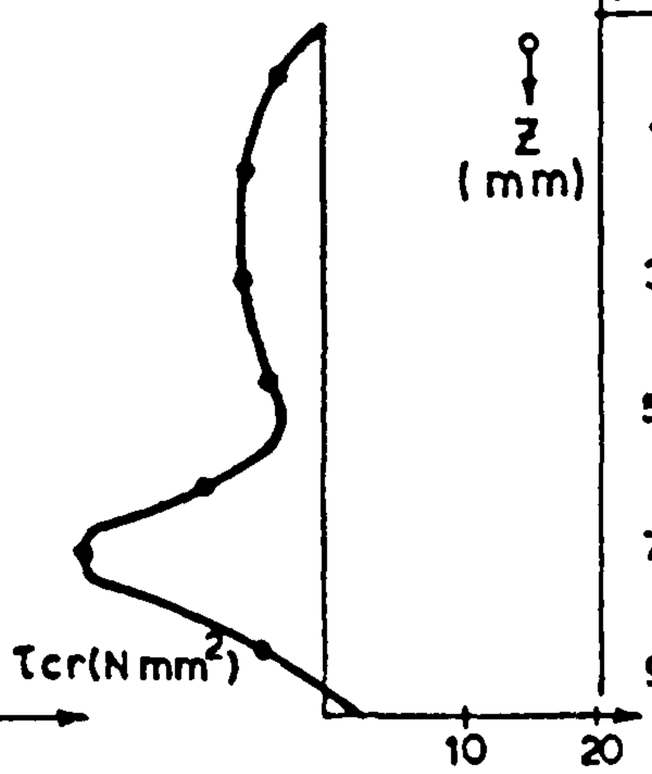

Z (mm)	ε_{yy} ($\mu\varepsilon$)
5	-0.5
15	-4
35	-7
55	-3
75	-19
95	+2

$\overline{x_4}, \overline{y_4}$: Fig 5.4.6

Section $\overline{x_4}=0$ $\overline{y_4}=18$mm. Distribution of concrete vertical strains

Z (mm)	ε_{zz} ($\mu\varepsilon$)
5	0
15	11
35	13
55	13
75	18
95	25

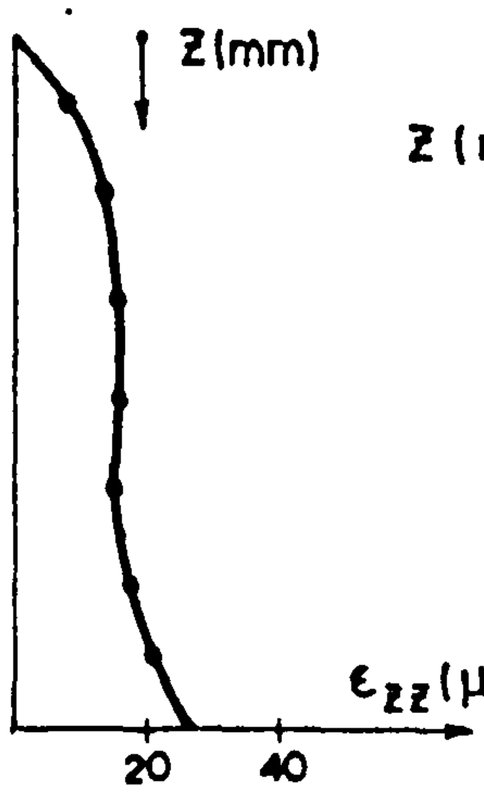

Section $\overline{x_4}=0$ $\overline{y_4}=18$mm. Distribution of concrete tangential strain

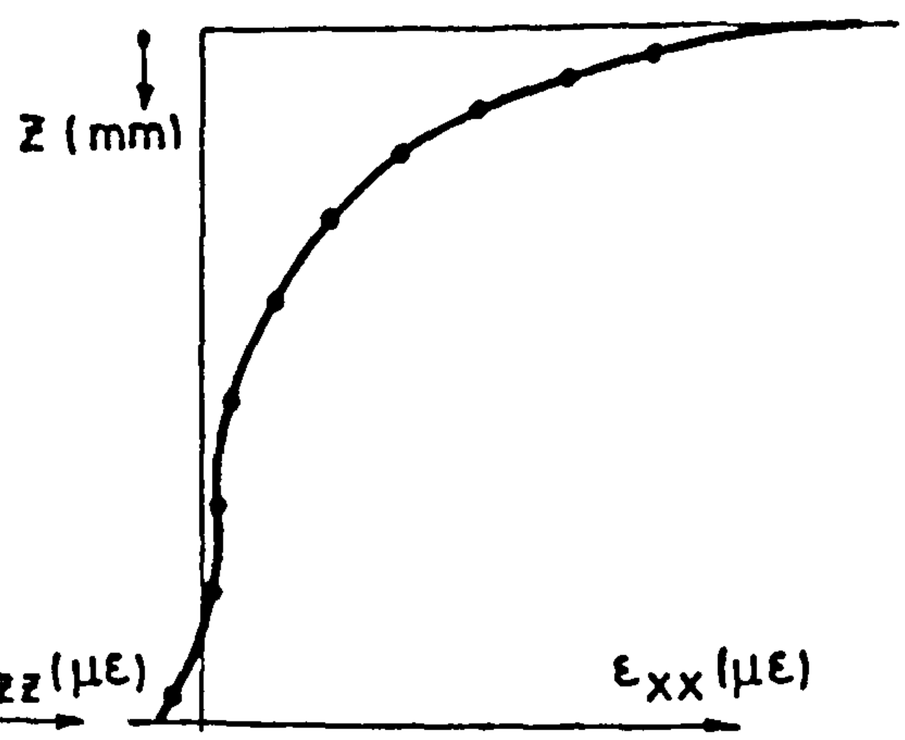

Z (mm)	ε_{xx} ($\mu\varepsilon$)
5	56
15	18
35	7
55	2
75	2
95	-3

Fig. 5.5 Distribution of steel, resin and concrete strains and of interfacial concrete-resin shear stresses derived from theoretical analysis of a particular system (d=12mm, d_o=16mm, t=2mm, l=100mm).

z = 0 plane

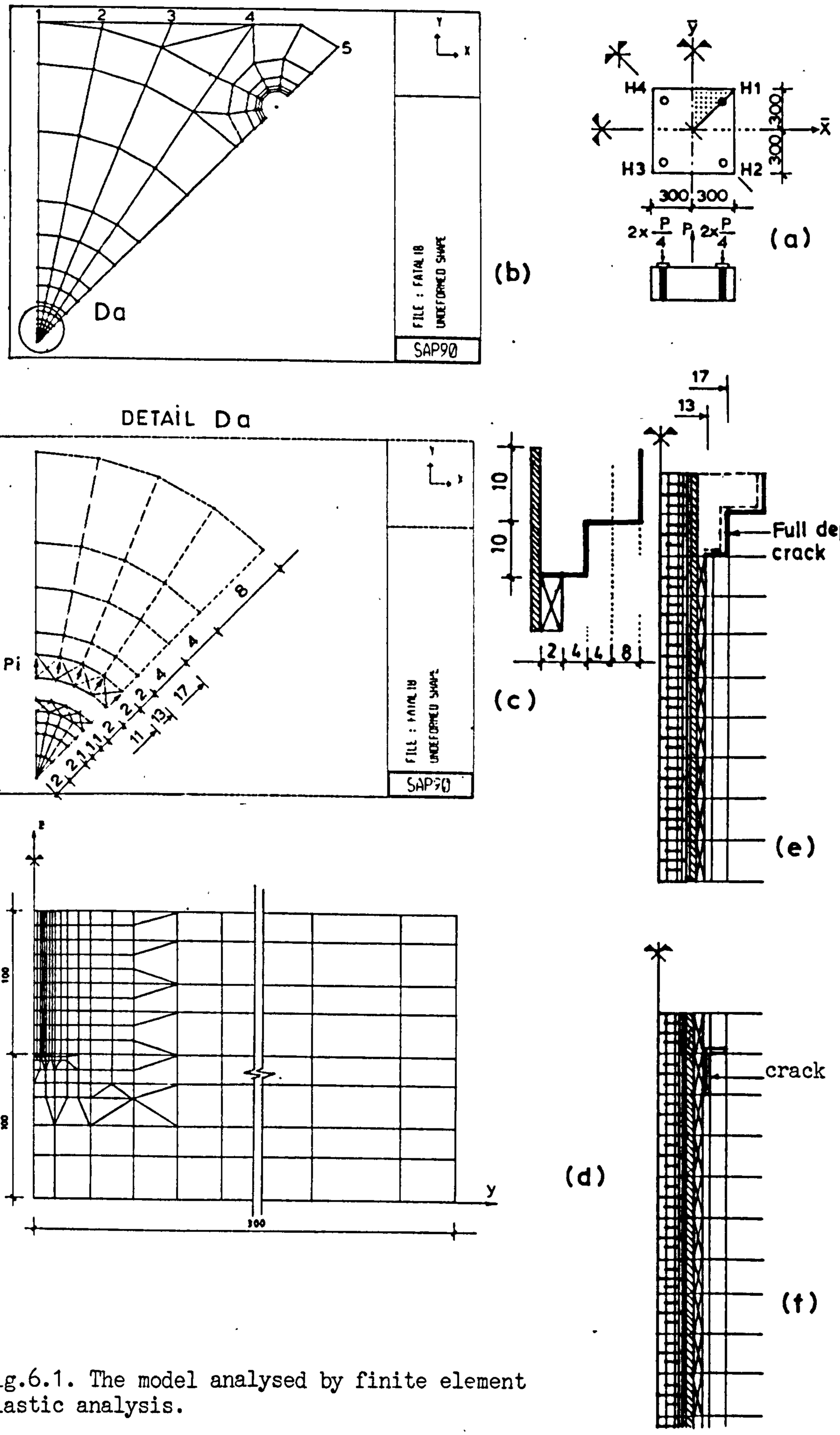

Fig.6.1. The model analysed by finite element elastic analysis.

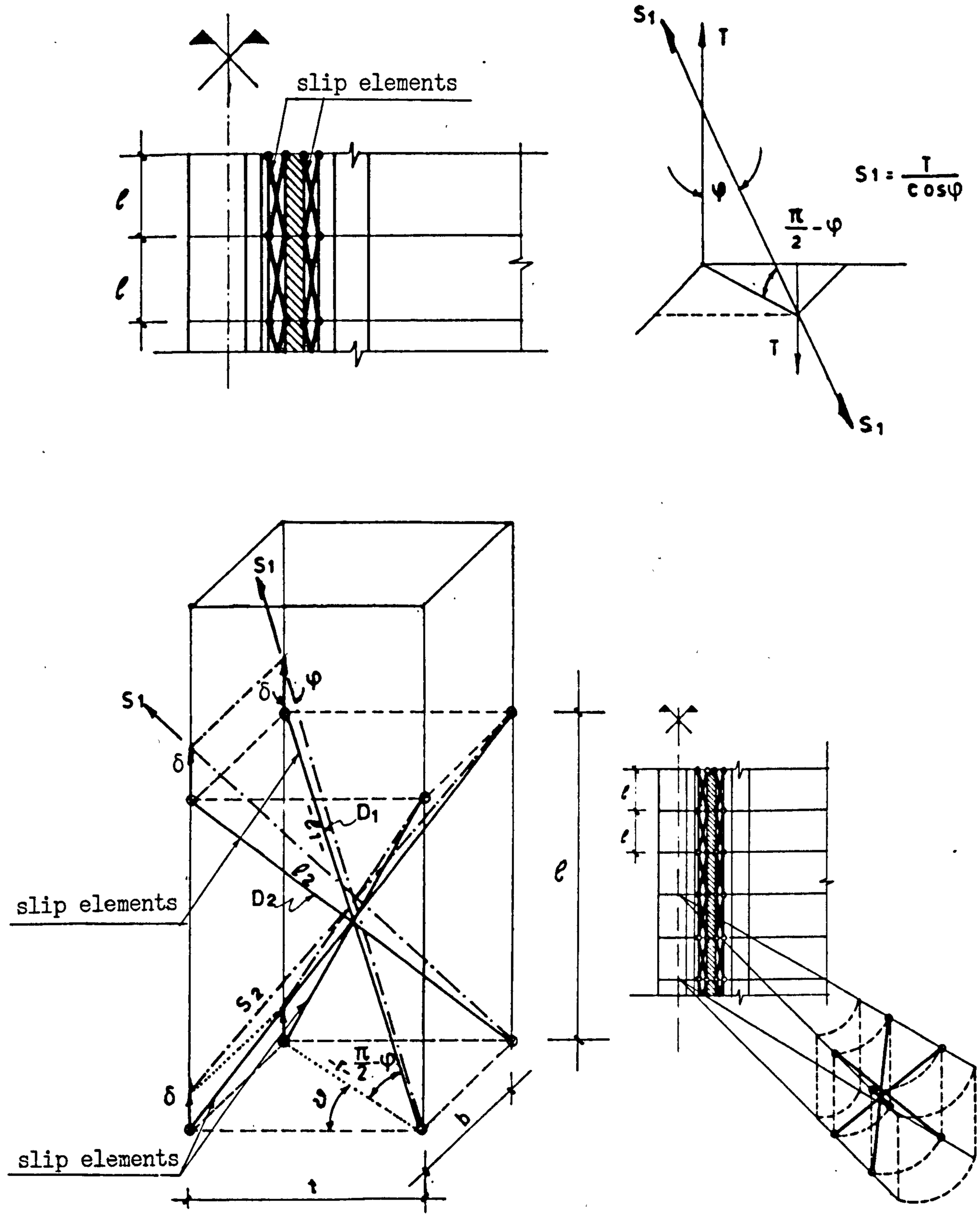

Fig.6.2. The slip elements used in the finite element elastic analysis.

(6.3.a) Finite element models analyzed

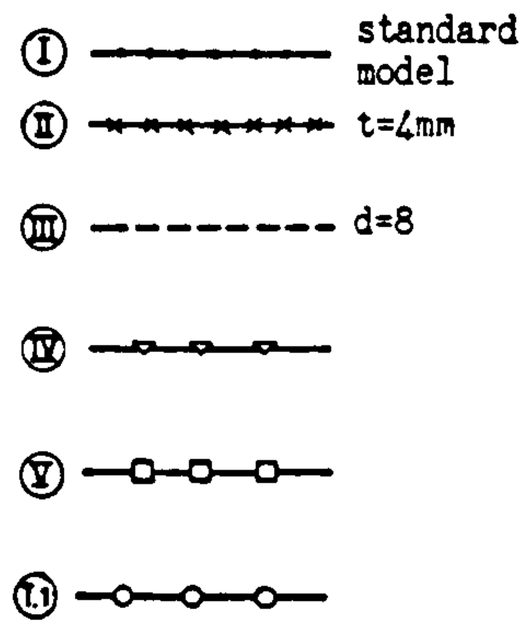

	Variable	d (mm)	t (mm)	l (mm)
I	standard model	12	2	100
II	thickness	12	4	100
III	diameter	8	2	100
IV	fully developed crack	12	2	100
V	stabilized crack	12	2	100
VI	standard model with stiffness of the tensile slip elements equal to that of shear slip elements $a_t = a$			

(6.3.b)
Steel strain ε_s ($\mu\varepsilon$) at P=10kN

z	FE mod I	FE mod II	FE mod III
5	791	792	1243
15	629	634	1044
25	607	617	981
35	483	497	806
45	436	454	730
55	336	356	574
65	276	298	487
75	187	207	337
85	121	138	234
95	36	40	67

(6.3 c)
Steel strain ε_s ($\mu\varepsilon$) distribution at P=10kN

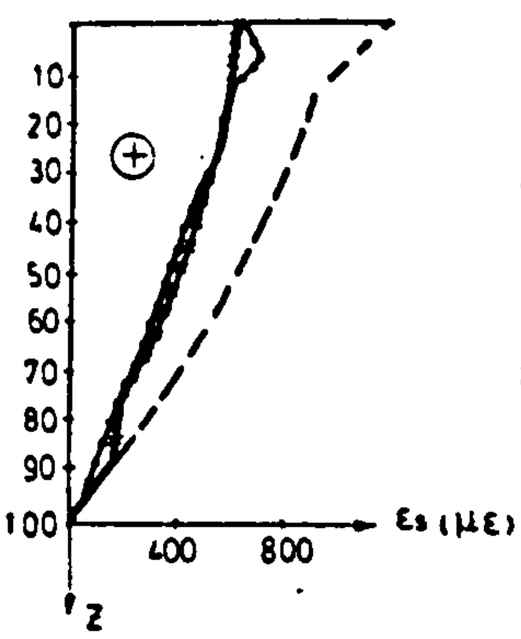

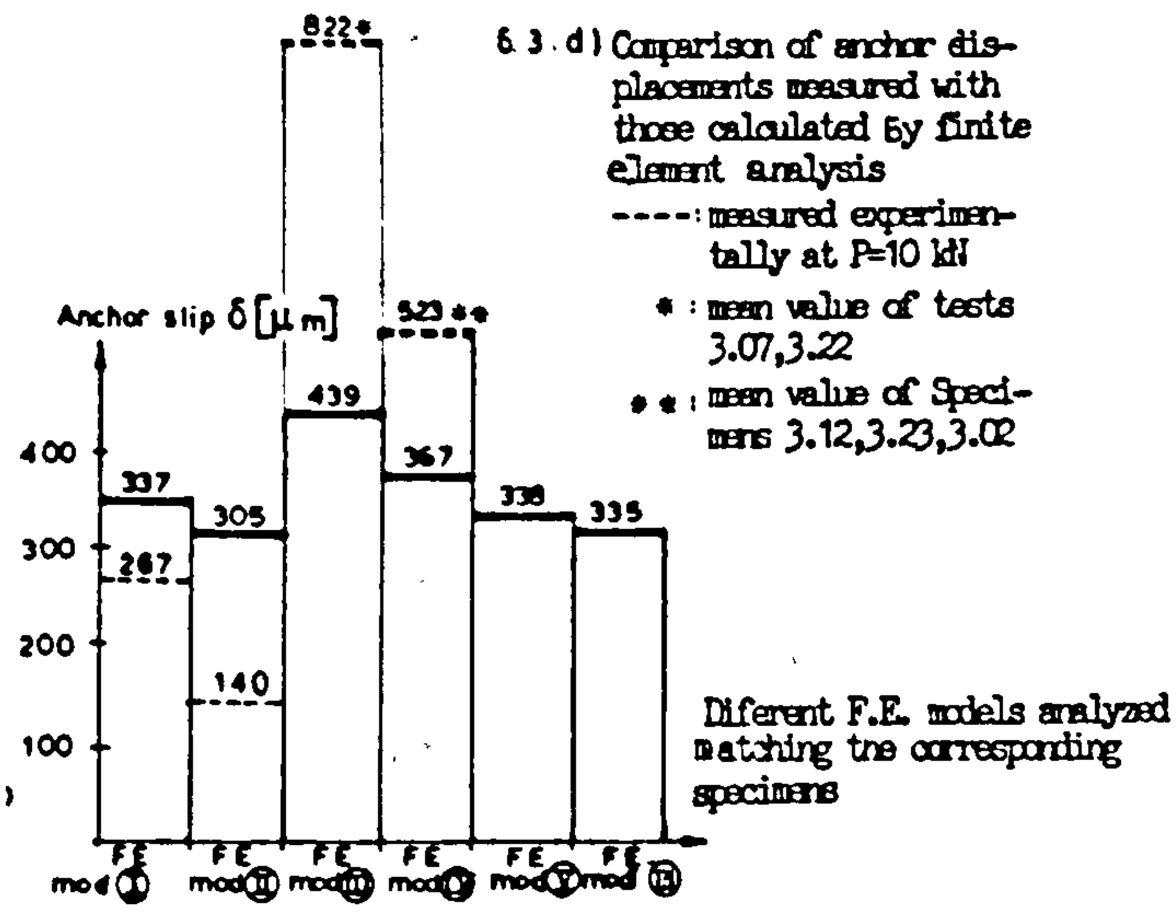

(6.3.d) Comparison of anchor displacements measured with those calculated by finite element analysis

----: measured experimentally at P=10 kN

*: mean value of tests 3.07, 3.22

**: mean value of Specimens 3.12, 3.23, 3.02

Diferent F.E. models analyzed matching the corresponding specimens

(6.3.f)
Resin strain ε_r ($\mu\varepsilon$) distribution

(6.3 e)
Resin strain ε_r ($\mu\varepsilon$) at P=10kN

z	FE mod. I	FE mod II	FE mod III	FE mod. VI
5	70	70	33	70
15	130	116	11	130
25	195	63	132	196
35	189	122	49	190
45	152	137	140	154
55	153	192	96	160
65	108	278	254	120
75	129	387	352	157
85	126	395	828	186
95	134	857	1567	246

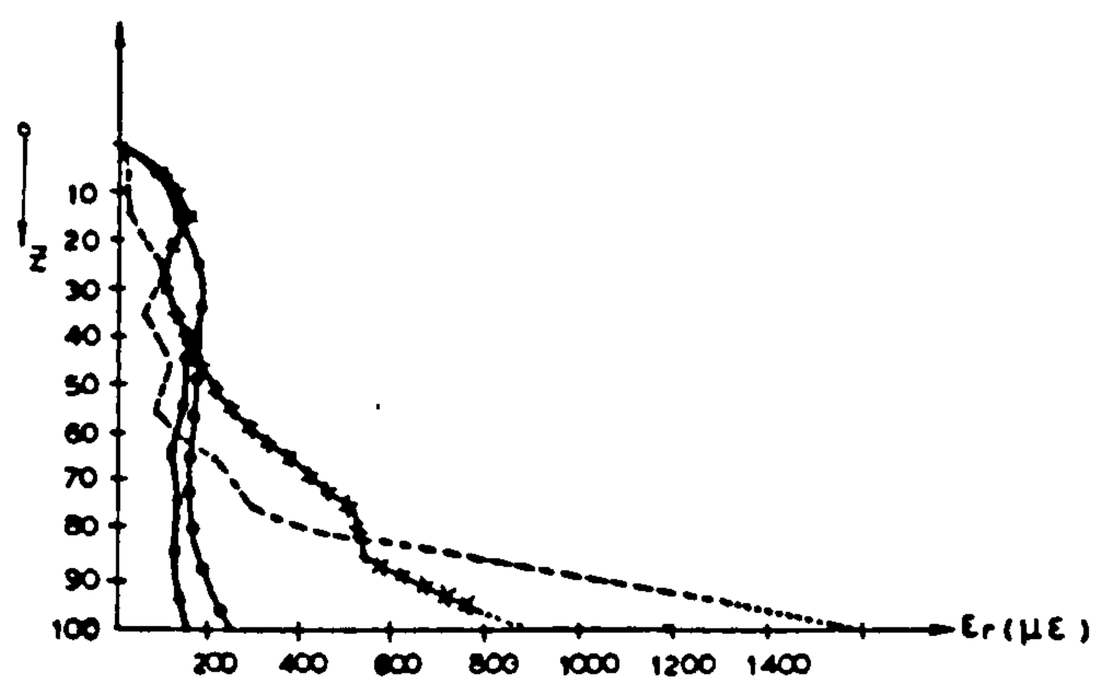

Fig.6.3. Results of finite elements elastic analysis (steel and resin strain distribution) due to an axial pull-out load P=10 kN

—•—•— : Model I/ Standard
—x—x— : Model II/ t=4mm
– – – – : Model III/d=8mm

Section y = 18mm

(6.4a)

Concrete-resin interfacial shear stress $\tau_{c,r}$(N/mm^2) at P: 10 kN

z	FE mod (I)	FE mod (II)	FE mod (III)
5	1.56	0.95	1.96
15	1.87	1.33	2.39
25	1.87	1.30	2.28
35	1.84	1.29	2.31
45	1.83	1.24	2.33
55	1.78	1.19	2.23
65	1.80	1.12	1.87
75	1.70	1.03	2.06
85	1.79	0.87	1.04
95	1.35	0.77	1.18

(6.4b)

Distribution of concrete-resin interfacial shear stress $\tau_{c,r}$(N/mm^2)

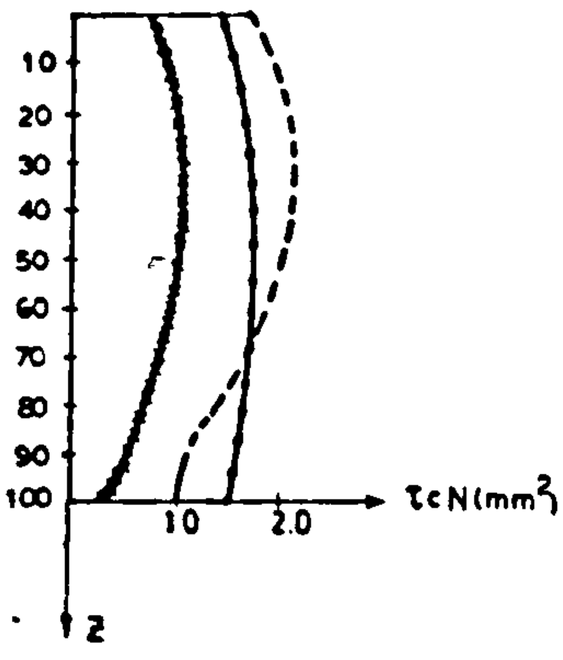

(6.4c)

Distribution of concrete radial strain ε_{yy}(με) at P=10 kN

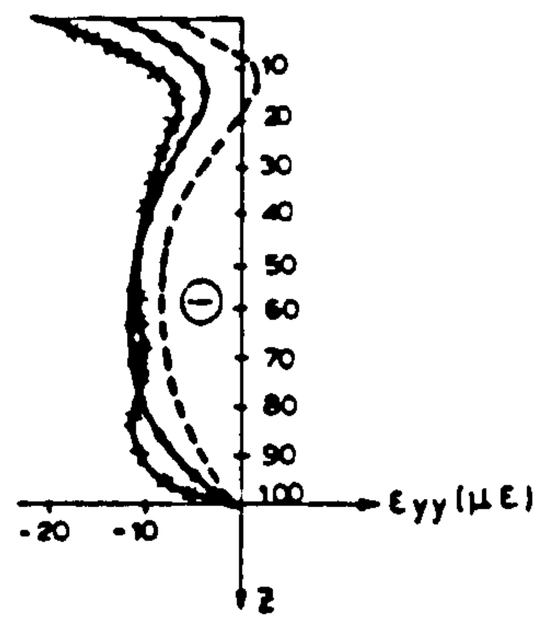

(6.4d)

Concrete radial strains ε_{yy}(με) at P=10 kN

z	FE mod (I)	FE mod (II)	FE mod (III)
5	-15	-18	-7
15	-4	-6	1
25	-8	-9	-3
35	-10	-10	-6
45	-11	-11	-7
55	-12	-11	-7
65	-12	-11	-7
75	-13	-11	-7
85	-12	-12	-7
95	-4	-10	-7

Section y=18 mm

(6.4.e)

Concrete vertical strain ε_{zz}(με) at P=10 kN

z	FE mod (I)	FE mod (II)	FE mod (III)
5	2	3	2
15	7	8	7
25	9	9	9
35	9	8	9
45	9	8	9
55	9	9	10
65	10	9	10
75	13	10	11
85	18	8	11
95	22	8	11

(6.4.f)

Distribution of Concrete vertical strain ε_{zz}(με) at P=10 kN

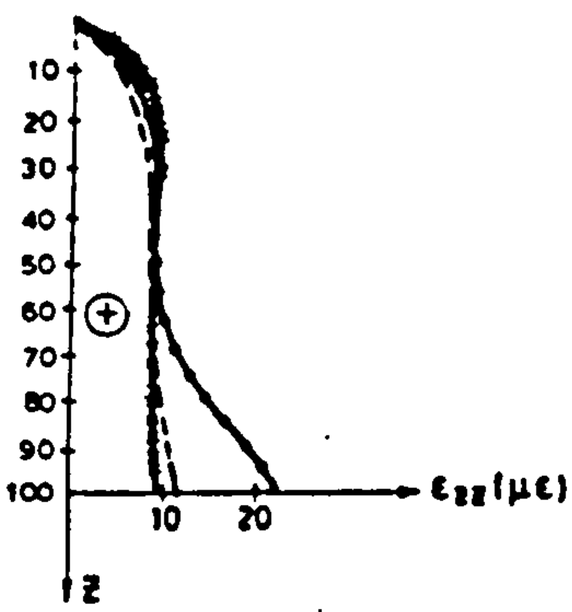

(6.4.g)

Distribution of concrete tangential strain ε_{xx}(με) at P=10 kN

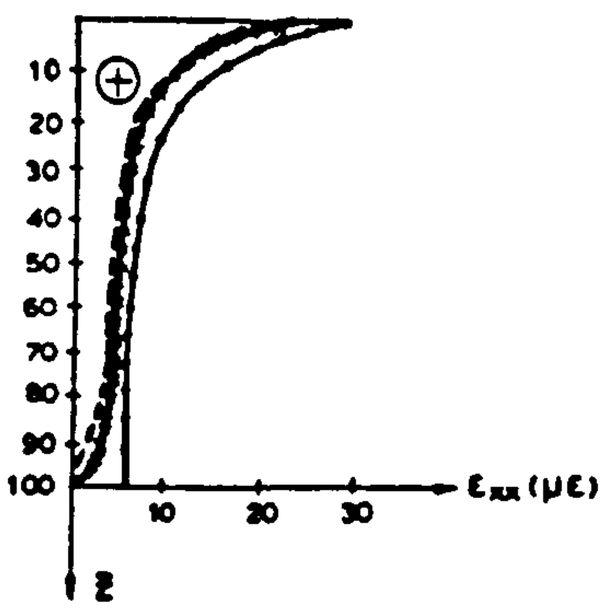

(6.4.h)

Concrete tangential strain ε_{xx}(με) at P=10 kN

z	FE mod (I)	FE mod (II)	FE mod (III)
5	22	20	19
15	9	8	7
25	7	6	6
35	6	5	5
45	6	5	5
55	6	5	4
65	5	4	4
75	5	4	4
85	5	4	4
95	4	2	3

Fig.6.4. Results of finite elements elastic analysis (interfacial shear stress and concrete strains distribution) due to an axial pull-out load P=10 kN

(6.5.a) Finite element models analyzed

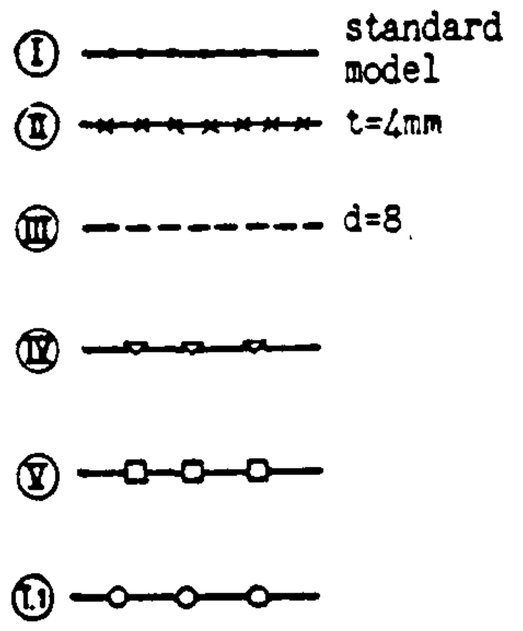

	Variable	d (mm)	t (mm)	l (mm)
I	standard model	12	2	100
II	thickness	12	4	100
III	diameter	8	2	100
IV	fully developed crack	12	2	100
V	stabilized crack	12	2	100
VI	standard model with stiffness of the tensile slip elements to that of shear slip elements at a			

(6.5.b)
Steel strain $\varepsilon_s(\mu\varepsilon)$ at P= 10 kN

z	FE mod I	FE mod IV	FE mod V
5	791	799	740
15	629	652	628
25	607	641	608
35	483	520	484
45	436	472	436
55	336	367	336
65	276	300	275
75	187	205	187
85	121	131	121
95	36	40	36

(6.5.c)
Steel strain $\varepsilon_s(\mu\varepsilon)$ distribution at P=10kN

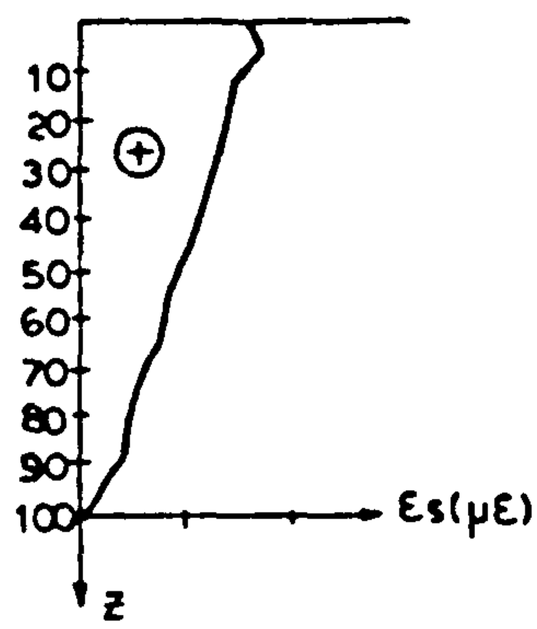

(6.5.d)
Resin strain $\varepsilon_r(\mu\varepsilon)$ at P=10 kN

z	mod I	mod IV	mod V
5	70	1661	77
15	130	1856	134
25	195	2580	205
35	184	1378	201
45	152	687	161
55	153	429	158
65	108	227	110
75	129	196	130
85	126	159	126
95	134	153	134

(6.5.e)
Resin strain $\varepsilon_r(\mu\varepsilon)$ distribution ε_r at P=10 kN.

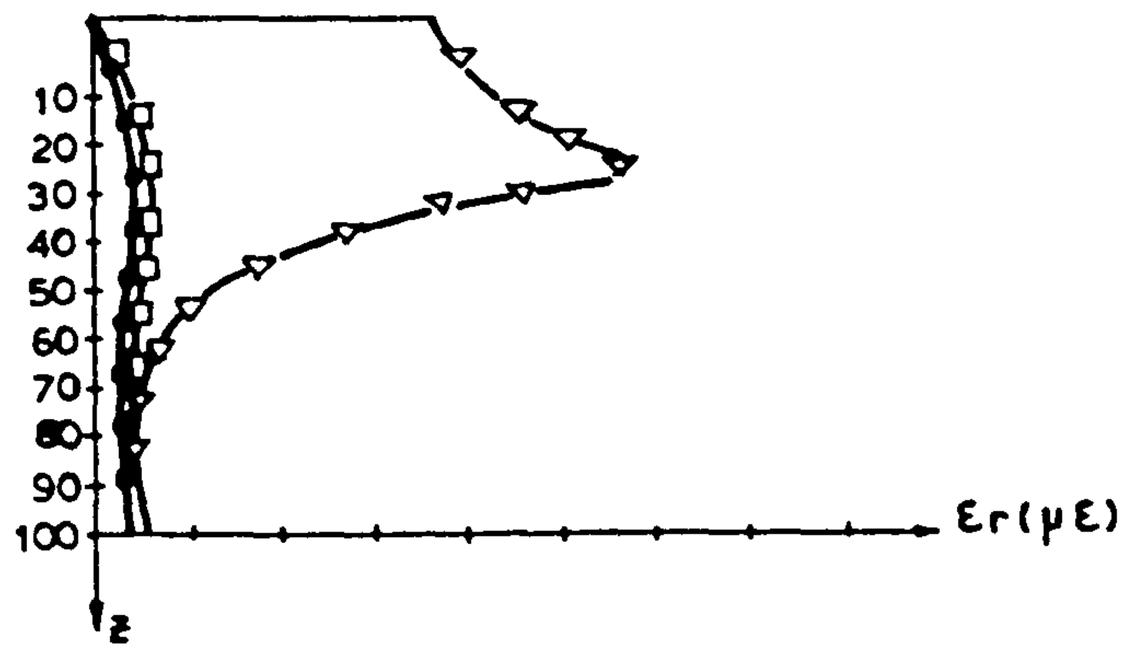

Fig.6.5. Results of finite elements elastic analysis (steel and resin strain distribution) due to an axial pull-ut load P=10 kN

(6.6.a)

Concrete-resin interfacial shear stress τ_{cr} (N/mm²) at P = 10 kN

z	FE mod I	FE mod IV	FE mod V
5	156		194
15	187	–	233
25	187	396	189
35	184	1.88	201
45	183	236	168
55	178	190	187
65	180	207	167
75	170	184	181
85	179	1.99	134
95	135	146	179

(6.6.b) Distribution of Concrete-resin interfacial shear stress $\tau_{c,r}$ (N/mm²) at P = 10 kN

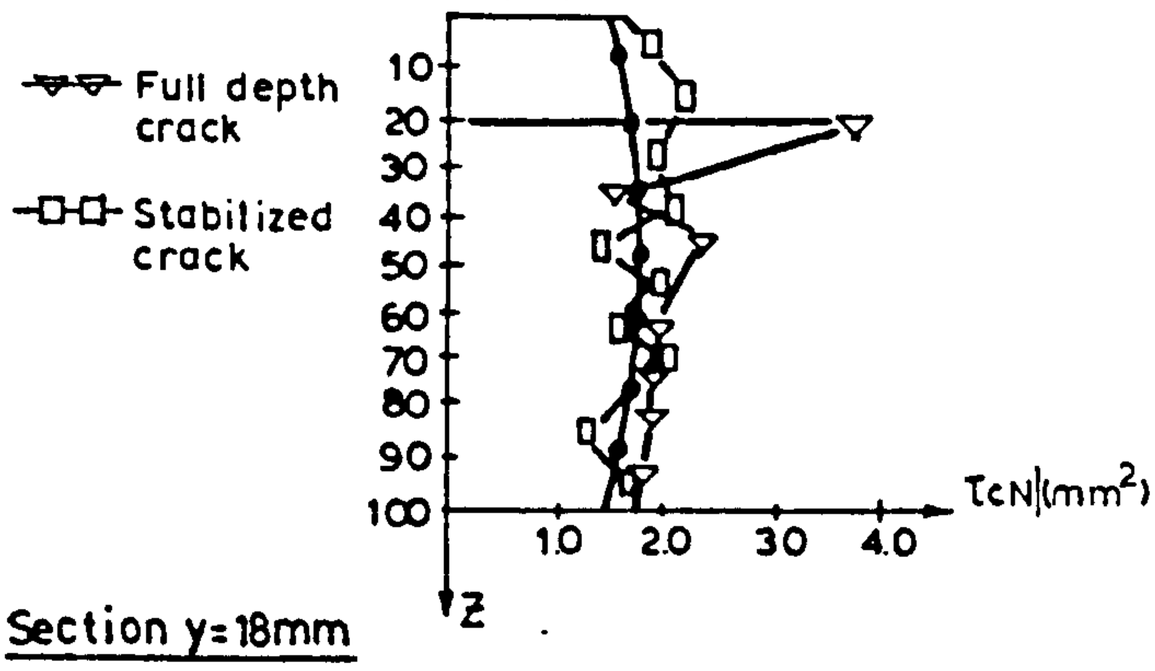

Section y = 18mm

(6.6.c)

Concrete radial strains ε_{yy} (με) at P = 10 kN

z	FE mod I	FE mod IV	FE mod V
5	-15	–	-20
15	-4	-17	-5
25	-8	-24	-14
35	-10	-3	-16
45	-11	-15	-8
55	12	-16	14
65	-12	-17	-14
75	-13	-18	-15
85	-12	-19	-14
95	-4	-17	-5

(6.6.d) Distribution of Concrete radial strain ε_{yy} (με) at P = 10 kN

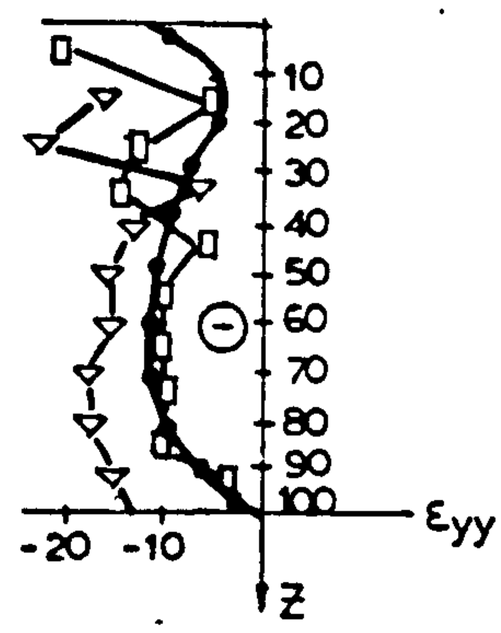

(6.6.e)

Concrete vertical strain ε_{zz} (με) at P = 10 kN

z	FE mod I	FE mod IV	FE mod V
5	2	–	-4
15	7	-30	+13
25	9	-19	+16
35	9	+5	-5
45	9	+11	+11
55	9	+8	+9
65	10	+11	+11
75	13	+12	+13
85	18	+19	+18
95	22	+23	+22

(6.6.f) Distribution of concrete vertical strain ε_{zz} (με) at P = 10 kN

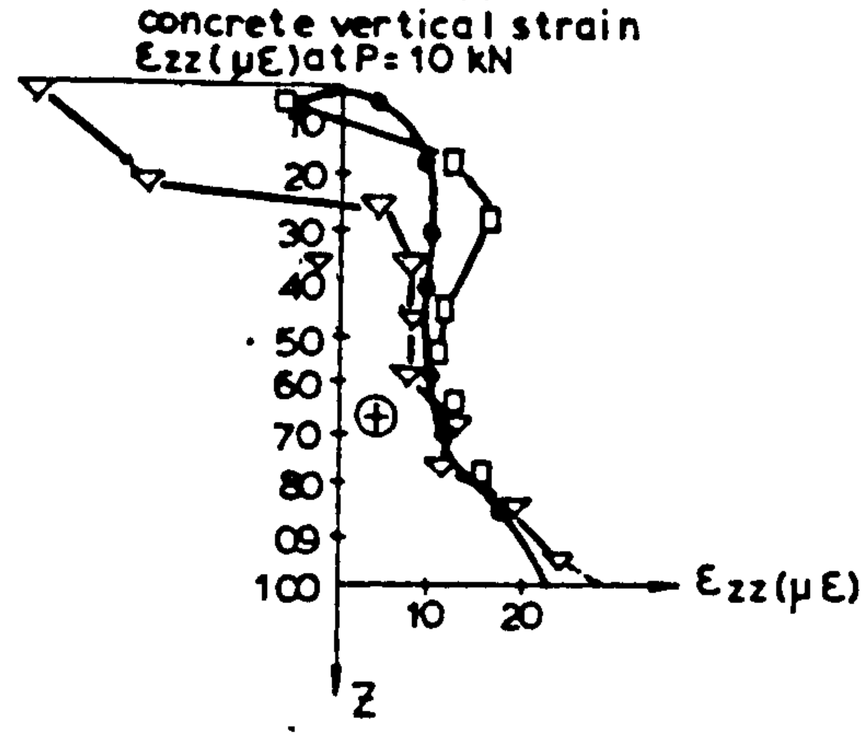

(6.6.g)

Concrete tangential strain ε_{xx} (με) at P = 10 kN

z	FE mod I	FE mod IV	FE mod V
5	22	–	18
15	9	24	9
25	7	4	8
35	6	7	6
45	6	7	7
55	6	8	6
65	5	8	6
75	5	7	6
85	5	7	6
95	4	5	4

(6.6.h) Distribution of concrete tangential strain ε_{xx} (με) at P = 10 kN

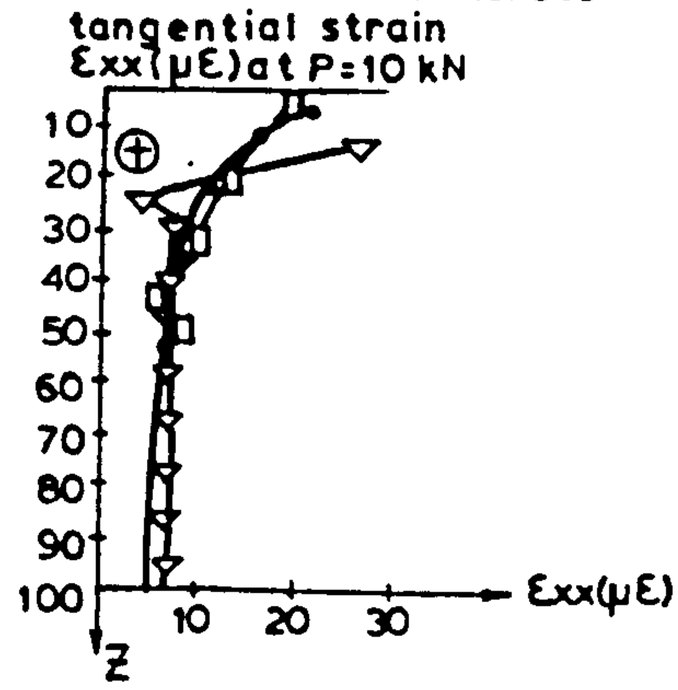

Fig.6.6. Results of finite elements elastic analysis (interfacial shear stress and concrete strains distribution) due to an axial pull-out load P=10 kN

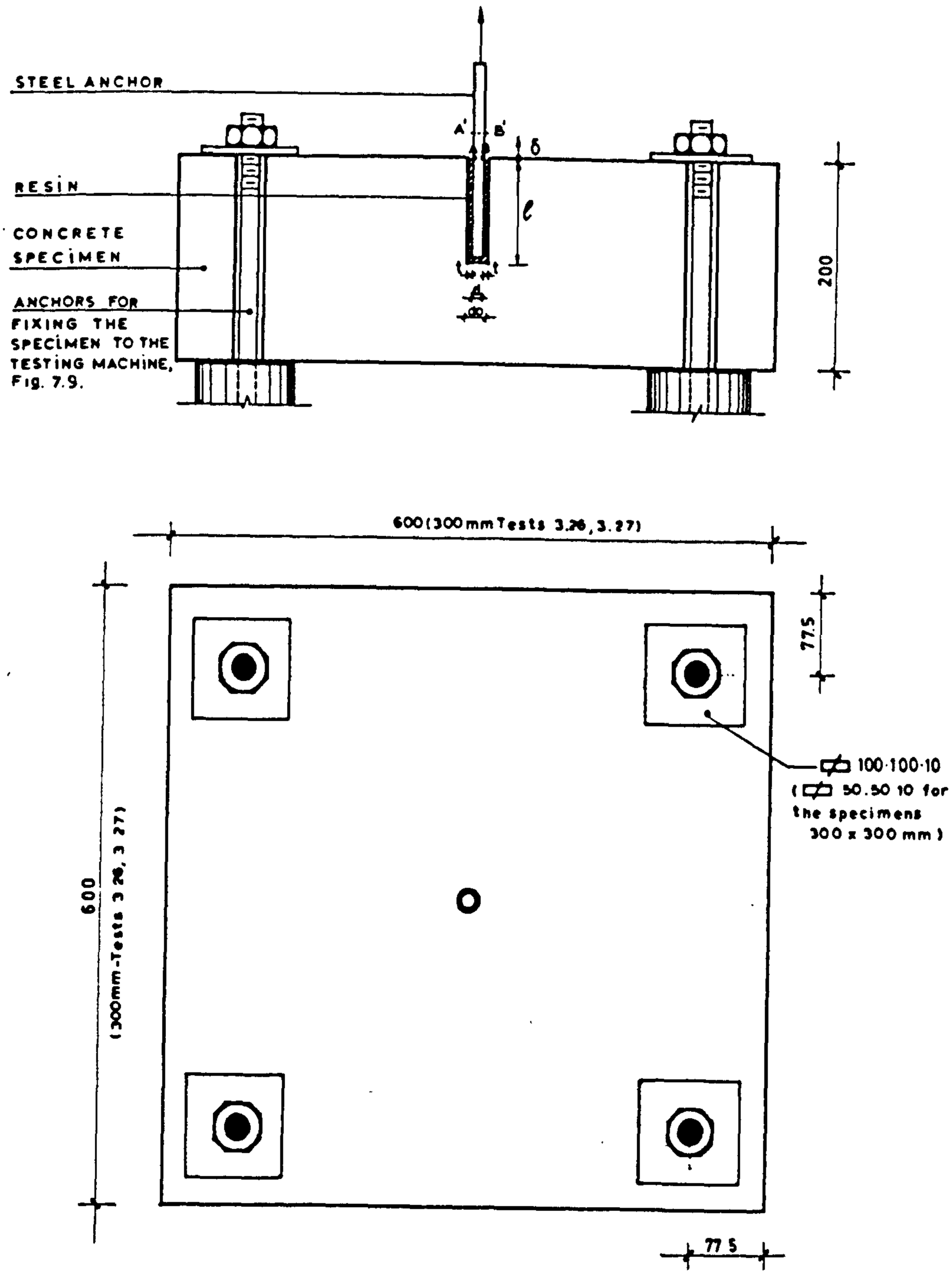

Fig.7.1. Outline sketch of the specimen.

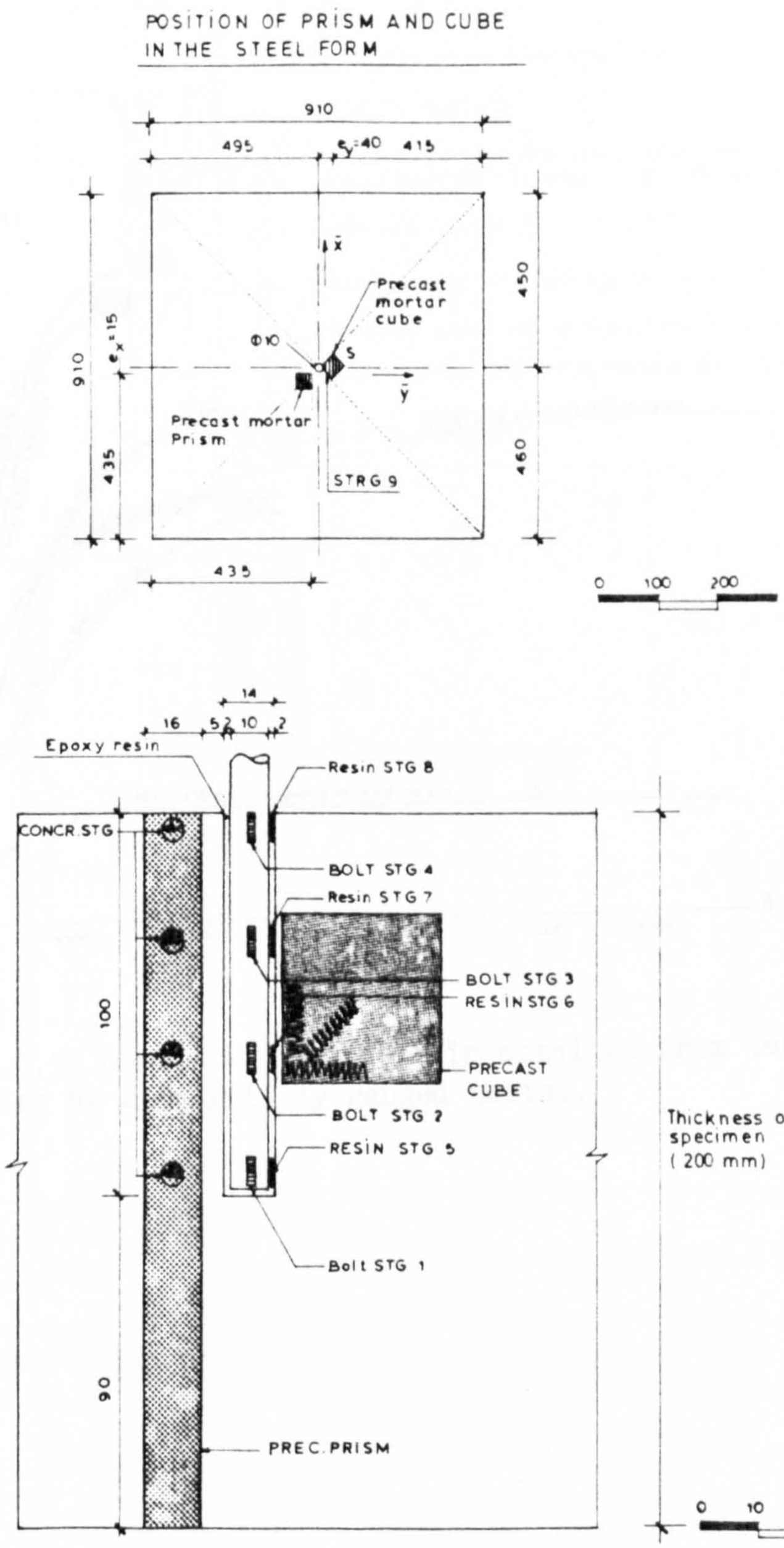

Fig.7.2. Precast mortar cube and prism for carrying the concrete strain gauges.
Test series No 1.

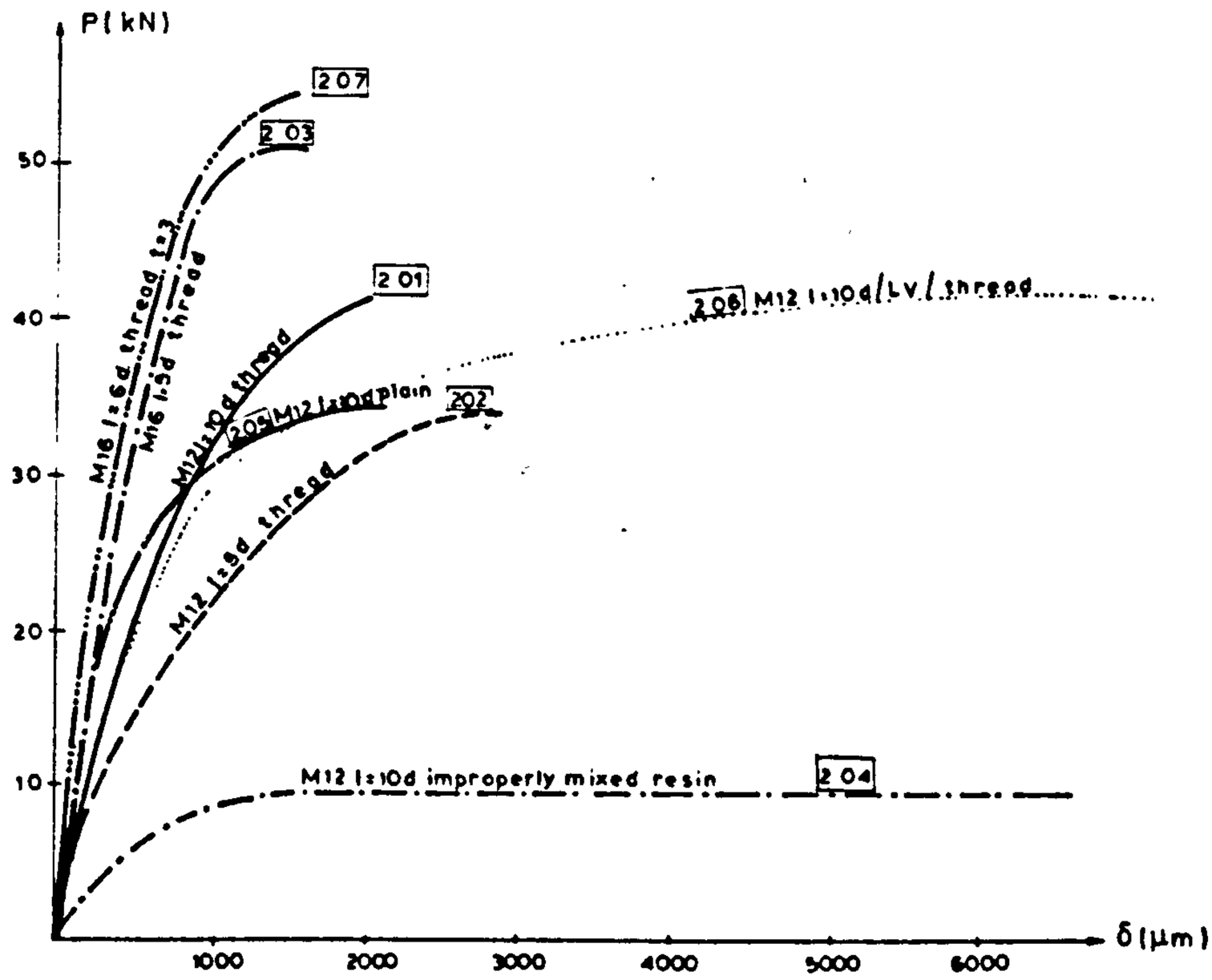

Fig.7.3. Load-slip relationship obtained from test series No 2 (partially gauged tests).

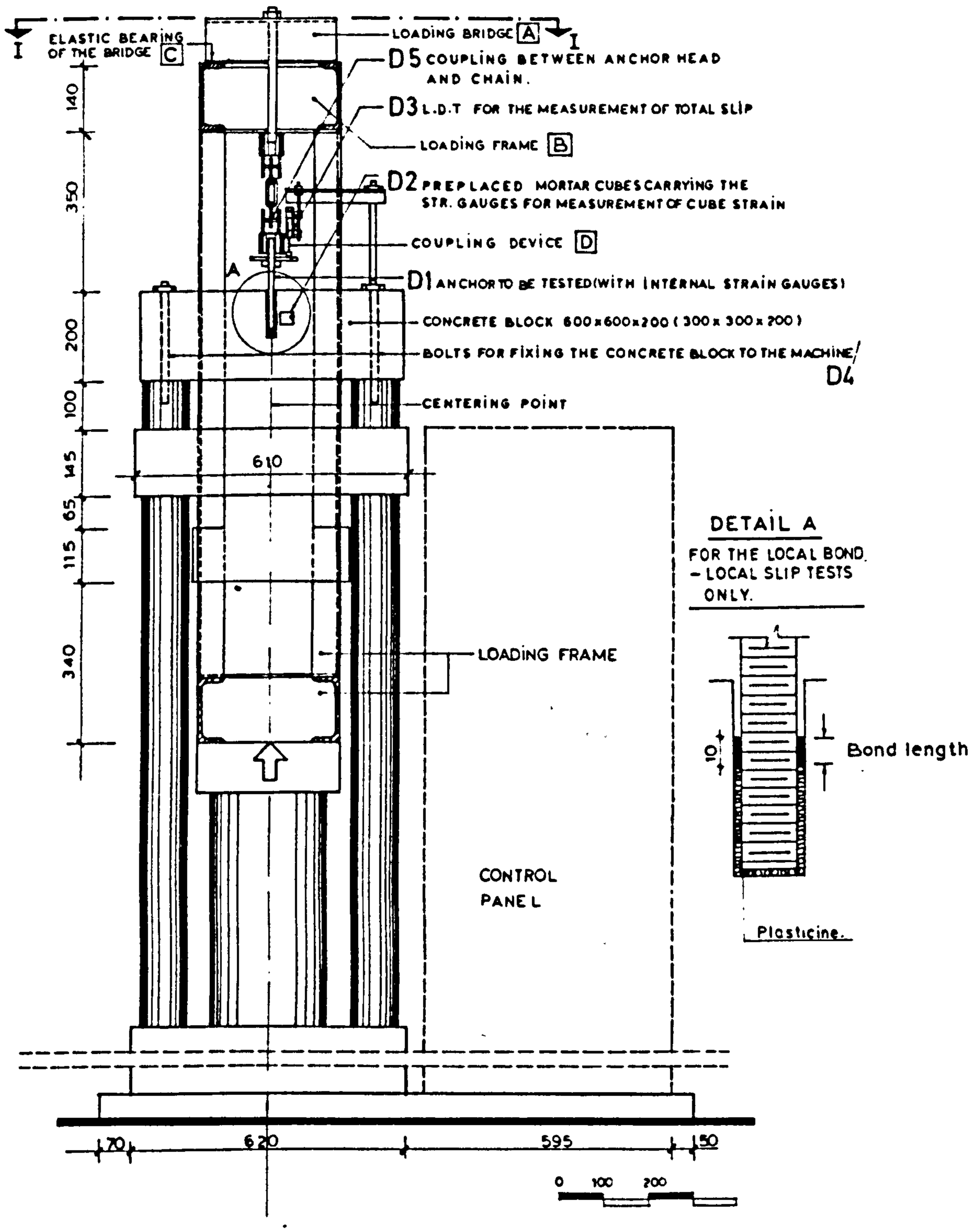

Fig.7.4. Experimental set up.

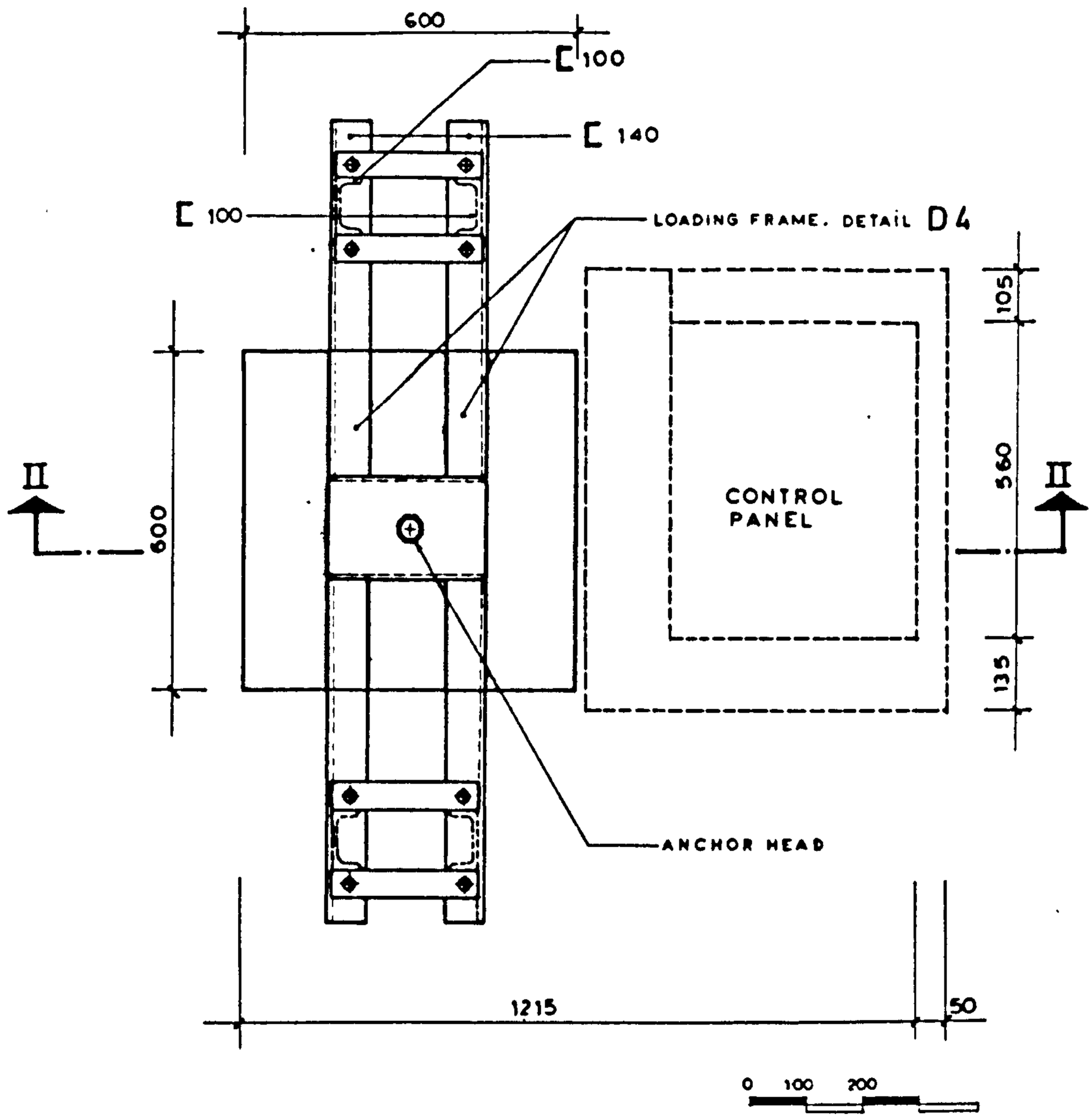

Fig.7.5. Elevation I-I, fig 7.4.

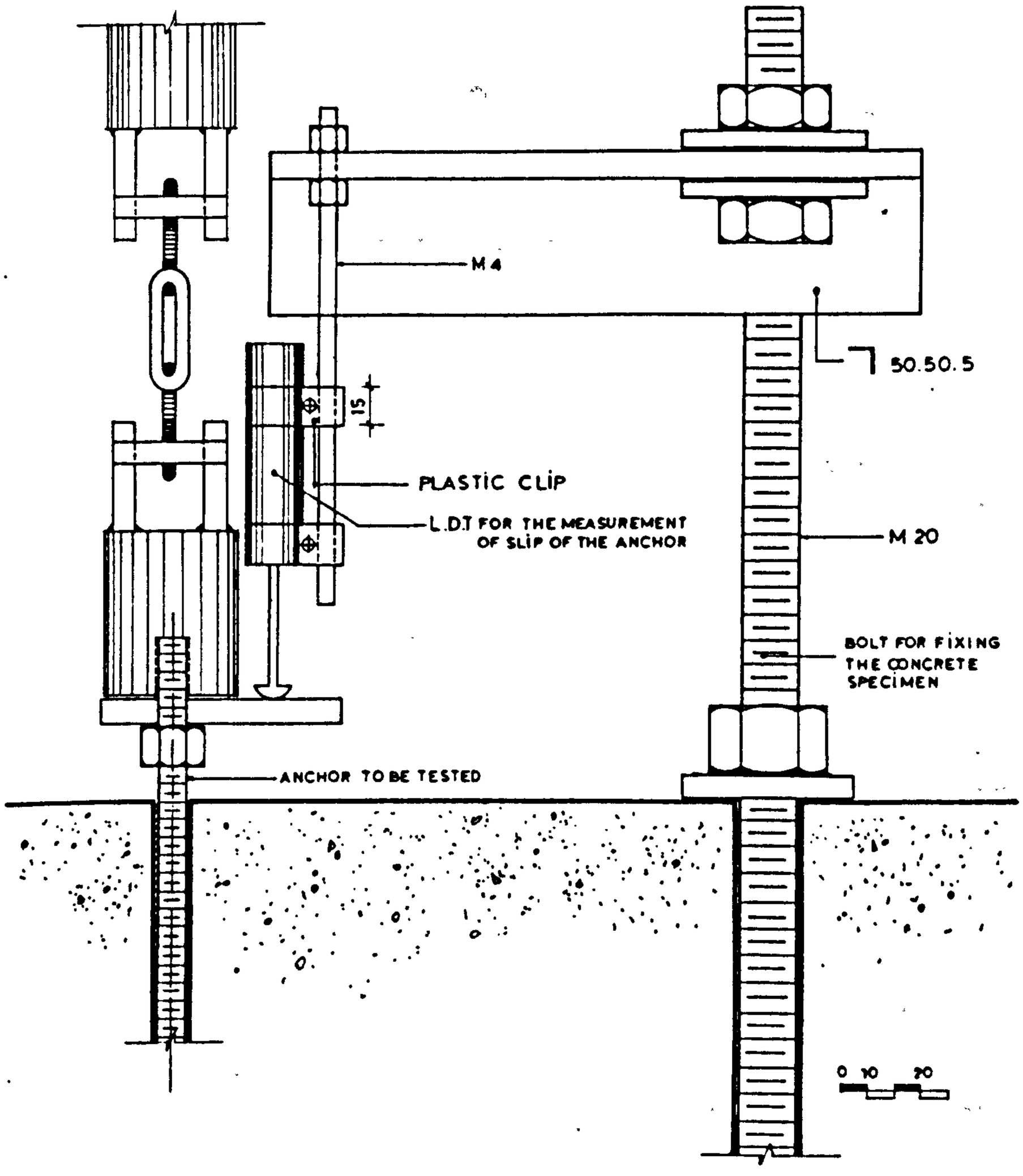

Fig.7.6. Detail D3 of the coupling device and the LDT for the measurement of the total slip.

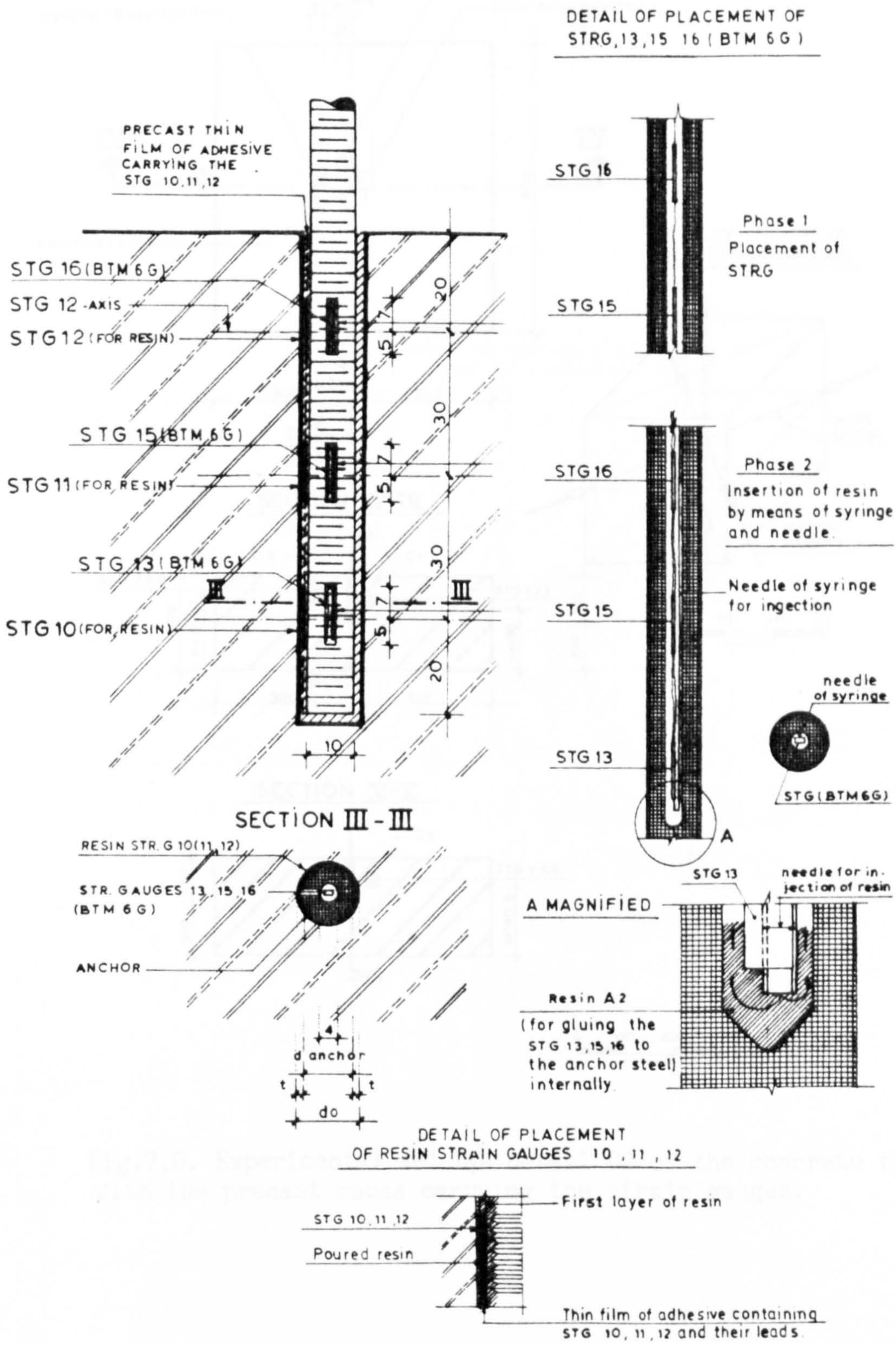

Fig.7.7. Experimental set up. Detail D1 of the steel and resin strain gauges

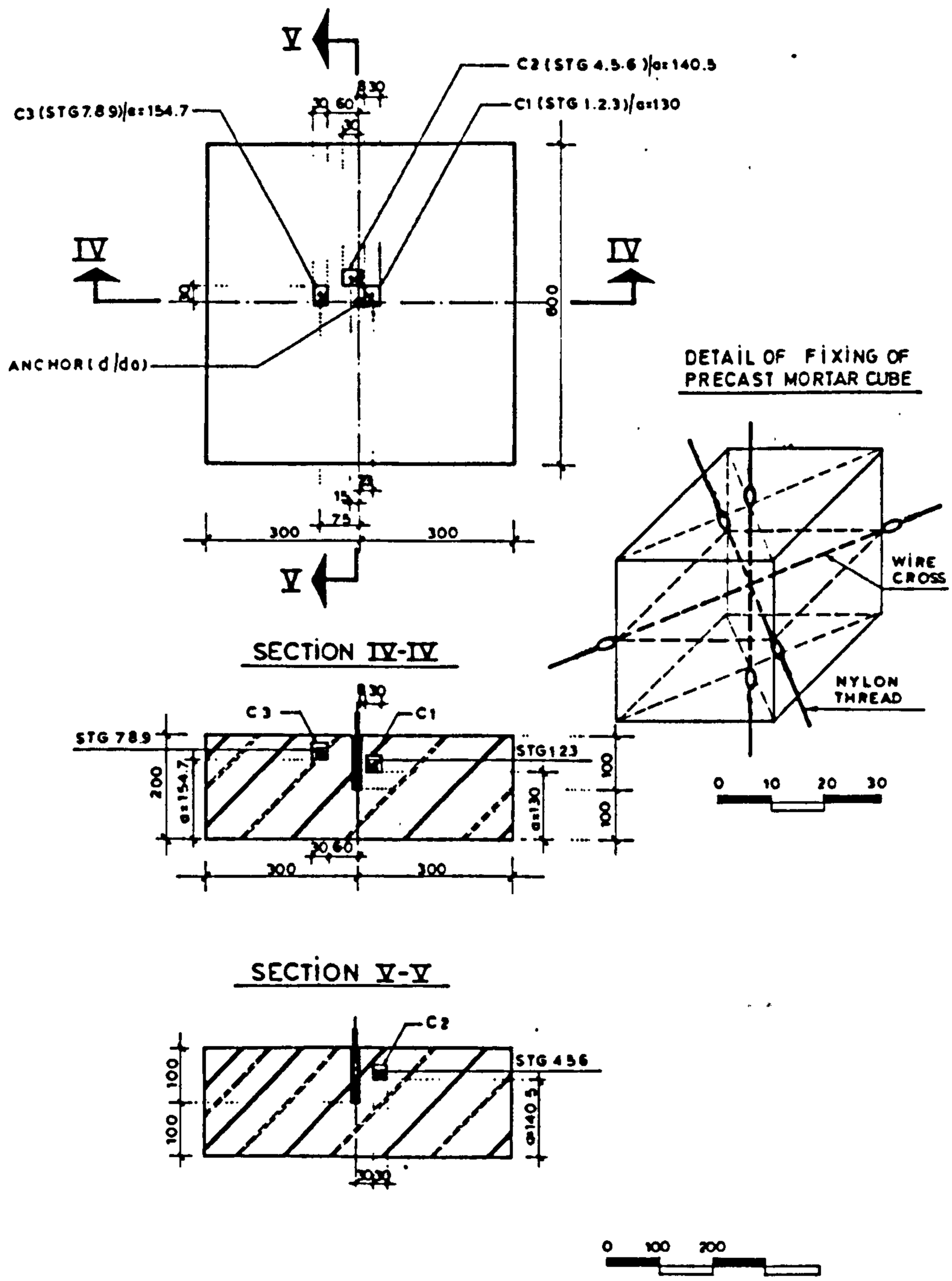

Fig.7.8. Experimental set up. Detail D2 of the concrete block with the precast cubes carrying the strain gauges.

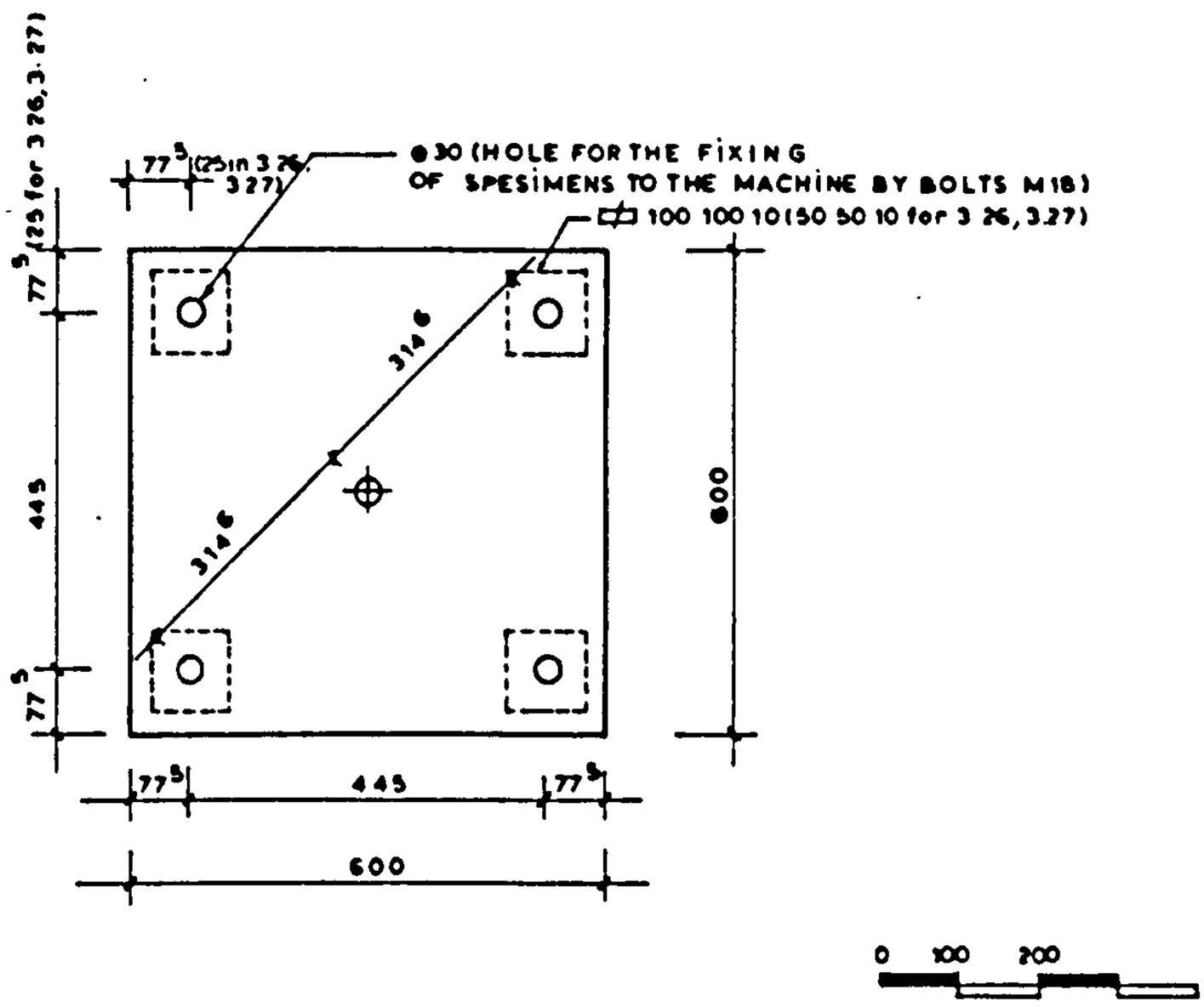

Fig.7.9. Detail D4.Fixing of concrete block to the loading machine.

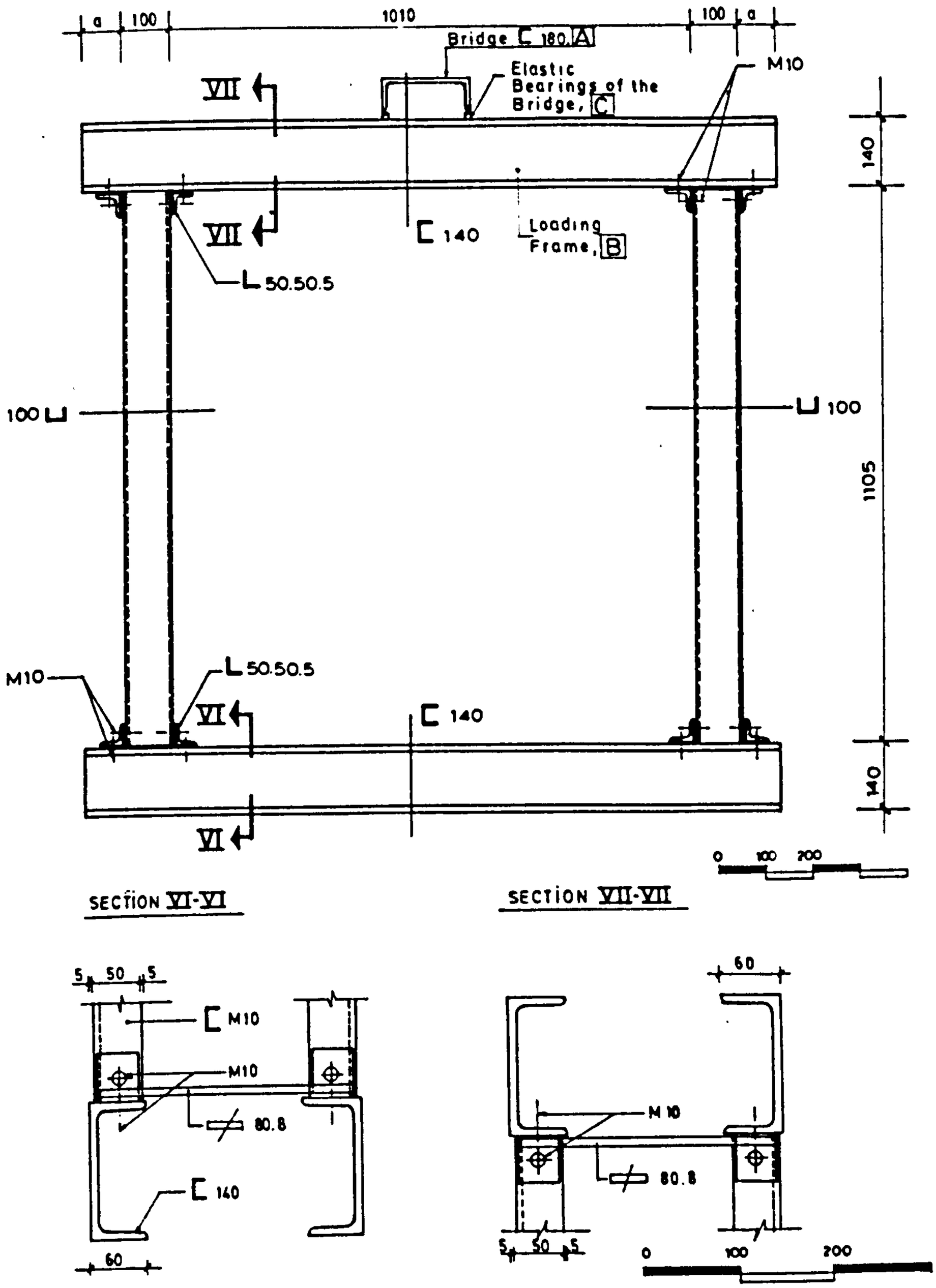

Fig.7.10. Loading frame converting the upward movement of the piston of the machine to tension.

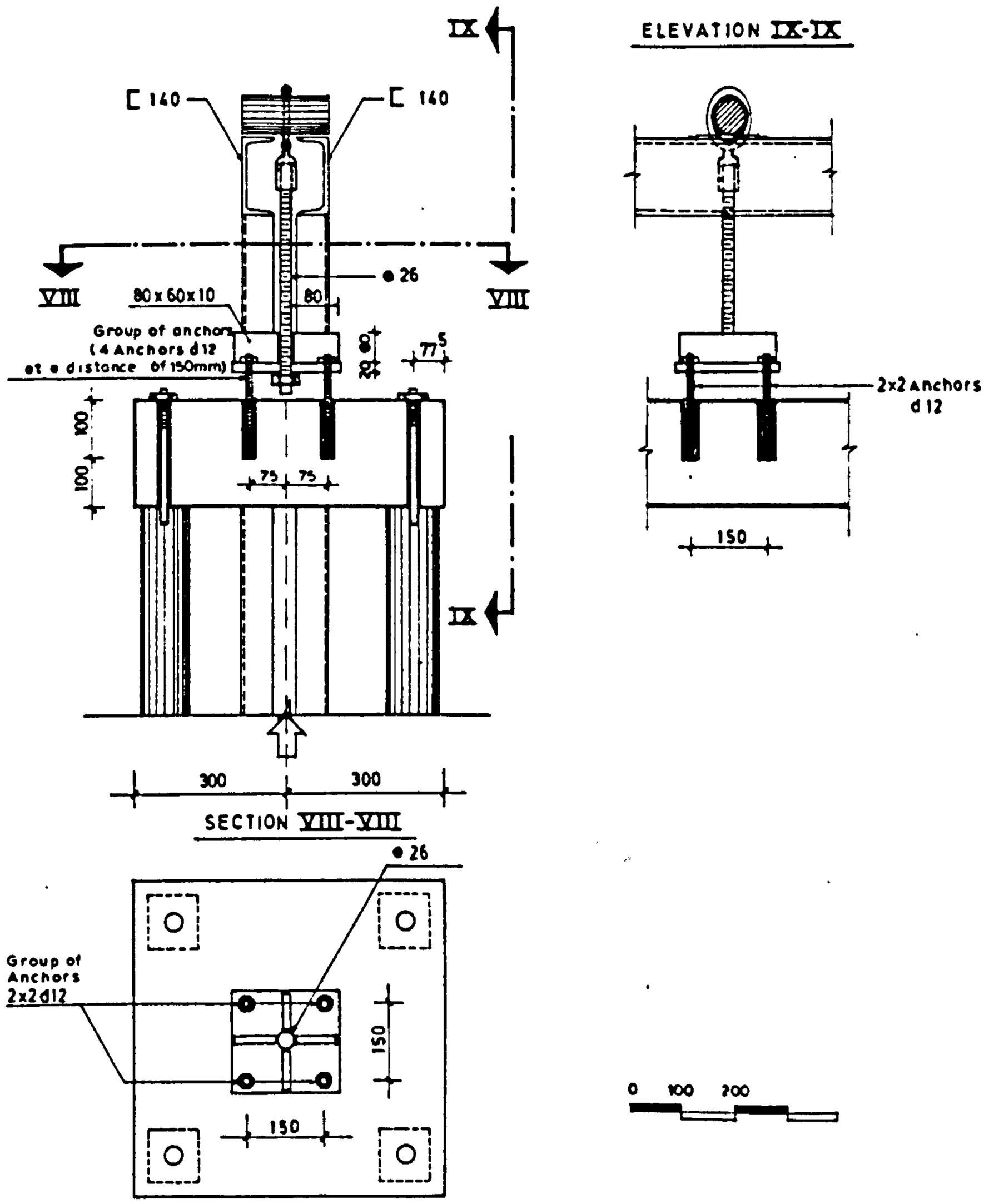

Fig.7.11. Experimental set up for pull-out of group of anchors (specimen 3.30.).

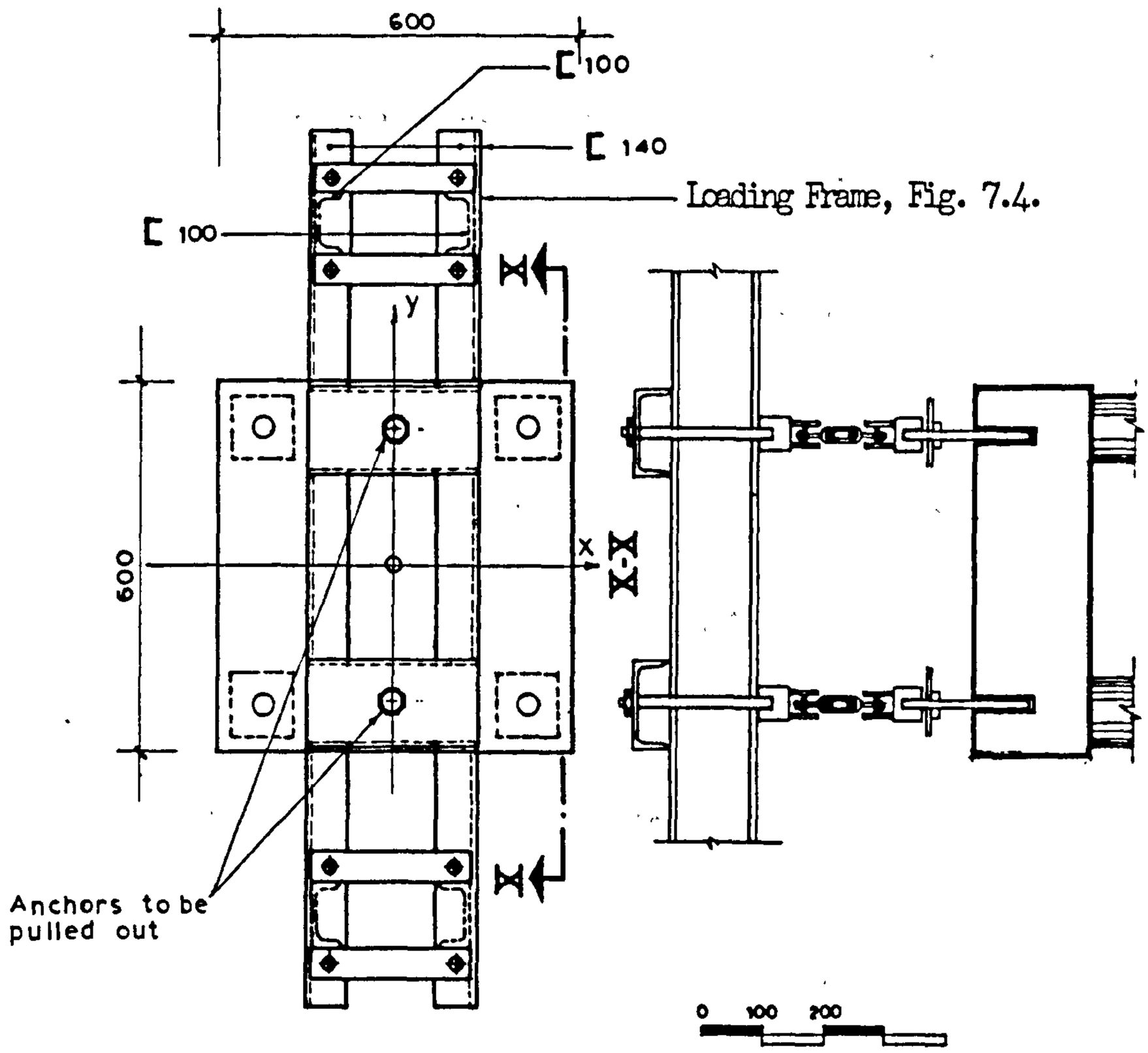

Fig.7.12. Experimental set up for the pull-out of the anchors placed near the edge (specimen 3.31).

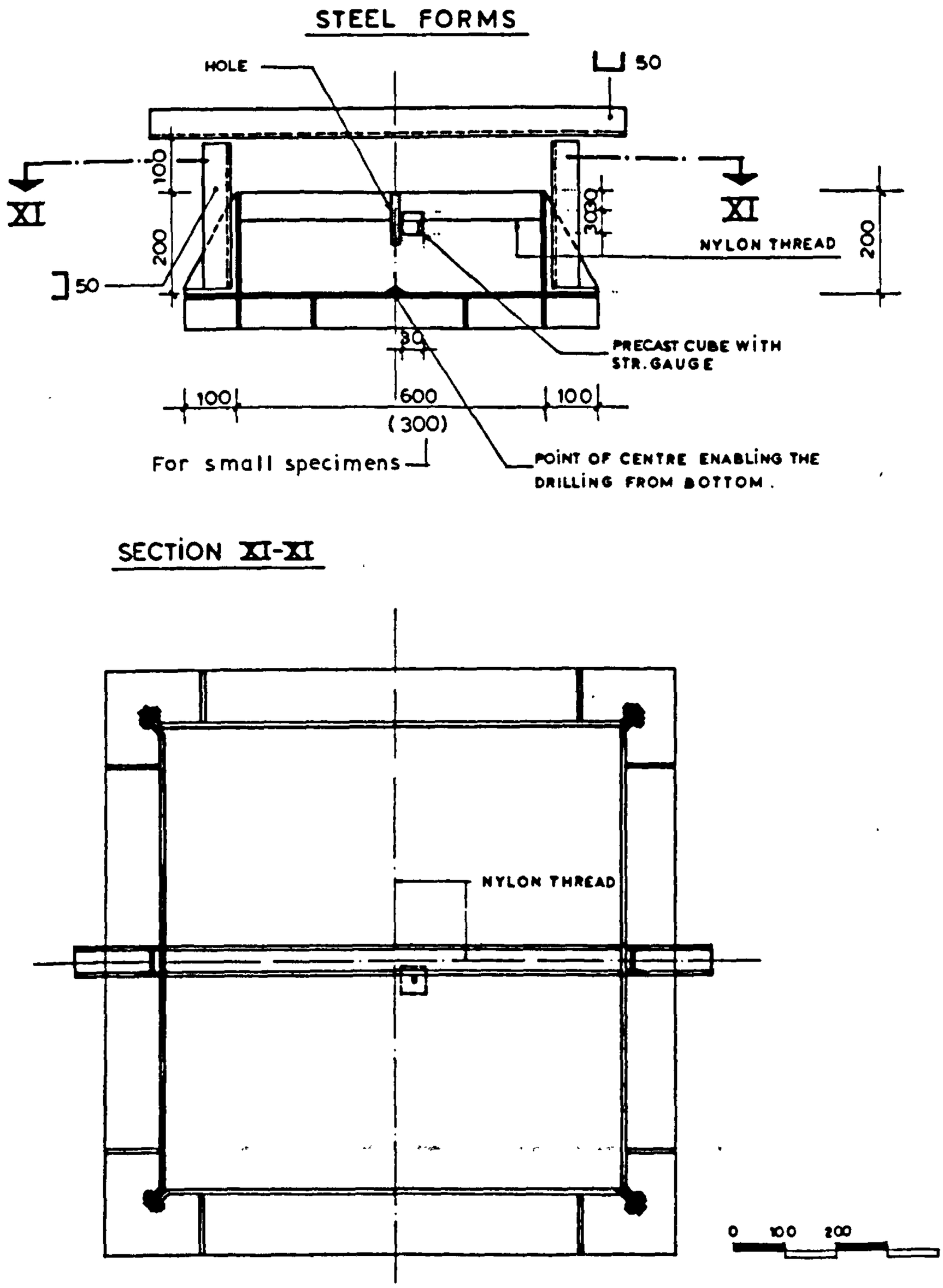

Fig.7.13. Formwork for casting the concrete blocks and fixing the precast mortar cubes.

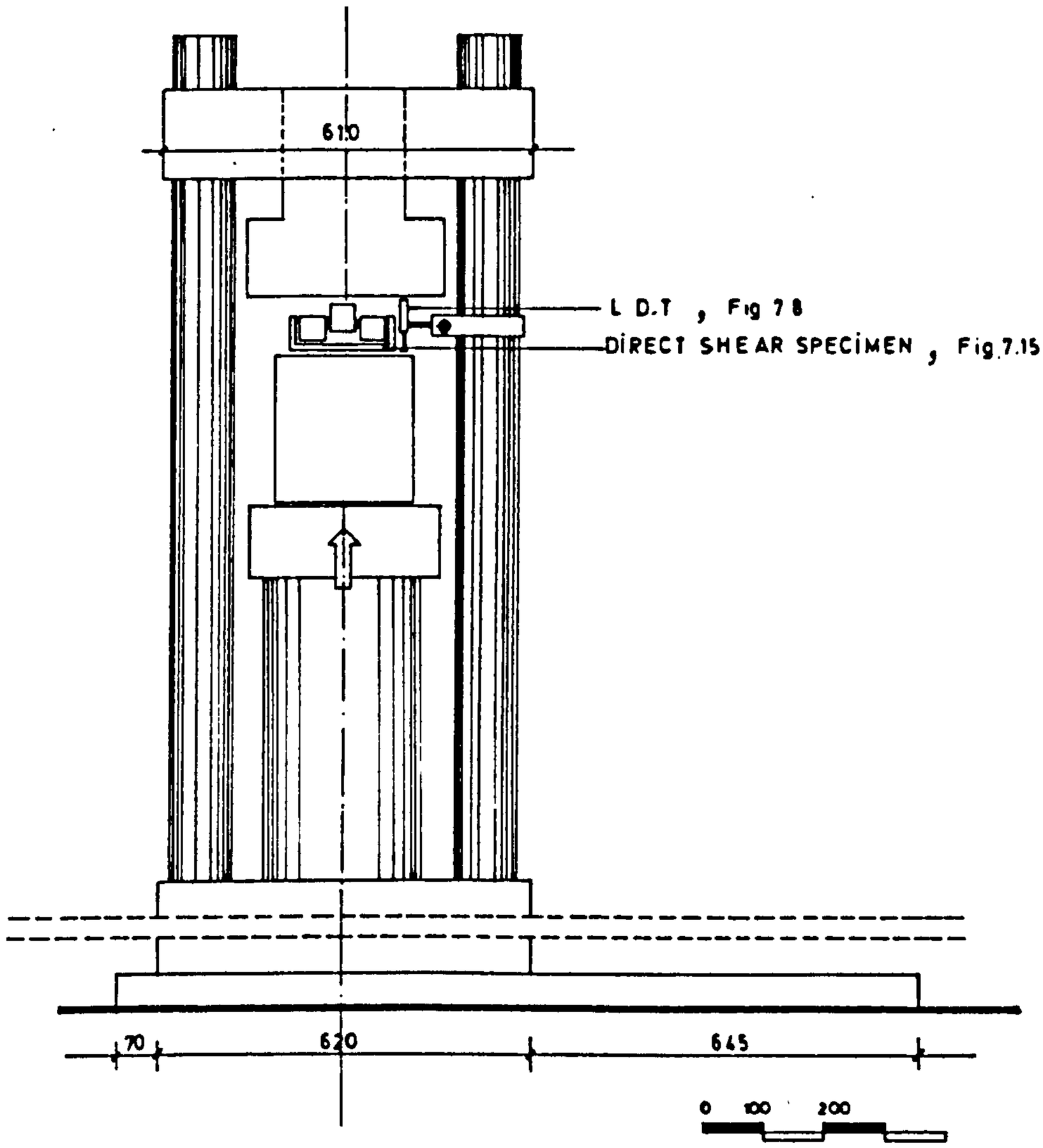

Fig.7.14. Direct shear tests.

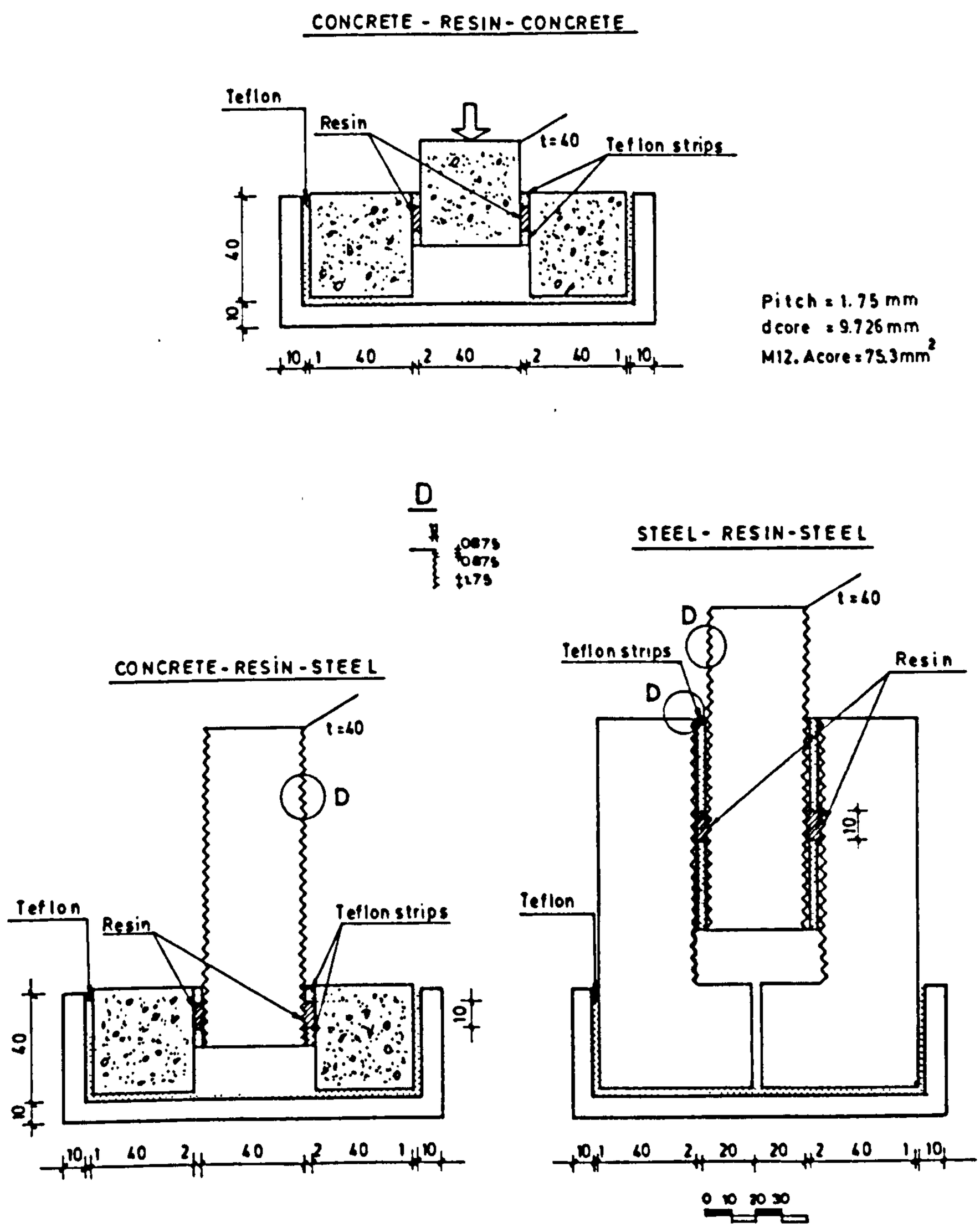

Fig.7.15. Direct shear specimens used.

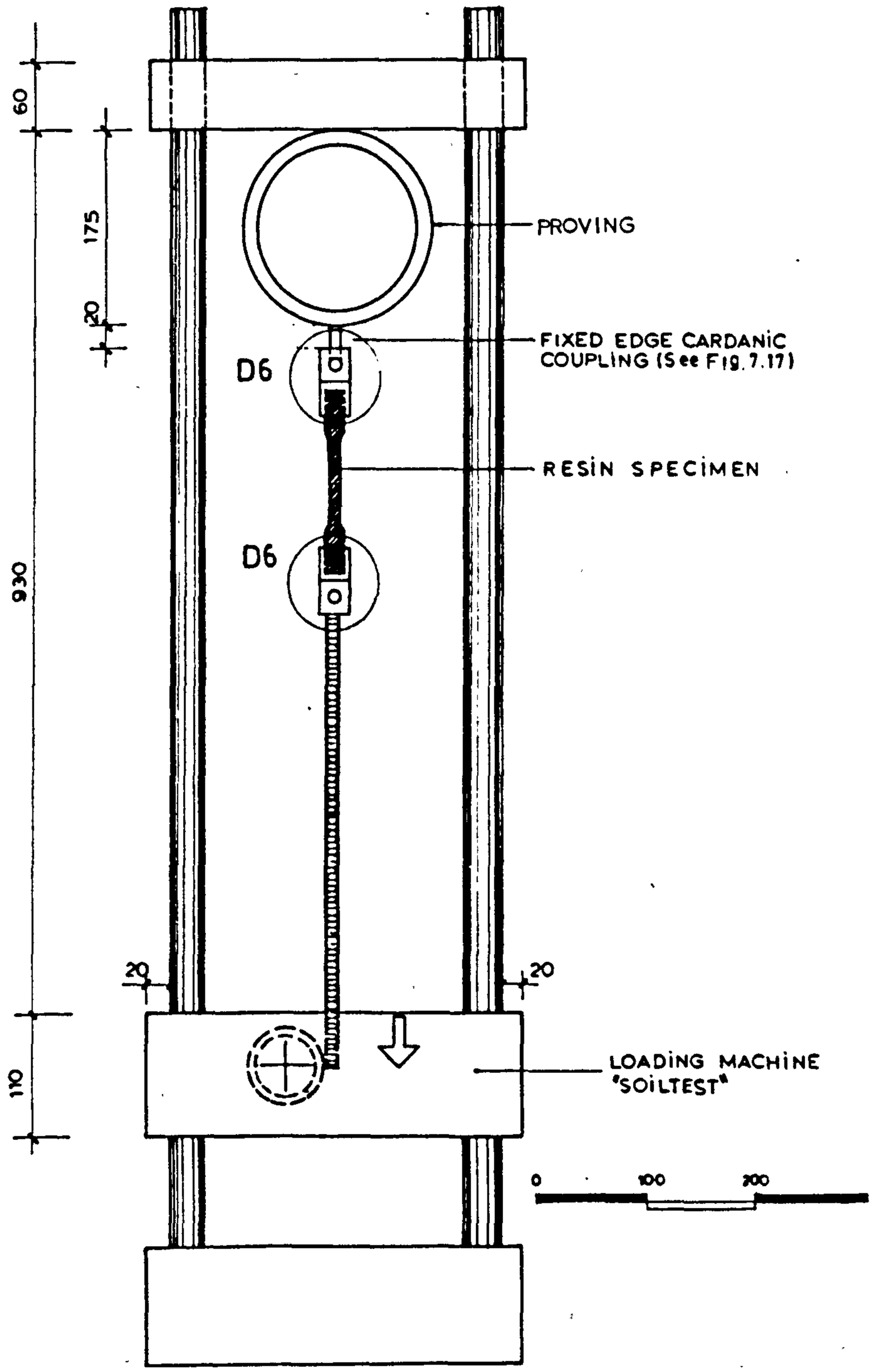

Fig.7.16. Resin tensile test.

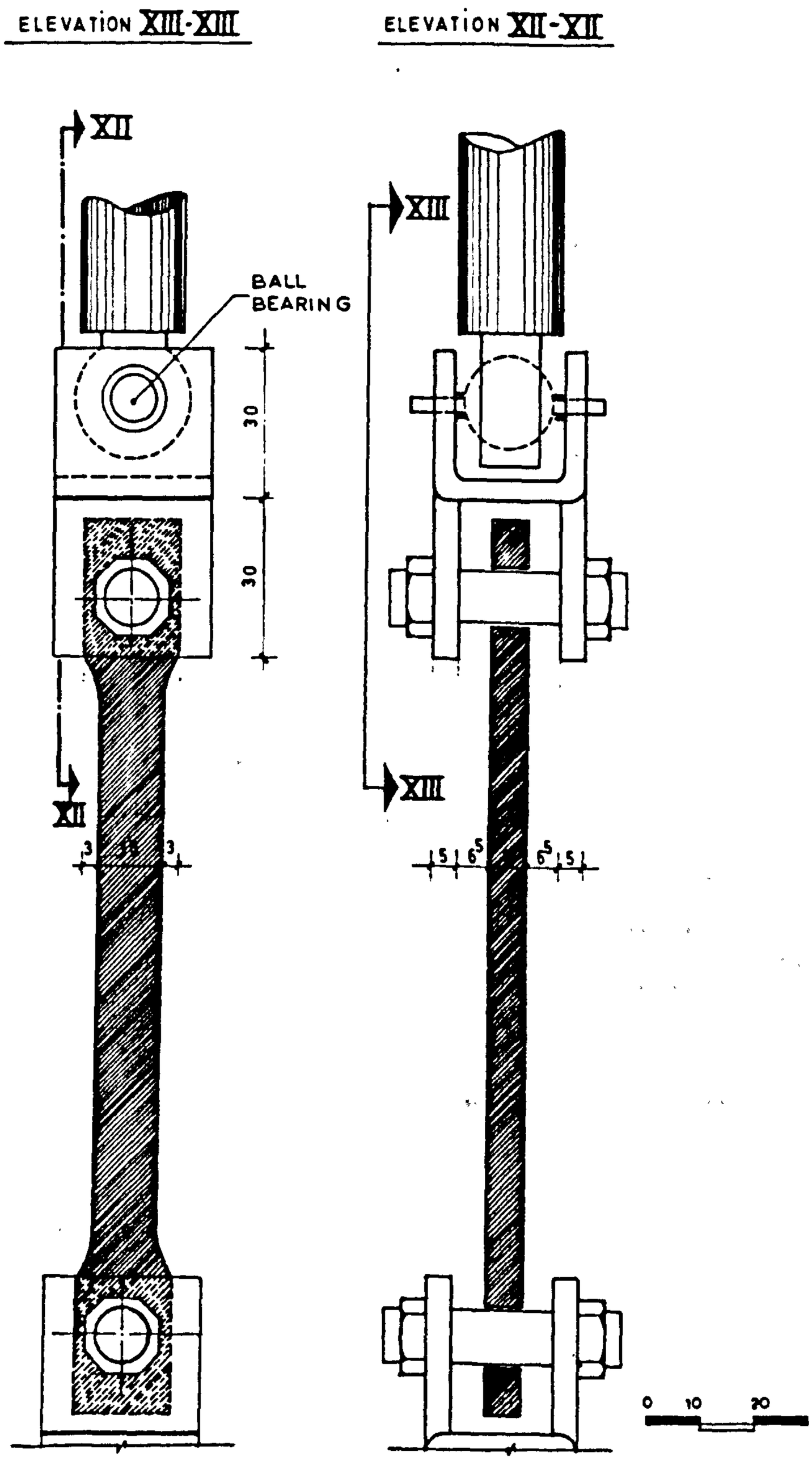

Fig.7.17. Resin tensile set up.Detail D6.

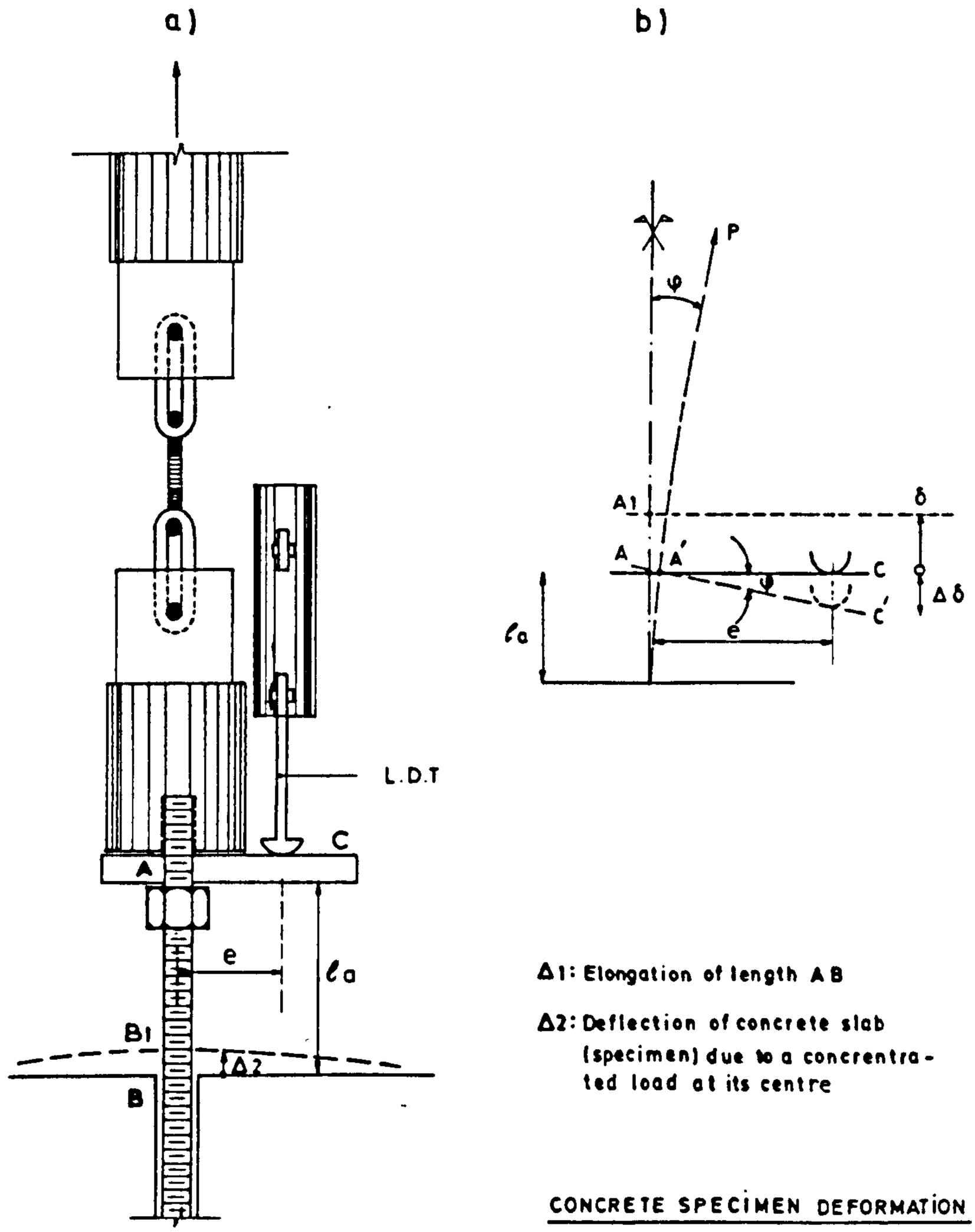

Δ1 (μm) / ℓa = 15 mm

	P=10KN	P=20KN	P=30KN	P=40KN
Φ 8	15	30	45	
Φ 10	9	18	27	
Φ 12	6	12	18	24

$$\frac{\Delta 2\,(\mu m)}{P = 10\ KN} = 3\ \mu m.$$

Fig.7.18. Effect of : a) Anchor free length and deflection of concrete specimen. b) Eccentricity of the needle of LDT.

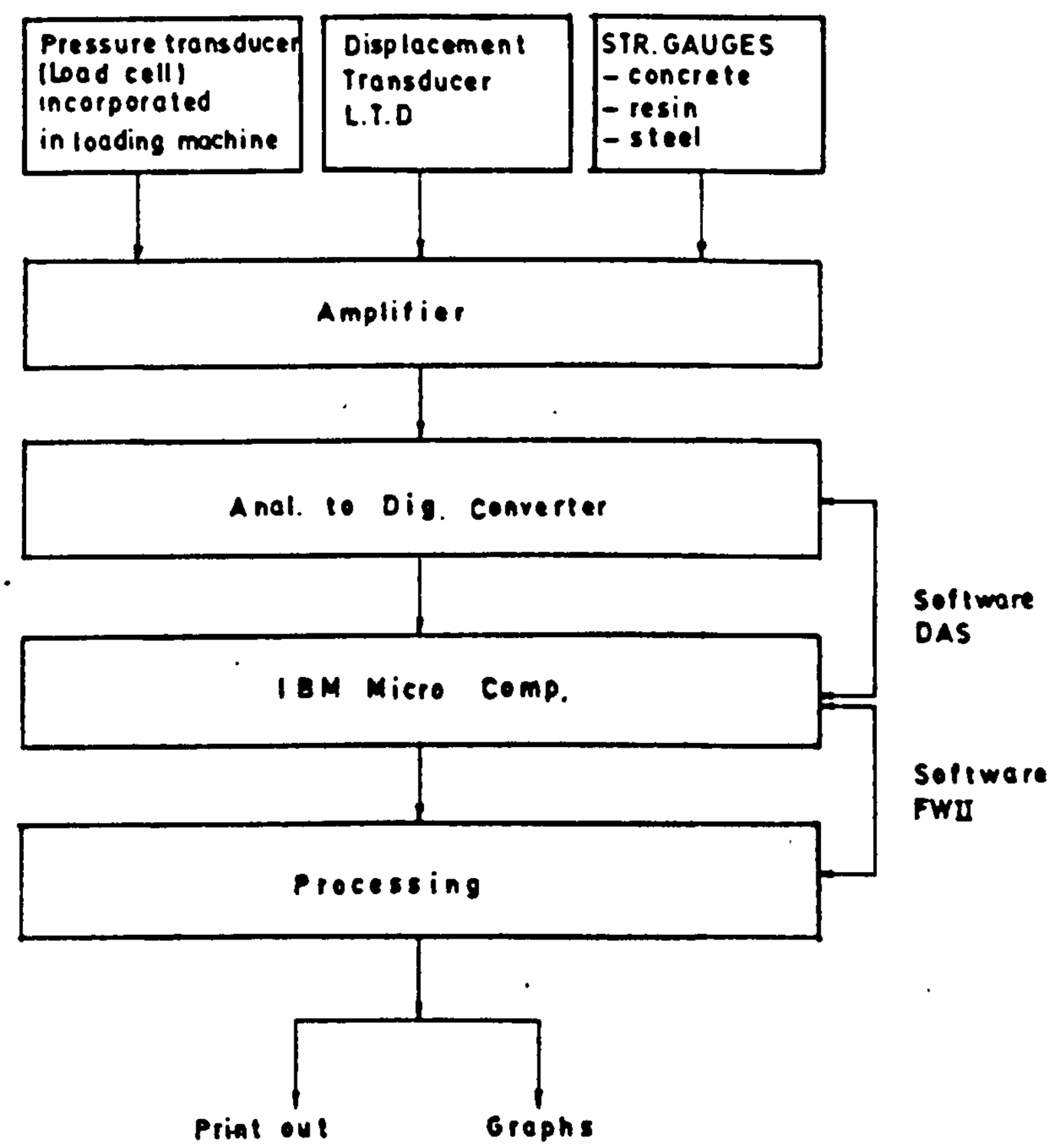

Fig.7.19. Configuration of the data acquisition and recording system.

TEST 2.01

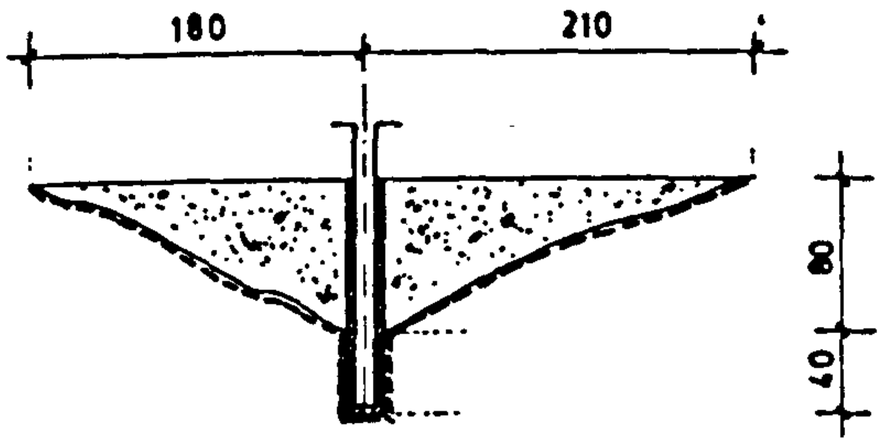

1	Embedm. length [mm]	: 120
2	Type of Anchor	:Thread
3	Diameter of Anchor [mm]	: 12
4	Cap/hole diameter [mm]	: 2/16
5	Epoxy Resin	: C1380
6	Method of insertion of Resin	:Pour
7	Concrete Compr.Str. [MPa]	: 28.0
8	Pault [kN]	:39.0
9	Mode of Failure	:I+C+R

10

P[kN]	δ(μm)
5.0	180
10.0	330
20.0	540
30.0	880
39.0	1089

TEST 2.02

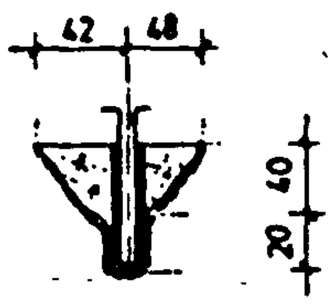

1	Embedm. length [mm]	: 60
2	Type of Anchor	:Thread
3	Diameter of Anchor [mm]	: 12
4	Cap/hole diameter [mm]	: 2/16
5	Epoxy Resin	: C1380
6	Method of insertion of resin	: Pour.
7	Concrete Compr.Str. [MPa]	:30.2
8	Pult [kN]	:30.0
9	Mode of failure	:I+C+R

TEST 2.03

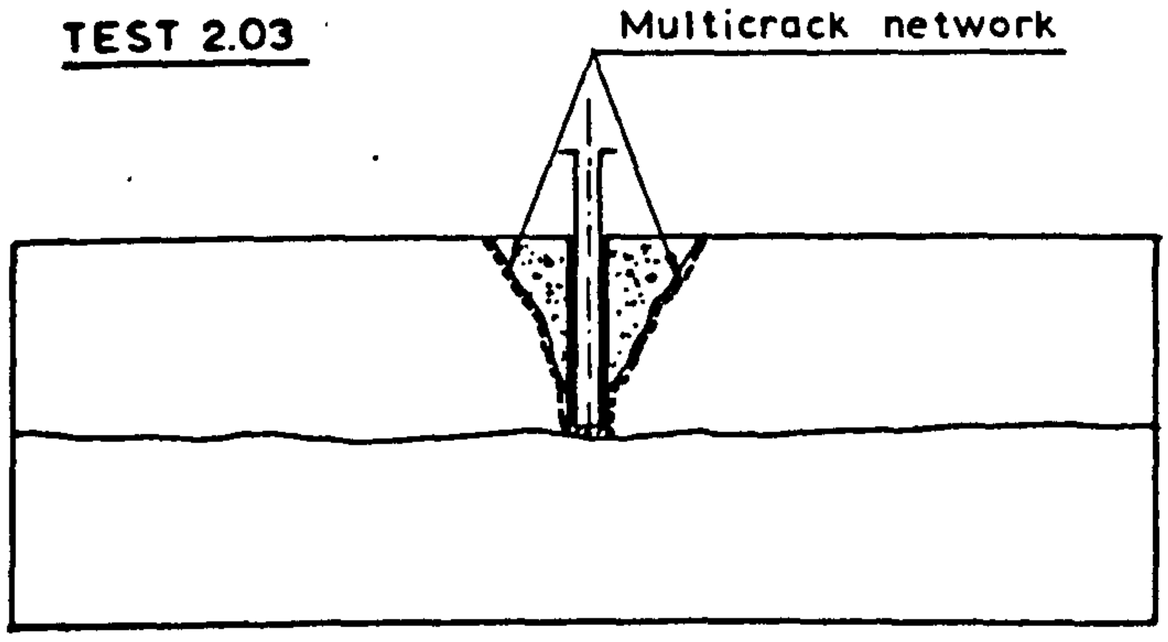

1	Embedm. length [mm]	: 80
2	Type of Anchor	: Treed
3	Diameter of Anchor [mm]	: 16
4	Cap/hole diameter [mm]	: 3/22
5	Epoxy Resin	: C1380
6	Method of insertion of resin	: Pour.
7	Concrete Compr. Str. [MPa]	: 27.5
8	Pult [kN]	: 47.6
9	Mode of failure	: Split

10

P[k N]	δ[μm]
10.0	51
20.0	100
30.0	190
40.0	320
47.6	880

Fig.7.20. Test series No 2.Details of tests.

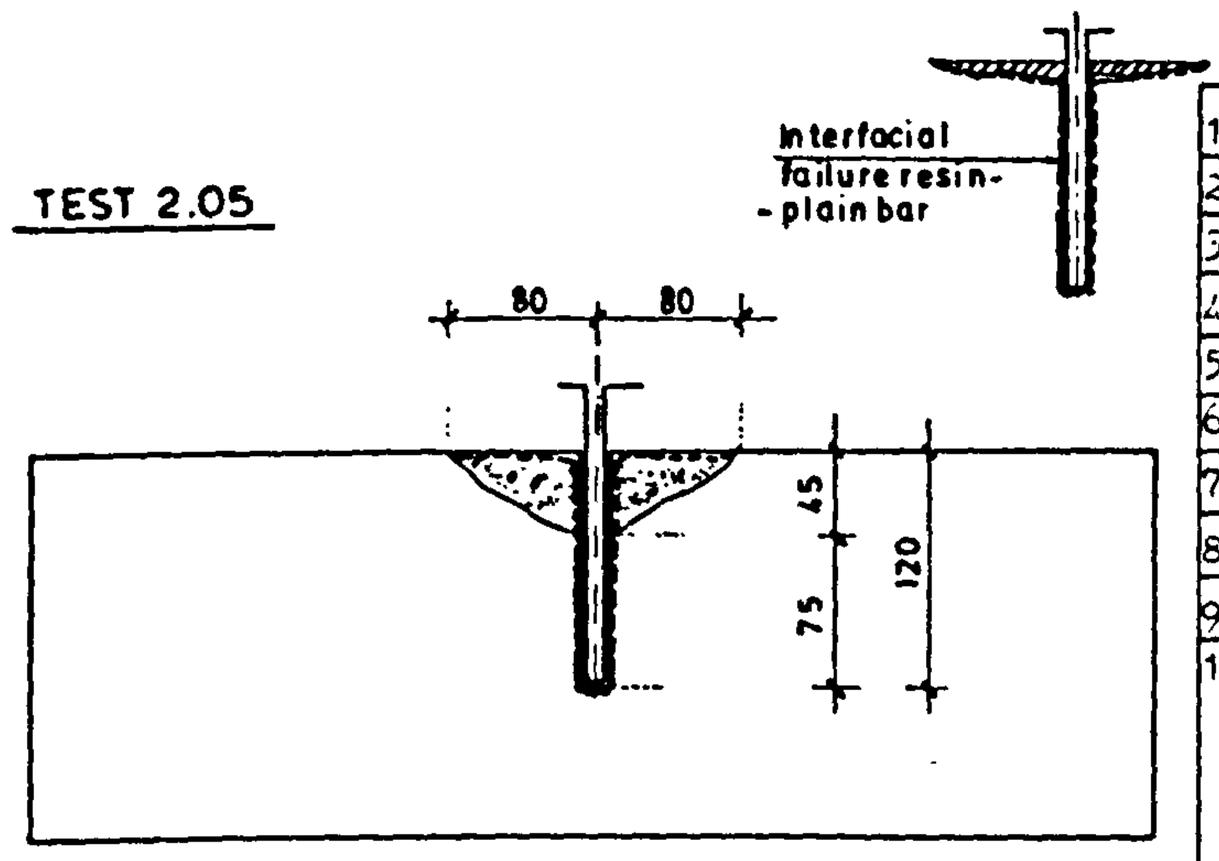

1	Embedm. length [mm]	: 120
2	Type of Anchor	: Plain
3	Diameter of Anchor [mm]	: 12
4	Gap/hole diameter [mm]	: 2/16
5	Epoxy Resin	: C1380
6	Method of insertion of resin	: Pour.
7	Concrete Compr. Str. [MPa]	: 26.5
8	Pult [kN]	: 34.4
9	Mode of failure	: I+R

10

P[kN]	δ[μm]
5.0	50
10.0	99
20.0	157
30.0	637
34.4	1957

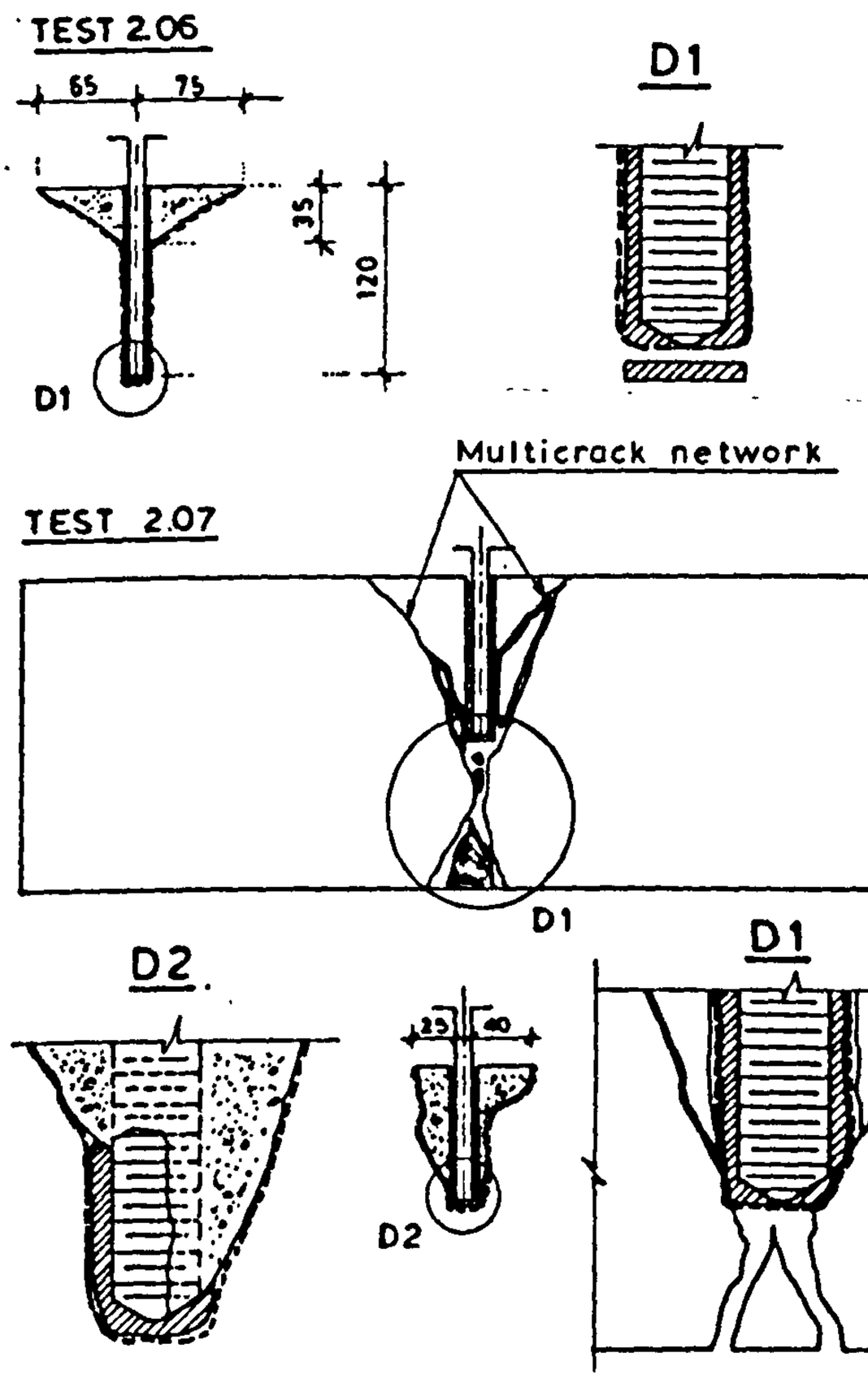

1	Embedm. length [mm]	: 120
2	Type of Anchor	: Tread
3	Diameter of Anchor [mm]	: 12
4	Gap/hole diameter [mm]	: 2/16
5	Epoxy Resin	: LV
6	Method of insertion of resin	: Pour.
7	Concrete Compr. Str. [MPa]	: 26.0
8	Pult [kN]	: 41.3
9	Mode of failure	: I+C+R

10

P[kN]	δ[μm]
10.0	100
20.0	390
30.0	1040

1	Embedm. length [mm]	: 100
2	Type of Anchor	: Tread
3	Diameter of Anchor [mm]	: 16
4	Gap/hole diameter [mm]	: 3/22
5	Epoxy Resin	: C1380
6	Method of insertion of resin	: Pour
7	Concrete Compr. Str. [MPa]	: 31.0
8	Pult [kN]	: 53.0
9	Mode of failure	: Split

10

P[kN]	δ[μm]
10.0	80
20.0	240
30.0	490
40.0	760

Fig.7.21. Test series No 2.Details of the tests.

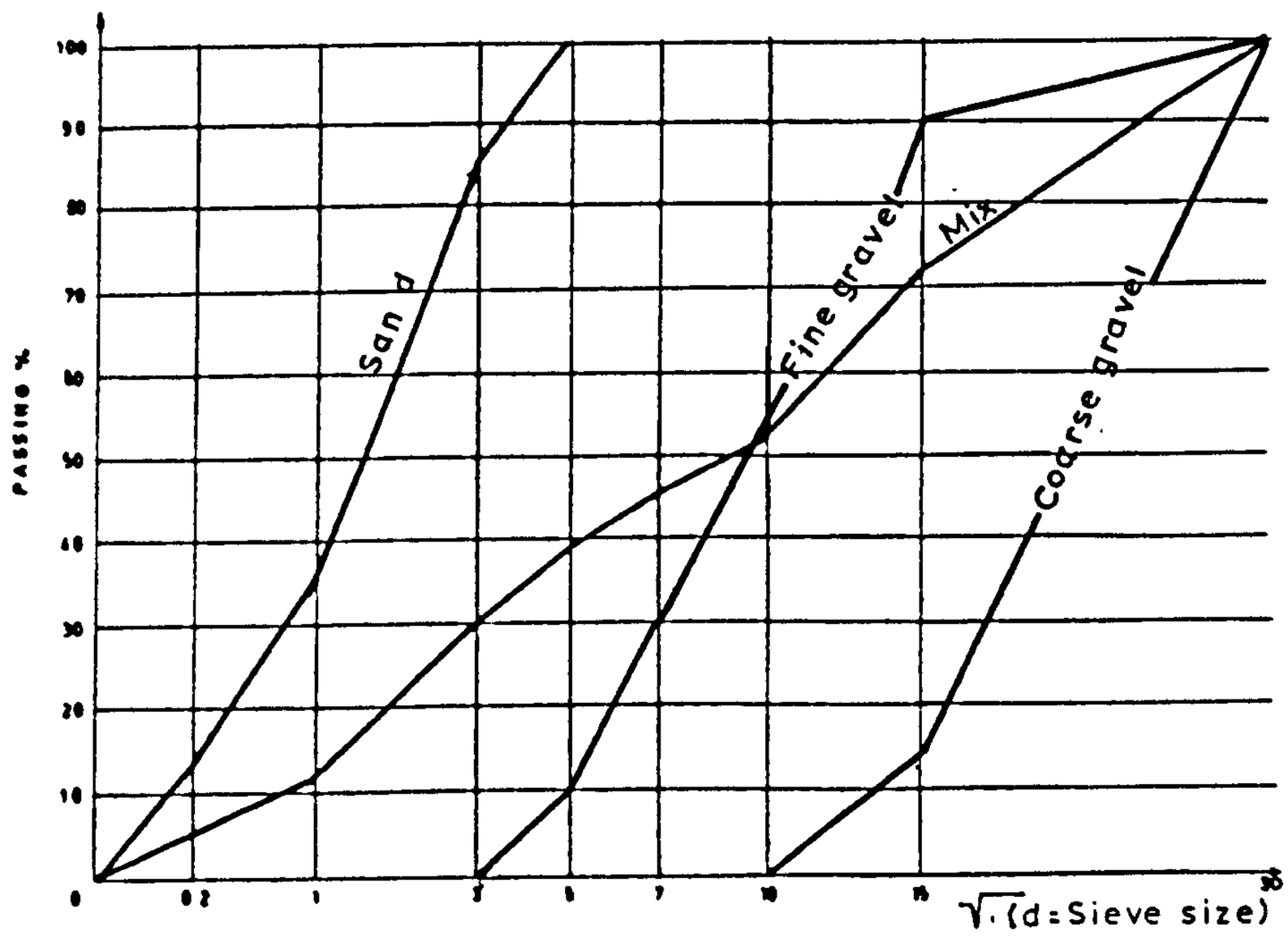

Fig.7.22. Grading of the aggregates used.

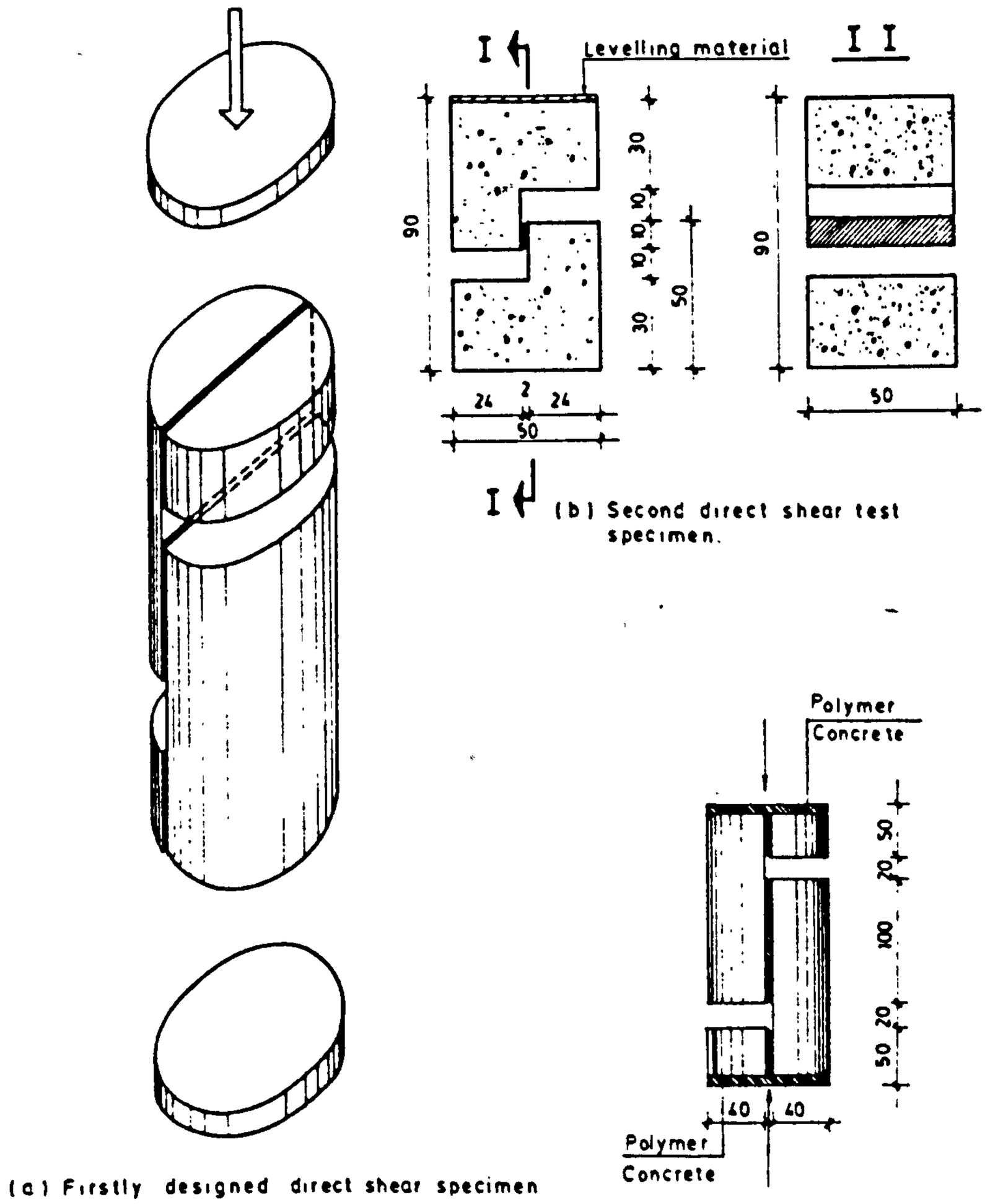

Fig.7.23.Initial specimens for the direct shear test.

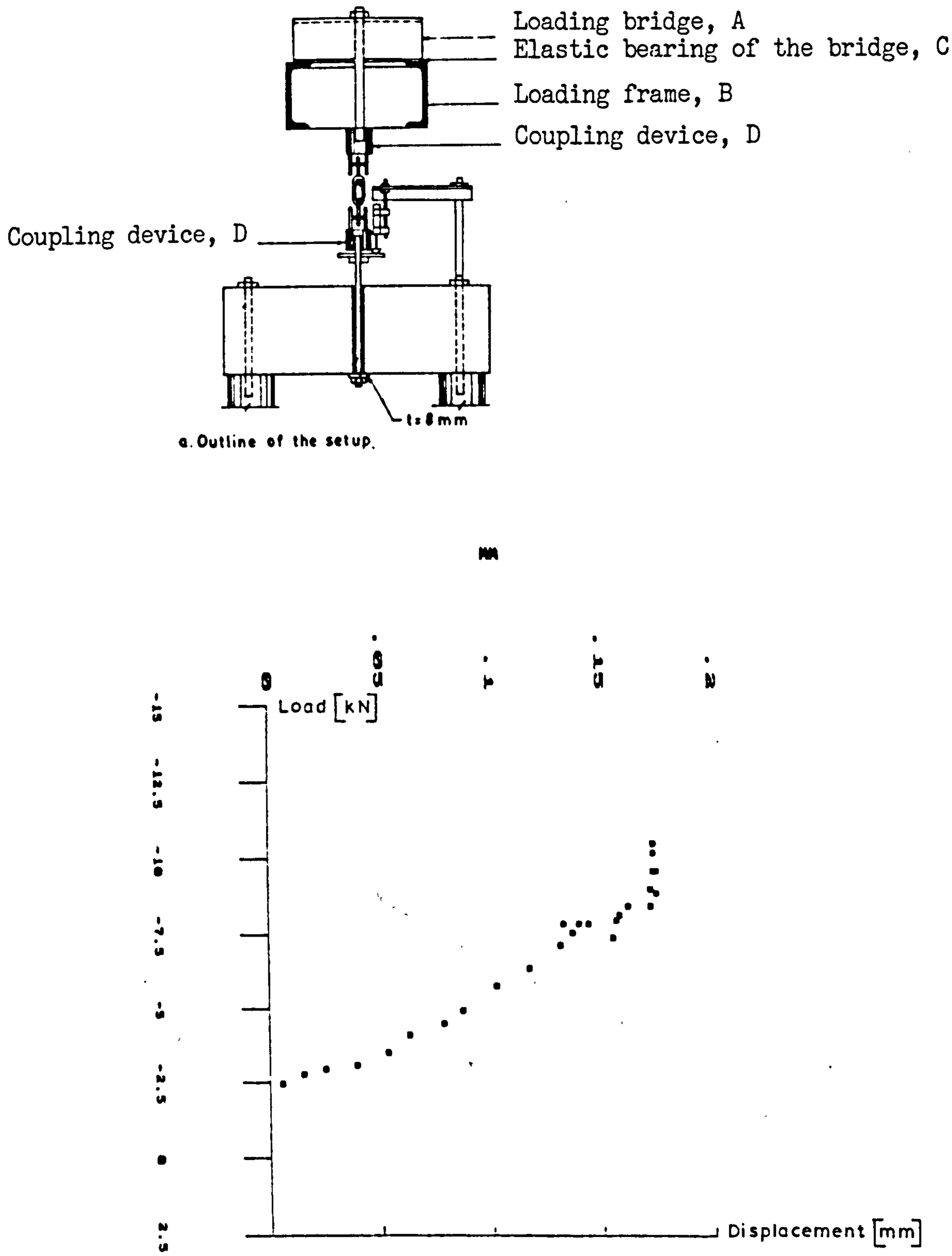

Fig.7.24. Calibration of the tension transfer system.

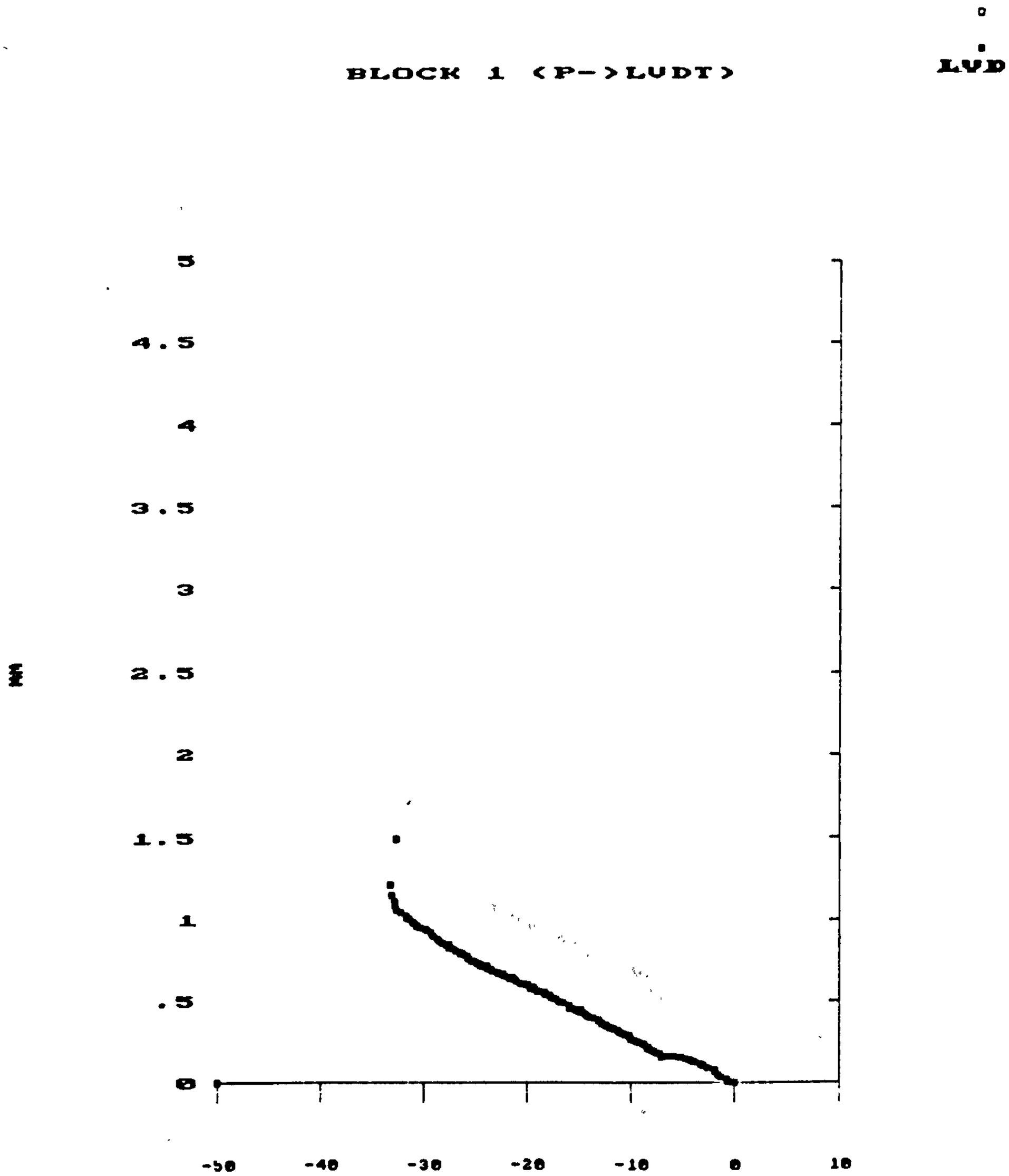

Fig. 7.25

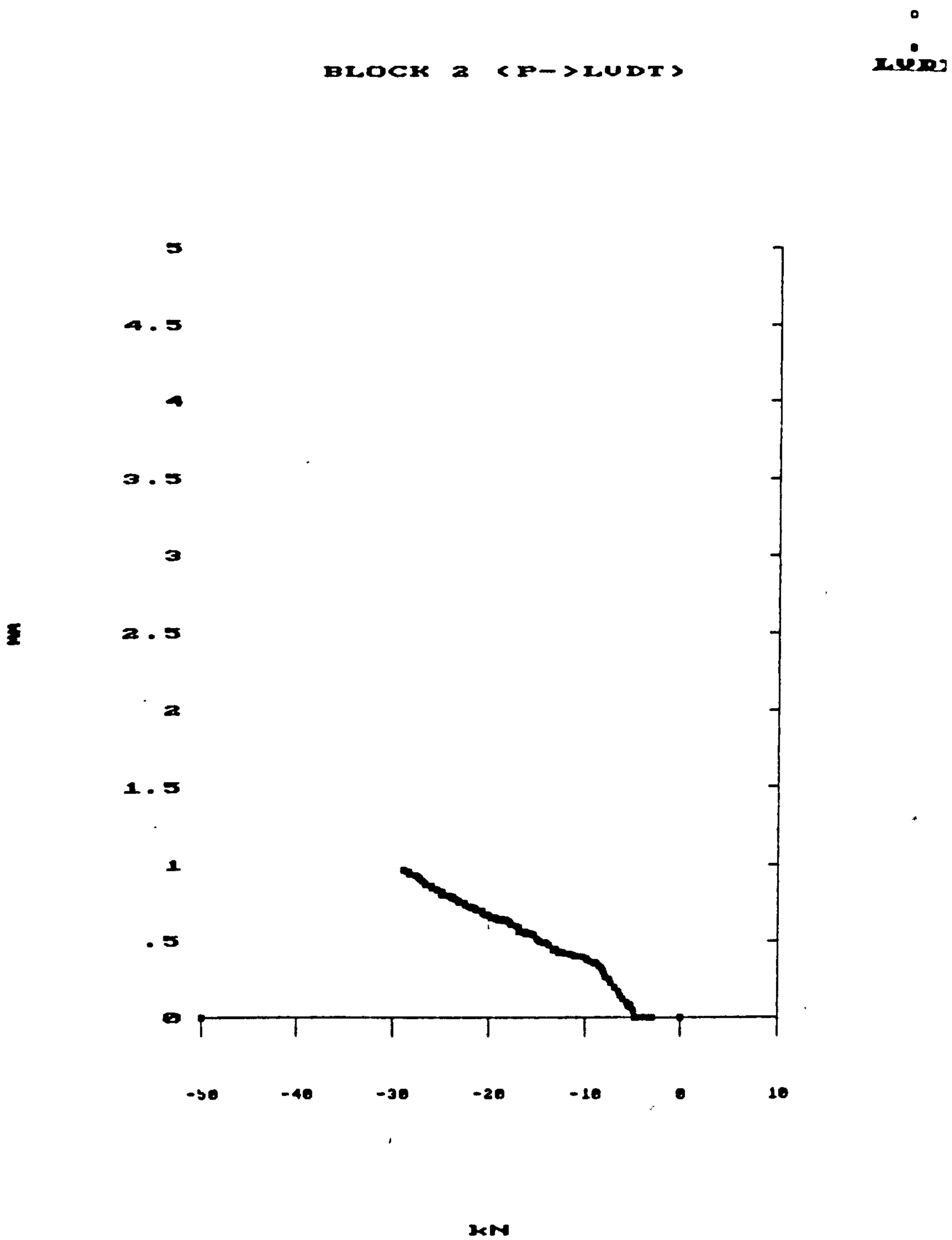

Fig. 7.26

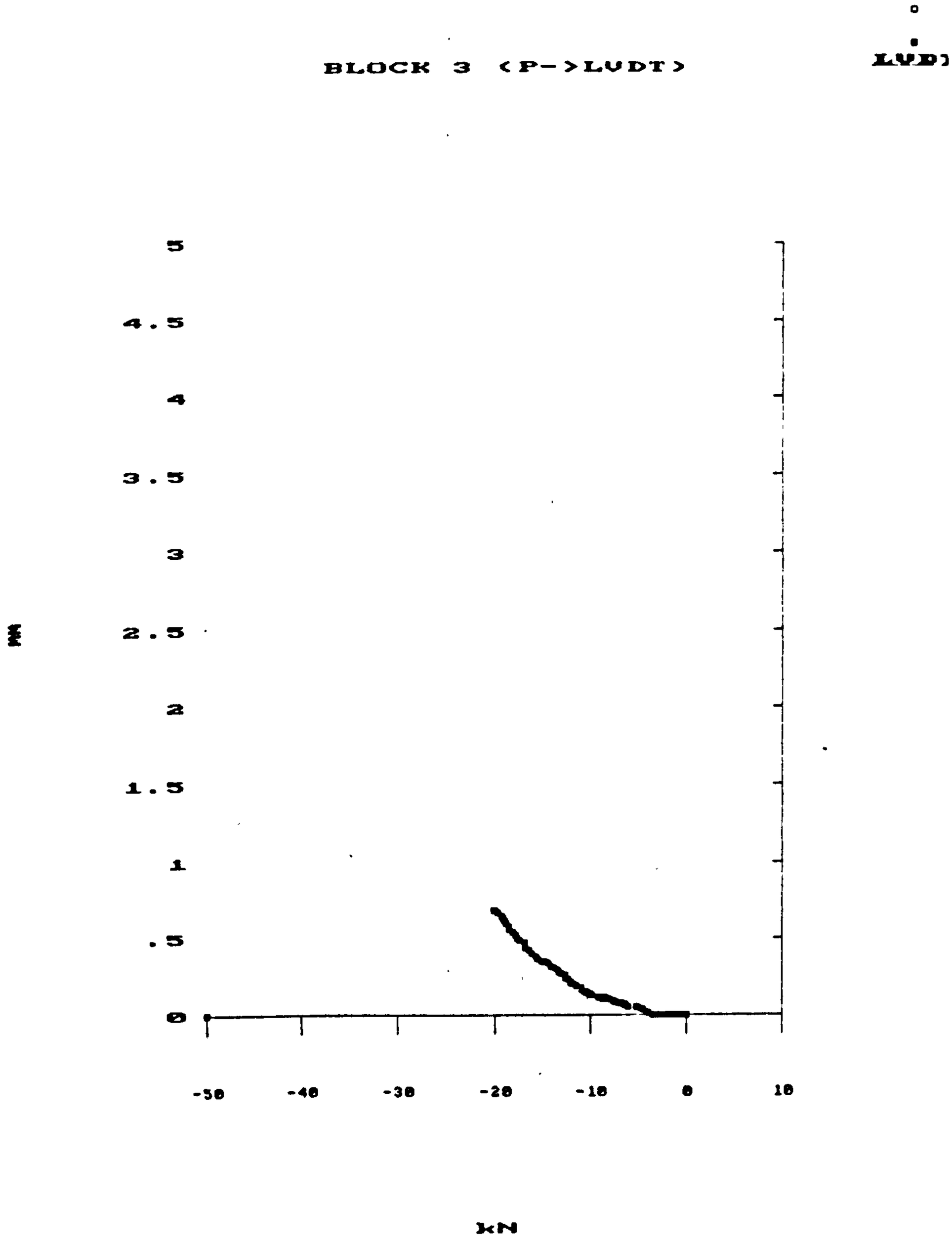

Fig. 7.27

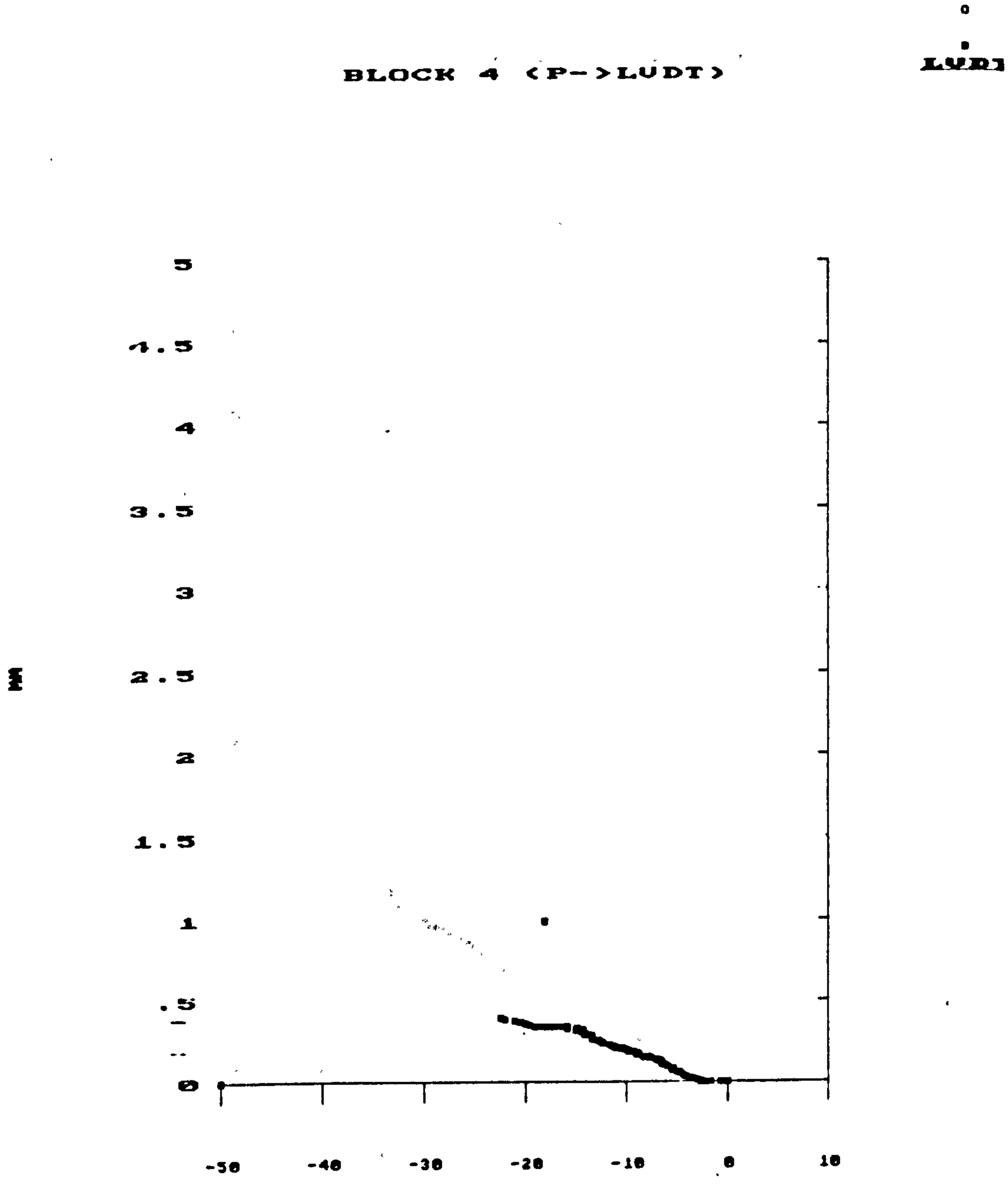

Fig. 7.28

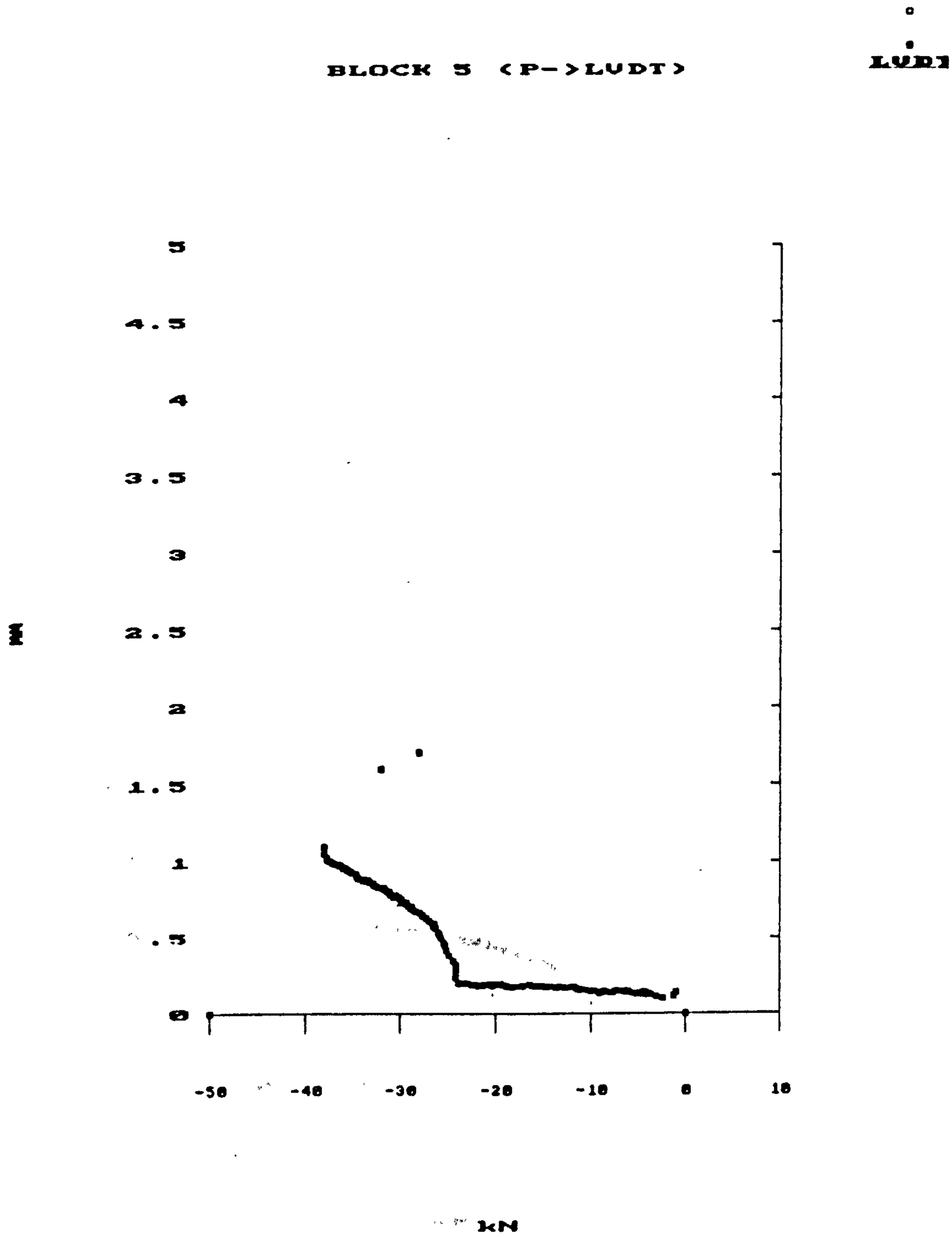

Fig. 7.29

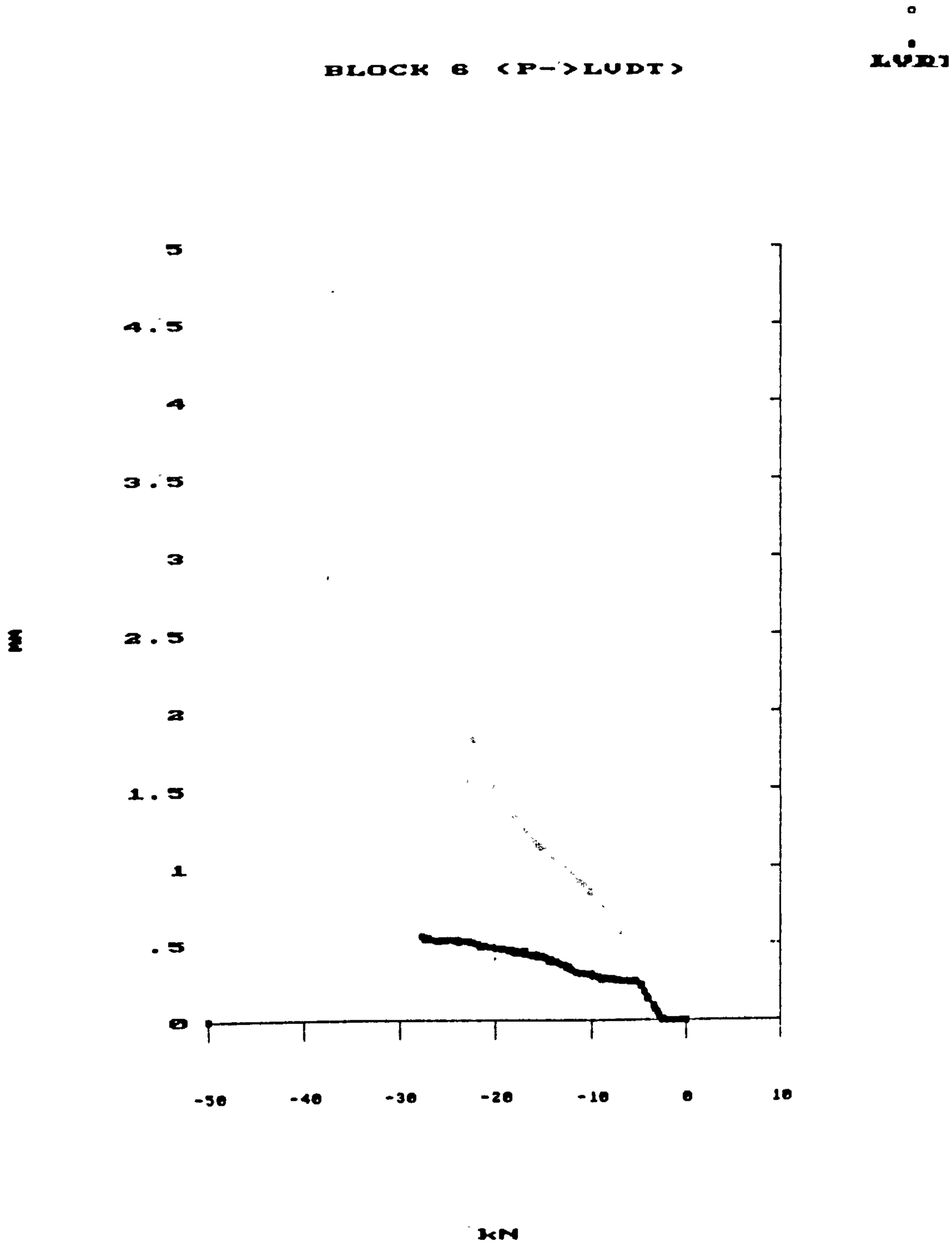

Fig. 7.30

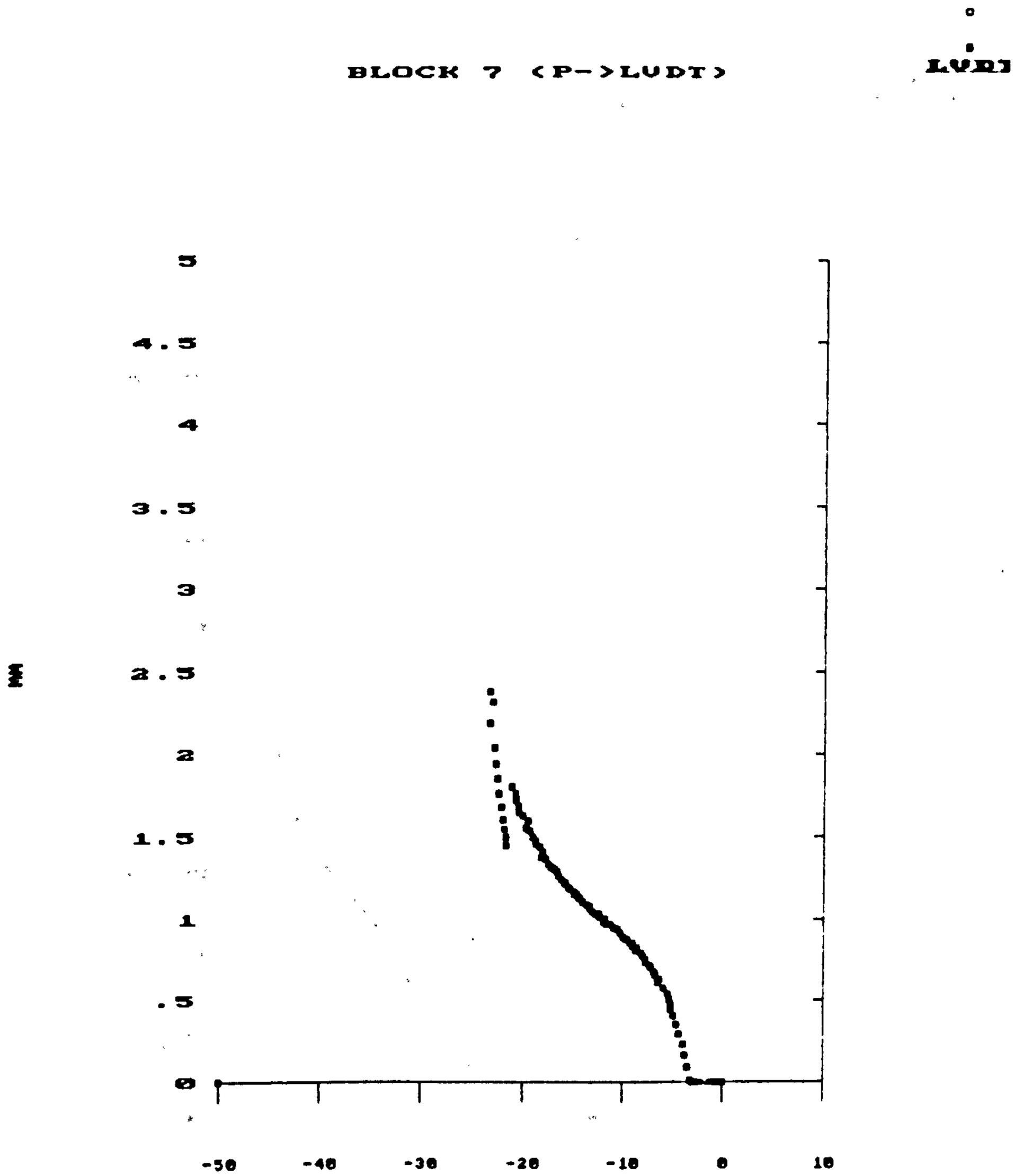

Fig. 7.31

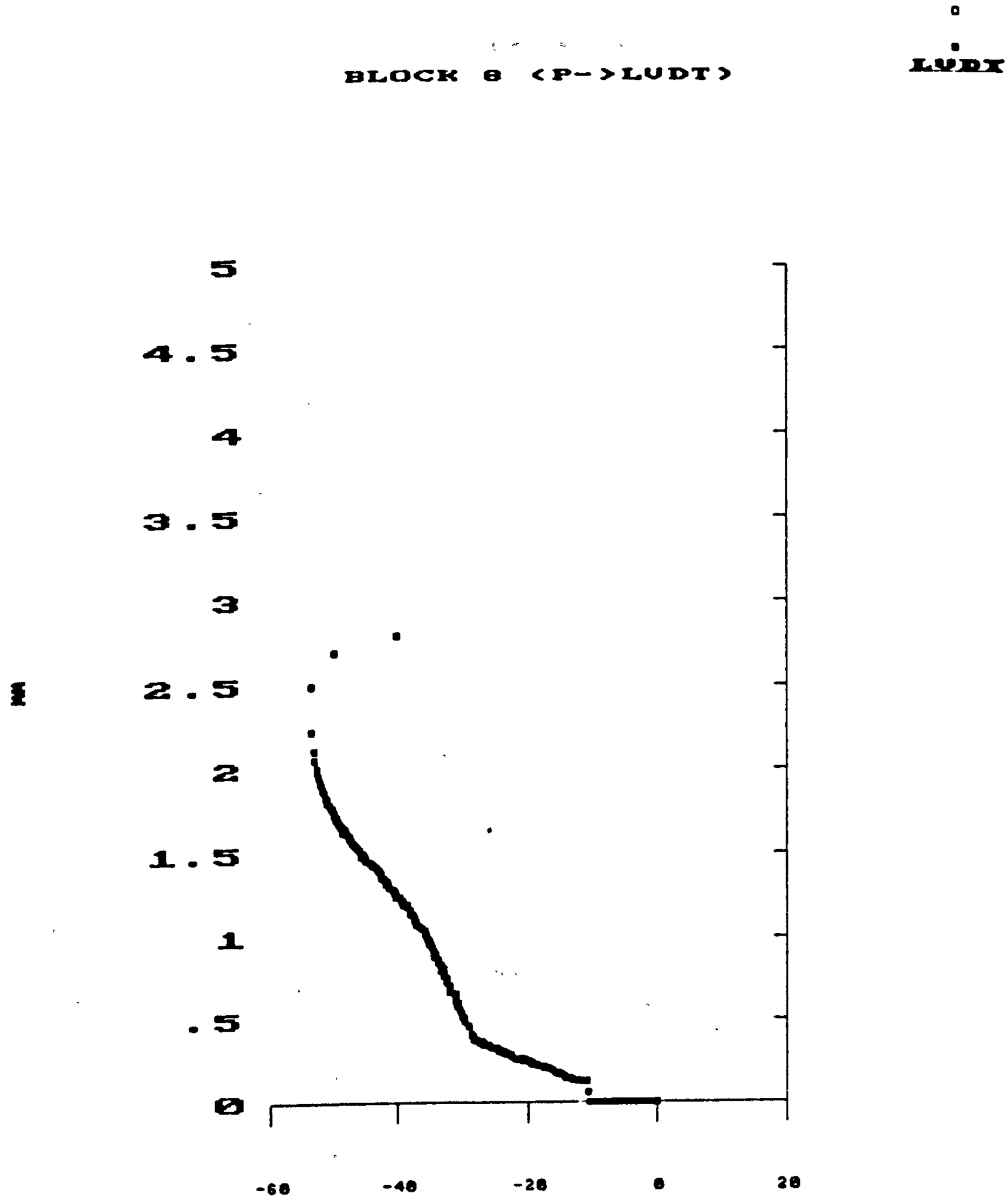

Fig. 7.32

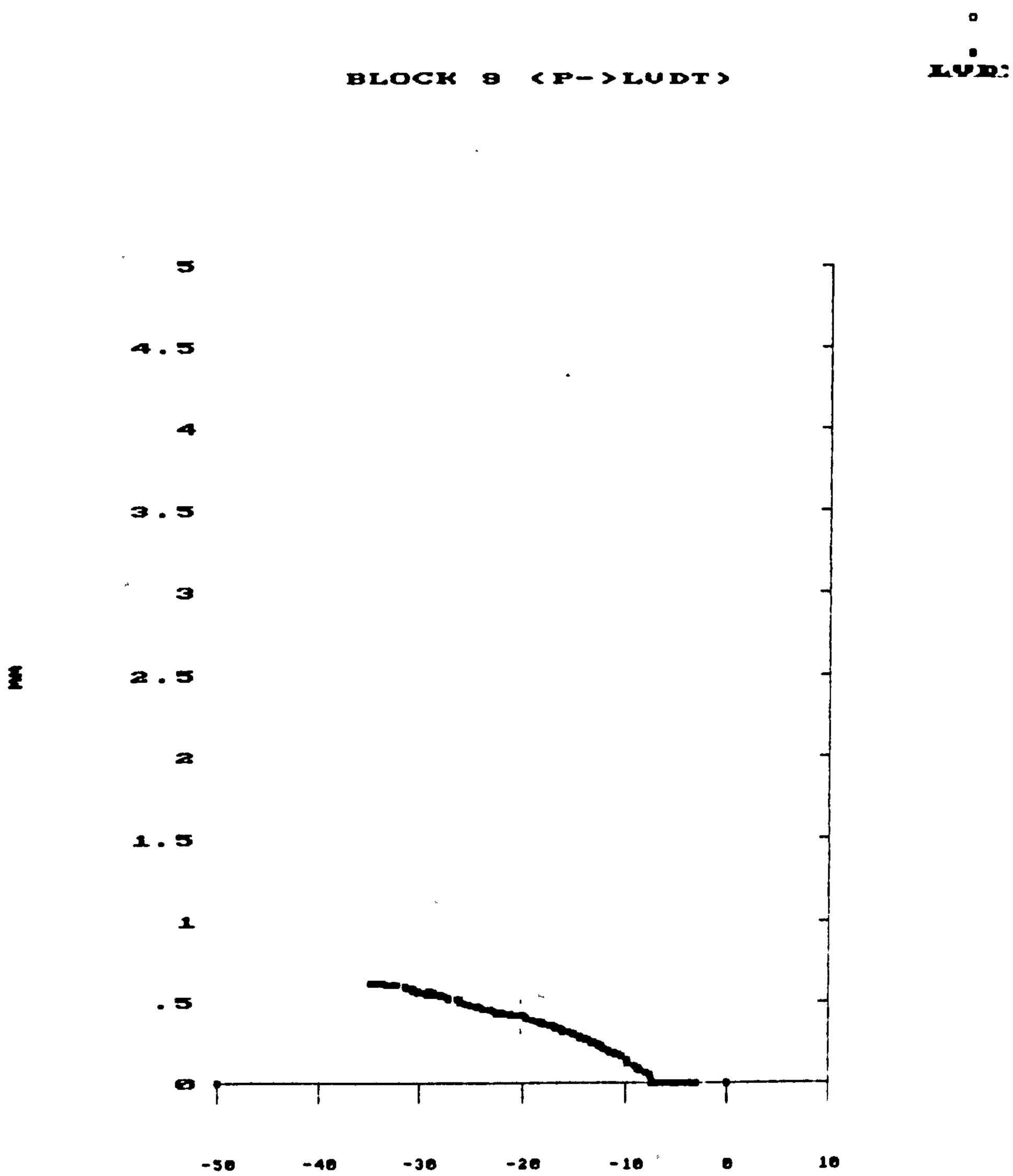

Fig. 7.33

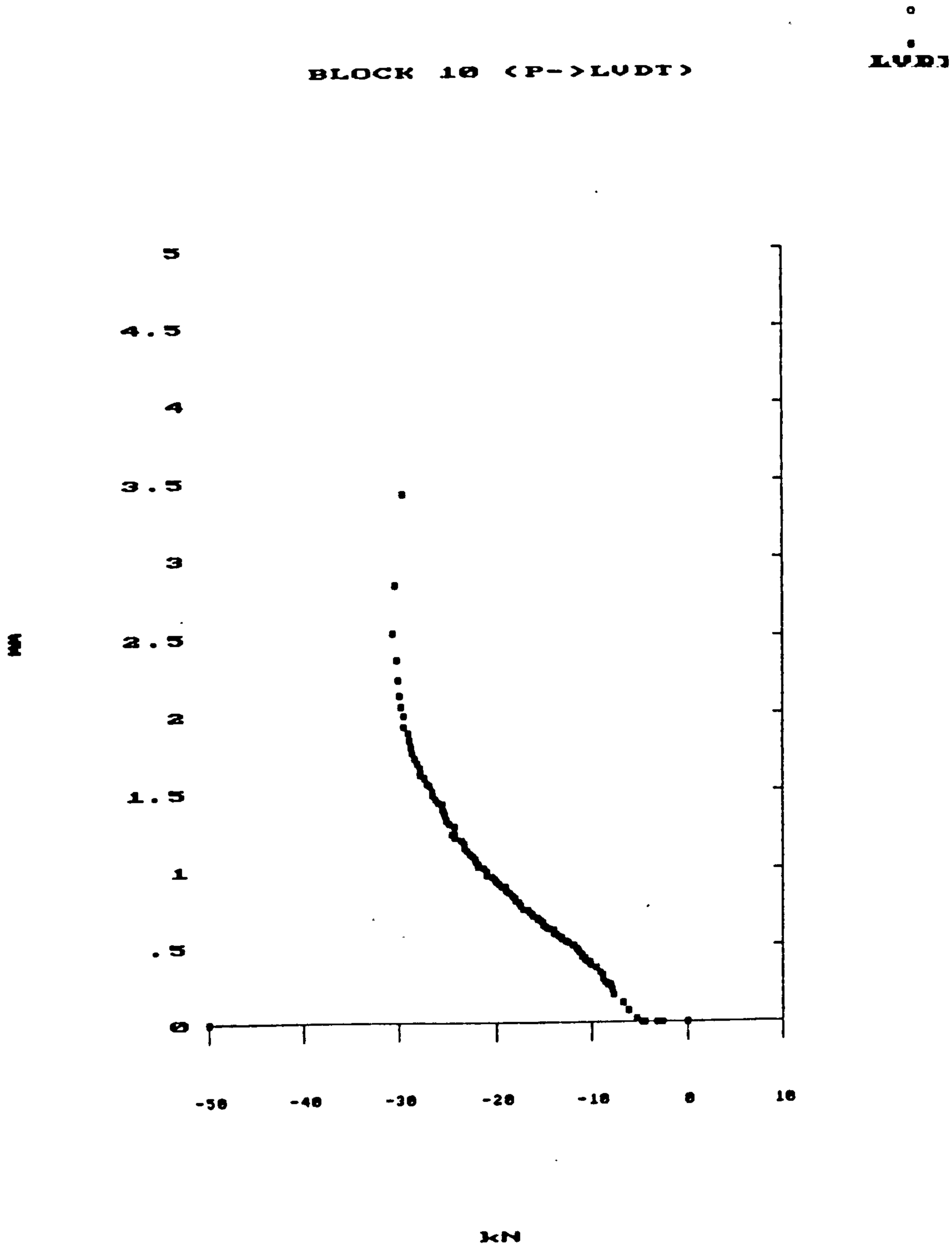

Fig. 7.34

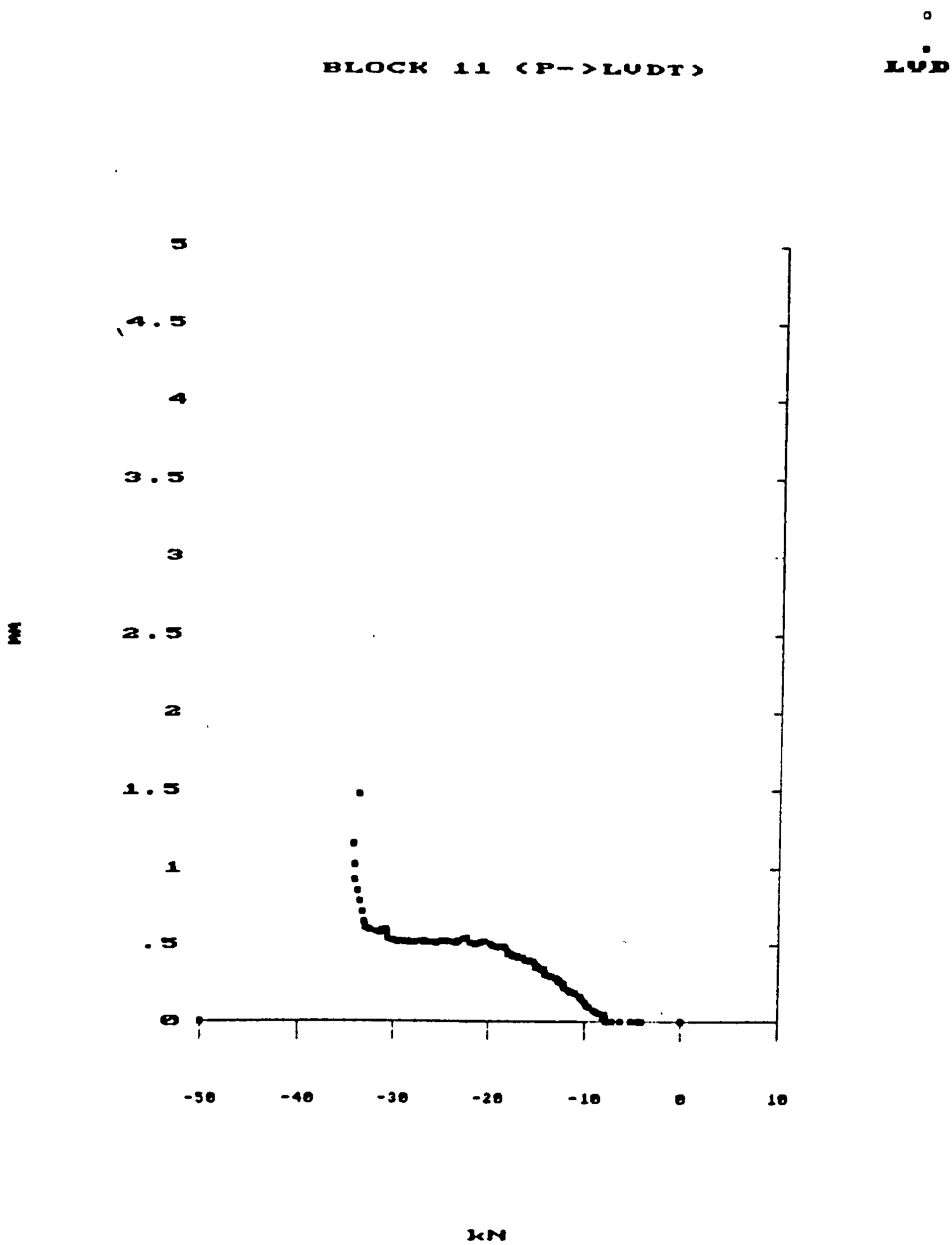

Fig. 7.35

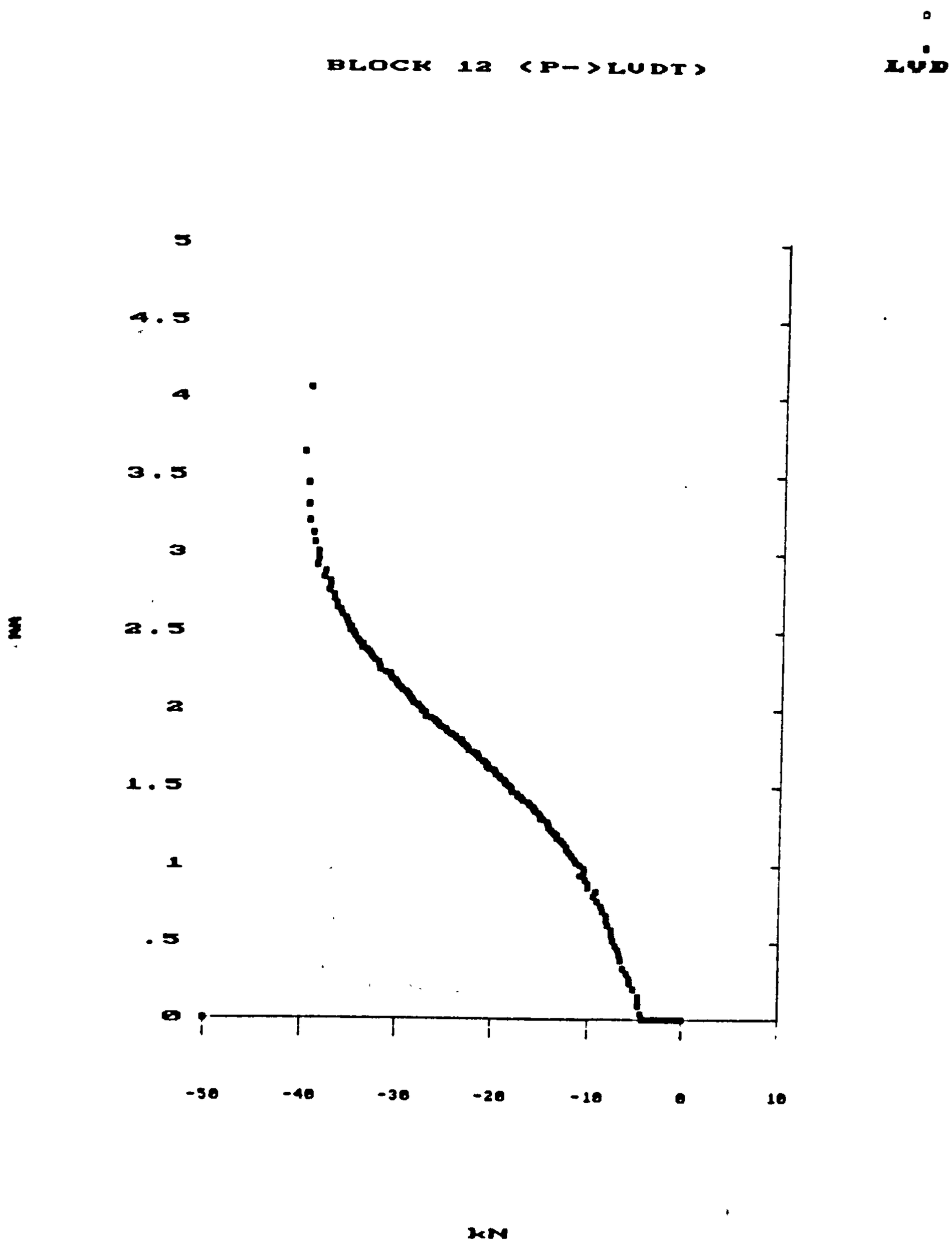

Fig. 7.36

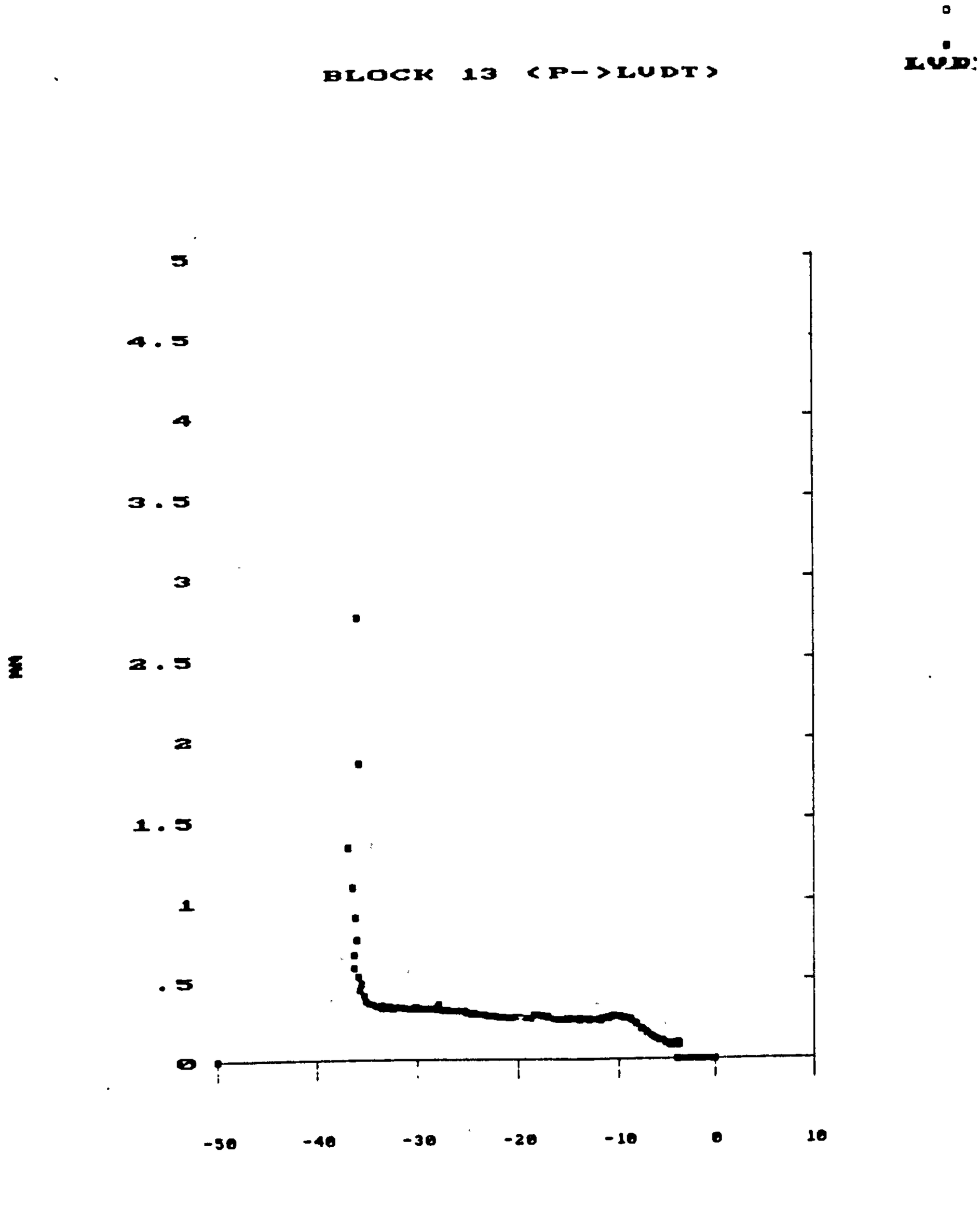

Fig. 7.37

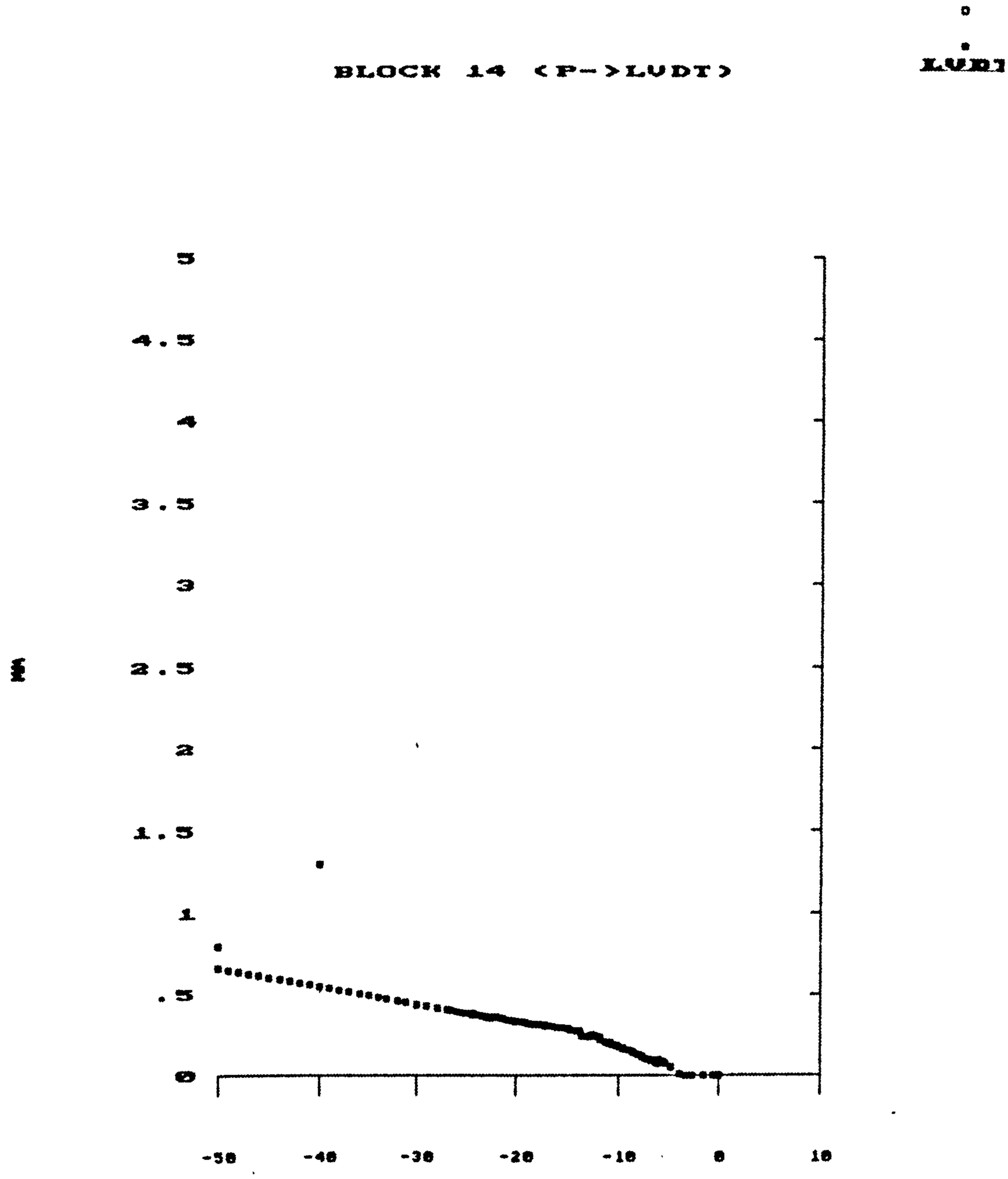

Fig. 738

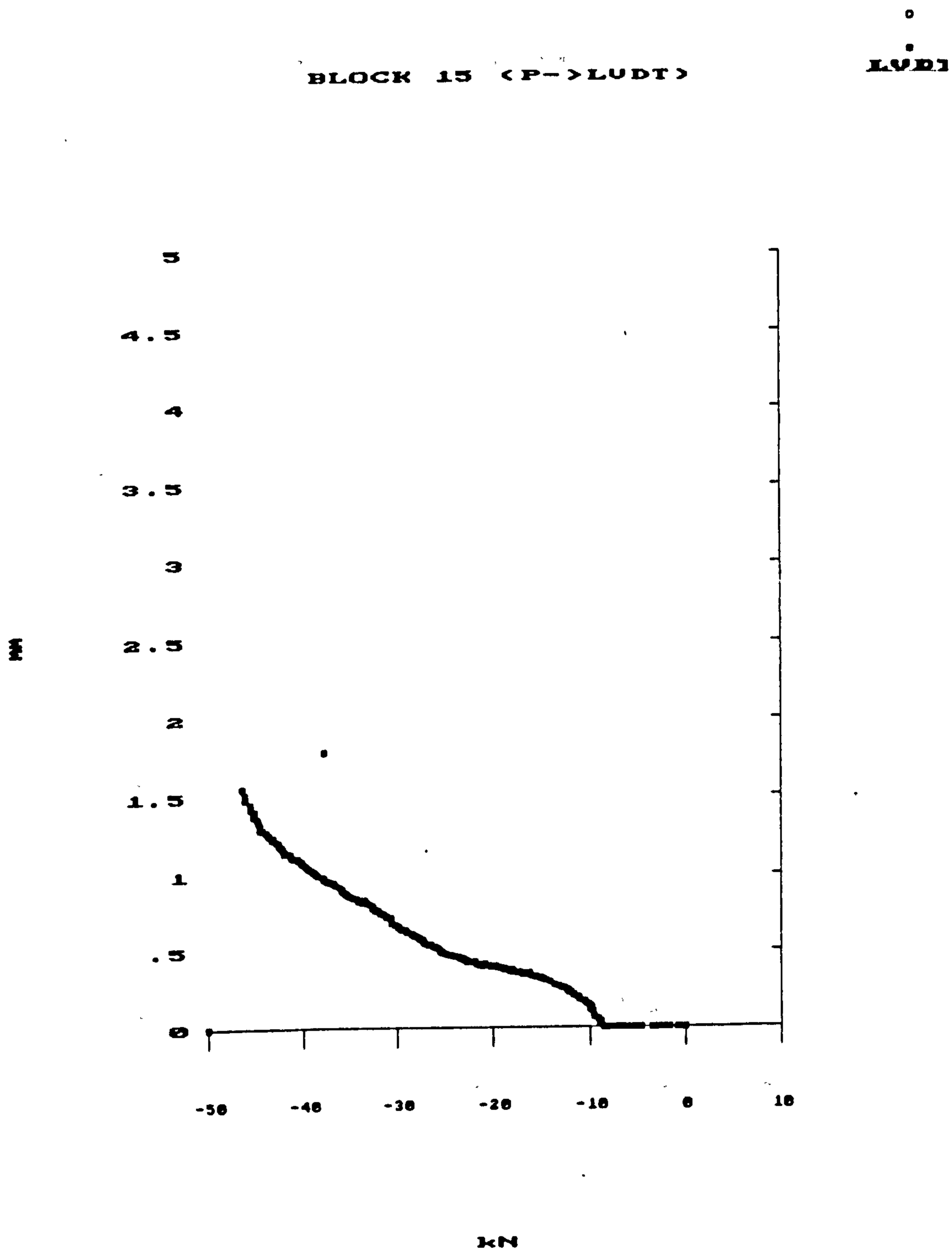

Fig. 7 39

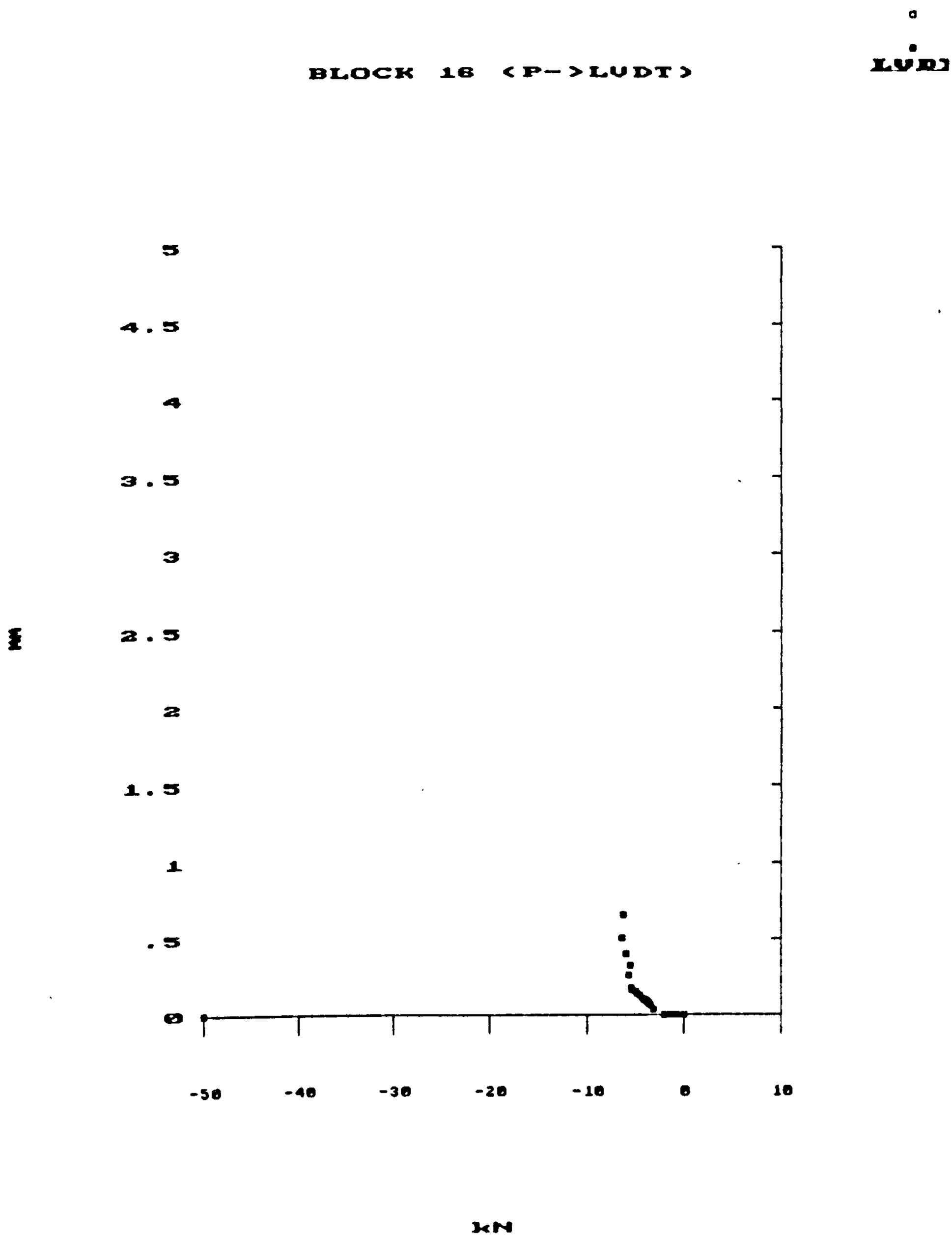

Fig 7.40

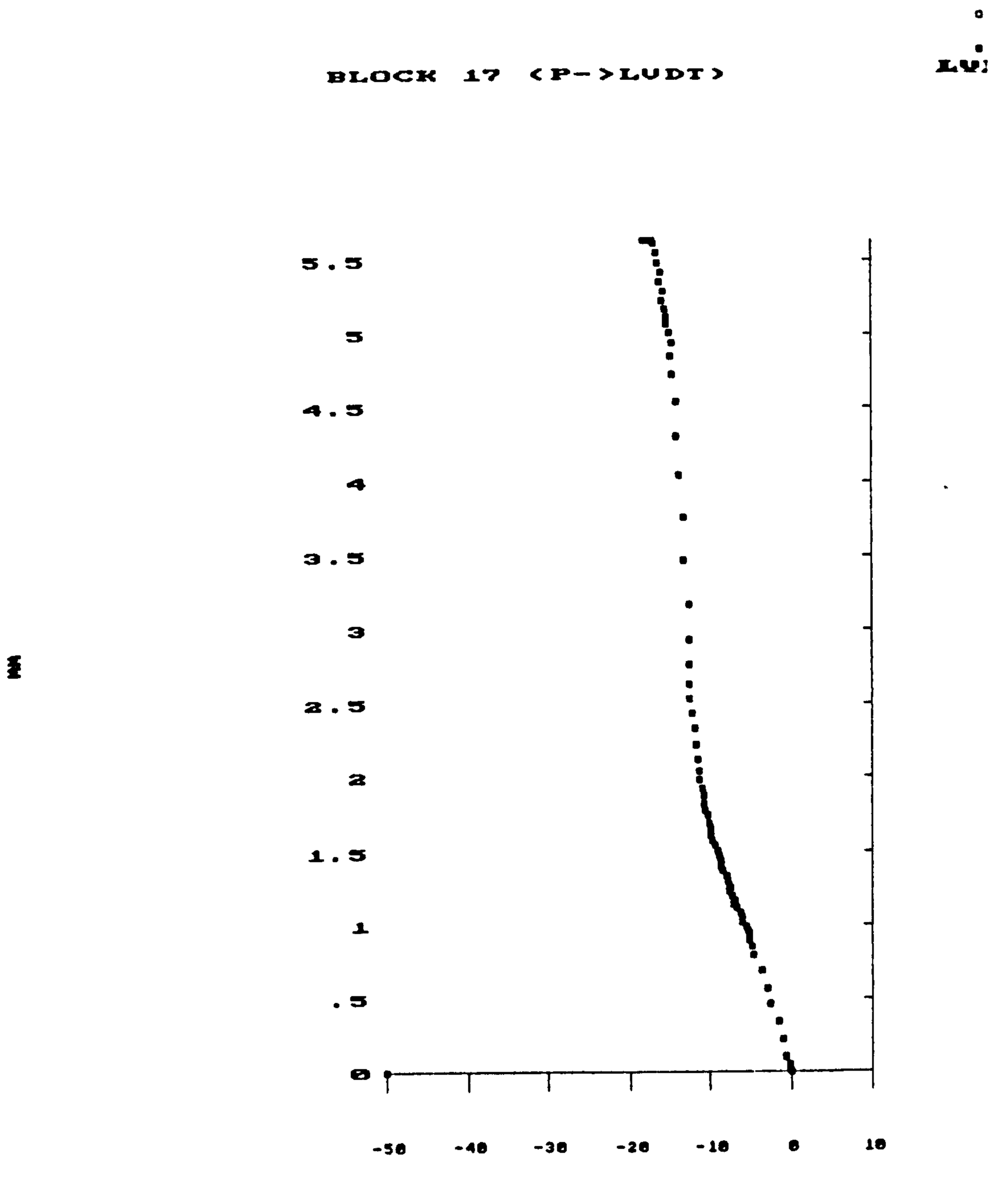

Fig. 7.41

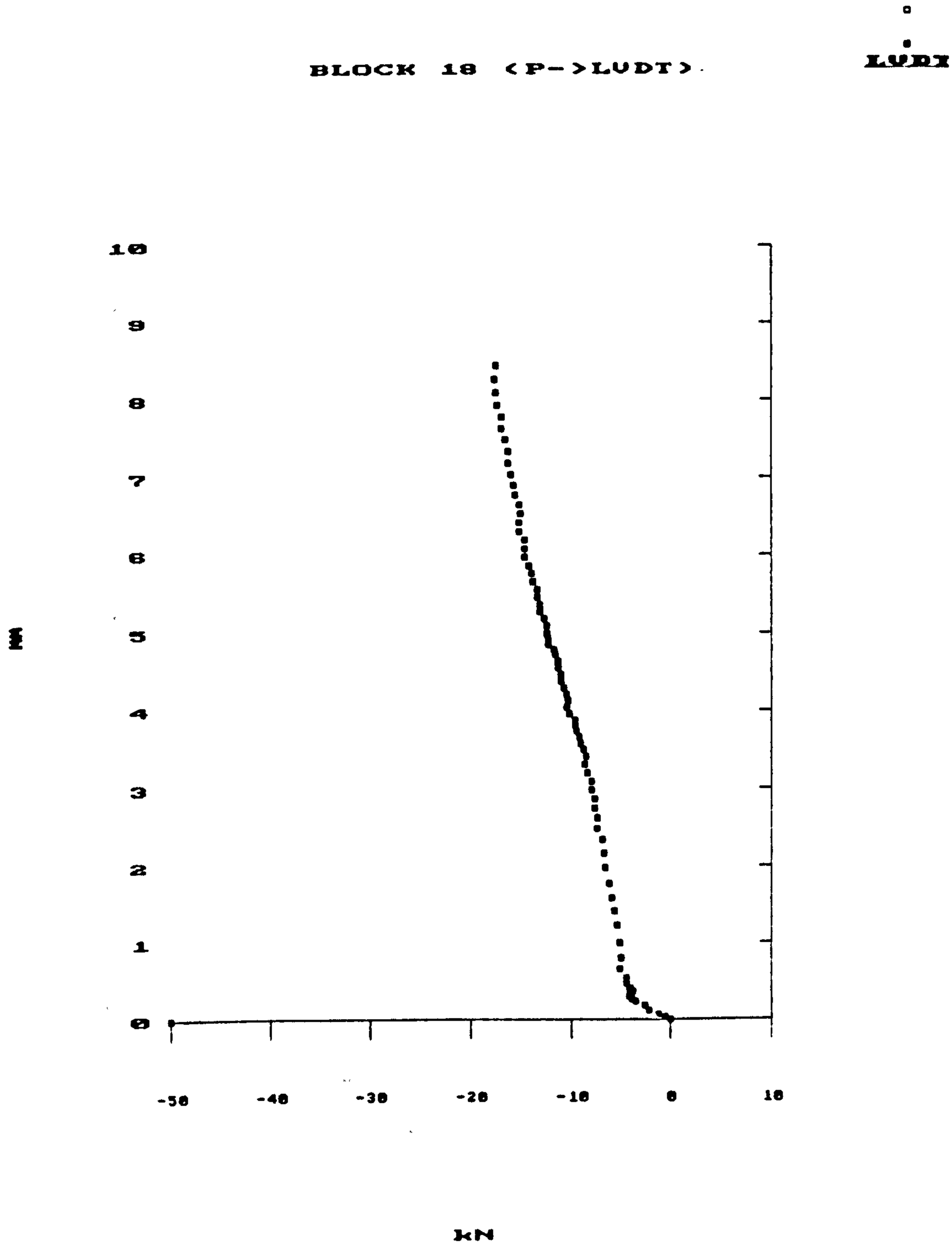

Fig 7.42

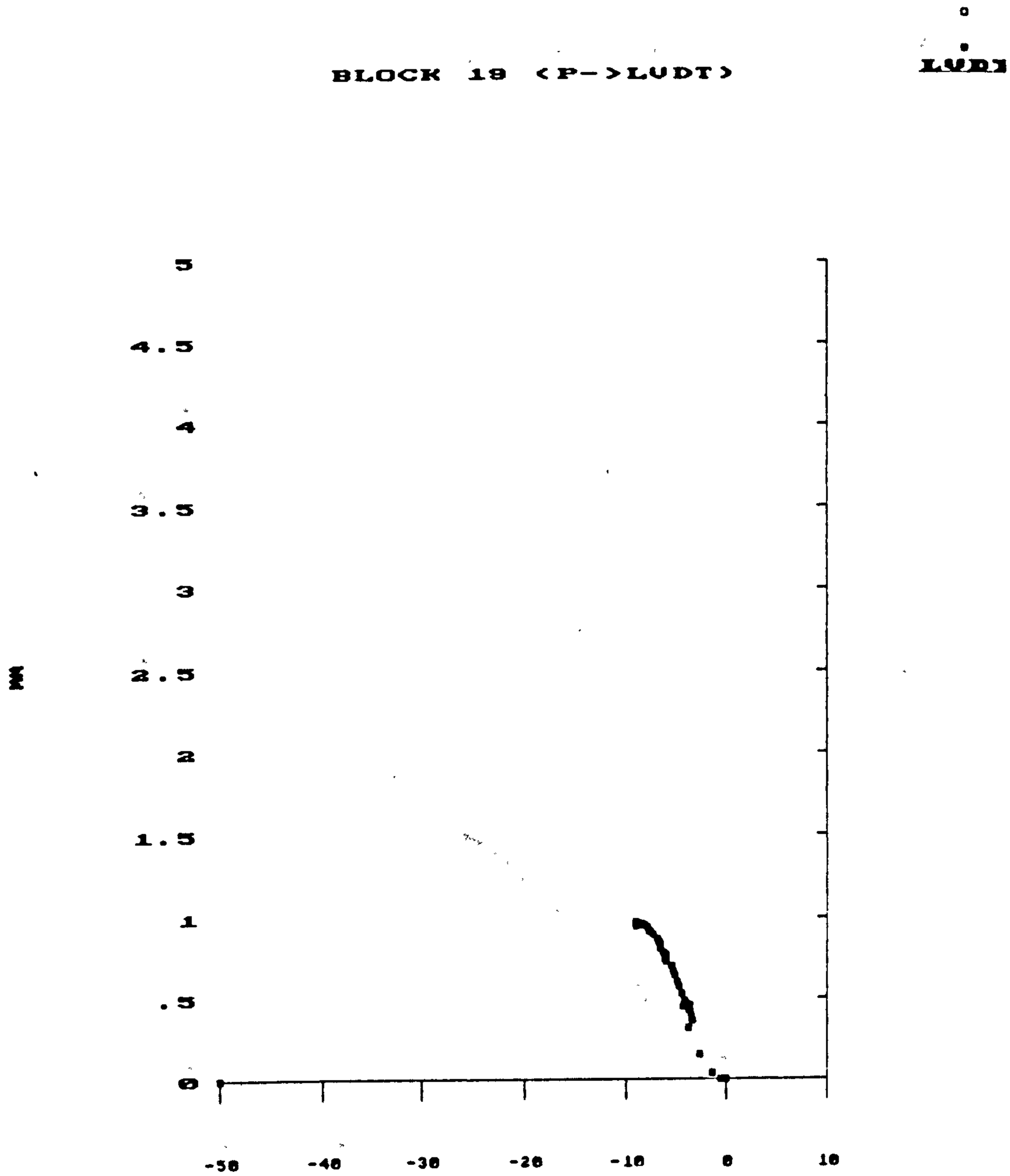

Fig 7 43

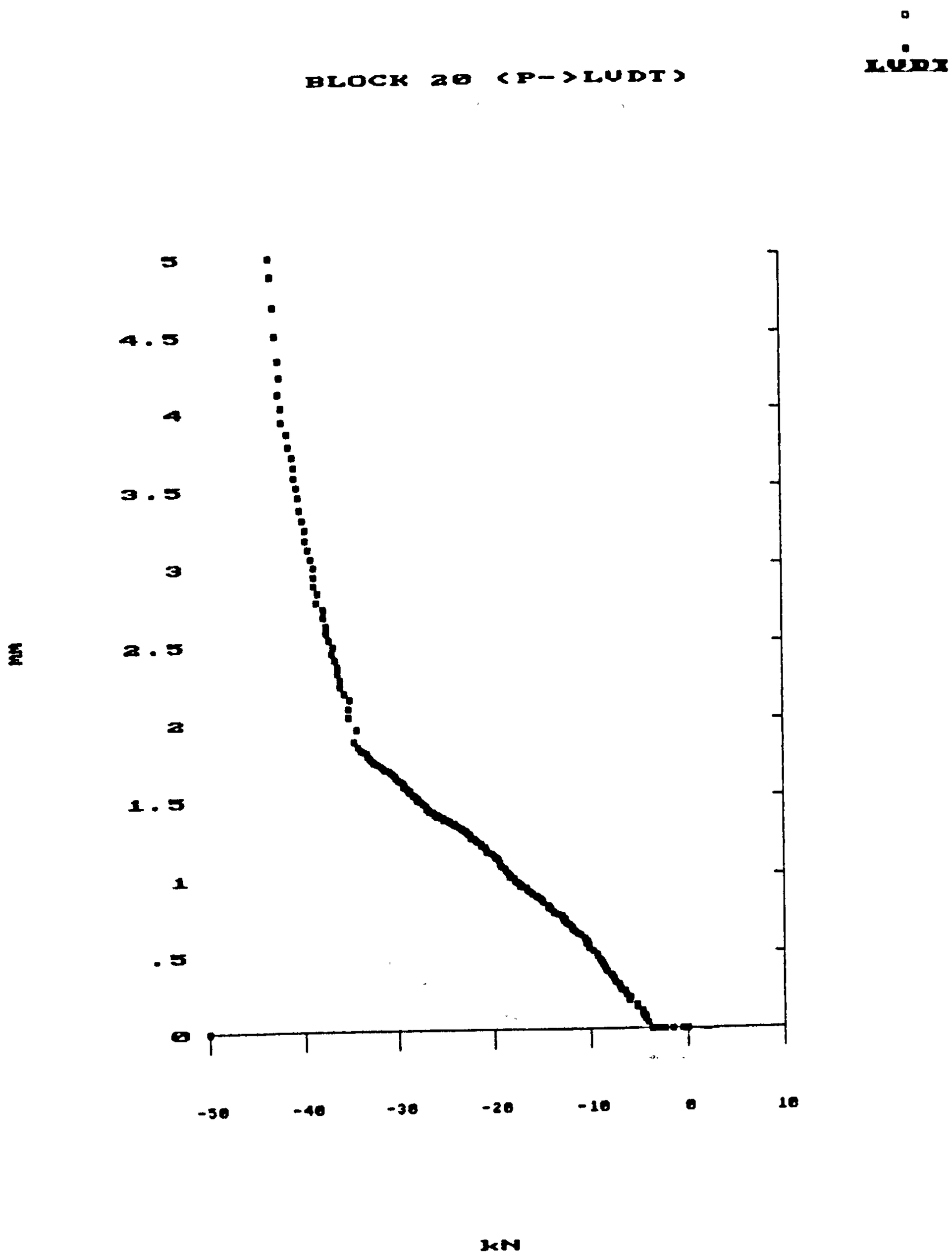

Fig 7.44

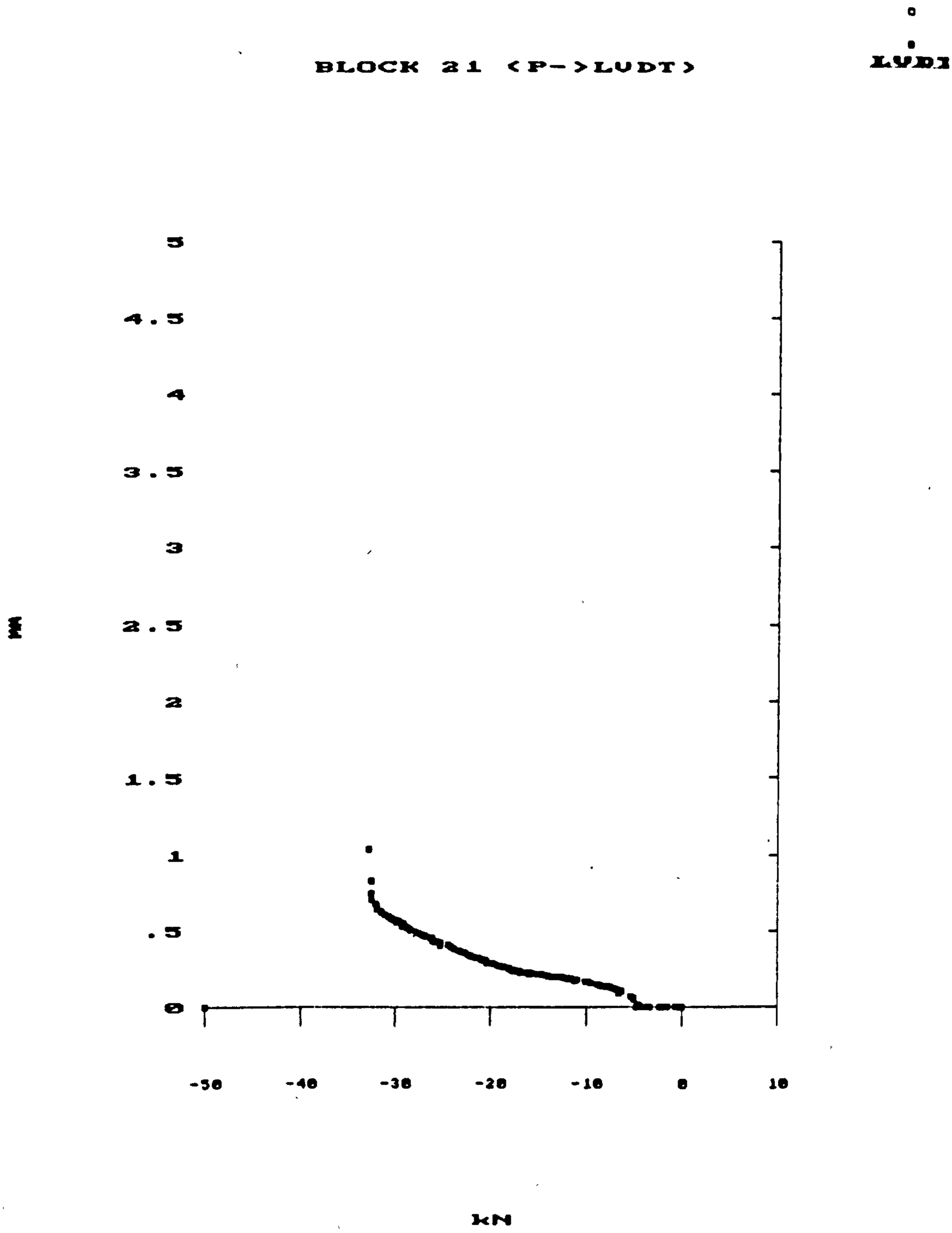

Fig. 7. 45

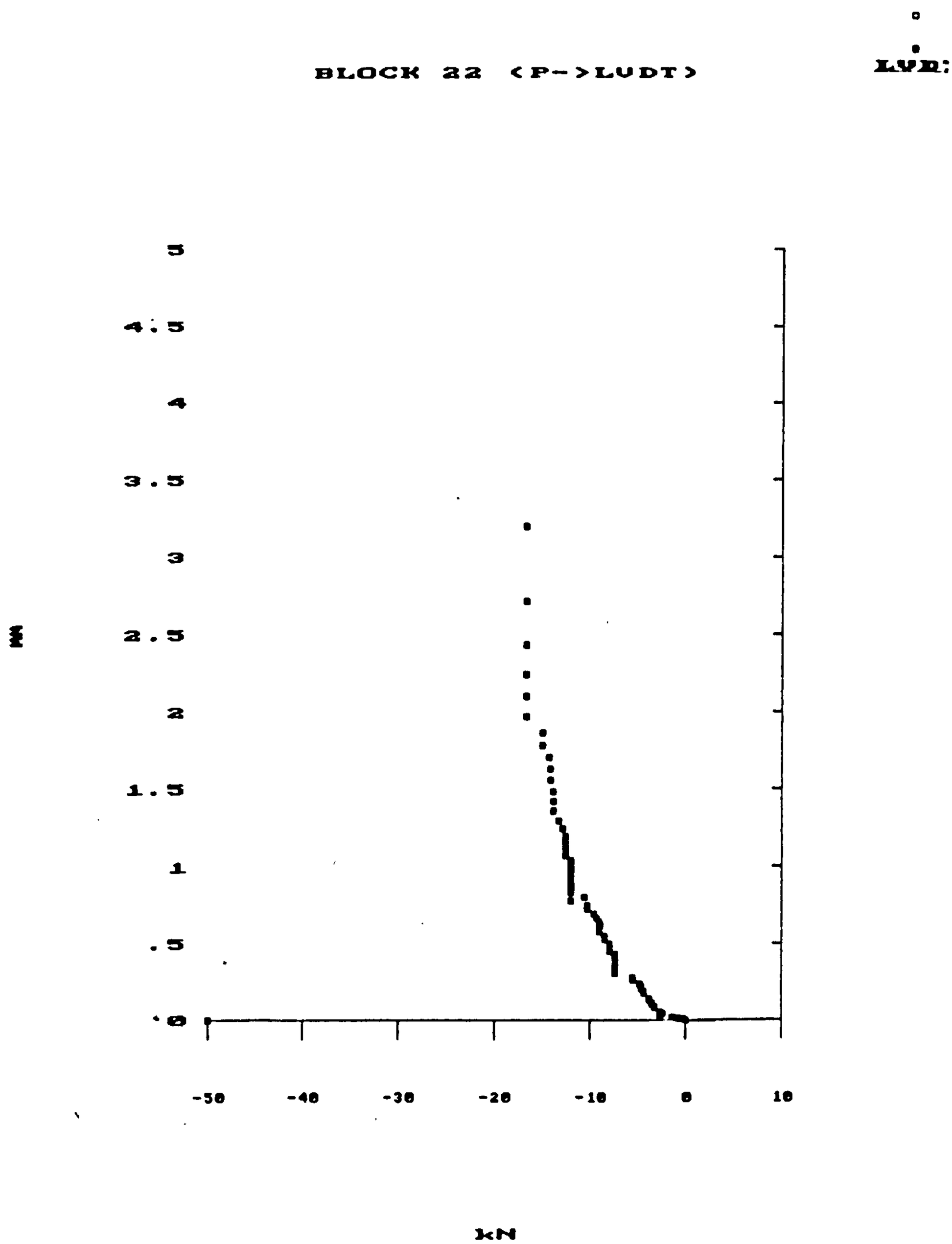

Fig. 7.46

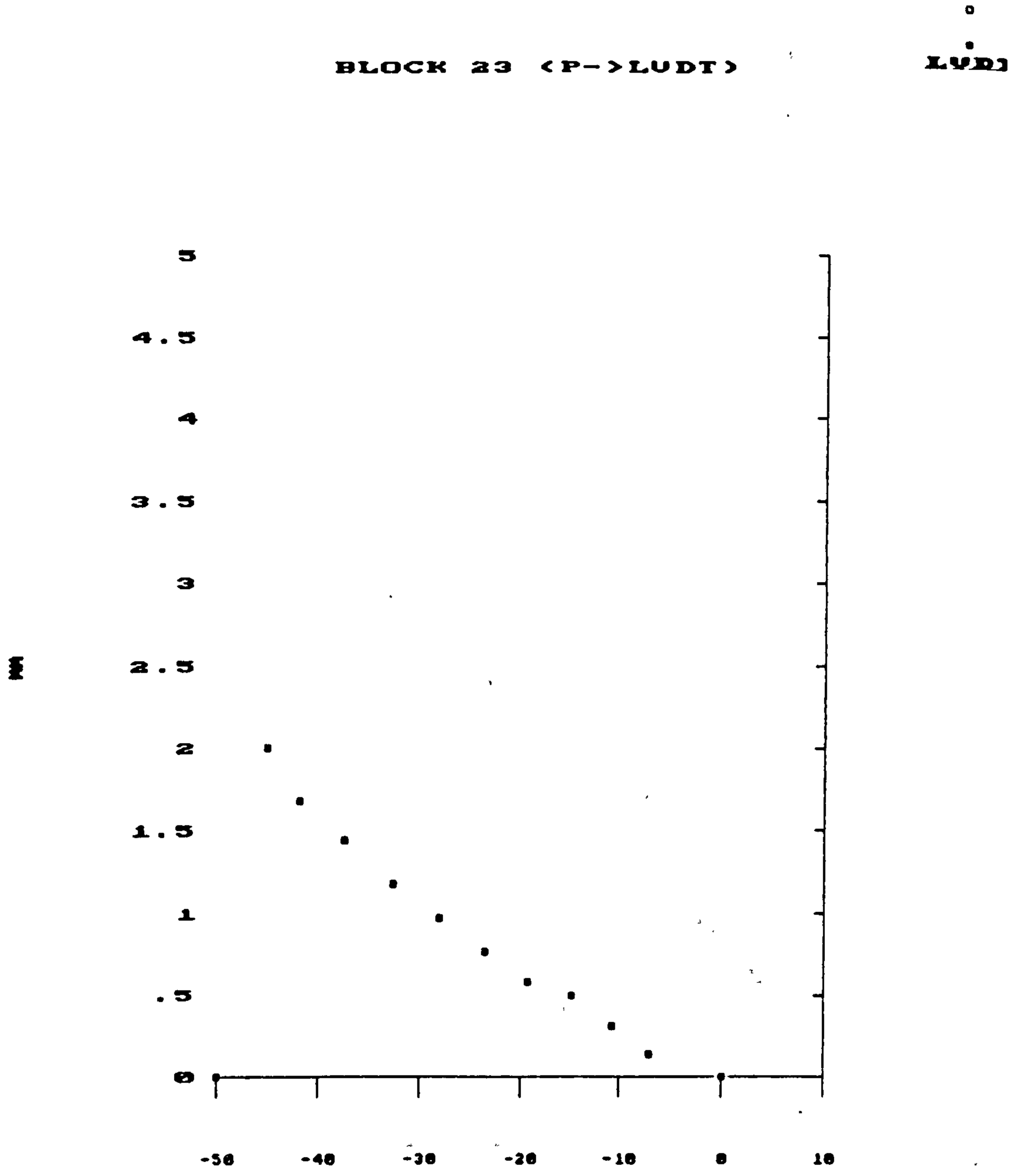

Fig 7.47

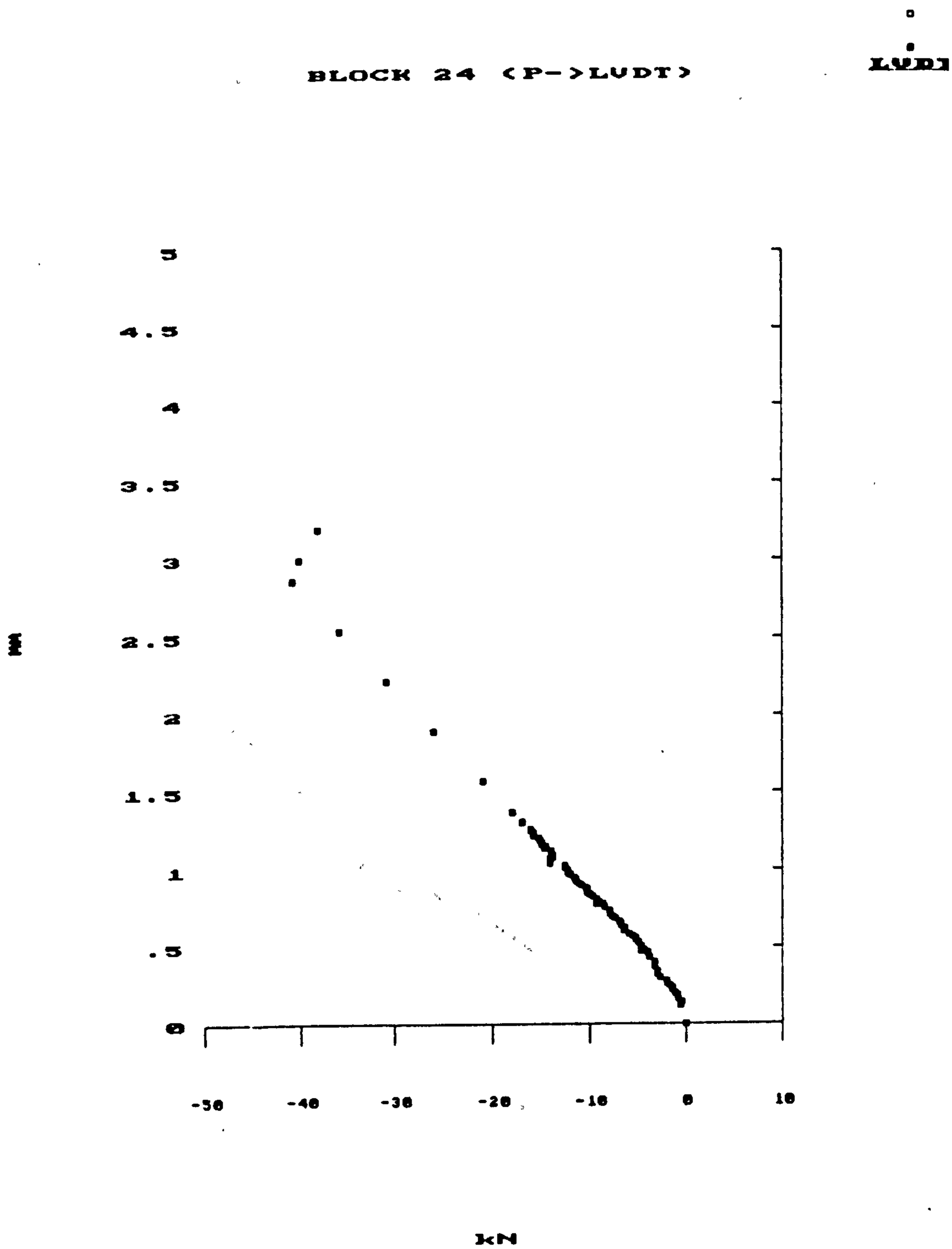

Fig. 7.48

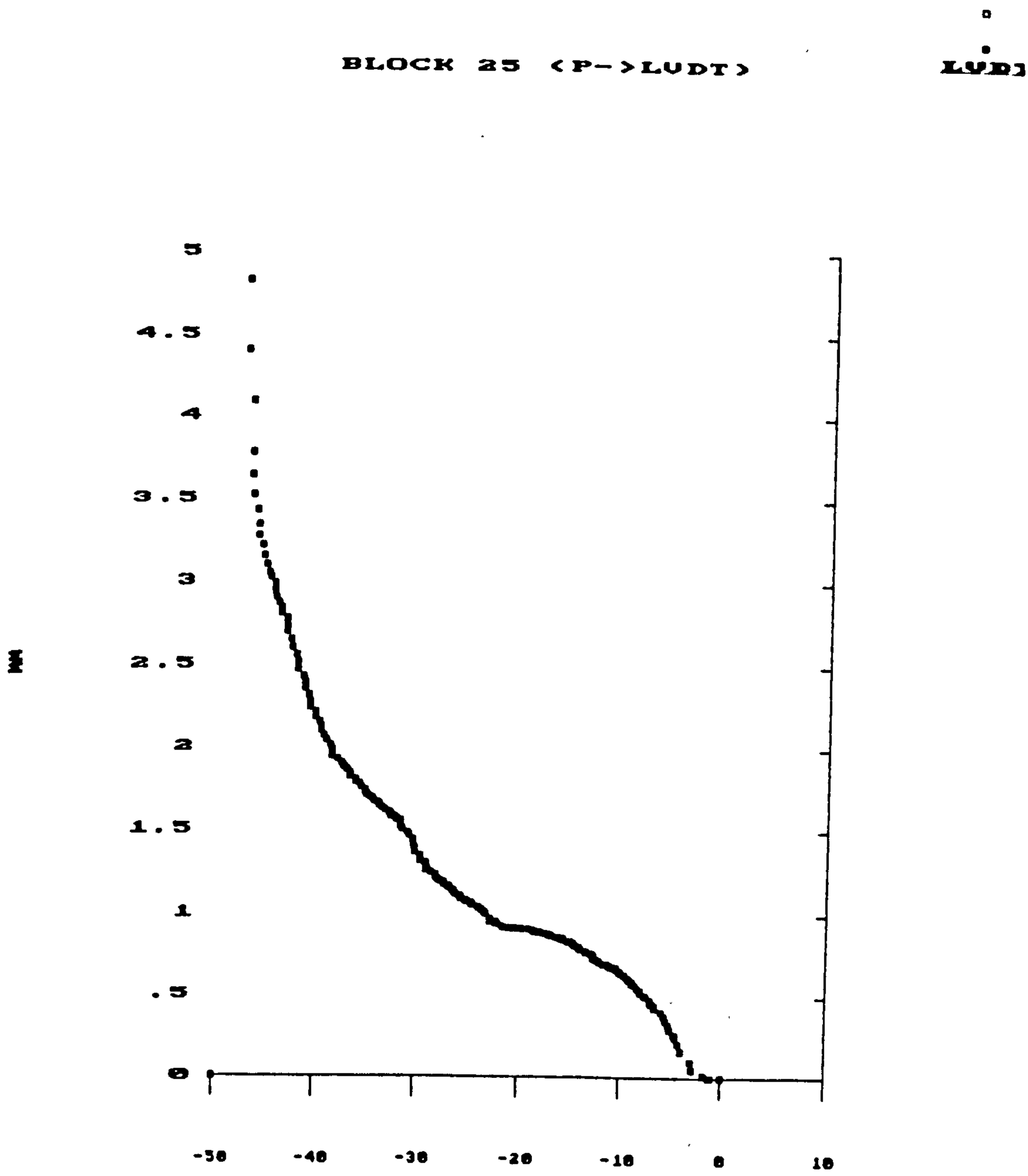

Fig. 7.49

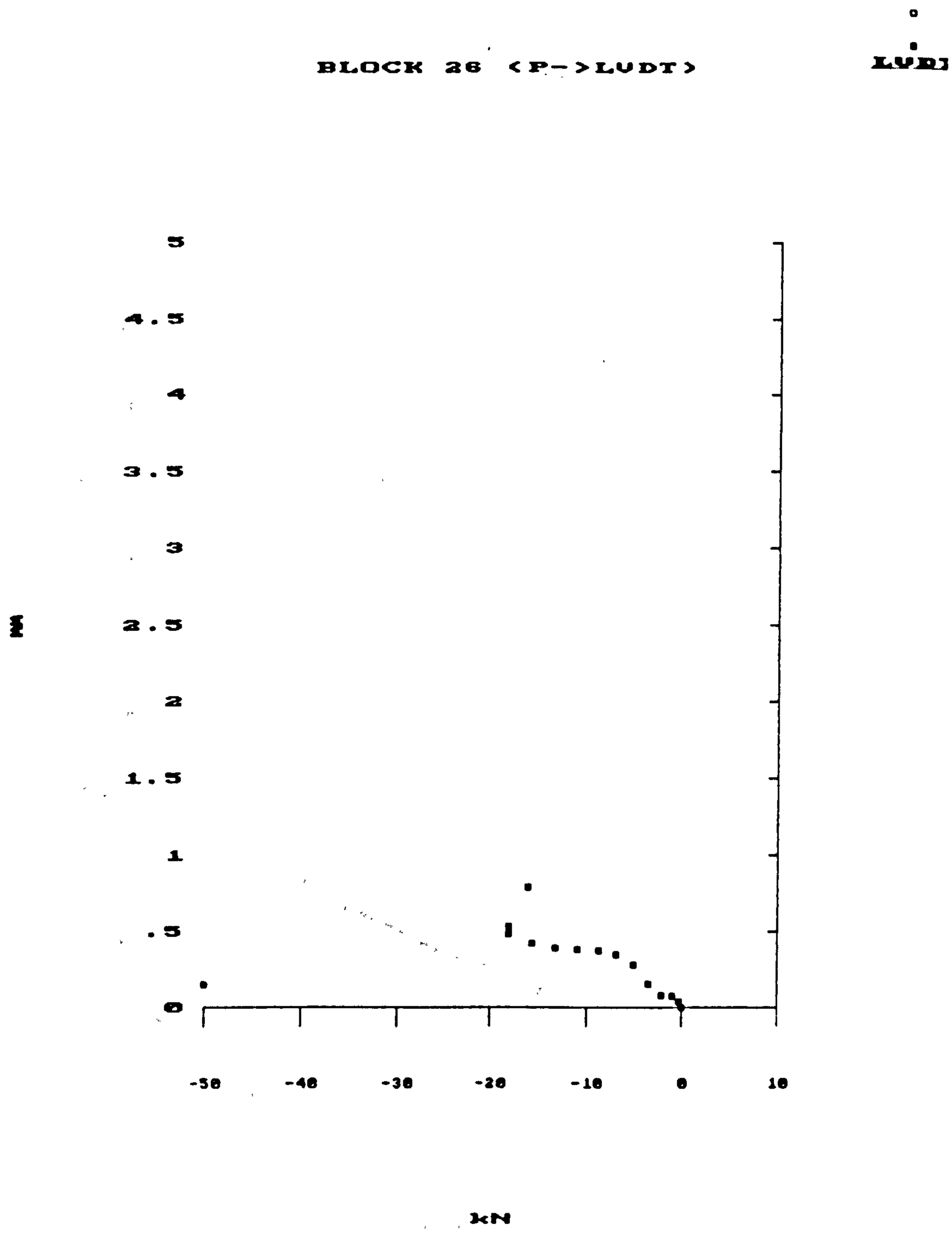

Fig. 7.50

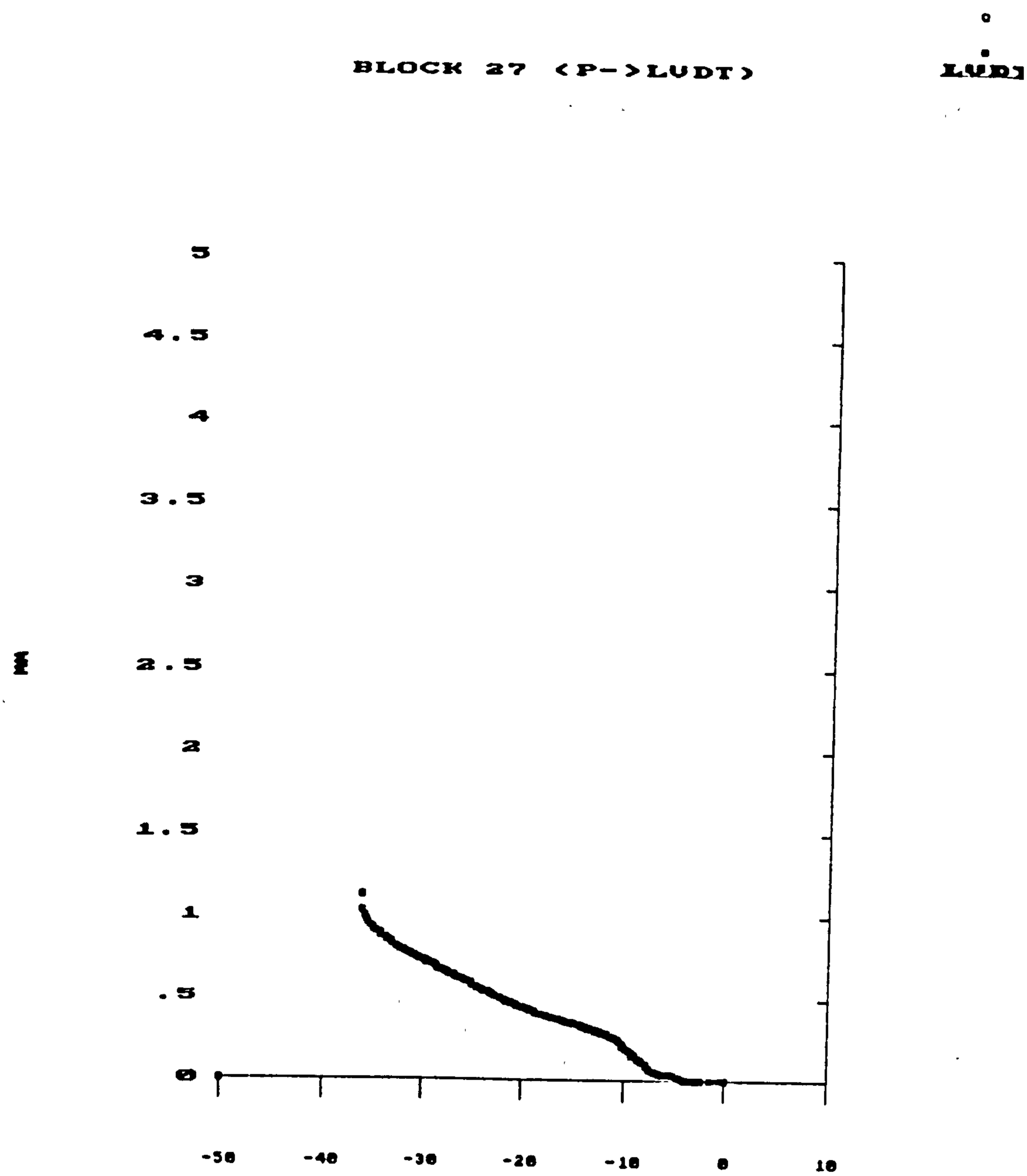

Fig. 7. 51

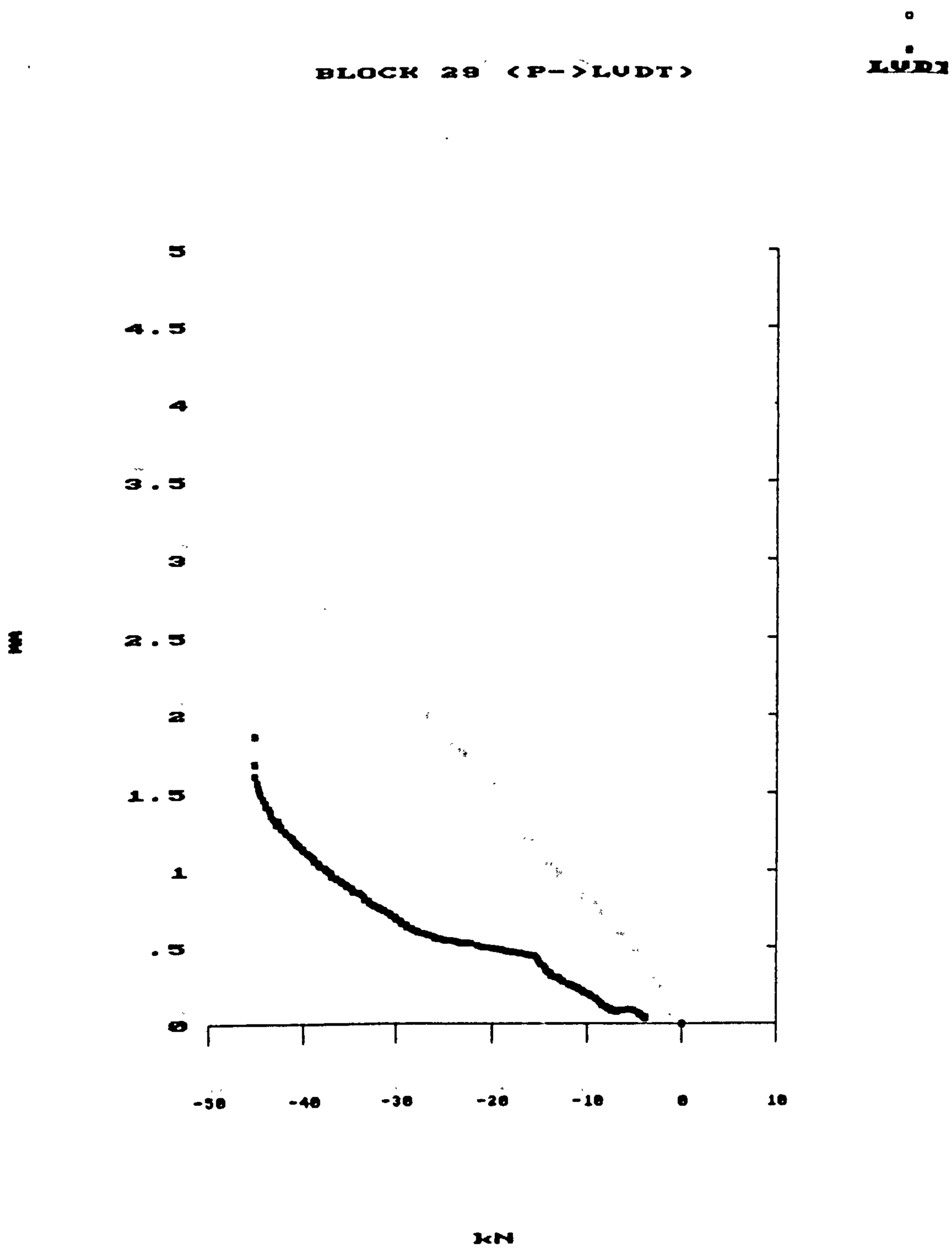

Fig. 7.52

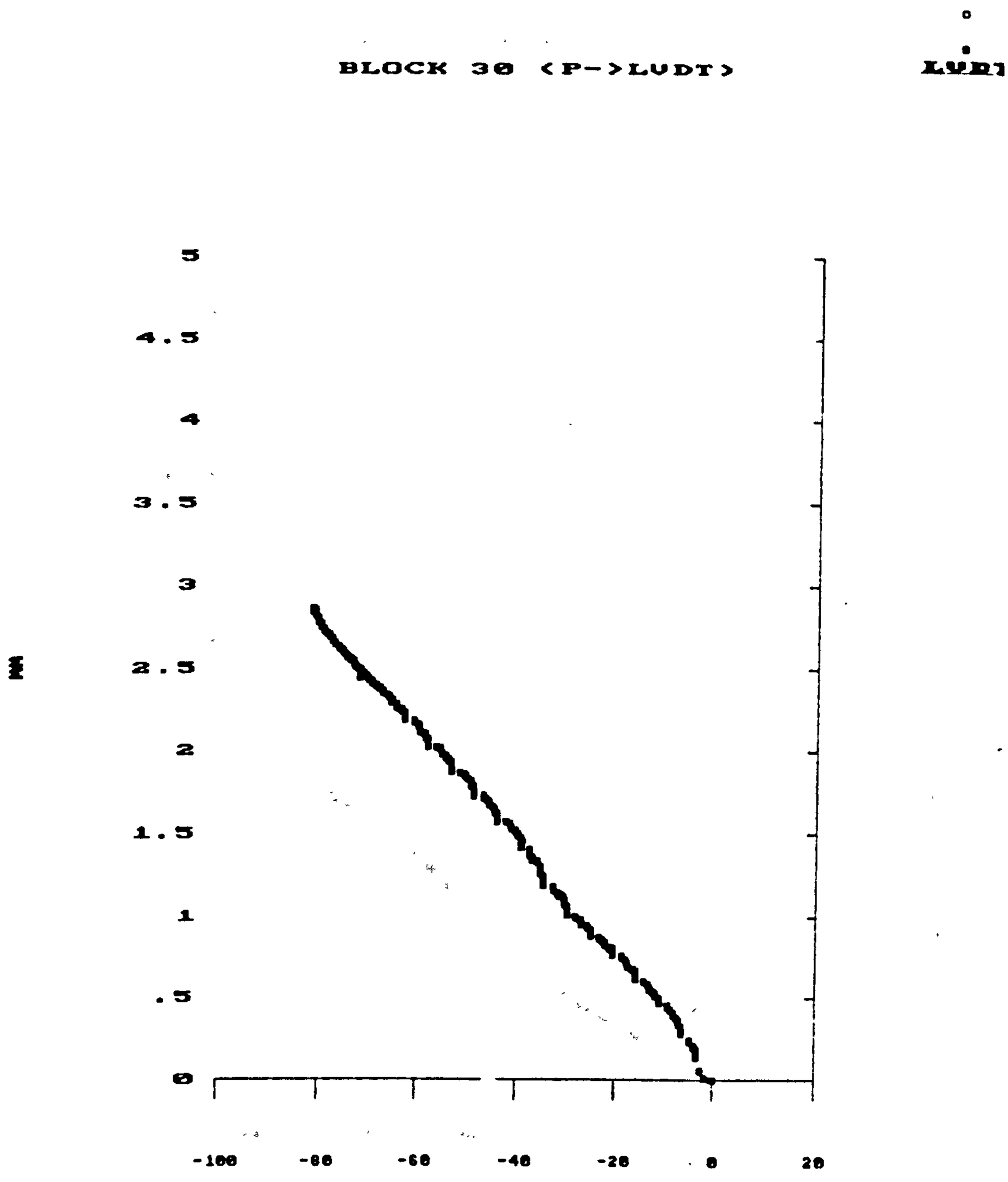

Fig. 7.53

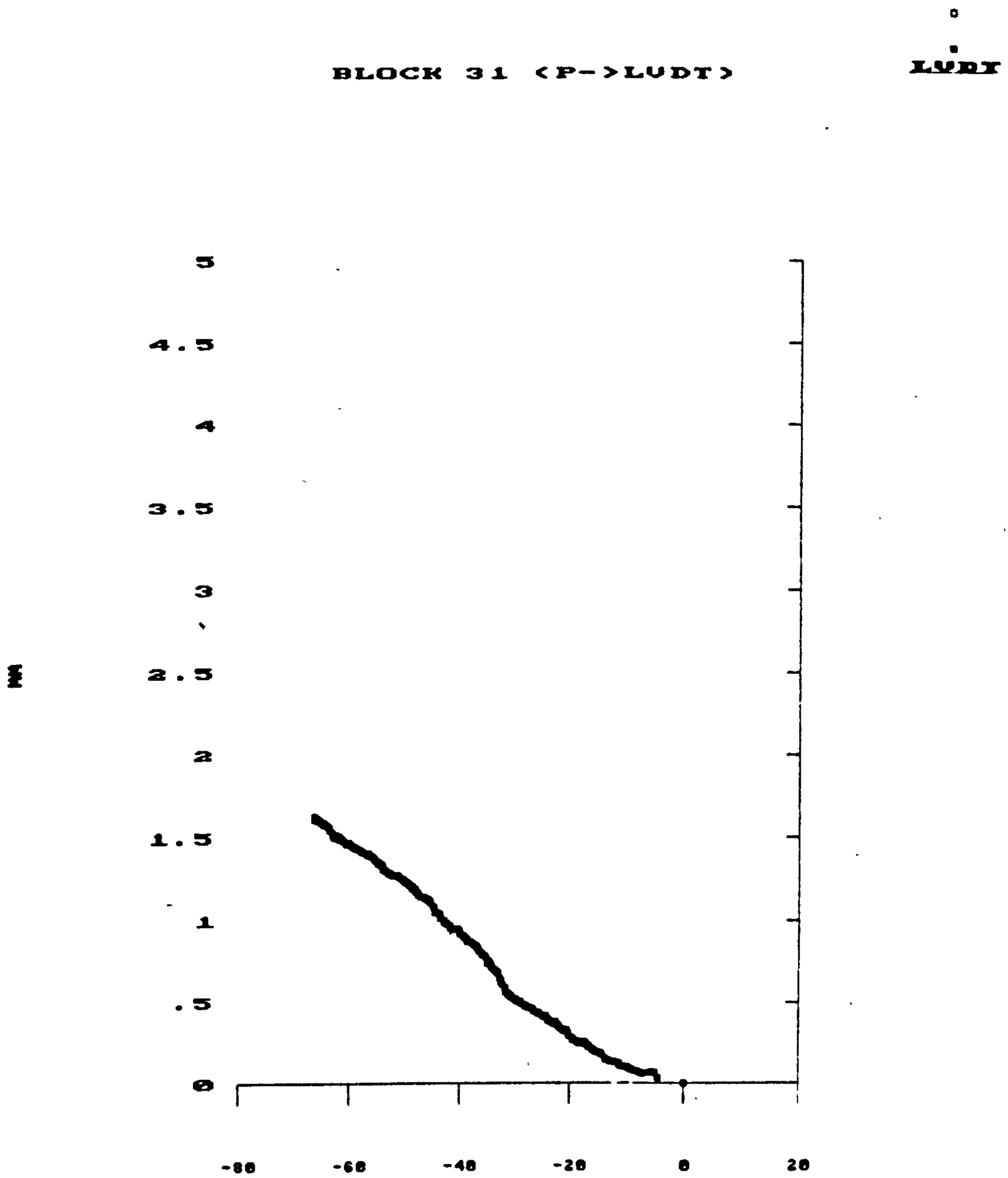

Fig. 7.54

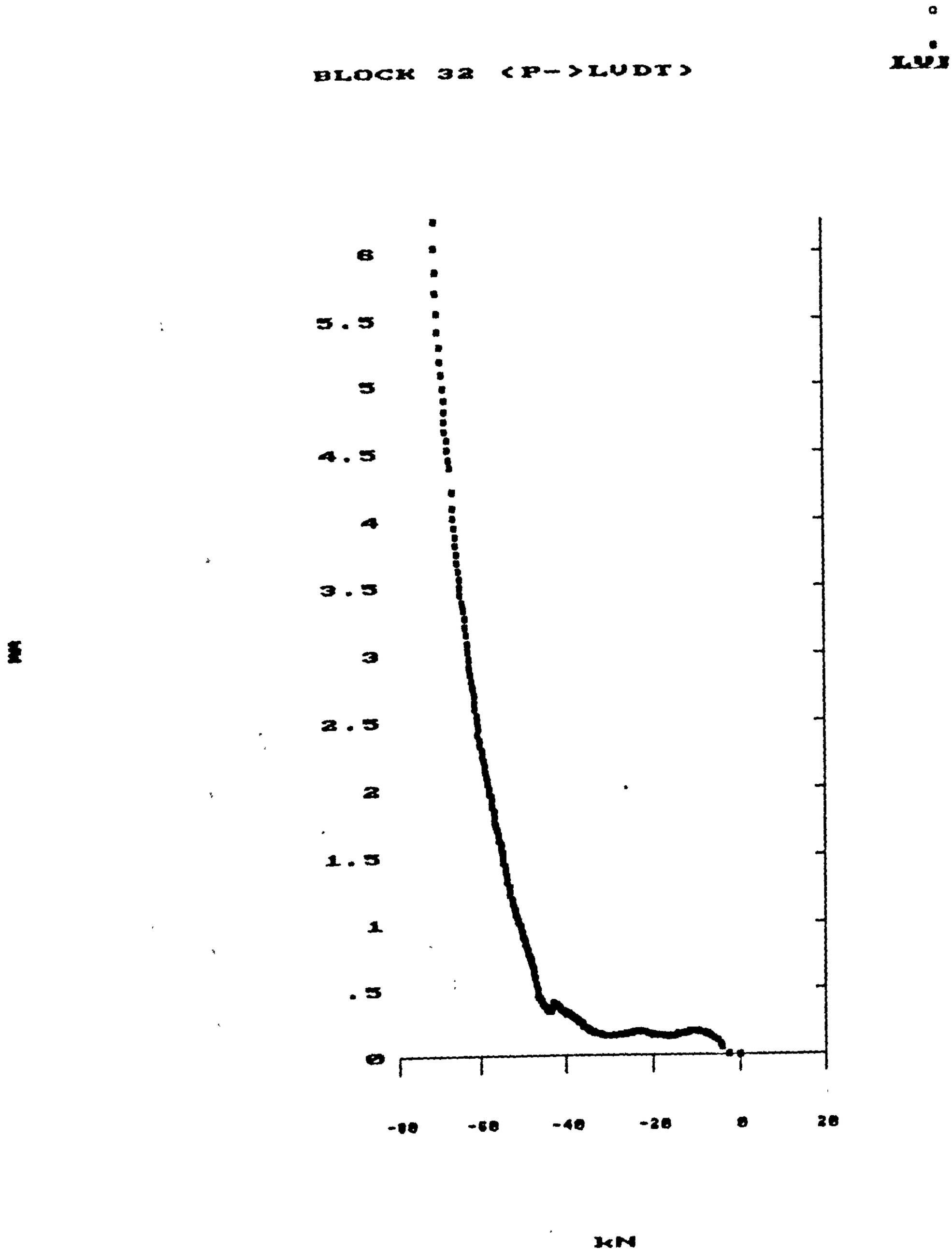

Fig. 7.55

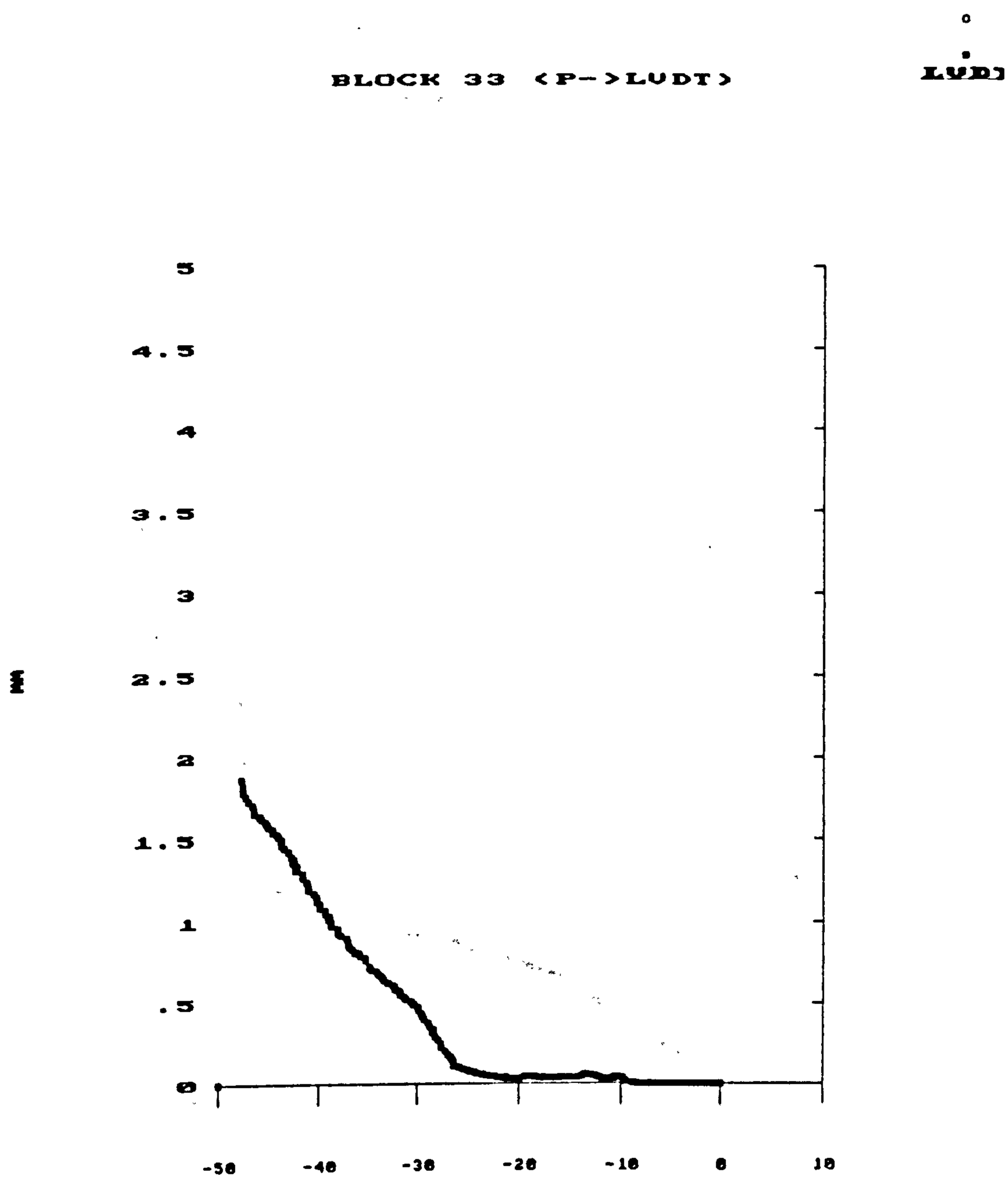

Fig. 7.56

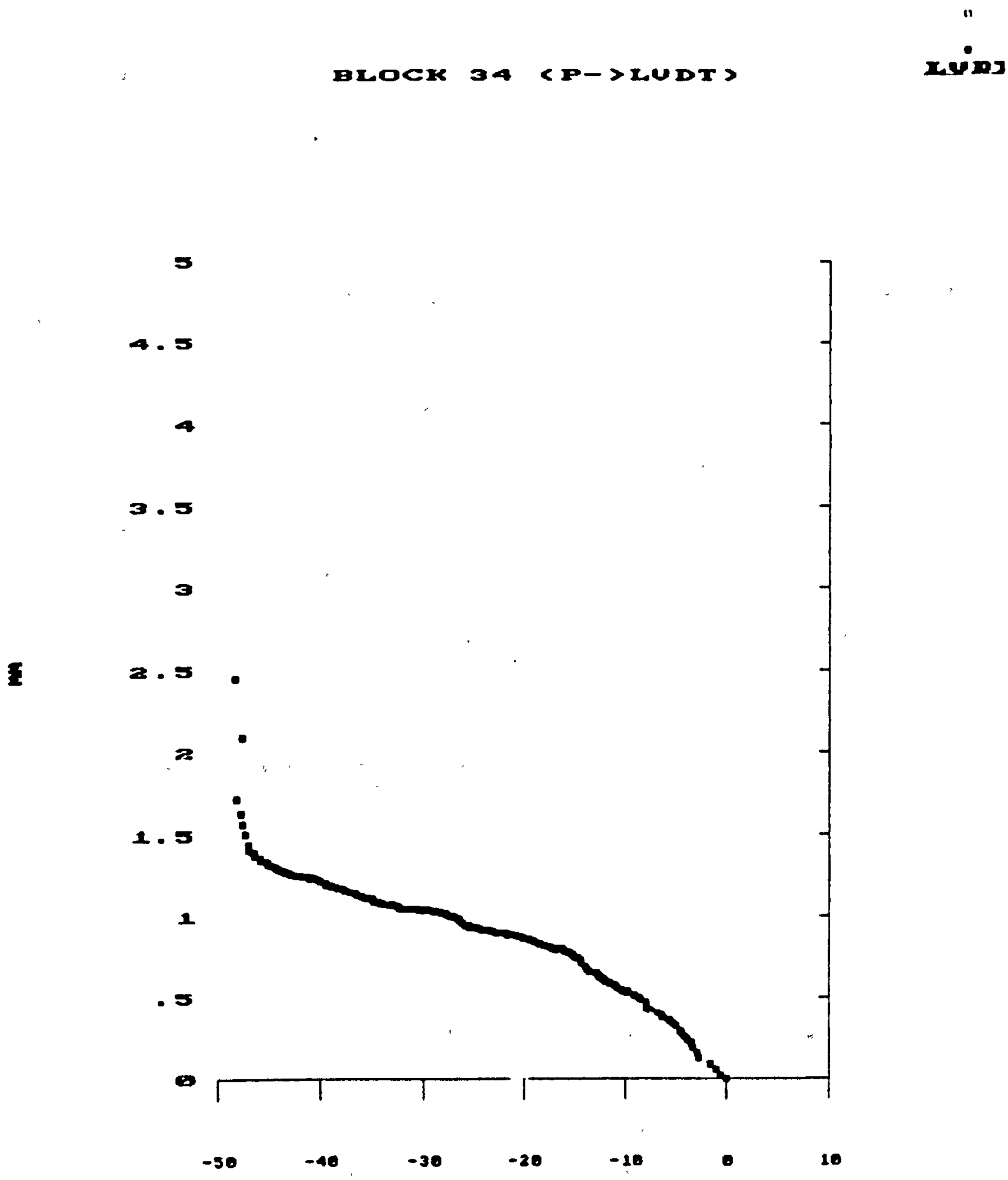

Fig. 7.57

Specimen 3.01 (O)

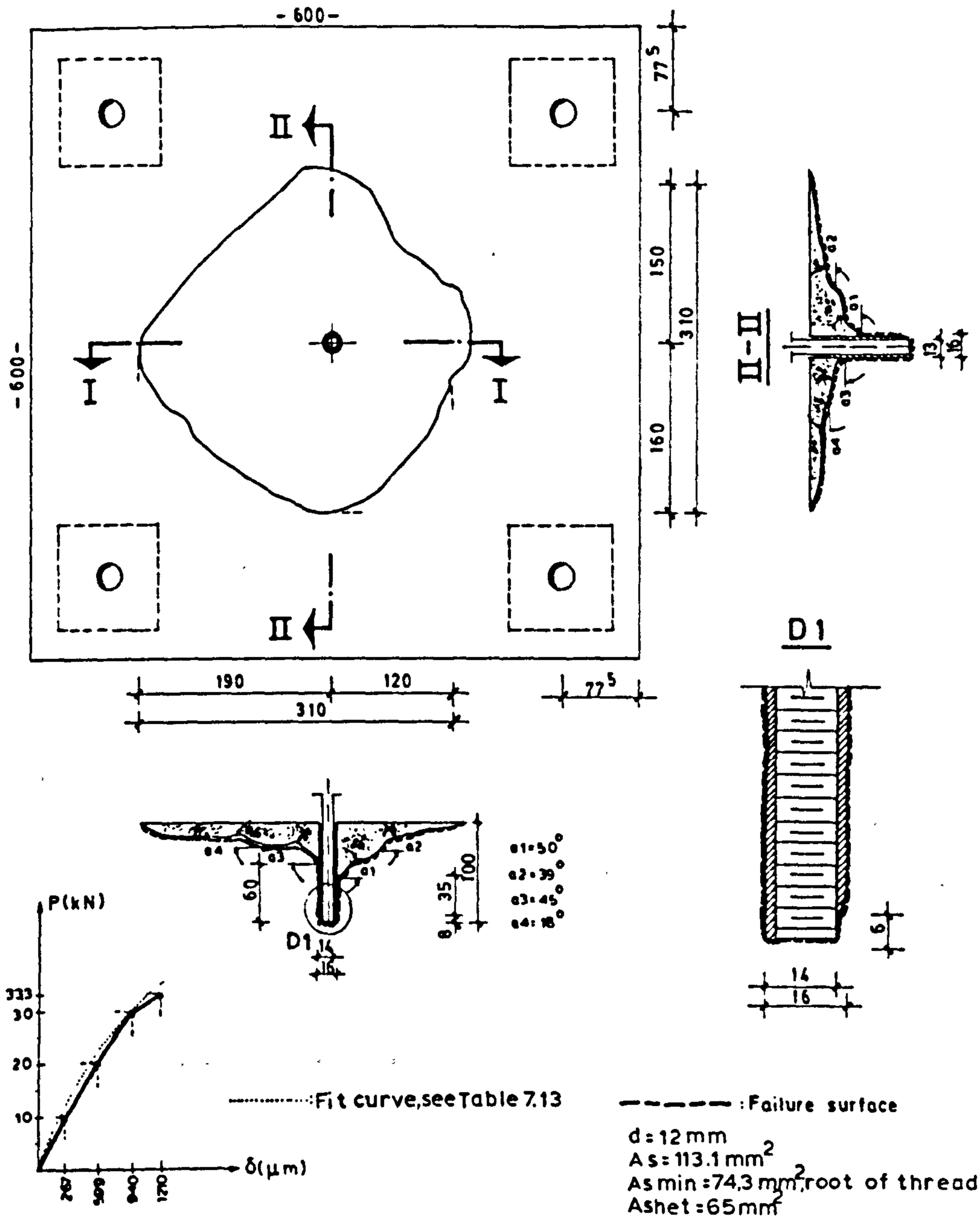

d = 12 mm
As = 113.1 mm²
As min = 74.3 mm², root of thread
Ashet = 65 mm²

Embedment length (mm): 100=(8.3)d	Method of drilling : Perc.Dr		
Type of Anchor : Thread	Method of insert. of resin: Pouring		
Anchor diameter (mm) : 12	Concrete compr.str (MPa) : 19.56		
Gap/diam of hole (mm): 2/16	Concrete tens.str. (MPa) : 2.63		
Adhesive : C 1380	Mode of failure : I+C+R		

P(kN)	δ(μm)	P(kN)	δ(μm)
5.0	161	25.0	745
10.0	267	30.0	940
15.0	445	33.3	1210
20.0	599		

Fig. 7.58

Specimen 3.02 (◐)

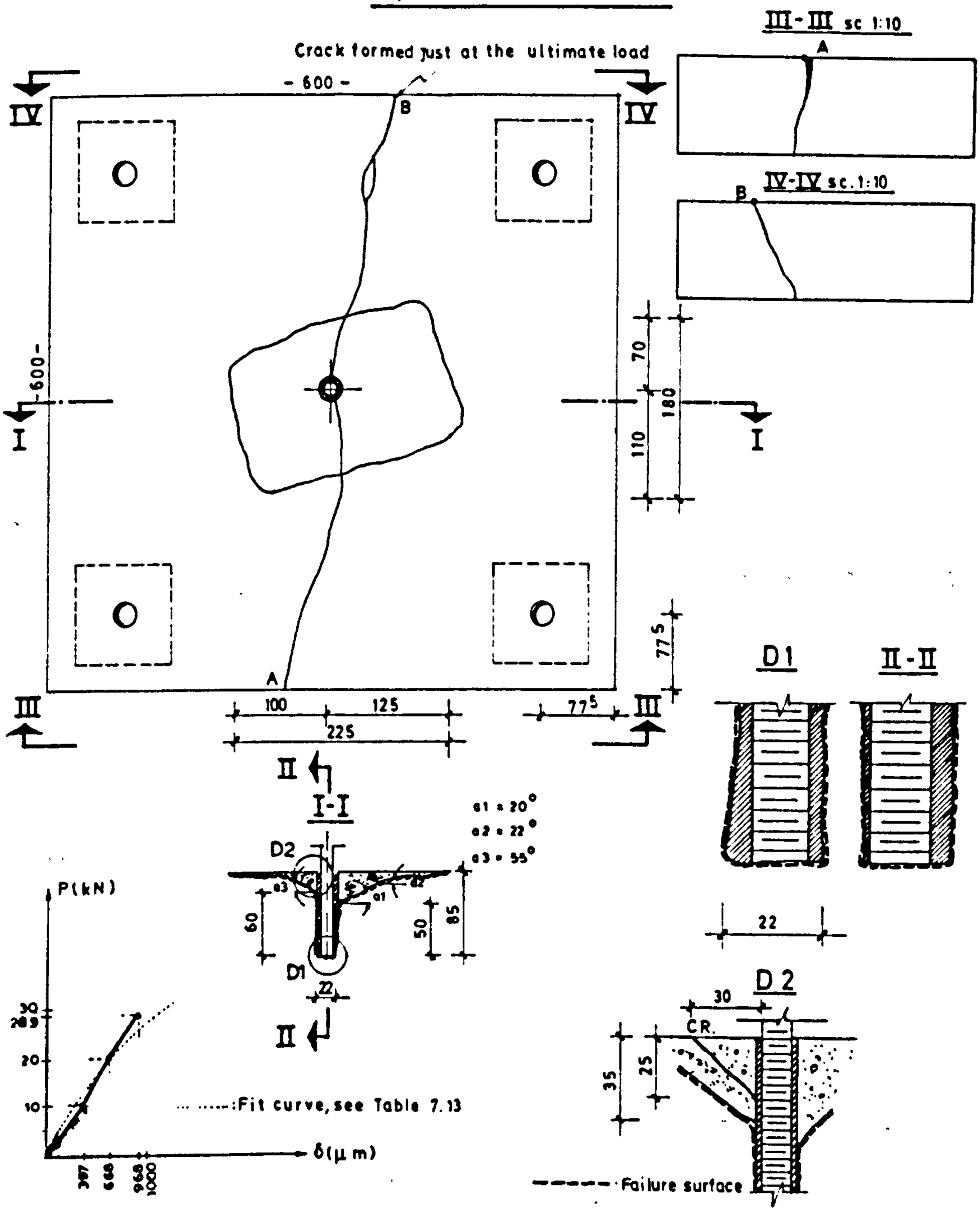

Embedment length (mm)	84=7d
Type of Anchor (mm)	:Tread.
Anchor diameter (mm)	:12
Gap/diam. of hole (mm)	:2/16
Adhesive	:C1380

Method of drilling	:Perc.Dr.
Method of insert. of resin	:Pouring
Concrete compr.str (MPa)	:20.38
Concrete tens.str. (MPa)	:2.96
Mode of failure	:I+C+R+SpA

P(kN)	δ(um)	P(kN)	δ(um)
5.0	102	25.0	857
10.0	397	28.9	968
15.0	521		
20.0	668		

Fig.7.59

Specimen 3.03 (◑)

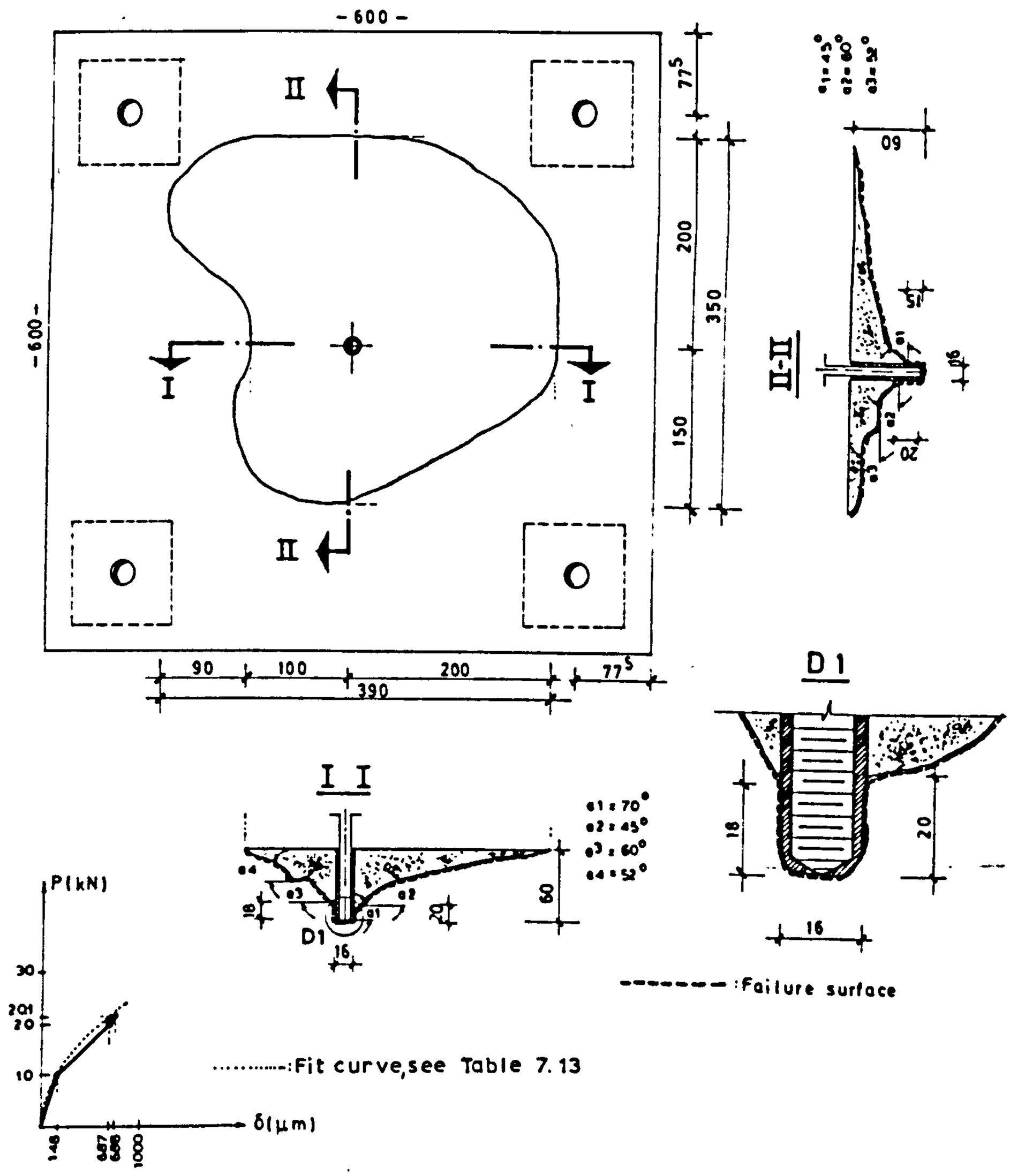

Embedment length (mm)	60=5d	Method of drilling	:Perc.Dr
Type of Anchor (mm)	:Thread.	Method of insert.of resin	:Pouring
Anchor diameter (mm)	:12	Concrete compr.str (MPa)	:21.29
Gap/diam of hole (mm)	:2/16	Concrete tens.str (MPa)	:2.64
Adhesive	:C1380	Mode of failure	:I+C+R

P(kN)	δ(μm)	P(kN)	δ(μm)
5.0	50	15.0	351
7.5	89	17.5	487
10.0	148	20.0	687
12.5	234	20.1	688

Fig. 7.60

Specimen 3.04 (□)

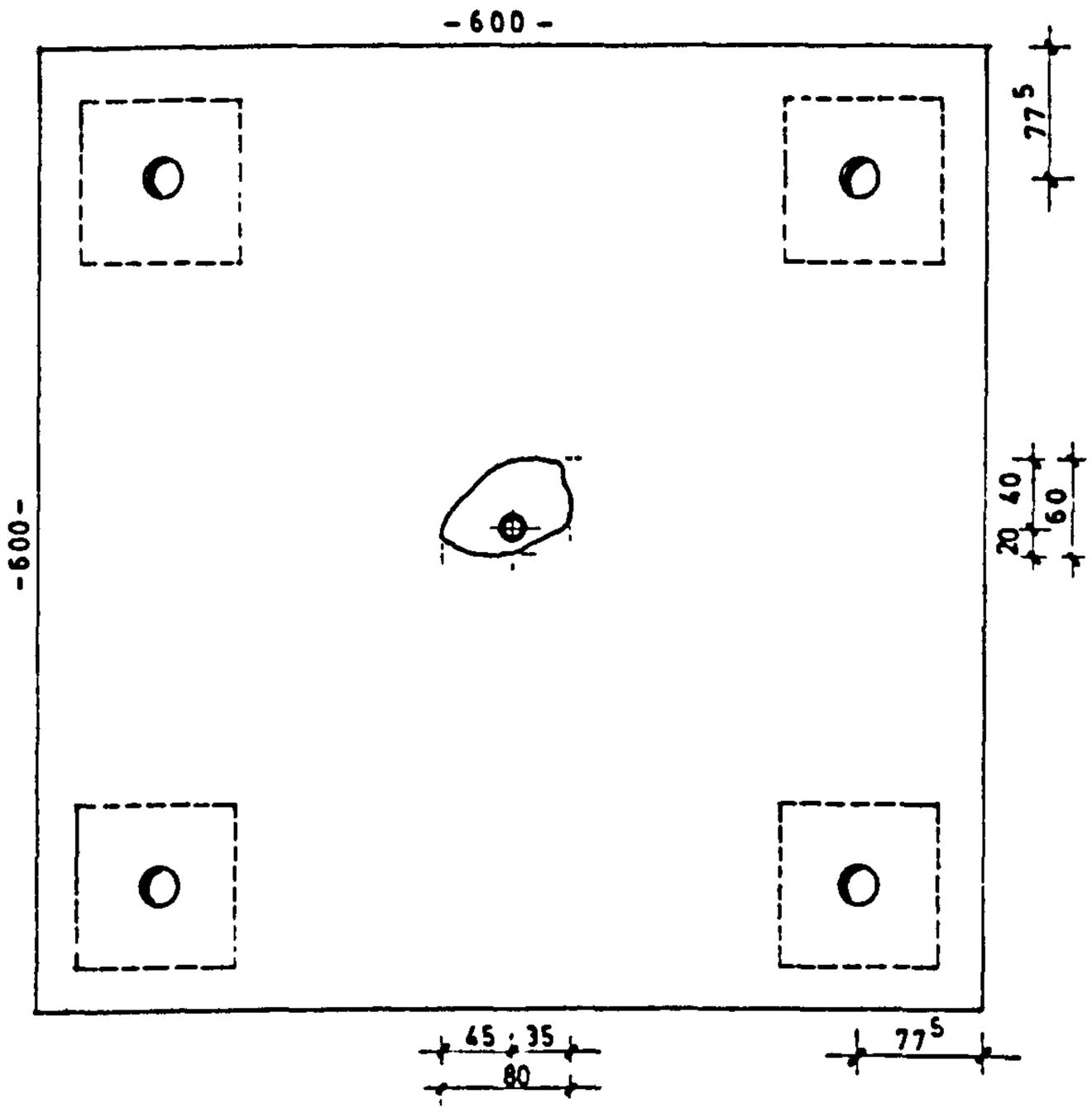

Pull out of the anchor

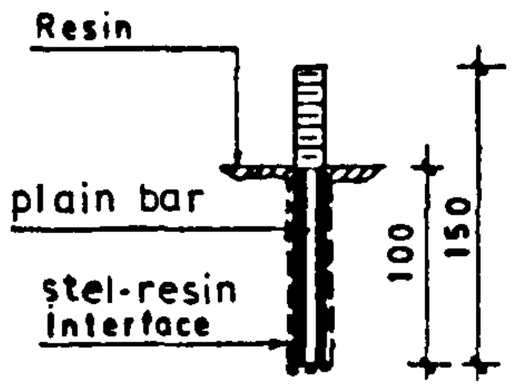

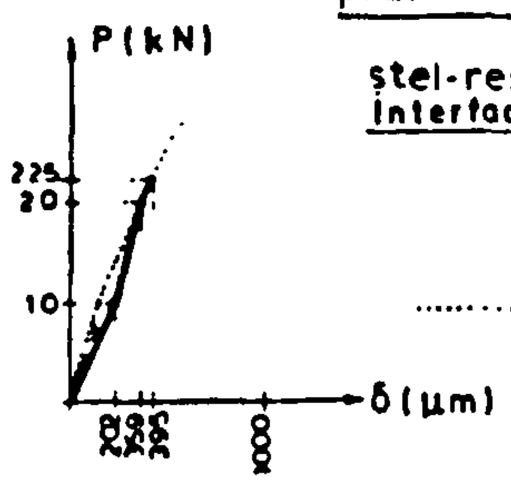

Failure surface

.....:Fit curve, see Table 7.13

Embedment length (mm)	:100=(8.3)d
Type of Anchor	:Plain b.
Anchor diameter (mm)	:12
Gap/diam.of hole (mm)	:2/16
Adhesive	:C1380

Method of drilling	:Perc.Dr
Method of insert.of resin	:Pour.
Concrete compr.str.(MPa)	:26.39
Concrete tens.str.(MPa)	:2.55
Mode of failure	: I

P(kN)	δ(μm)	P(kN)	δ(μm)
5.0	60	15.0	330
7.5	152	17.5	341
10.0	202	20.0	359
12.5	251	22.5	395

Fig.7.61

Specimen 3.05 (■)

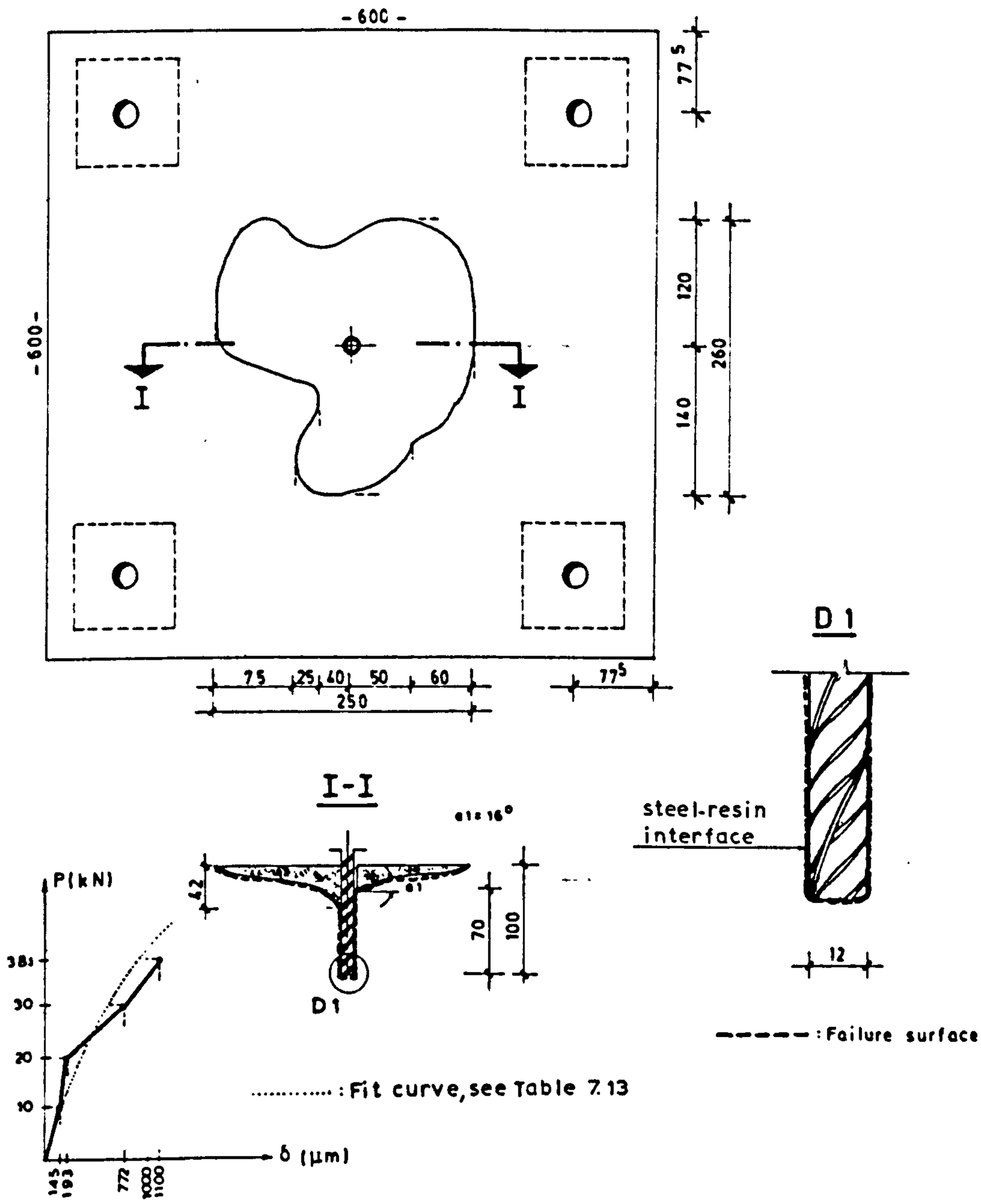

Embedment length(mm):	100=(8.3)d
Type of Anchor	:Ribbed
Anchor diameter (mm)	:12
Gap/diam.of hole(mm)	:2/16
Adhesive	:C1380

Method of drilling	:Perc.Dr
Method of insert.of resin	:Pouring
Concrete compr.str.(MPa)	:23.20
Concrete tens.str (MPa)	: 3.13
Mode of failure	:I+C+R

P(kN)	δ(μm)	P(kN)	δ(μm)
5.0	129	25.0	419
10.0	145	30.0	772
15.0	179	35.0	933
20.0	193	38.1	1100

Fig. 7.62

Specimen 3.06 (▬)

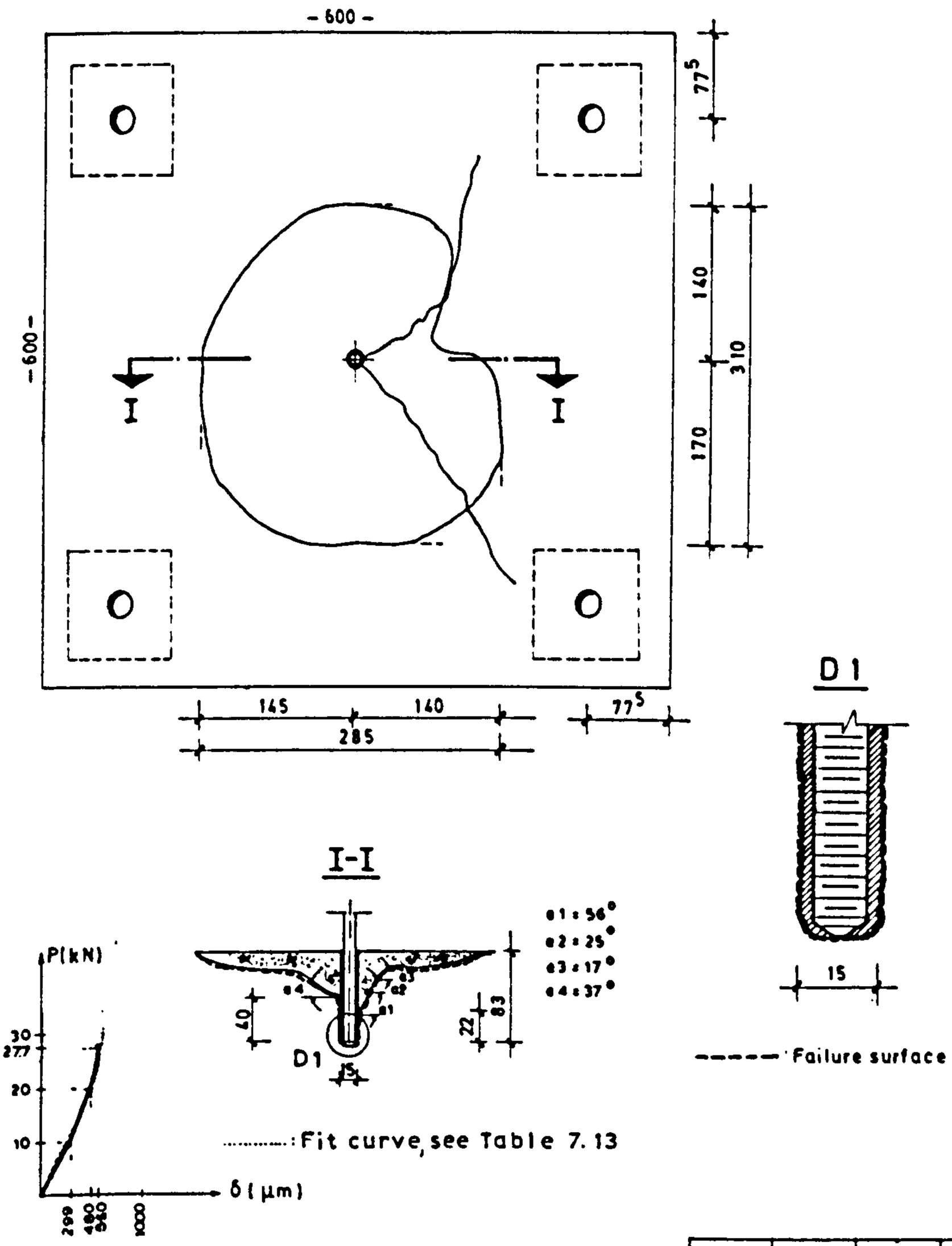

Embedment length	:83=(8.3)d
Type of Anchor	:Thread.
Anchor diameter (mm)	:10
Gap/diam.of hole (mm)	2/14
Adhesive	:C1380

Method of drilling	:Perc.Dr
Method of insert.of resin	:Pouring
Concrete compr.str.(MPa)	:23.11
Concrete tens.str.(MPa)	:2.71
Mode of failure	:I+C+R

P(kN)	δ(um)	P(kN)	δ(um)
5.0	247	17.5	440
7.5	264	20.0	480
10.0	299	22.5	510
12.5	355	25.0	530
15.0	410	27.7	550

Fig. 7.63

Specimen 3.07(▬)

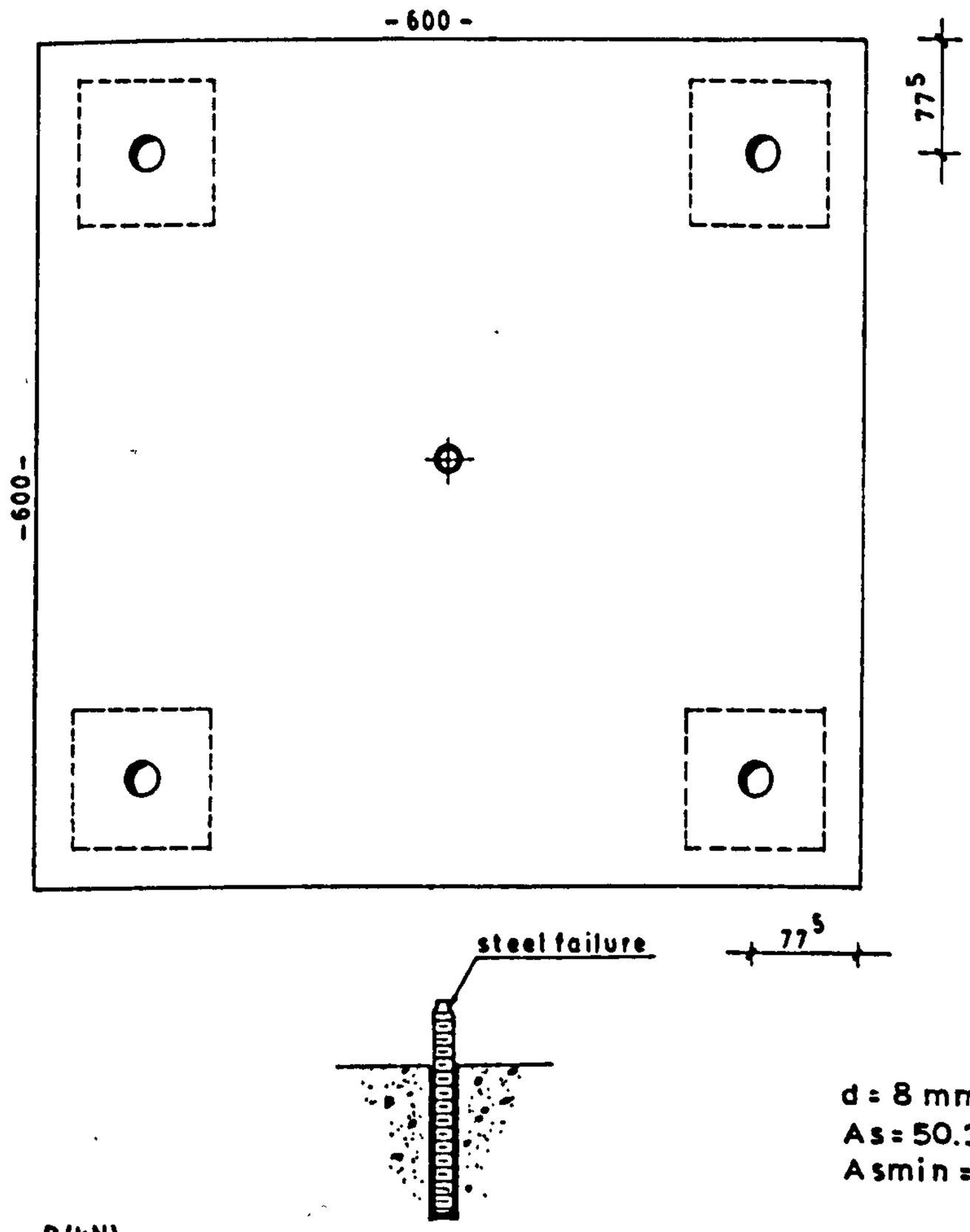

d = 8 mm
As = 50.3 mm²
Asmin = 31.9 mm², root of thread

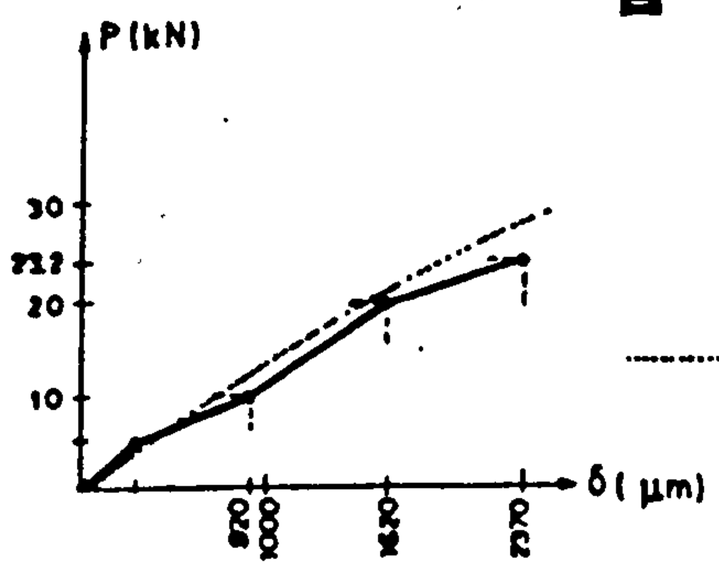

.....: Fit curve, see Table 7.13

Embedment length(mm):	66=(8.3)d
Type of Anchor	:Thread
Anchor diameter	:8
Gap/diam of hole(mm)	:2/12
Adhesive	:C1380

Method of drilling	:Perc.Dr
Method of insert.of resin	:Pouring
Concrete compr.str.(MPa)	:29.48
Concrete tens.str (MPa)	:3.68
Mode of failure	:S

P(kN)	δ(μm)	P(kN)	δ(μm)
5.0	407	15.0	1160
7.5	722	20.0	1620
10.0	920	22.5	1750
12.5	1020	23.2	2370

Fig.7.64

Specimen 3.08 (●)

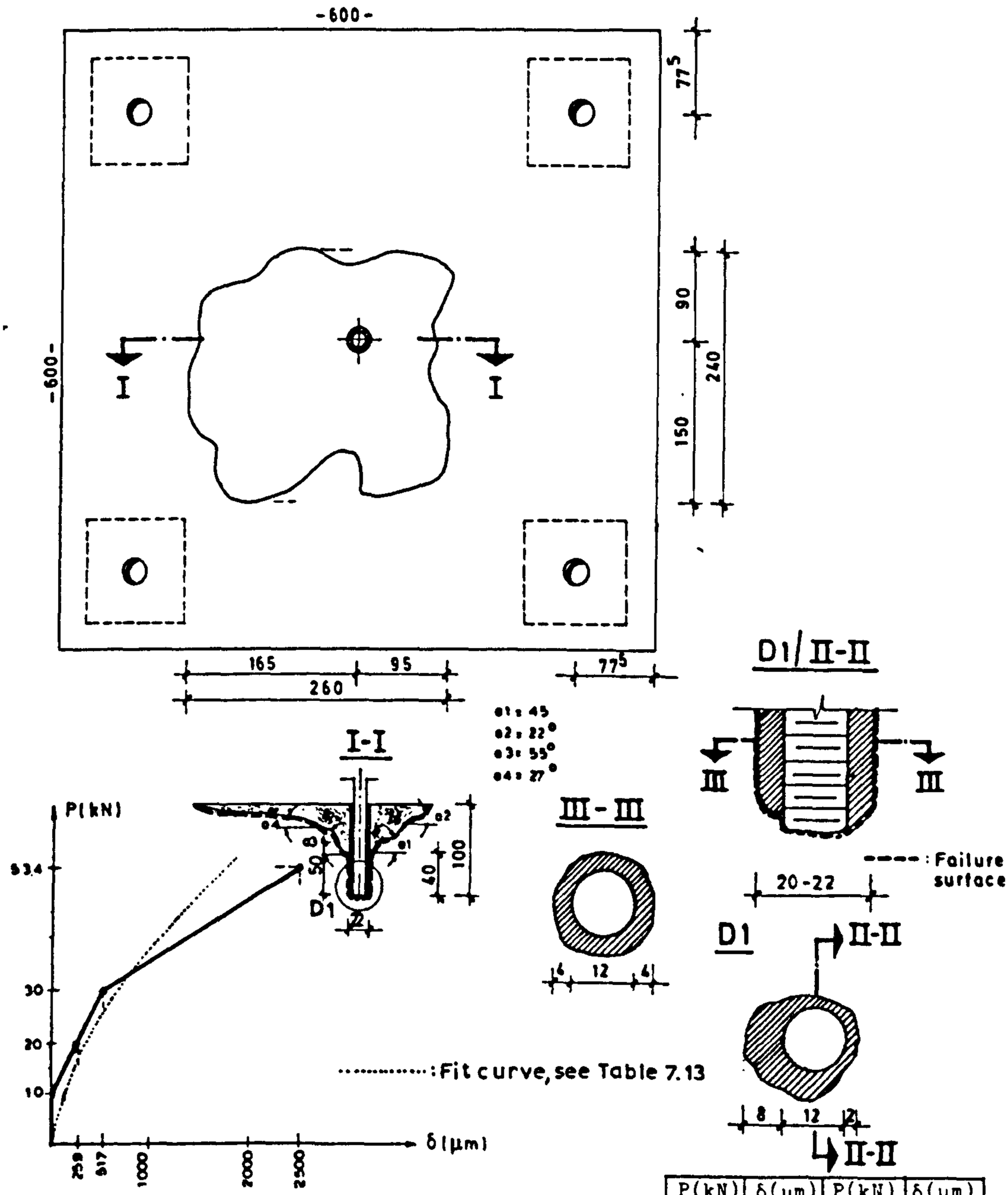

Embedment length (mm): 100=(8.3)d	
Type of Anchor (mm)	:Thread
Anchor diameter (mm)	:12
Gap/diam of hole (mm)	:4/20
Adhesive	:C1380

Method of drilling	:Perc.Dril
Methode of insert. of resin	:Pouring
Concrete compr.str. (MPa)	:28.76
Concrete tens.str. (MPa)	: 3.05
Mode of failure	:I+C+R

P(kN)	δ(um)	P(kN)	δ(um)
10.0	00.0	35.0	960
15.0	190	40.0	1240
20.0	260	45.0	1470
25.0	330	50.0	1740
30.0	518	53.4	2230

Fig. 7.65

Specimen 3.09 (◆)

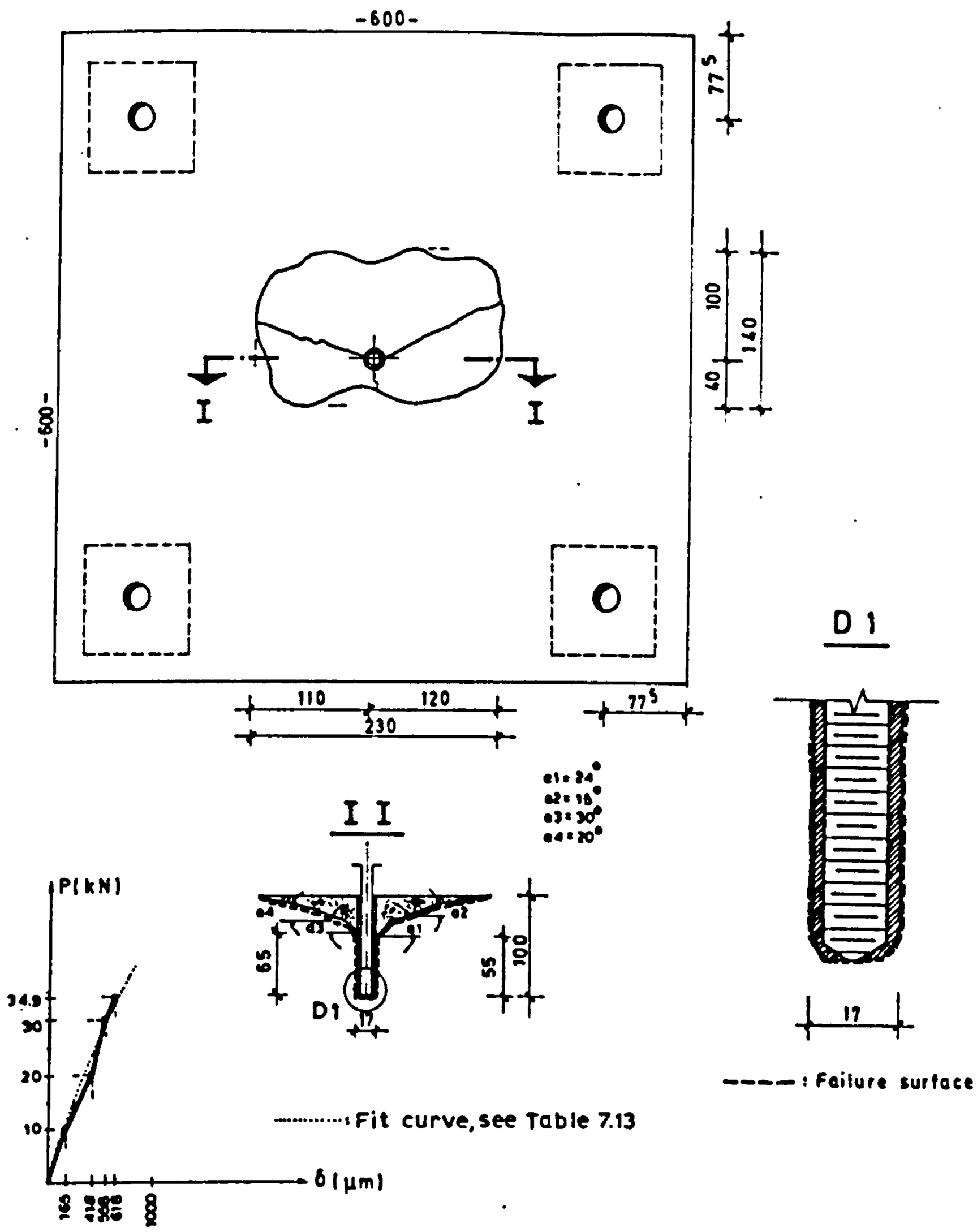

Embedment length (mm)	:100=(8.3)d	Method of drilling	:Perc.Dril	P(kN)	δ(µm)	P(kN)	δ(µm)
Type of Anchor	:Thread.	Method of insert. of resin	:Pouring	10.0	165	30.0	558
Anchor diameter (mm)	:12	Concrete compr.str.(MPa)	:31.67	15.0	308	34.9	618
Gap/diam of hole(mm)	:2/16	Concrete tens.str.(MPa)	: 2.76	20.0	418		
Adhesive	: LV	Mode of failure	:I+C+R	25.0	478		

Fig. 7.66

Specimen 3.10 (◆)

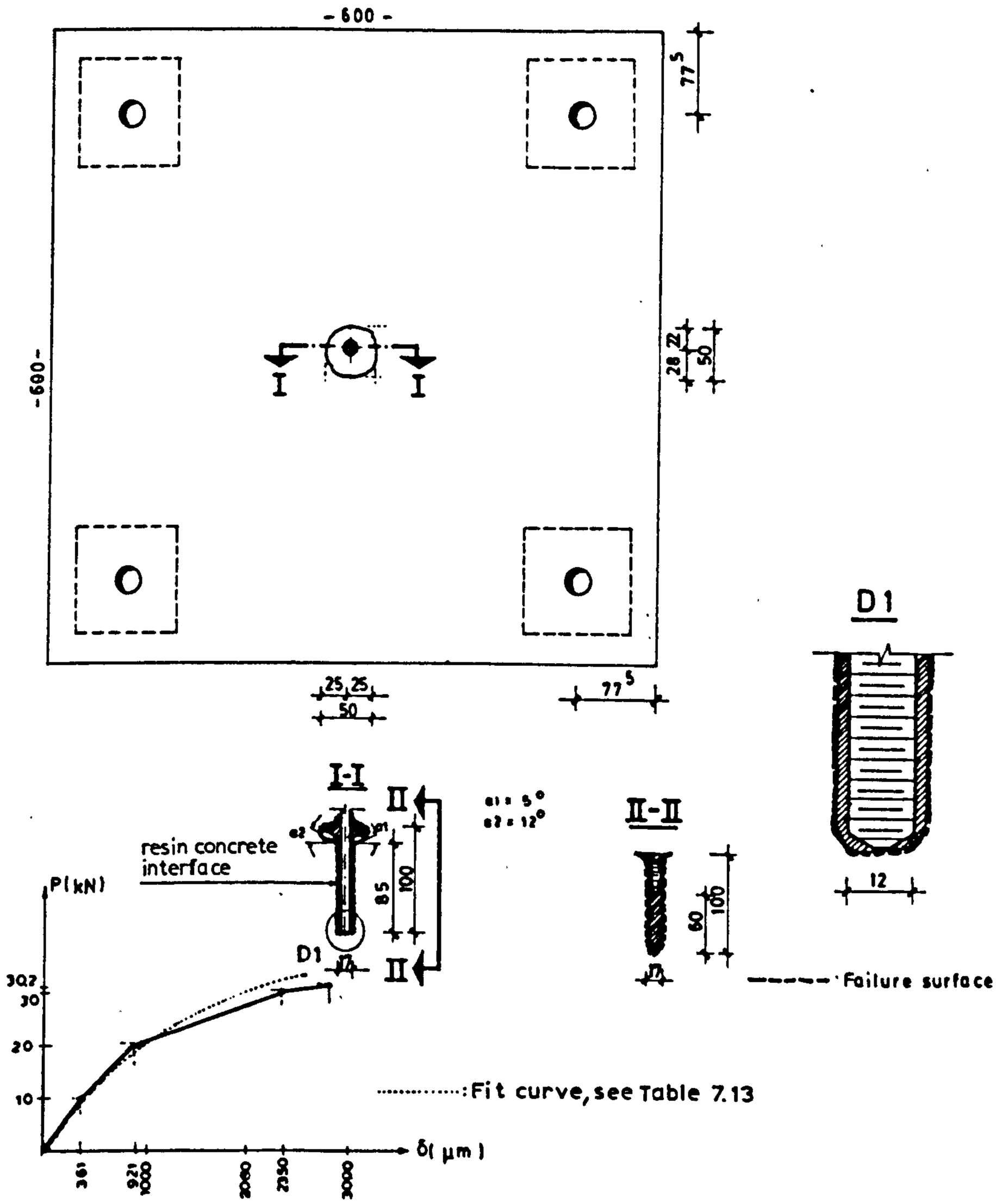

Embedment length (mm): 100=(8.3)d	
Type of Anchor	: Thread
Anchor diameter (mm)	: 12
Gap/diam. of hole (mm)	: 2/16
Adhesive	: GEL

Method of drill.	: Perc. Drill
Method of insert. of resin	: Coating
Concrete compr. str. (MPa)	: 25.30
Concrete tens. str. (MPa)	: 2.61
Mode of failure	: I

P(kN)	δ(μm)	P(kN)	δ(μm)
10.0	361	30.0	2350
15.0	639	30.2	2520
20.0	921		
25.0	1320		

Fig.7.67

Specimen 3.11 (⊕)

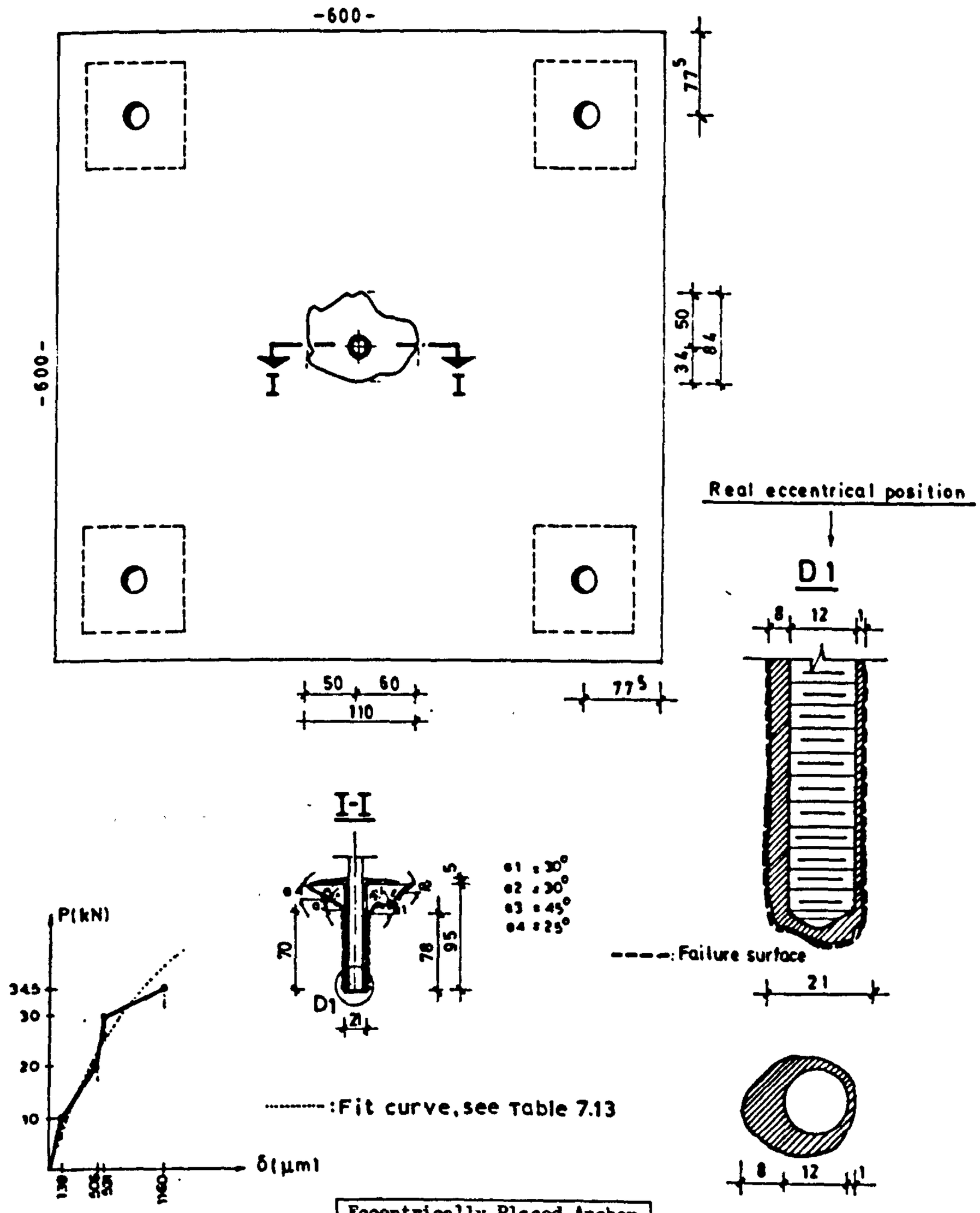

Embedment length(mm)	:100=(8.3)d
Type of Anchor	:Thread.
Anchor diameter (mm)	:12
Gap/diam.of hole(mm)	:4/20
Adhesive	:C1380

Eccentrically Placed Anchor	
Method of drilling	:Perc.Dri
Method of insert.of resin	:Pouring
Concrete compr.str.(MPa)	:28.48
Concrete tens.str.(MPa)	: 2.51
Mode of failure	:I+C+R

P(kN)	δ(μm)	P(kN)	δ(μm)
10.0	139	30.0	531
15.0	359	34.5	1160
20.0	506		
25.0	522		

Fig. 7.68

Specimen 3.12 (⊖)

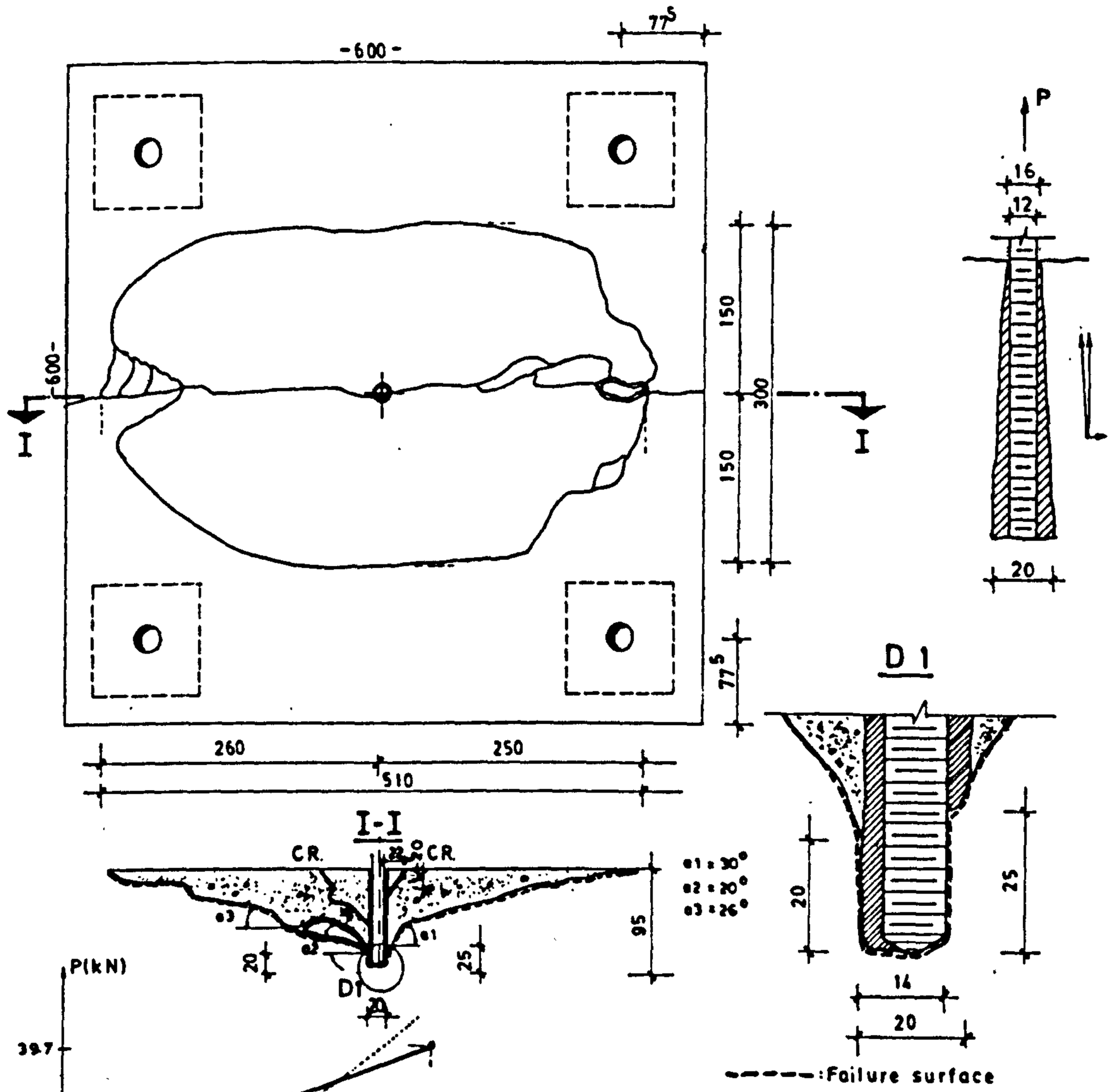

Embedment length (mm):	95=(7.9)d
Type of Anchor	:Thread
Anchor diameter (mm)	:12
Gap/diam.of hole (mm)	:2/16
Adhesive	:C1380

Method of drill.	:Perc.Dri
Method of insert.of resin	:Pouring
Concrete compr.str.(MPa)	: 21.93
Concrete tens.str.(MPa)	: 2.58
Mode of failure	:Split+R

P(kN)	δ(μm)	P(kN)	δ(μm)
10.0	861	35.0	2500
15.0	1300	37.5	2760
20.0	1610	39.0	3070
25.0	1850	39.7	3143
30.0	2150		

Fig.7.69

Specimen 3.13 (◇)

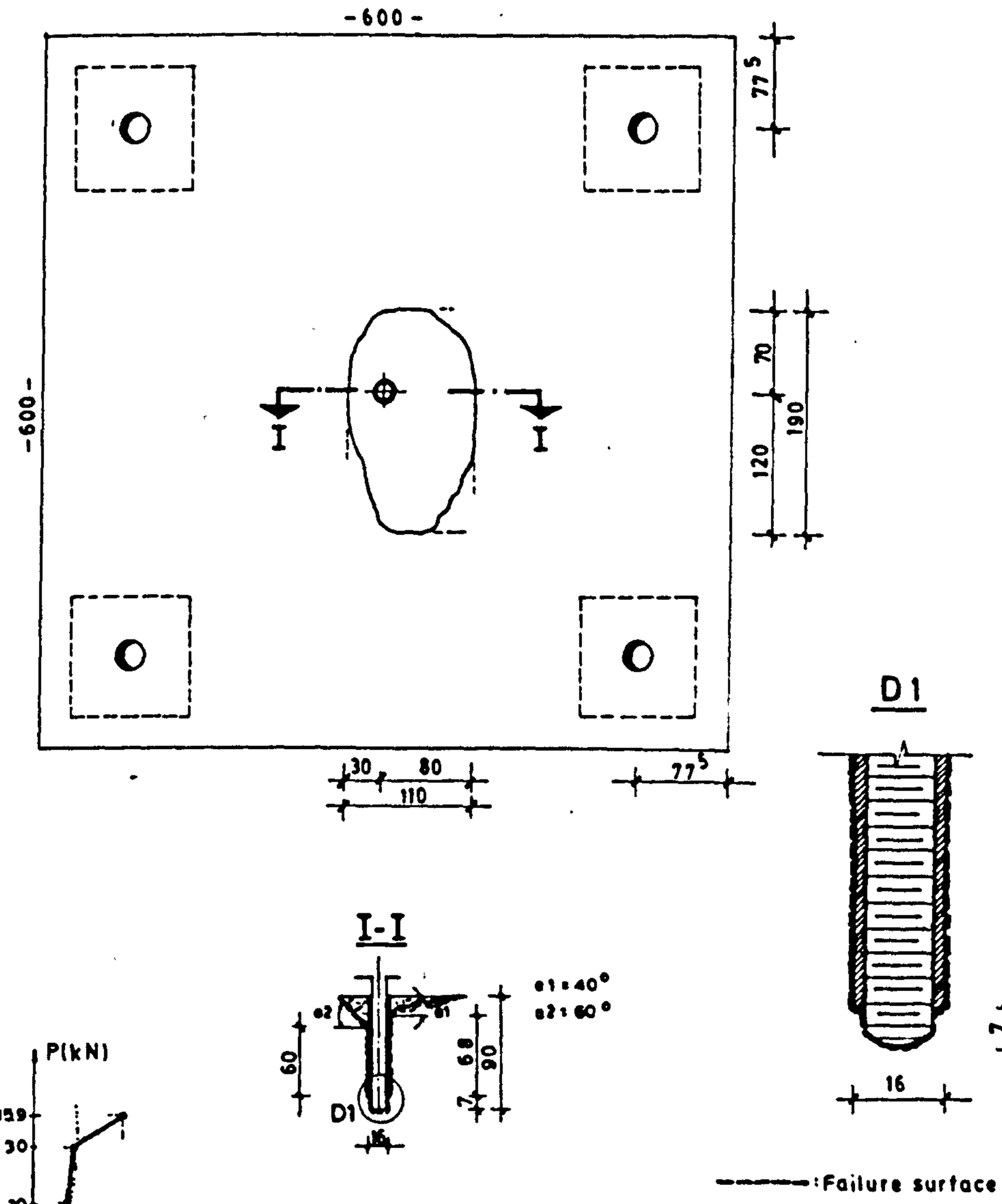

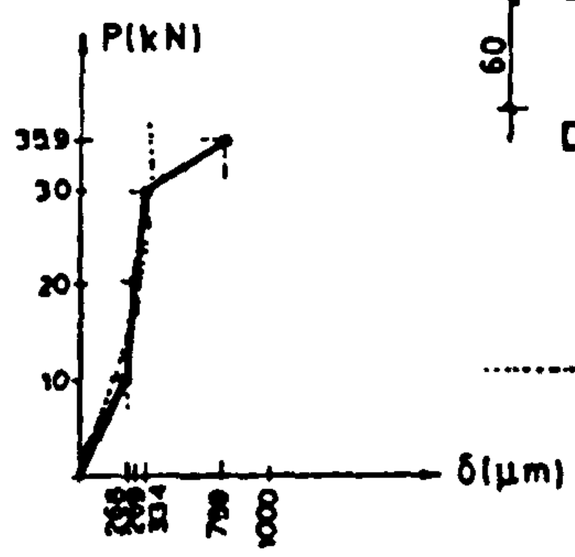

Embedment length (mm): 90=(7.5)d		Method of drilling	:Perc.Drill	P(kN)	δ(μm)	P(kN)	δ(μm)
Type of Anchor	:Thread	Method of insert. of resin	:Pouring	5.0	100	25.0	296
Anchor diameter (mm)	: 12	Concrete compr.str. (MPa)	: 37.90	10.0	268	30.0	334
Gap/diam. of hole (mm)	:2/16	Concrete tens.str. (MPa)	: 3.17	15.5	251	35.0	373
Adhesive	:C1380	Mode of failure	:I+C+R	20.0	265	35.9	759

Fig. 7.70

Specimen 3.14 (◆)

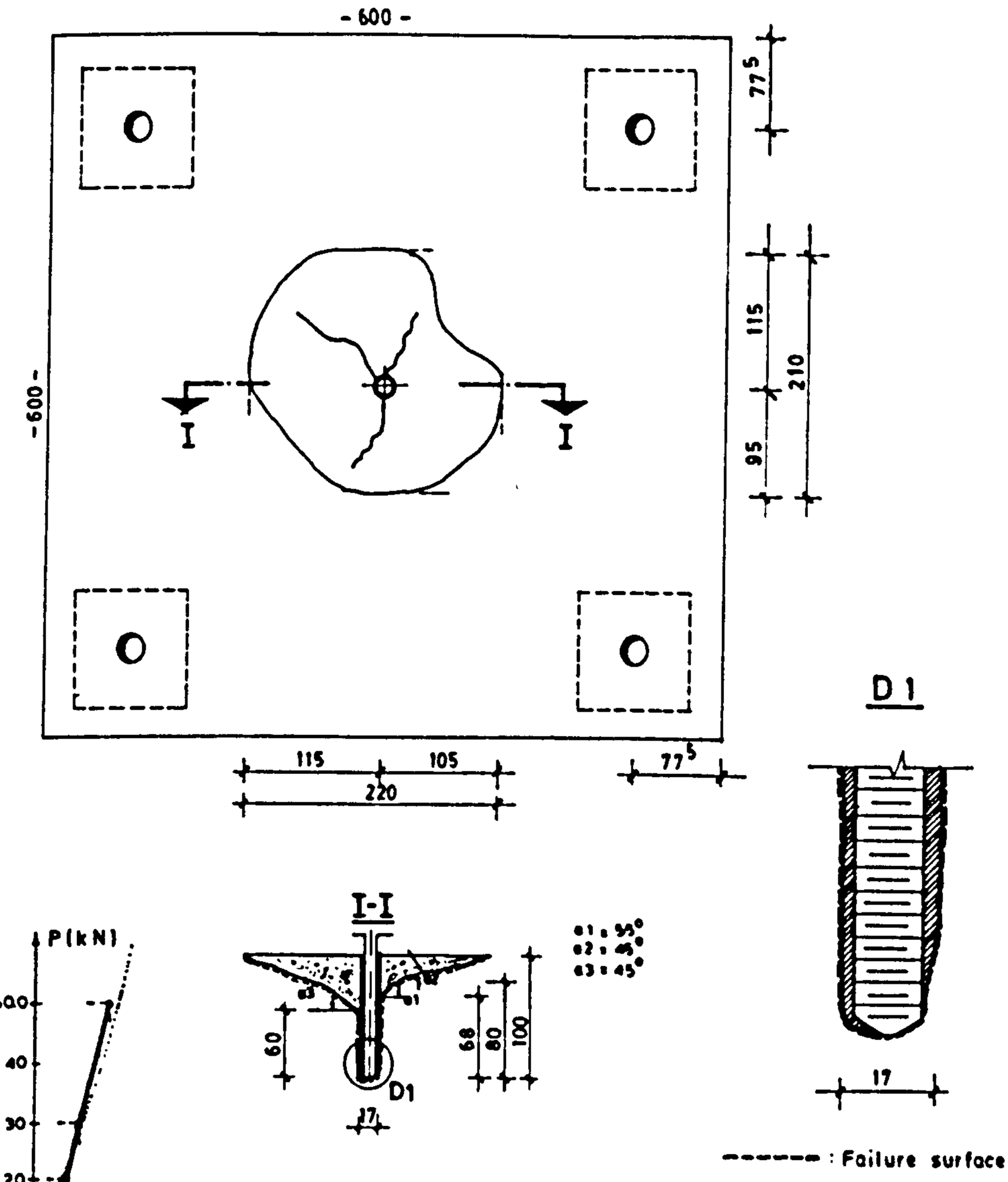

Embedment length(mm): 100=(8.3)d		Method of drilling	:Perc.Dr.	P(kN)	δ(μm)	P(kN)	δ(μm)
Type of Anchor	:Thread.	Method of insert.of resin	:Pouring	10.0	178	30.0	440
Anchor diameter (mm)	:12	Concrete compr.str.(MPa)	51.78	15.0	288	40.0	552
Gap/diam.of hole(mm)	:2/16	Concrete tens.str.(MPa)	: 3.69	20.0	330	45.0	607
Adhesive	:C1380	Mode of failure	:I+C+R	25.5	385	50.0	662

Fig.7.71

Specimen 3.15 (⊕)

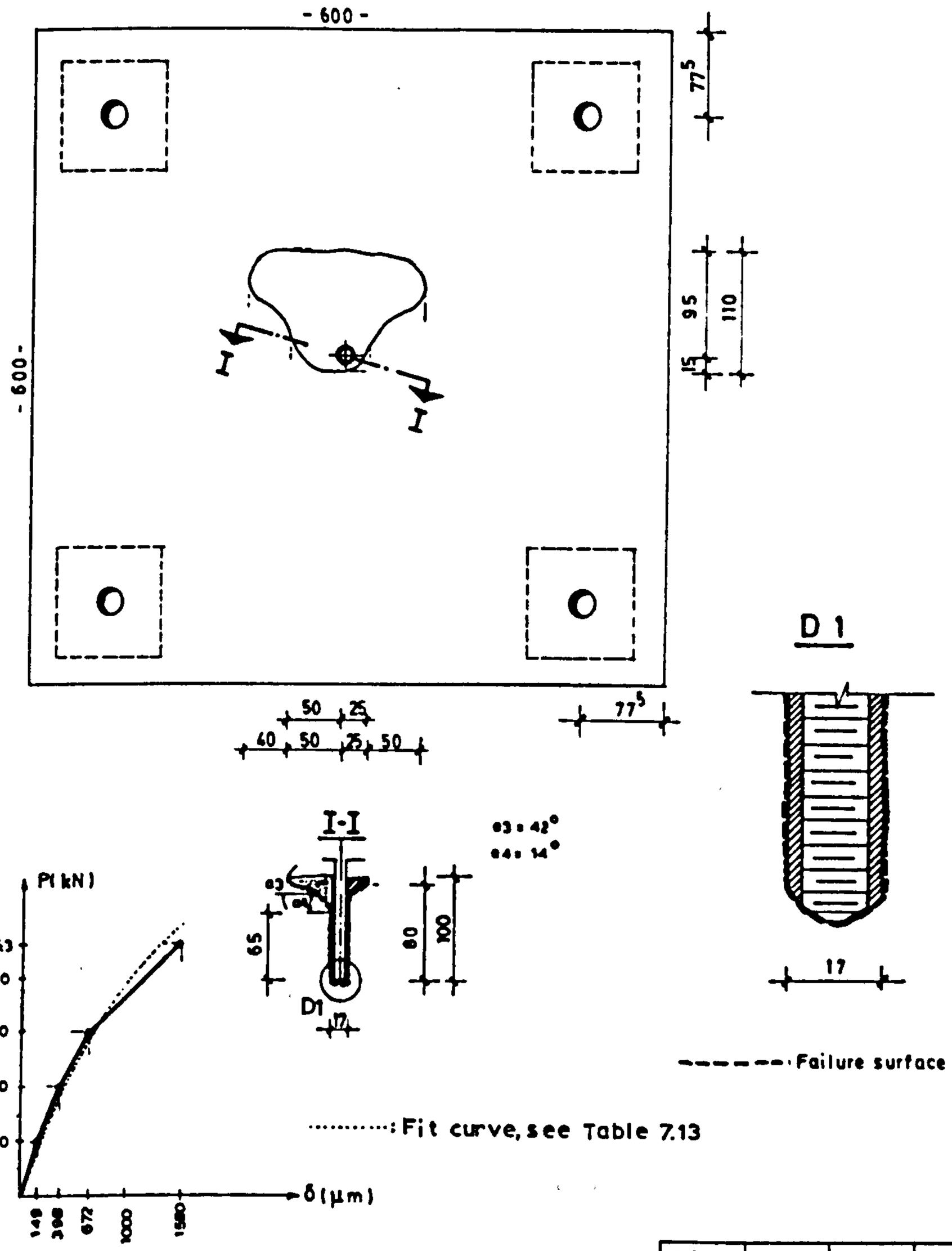

.....: Fit curve, see Table 7.13

Embedment length(mm):	100=(8.3)d
Type of Anchor	:Thread
Anchor diameter (mm):	12
Gap/diam.of hole(mm):	2/16
Adhesive	:C1380

Method of drilling	:Perc.Dr.
Method of insert.of resin:	Inject
Concrete compr.str.(MPa)	:21.48
Concrete tens.str.(MPa)	: 2.37
Mode of failure	:I+C+R

P(kN)	δ(μm)	P(kN)	δ(μm)
10.0	149	35.0	871
15.0	322	40.0	1080
20.0	398	45.0	1380
25.0	490	46.3	1550
30.0	672		

Fig. 7.72

Specimen 3.16 (◭)

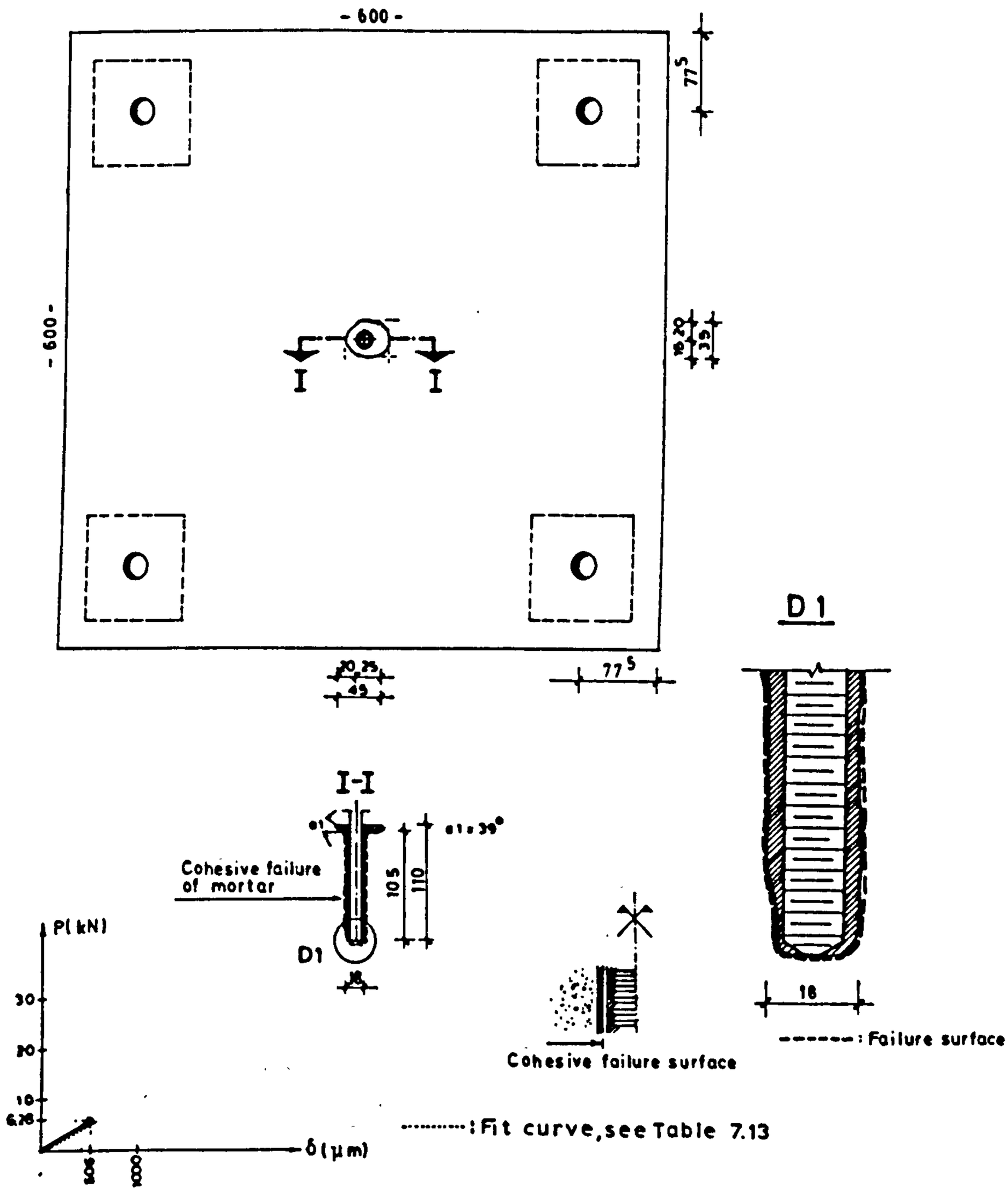

Embedment length(mm): 100=(8.3)d	Method of drilling : Perc.Dr.	P(kN)	δ(μm)	P(kN)	δ(μm)
Type of Anchor : Thread.	Method of insert. of resin: Pouring	6.28	506		
Anchor diameter (mm): 12	Concrete compr.str.(MPa) : 24.93				
Gap/diam. of hole(mm): 4/20	Concrete tens.str.(MPa) : 3.05				
Adhesive : Cem.gr.	Mode of failure : I				

Fig.7.73

Specimen 3.17 (△)

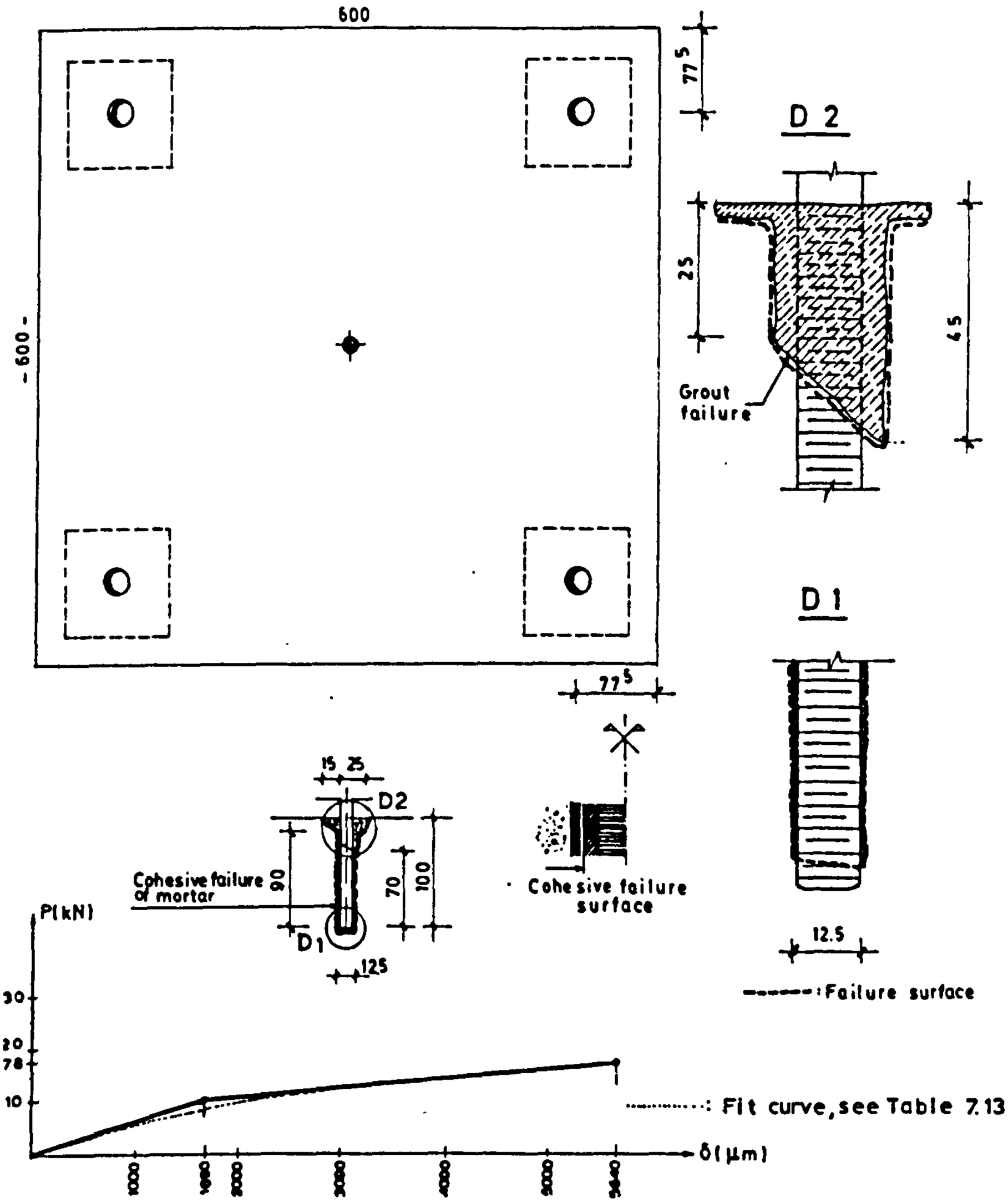

Embedment length (mm): 100=(8.3)d	Method of drilling : Perc.Dr.	P(kN)	δ(μm)	P(kN)	δ(μm)
Type of Anchor : Thread	Method of insert. of resin: Pouring	5.0	936	15.0	5070
Anchor diameter (mm) : 12	Concrete compr.str. (MPa) : 21.66	7.5	1170	17.8	5640
Gap/diam. of hole (mm): 4/20	Concret tens.str. (MPa) : 2.88	10.5	1690		
Adhesive : N.Sr.gr	Mode of failure : I+R	12.5	2530		

Fig.7.74

Specimen 3.18 (▲)

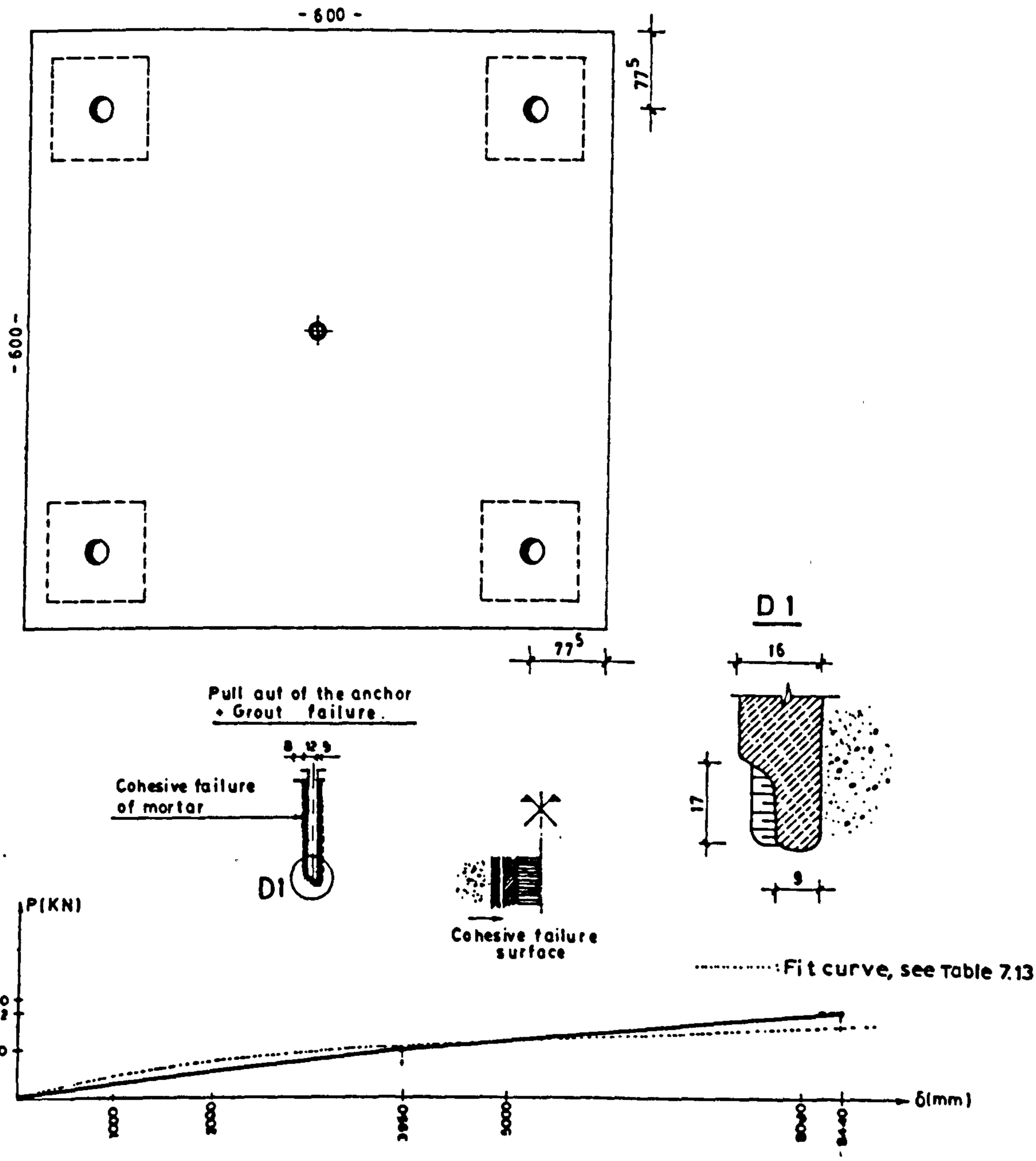

Embedment length(mm): 100=(8.3)d	Method of drilling :Perc.Dr.	P(kN)	δ(μm)	P(kN)	δ(μm)
Type of Anchor :Thread.	Method of insert.of resin :Pouring	5.0	1000	15.0	6650
Anchor diameter (mm): 12	Concrete compr.str.(MPa) :21.66	7.5	2500	15.2	8440
Gap/diam.of hole(mm): 4/20	Concrete tens.str.(MPa) : 2.88	10.0	3950		
Adhesive : Pol.Conc	Mode of failure :I+R	12.5	5180		

Fig.7.75

Specimen 3.19 ▲

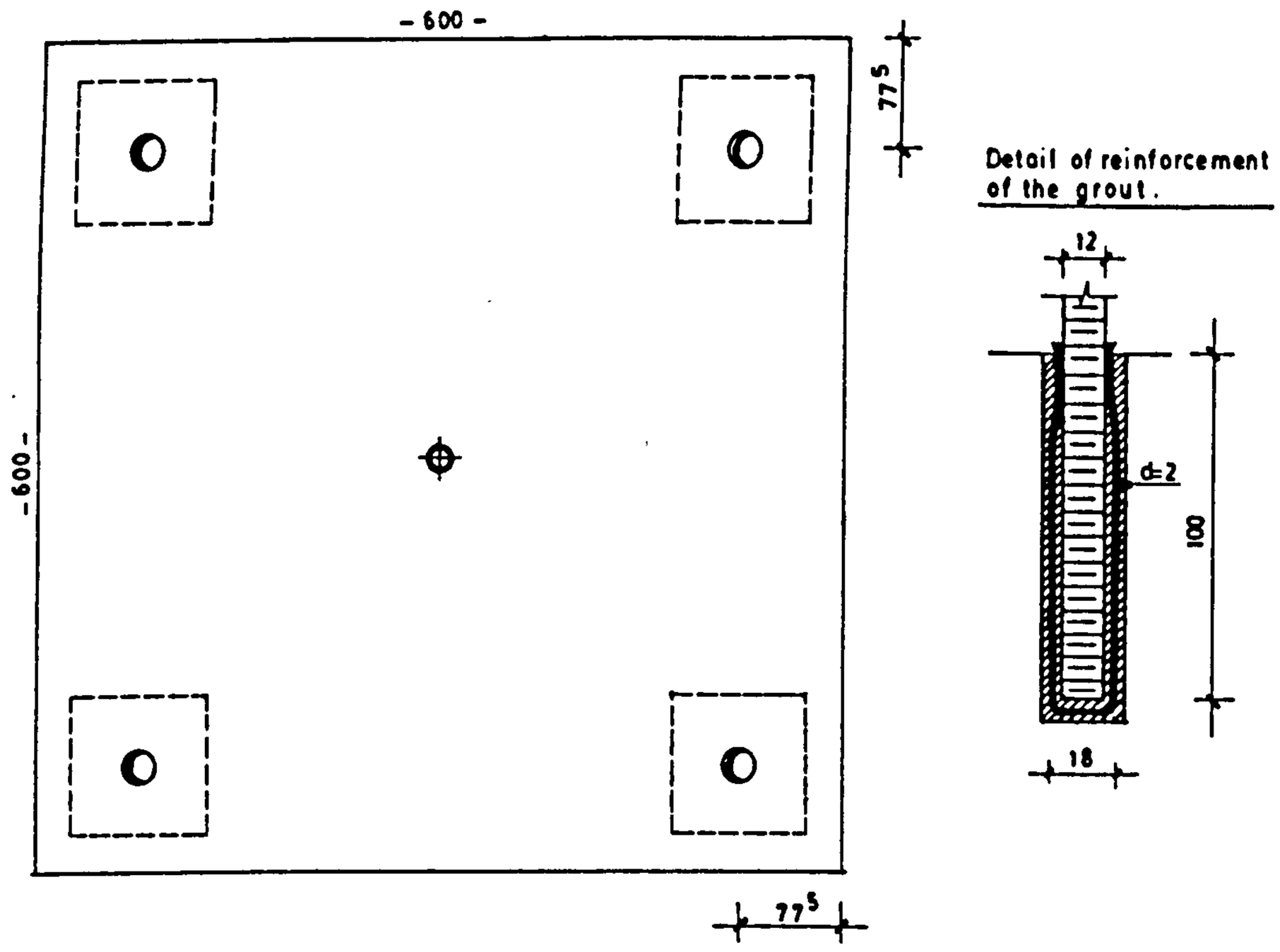

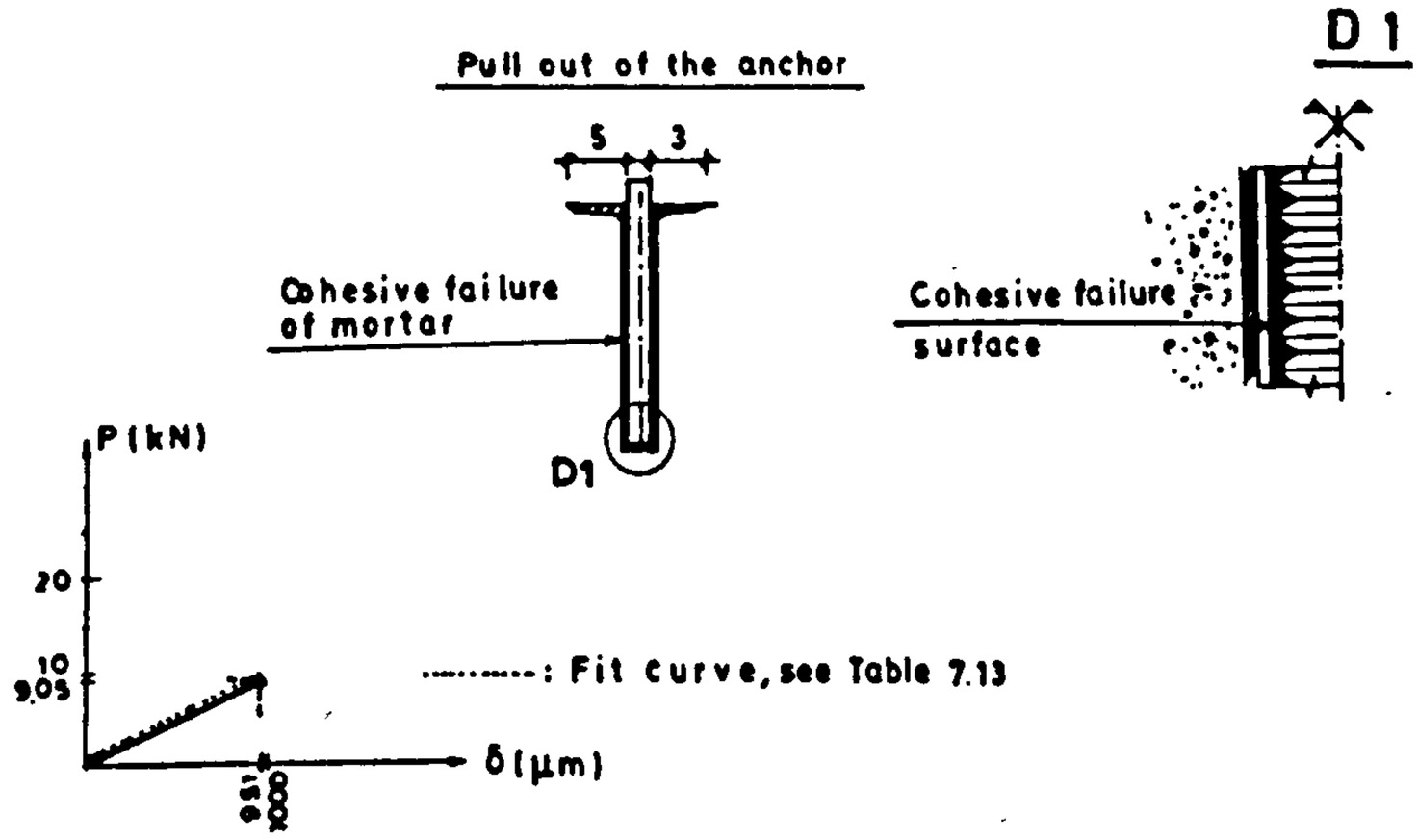

Embedment length(mm):100=(8.3)d	Method of drilling :Perc.Dr.	P(kN)	δ(µm)	P(kN)	δ(µm)
Type of Anchor :Thread.	Method of insert.of resin:Pouring	5.0	648		
Anchor diameter (mm):12	Concrete compr.str.(MPa) :21.66	7.5	914		
Gap/diam.of hole(mm):1/20	Concrete tens.str.(MPa) : 2.88	9.05	951		
Adhesive: Reinforced cem. gr.	Mode of failure :I				

Fig.7.76

Specimen 3.20 (◁)

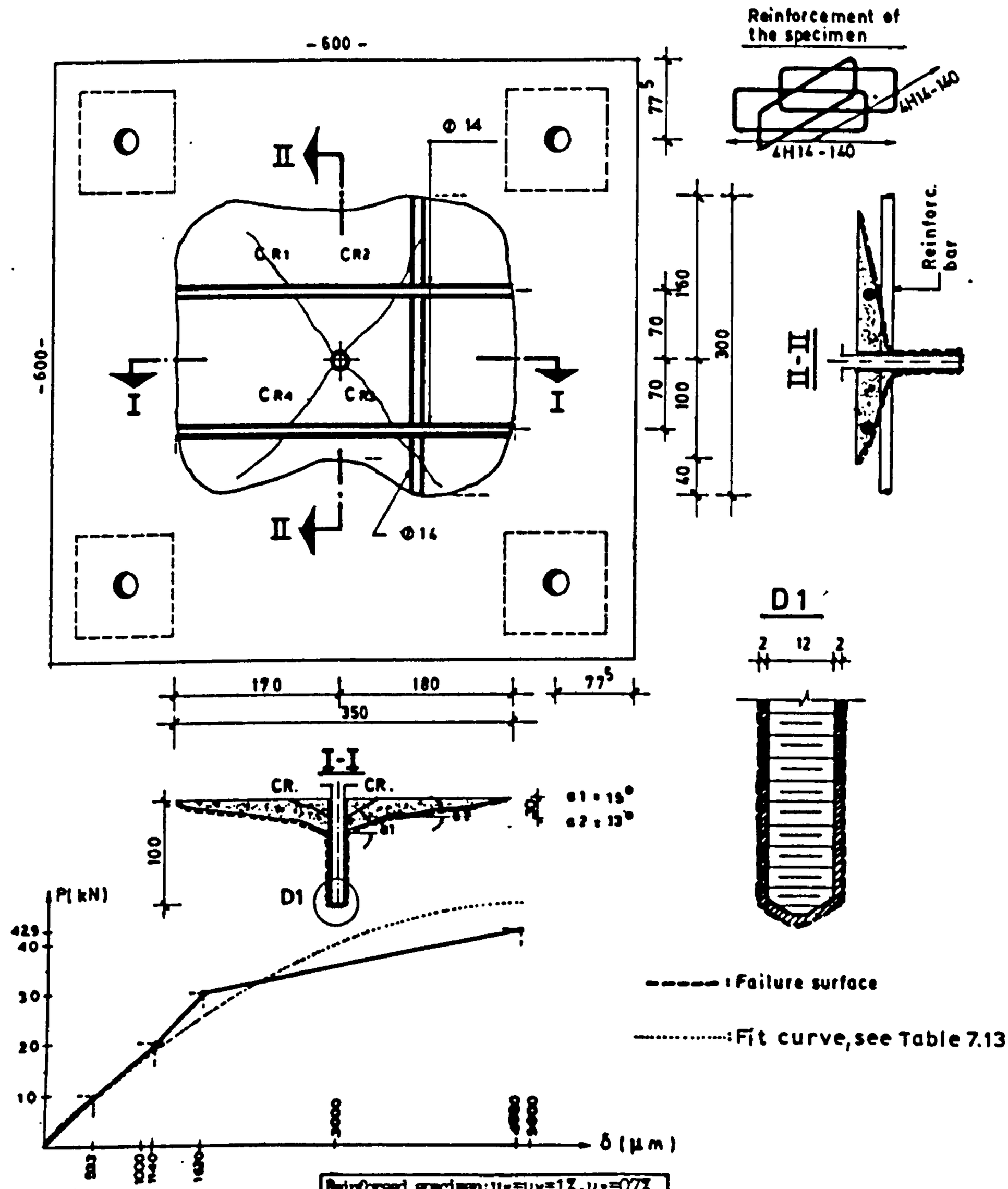

Embedment length(mm);	100=(8.3)d
Type of Anchor	:Thread.
Anchor diameter (mm):	12
Gap/diam.of hole(mm):	2/16
Adhesive	:C1380

Reinforced specimen: $\mu_x=\mu_y=1\%$, $\mu_z=0.7\%$

Method of drilling	: Perc.Dr.
Method of insert.of resin:	Pouring
Concrete compr.str.(MPa)	:26.07
Concrete tens.str.(MPa)	: 2.65
Mode of failure	:I+C+R+Spl.

P(kN)	δ(μm)	P(kN)	δ(μm)
10.0	533	30.0	1620
15.0	855	35.0	2030
20.0	1140	40.0	3370
25.5	1360	42.9	4880

Fig.7.77

Specimen 3.21 (◀)

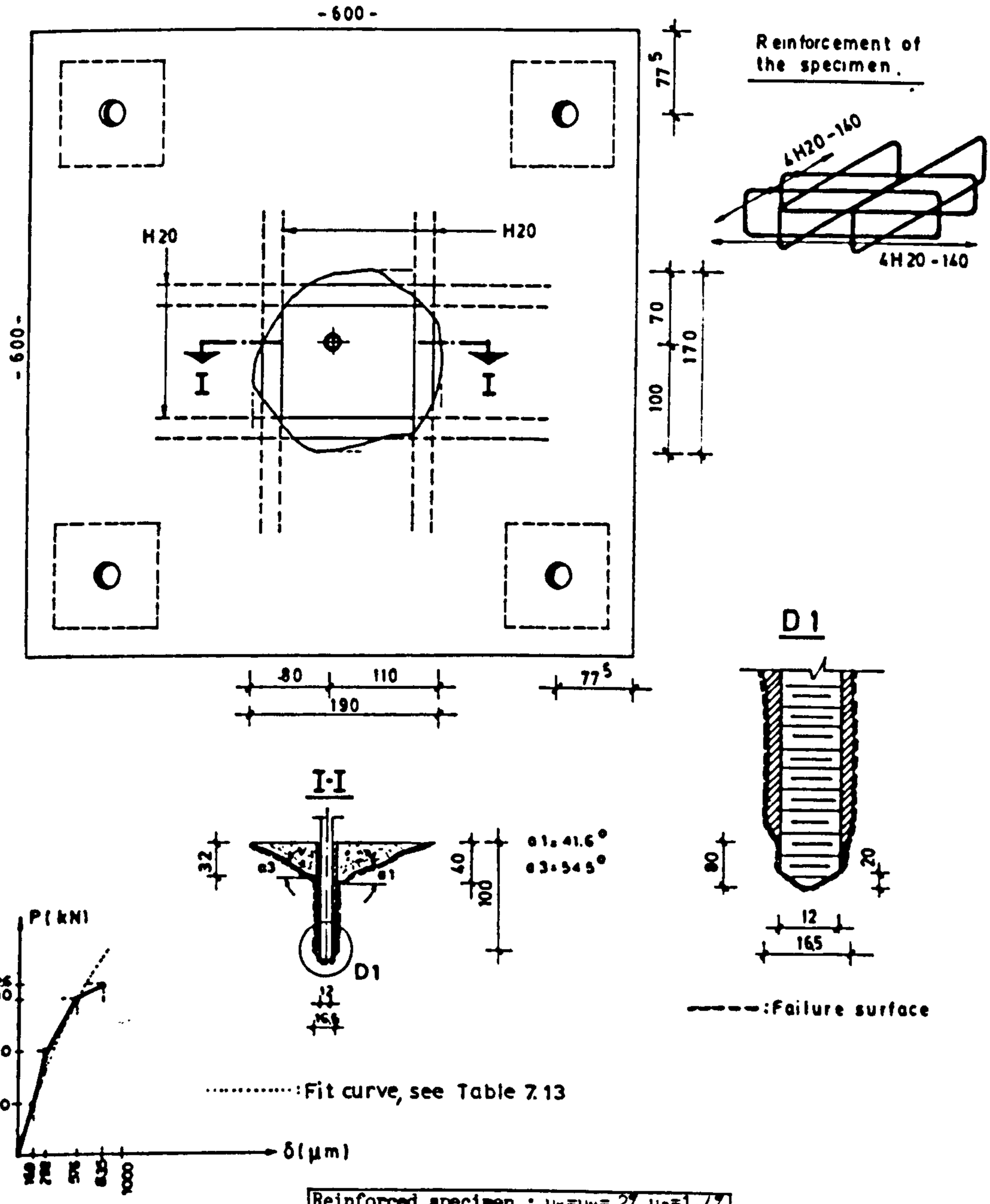

Embedment length(mm)	:100=(8,3)d
Type of Anchor	:Thread.
Anchor diameter(mm)	:12
Cap/diam.of hole(mm)	:2/16
Adhesive	:C1380

Reinforced specimen : $\mu_x=\mu_y=2\%, \mu_z=1.4\%$

Method of drilling	:Perc.Dr.
Method of insert.of resin	:Pouring
Concrete compr.str.(MPa)	:20.93
Concrete tens.str.(MPa)	:2.30
Mode of failure	:I+C+R

P(kN)	δ(μm)	P(kN)	δ(μm)
10.0	169	30.0	576
15.0	219	32.6	835
20.0	292		
25.0	406		

Fig.7.78

Specimen 3.22 (Φ)

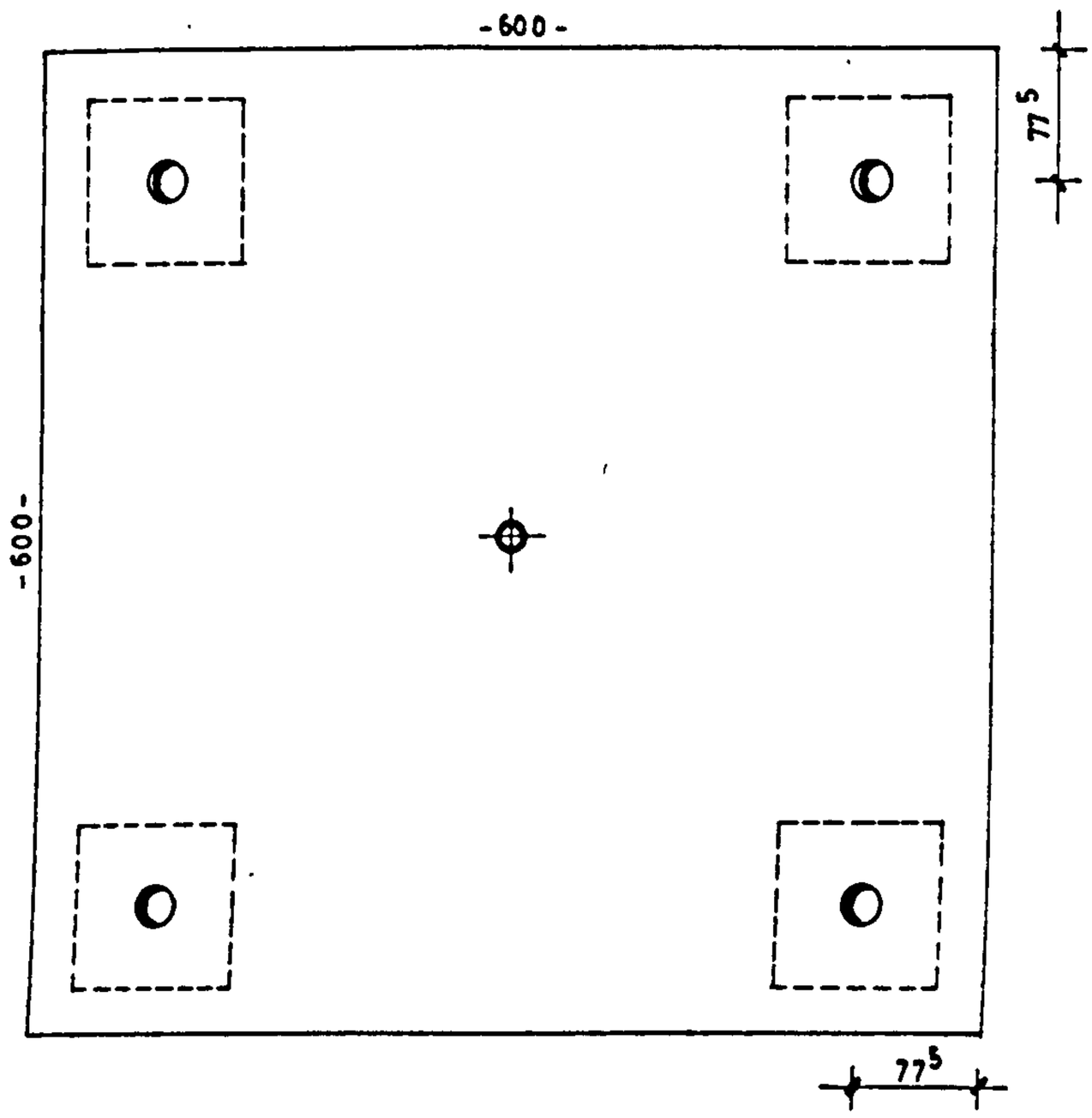

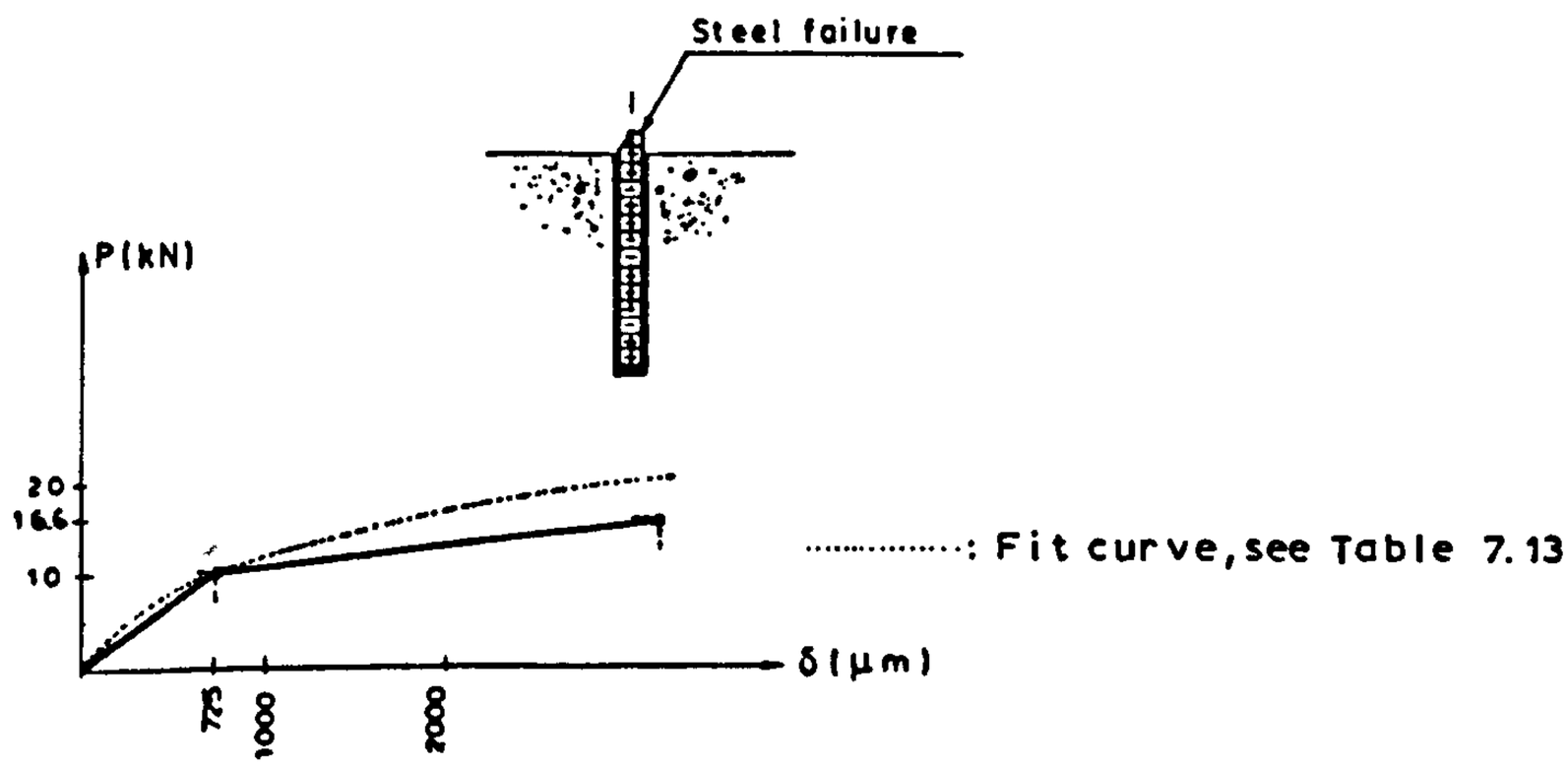

Embedment length(mm):90=(7.5)d	Method of drilling :Perc.Dr.	P(kN)	δ(μm)	P(kN)	δ(μm)
Type of Anchor :Thread.	Method of insert.of resin:Pouring	5.0	264	15.0	1860
Anchor diameter (mm):8	Concrete compr.str.(MPa) :20.65	7.5	433	16.6	2710
Gap/diam.of hole(mm):2/12	Concrete tens.str.(MPa) : 2.25	10.5	725		
Adhesive :C1380	Mode of failure : S	12.5	1070		

Fig.7.79

Specimen 3.23 (◆)

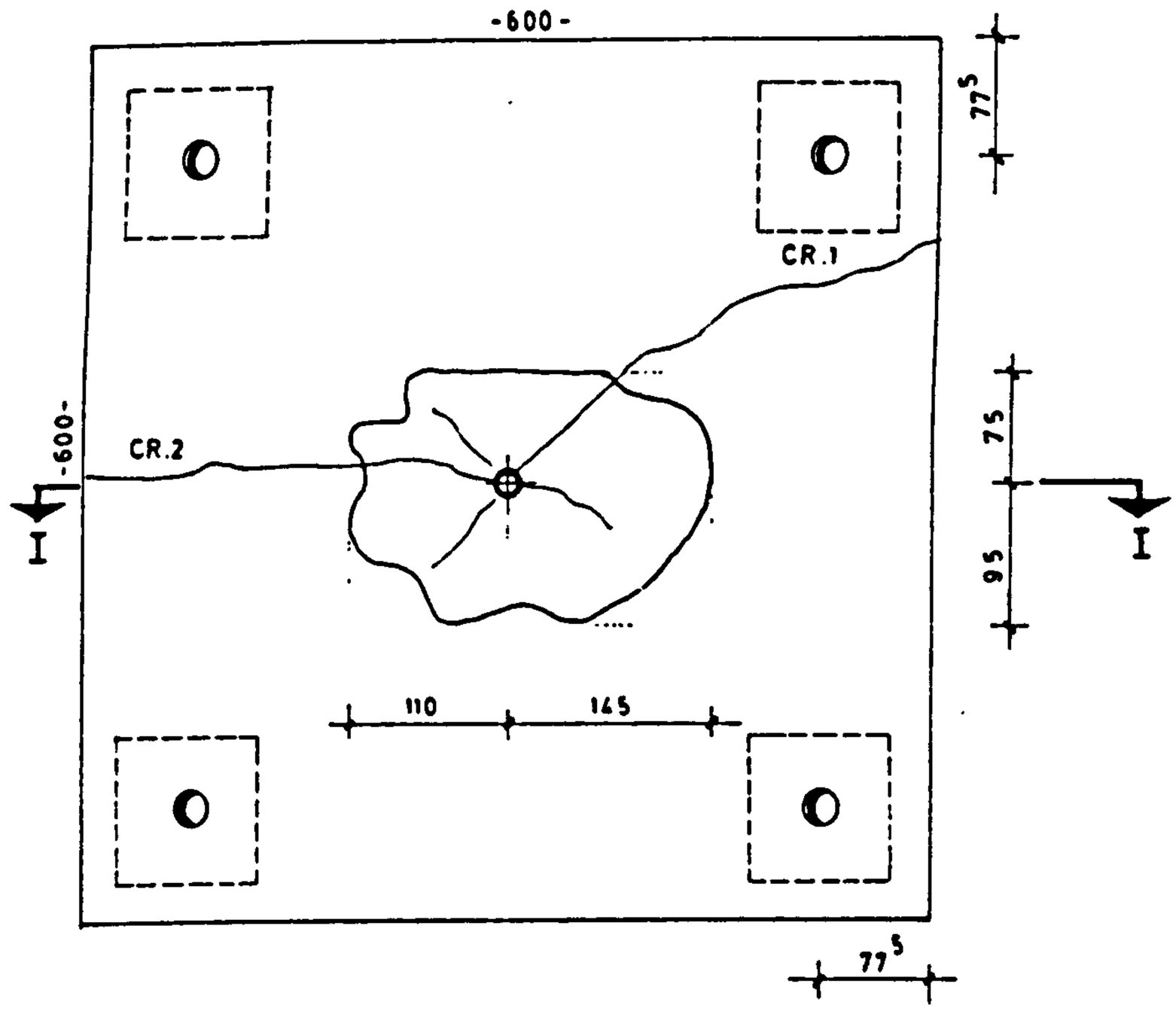

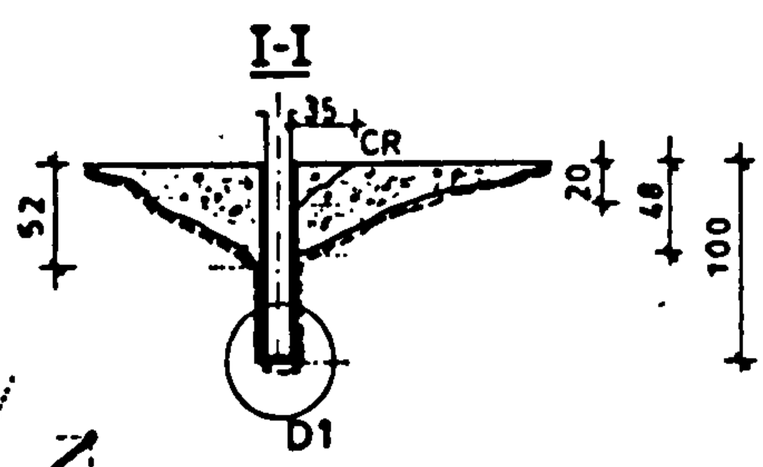

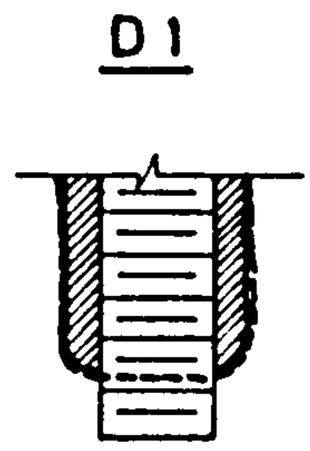

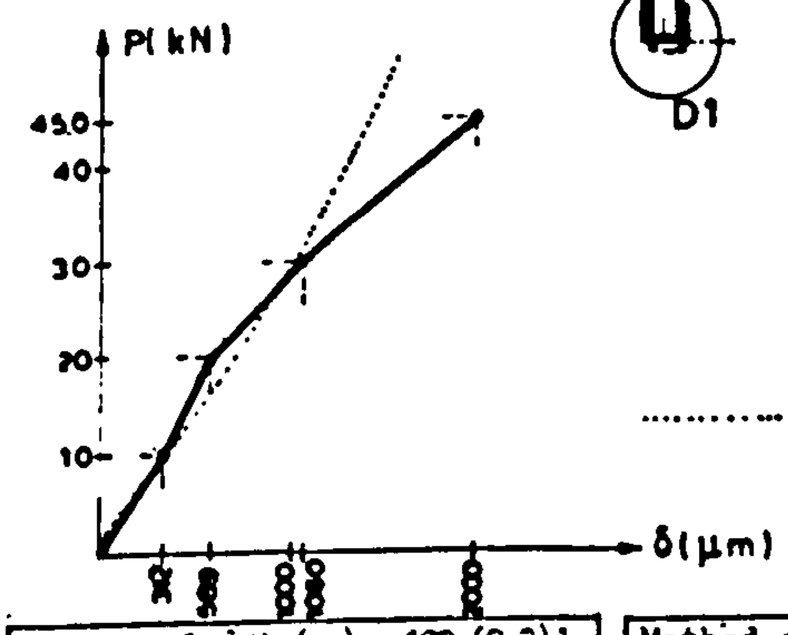

-·-·-·-: Failure surface

·····: Fit curve, see Table 7.13

Embedment length (mm)	: 100=(8.3)d
Type of Anchor	:Thread.
Anchor diameter	:12
Gap/diam.of hole(mm)	:2/16
Adhesive	:LV

Method of drilling	:Perc.Dr.
Method of insert.of resin	:Pouring
Concrete compr.str.(MPa)	:18.97
Concrete tens.str.(MPa)	: 2.15
Mode of failure	:I+C+R+Sp.

P(kN)	δ(μm)	P(kN)	δ(μm)
10.0	312	32.7	1180
25.0	501	37.4	1440
20.0	589	41.8	1680
28.0	977	45.0	2000

Fig. 7.80

Specimen 3.24 ( )

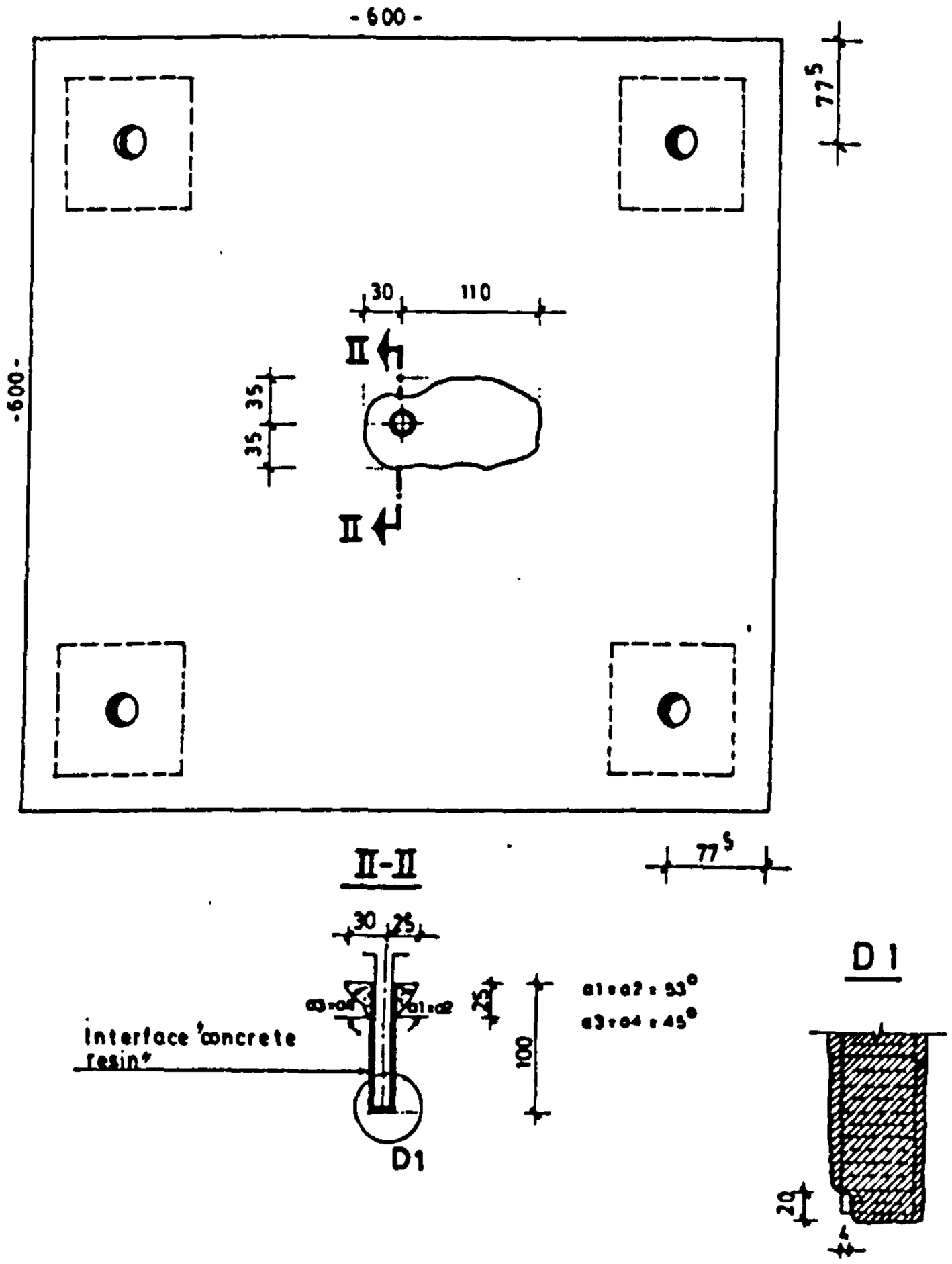

Embedment length (mm) : 100=(8.3)d	Method of drilling : Perc.Dr.	
Type of Anchor : Ribbed	Method of insert.of resin: Pouring	
Anchor diameter(mm) : 12	Concrete compr.str.(MPa) : 24.89	
Gap/diam.of hole(mm): 2/16	Concrete tens.str.(MPa) : 2.65	
Adhesive : C1380	Mode of failure : I+C+R	

Fig.7.81

Specimen 3.25 (❋)

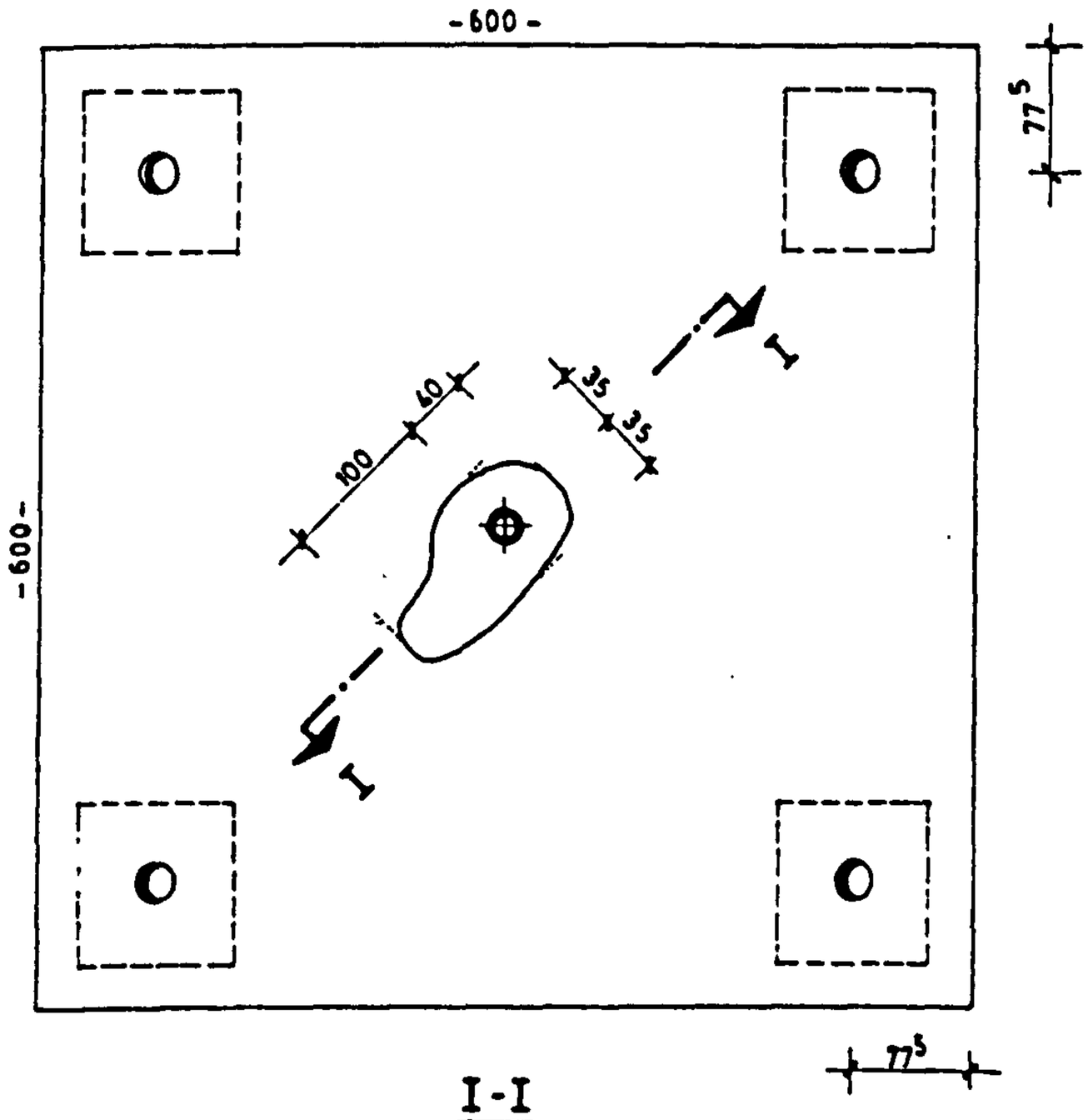

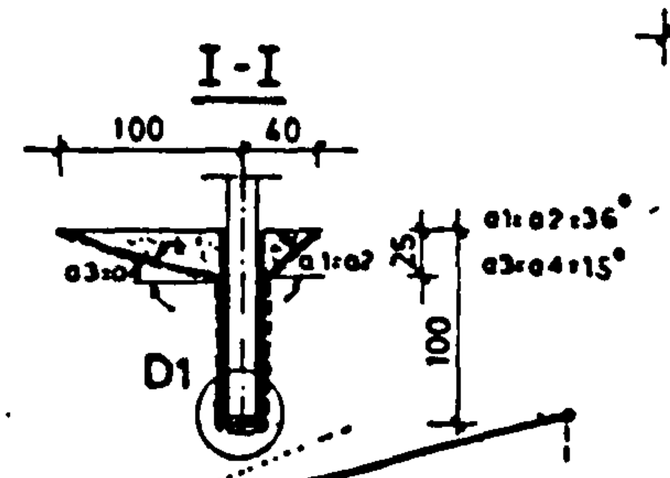

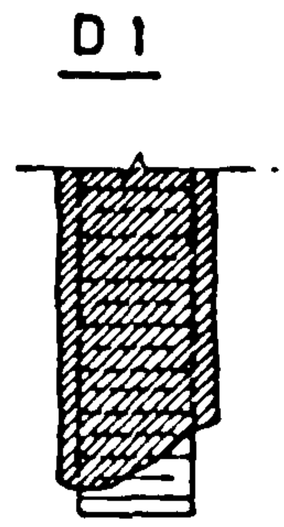

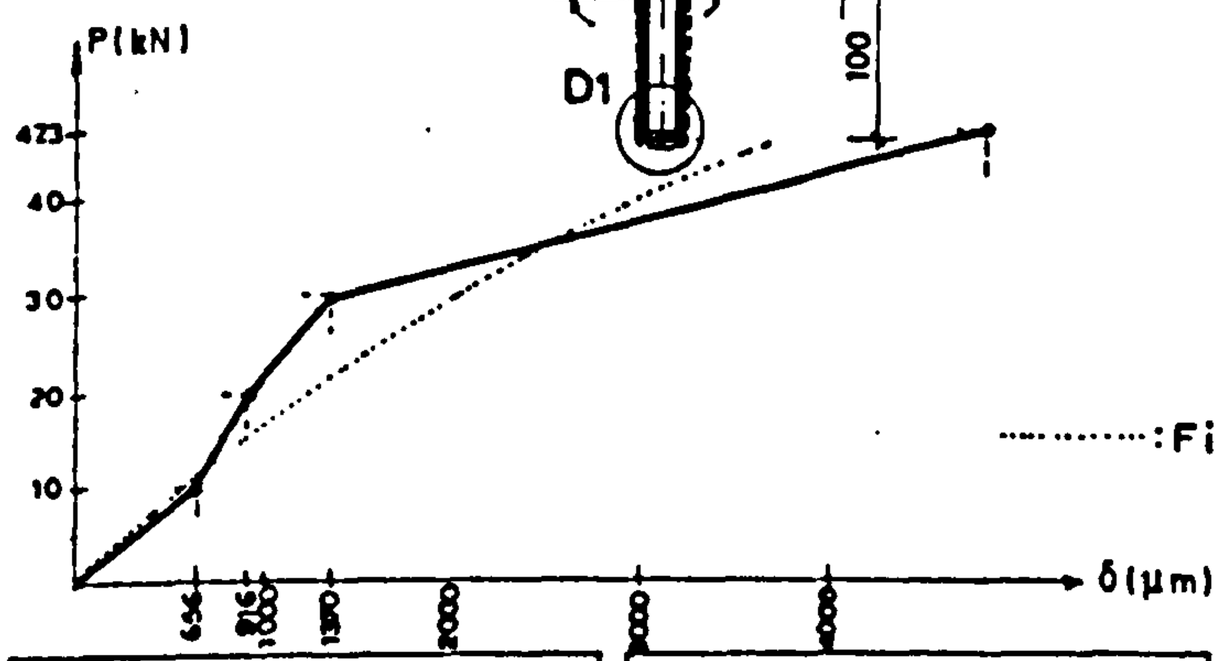

.....: Fit curve, see Table 7.13

Embedment length	:100=(8,3)d
Type of Anchor	:Thread
Anchor diameter(mm)	:12
Gap/diam.of hole(mm)	:1/20
Adhesive	:C1380

Method of drilling	:Diam.Dr
Method of insert.of resin	:Pouring
Concrete compr.str.(MPa)	:22.25
Concrete tens.str.(MPa)	: 2.25
Mode of failure	:I+C+R

P(kN)	δ(um)	P(kN)	δ(um)
10.0	656	35.0	1730
15.0	833	40.0	2180
20.0	916	45.0	3050
25.0	1080	47.3	4400
30.0	1370		

Fig.7.82

Specimen 3.26 (▷)

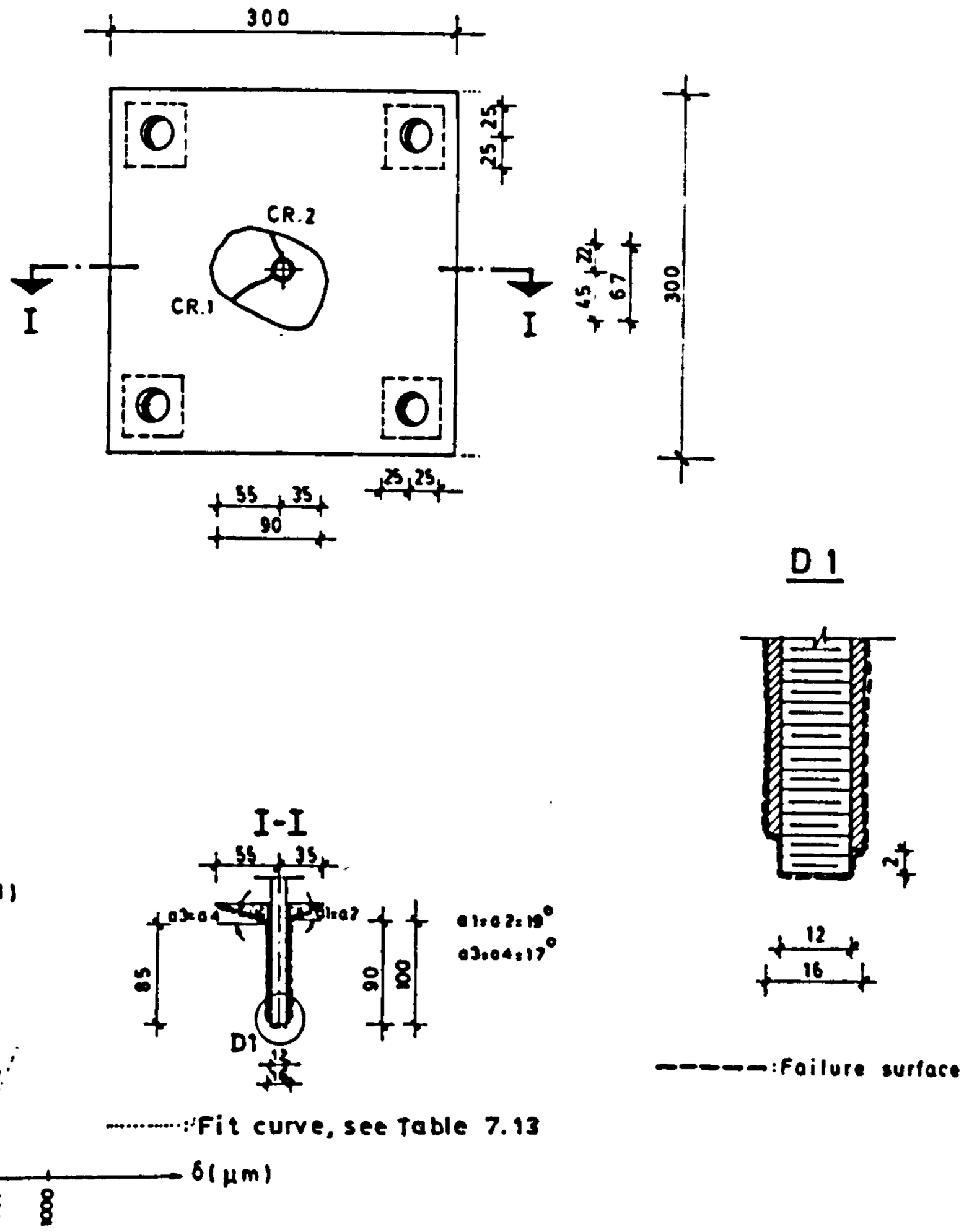

Embedment length(mm)	:100=(8.3)d
Type of Anchor	:Thread.
Anchor diameter (mm)	:12
Gap/diam.of hole(mm)	:2/16
Adhesive	:C1380

Small specimen 300×300×200

Method of drilling	:Perc.Dr.
Method of insert.of resin	:Pouring
Concrete compr.str.(MPa)	:20.02
Concrete tens.str.(MPa)	: 2.15
Mode of failure	:I+C+R+spl.

P(kN)	δ(μm)	P(kN)	δ(μm)
5.0	280	15.6	426
6.9	348	18.0	487
11.0	385		
18.0	487		

Fig.7.83

Specimen 3.27 (▶)

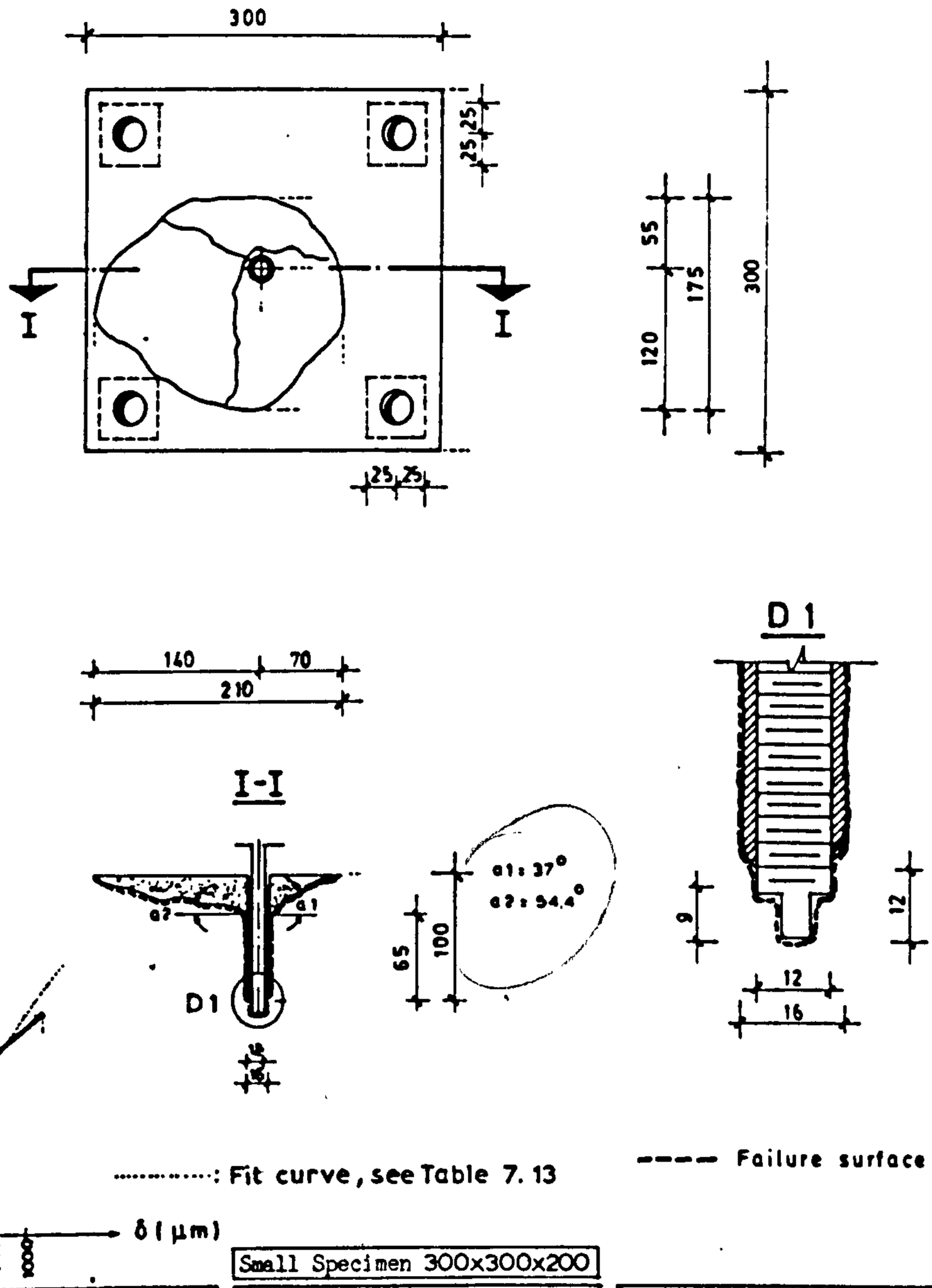

Embedment length (mm)	: 100=(8.3)d
Type of Anchor	:Thread
Anchor diameter(mm)	:12
Cap/diam.of hole (mm)	:4/20
Adhesive	:C1380

Small Specimen 300x300x200	
Method of drilling	:Perc.Dr
Method of insert.of resin	:Pouring
Concrete compr.str.(MPa)	:20.61
Concrete tens.str.(MPa)	: 2.40
Mode of failure	:I+C+R+Sp

P(kN)	δ(μm)	P(kN)	δ(μm)
10.0	205	30.0	744
15.5	348	35.5	922
20.5	447	36.2	1040
25.0	580		

Fig.7.84

Specimen 3.28 (中)

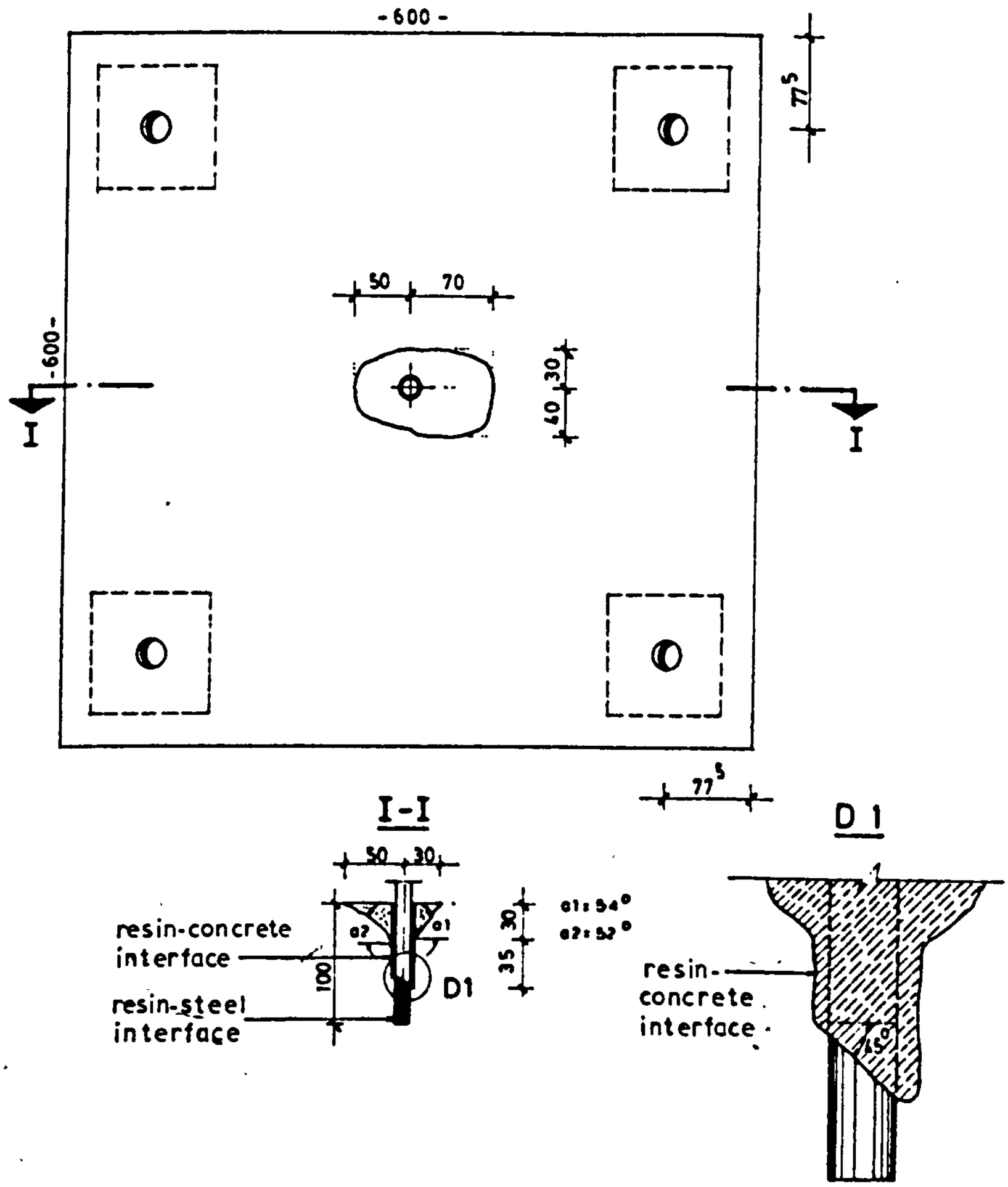

Embedment length(mm):	100=(8.3)d	Method of drilling	:Perc.Dr.	P(kN)	δ(μm)	P(kN)	δ(μm)
Type of Anchor	:Plain	Method of insert.of resin:	Pouring				
Anchor diameter (mm)	:12	Concrete compr.str.(MPa)	:22.84				
Gap/diam.of hole(mm)	:2/16	Concrete tens.str.(MPa)	: 2.65				
Adhesive	:C1380	Mode of failure	:I+C+R				

Fig.7.85

Specimen 3.29 (⊕)

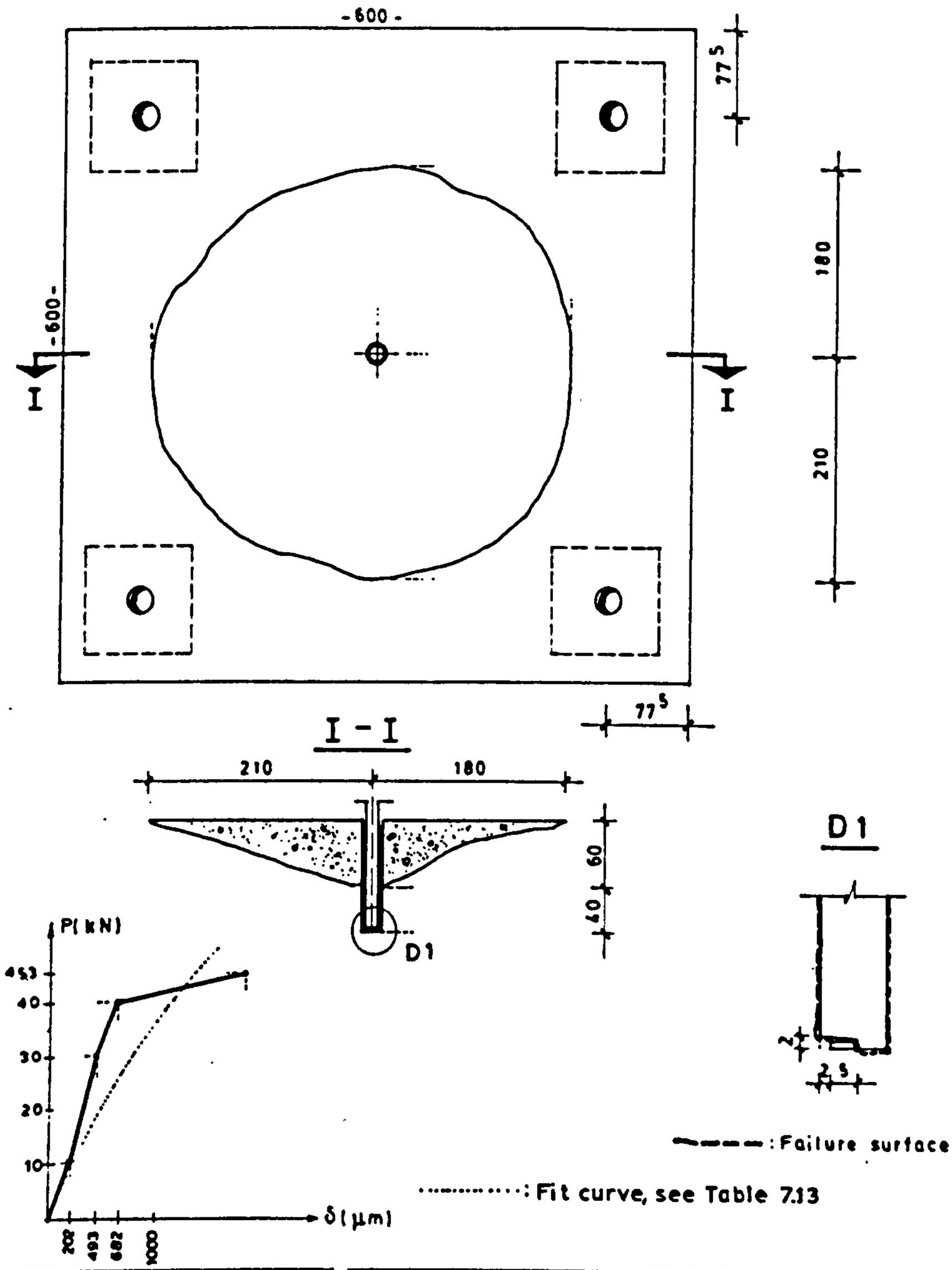

Embedment length (mm) : 100=(8.3)d	Method of drilling :Perc.Dr.	P(kN)	δ(µm)	P(kN)	δ(µm)
Type of Anchor :Thread	Method of insert.of resin.Pouring	10.0	202	30.0	682
Anchor diameter(mm) :12	Concrete compr.str.(MPa):24.25	15.0	408	35.0	886
Gap/diam.of hole(mm):2/16	Concrete tens.str.(MPa) : 2.60	20.0	493	40.0	1130
Adhesive : LV	Mode of failure :I+C+R	25.0	546	45.3	1610

Fig.7.86

Specimen 3.30 (+)

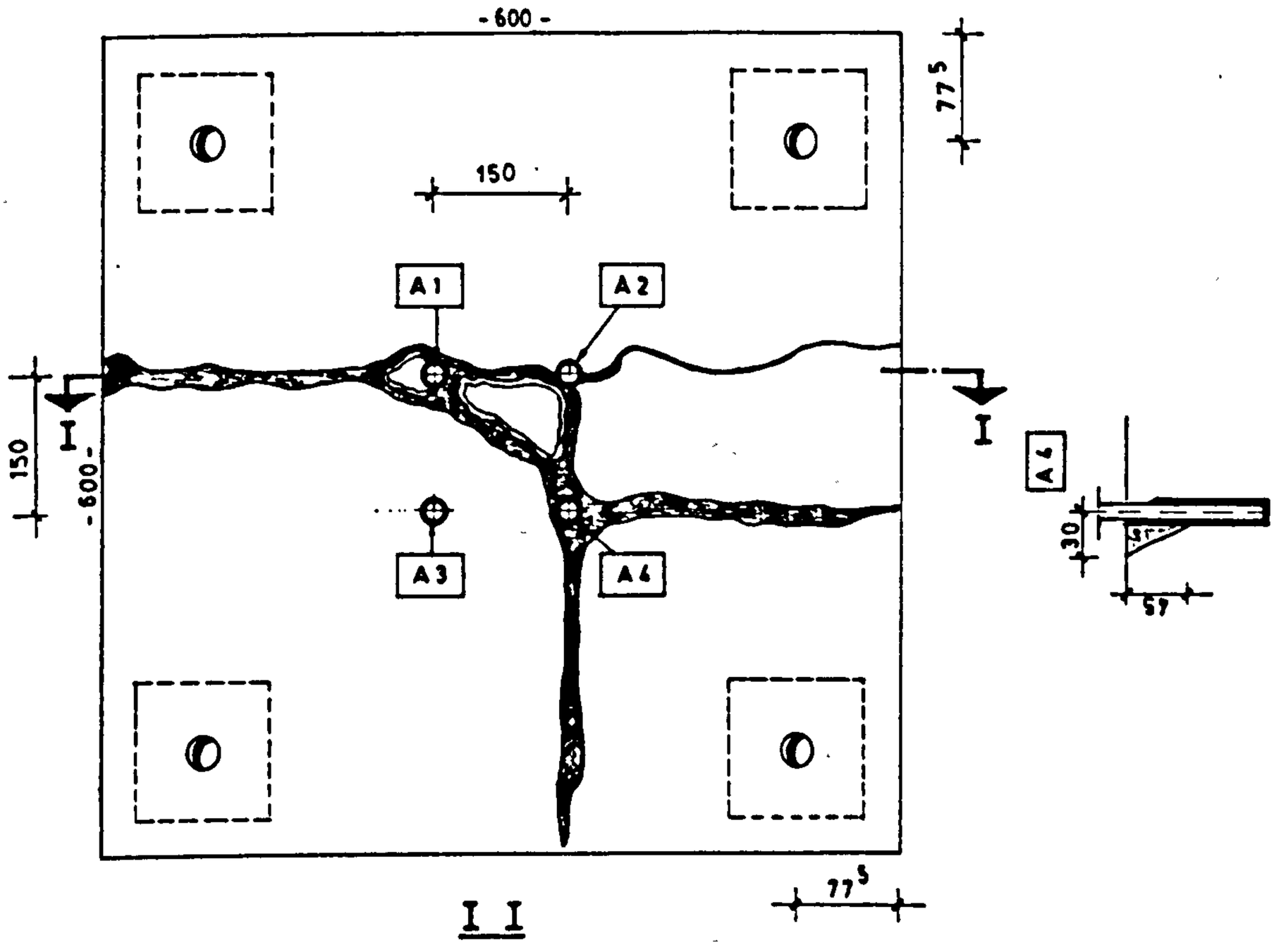

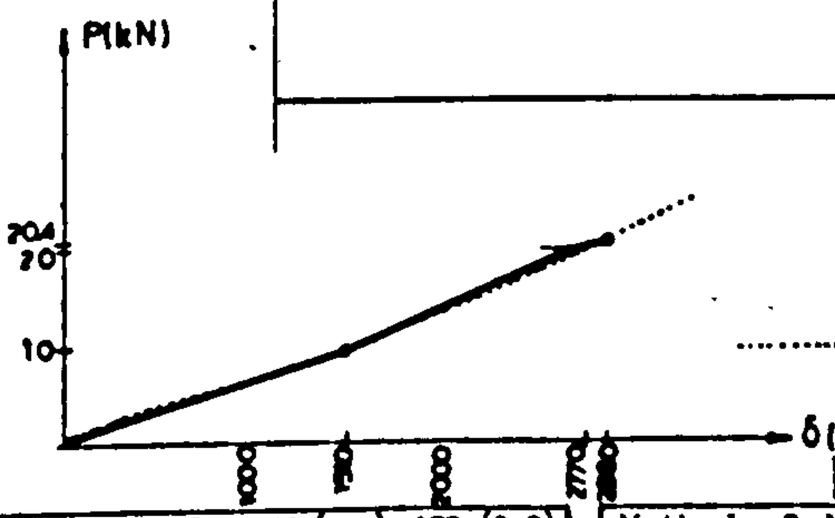

——— : Failure surface

..... : Fit curve, see Table 7.13

Embedment length(mm)	:100=(8.3)d
Type of Anchor	:Thread
Anchor diameter(mm)	:12
Gap/diam.of hole(mm)	:2/16
Adhesive	

Group of ANCHORS	
Method of drilling	:Perc.Dr.
Method of insert.of resin	:Pouring
Concrete compr.str.(MPa)	:20.61
Concrete tens.str.(MPa)	: 2.70
Mode of failure	:I+C+R+SD1

P(kN)	δ(μm)	P(kN)	δ(μm)
5.0	767	15.0	2160
7.5	1070	17.5	2440
10.0	1510	20.0	2770
12.5	1830	20.4	2860

Fig.7.87

Specimen 3.31 (⊠)

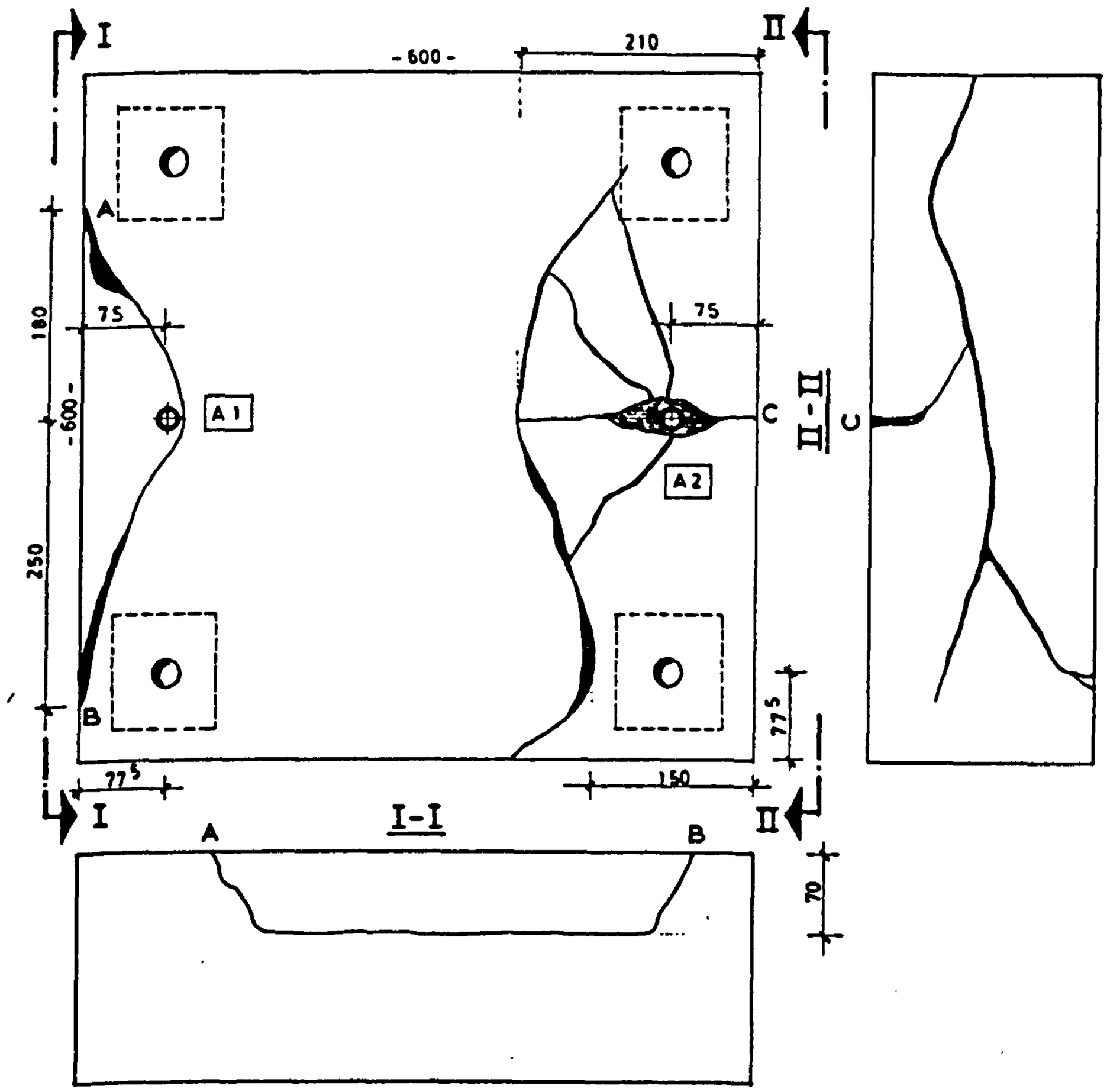

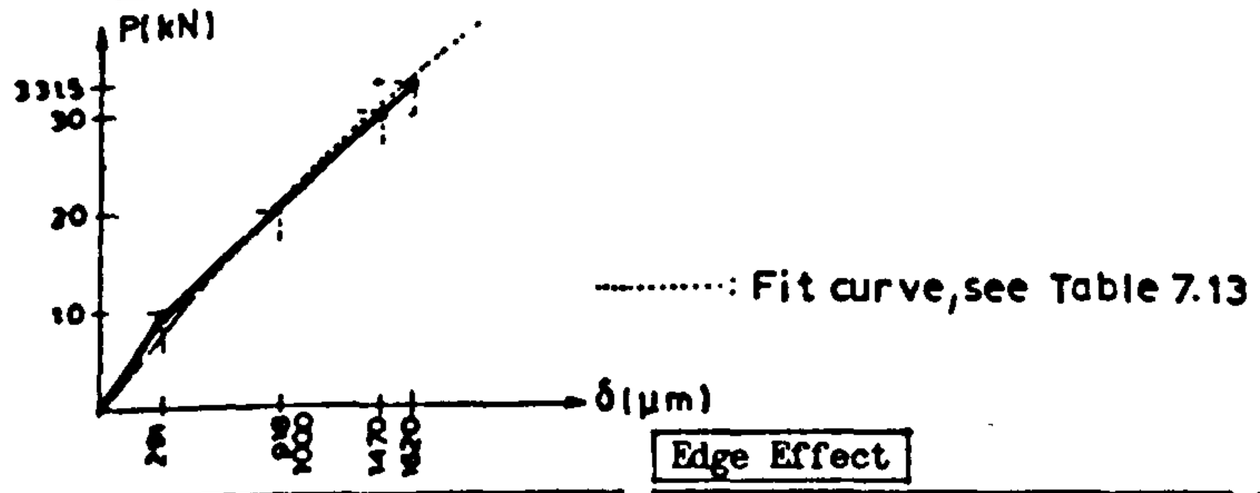

Embedment length(mm)	: 100=(8.3)d
Type of Anchor	:Thread
Anchor diameter (mm)	:12
Gap/diam.of hole(mm)	:2/16
Adhesive	:C1380

Edge Effect

Method of drilling	:Perc.Dr.
Method of insert.of resin	:Pouring
Concrete compr.str.(MPa)	:24.89
Concrete tens.str.(MPa)	: 2.55
Mode of failure	:Split.

P(kN)	δ(μm)	P(kN)	δ(μm)
5.0	101	25.0	1240
10.0	290	30.0	1470
15.0	521	33.15	1620
20.5	918		

Fig.7.88

Specimen 3.32

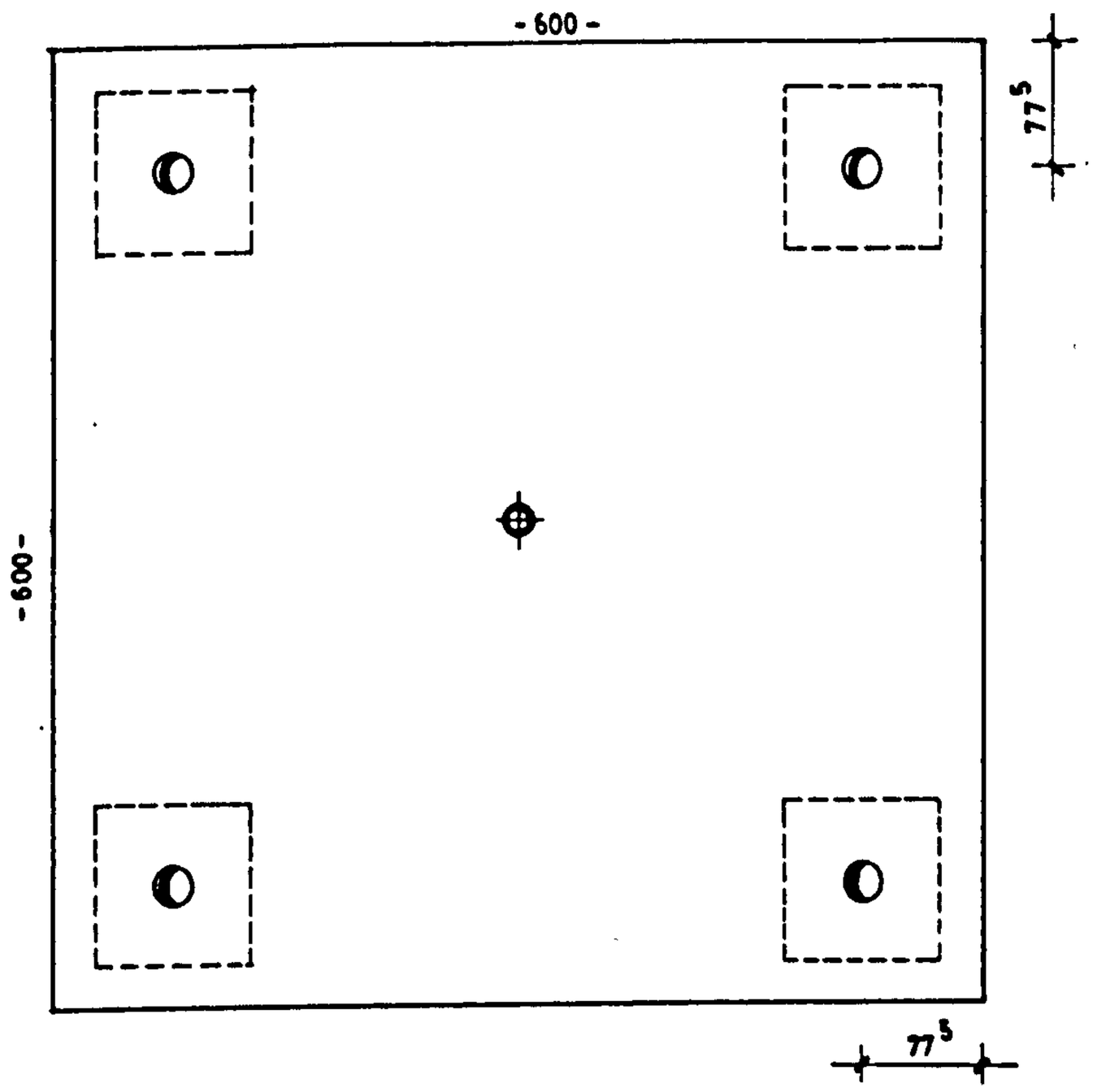

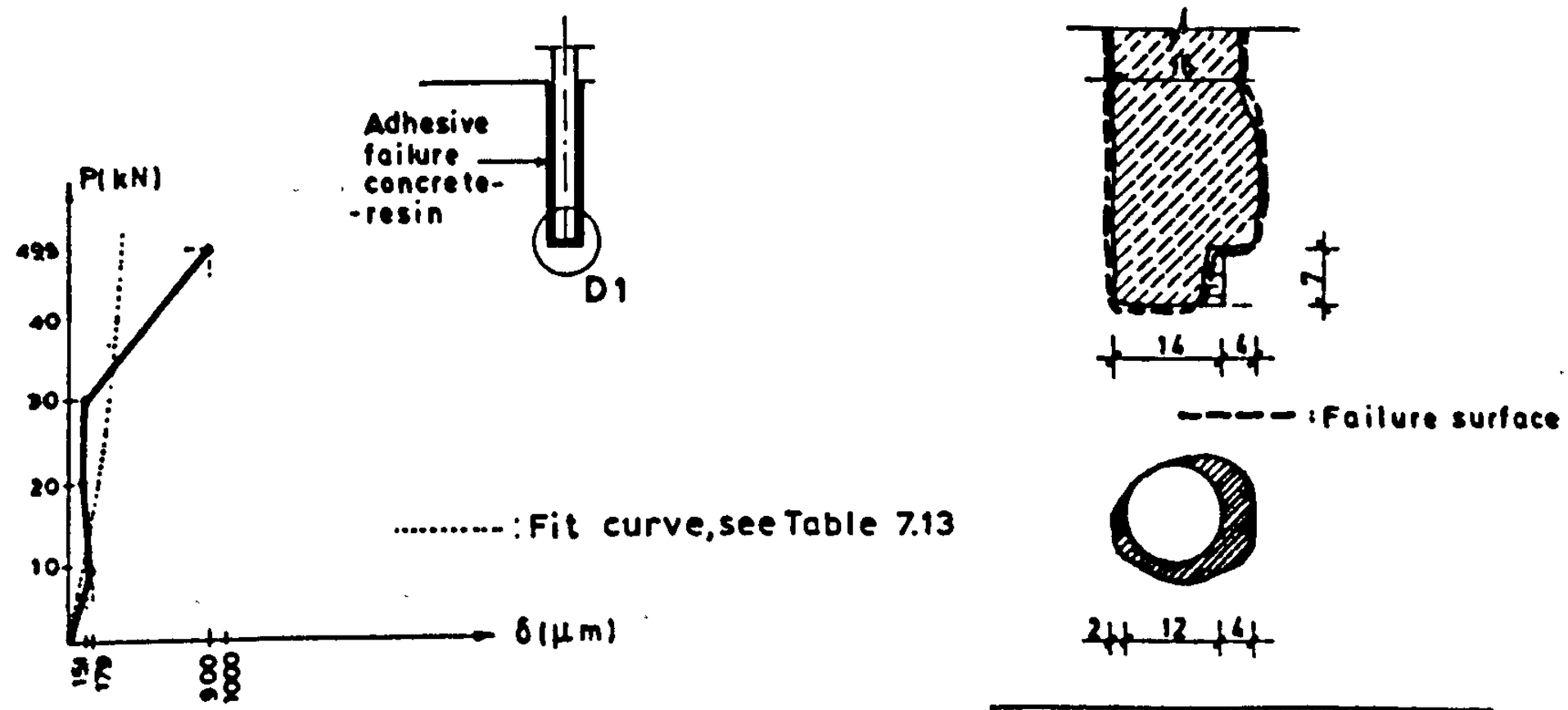

Embedment length (mm) : 100=(8.3)d	
Type of Anchor	:Thread
Anchor diameter (mm)	:12
Gap/diam.of hole(mm)	:2/16
Adhesive	:C1380

Method of drilling	:Perc.Dr.
Method of insert.of resin	:Pouring
Concrete compr.str.(MPa)	62.45
Concrete tens.str.(MPa)	: 3.59
Mode of failure	:I + R

P(kN)	δ(μm)	P(kN)	δ(μm)
10.0	179	35.0	201
15.0	145	40.0	313
20.0	151	45.0	386
25.0	166	49.5	889
30.0	151		

Fig. 7.89

Specimen 3.33 (⊕)

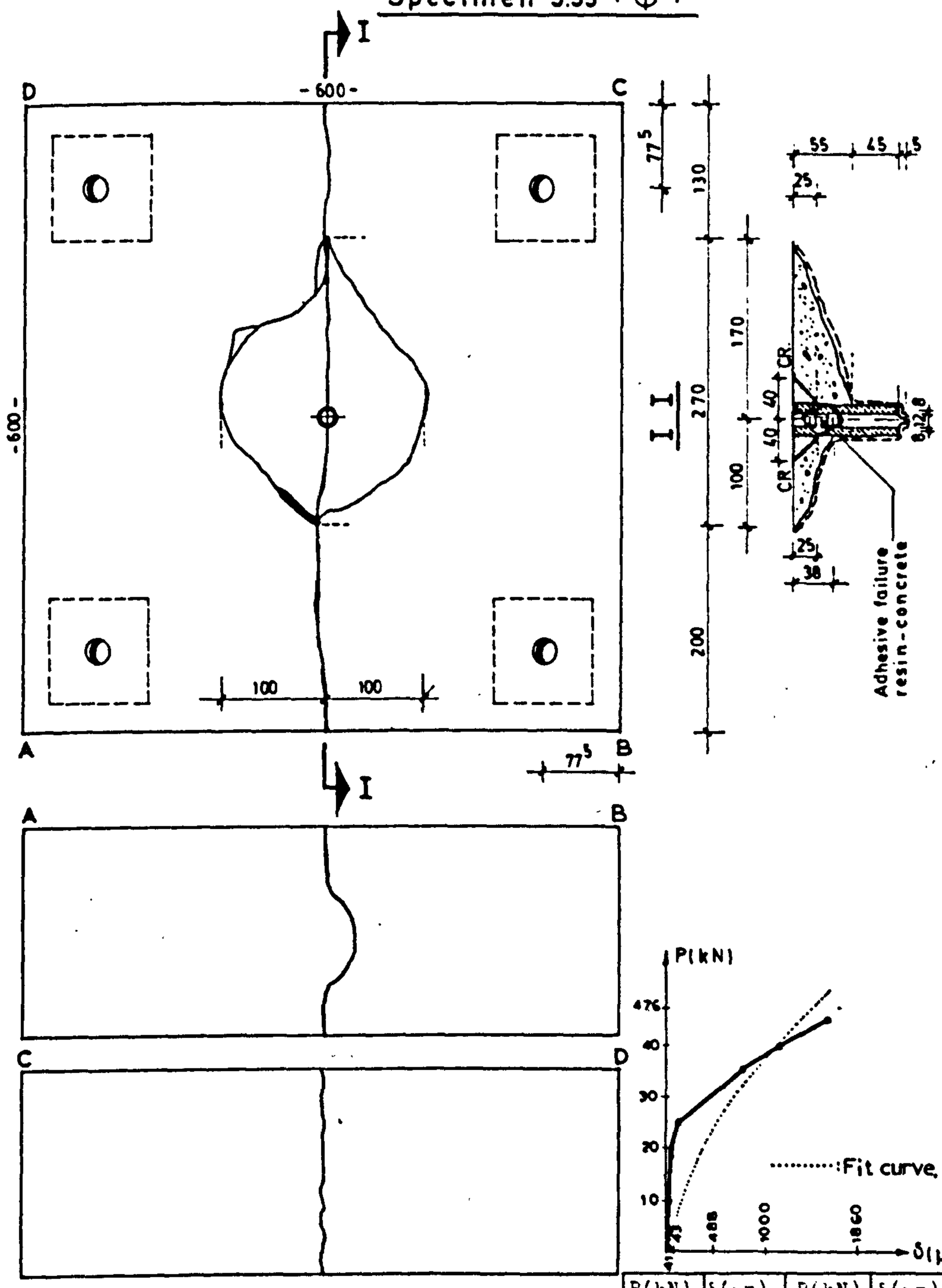

Embedment length (mm)	: 100=(8.3) d
Type of Anchor	: Thread
Anchor diameter (mm)	: 12
Cap/diam.of hole(mm)	: 8/25
Adhesive	: C1380

Method of drilling	: Perc.Dr
Method of insert.of resin	: Pouring
Concrete compr.str.(MPa)	: 27.61
Concrete tens.str.(MPa)	: 2.67
Mode of failure	: I+C+R Spl

P(kN)	δ(μm)	P(kN)	δ(μm)
10.0	41	35.0	760
15.0	42	40.0	1130
20.0	43	45.0	1570
25.0	105	47.6	1860
30.0	488		

Fig.7.90

Specimen 3.34 (⊗)

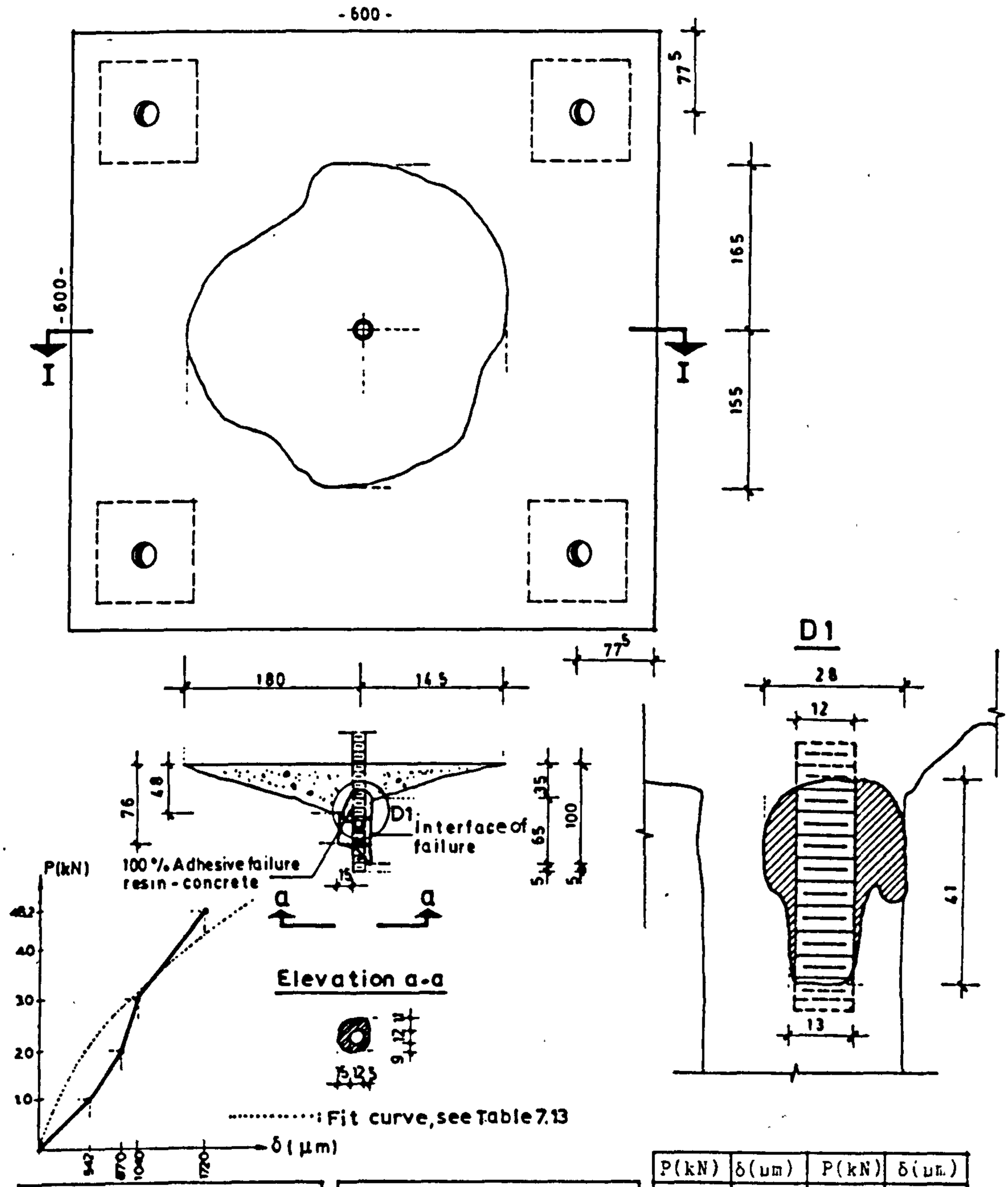

Embedment length (mm)	: 100=(8.3)d
Type of Anchor	: Thread
Anchor diameter (mm)	: 12
Gap/diam. of hole (mm)	: 10/32
Adhesive	: C1380

Method of drilling	: Perc.Dr
Method of inser. of resin	: Pouring
Concrete compr. str. (MPa)	: 26.55
Concrete tens. str. (MPa)	: 3.25
Mode of failure	: I+C+R

P(kN)	δ(µm)	P(kN)	δ(µm)
10.0	542	35.0	1110
15.0	763	40.0	1220
20.0	870	45.0	1320
25.0	935	48.2	1720
30.0	1040		

Fig.7.91

TEST 4.01 - Partially bonded anchor

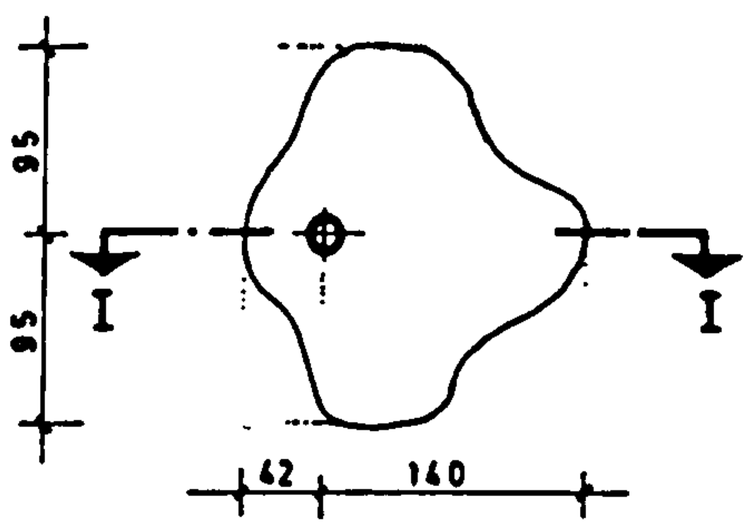

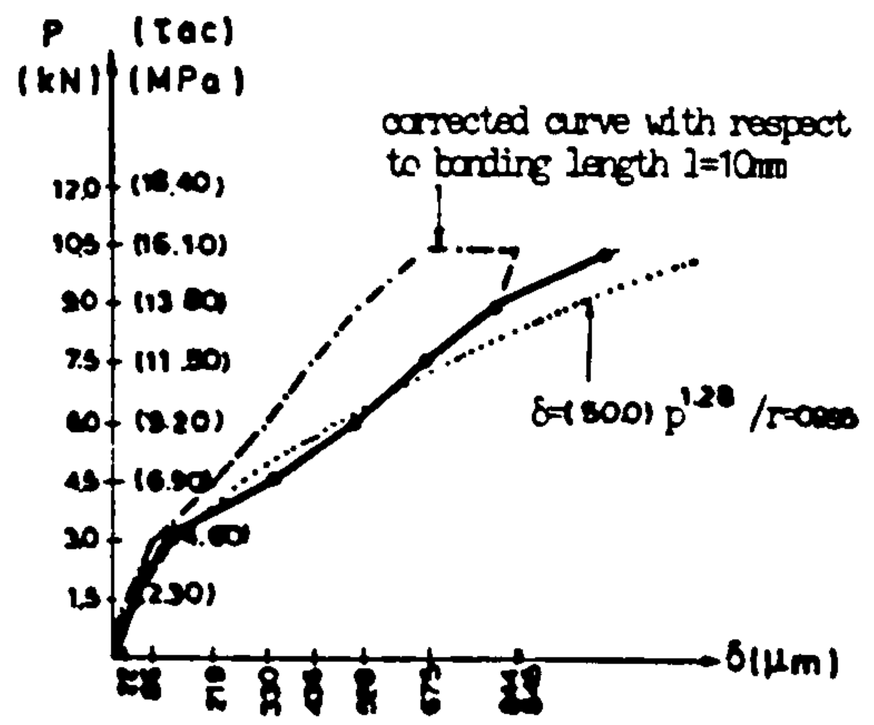

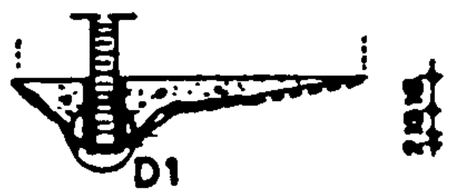

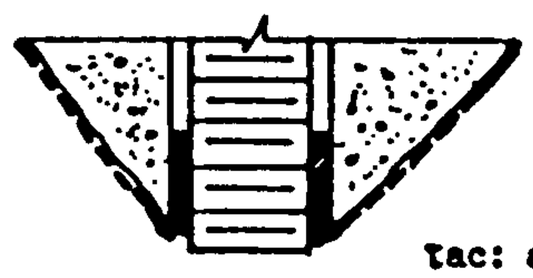

P=1,5

$\tau = \frac{1500}{3{,}14 \times 12 \times 13} = 3{,}06$ MPa

$\tau ac = \frac{1500}{3{,}14 \times 16 \times 13} = 2{,}30$ MPa

τac: at the concrete - resin interface.

				Py	Tac	δ	P	Tac	δ
		Mode of failure: C		[kN]		[μm]	[kN]		[μm]
Bond length [mm]	: 13	Method of drill	: Per.dr	15	2.99	22(34)	7.5	14.93	436(671)
Type of Anchor	: Thread	Method of insert.of resin	: Pour	30	5.97	86(132)	9.0	17.91	528(812)
Anchor diameter [mm]	: 12	Concrete Compr. Str. [MPa]	: 19.56	45	8.95	219(336)	10.2	20.30	844(1298)
Gap/hole diameter [mm]	: 2/16	Concrete tensil Str. [MPa]	: 2.63	60	11.94	330(508)			
Adhesive	: C1380	Concrete Specimen	: 3.01						

( ): correctedvalues of δ

TEST 4.02 - Partially bonded anchor

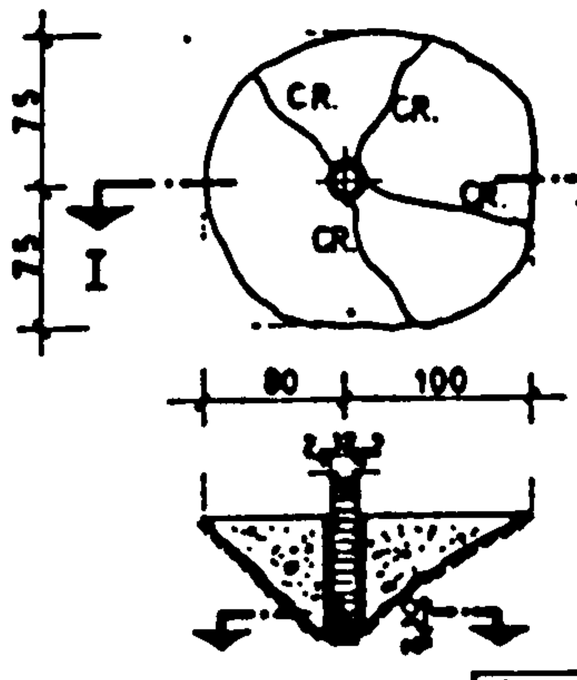

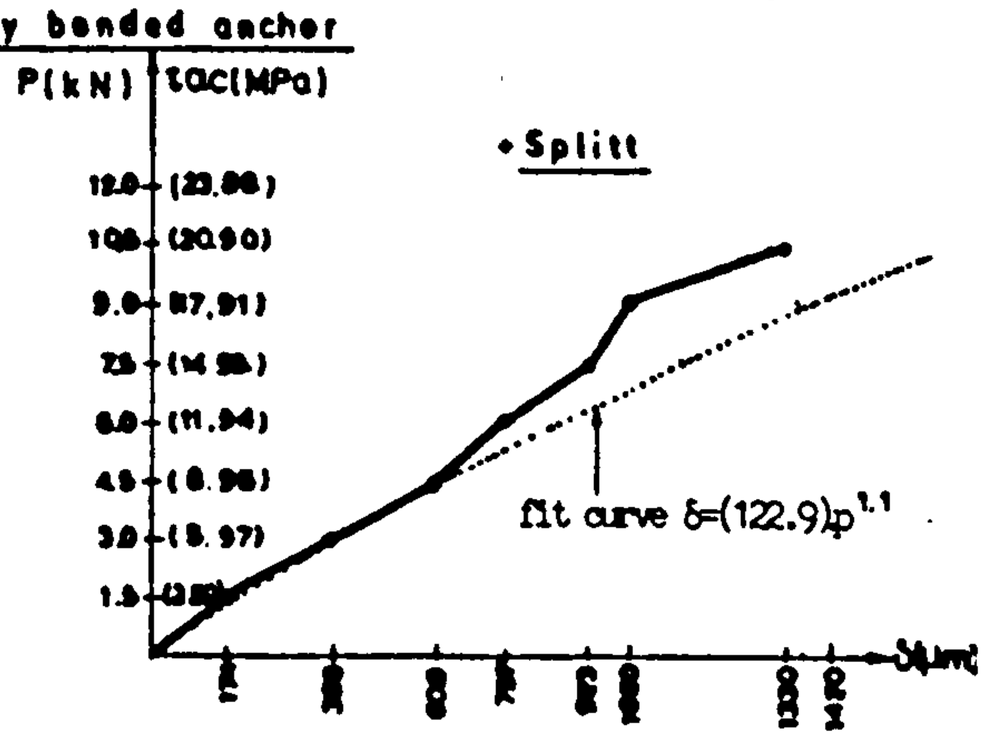

				P	Tac	δ	P	Tac	δ
		Mode of failure: C+R+Split.		[kN]	[MPa]	[μm]	[kN]	[MPa]	[μm]
Bond length [mm]	: 10	Method of drill	: Per.	15	2.99	174	7.5	14.93	923
Type of Anchor	: Thread	Method of insert.of resin	: Pour	30	5.97	393	9.0	17.91	1060
Anchor Diameter [mm]	: 12	Concrete Compr. Str. [MPa]	: 51.78	45	8.95	609	10.5	20.90	1330
Gap/hole diameter [mm]	: 2/16	Concrete tensil Str. [MPa]	: 3.69	60	11.94	757			
Adhesive	: C1380	Concrete Specimen	: 3.14						

Fig. 7.92

TEST 4.03 - Partially bonded anchor

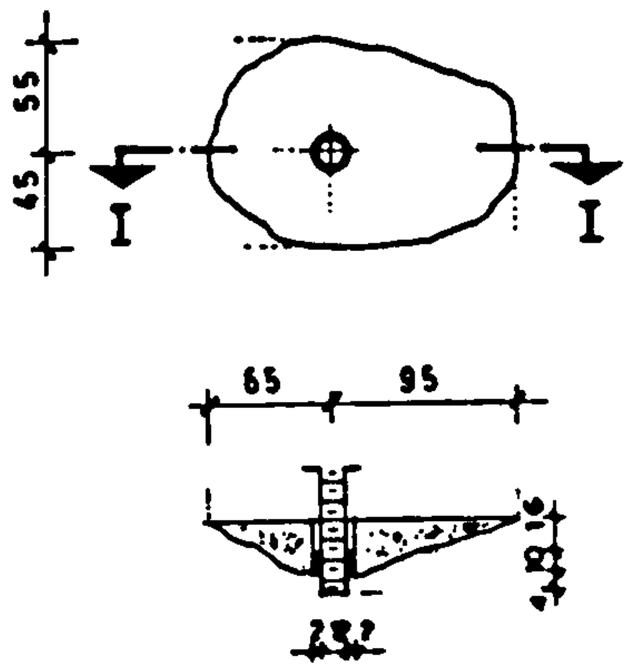

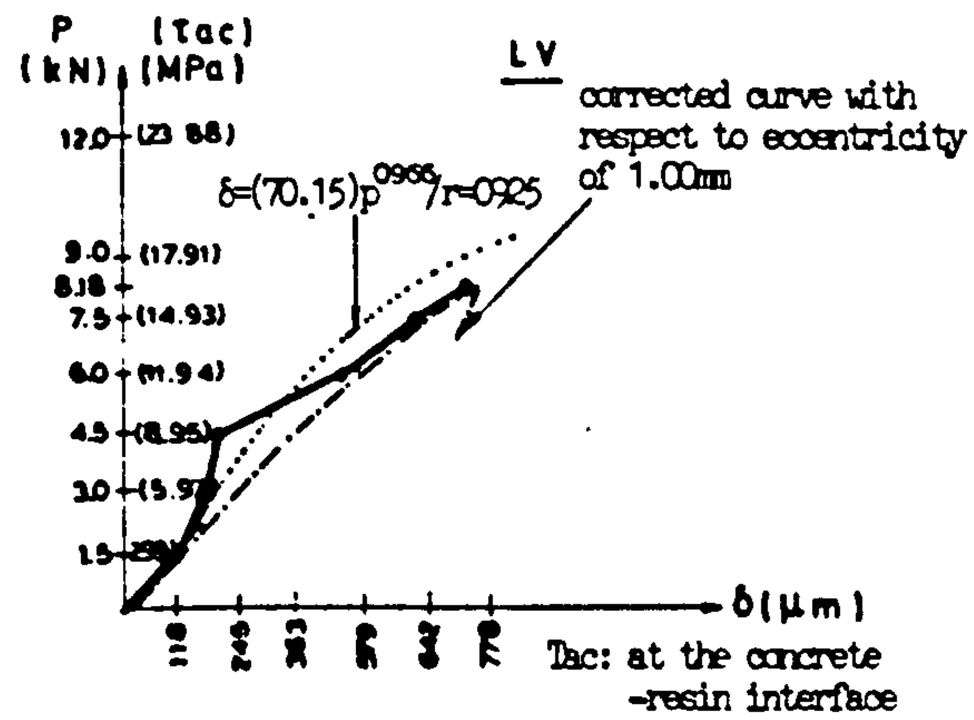

Eccentricity of 1mm		Mode of failure: C		P [kN]	Tac [MPa]	δ [μm]	P [kN]	Tac [MPa]	δ [μm]
Bond length [mm]	: 10	Method of dril	: Per.dr	1.5	2.99	118(123)	7.5	14.93	642(629)
Type of Anchor	: Tread	Method of insert. of resin	: Pour	3.0	5.97	245(169)	8.18	16.30	778(763)
Anchor diameter [mm]	: 12	Concrete Compr. Str. [MPa]	: 21.29	4.5	8.95	363(213)			
Gap/hole diam. [mm]	: 2/16	Concrete tensil Str. [MPa]	: 2.64	6.0	11.94	579(509)			
Adhesive	LV	Concrete Specimen	: 3.03						

( ): Corrected values of δ see Appendix H

TEST 4.04 - Partially bonded anchor

Plain bar

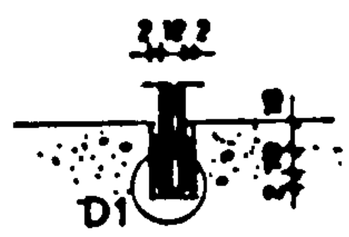

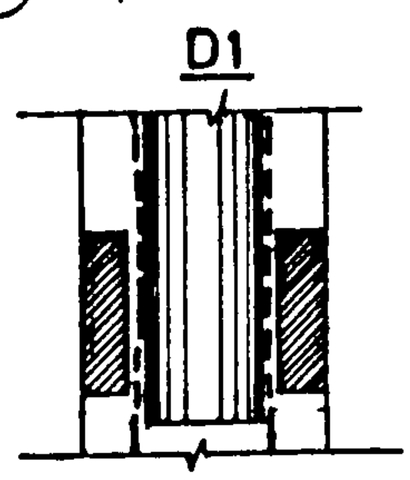

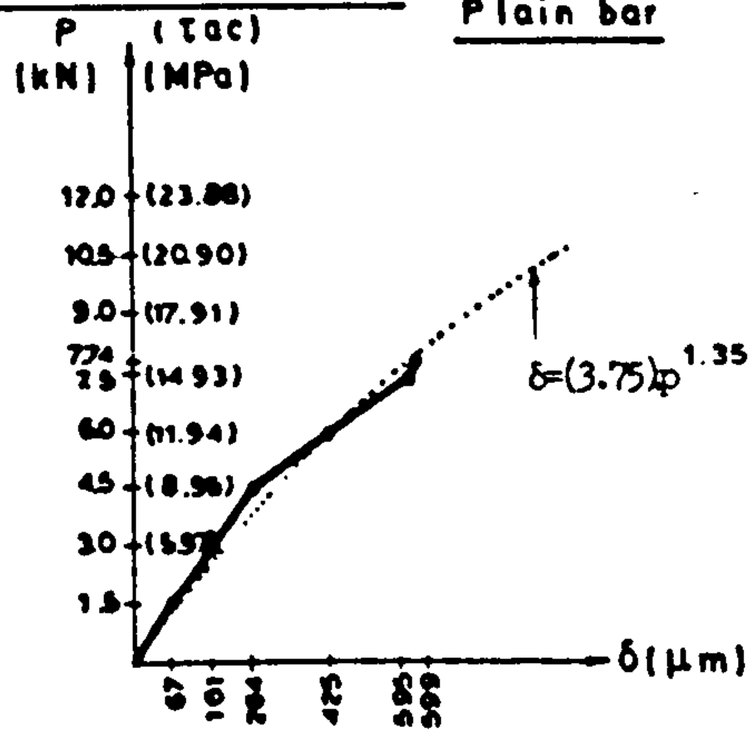

		Mode of failure: I		P [kN]	Tac [MPa]	δ [μm]	P [kN]	Tac [MPa]	δ [μm]
Bond length [mm]	: 10	Method of dril	: Per. dr	1.5	2.99	67	7.5	14.93	593
Type of Anchor	: Plain	Method of insert. of resin	: Pour	3.0	5.97	161	7.74	15.43	549
Anchor diameter [mm]	: 12	Concrete Compr. Str. [MPa]	: 20.60	4.5	8.95	264			
Gap/hole diam. [mm]	: 2/16	Concrete tensil Str. [MPa]	: 2.25	6.0	11.95	425			
Adhesive	: CT380	Concrete Specimen	: 3.22						

Fig. 7.93

TEST 4.05 - Partially bonded anchor

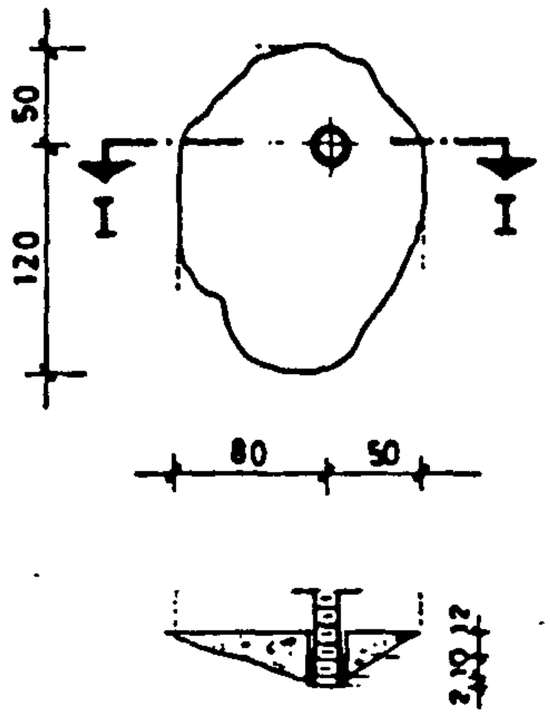

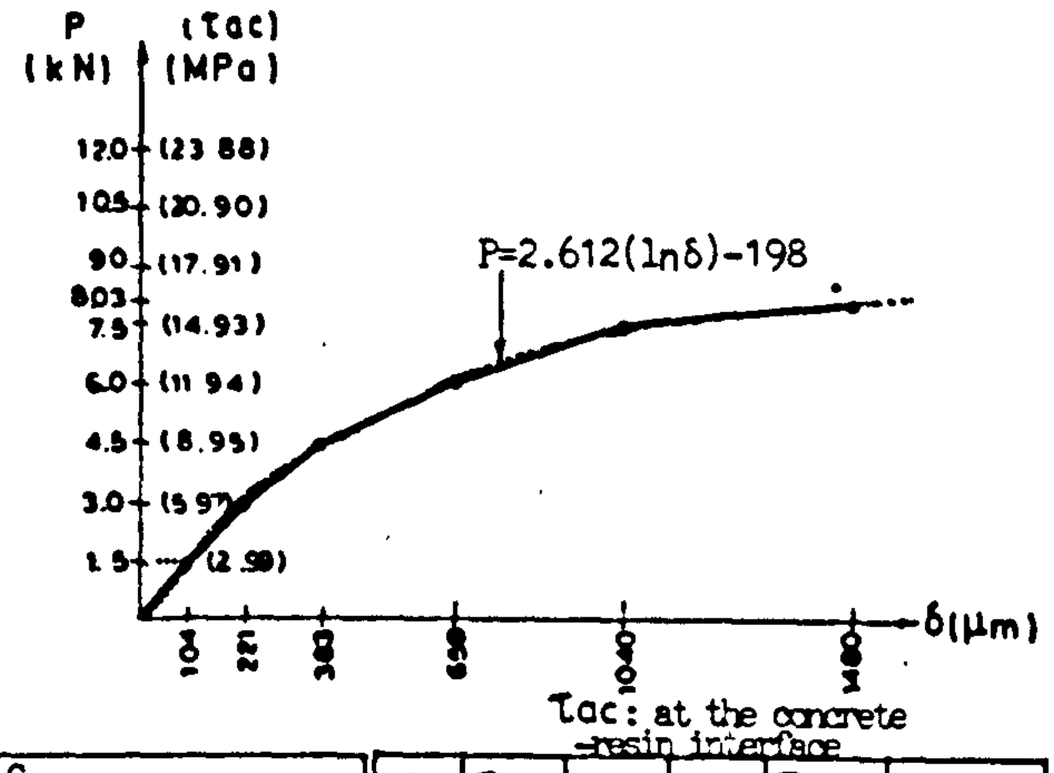

				P	τac	δ	P	τac	δ
		Mode of failure: C							
Bond length [mm]	: 10	Method of dril	:Per. dr	[kN]	[MPa]	[μm]	[kN]	[MPa]	[μm]
Type of Anchor	: Tread	Method of insert. of resin	:Cart	δ1.5	2.99	104	7.5	14.93	1040
Anchor diameter [mm]	: 12	Concrete Compr. Str. [MPa]	:22.25	δ3.0	5.97	221	8.03	16.00	1430
Cap/hole diam. [mm]	: 2/16	Concrete tensil Str. [MPa]	: 2.25	δ4.5	8.95	333			
Adhesive	: CEL	Concrete Specimen	: 3.25	δ6.0	11.95	658			

TEST 4.07 - Partially bonded anchor

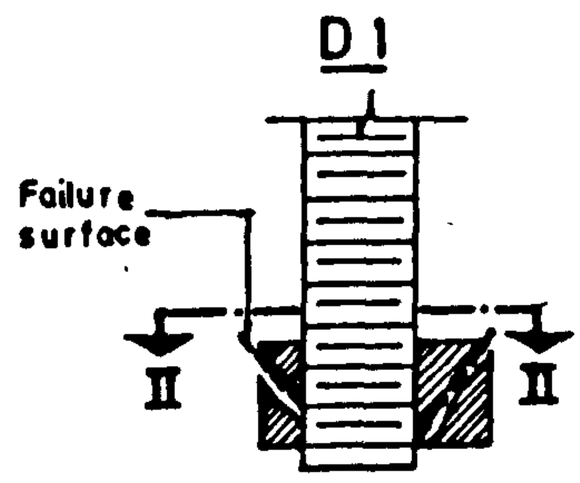

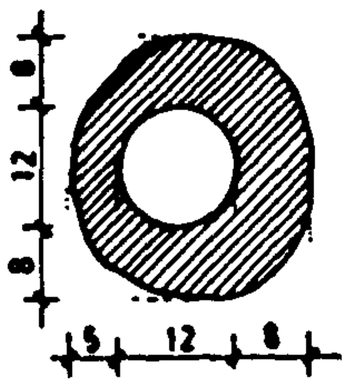

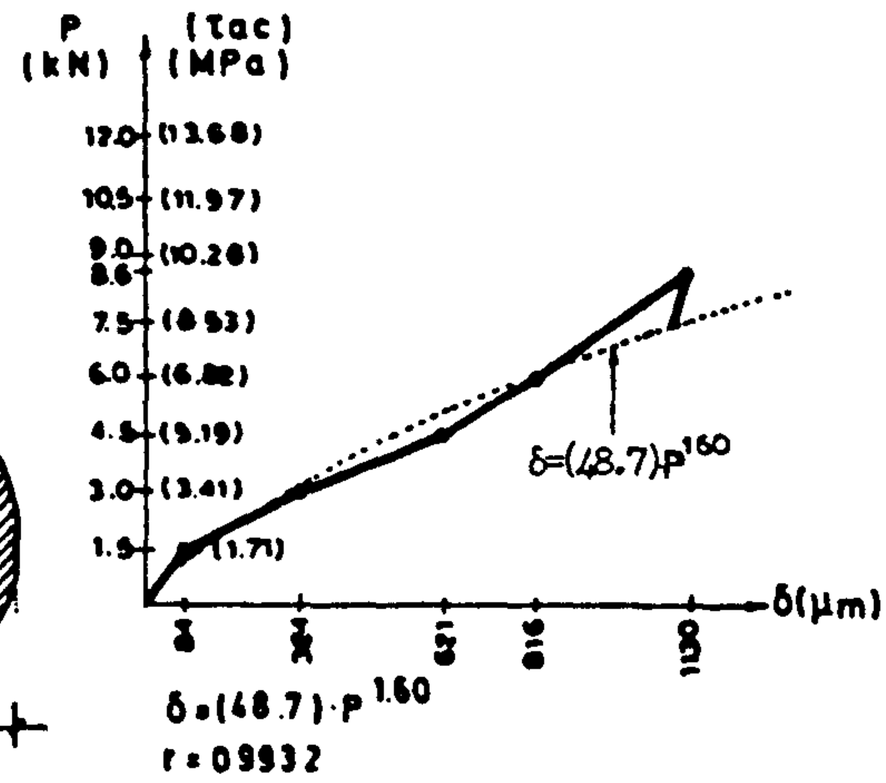

				P	τac	δ	P		δ
Bond length [mm]	: 10	Method of dril	: Per.dr	[kN]	[MPa]	[μm]	[kN]	[MPa]	[μm]
Type of Anchor	:Tread	Method of insert.of resin	: Pour	1.5	1.71	84	7.5	8.53	1130
Anchor Diameter [mm]	: 12	Concrete Compr. Str. [MPa]	:23.11	3.0	3.41	324	8.6	9.78	1300
Cap/hole diam. [mm]	: 8/28	Concrete tensil Str. [MPa]	: 2.71	4.5	5.19	621			
Adhesive	: C1380	Concrete Specimen	: 3.06	6.0	6.82	816			

Fig.7.94

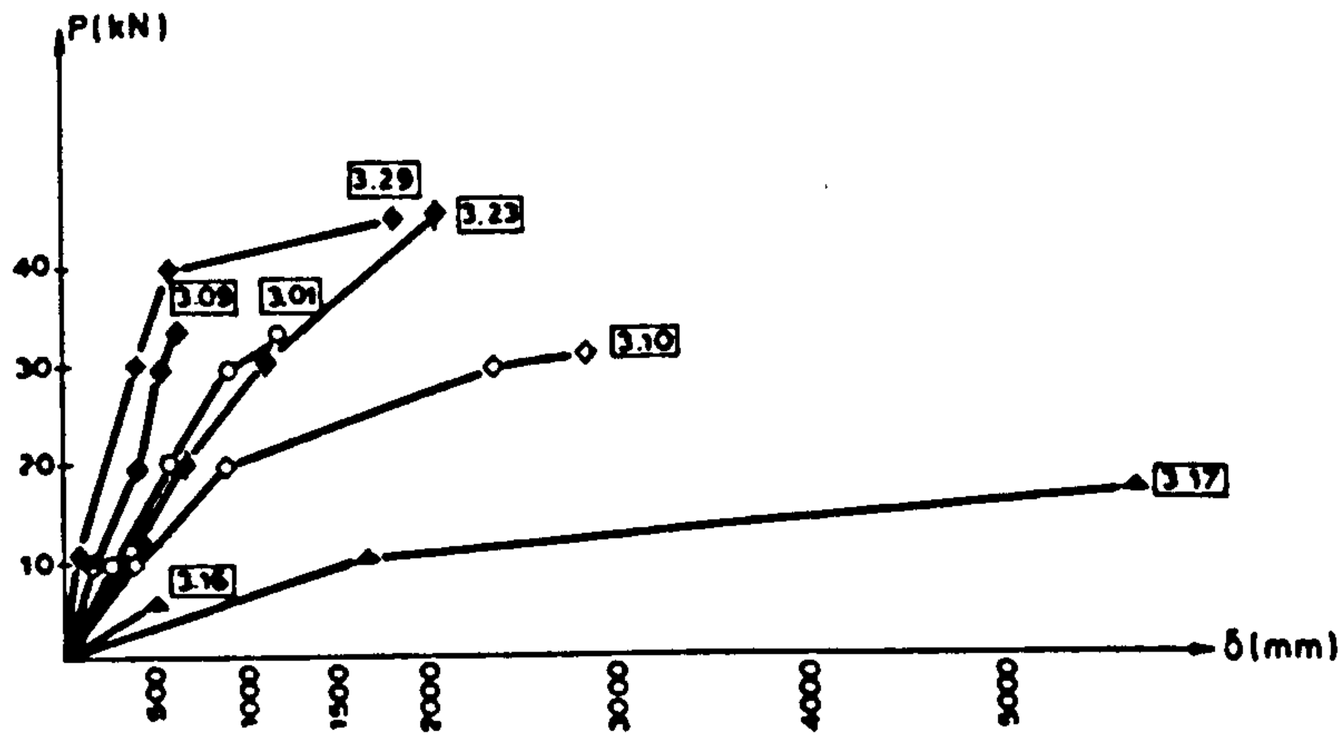

	Sp.	Emb.le.	Typ.of Anchor	Diam.of Anchor	Cap/dia.of Anchor	Epoxy	Method of Insert.	Method of Dril.	fcc	fst	δ10	δ20	δ30	δ40	δy
○	3.01	100=(8.3)d	Thr.	12	2/16	C1380	Pour.	Perc.	19.56	2.63	267	599	940		1210
◆	3.09	100=(8.3)d	Thr.	12	2/16	LV	Pour	Perc.	31.67	2.76	165	418	558		618
◆	3.10	100=(8.3)d	Thr.	12	2/16	GEL	Coat	Perc.	25.30	2.61	361	921	2350		2830
▲	3.16	100=(8.3)d	Thr.	12	4/20	[illegible]	Pour	Perc.	24.93	3.05					506
▲	3.17	100=(8.3)d	Thr.	12	4/20	[illegible]	Pour	Perc.	21.66	2.88	1690				5640
◆	3.23	100=(8.3)d	Thr.	12	2/16	LV	Pour	Perc.	18.97	2.15	312	589	1060		2000
◆	3.29	100=(8.3)d	Thr.	12	2/16	LV	Pour	Perc.	24.25	2.60	202	493	682		1860

Fig.7.95. Comparison of the fundamental law P=P(δ) for different types of adhesive.

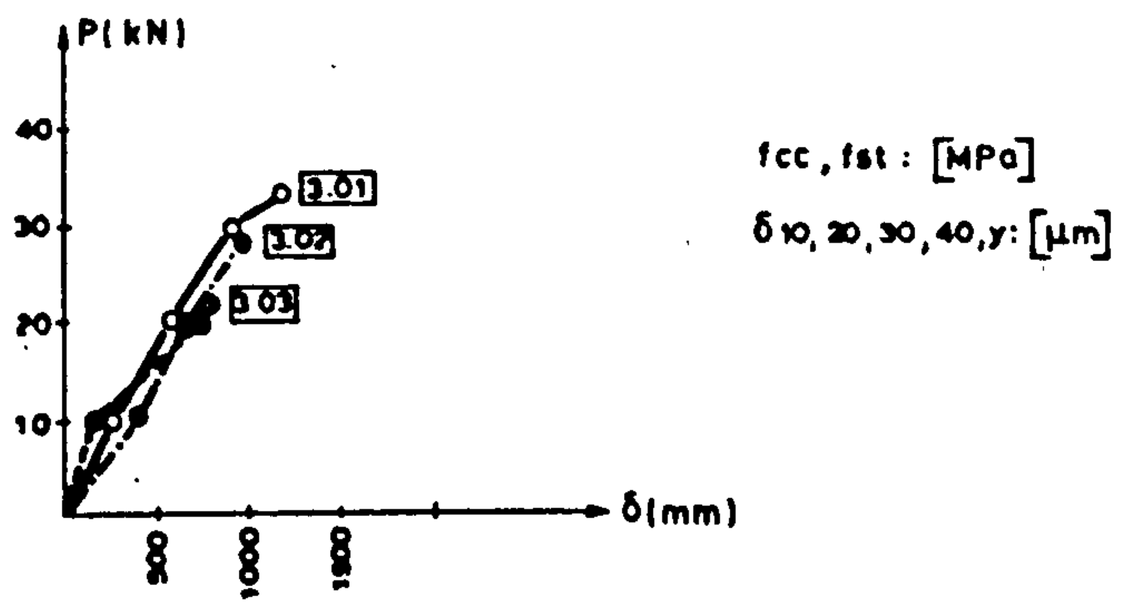

	Sp.	Emb.le.	Typ.of Anchor	Diam.of Anchor	Cap/dia. of Anchor	Epoxy	Method of Insert.	Method of Dril	fcc	fst	δ10	δ20	δ30	δy
○	3.01	100=(8.3)d	Thr.	12	2/16	C1380	Pour	Perc.	19.56	2.63	267	599	940	1210
●	3.02	84=7d	Thr.	12	2/16	C1380	Pour	Perc.	20.38	2.96	397	668		[illegible]
●	3.03	60=5d	Thr.	12	2/16	C1380	Pour	Perc.	21.29	2.64	148	687		688

Fig.7.96. Comparison of the fundamental law for different values of embedment length.

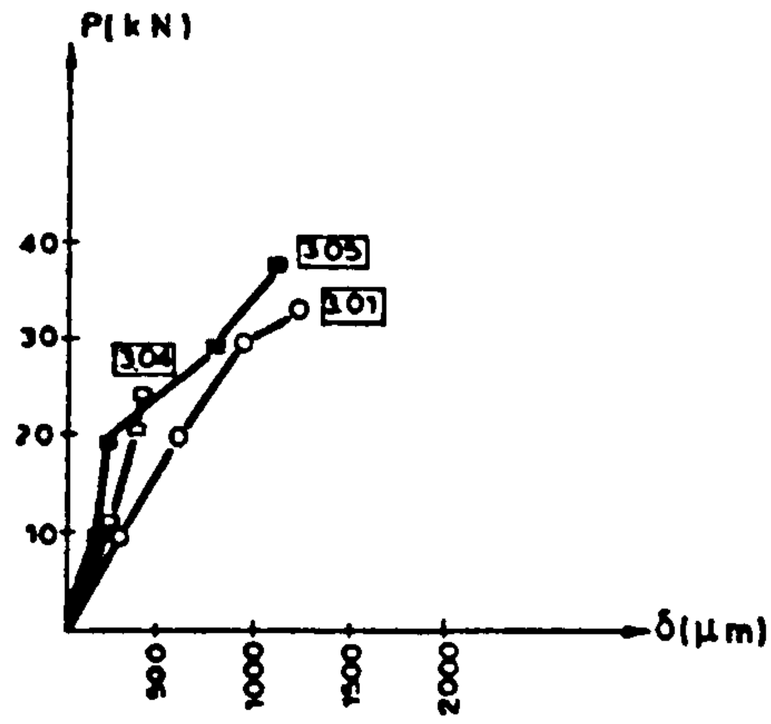

Sp.	Emb.le.	Typ.of Anchor	Diam.of Anchor	Gap/dia.of Anchor	Epoxy	Method of Insert.	Method of Drill	fcc	fst	δ10	δ20	δ30	δy	Py
○ 3.01	100=(8.3)d	Thr.	12	2/16	C1380	Pour	Perc.	19.56	2.63	267	599	940	1210	33.3
□ 3.04	100=(8.3)d	Plain b.	12	2/16	C1380	Pour	Perc.	26.39	2.55	202	359		395	22.5
■ 3.05	100=(8.3)d	Ribbed	12	2/16	C1380	Pour	Perc.	23.20	3,13	145	193	772	1100	18.1

Fig.7.97. Comparison of the fundamental law P=P(δ) for different types of anchor.

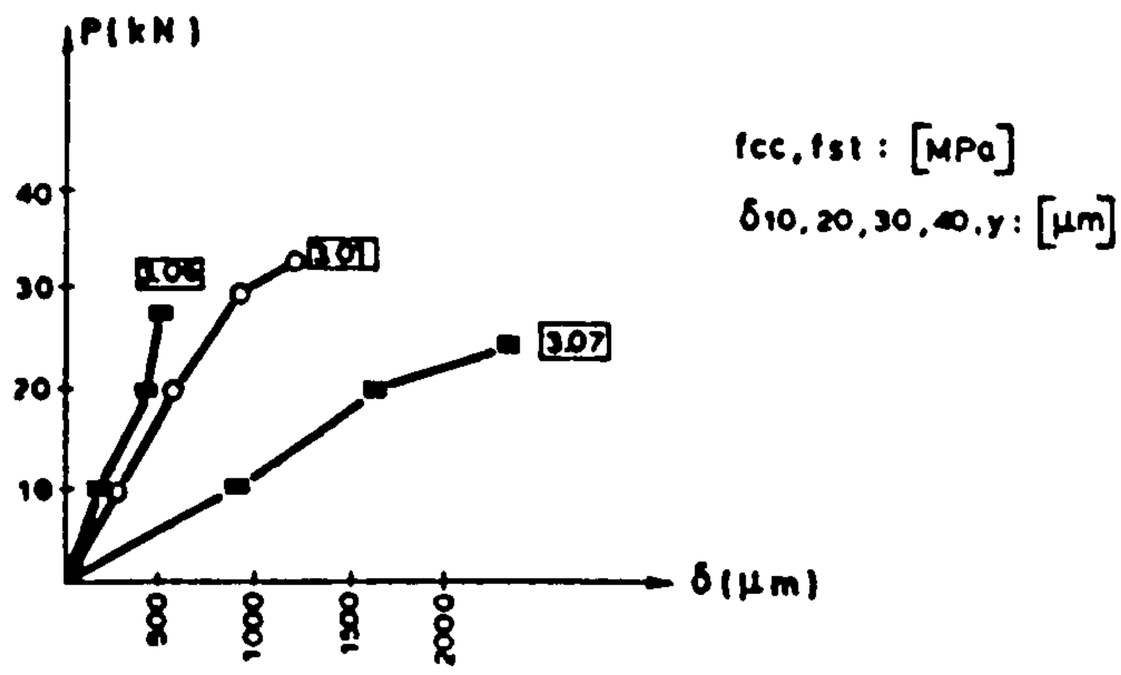

Sp.	Emb.le.	Typ.of Anchor	Diam.of Anchor	Gap/dia.of Anchor	Epoxy	Method of Insert.	Method of Drill	fcc	fst	δ10	δ20	δ30	δy
○ 3.01	100=(8.3)d	Thr.	12	2/16	C1380	Pour	Perc.	19.56	2.63	267	599	940	1210
■ 3.06	83=(8.3)d	Thr.	10	2/14	C1380	Pour	Perc.	23.11	2.71	299	480		550
■ 3.07	66=(8.3)d	Thr.	8	2/12	C1380	Pour	Perc.	29.48	3.68	920	1620		2370

Fig.7.98. Comparison of the fundamental law for different anchor diameters.

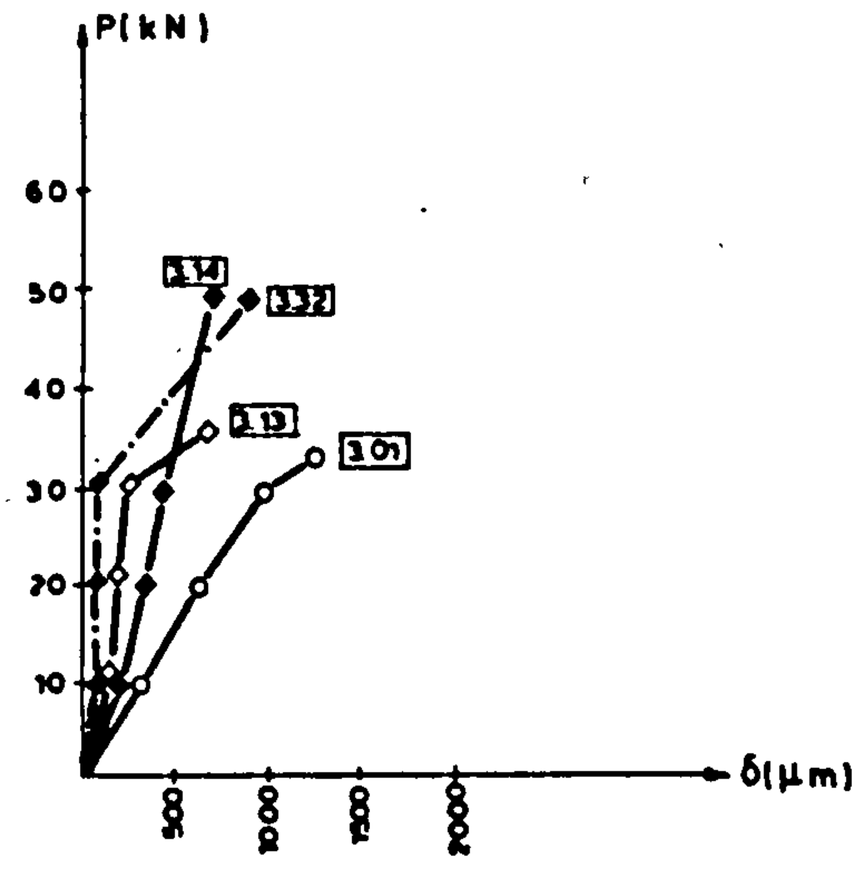

	Sp.	Emb.le.	Typ.of Anchor	Diam.of Anchor	Gap/dia.of Anchor	Epoxy	Method of Insert.	Method of Drill	fcc	fst	δ10	δ20	δ30	δ40	δy
○	3.01	100=(8.3)d	Thr.	12	2/16	C1380	Pour	Perc.	19.56	2.63	267	599	940		1210
◇	3.13	90=(7.5)d	Thr.	12	2/16	C1380	Pour	Perc.	37.90	3.17	268	265	334		759
◆	3.14	100=(8.3)d	Thr.	12	2/16	C1380	Pour	Perc.	51.78	3.69	178	330	440		662
◆	3.32	100	Thr.	12	2/16	C1380	Pour	Perc.	62.45	7.90	179	151	151		911

Fig.7.99. The effect of concrete strength on the fundamental law P=P(δ).

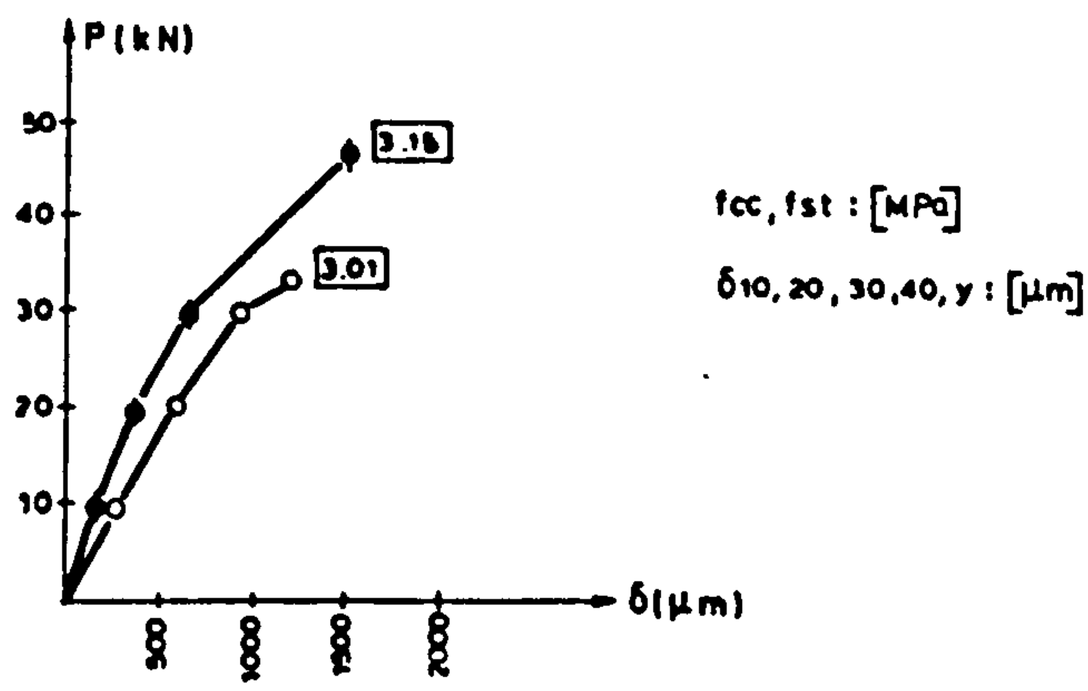

	Sp.	Emb.le	Typ.of Anchor	Diam.of Anchor	Gap/dia.of Anchor	Epoxy	Method of Insert.	Method of Drill	fcc	fst	δ10	δ20	δ30	δ40	δy
○	3.01	100=(8.3)d	Thr.	12	2/16	C1380	Pour	Perc.	19.56	2.63	267	599	940		1210
◆	3.15	100=(8.3)d	Thr.	12	2/16	C1380	Injec.	Perc.	21.48	2.37	149	398	672		1550

Fig.7.100. The effect of the method of insertion of resin on the P=P(δ) relationship.

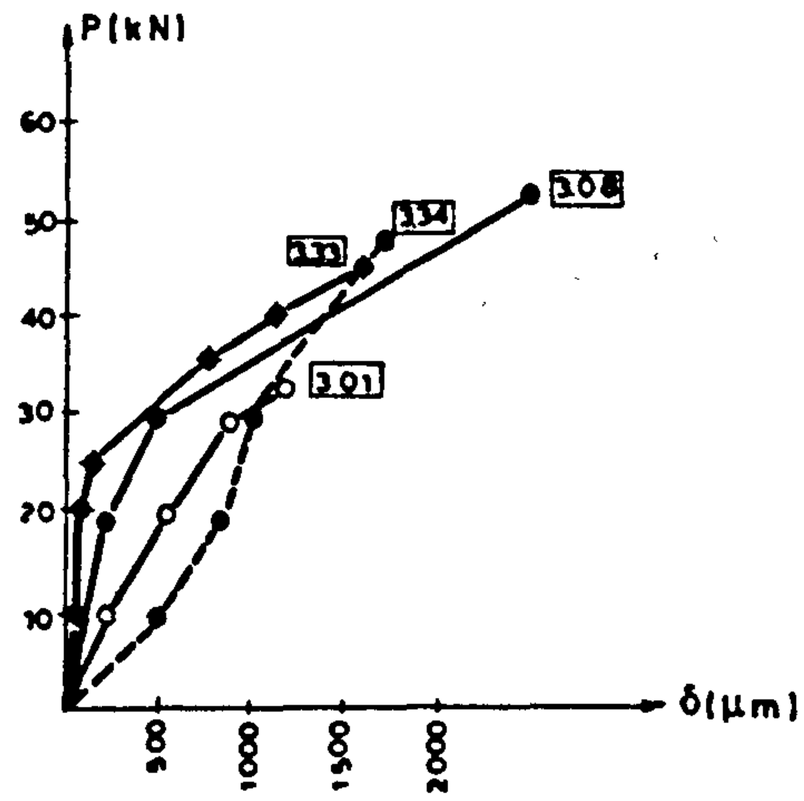

Sp.	Emb.le.	Typ.of Anchor	Diam.of Anchor	Cap/dia.of Anchor	Epoxy	Method of Insert.	Method of Dril	fcc	fst	δ10	δ20	δ30	δy
○ 3.01	100=(8.3)d	Thr.	12	2/16	C1380	Pour	Perc.	19.56	2.63	267	599	940	1210
● 3.08	100=(8.3)d	Thr.	12	4/20	C1380	Pour	Perc.	28.76	3.05	000	259	517	2230
◆ 3.33	100=(8.3)d	Thr.	12	8/28	C1380	Pour	Perc.	27.61	2.67	41	43	488	1860
● 3.34	100=(8.3)d	Thr.	12	10/32	C1380	Pour	Perc.	26.55	3.25	542	870	1040	1720

Fig.7.101. The influence of thickness of resin on the P=P(δ) relationship.

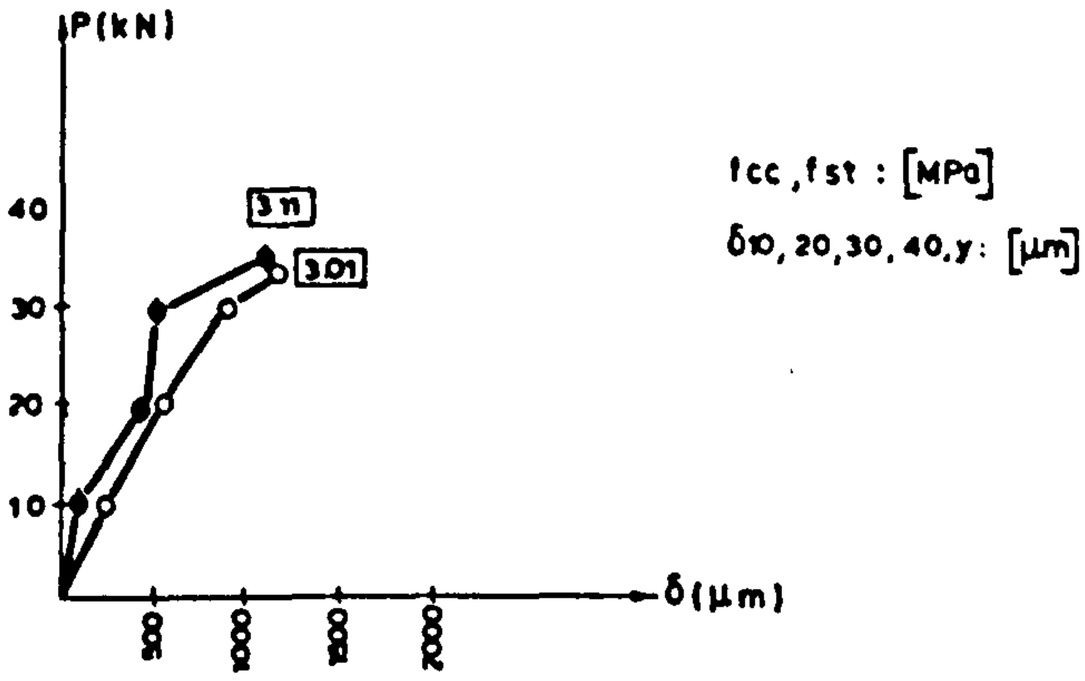

Sp.	Emb.le.	Typ.of Anchor	Diam.of Anchor	Cap/dia.of Anchor	Epoxy	Method of Insert.	Method of Dril	fcc	fst	δ10	δ20	δ30	δy
○ 3.01	100=(8.3)d	Thr.	12	2/16	C1380	Pour	Perc.	19.56	2.63	267	599	940	1210
◆ 3.11	100=(8.3)d	Thr.	12	4/20	C1380	Pour Eccentric	Perc.	28.48	2.51	139	506	531	1160

Fig.7.102. The influence of the eccentricity of the anchor on the P=P(δ) curve.

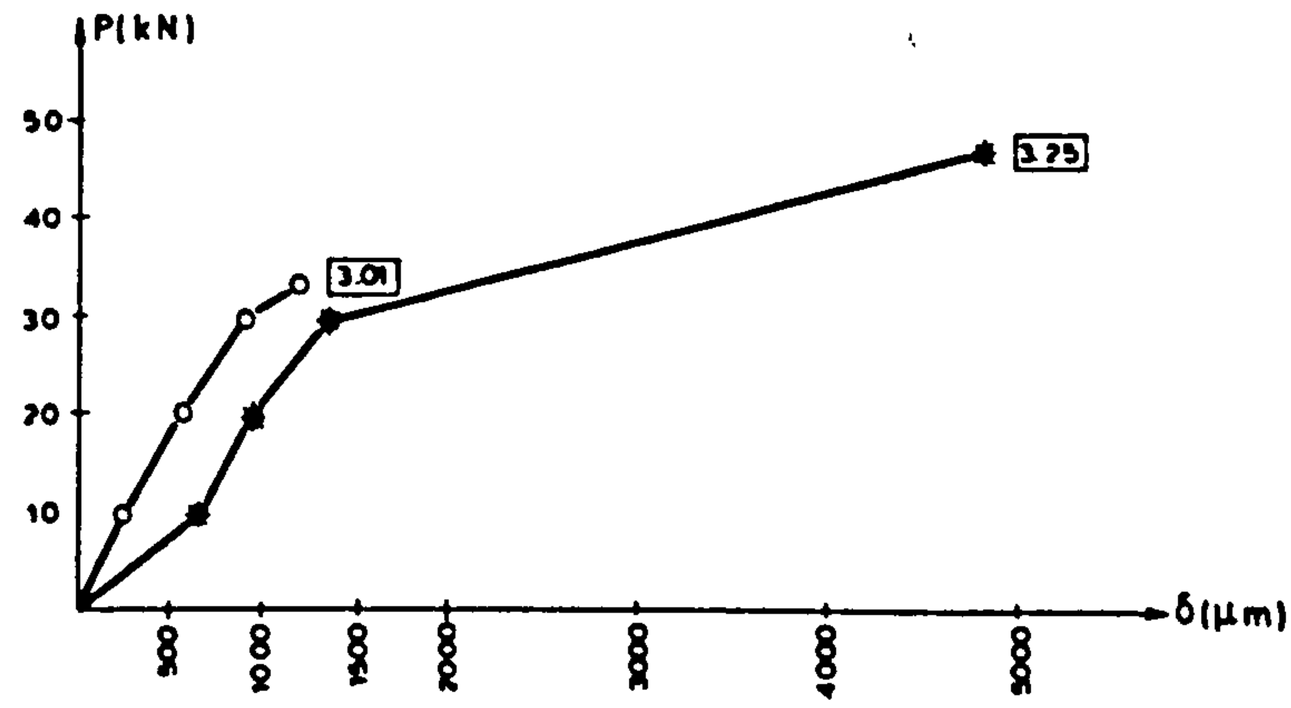

Sp.	Emb.le.	Typ.of Anchor	Diam.of Anchor	Cap/dia.of Anchor	Epoxy	Method of Insert.	Method of Dril.	f_{cc}	f_{st}	δ10	δ20	δ30	δy
○ 3.01	100=(8.3)d	Thr.	12	2/16	C1380	Pour	Perc.	19.56	2.63	267	599	940	1210
● 3.25	100=(8.3)d	Thr.	12	4/20	C1380	Pour	Diam.dr	22.25	2.25	656	916	1370	4830

Fig.7.103. The influence of the method of drilling.

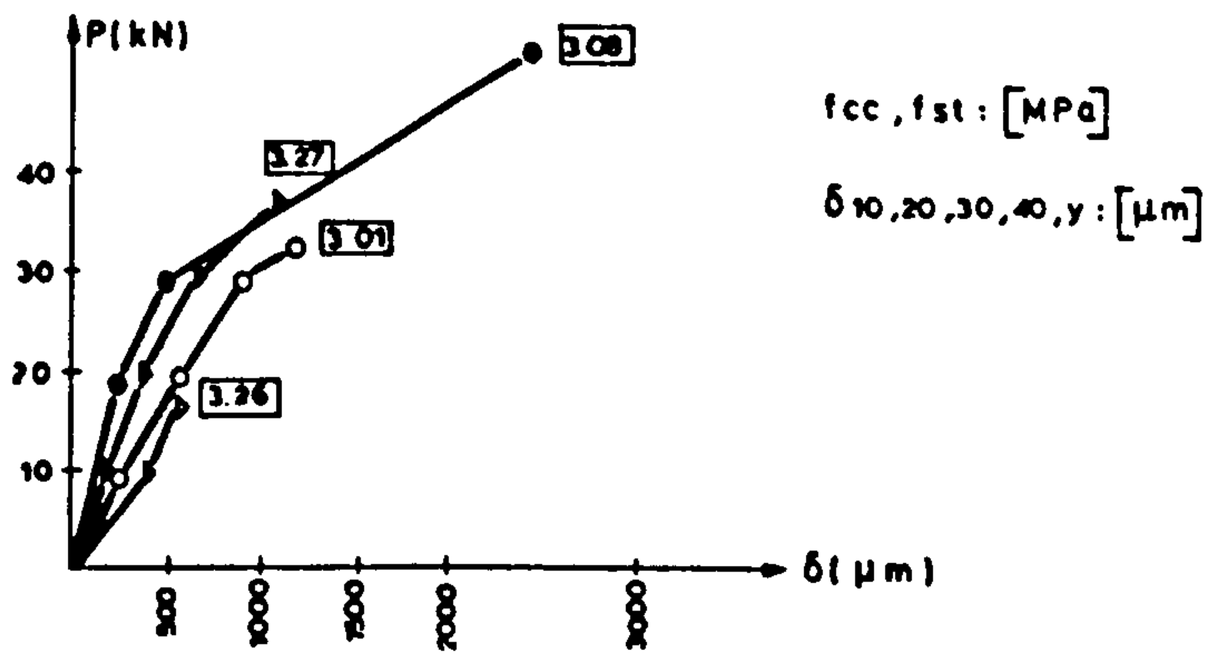

Sp.	Emb.le.	Typ.of Anchor	Diam.of Anchor	Cap/dia.of Anchor	Epoxy	Method of Insert.	Method of Drill	f_{cc}	f_{st}	δ10	δ20	δ30	δy
○ 3.01	100=(8.3)d	Thr.	12	2/16	C1380	Pour	Perc.	19.56	2.63	267	599	940	1210
● 3.08	100=(8.3)d	Thr.	12	4/20	C1380	Pour	Perc.	26.76	3.05	000	259	517	2230
▶ 3.26	100=(8.3)d	Thr.	12	2/16	C1380	Pour	Perc.	20.02	2.15	385			536
▶ 3.27	100=(8.3)d	Thr.	12	4/20	C1380	Pour	Perc.	20.61	2.40	205	447	744	1130

Fig.7.104. The effect of the size of specimen on the relationship R=P(δ).

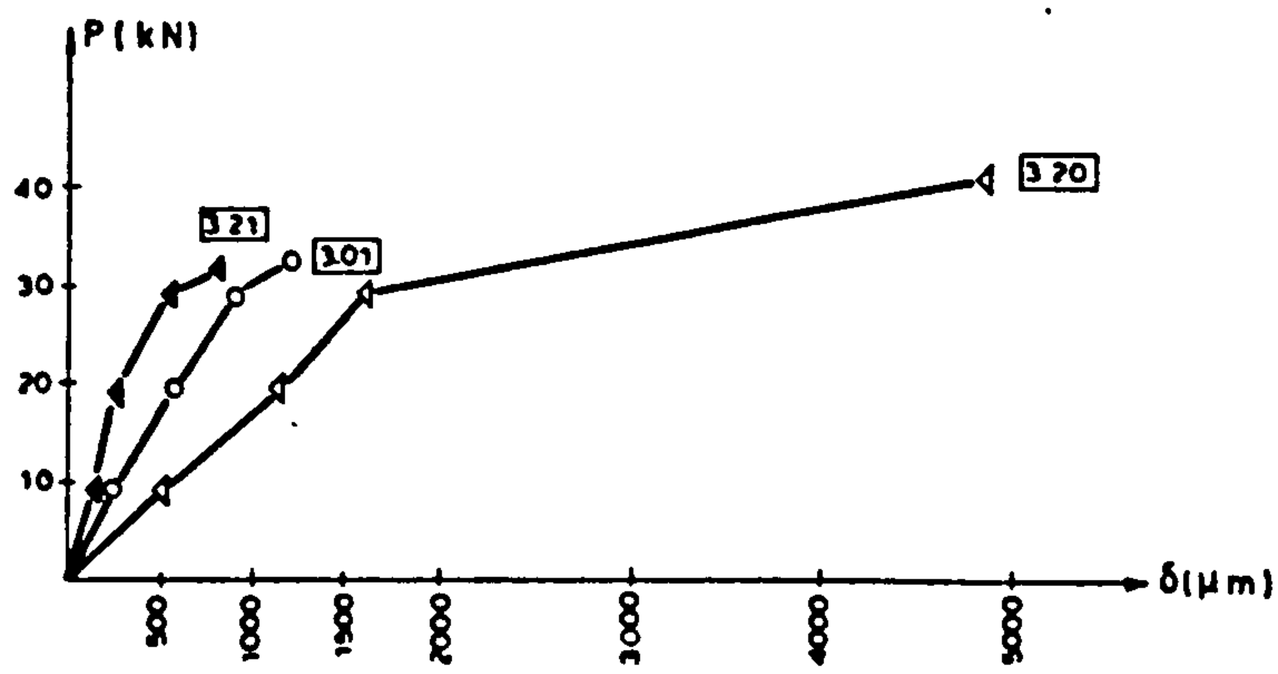

	Sp.	Emb.le.	Typ.of Anchor	Diam.of Anchor	Gap/dia.of Anchor	Epoxy	Method of Insert.	Method of Dril	f_{cc}	f_{st}	δ10	δ20	δ30	δy	μ_{xy}
○	3.01	100=(8.3)d	Thr.	12	2/16	C1380	Pour	Perc.	19.56	2.63	267	599	940	1210	0
◀	3.20	100=(8.3)d	Thr.	12	2/16	C1380	Pour	Perc.	26.07	2.65	533	1140	1620	4880	1%
◀	3.21	100=(8.3)d	Thr.	12	2/16	C1380	Pour	Perc.	20.93	2.30	169	292	576	835	2%

Fig.7.105. The effect of the amount of reinforcement.

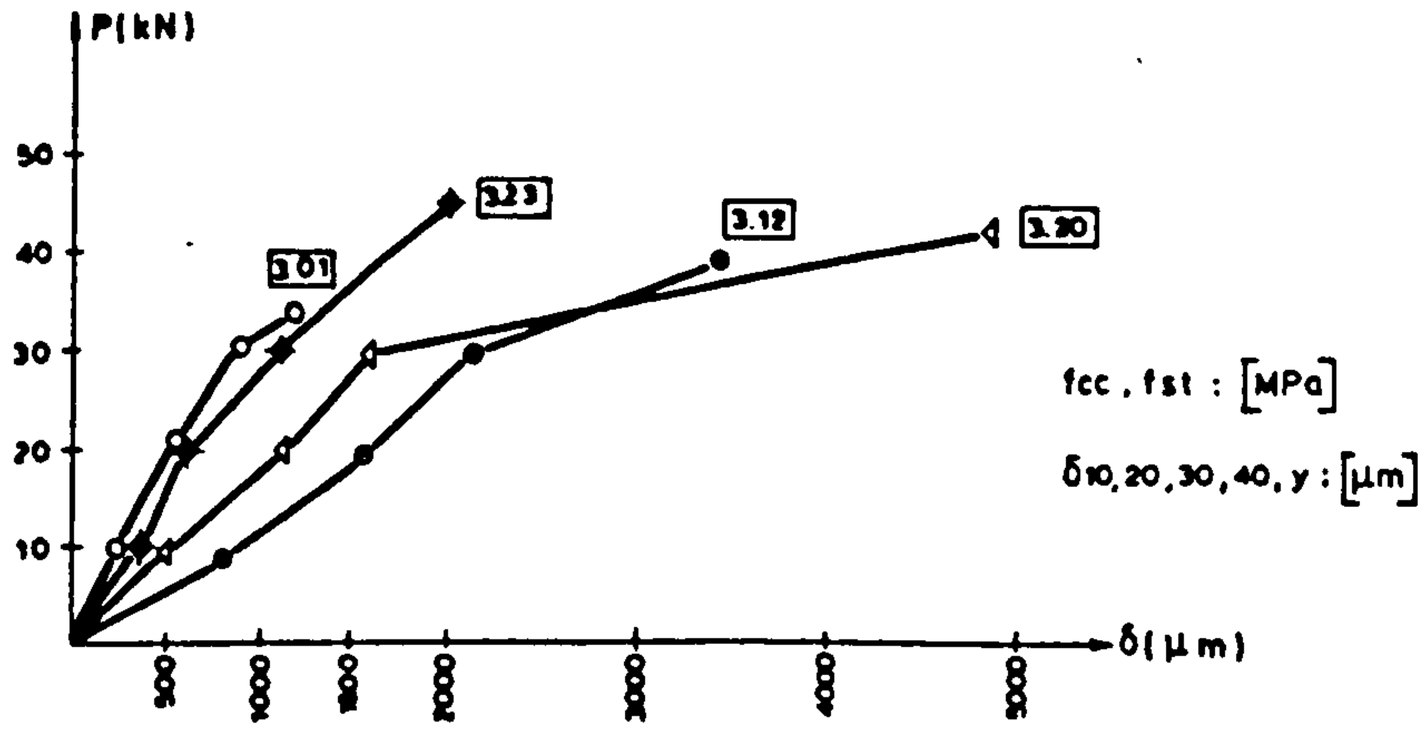

	Sp.	Emb.le.	Typ.of Anchor	Diam.of Anchor	Gap/dia.of Anchor	Epoxy	Method of Insert.	Method of Dril	f_{cc}	f_{st}	δ10	δ20	δ30	δy	mode
○	3.01	100=(8.3)d	Thr.	12	2/16	C1380	Pour	Perc.	19.56	2.63	267	599	940	1210	I•C•R
●	3.12	95=(7.9)d	Thr.	12	2/16	C1380	Pour	Perc.	21.93	2.58	861	1610	2150	3450	spl.•R
◀	3.20	100=(8.3)d	Thr.	12	2/16	C1380	Pour	Perc.	26.07	2.65	533	1140	1620	4880	spl.•R
◆	3.23	100=(8.3)d	Thr.	12	2/16	C1380	Pour	Perc.	18.97	2.15	312	589	1060	2000	I•C•R•Spl

Fig.7.106. The relationship P=P(δ) for different modes on failure

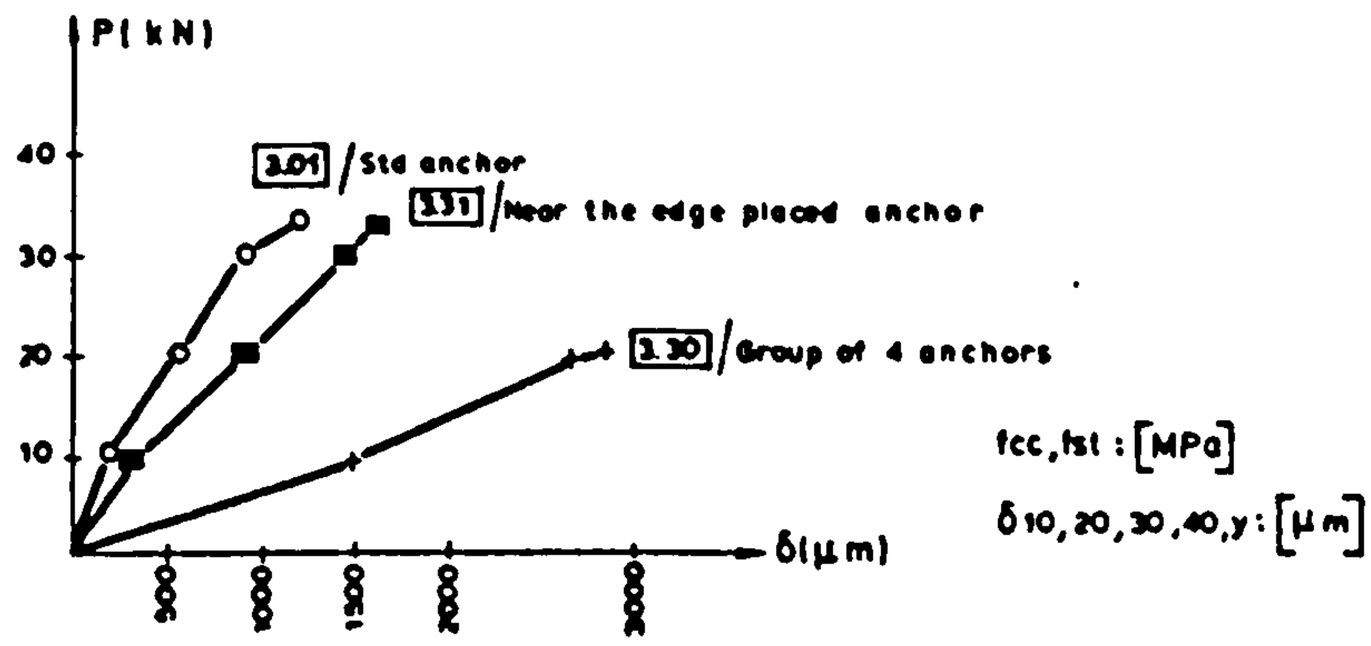

Sp.		Emb.le.	Typ.of Anchor	Diam.of Anchor	Cap/dia.of Anchor	Epoxy	Method of Insert.	Method of Drill	fcc	fst	δ10	δ20	δ30	δy
○	3.01	100=(8.3)d	Thr.	12	2/16	C1380	Pour	Perc.	19.56	2.63	267	599	940	1210
+	3.30	100=(8.3)d	Thr.	12	2/16	C1380	Pour	Perc.	20.61	2.70	1510	2770		2860
■	3.31	100=(8.3)d	Thr.	12	2/16	C1380	Pour	Perc.	24.89	2.55	291	918	1470	1620

Fig.7.107. The group and the edge effect on the P=P(δ) relationship.

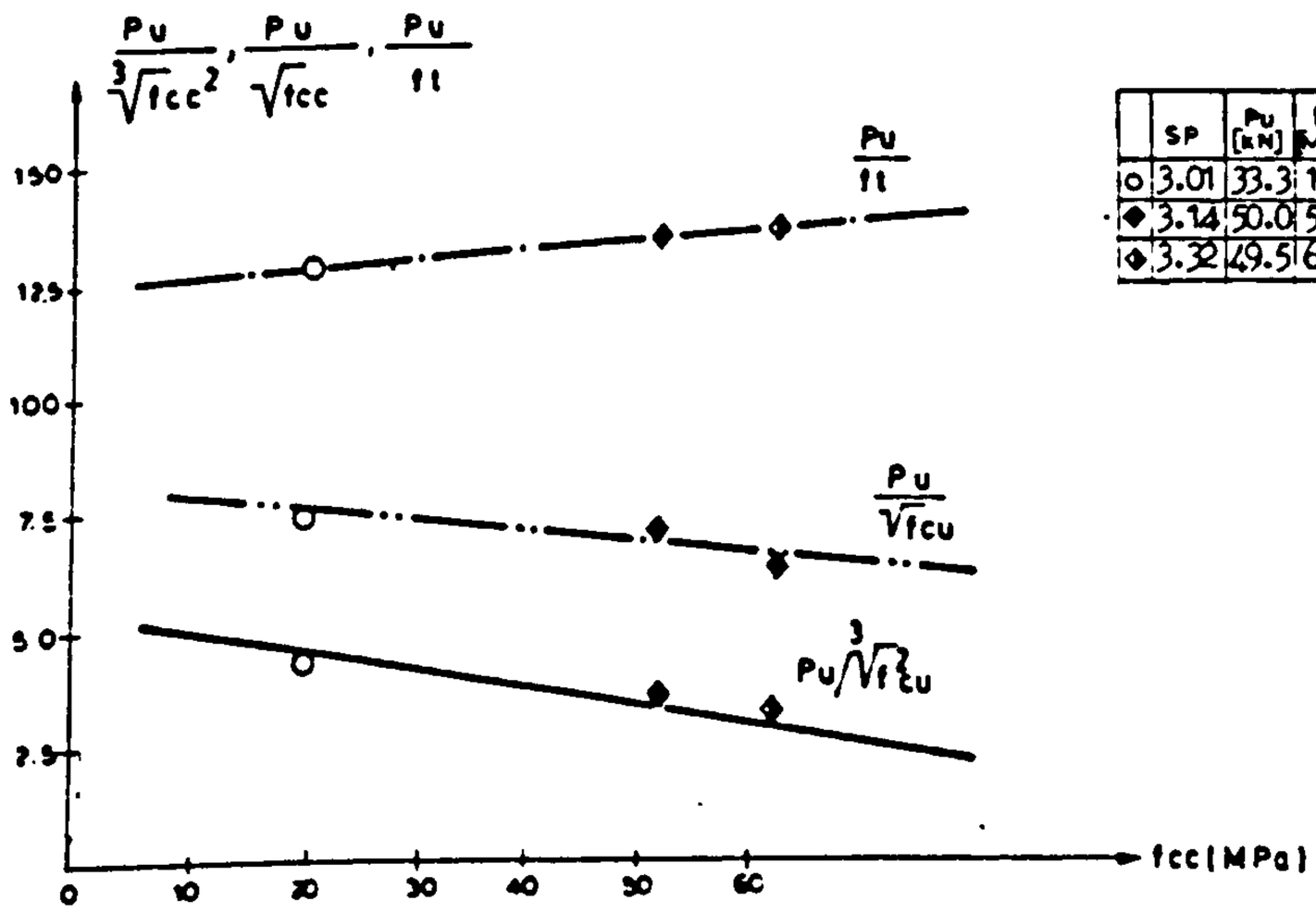

	SP	Pu [kN]	fcc [MPa]	∛fc²	ft [MPa]	√fc	Pu/∛fc²	Pu/ft	Pu/√fc
o	3.01	33.3	19.56	7.27	2.63	4.42	4.56	12.66	7.54
◆	3.14	50.0	51.78	13.91	3.69	7.20	3.59	13.55	6.94
◆	3.32	49.5	62.45	15.76	3.59	7.90	3.14	13.78	6.26

Fig.7.108. Dependence of ultimate pull-out load on concrete strength.

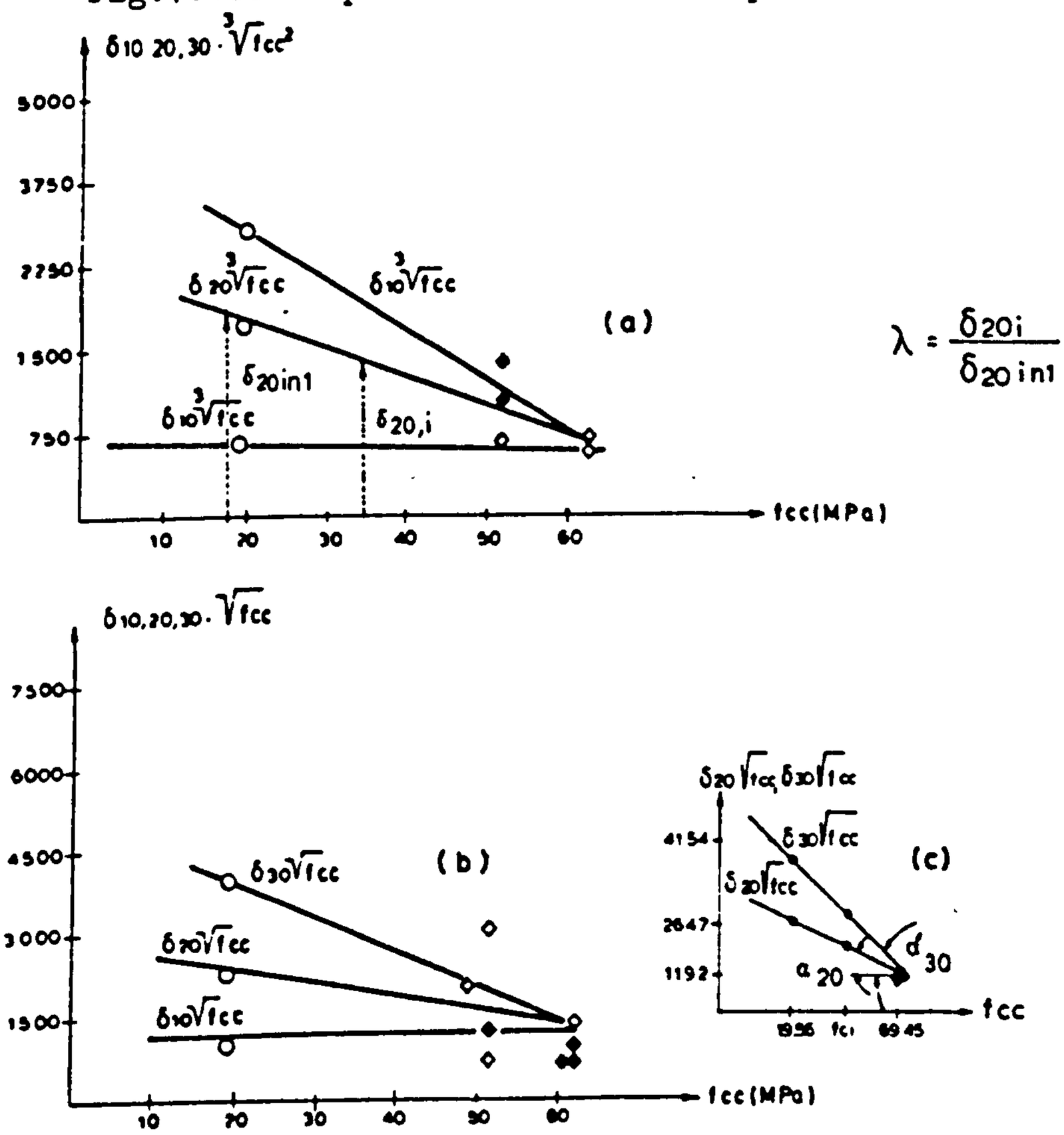

	SPo	fcc	∛fcc	√fcc	δ10 [μm]	δ20 [μm]	δ30 [μm]	δ10∛fcc	δ20∛fcc	δ30∛fcc	δ10√fcc	δ20√fcc	δ30√fcc
o	3.01	19.56	2.69	4.42	267	599	940	716	1611	2529	1180	2647	4154
◆	3.14	51.78	3.72	7.20	178	330	440	662	1227	1636	1281	2376	3168
◆	3.32	69.45	4.10	7.90	179	151	151	734	619	619	1414	1192	1192

Fig.7.109. Effect of concrete strength on anchors displacement.

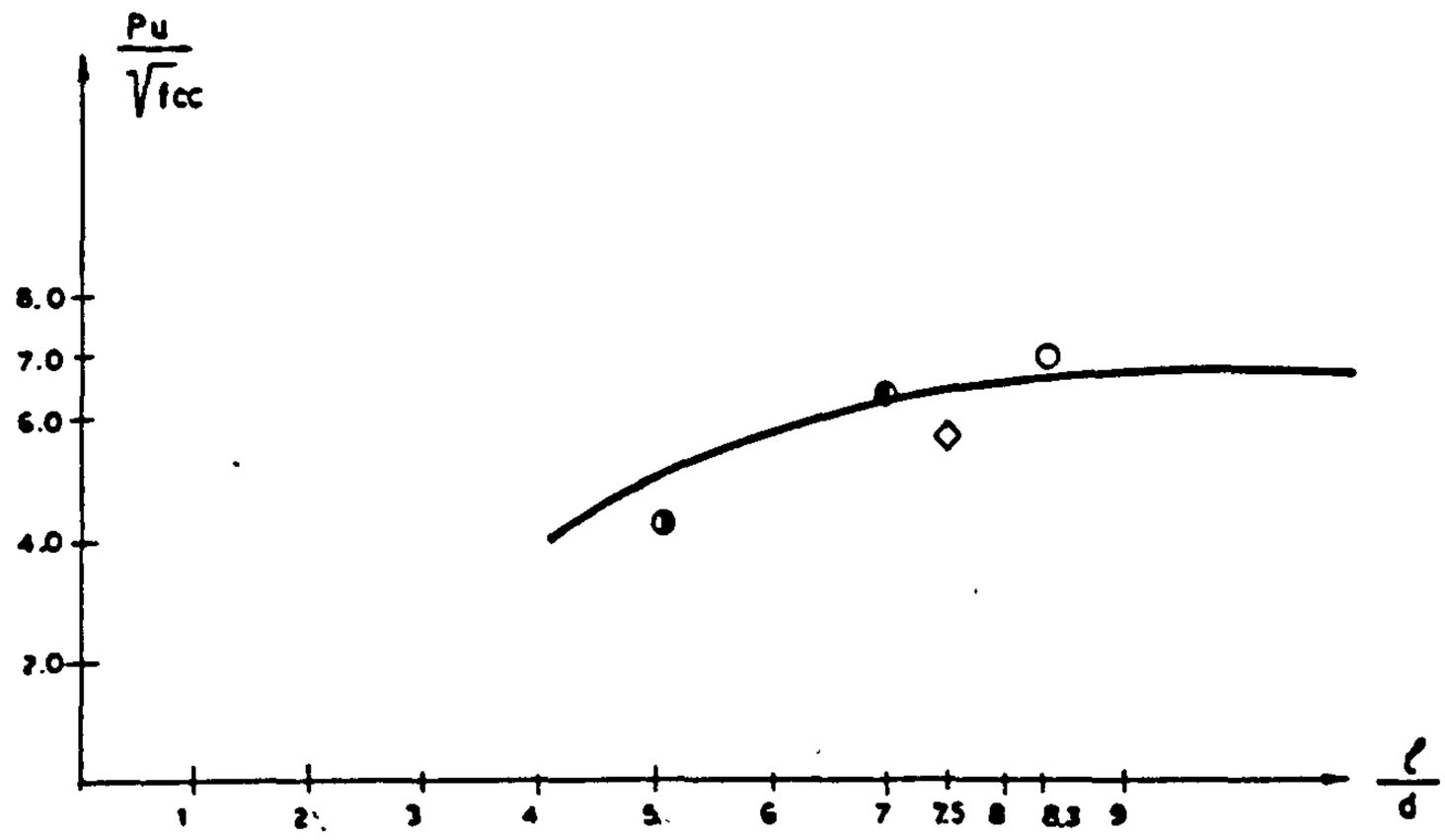

Fig.7.110. Effect of embedment length on the ultimate pull-out load.

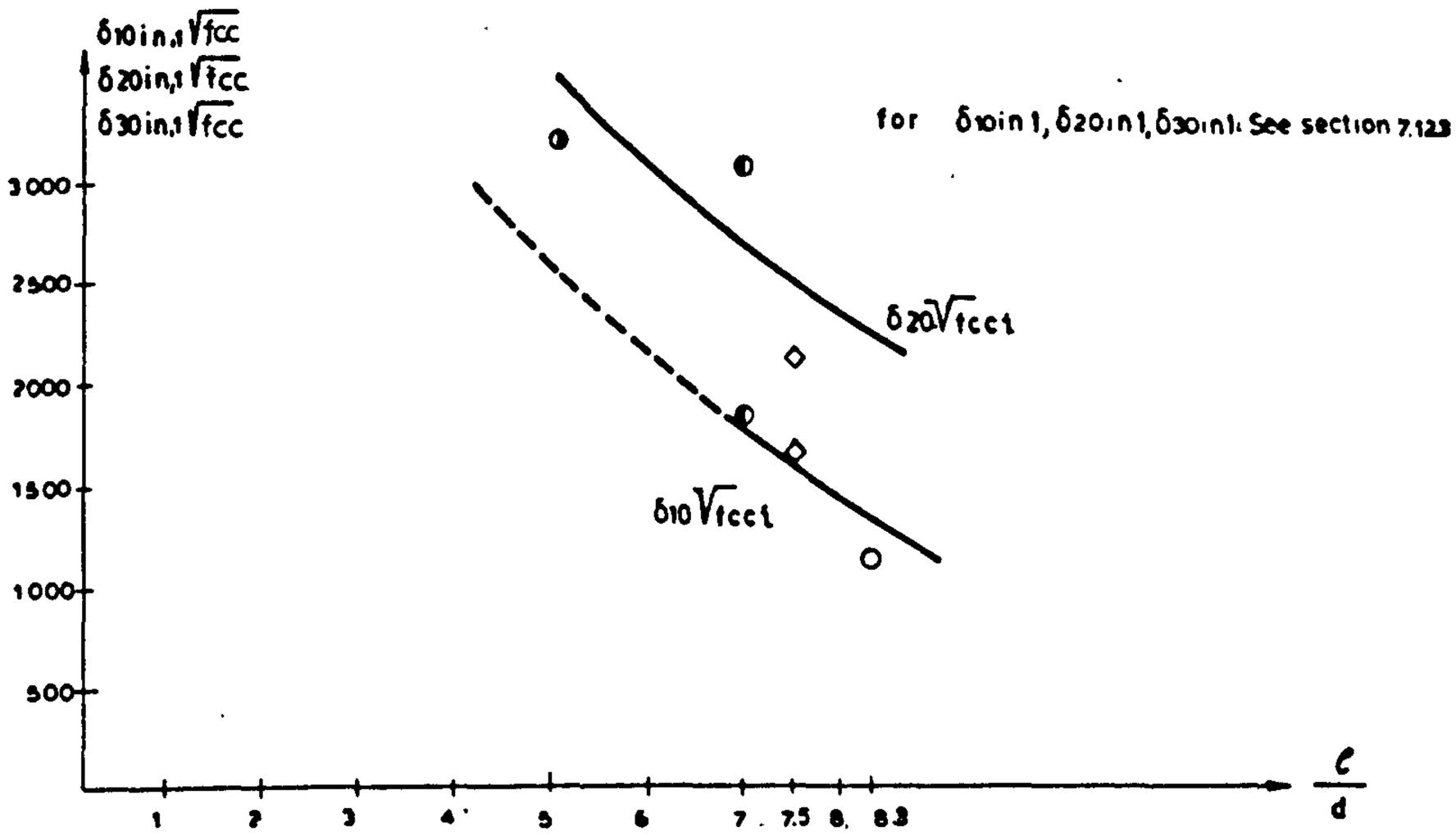

Fig.7.111. Effect of embedment length on the anchor displacement.

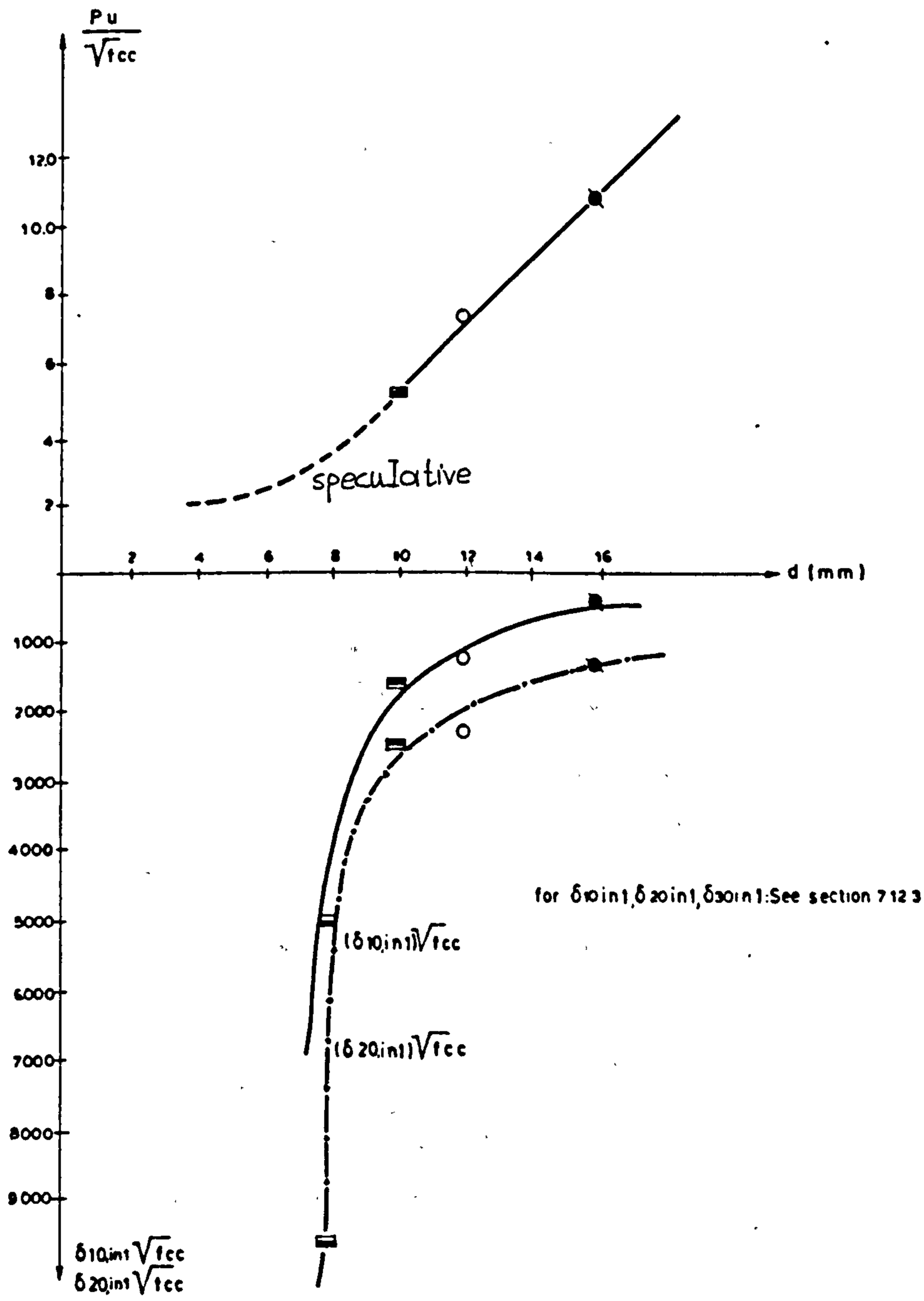

Fig.7.112. Effect of the diameter of anchor on the ultimate pull-out value and on the anchor displacement.

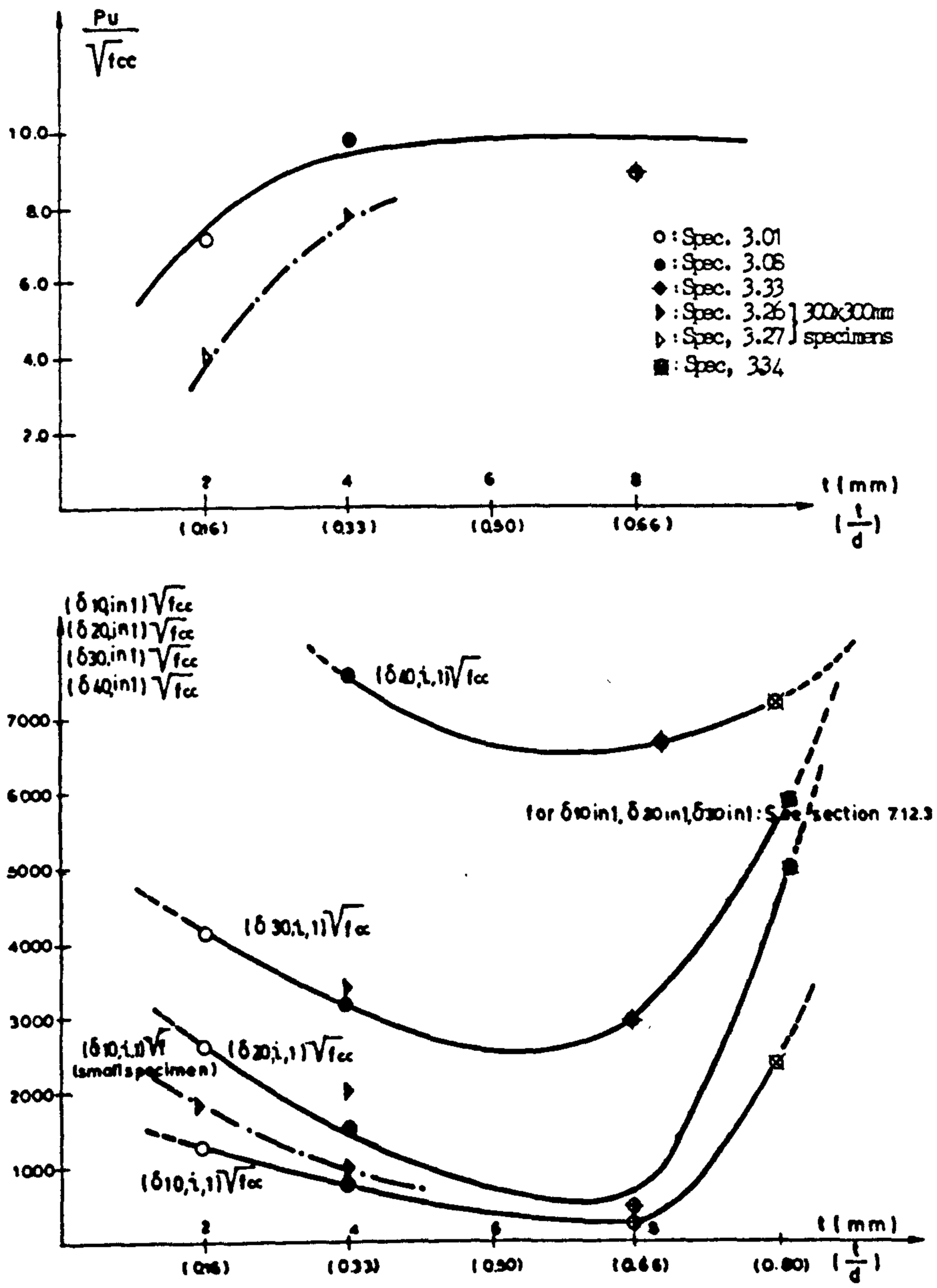

Fig.7.113. Effect of thickness or resin on the ultimate pull-out load and on the anchor displacement

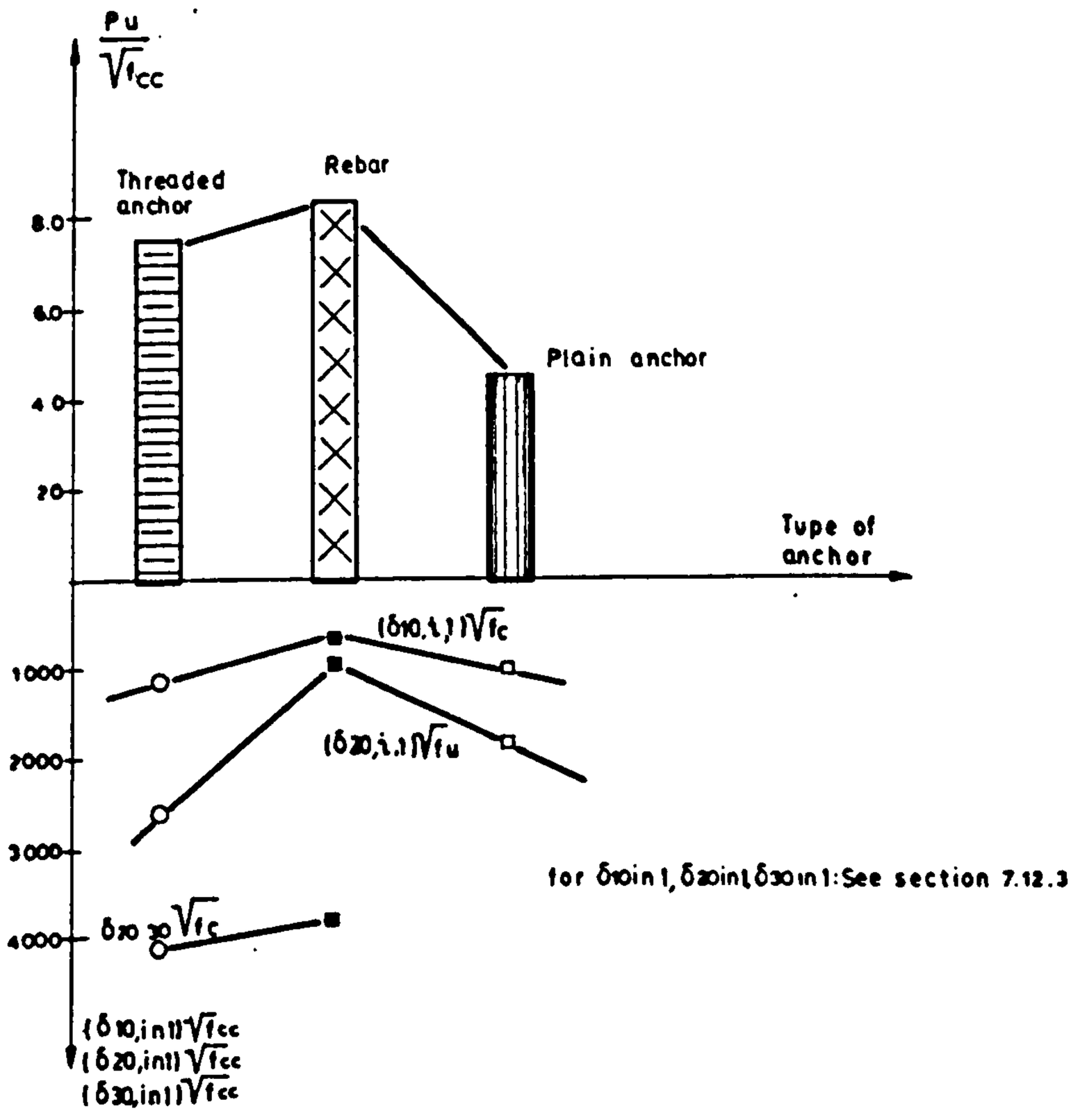

Fig.7.1.14. Effect of the type of the anchor.

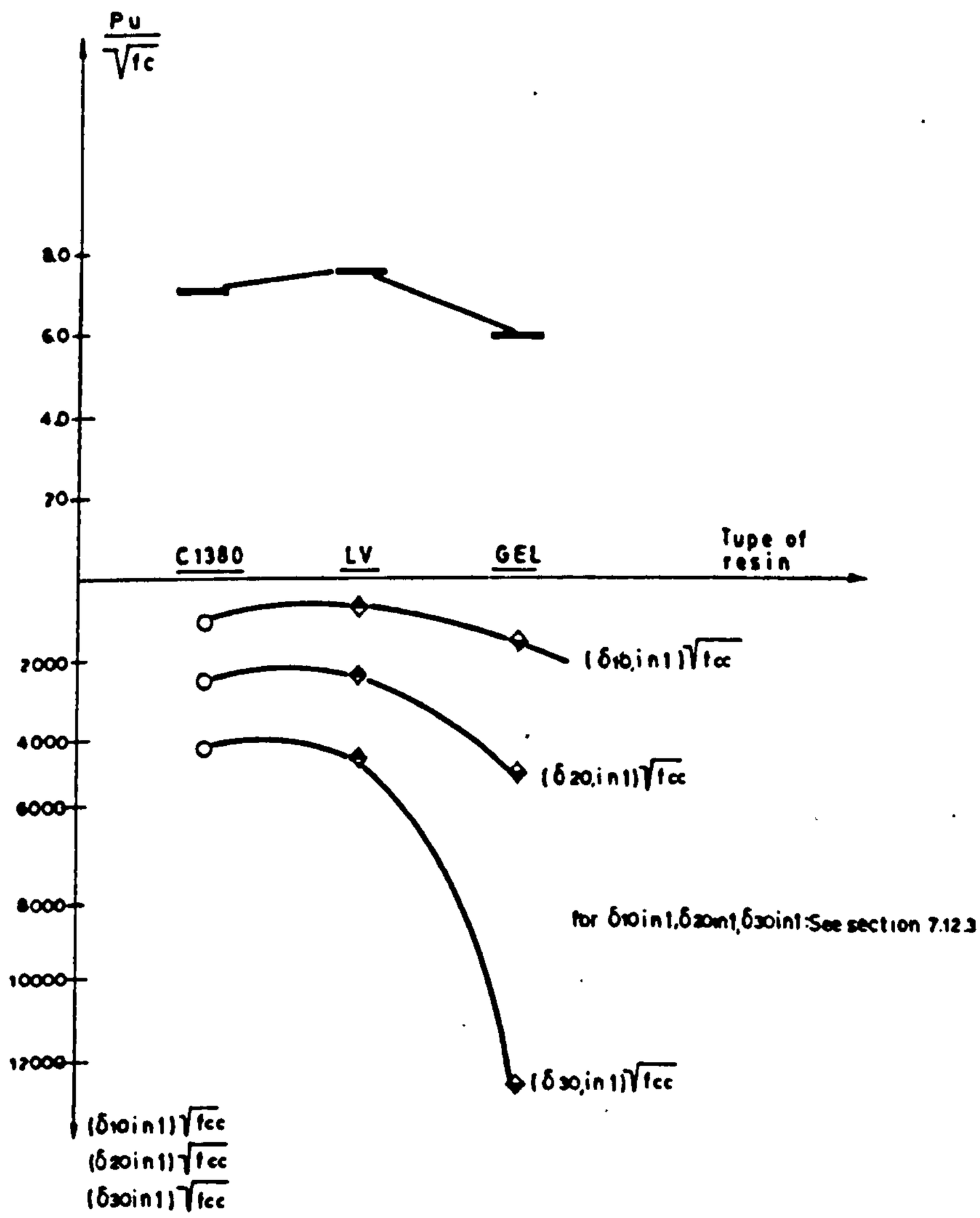

Fig.7.115. Effect of the type of adhesive.

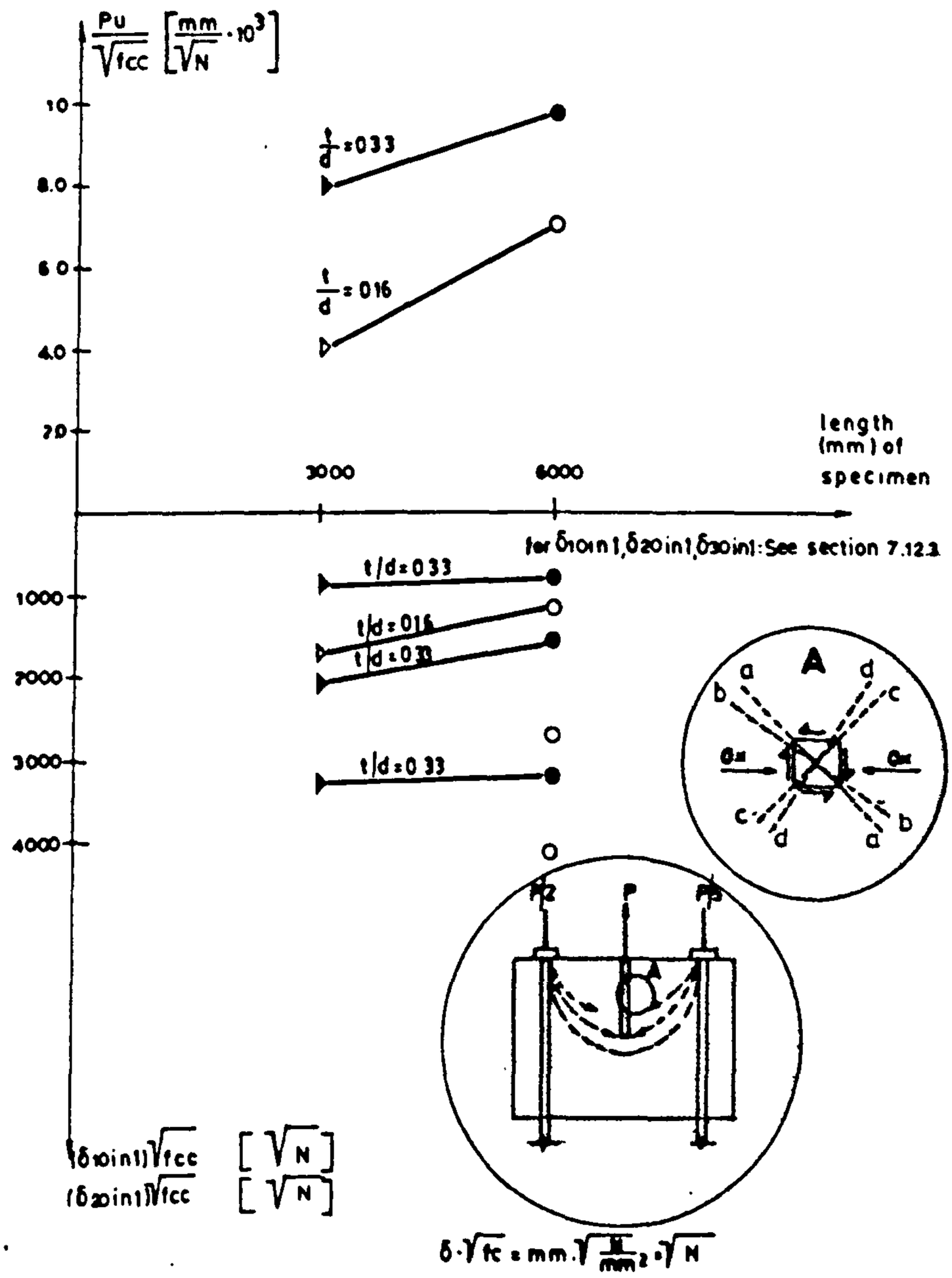

Fig.7.116. Effect of the size of the specimen.

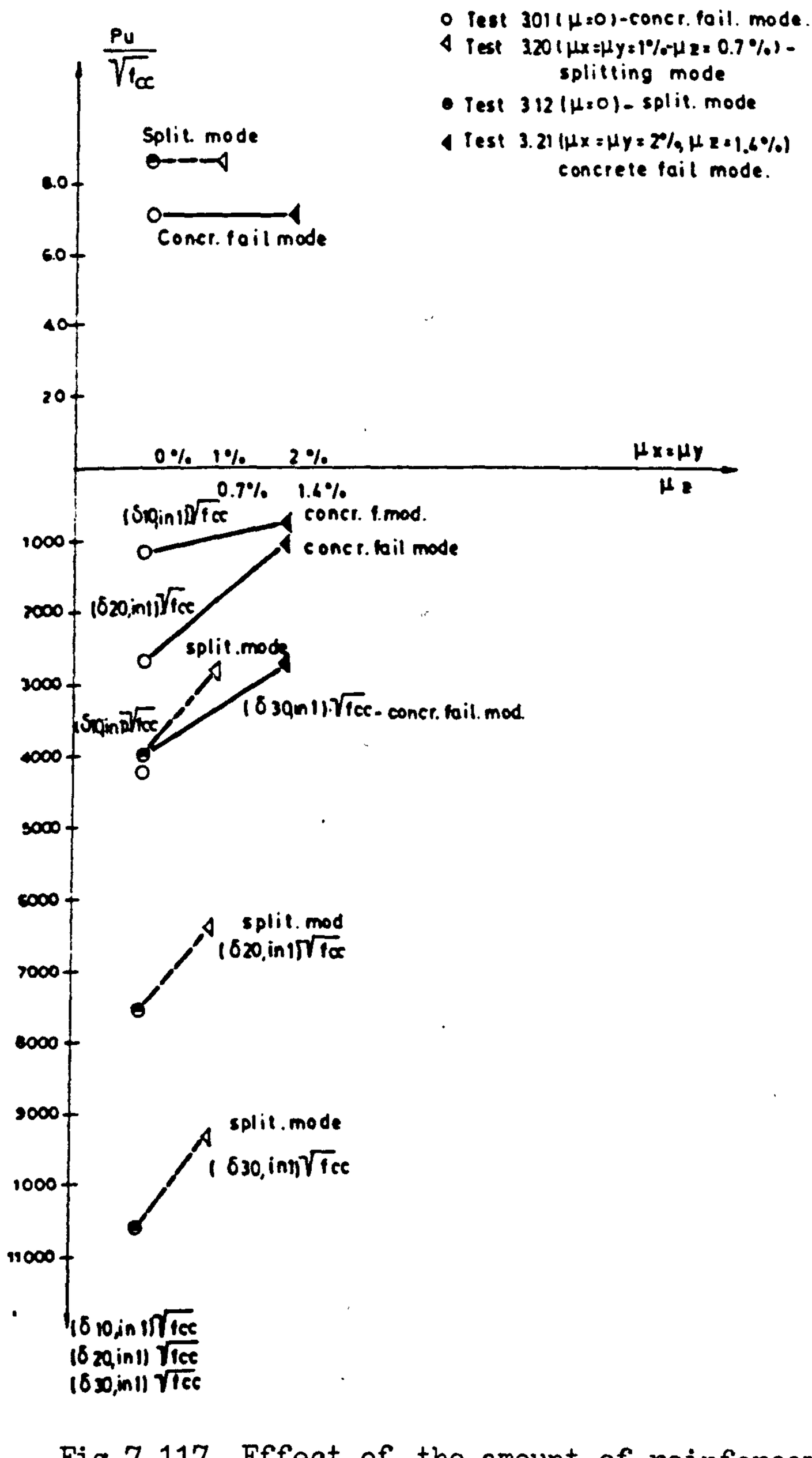

Fig.7.117. Effect of the amount of reinforcement.

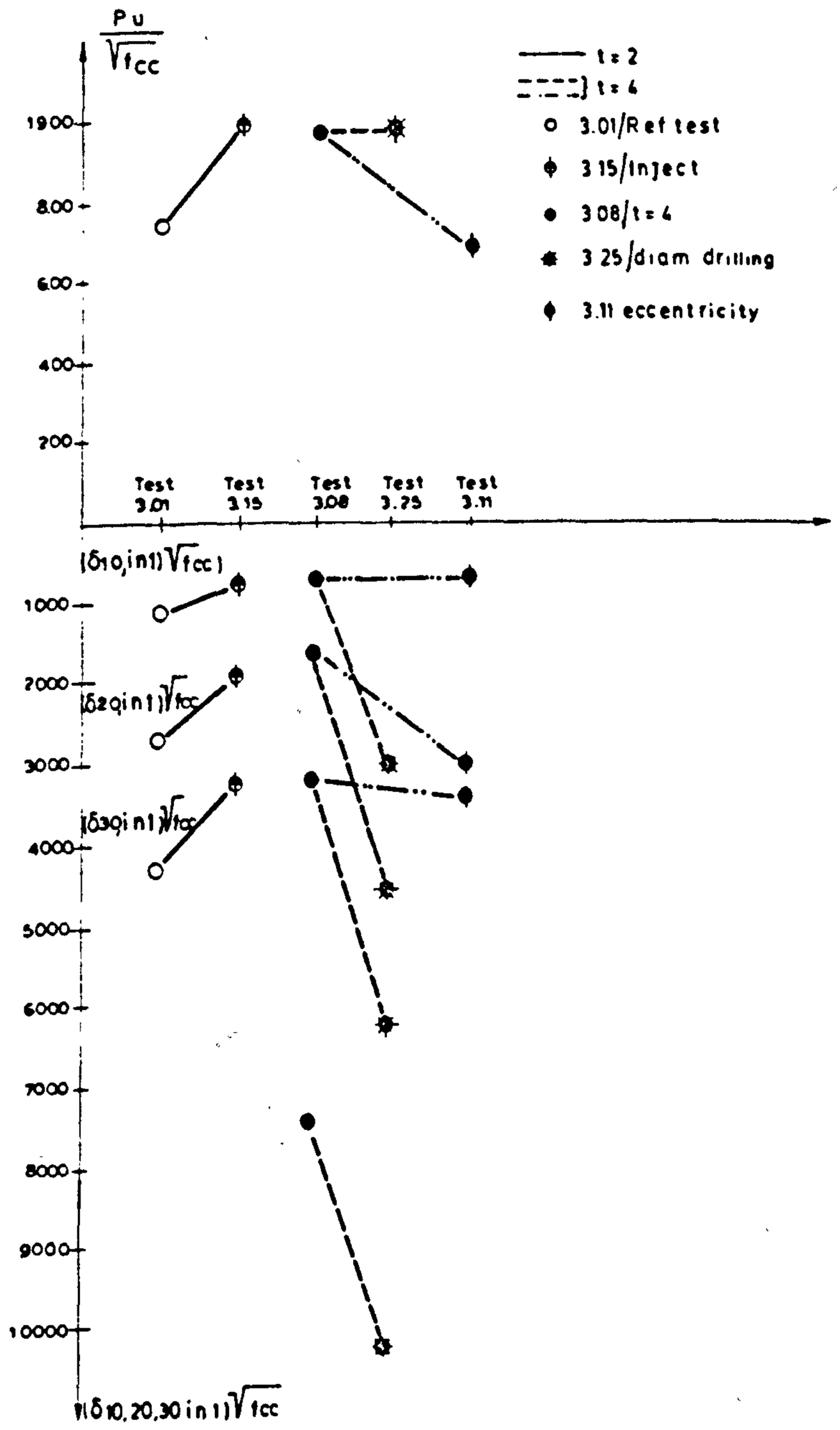

Fig.7.118. Effect of the method of drilling, the injection of resin and eccentricity of the anchor.

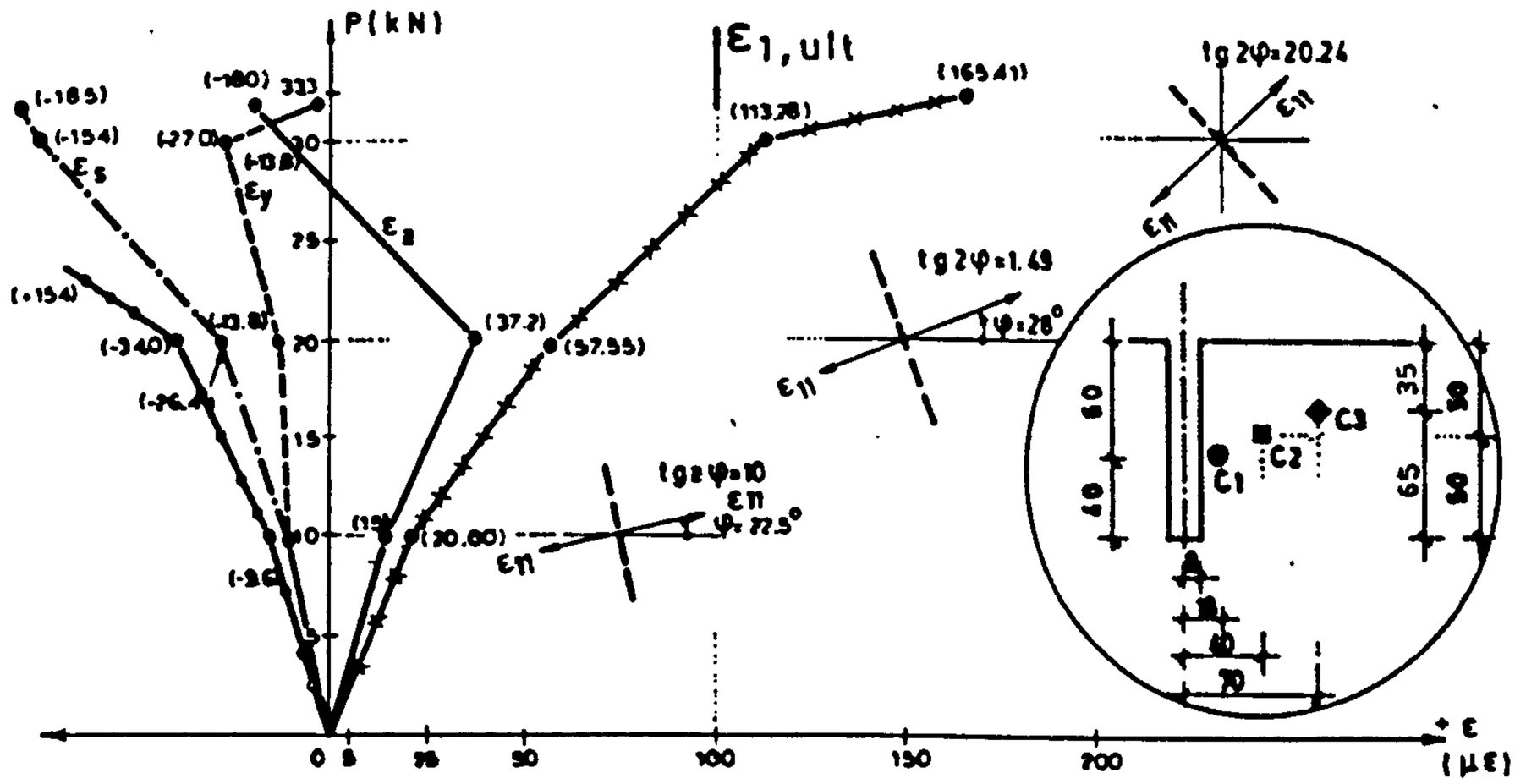

Fig.7.119. Specimen 3.01 (STD TEST) - Point C1
Distribution of concrete strains ε_{zz}, ε_{yy}, ε_{ss}, ε_{11}, ε_{22}
and inclination of principal strains

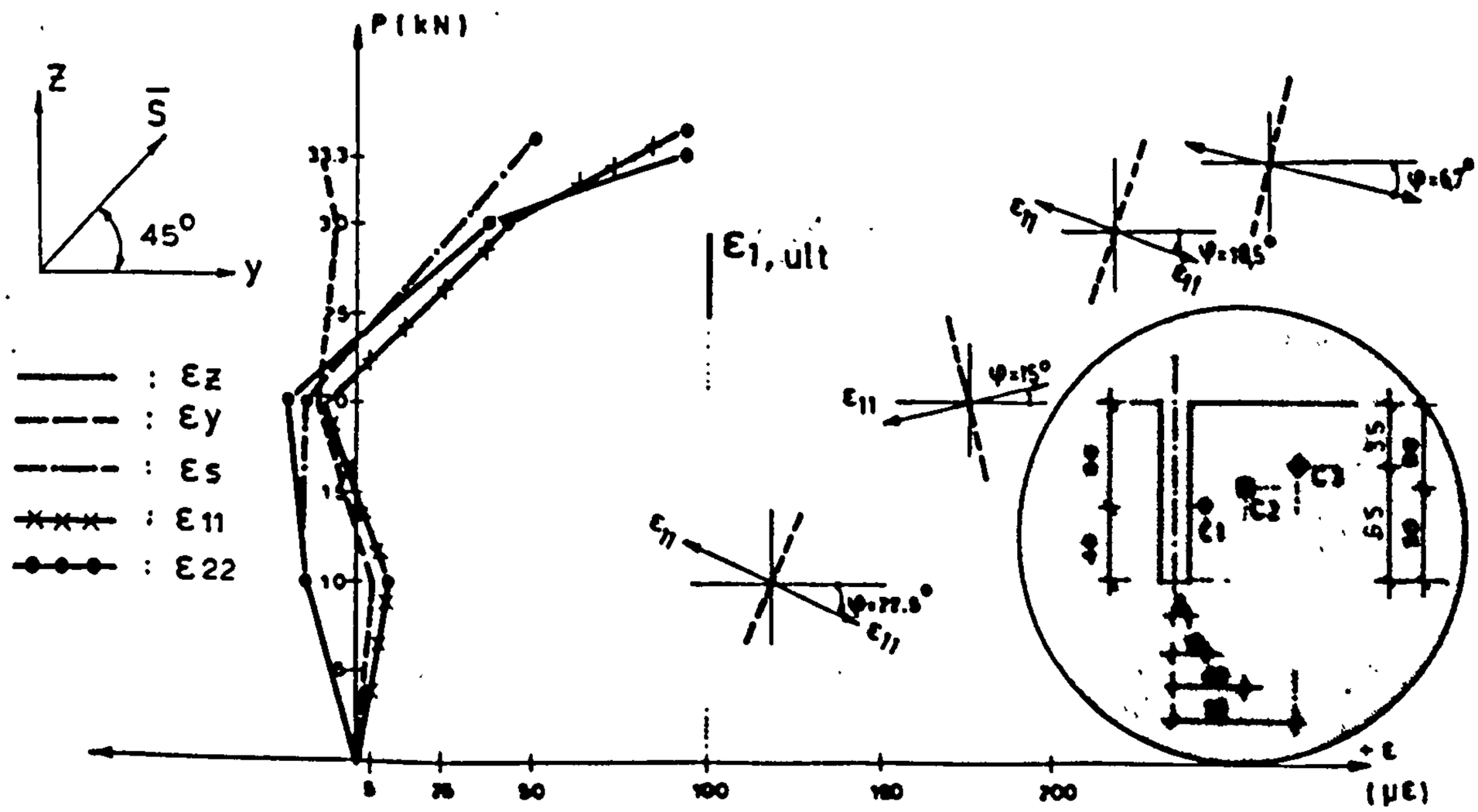

Fig.7.120. Specimen 3.01 (STD TEST) - Point C3
Distribution of concrete strains ε_{zz}, ε_{yy}, ε_{ss}, ε_{11}, ε_{22}
and inclination of principal strains.

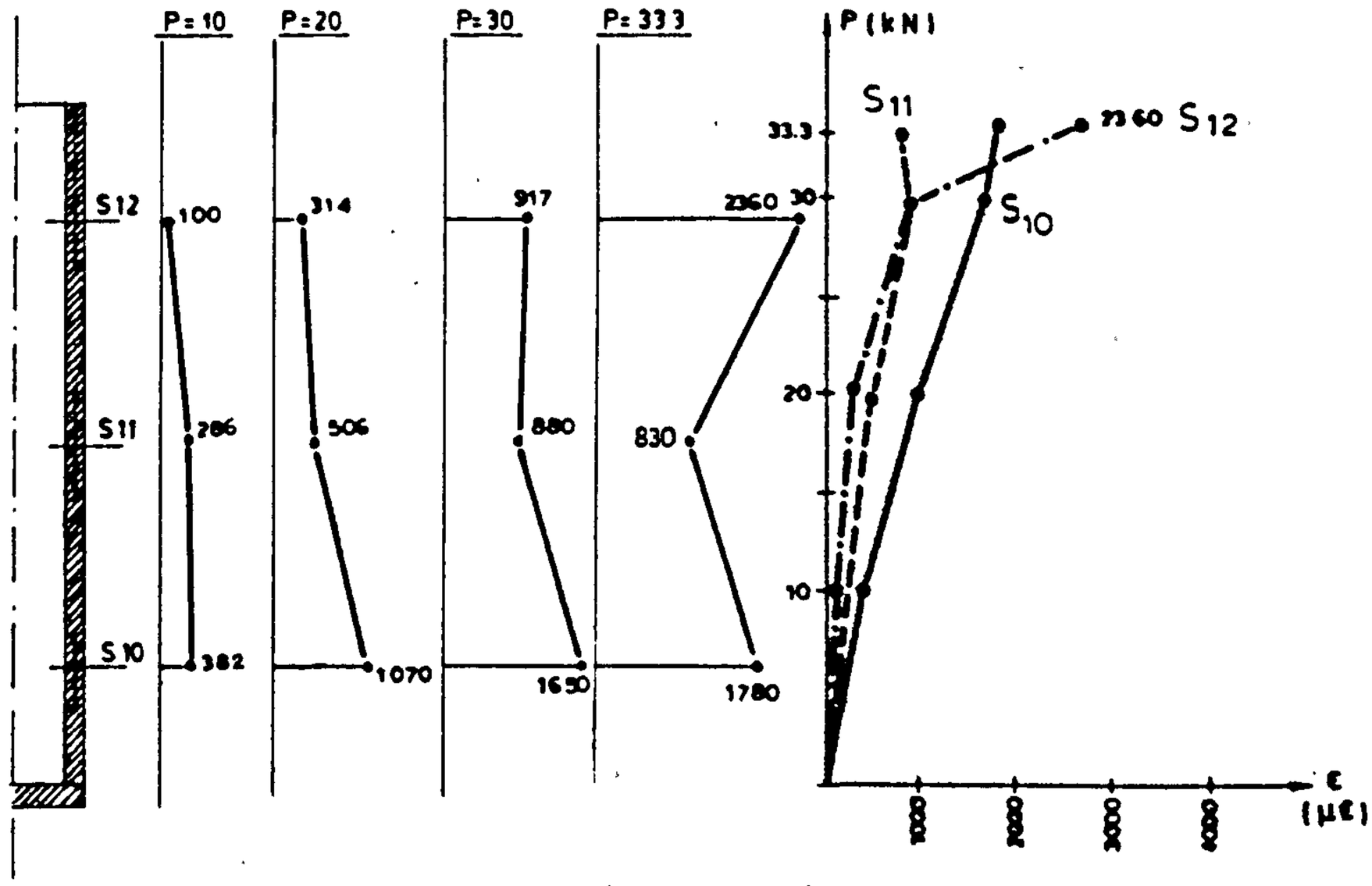

Fig.7.121. Specimens 3.01 (STD TEST). Distribution of resin strains along the resin shell

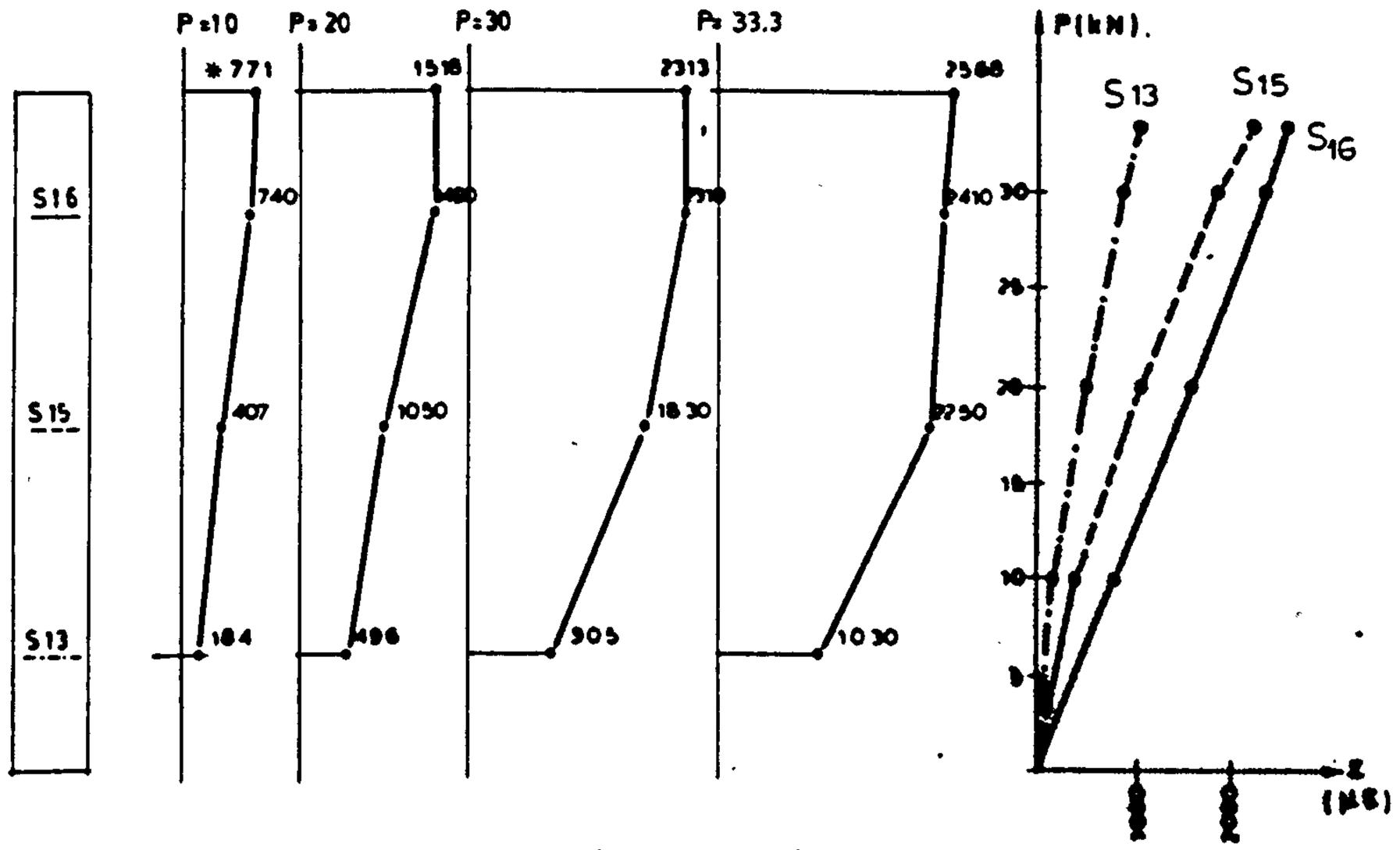

Fig.7.122. Specimens 3.01 (STD TEST). Distribution of anchor strains.
*Calculated at free end.

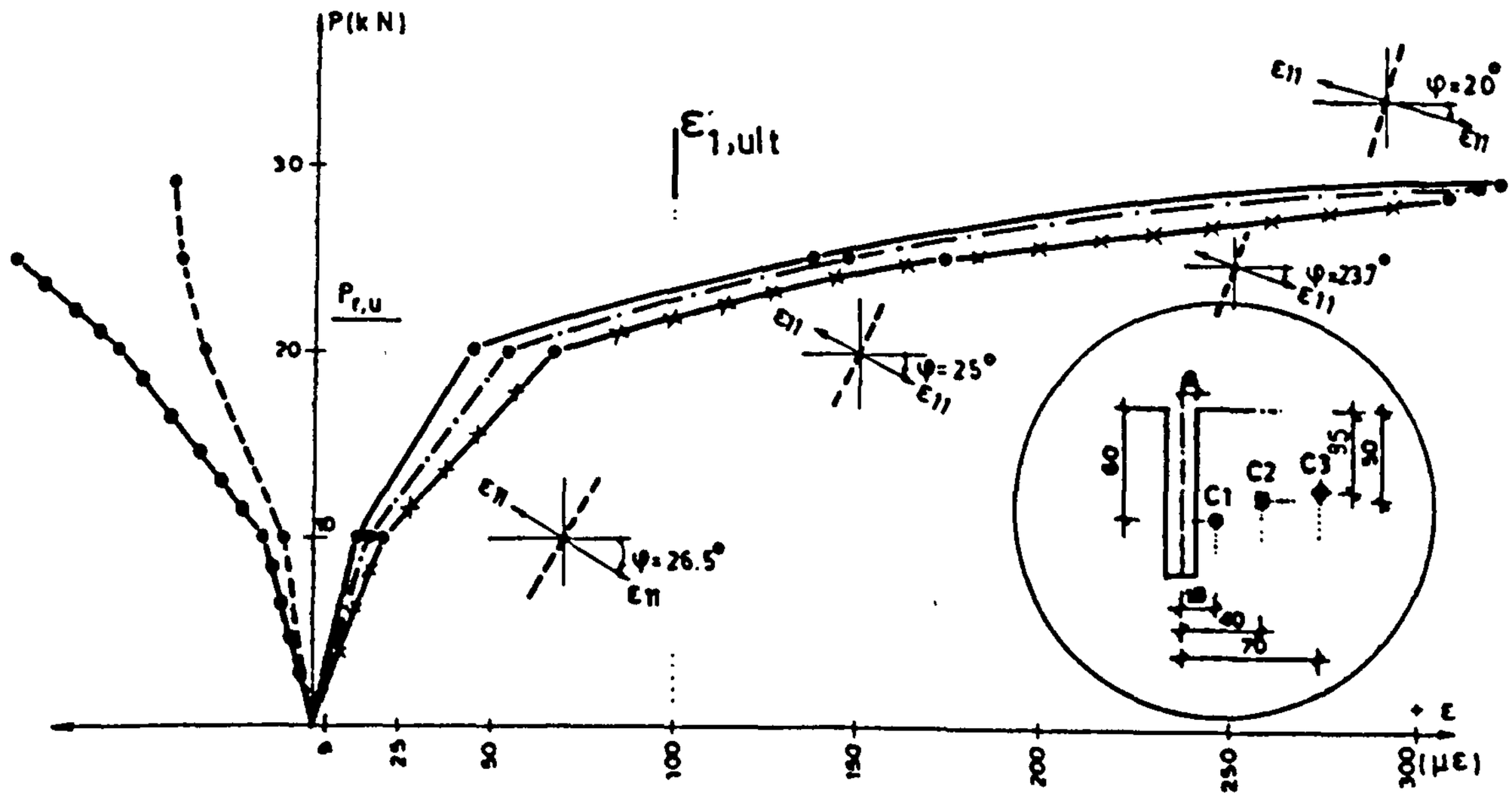

Fig.7.123. Specimen 3,02 (l=7,0d) Point C1 in concrete. Distribution of strains ε_{zz}, ε_{yy}, ε_{ss}, ε_{11}, ε_{22} and inclination of principal stress.

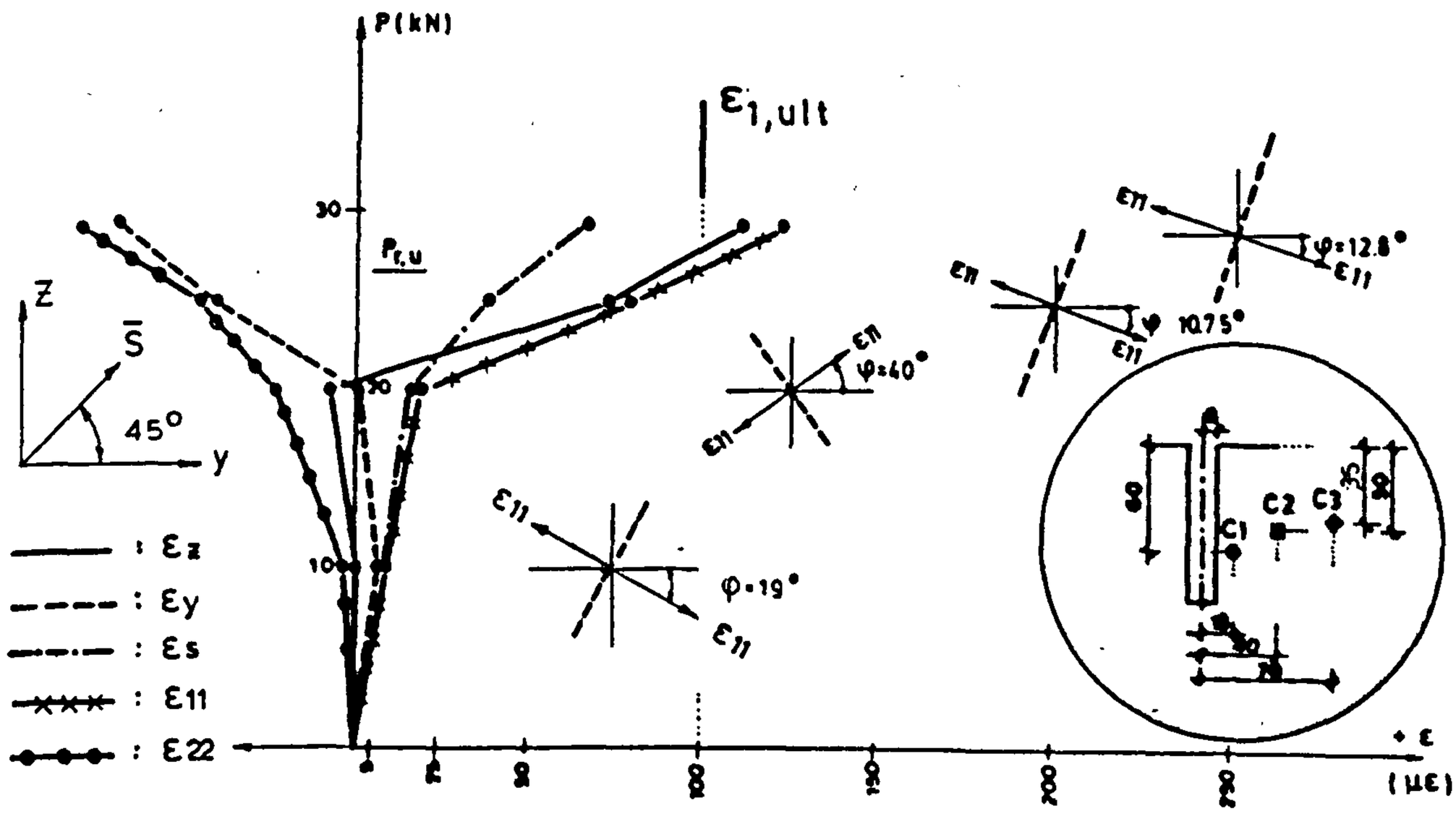

Fig.7.124. Specimen 3.02 (l=7.0 d) Point C2 in concrete Distribution of strains ε_{zz}, ε_{yy}, ε_{ss}, ε_{11}, ε_{22} and inclination of principal strains.

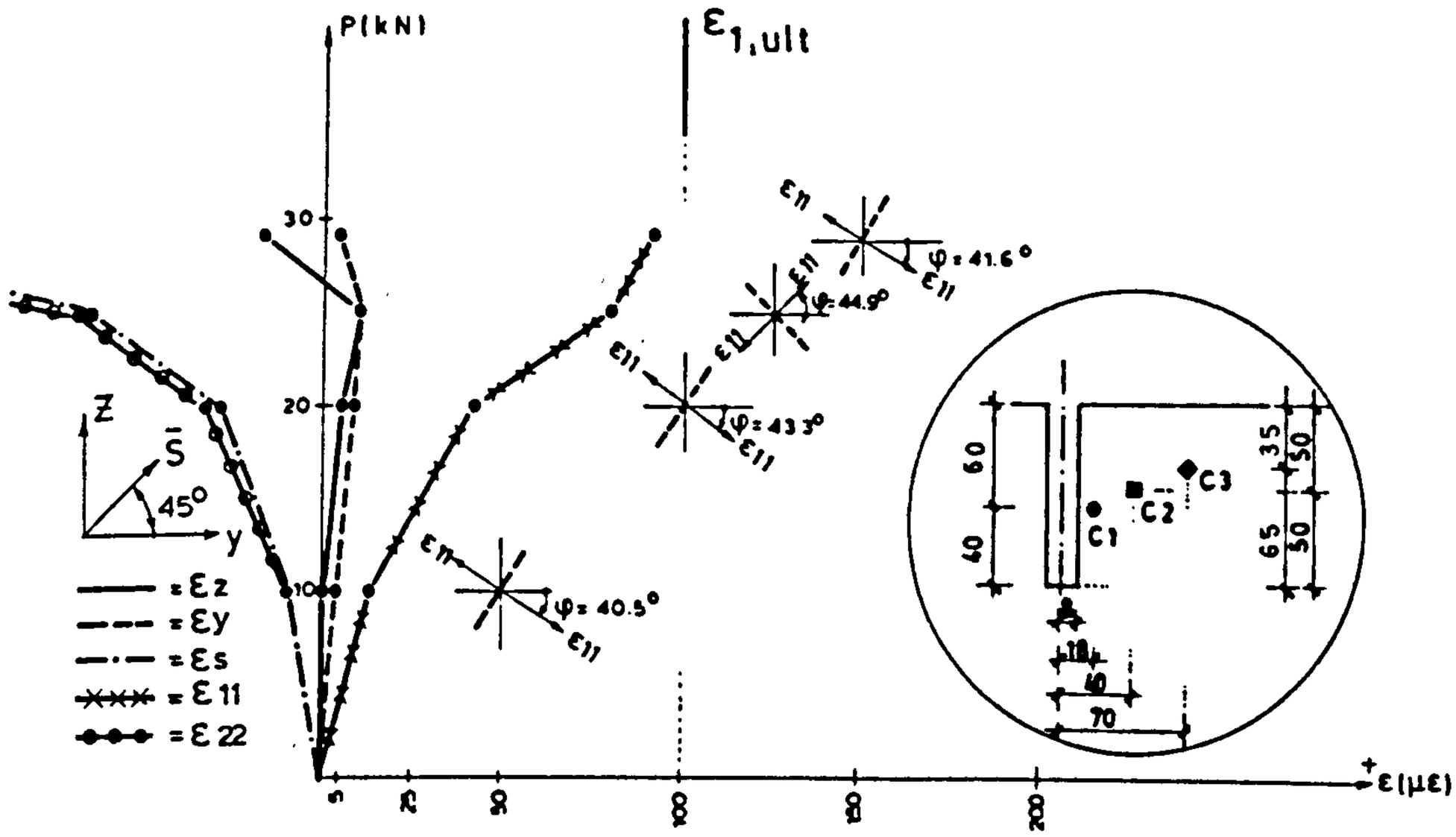

Fig.7.125. Specimen 3.02 (l=7.0 d). Point C3 in concrete. Distribution of strains ε_{zz}, ε_{yy}, ε_{ss}, ε_{11}, ε_{22} and inclination of principal strains

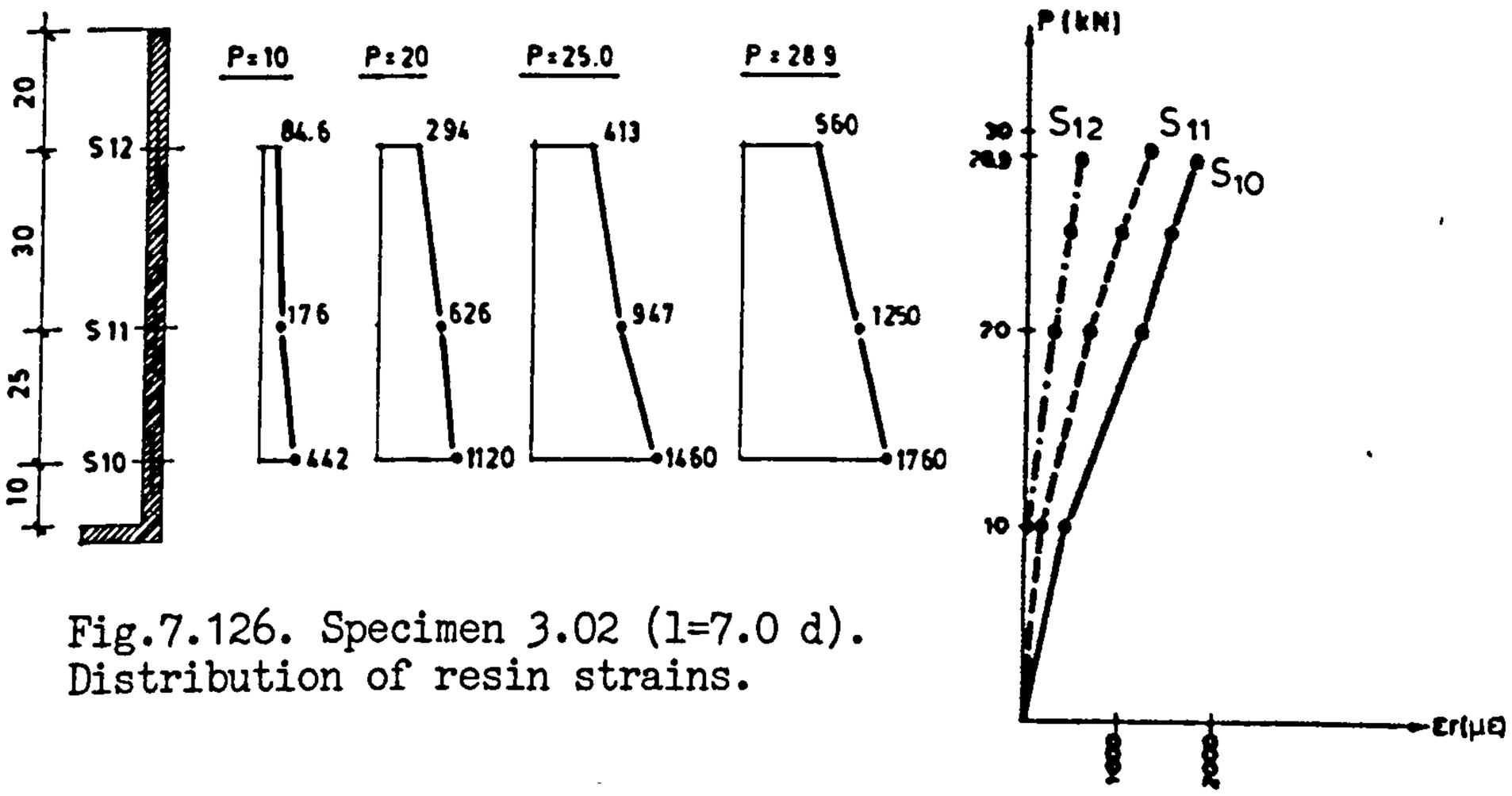

Fig.7.126. Specimen 3.02 (l=7.0 d). Distribution of resin strains.

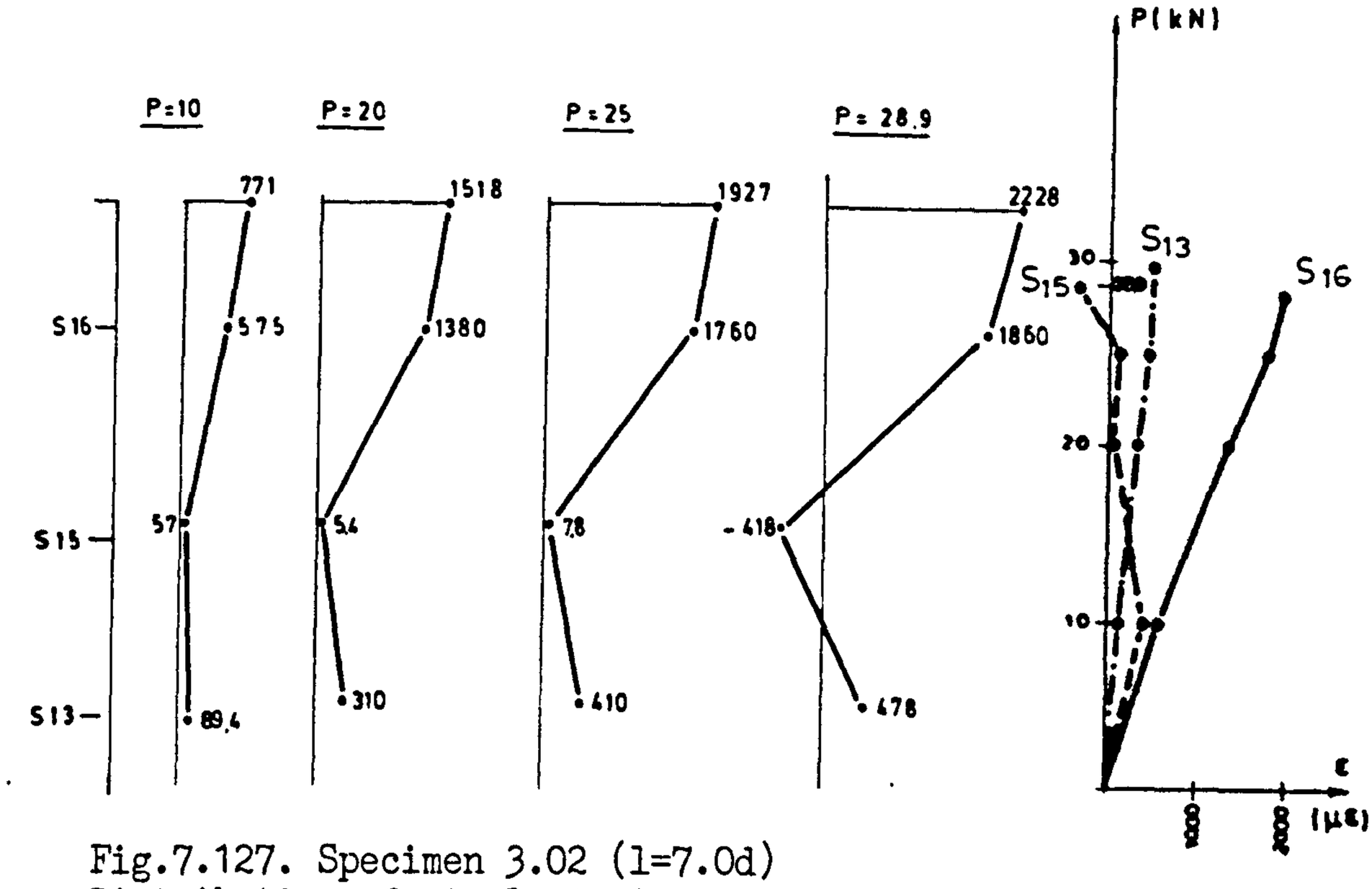

Fig.7.127. Specimen 3.02 (l=7.0d)
Distribution of steel strains.

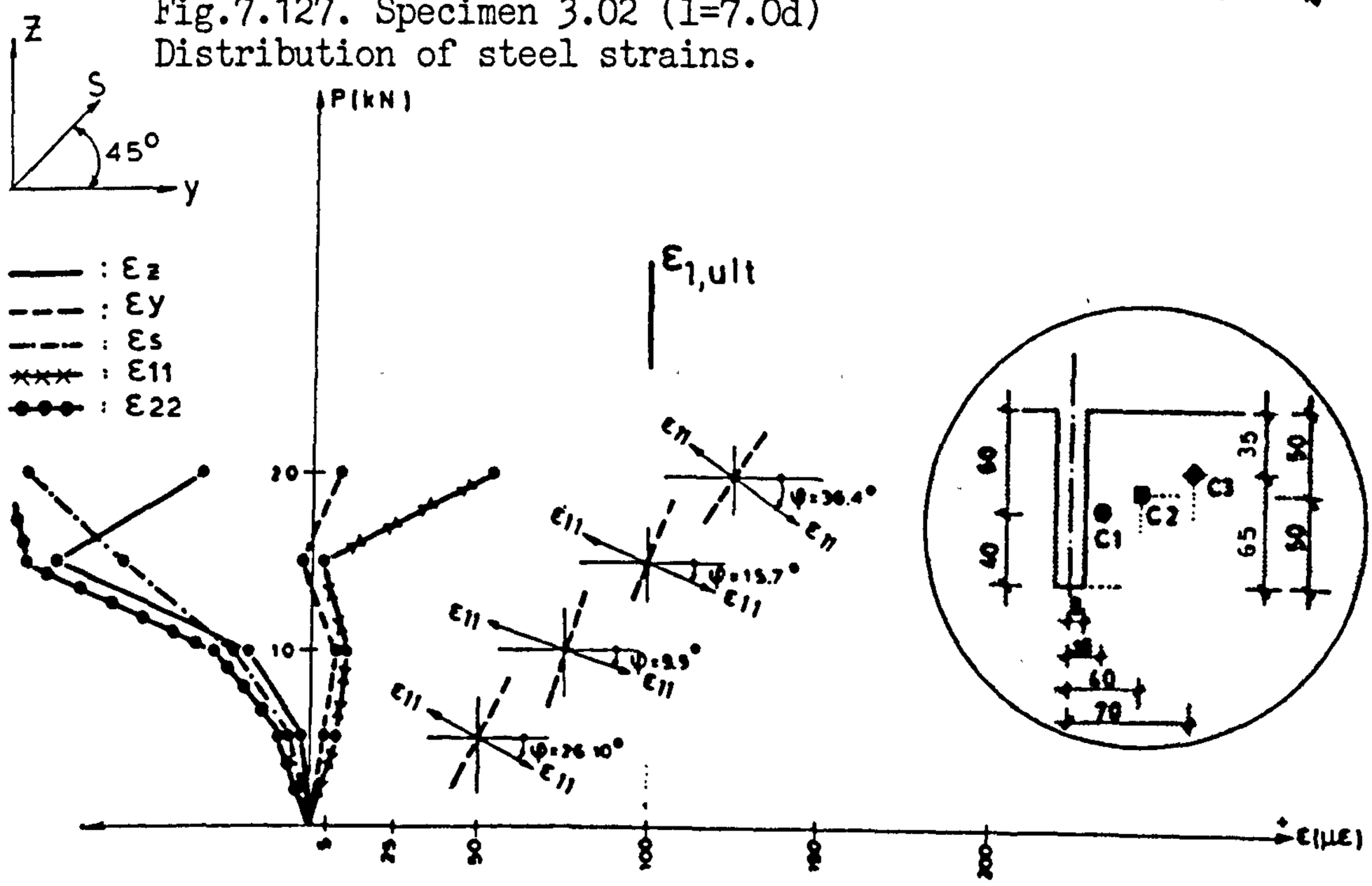

Fig.7.128. Specimen 3.03 (l=5d) - Point C3 in concrete.
Distribution of concrete strains ε_{zz}, ε_{yy}, ε_{ss}, ε_{11}, ε_{22} and inclination of principal strains.

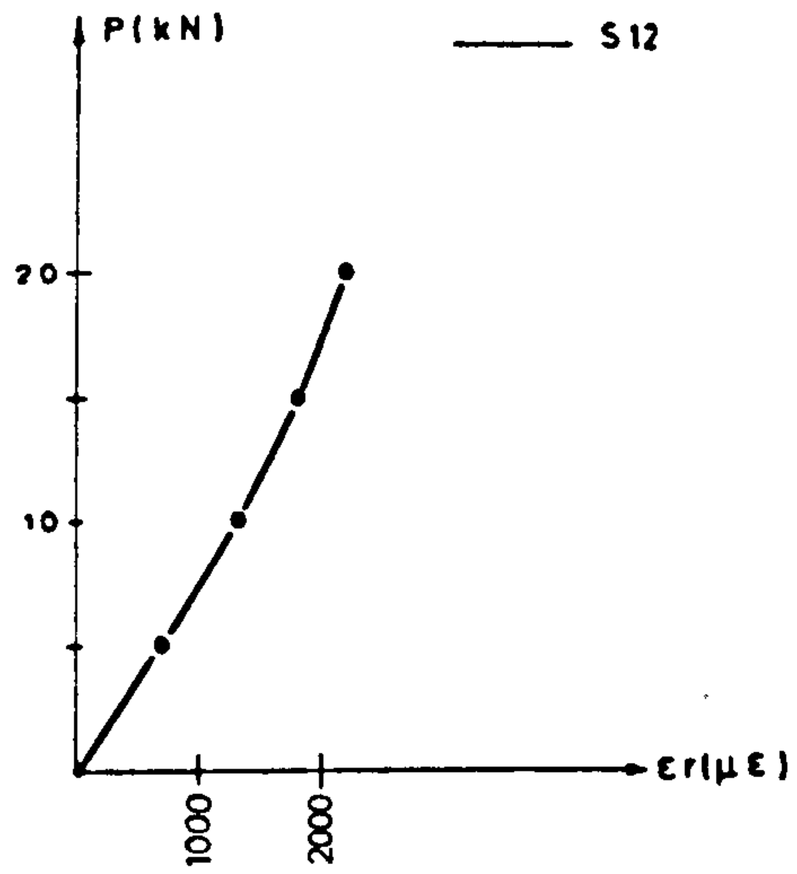

Fig.7.129. Specimen 3.03 (l=5d)
Resin strains in the lower strain gauge.

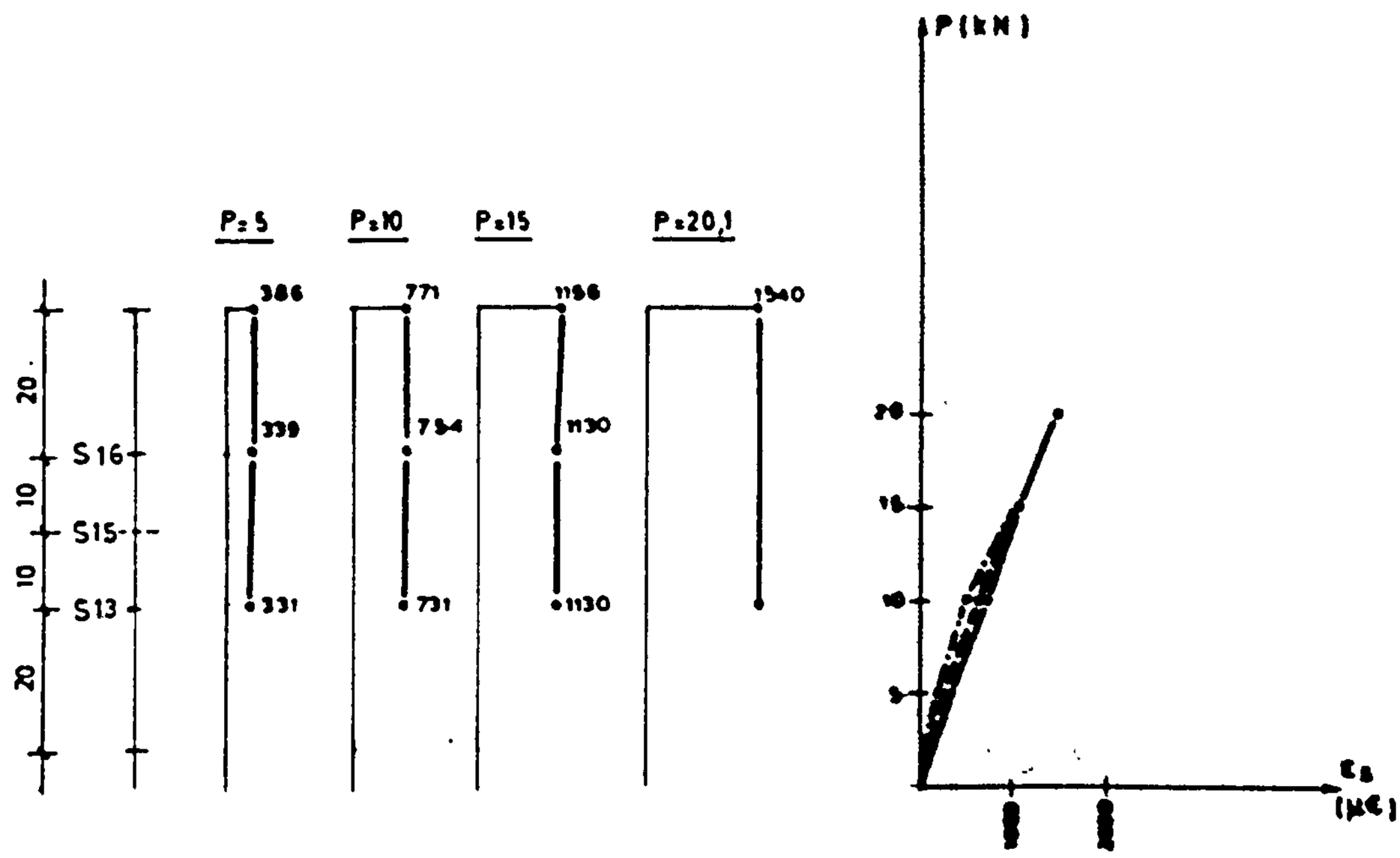

Fig.7.130. Specimen 3.03 (l=5d)
Distribution of steel strains (με)

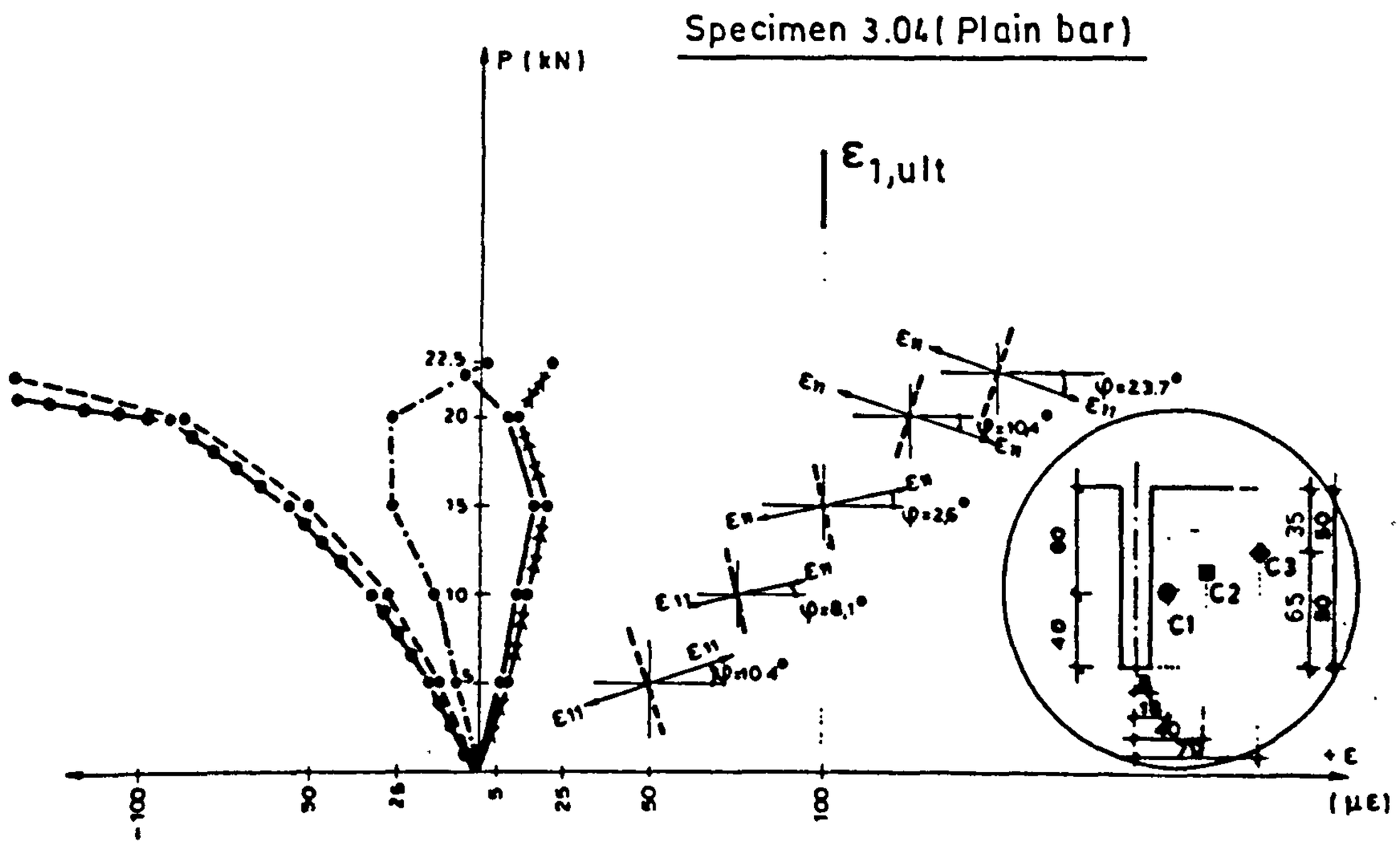

Fig.7.131. Specimen 3.04 point C1. Strains ε_{zz}, ε_{yy}, ε_{ss}, ε_{11}, ε_{22} and inclination of principal strains of concrete.

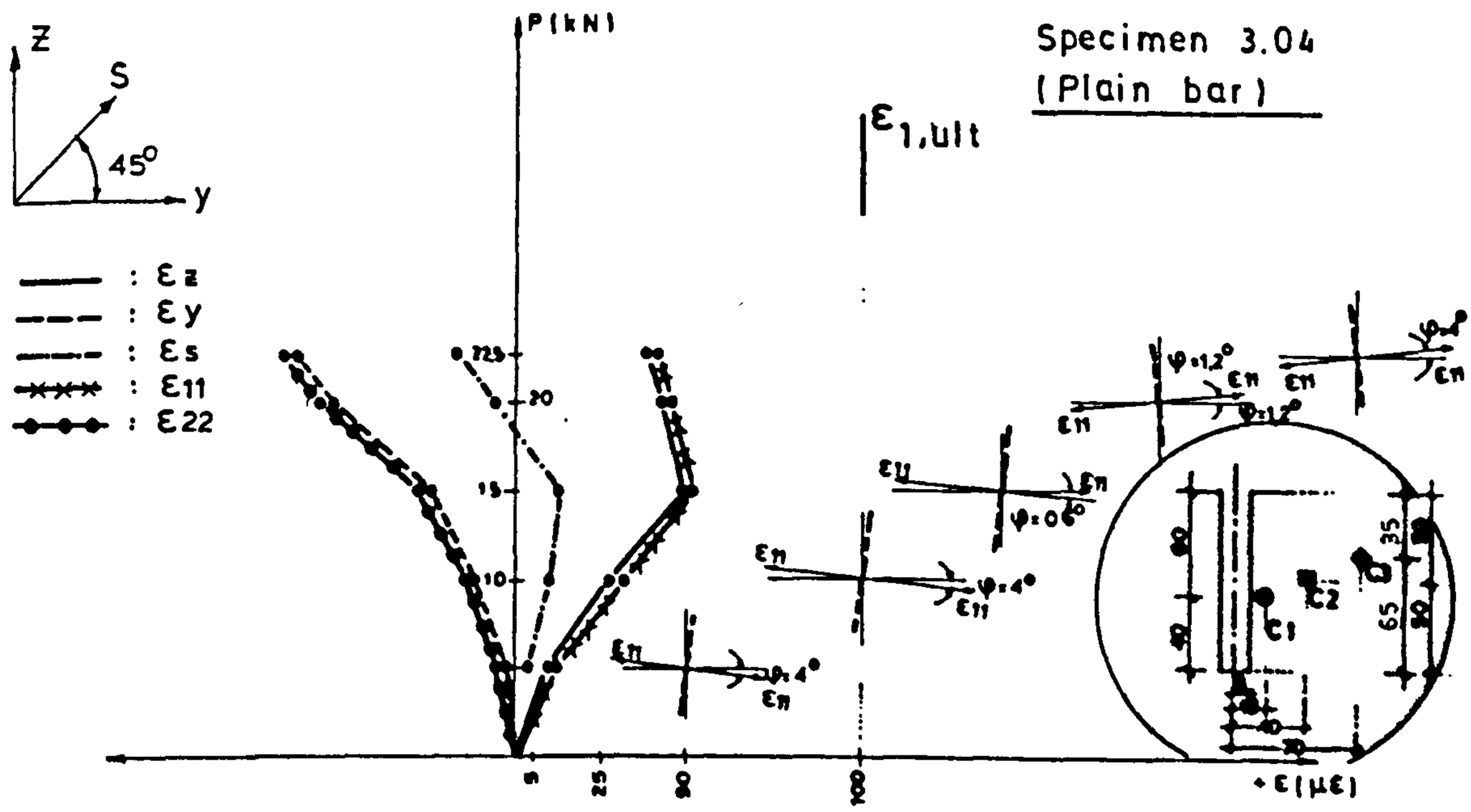

Fig.7.132. Specimen 3.04 point C2. Strains ε_{zz}, ε_{yy}, ε_{ss}, ε_{11}, ε_{22} and inclination of principal strains of concrete.

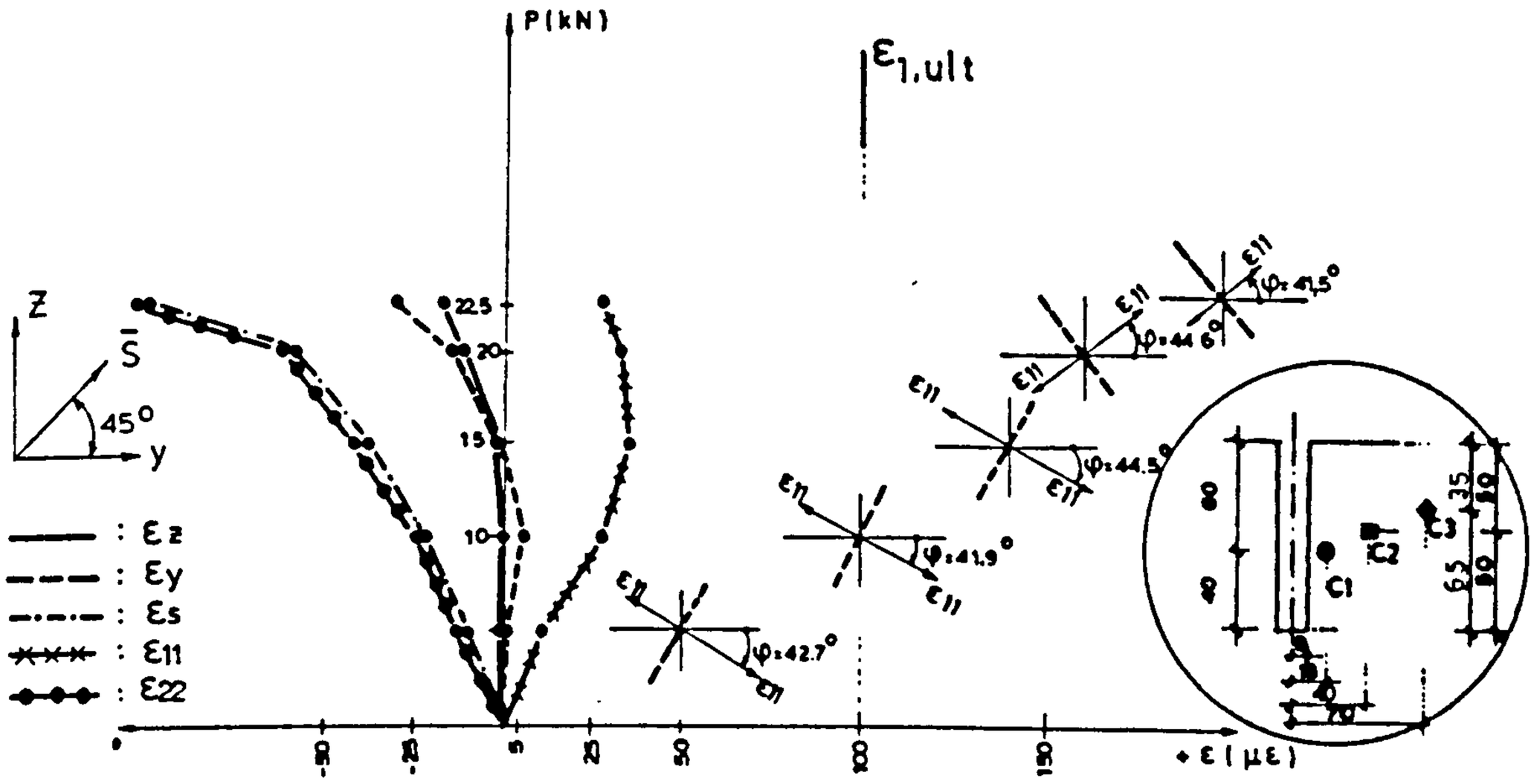

Fig.7.133. Specimen 3.04 (plain bar) point C3. Strains ε_{zz}, ε_{yy}, ε_{ss}, ε_{11}, ε_{22} and inclination of principal strains of concrete.

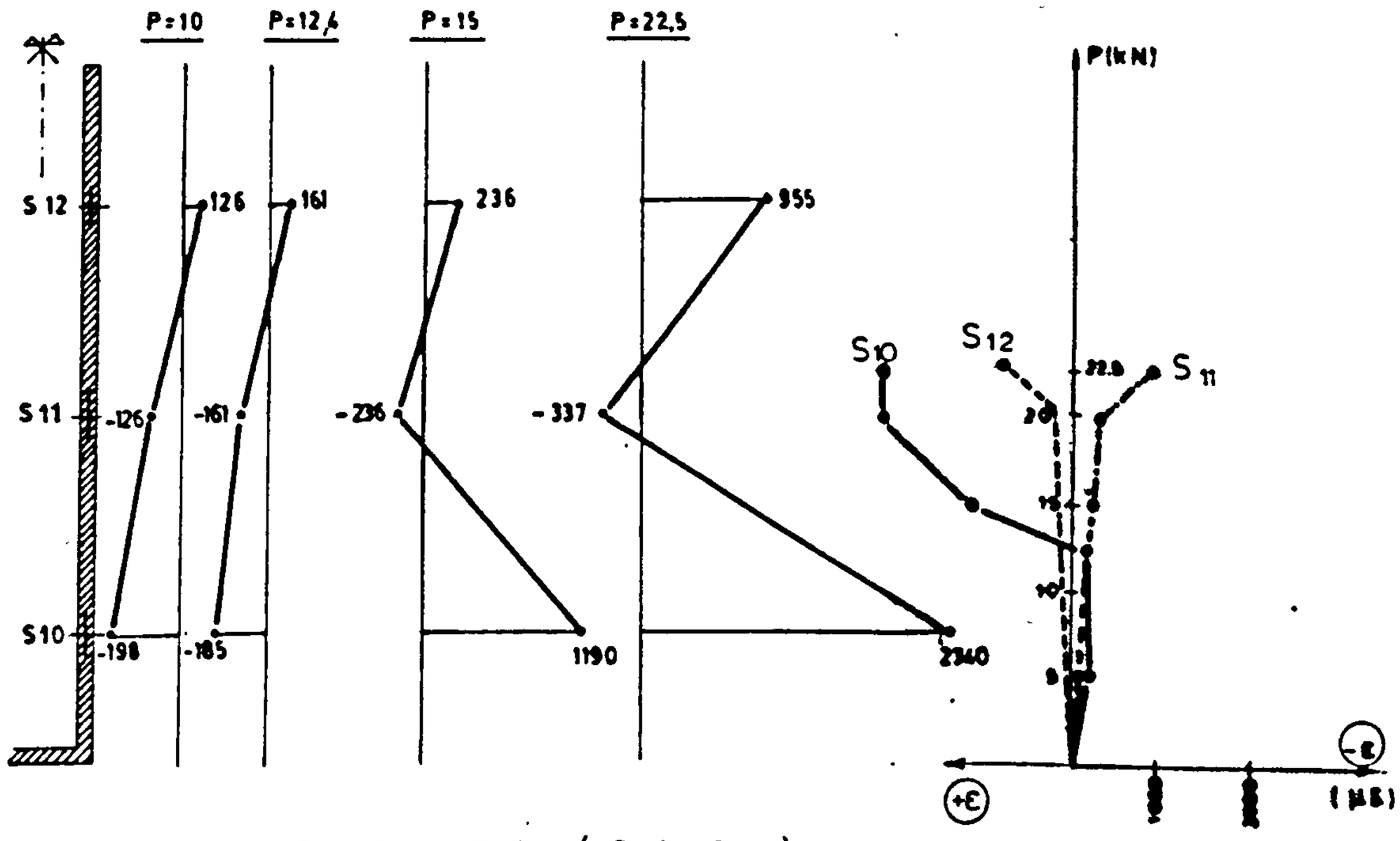

Fig.7.134. Specimen 3.04 (plain bar) Distribution of resin strains.

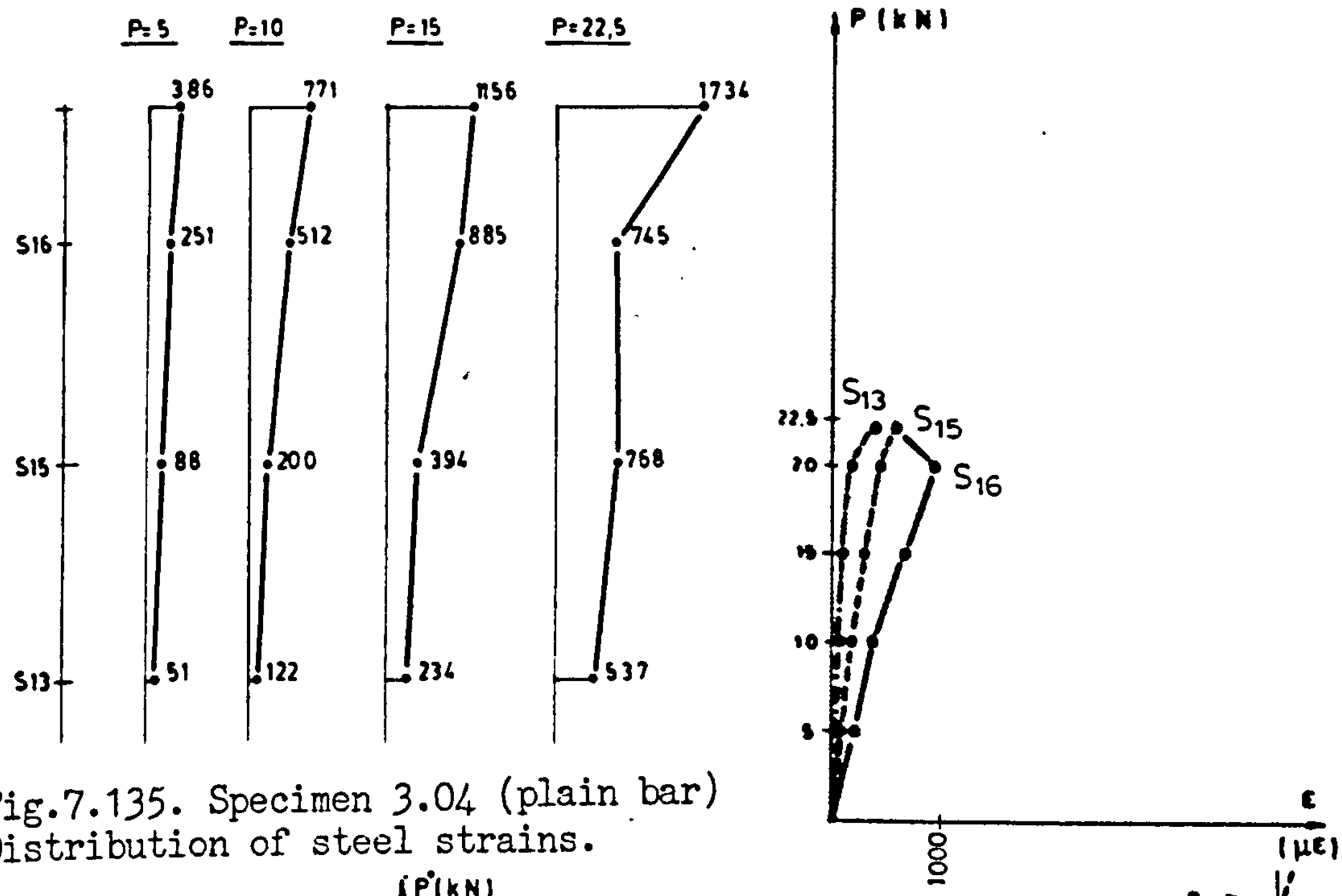

Fig.7.135. Specimen 3.04 (plain bar)
Distribution of steel strains.

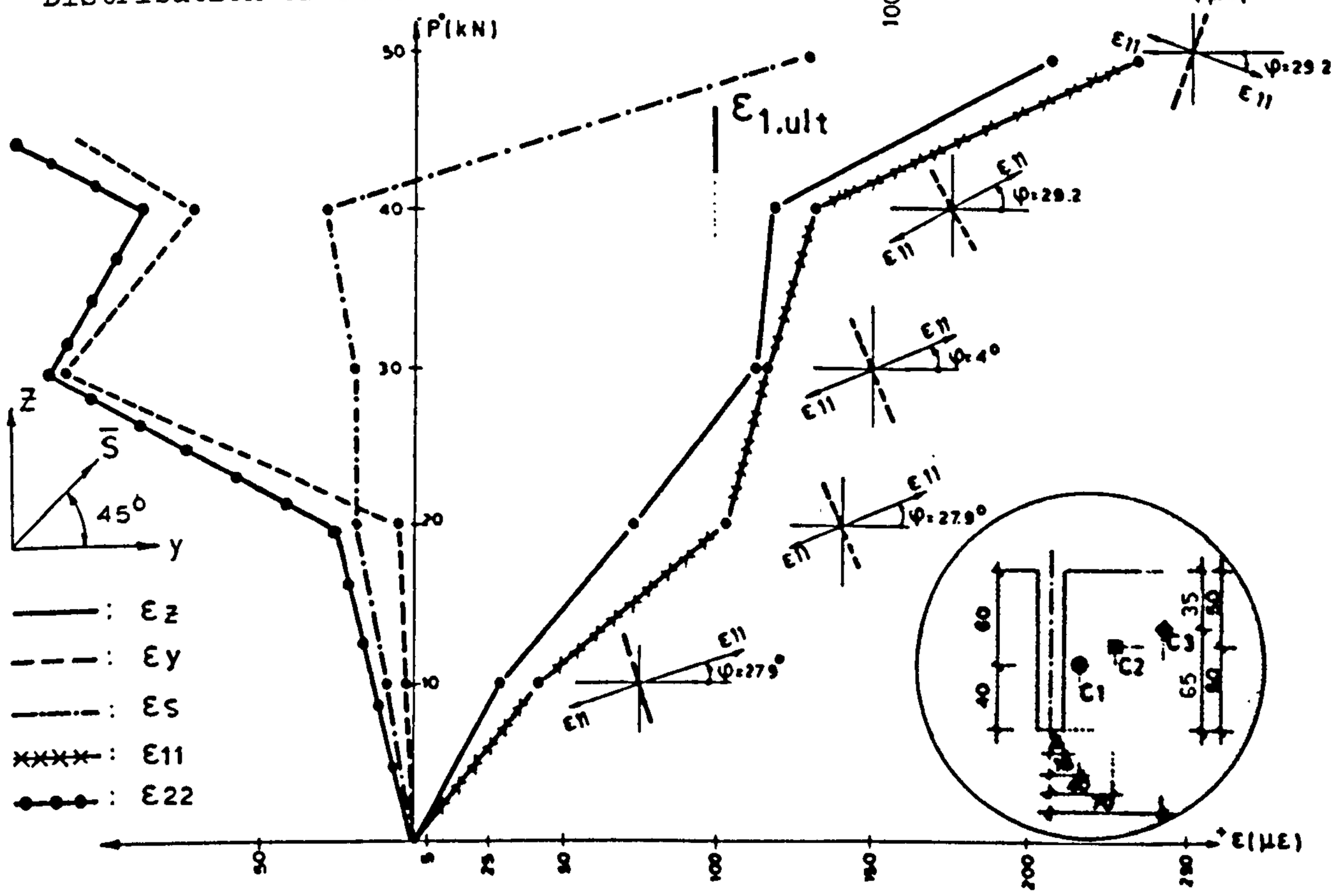

Fig.7.136. Specimen 3.14 (C50) point C1. Strains ε_{zz}, ε_{yy}, ε_{ss}, ε_{11}, ε_{22} and inclination of principal strains of concrete.

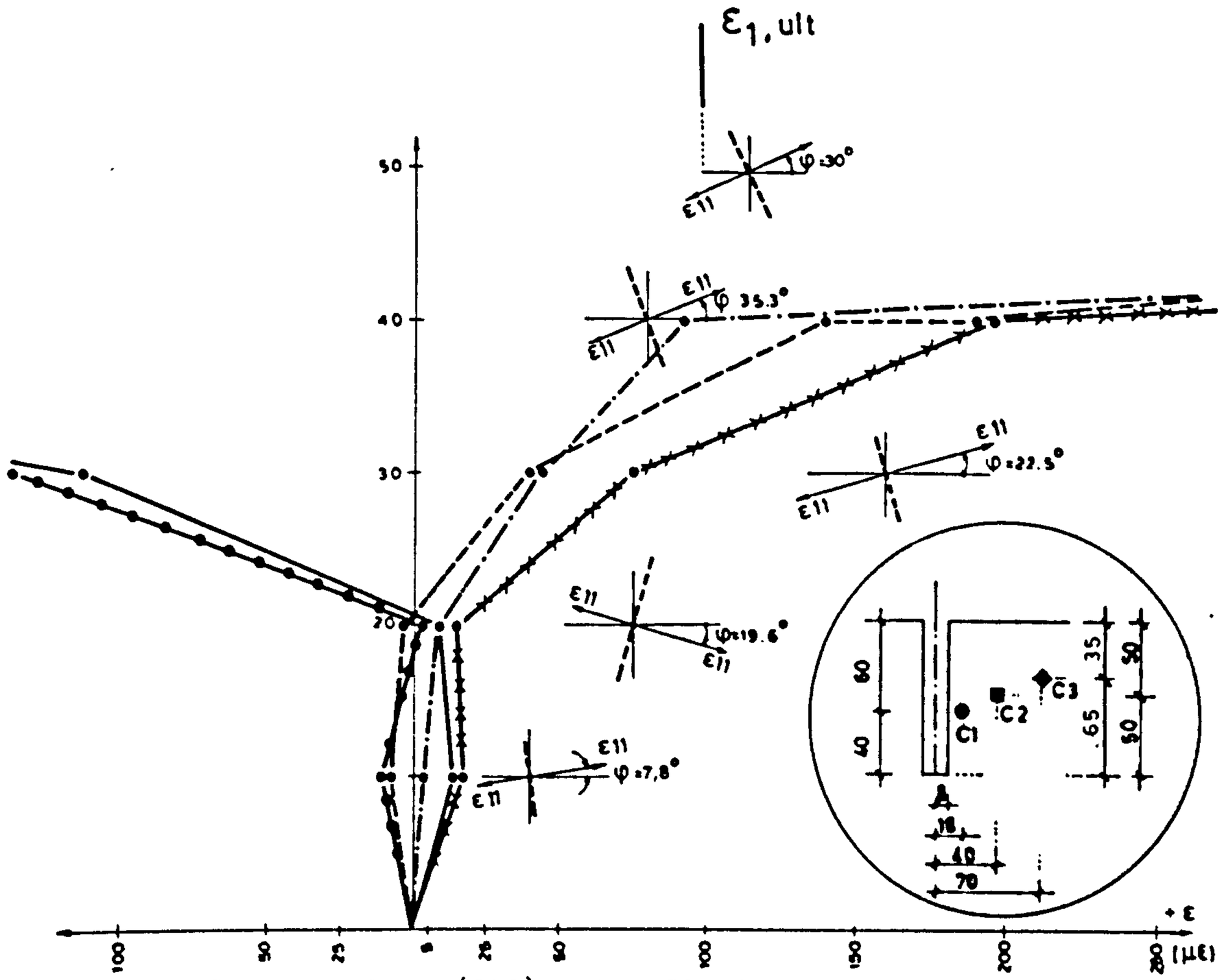

Fig.7.137. Specimen 3.14 (C50) point C2. Concrete strains.

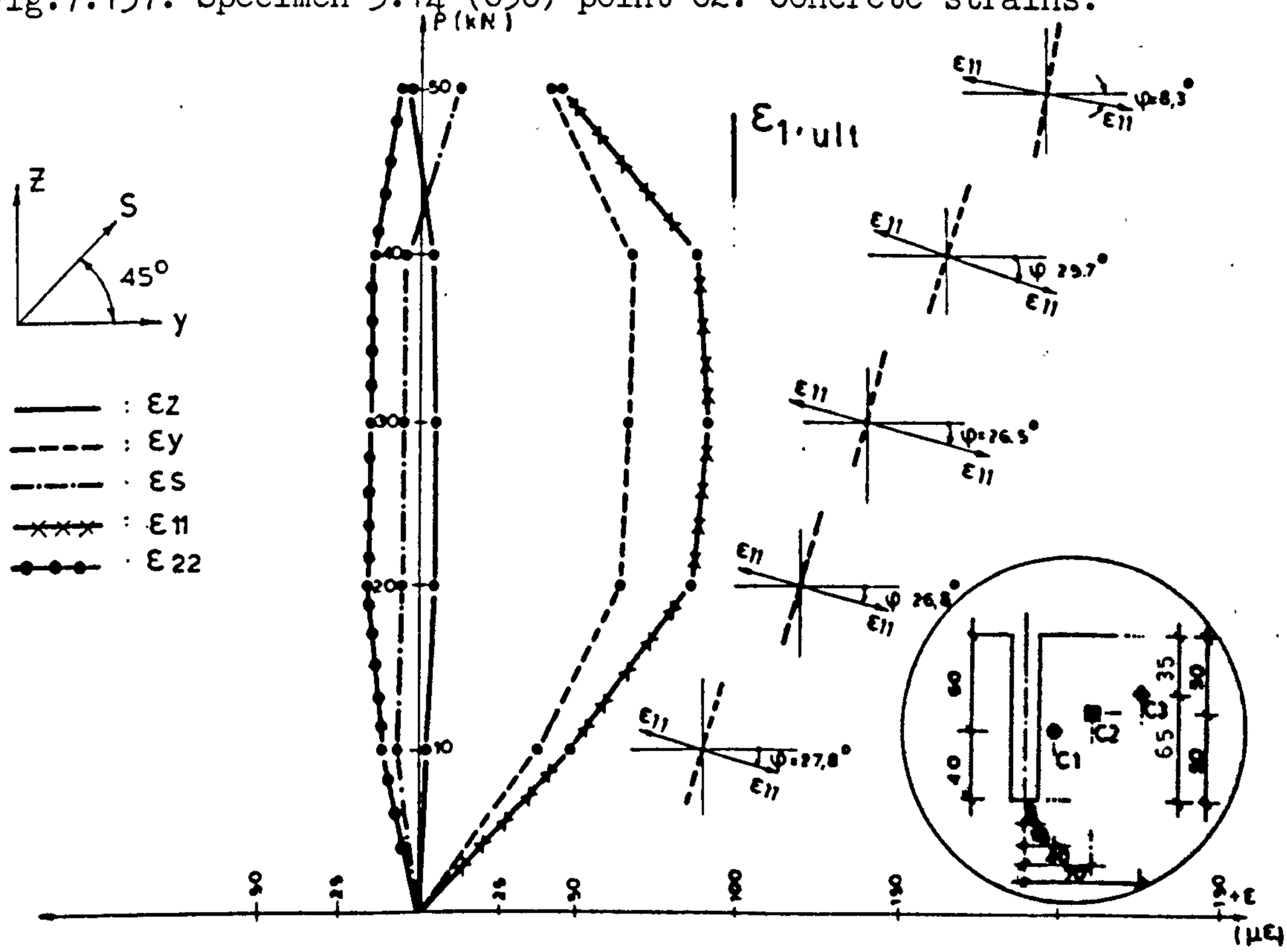

Fig.7.138. Specimen 3.14 (C50) point C3. Strains ε_{zz} , ε_{yy} , ε_{ss} ε_{11} , ε_{22} and inclination of principal strains of concrete.

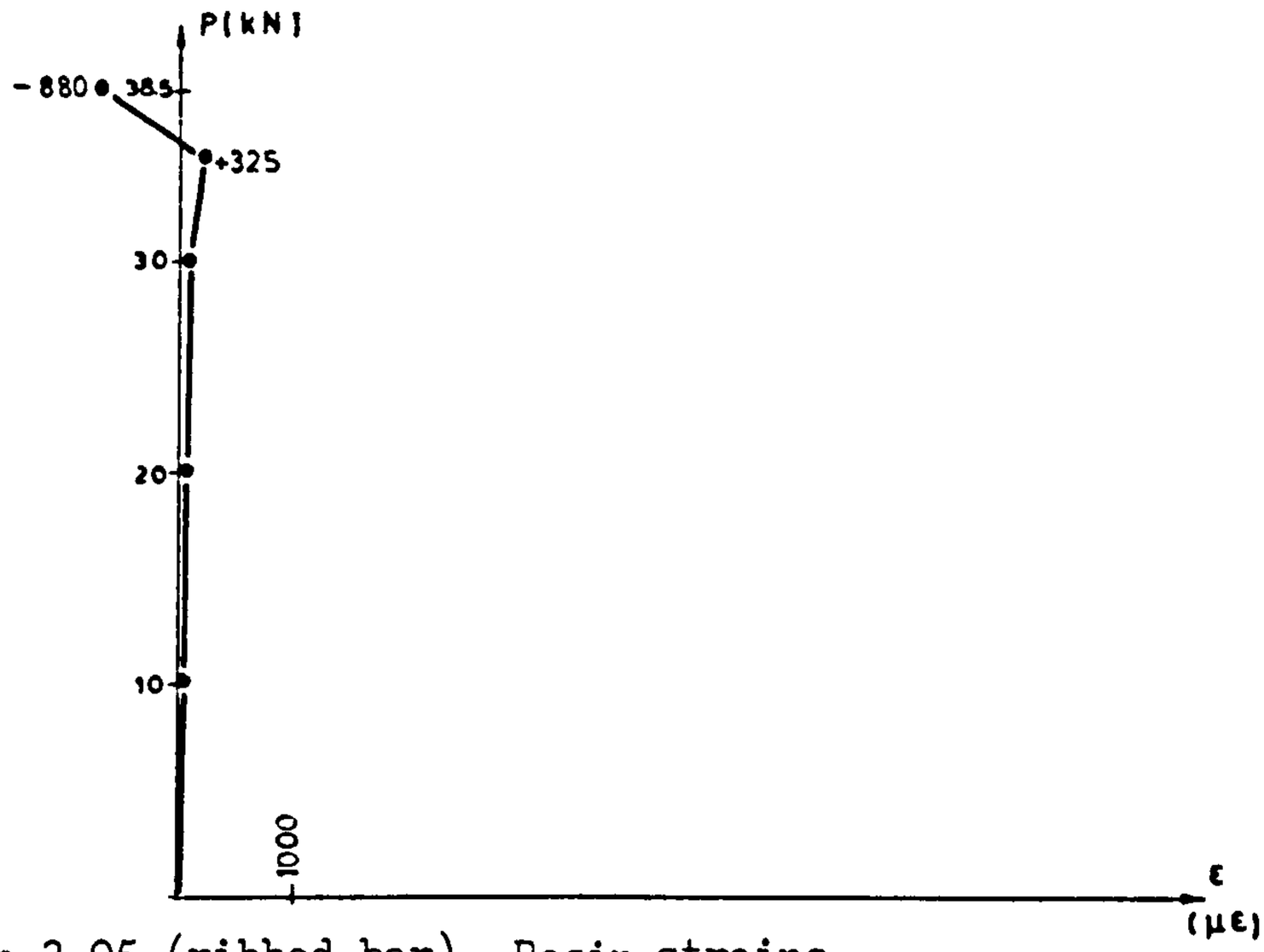

Fig.7.139. Specimen 3.05 (ribbed bar). Resin strains.

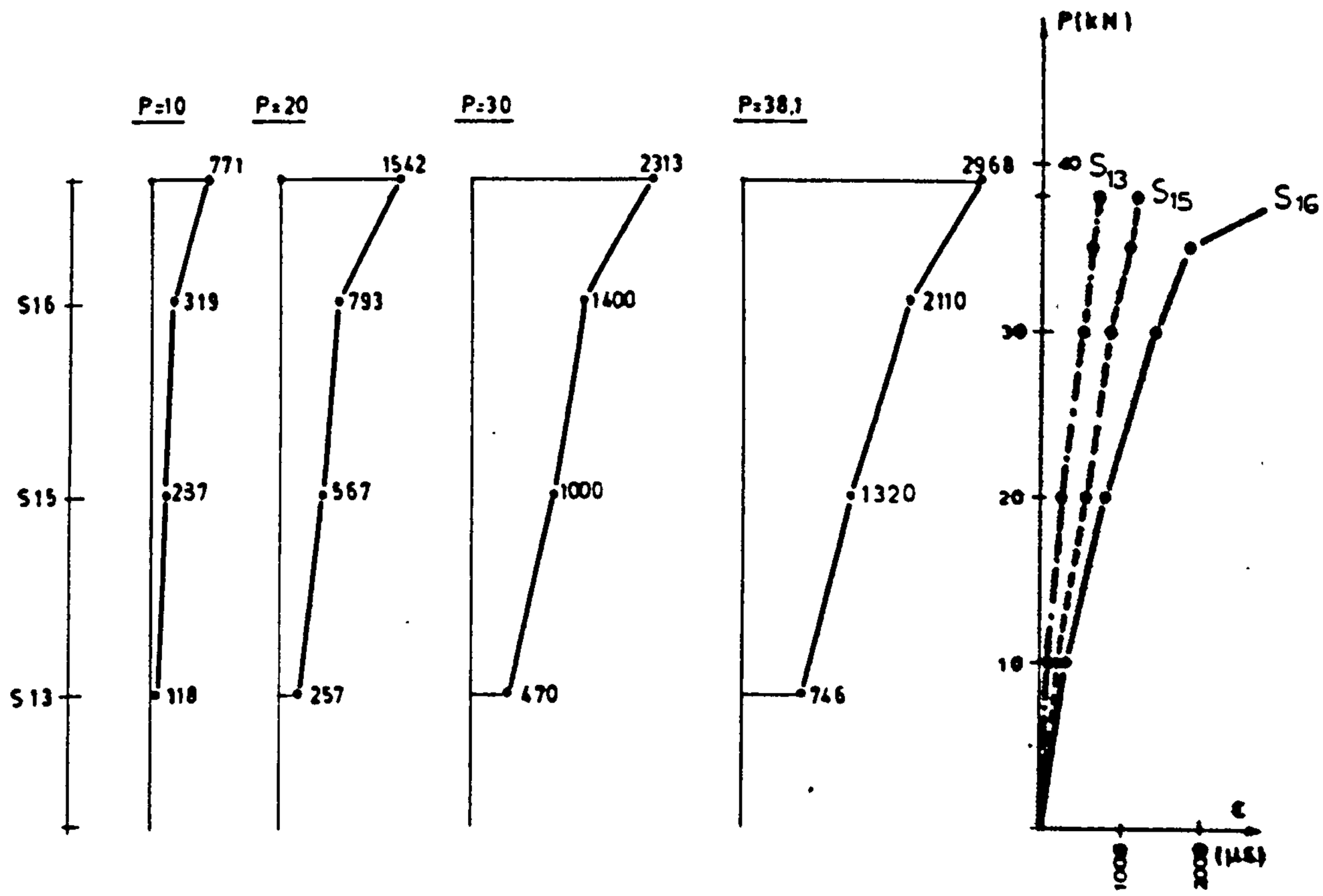

Fig.7.140. Specimen 3.05 (ribbed bar). Steel strains.

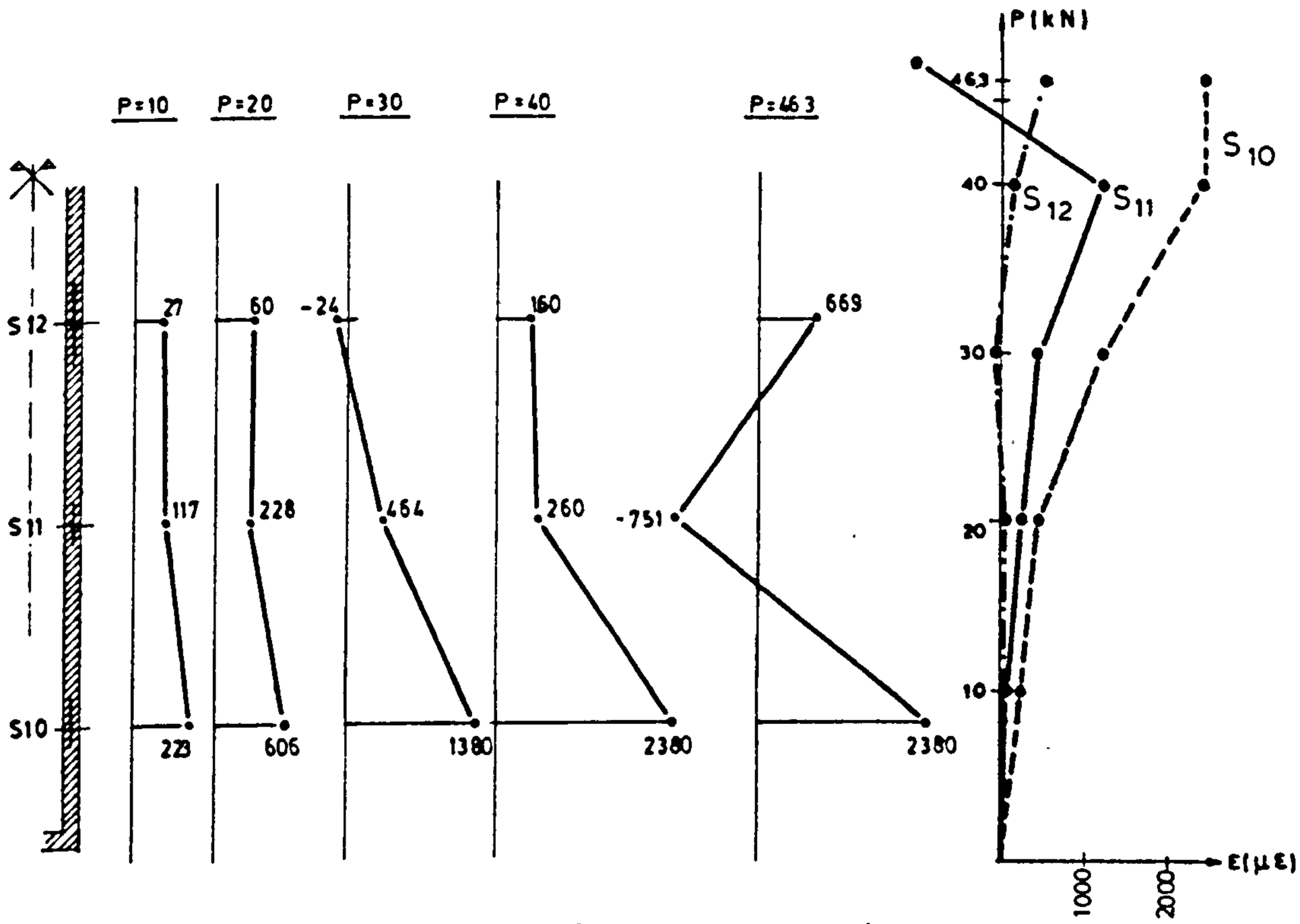

Fig.7.141. Specimen 3.15 (injected resin). Resin strains.

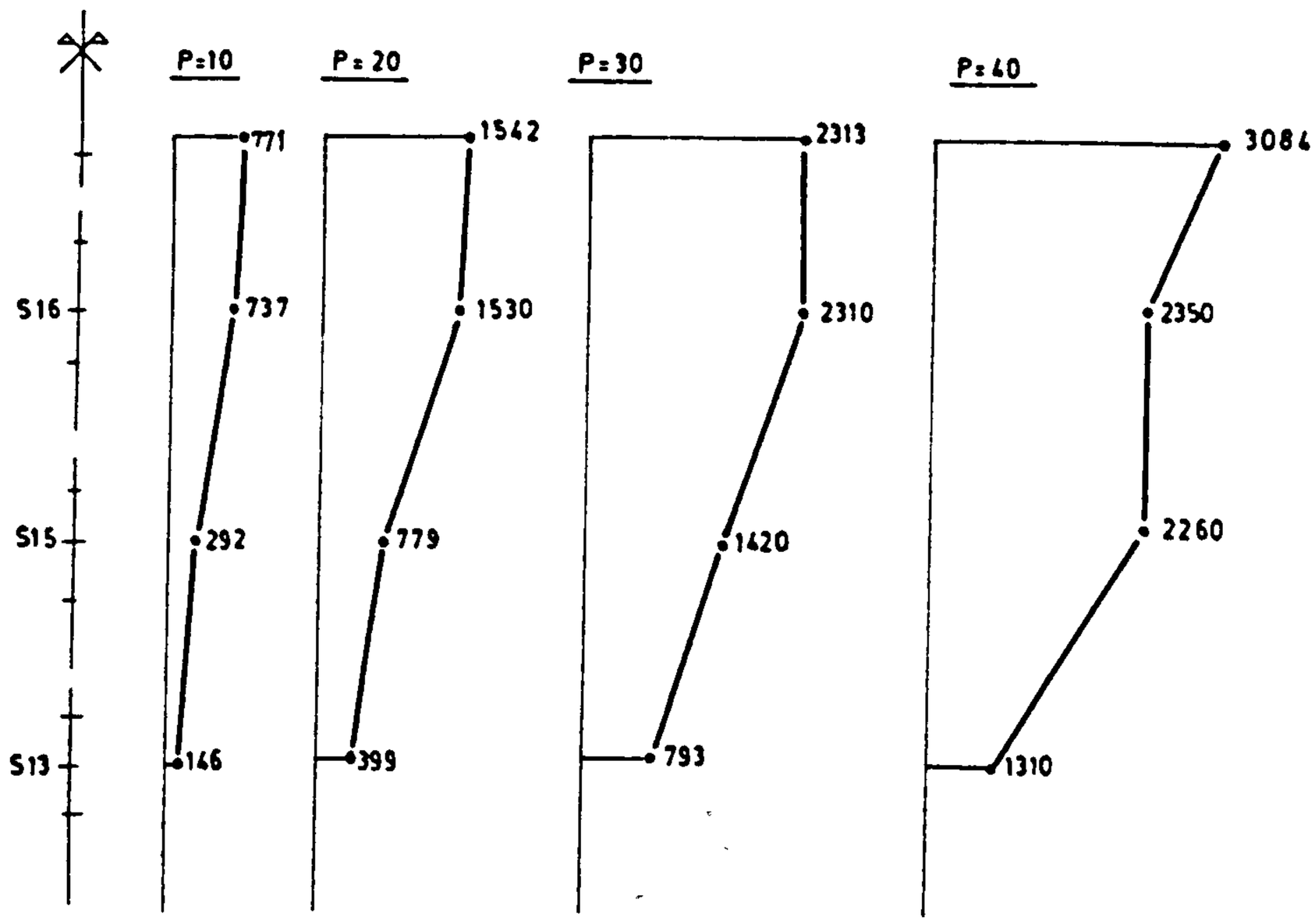

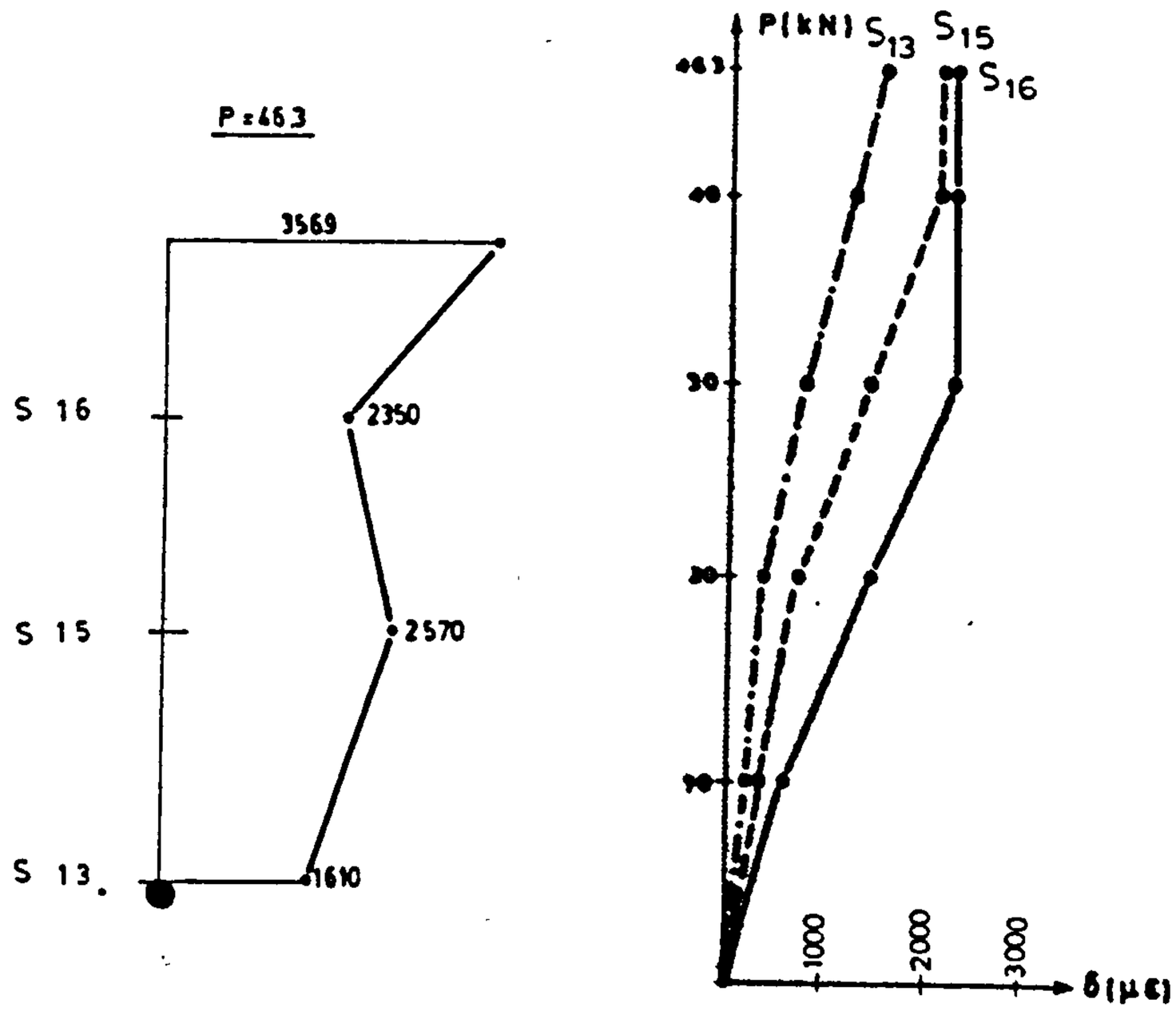

Fig.7.142. Specimen 3.15 (injected resin). Steel strains.

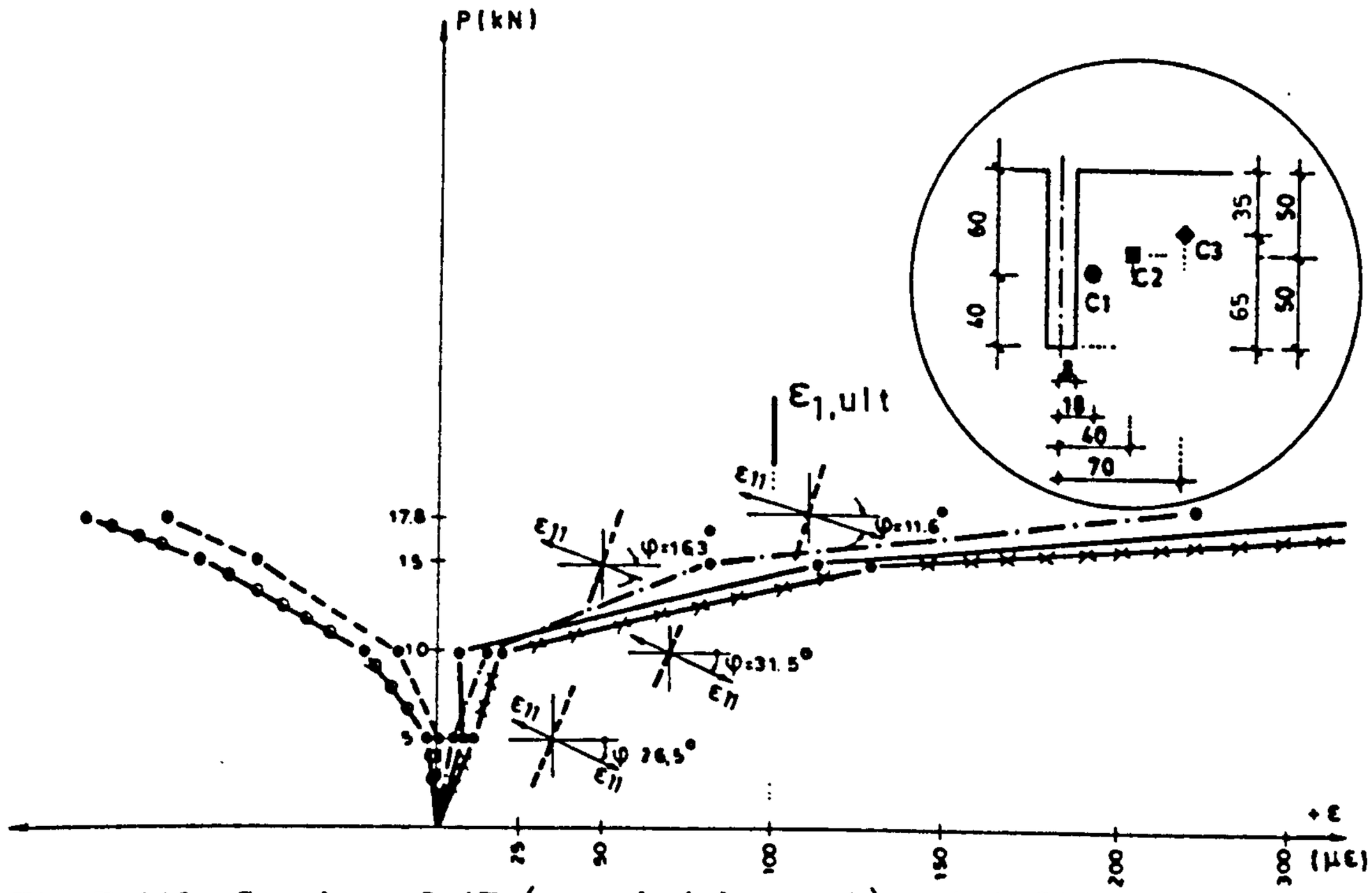

Fig.7.143. Specimen 3.17 (non shrink grout) point C1. Strains ε_{zz}, ε_{yy}, ε_{ss}, ε_{11}, ε_{22} and inclination of principal strains of concrete.

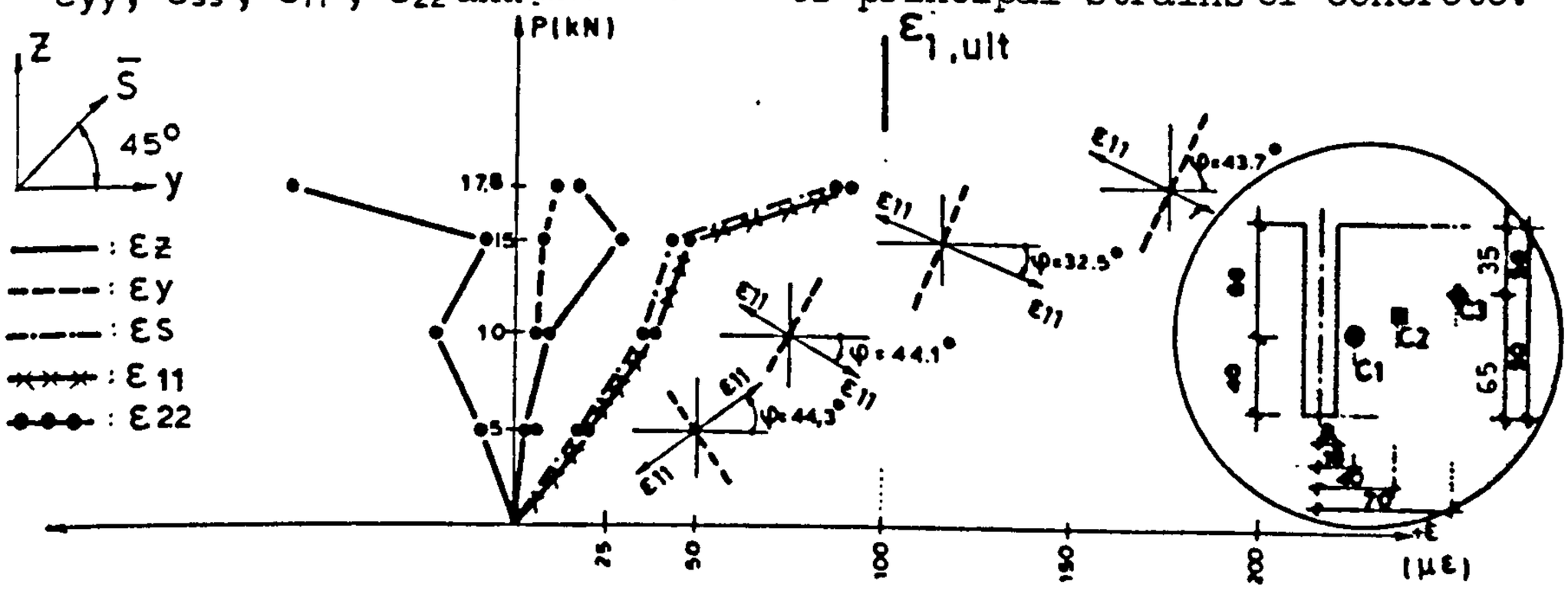

Fig.7.144. Specimen 3.17 (non shrink grout)-point C2. Strains ε_{zz}, ε_{yy}, ε_{ss}, ε_{11}, ε_{22} and inclination of principal strains of concrete.

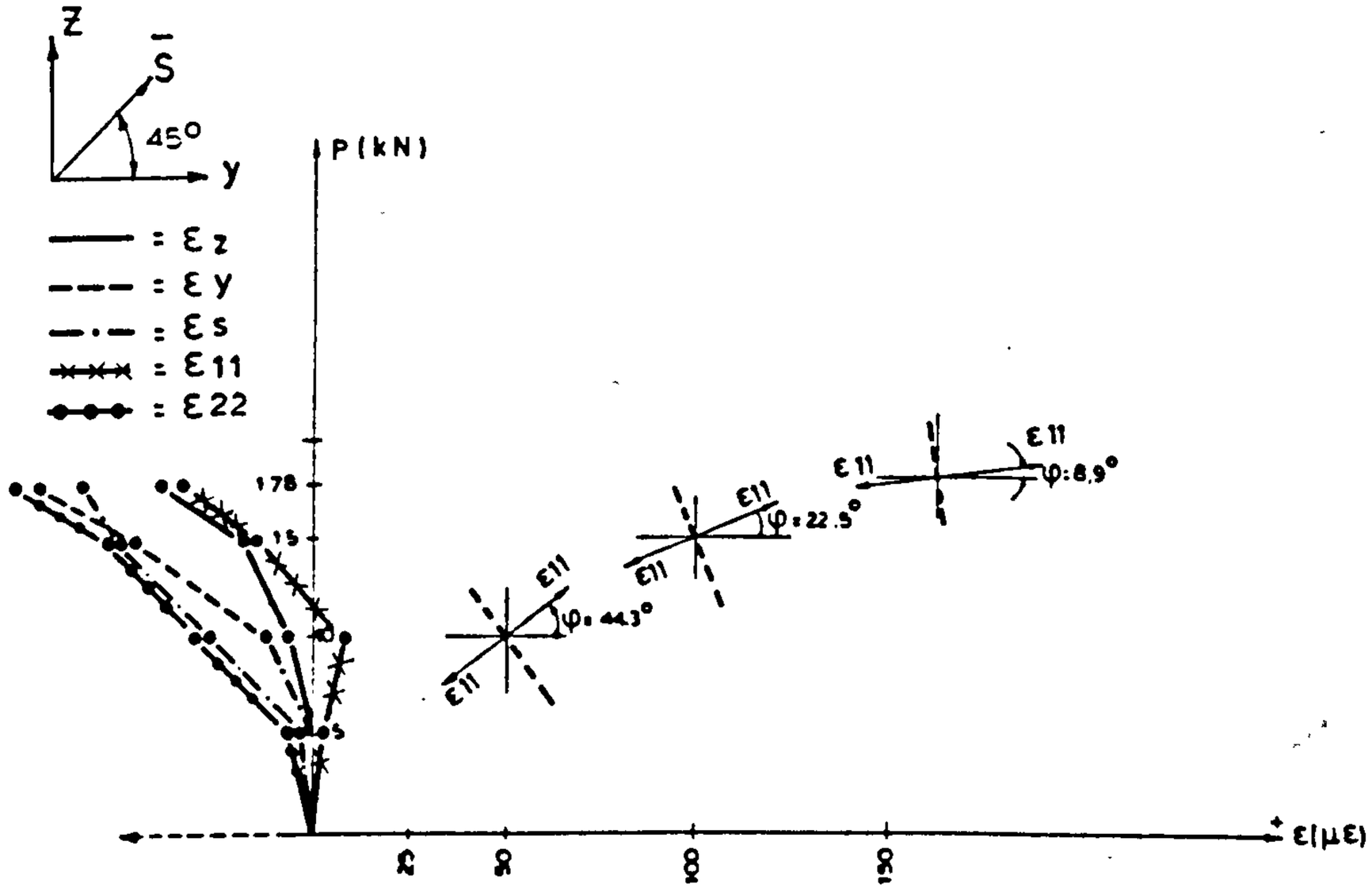

Fig.7.145. Specimen 3.17,(non shrink grout),point C3.
Concrete strains.

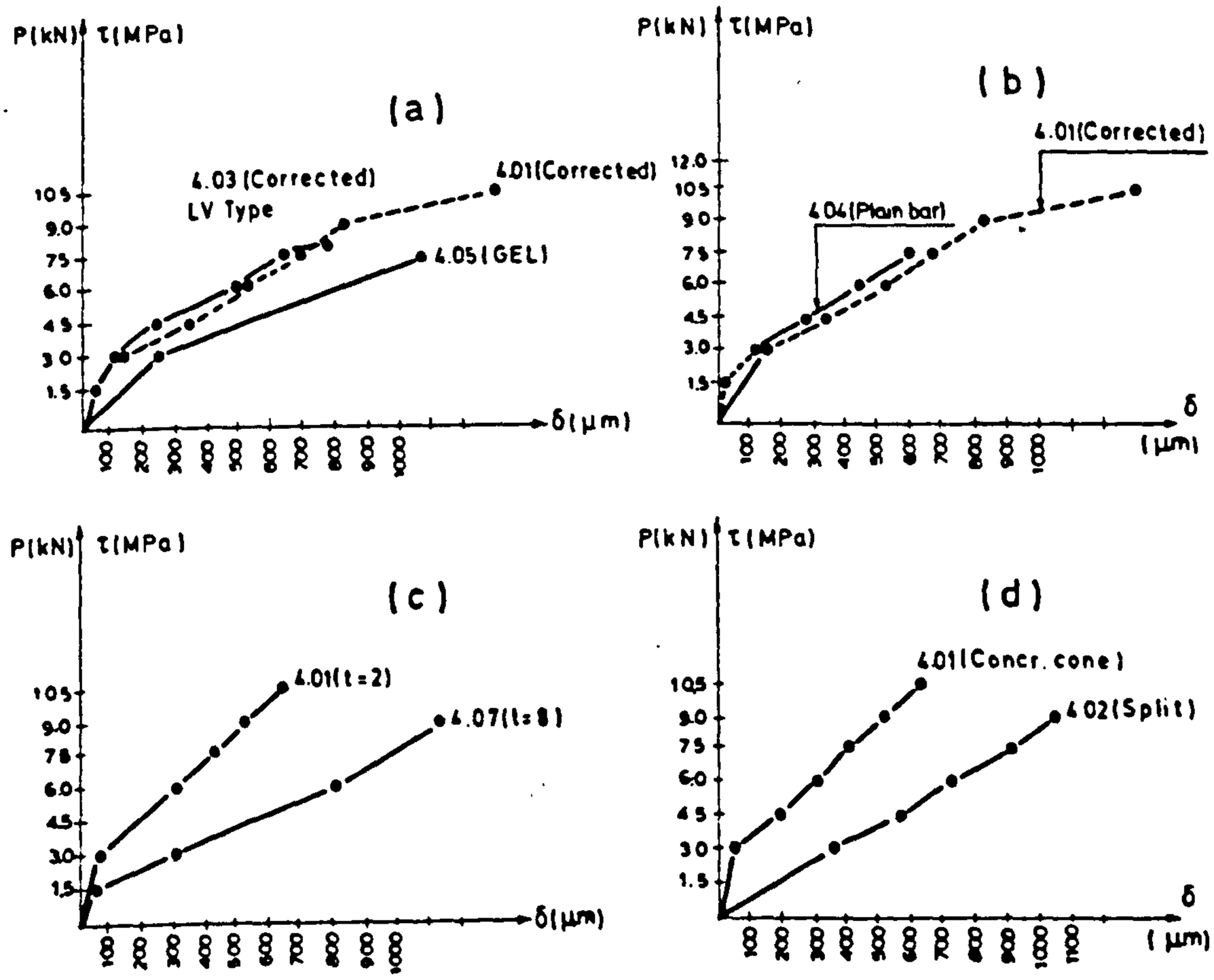

Fig.7.146. Partially bonded anchors. P=P(δ) and τ = τ (δ) relationships obtained experimentally.

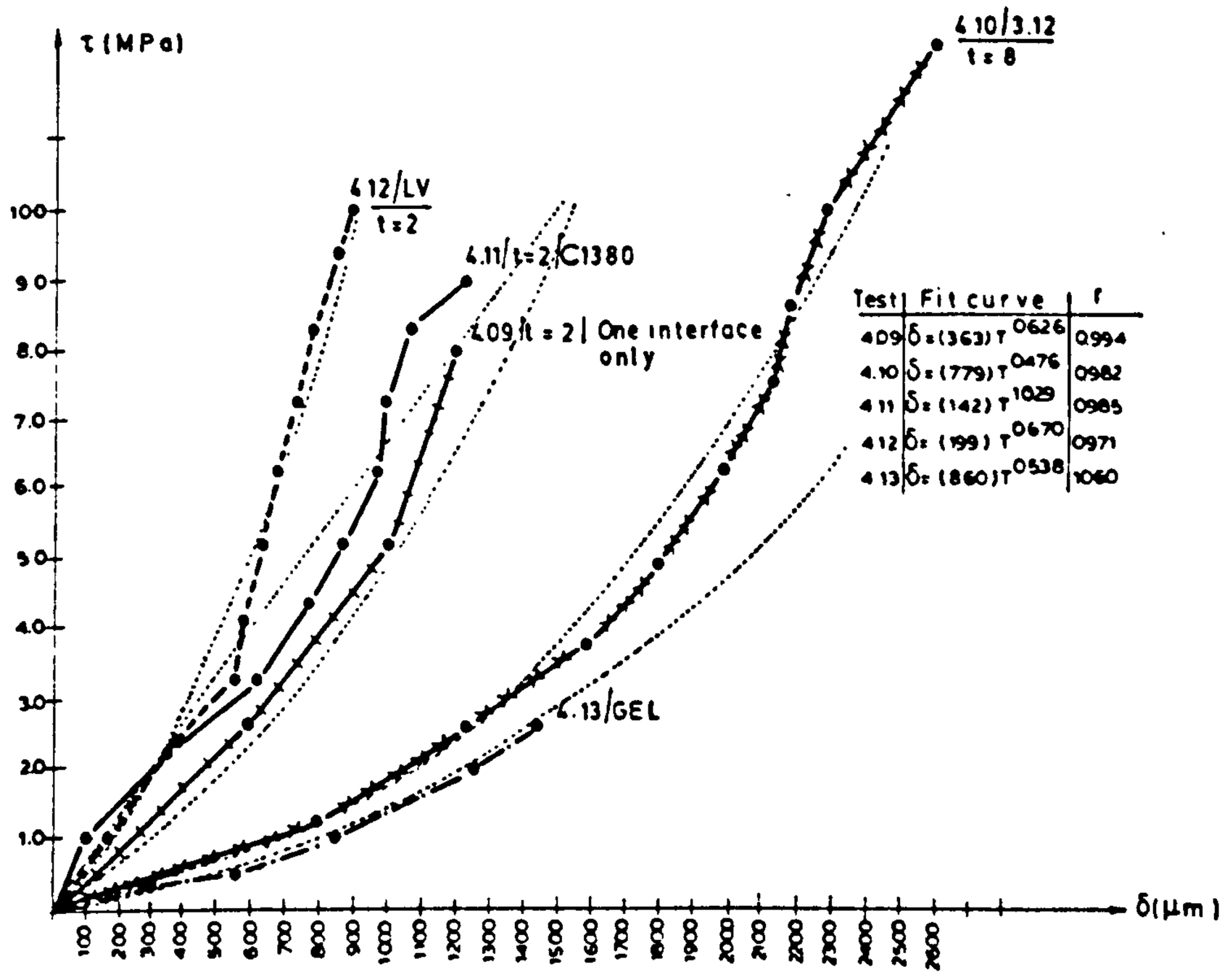

Fig.7.147. Local bond - local slip for concrete to concrete adhesive joints.

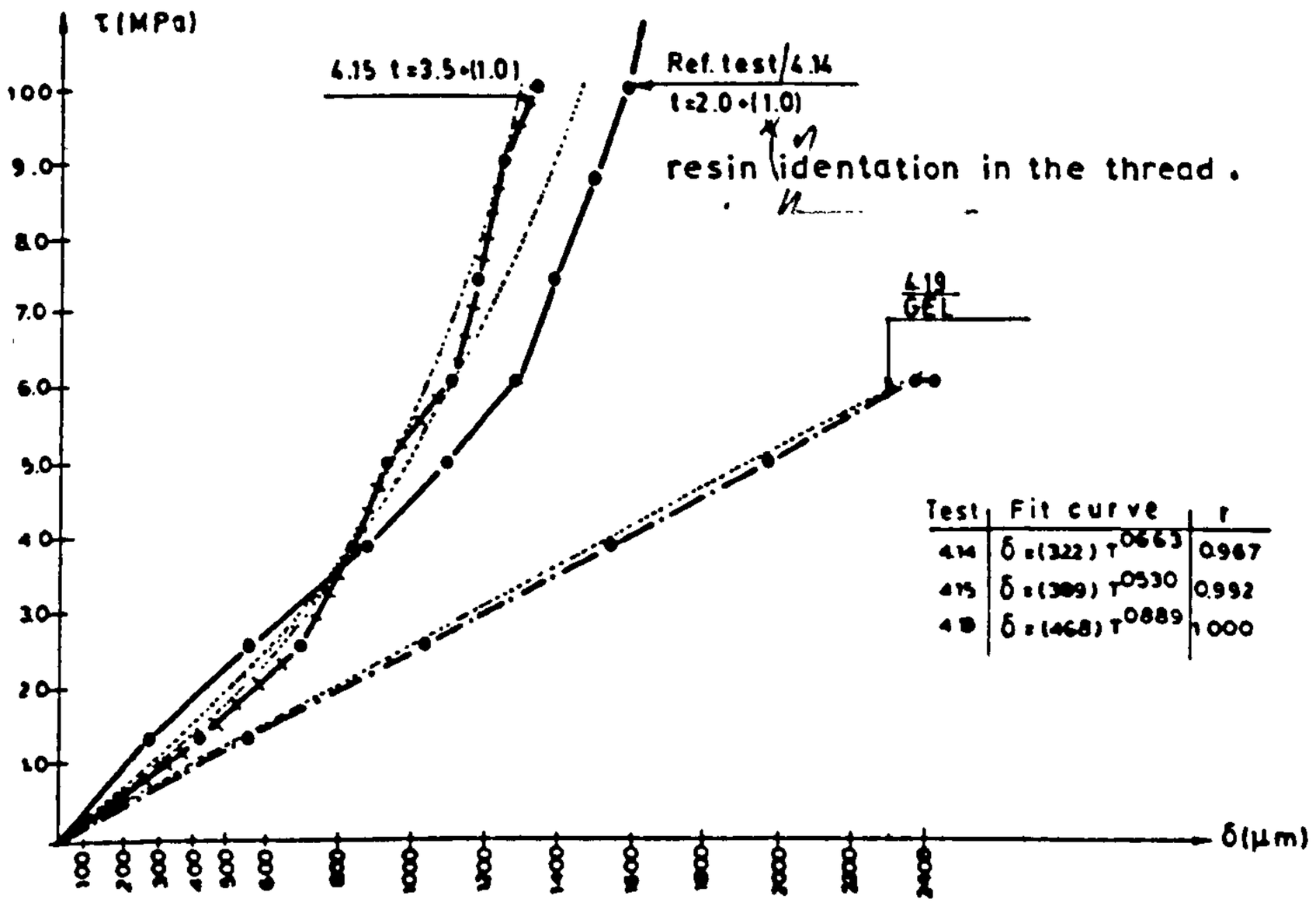

Fig.7.148. Local bond - local slip for concrete to steel adhesive joints.

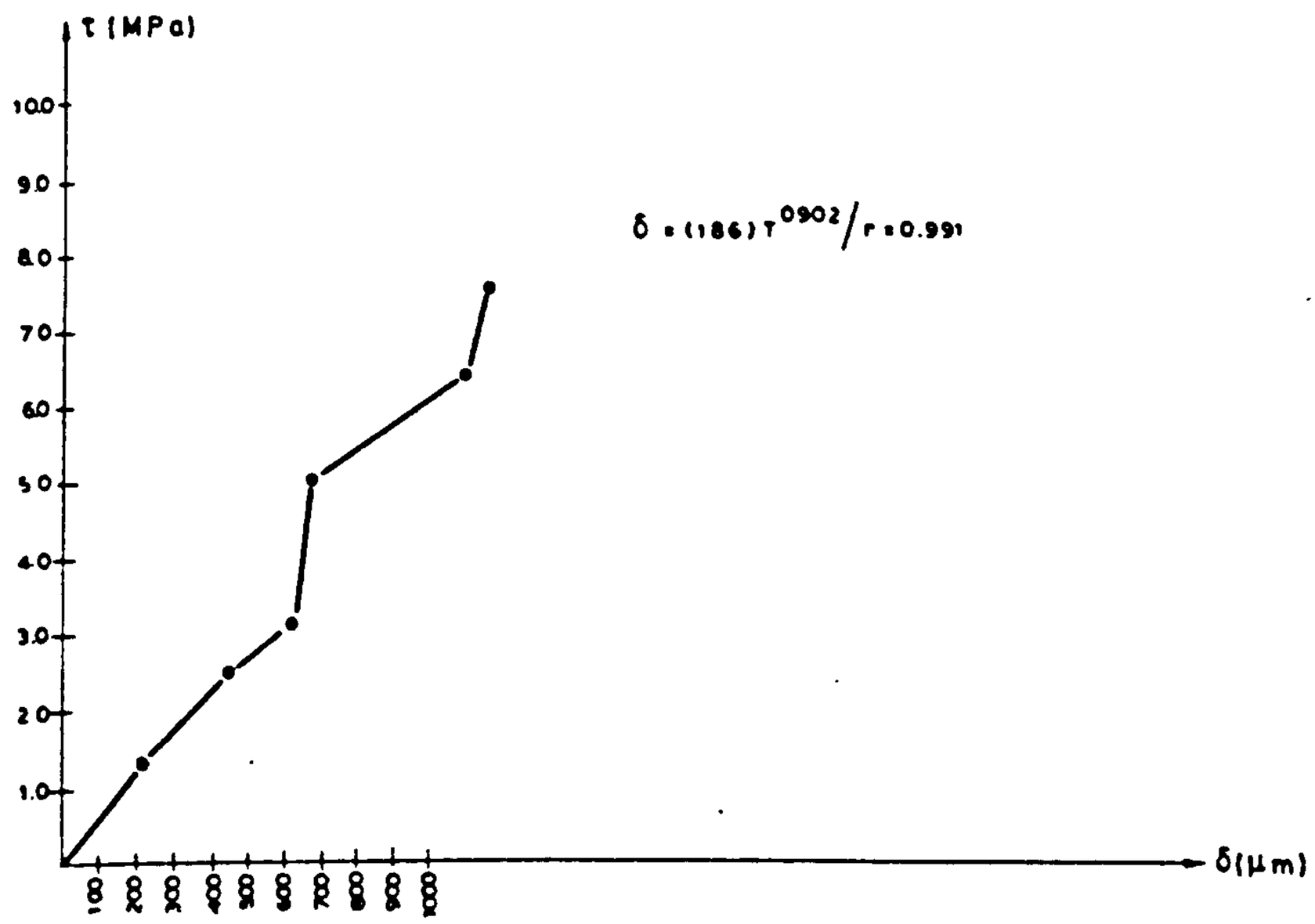

Fig.7.149. Local bond/local slip for steel to steel adhesive joints.

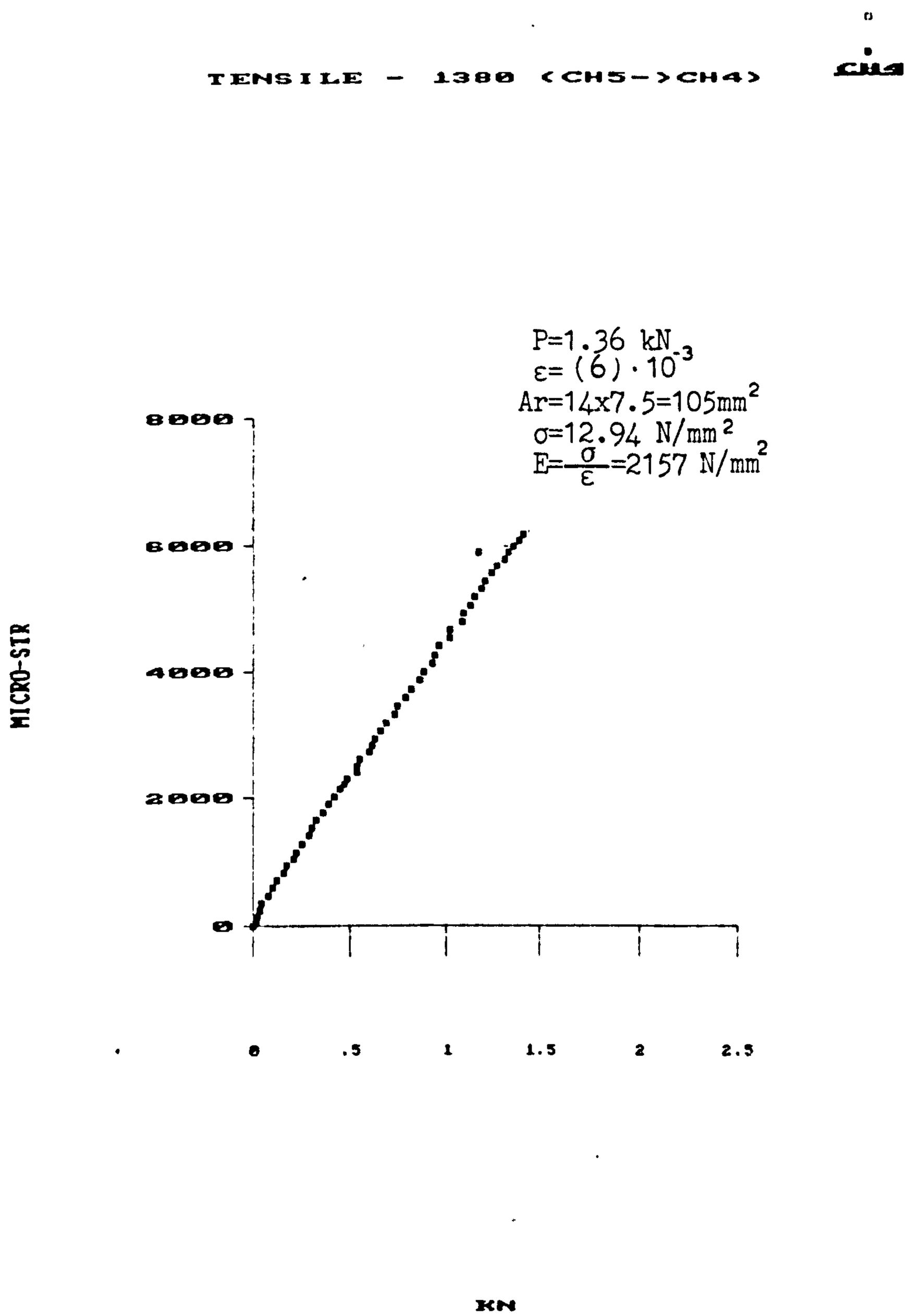

Fig.7.150. Resin C 1380. Tensile test.

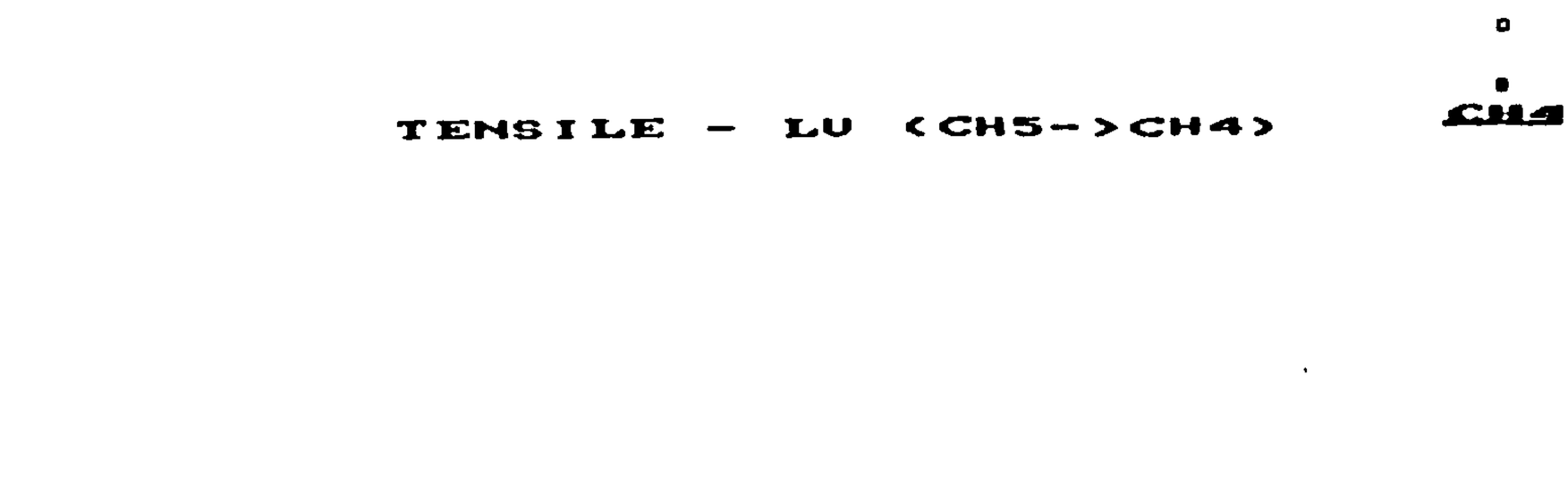

P= 1.3 kN
$\varepsilon=(5.334)\cdot 10^{-3}$
Ar= 13x8=104 mm^2
σ= 12.48 N/mm^2
E= 2340 N/mm^2

Fig.7.151. Resin LV. Tensile test.

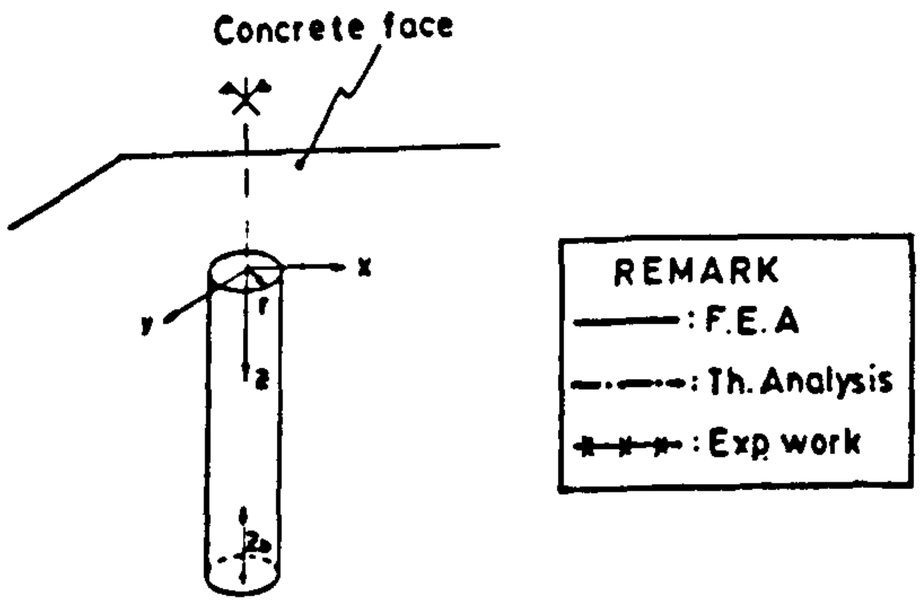

Values of the anchor steel strain ε_{zs} [$\mu\varepsilon$]

	P= 10kN			P=20 kN			P=30 kN		
z	EXP	TH.A	FEA	EXP	TH.A	FEA	EXP	TH.A	FEA
0	771	771		1542	1542		2313	2313	
5			791			1562			2373
10		685			1370			2055	
15			628			1256			1884
20	740	600		1490	1200		2310	1800	
25			607			1214			1821
30		520			1040			1560	
35			483			966			1449
40		440			880			1320	
45			436			872			1308
50	407	364		1050	728		1830	1092	
55			336			672			1008
60		285			570			855	
65			276			552			828
70		216			432			648	
75			187			374			561
80	184	143		496	286		905	429	
85			121			242			363
90		71			142			213	
95			36			72			108
100		0			0			0	

(8.1.a) Distribution of the steel strains ε_{zs},($\mu\varepsilon$)/X=0, y=0

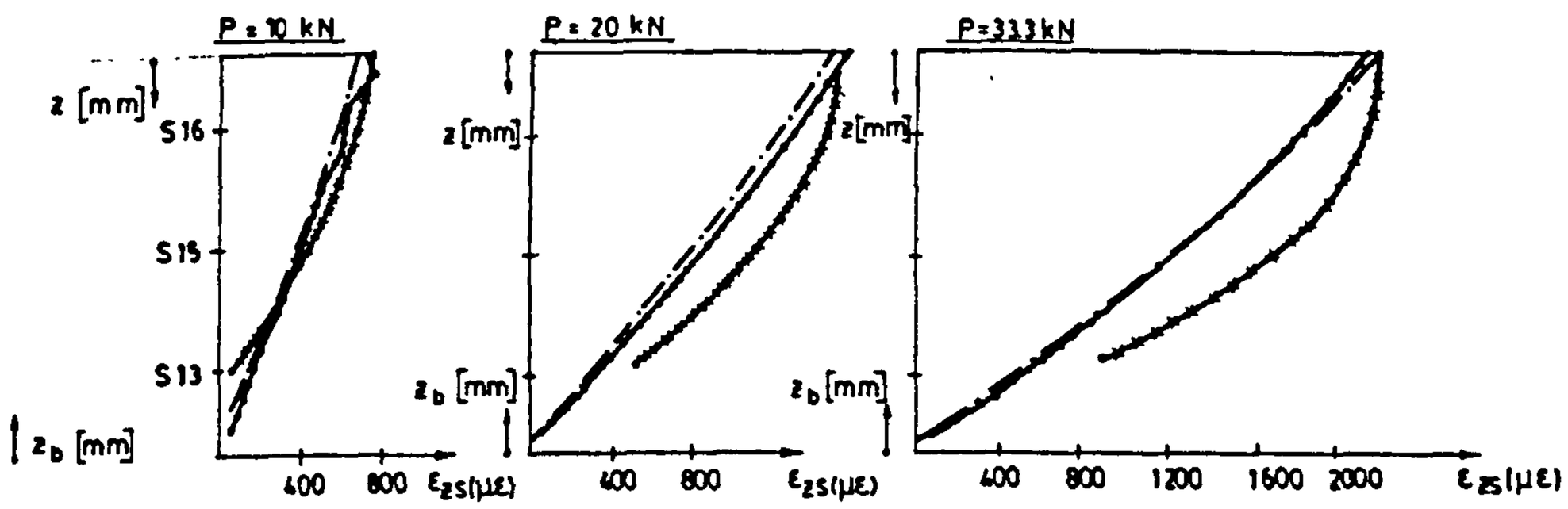

(8.1.b.) Distribution of the resin tensile strains ε_r ($\mu\varepsilon$) at r=7mm (middle of resin thickness)

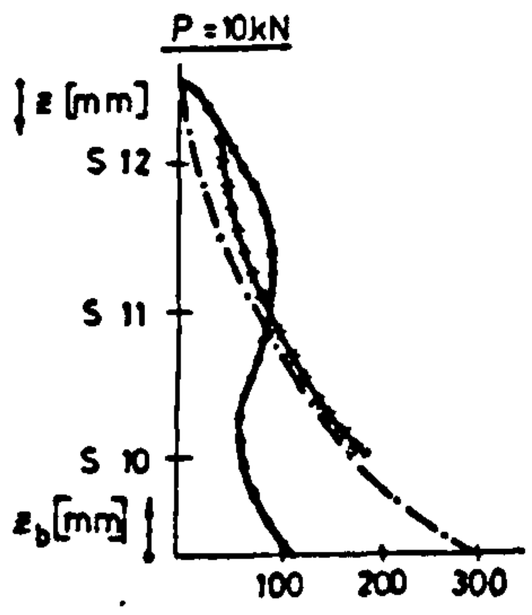

ε_r ($\mu\varepsilon$)

	P = 10 kN			P = 20 kN			P = 30 kN		
z	EXP	TH.A	FEA	EXP	TH.A	FEA	EXP	TH.A	FEA
0		0			0			0	
5			70			140			210
10		8			16			24	
15			129			258			387
20	100	44		314	88		917	132	
25			195			390			585
30		84			168			252	
35			188			376			564
40		113			226			339	
45			152			304			456
50	286	146		506	292		880	438	
55			153			306			459
60		177			354			531	
65			108			216			324
70		208			416			624	
75			129			258			367
80	382	238		1070	476		1650	714	
85			126			252			378
90		298			596			894	
95			134			268			402
100		300							

(8.1.c) Ancor displacement at P= 10,20,30 kN

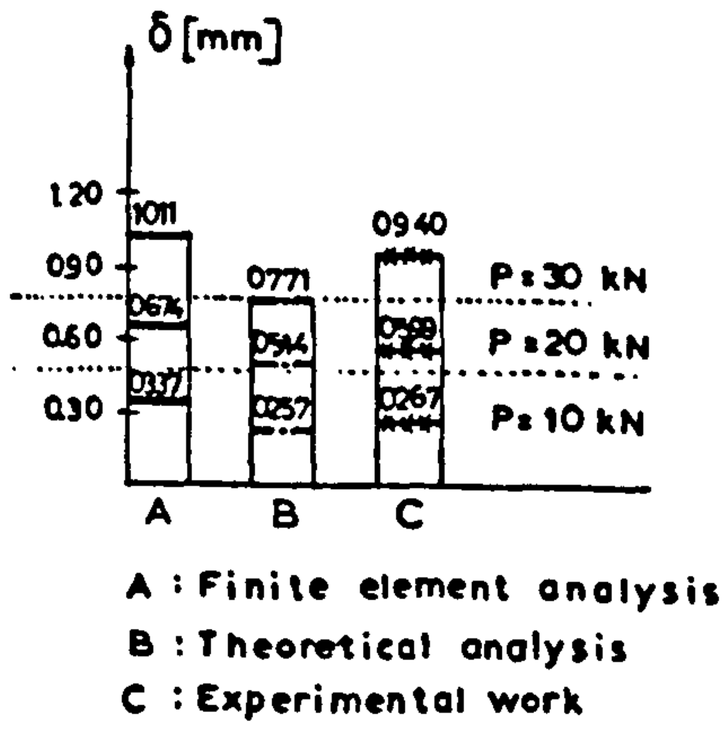

Fig.8.1. Comparison of the steel strains and displacement and resin strains derived from theoretical and finite element analyses with those obtained experimentally.

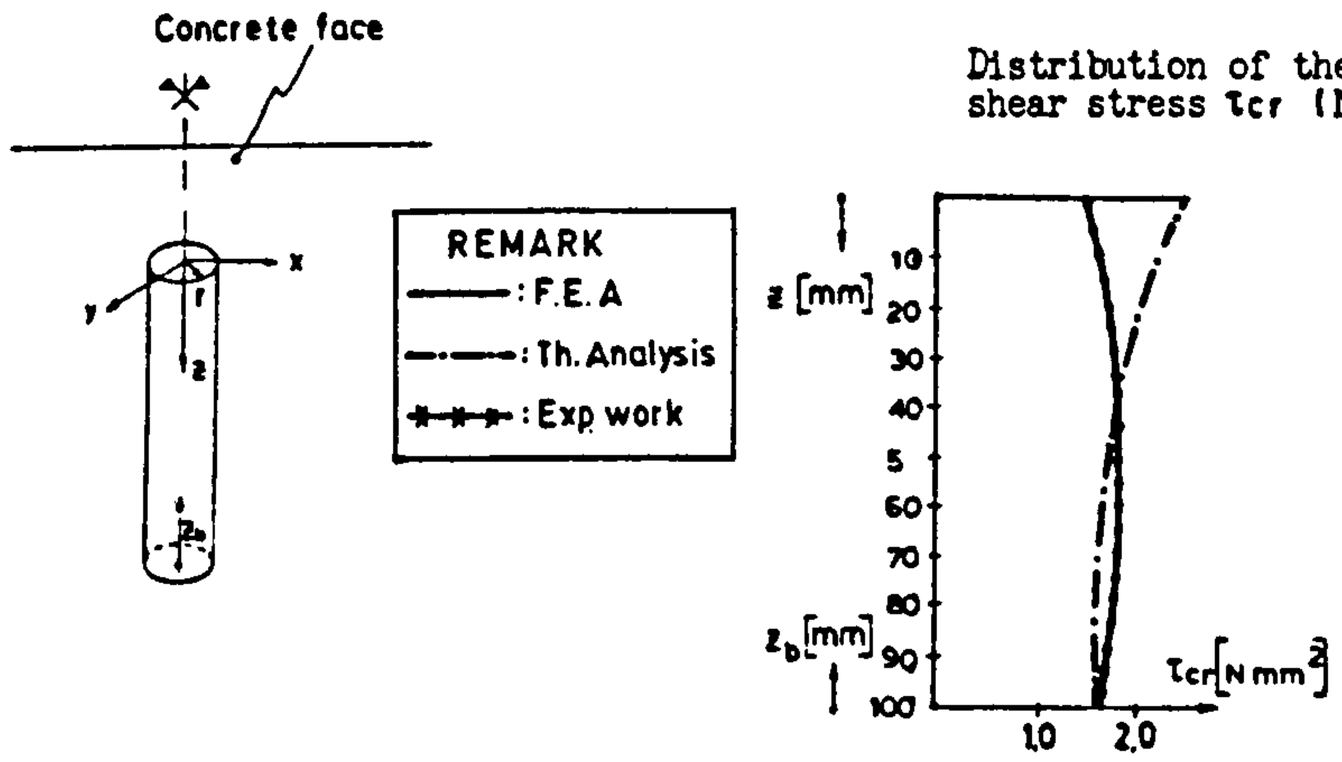

Distribution of the concrete resin interfacial shear stress τ_{cr} (N/mm^2) at r=8mm. P=10 kN

	TH.A.	F.E.A
0	2.24	
5		1.56
10	2.21	
15		1.90
20	2.13	
25		1.90
30	2.06	
35		1.83
40	2.00	
45		1.82
50	1.95	
55		1.78
60	1.91	
65		1.80
70	1.88	
75		1.69
80	1.86	
85		1.80
90	1.84	
95		1.35
100	1.84	

Distribution of concrete strains at P=10 kN at x=0, y=18mm

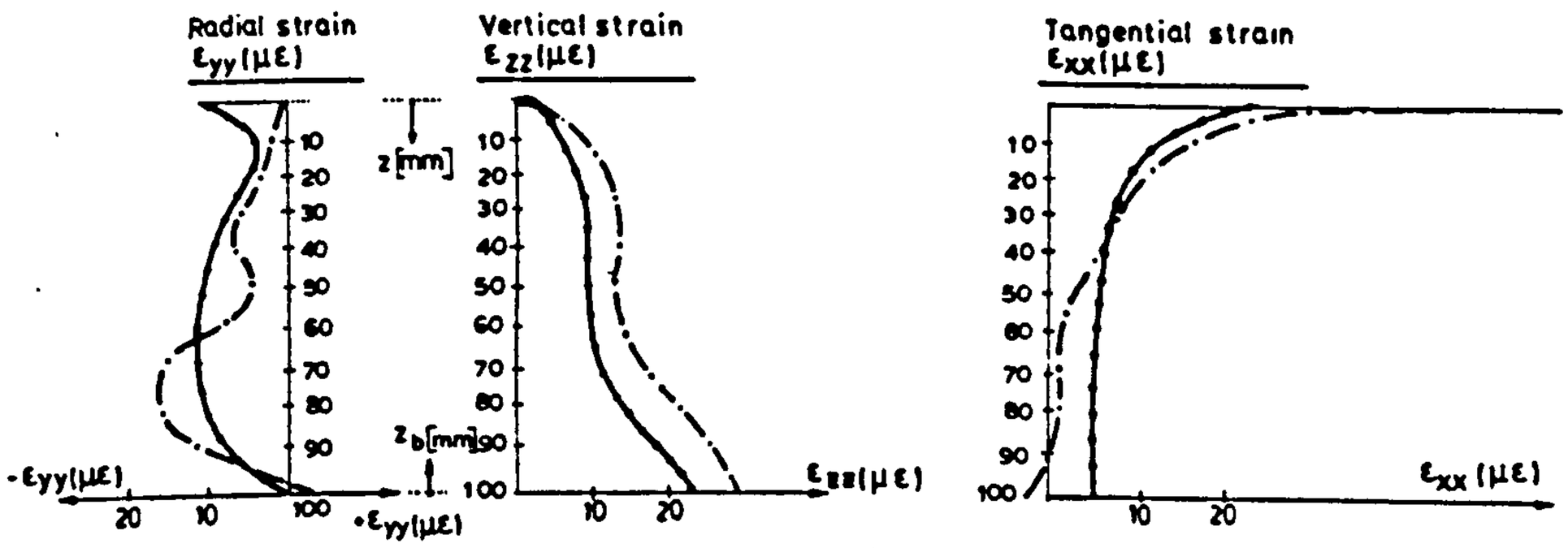

Values of concrete radial ε_{yy}, vertical ε_{zz} and targential ε_{xx} strains at x=0, y=18mm at P= 10, 20, 30 kN

	P = 10 kN									P = 20 kN									P = 30 kN								
	EXPER.			F.E.A			TH. ANAL.			EXPER.			F.E.A			TH. ANAL.			EXPER.			F.E.A			TH. ANAL.		
Z	ε_{xx}	ε_{yy}	ε_{zz}	ε_{xx}	ε_{yy}	ε_{zz}	ε_{xx}	ε_{yy}	ε_{zz}	ε_{xx}	ε_{yy}	ε_{zz}	ε_{xx}	ε_{yy}	ε_{zz}	ε_{xx}	ε_{yy}	ε_{zz}	ε_{xx}	ε_{yy}	ε_{zz}	ε_{xx}	ε_{yy}	ε_{zz}	ε_{xx}	ε_{yy}	ε_{zz}
0							56	-05	0							112	-1	0							168	-15	0
5				21	-15	2	(45)						42	-30	4							63	-45	6			
10																											
15				9	-4	7	18	-4	11				18	-8	14	36	-8	22				27	-12	21	54	-12	83
20																											
25				7	-8	9							14	-16	18							21	-24	27			
30																											
35				6	-10	9	7	-7	13				12	-20	18	14	-14	26				18	-30	27	21	-21	39
40																											
45				6	-11	9							12	-22	18							18	-33	27			
50																											
55				6	-12	9	2	-3	13				12	-24	18	4	-6	26				18	-36	27	6	-9	39
60	-9,60	15								-14	37								-27	-14							
65				6	-12	10							12	-24	20							18	-36	30			
70																											
75				5	-13	13	2	-19	18				10	-26	26	4	-38	36				15	-39	39	6	-57	54
80																											
85				5	-12	18							10	-24	36							15	-36	54			
90																											
95				4	-4	22	-3	2	25				6	-8	44	-6	4	50				12	-12	66	-9	6	75
100	0									0									0								

Fig.8.2. Comparison of the interfacial concrete - resin shear stresses calculated by theoretical and finite element analyses, and of concrete strains derived from both analyses with those obtained experimentally.

Plate 1. The experimental set up.

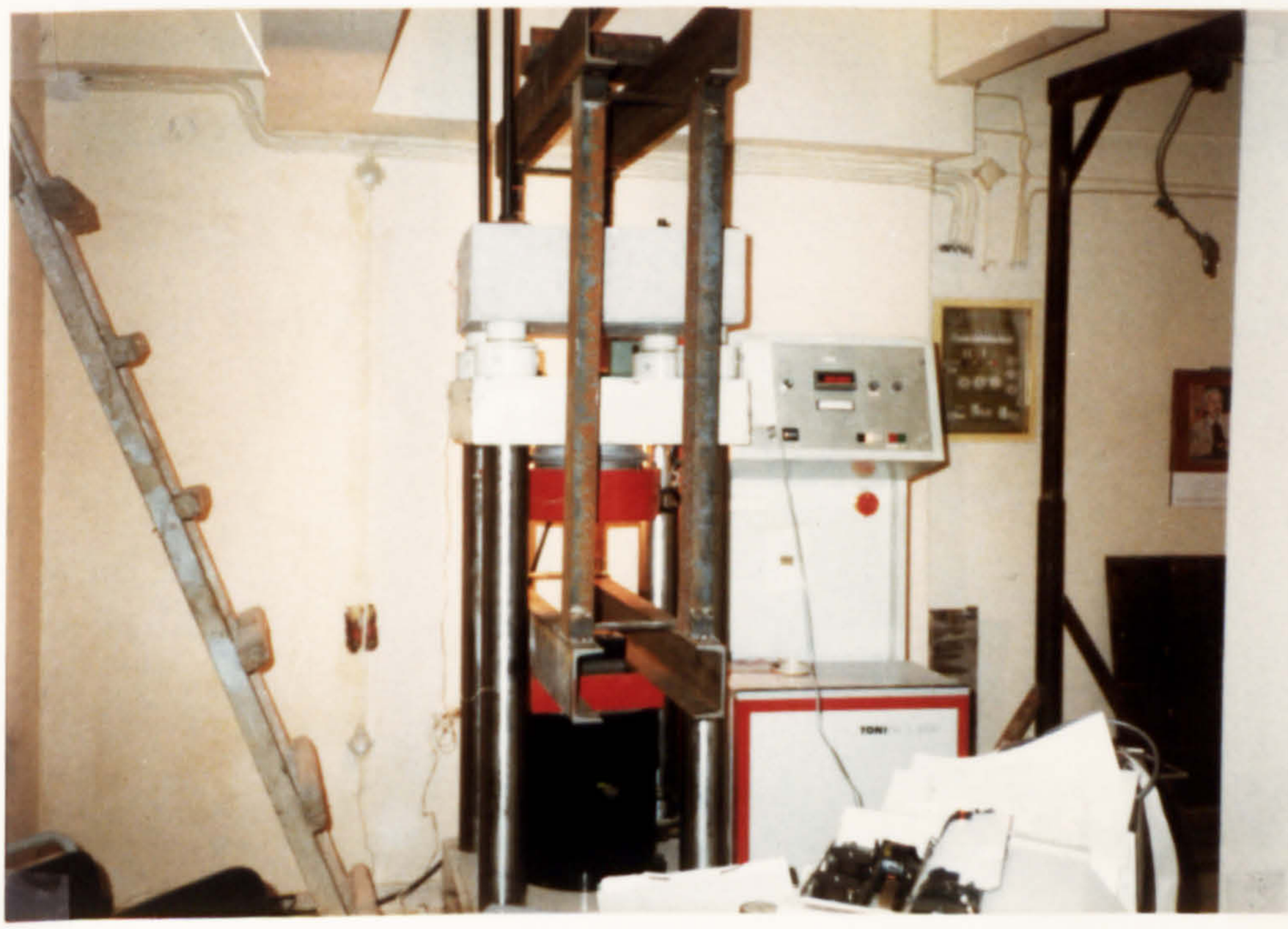

Plate 2. The experimental set up.

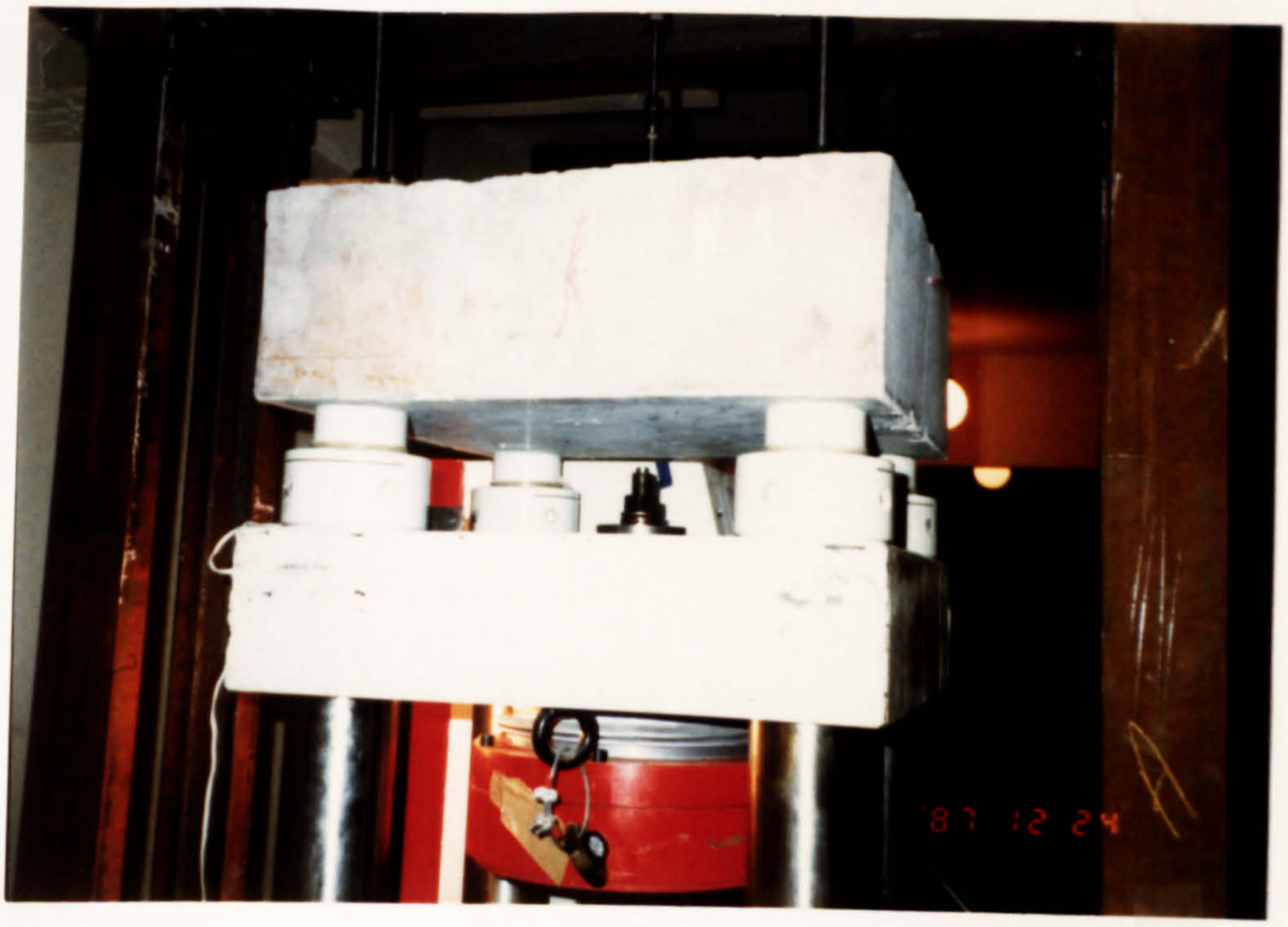

Plate 3. Fixing of concrete specimen on the testing machine.

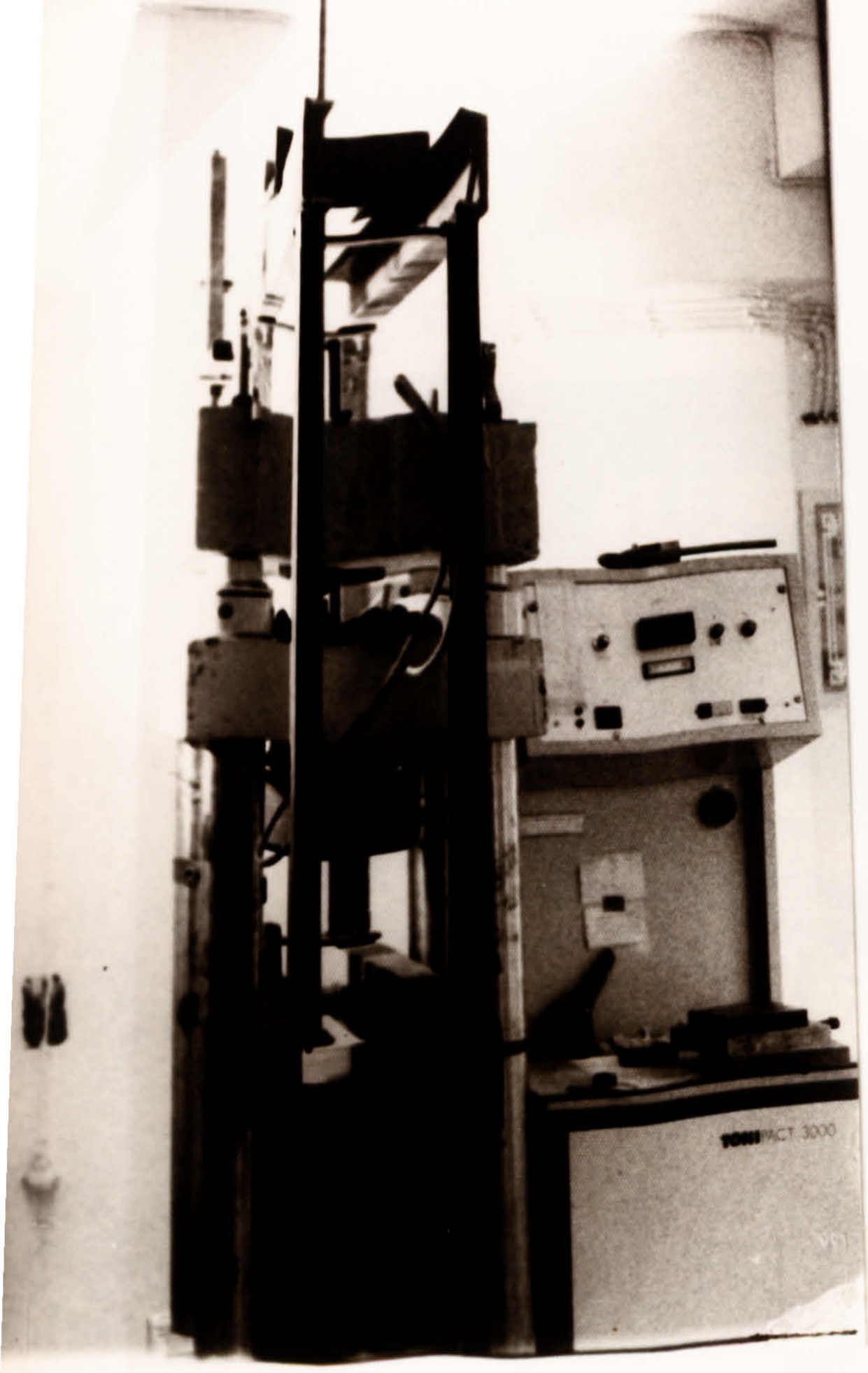

4.1

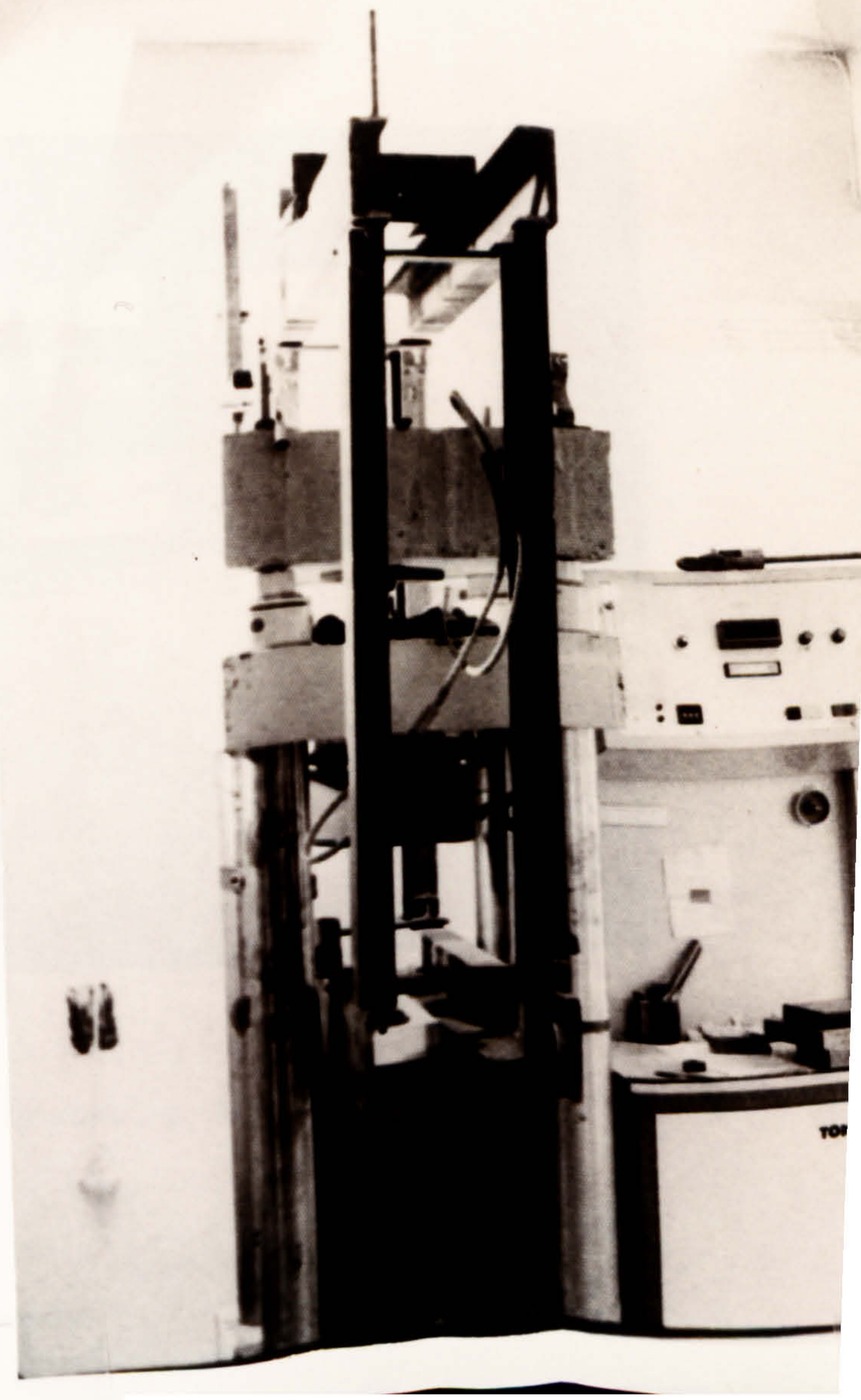

4.2

Plate 4. Details of the experimental set up

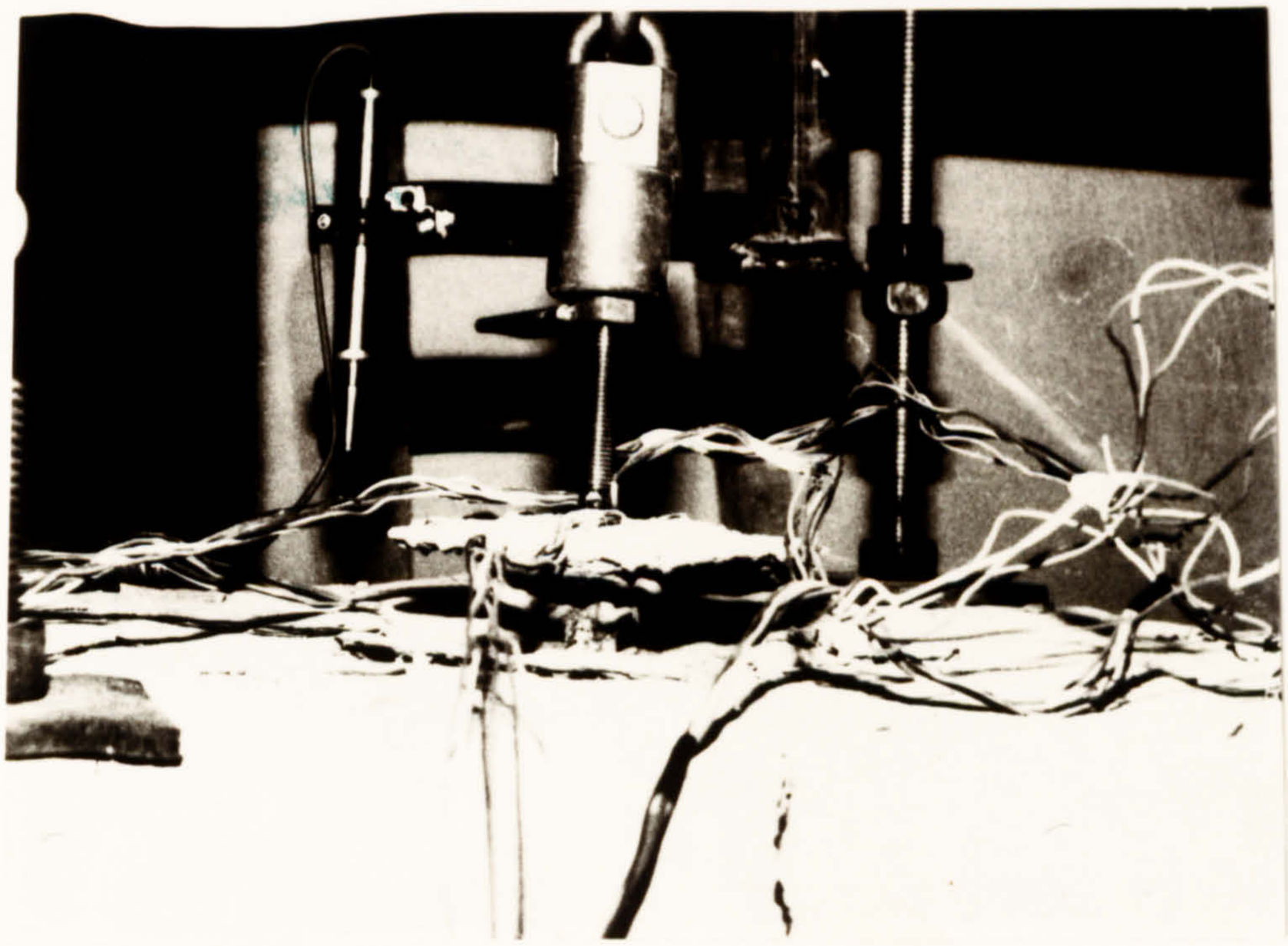

5.1

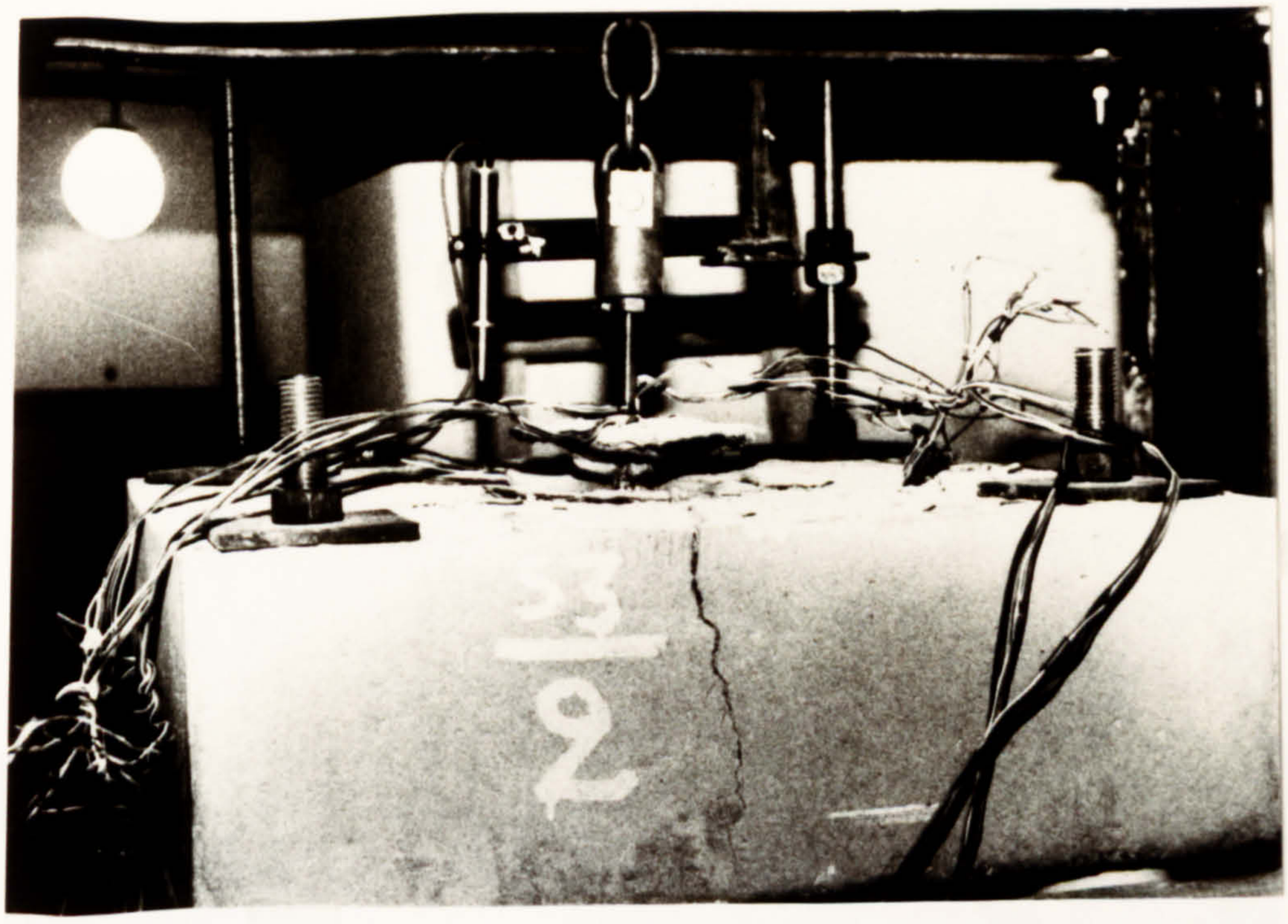

5.2

Plate 5. Detail of the slip measuring device (LDT).

Plate 6. Failure surface with the precast mortar cube carrying the concrete strain gauges.

Plate 7. Failure surface with the precast mortar cube carrying the concrete strain gauges.Close-up.

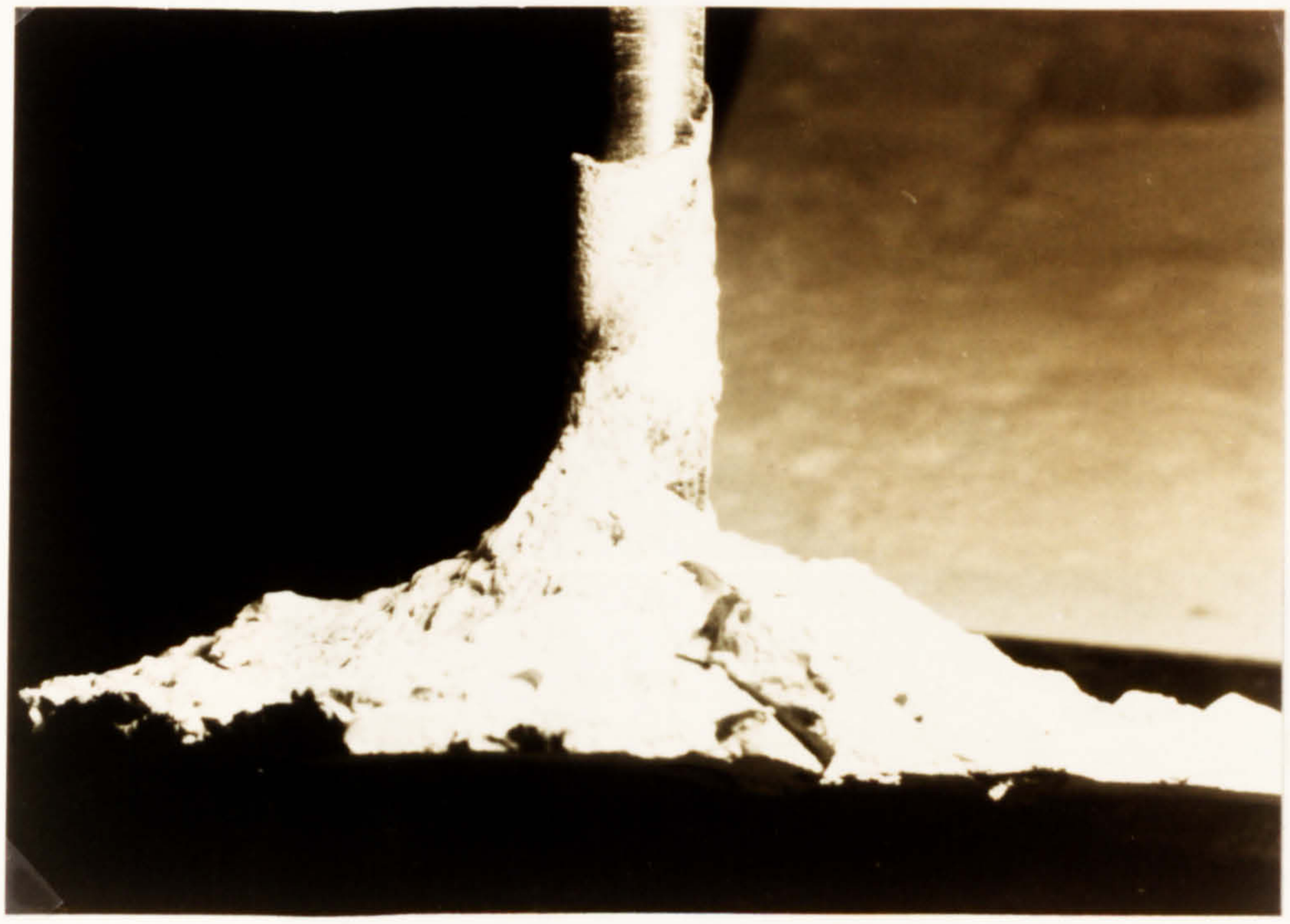

Plate 8. Typical combined mode of failure.

Plate 9. Typical combined mode of failure. Close-up.

10.1

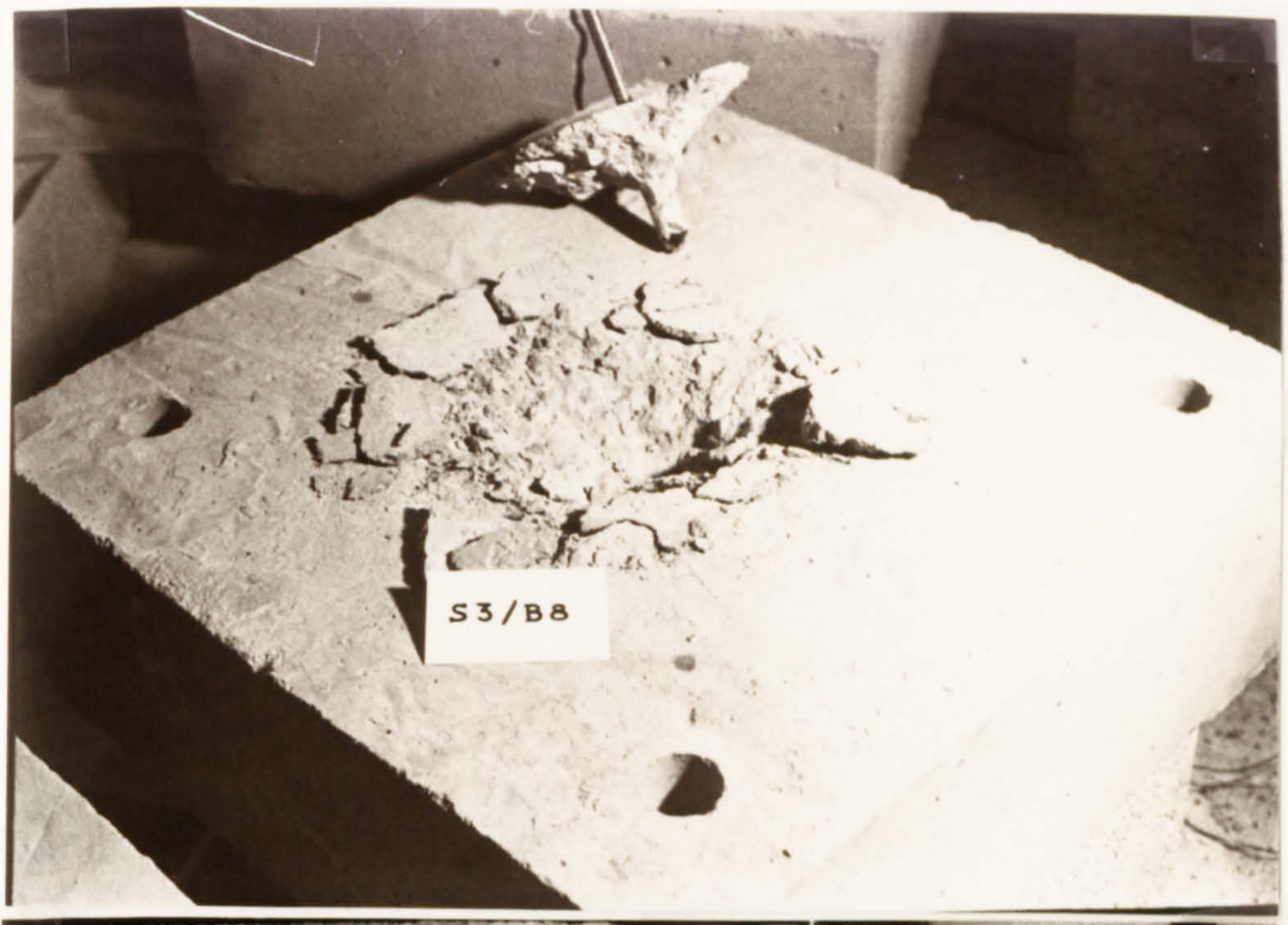

10.2

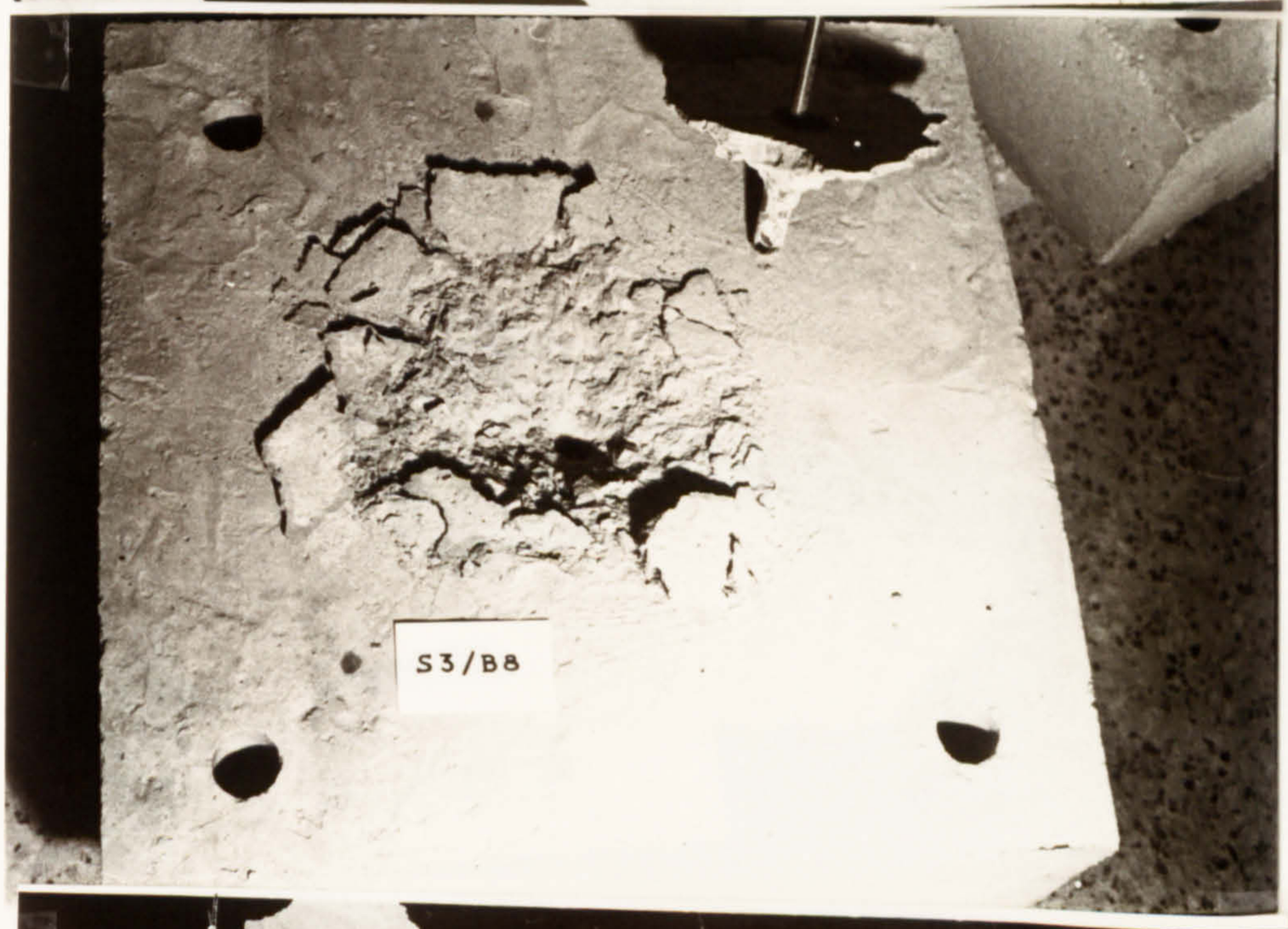

10.3

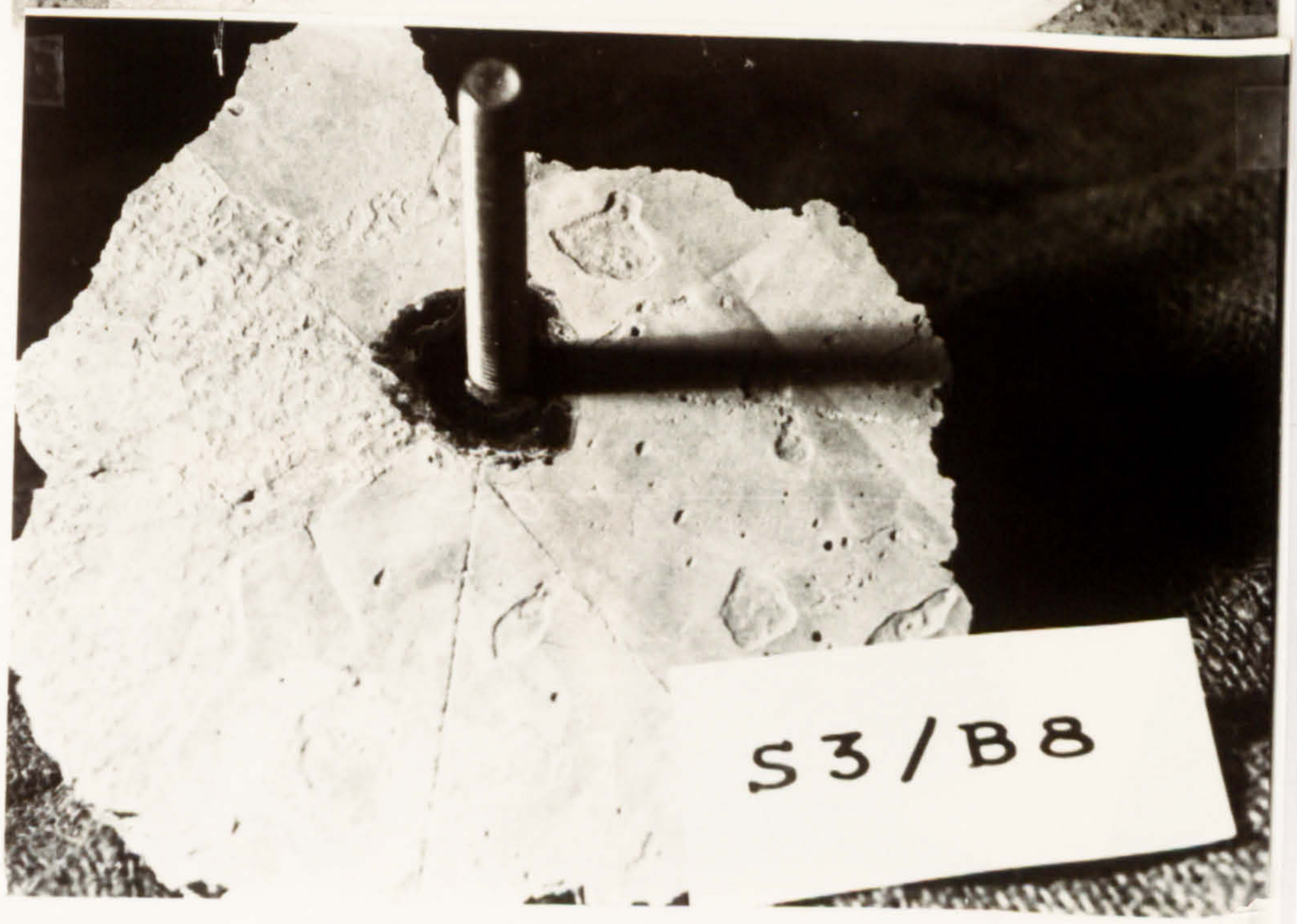

Plate 10. Typical combined mode of failure

11.1

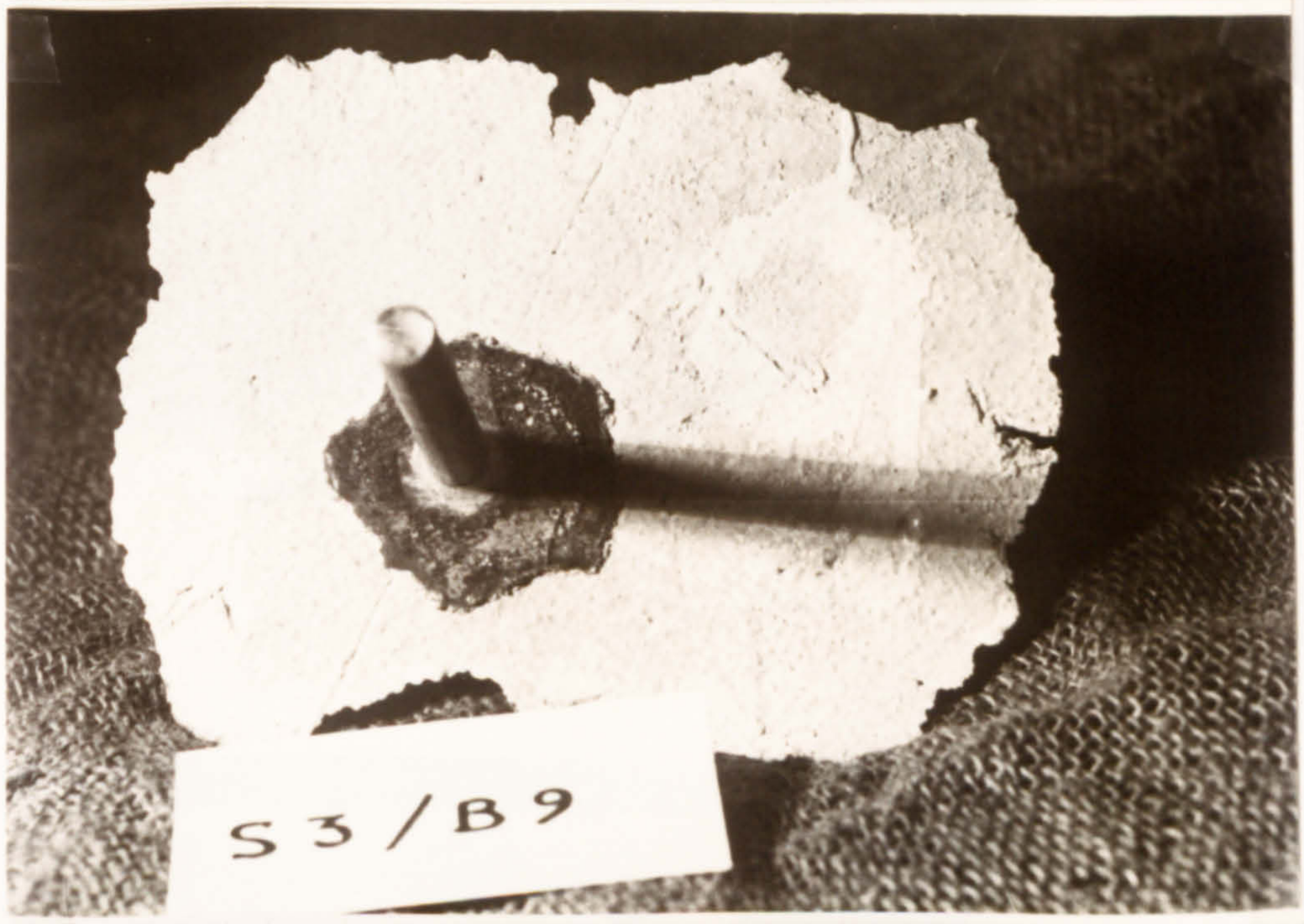

11.2

11.3

Plate 11. Typical combined mode of failure.

12.1

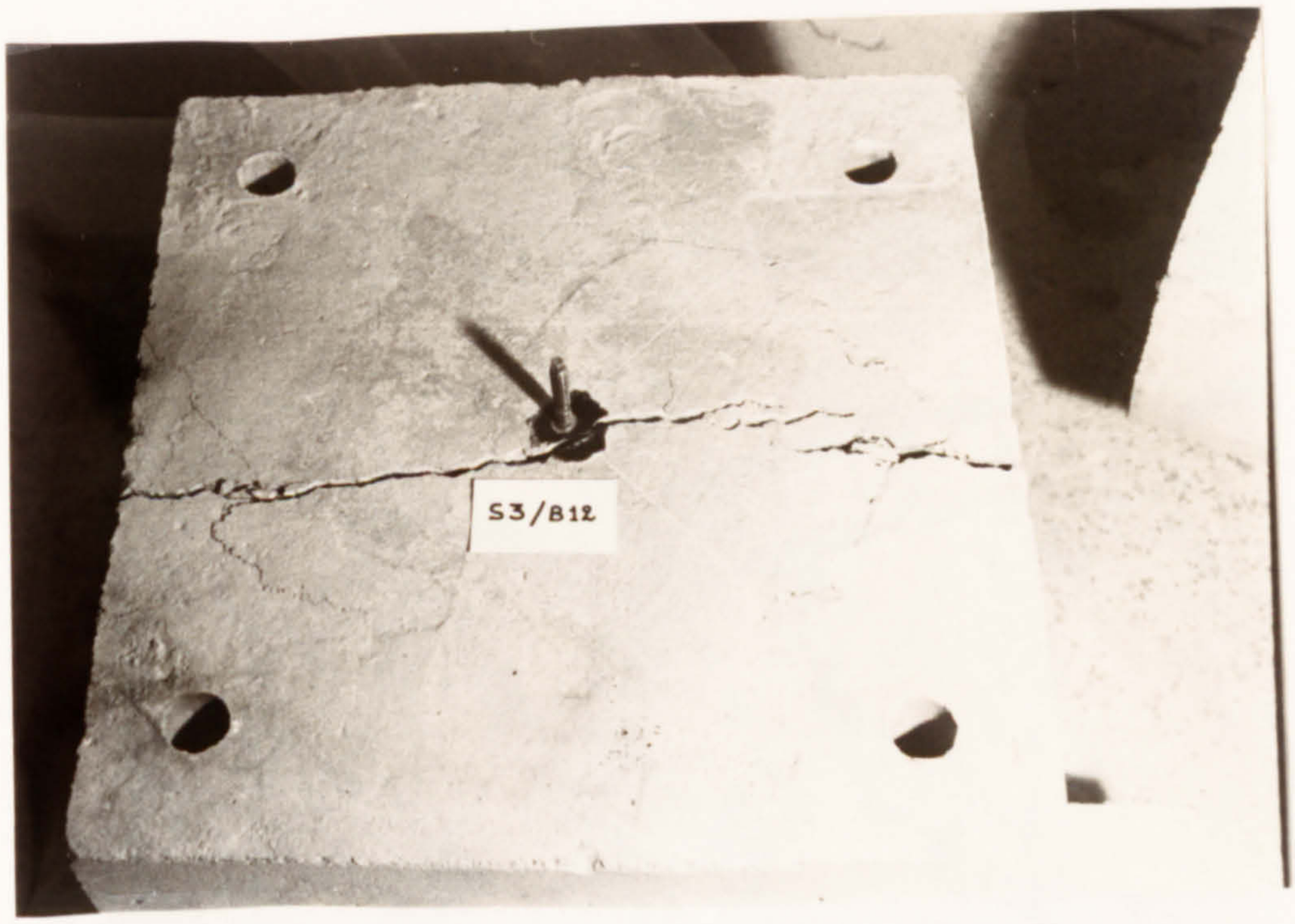

12.2

Plate 12. Split specimen.

Plate 13. Failure surface of split specimen.

Plate 14. Failure surface of split specimen. Close-up.

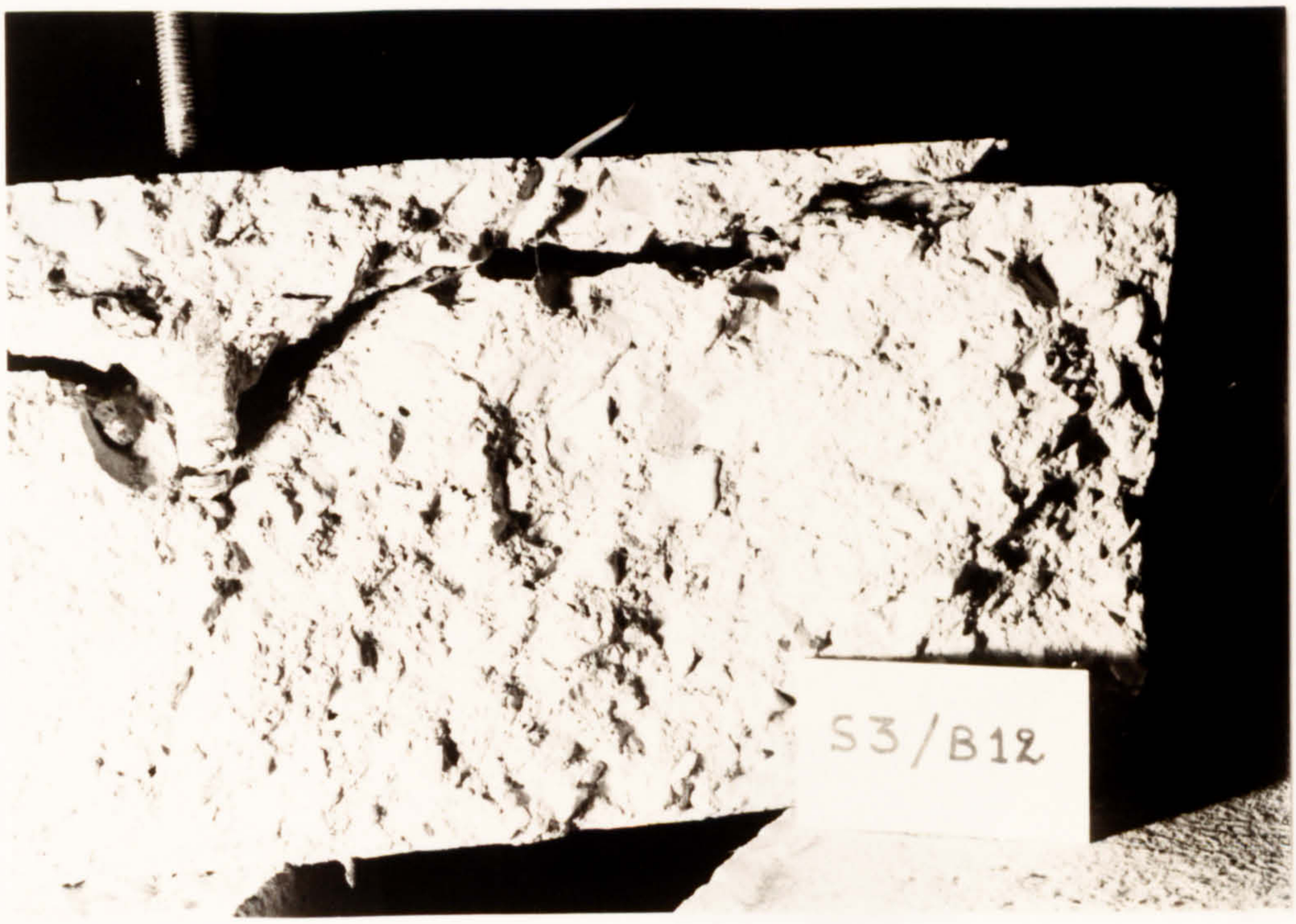

15.1

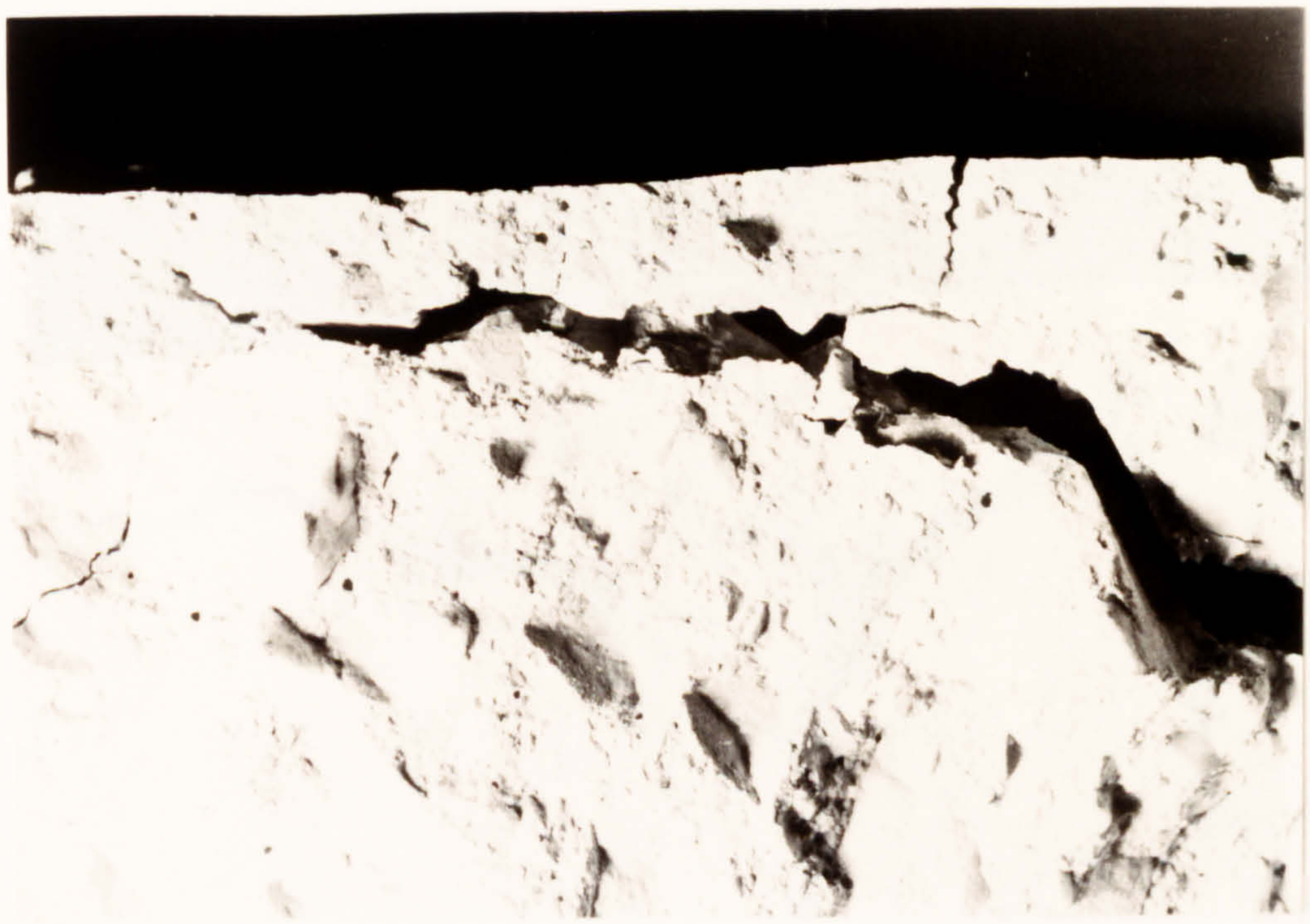

15.2

Plate 15. Details of split specimen.

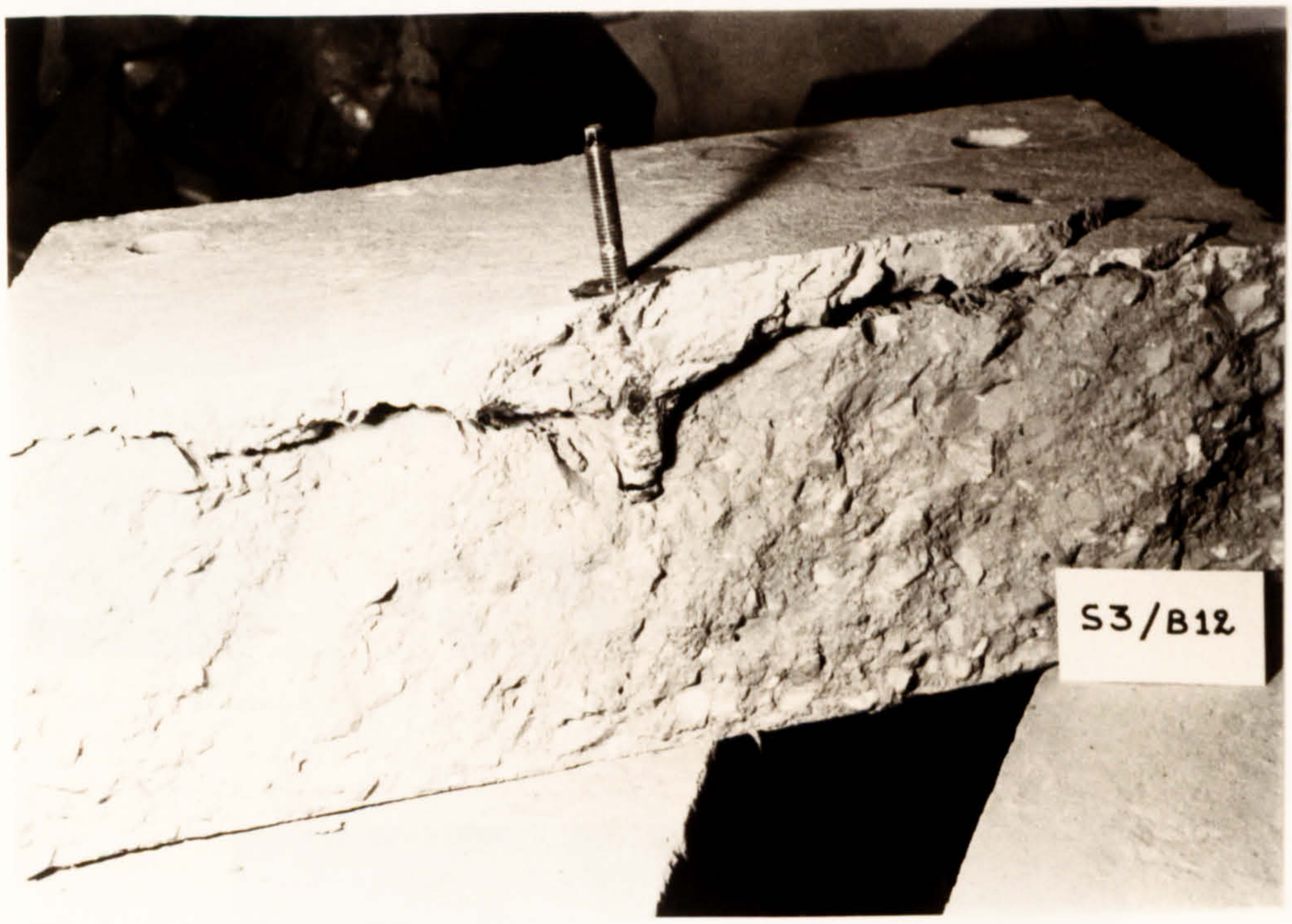

16.1

16.2

Plate 16. Details of split specimen.

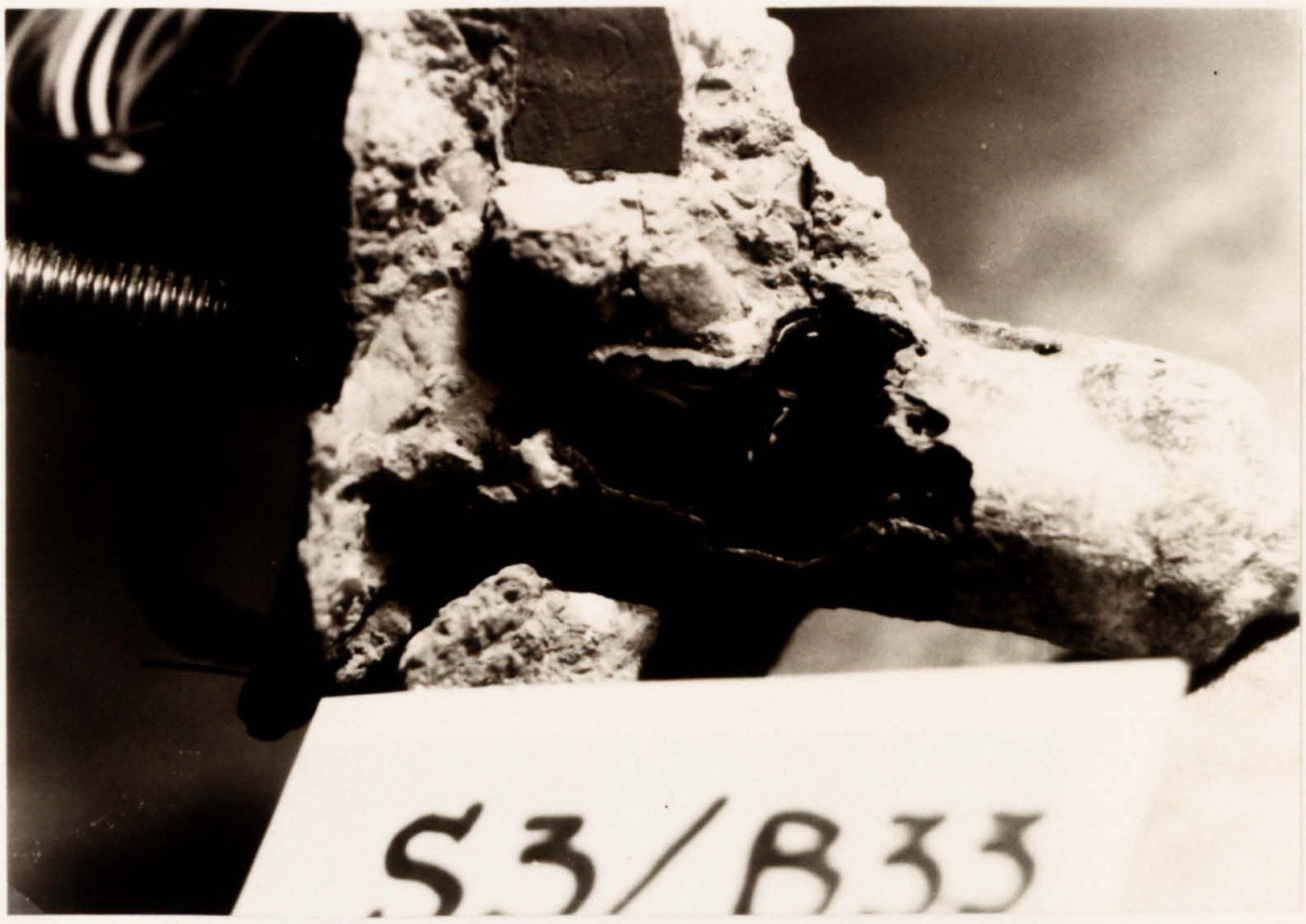

17.1

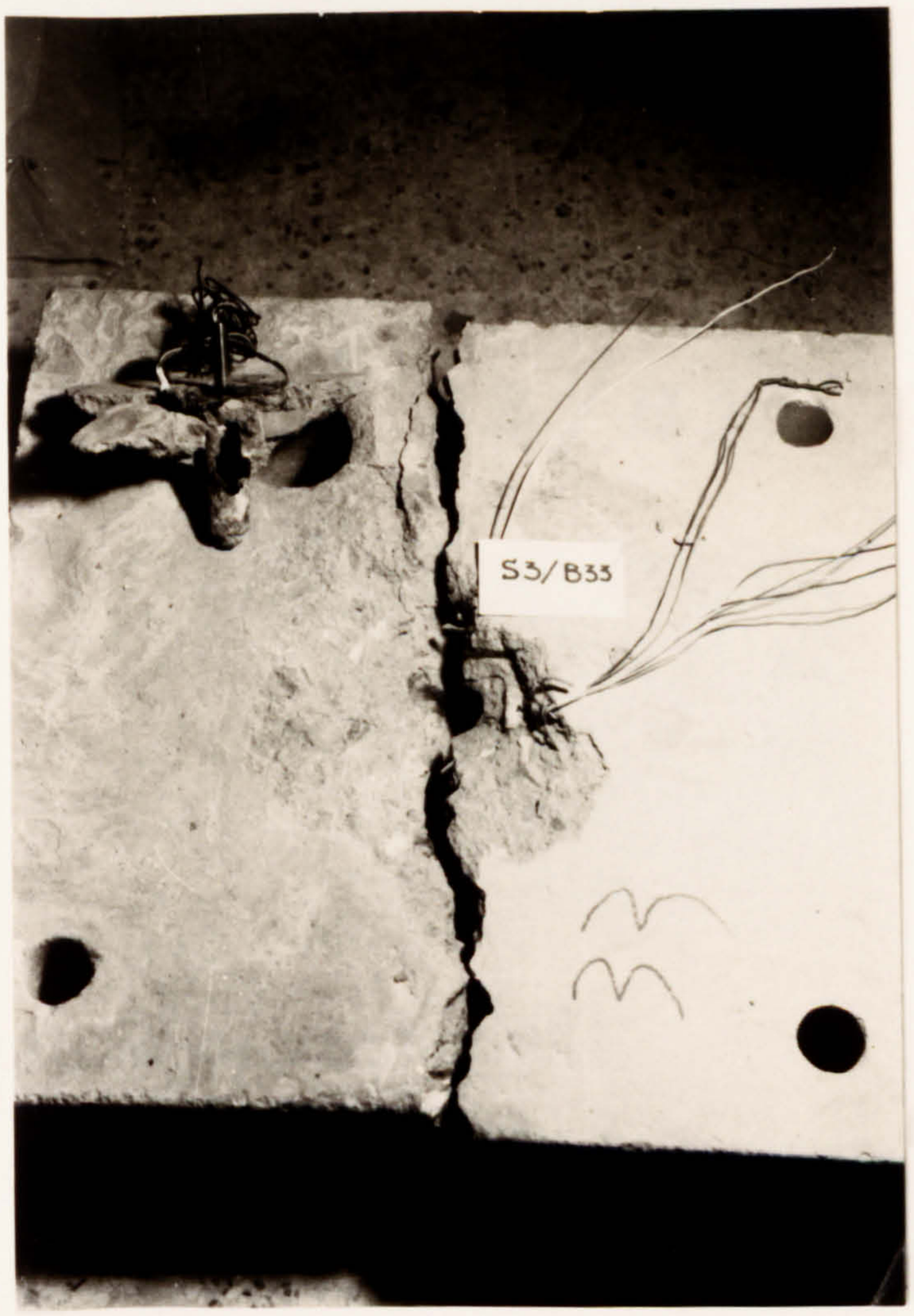

17.2

Plate 17. Split specimen.

Plate 18. Typical bond failure.

19.1

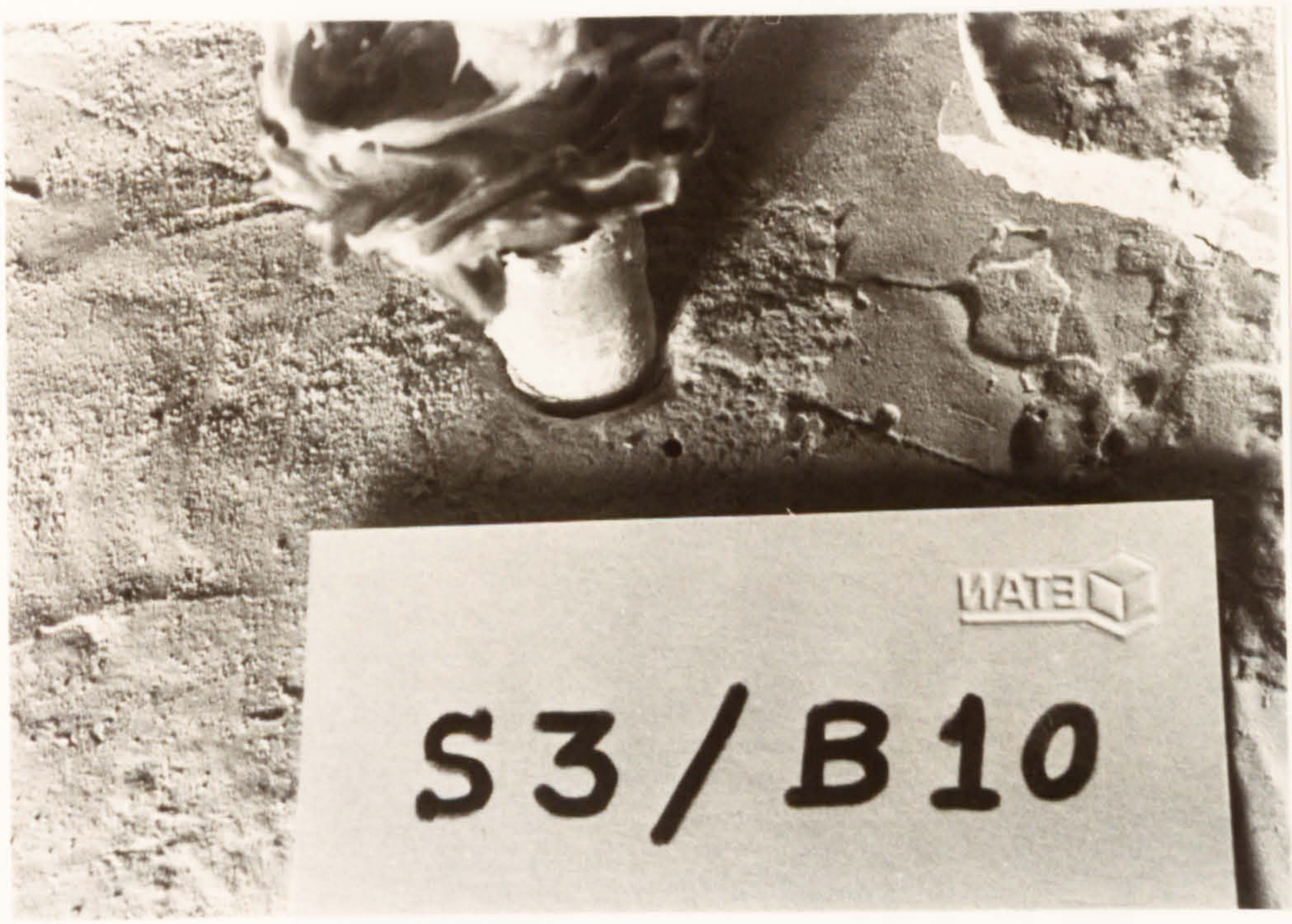

19.2

Plate 19. Typical bond failure.

20.1

20.2

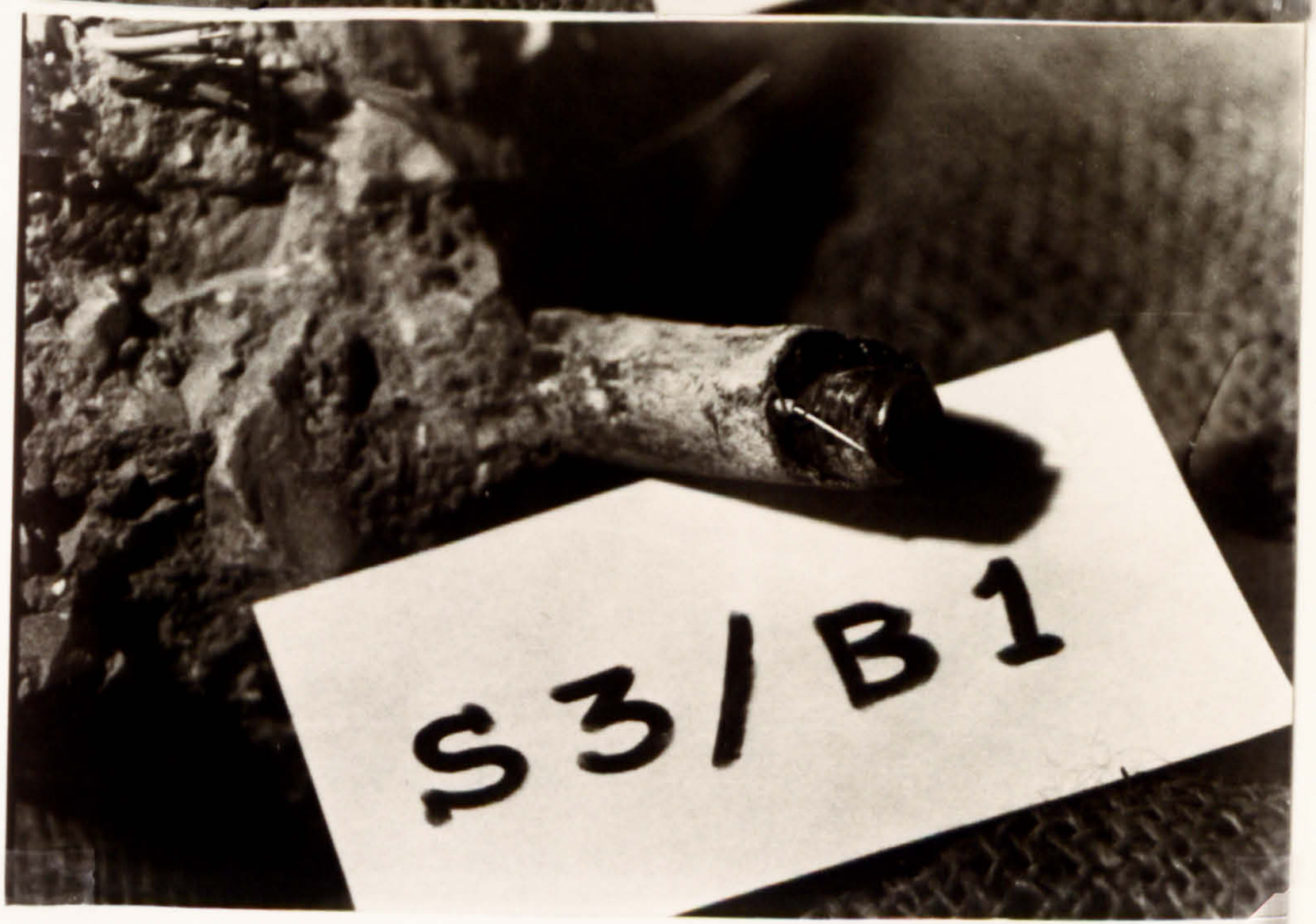

20.3

Plate 20. Typical combined mode of failure.

21.1

21.2

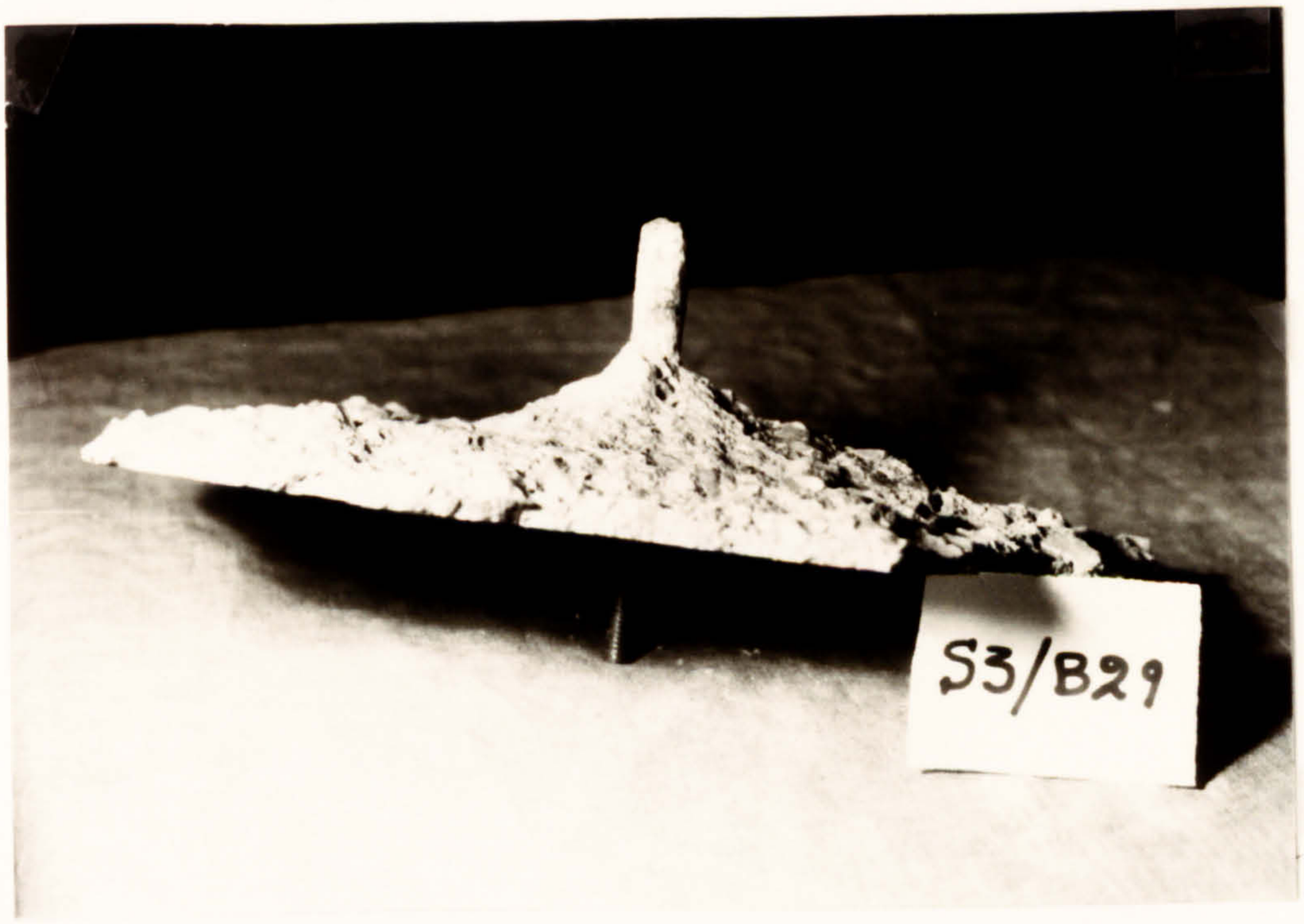

21.3

Plate 21. Double cone of concrete failure.

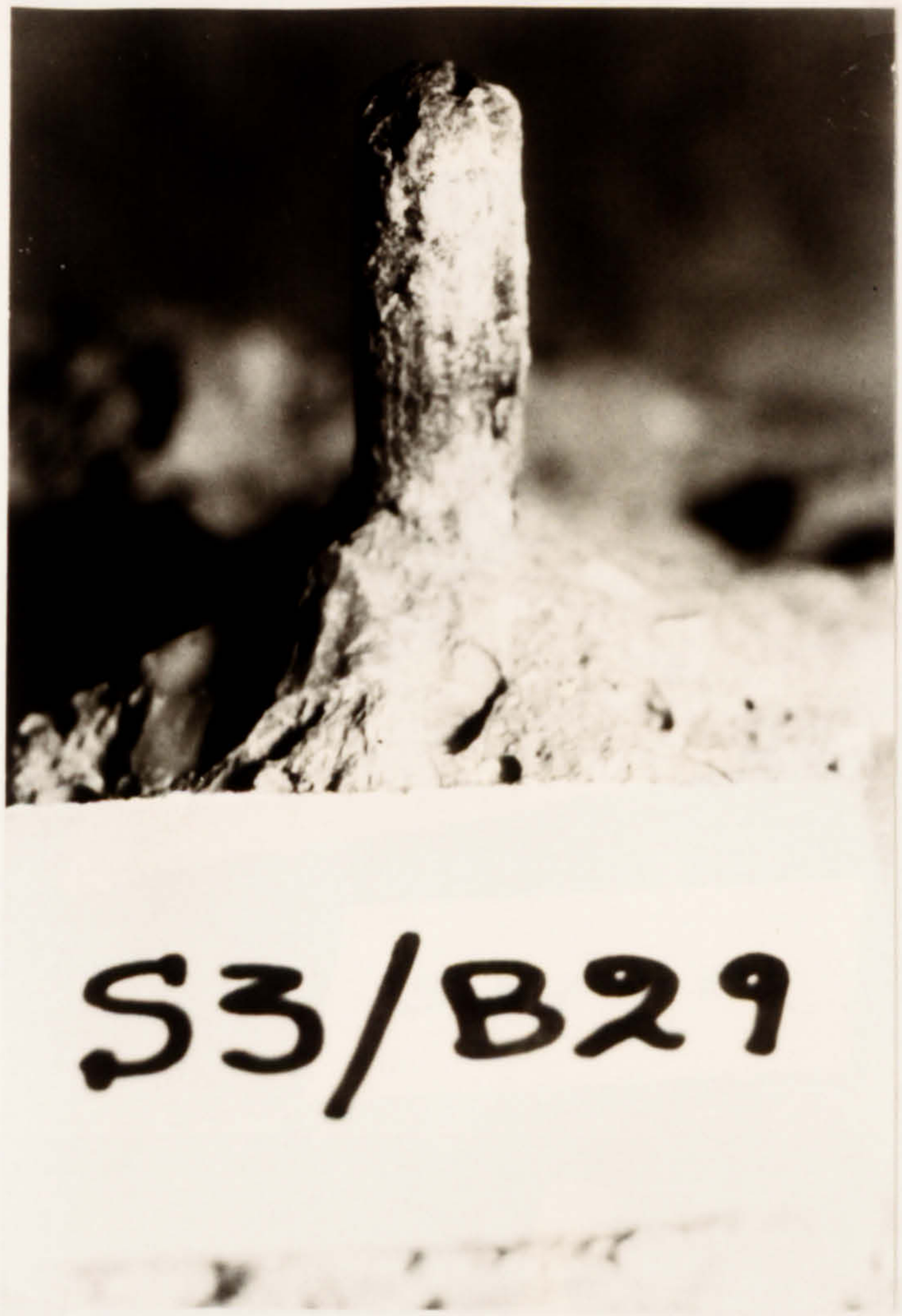

Plate 22. Detail of the double cone of failure.

23.1

23.2

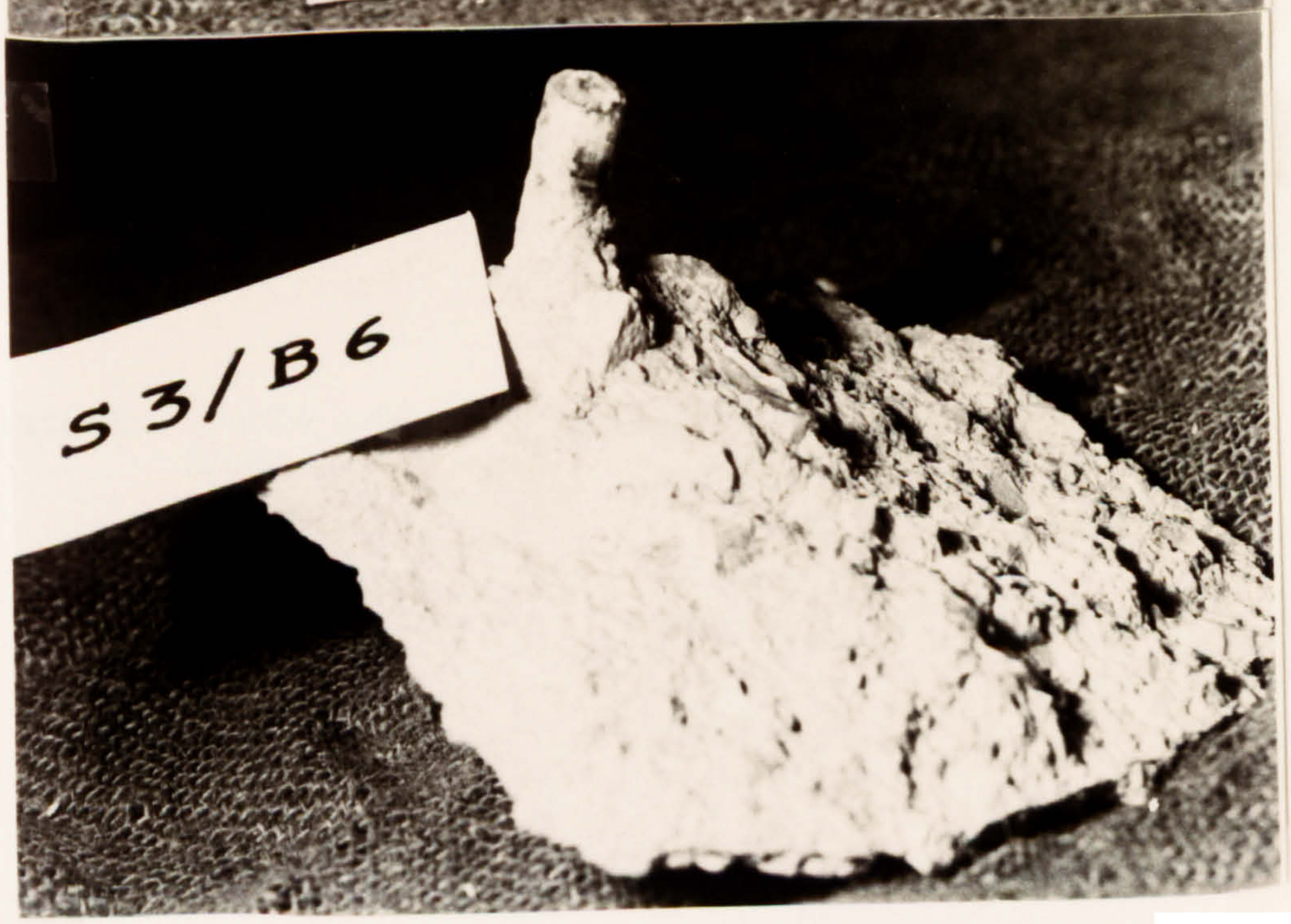

23.3

Plate 23. Double cone of concrete failure.

Plate 24. Double cone of concrete failure.
Close-up.

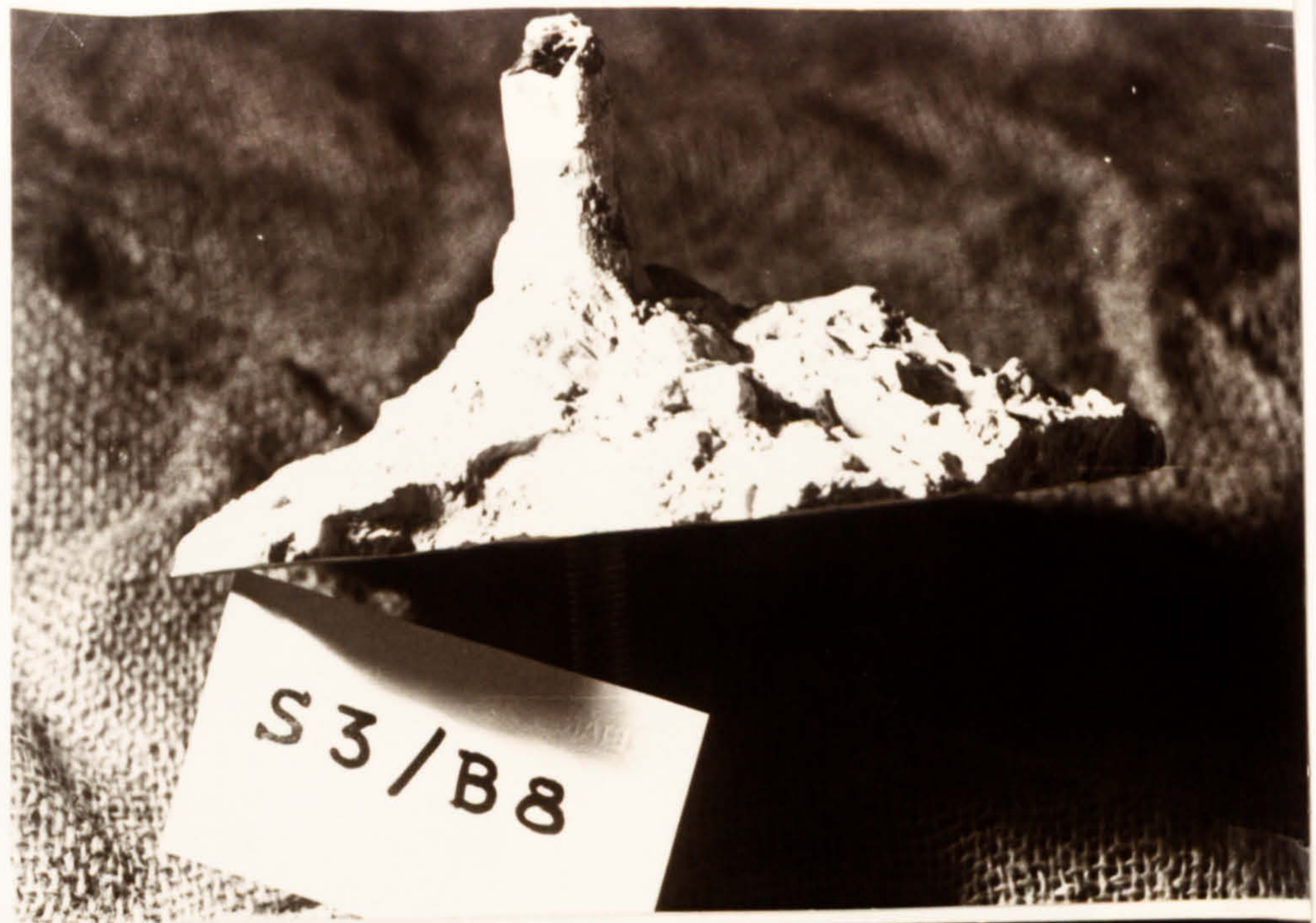

25.1

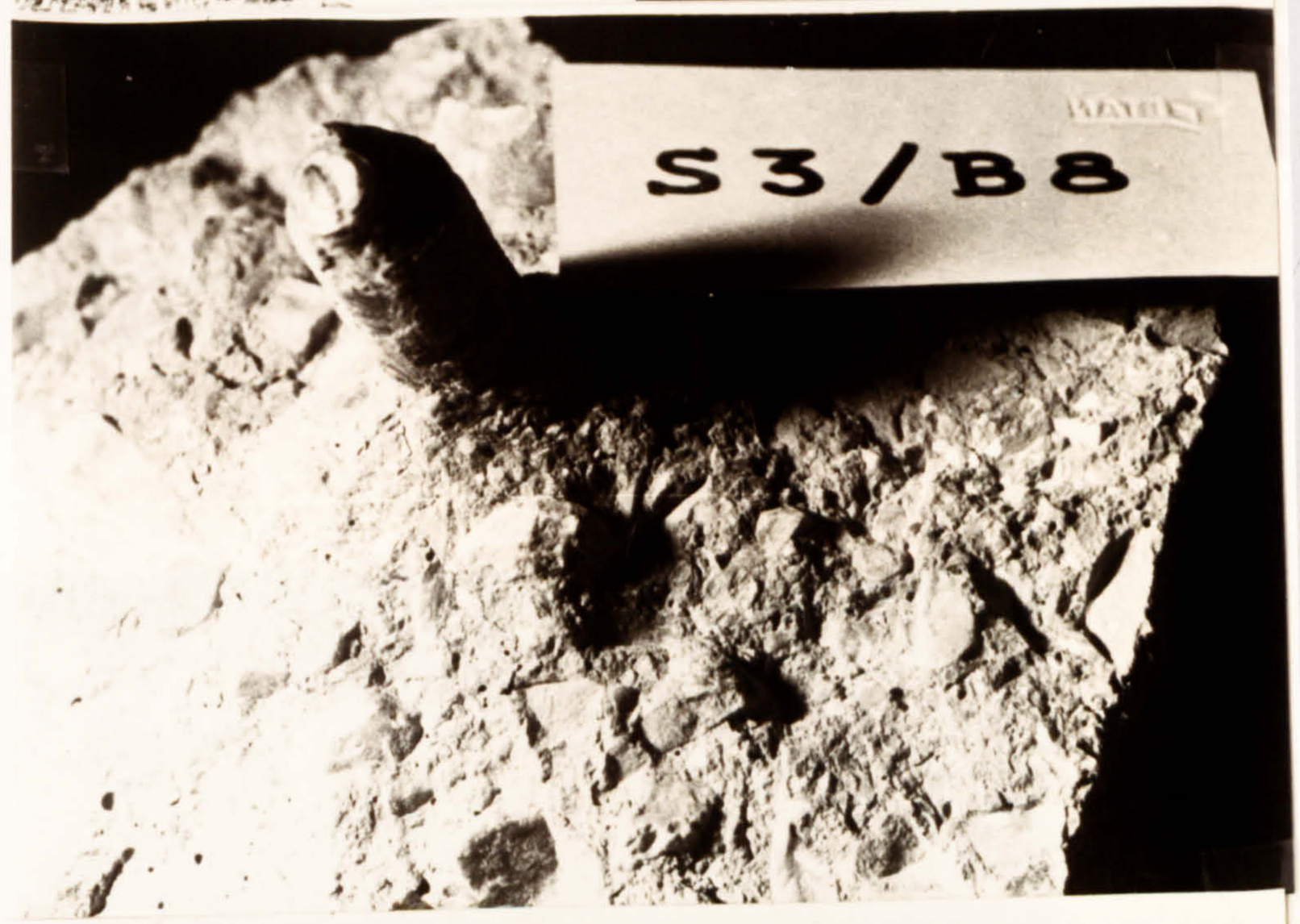

25.2

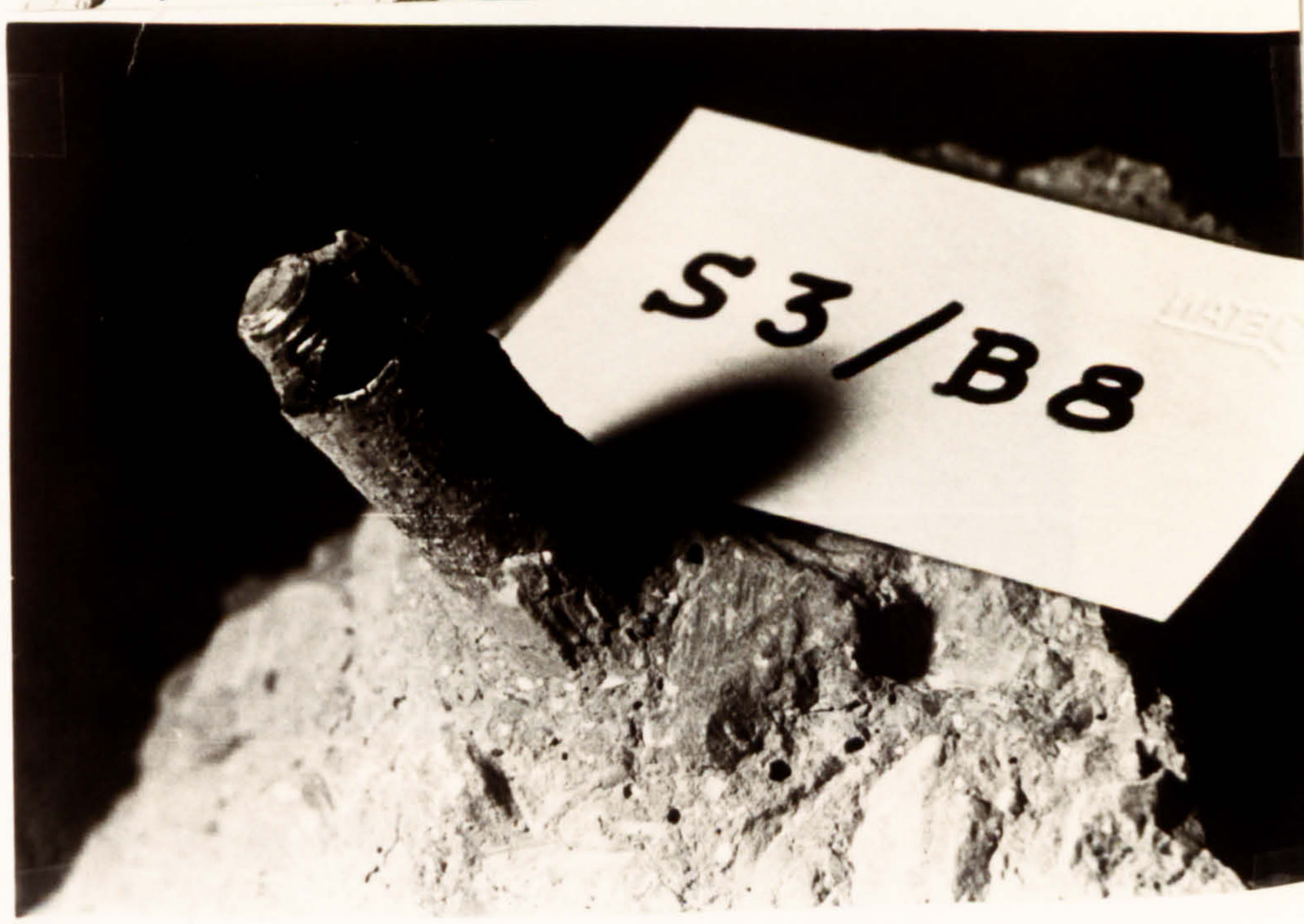

25.3

Plate 25. Concrete failure cone.

Plate 26. Resin failure at the bottom.

Plate 27. Resin failure at the bottom.

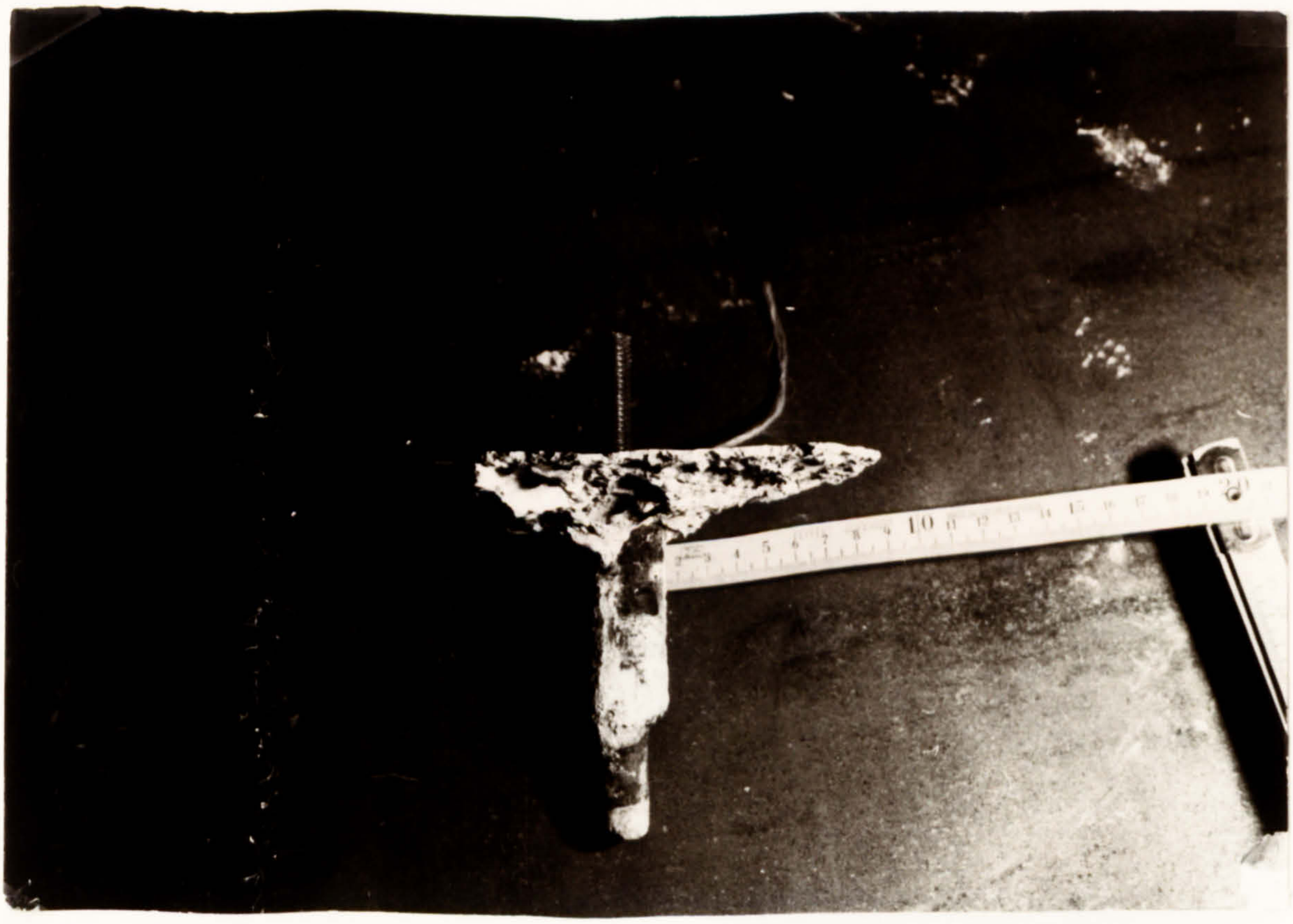

28.1

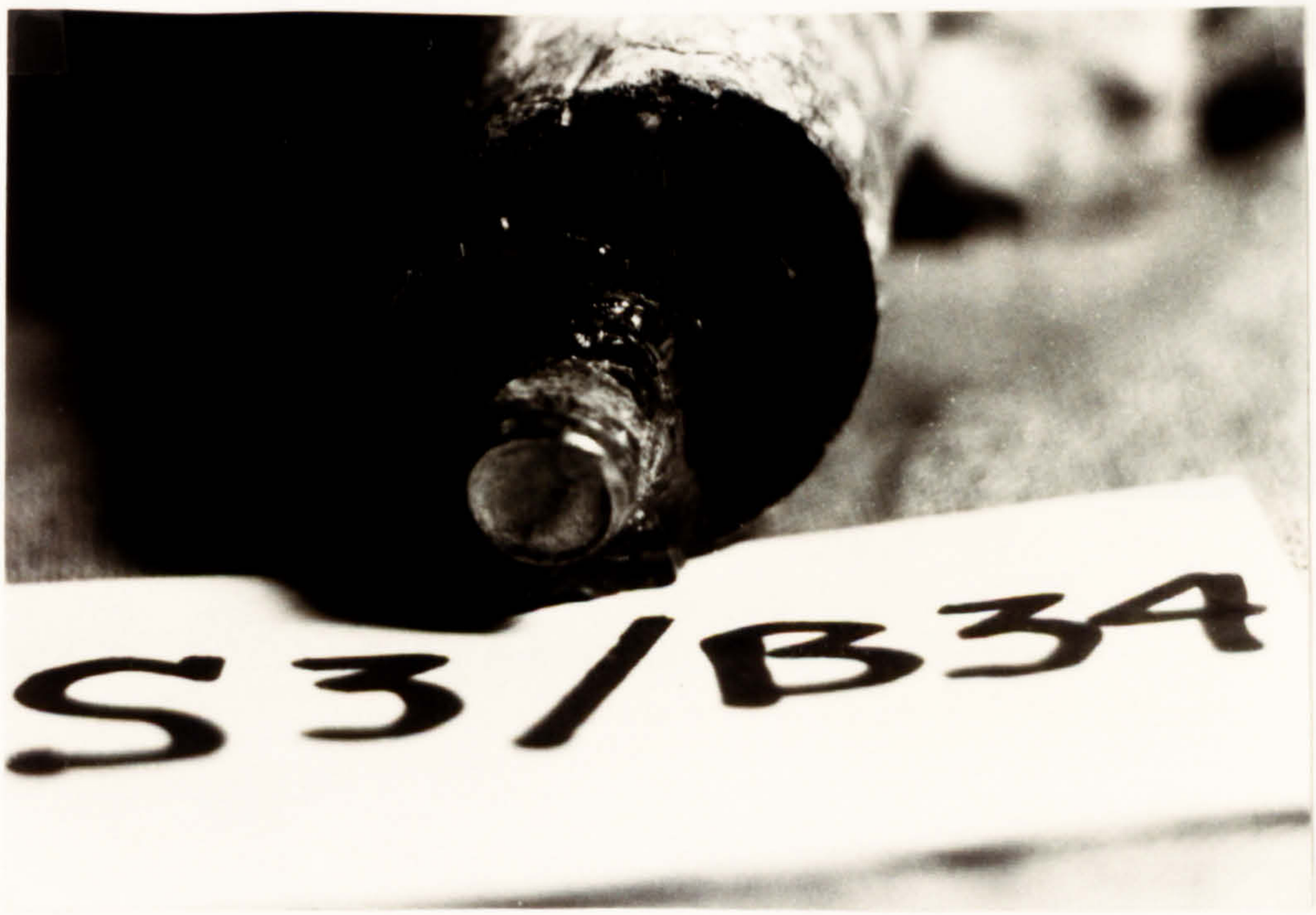

28.2

Plate 28. Detail of resin failure at the bottom.

Plate 29. Detail of the resin failure at the bottom.

Plate 30. Detail of resin failure at the bottom of split specimen.

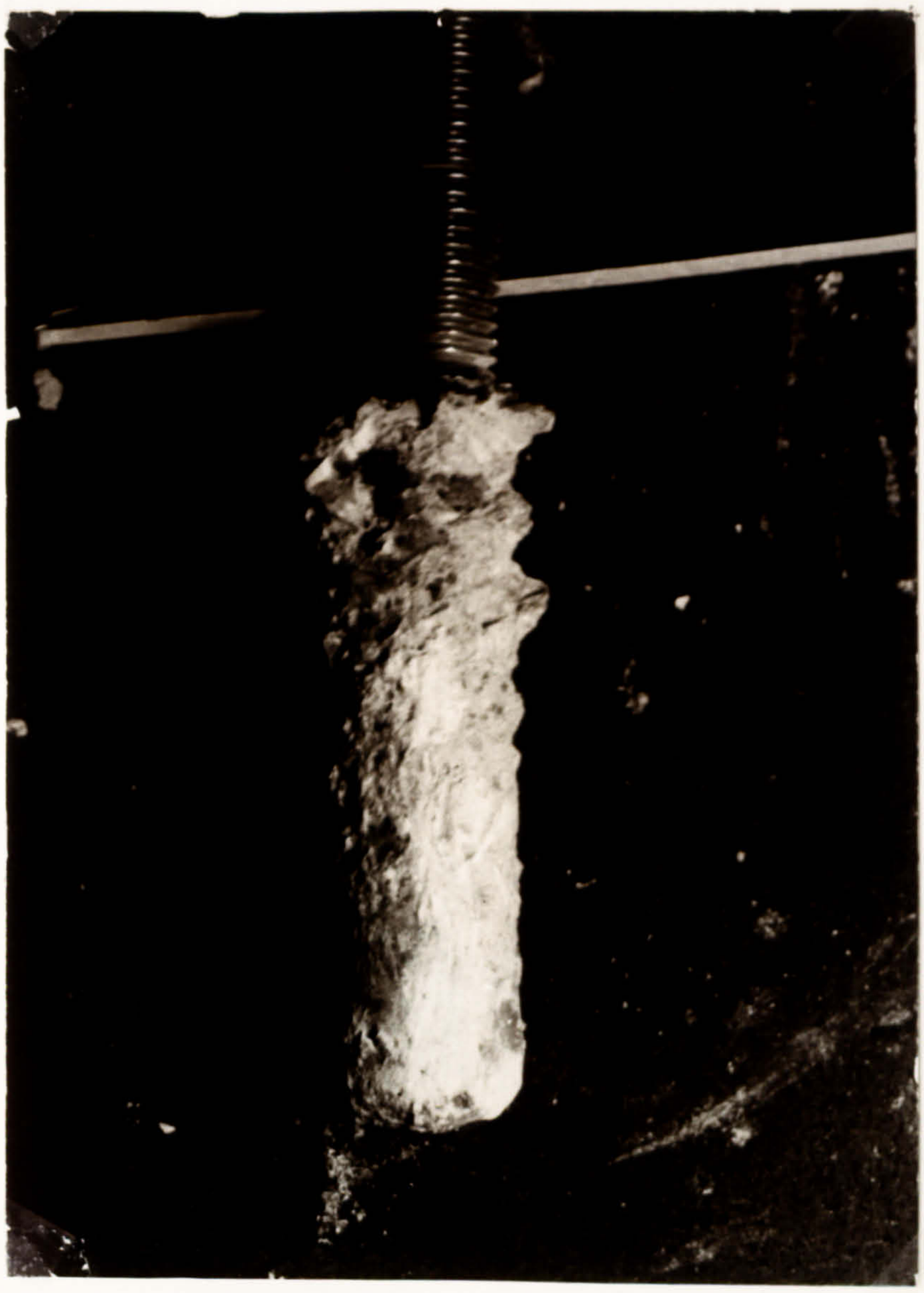

Plate 31. Detail of bond failure.

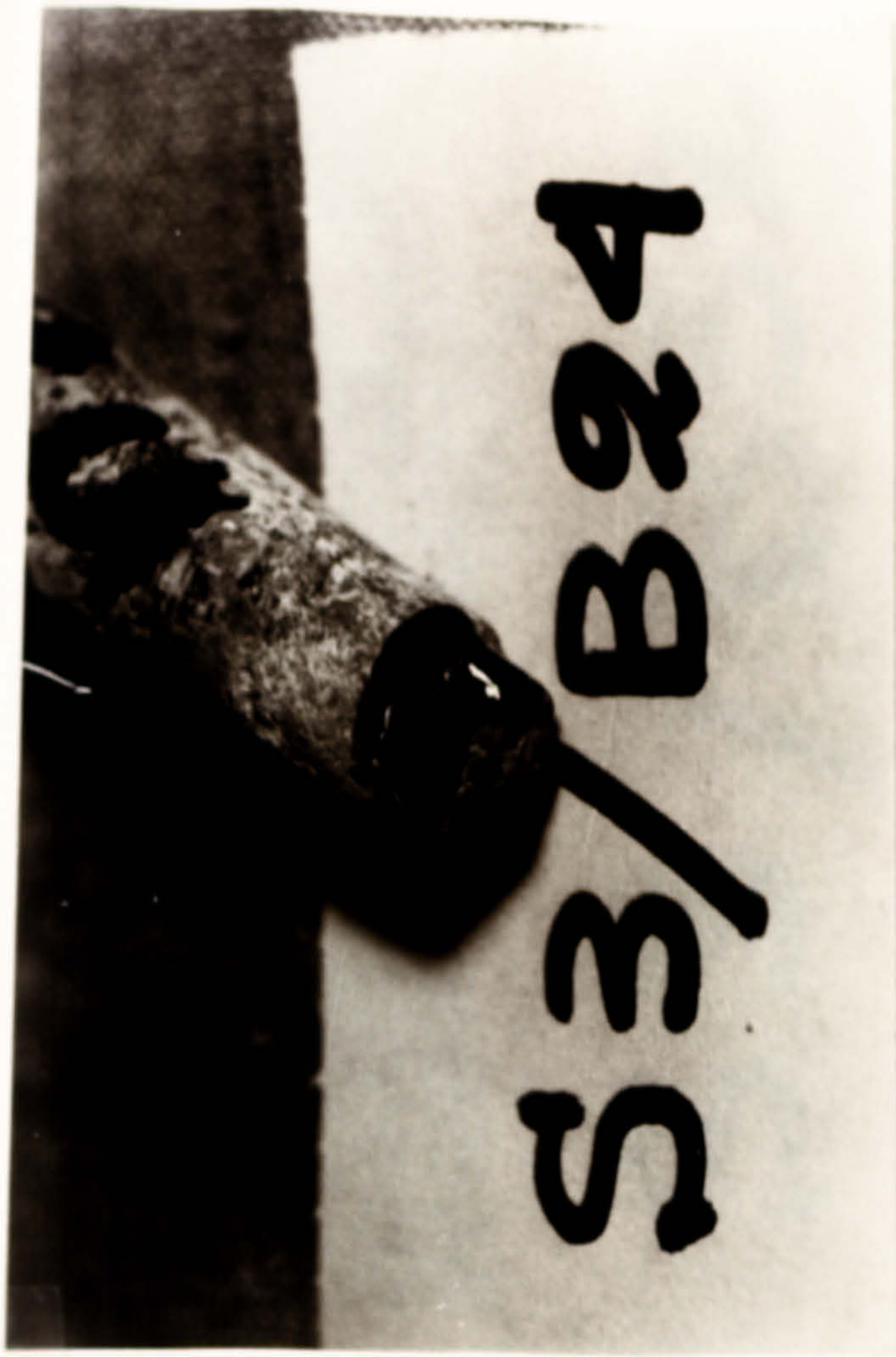

Plate 32. Resin failure of the bottom.

Plate 33. Details of the ribbed bar-resin interface.

Plate 34. Details of the ribbed bar-resin interface. Close-up.

B392

Plate 35. Failure of resin in the case of threaded anchor.

Plate 36. Detail of the threaded anchor - resin interface.

Plate 37. Details of the threaded anchor - resin interface.

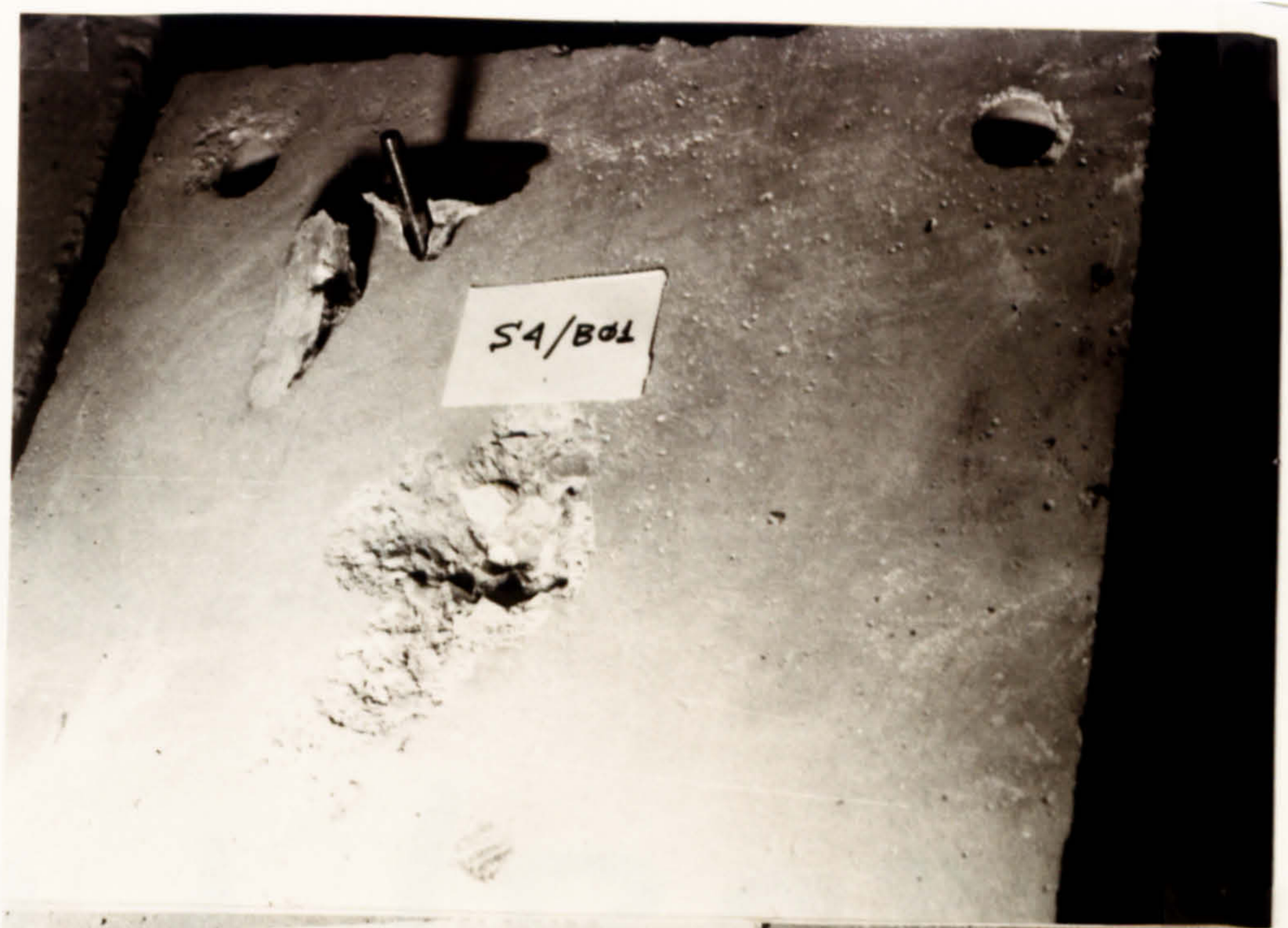

38.1

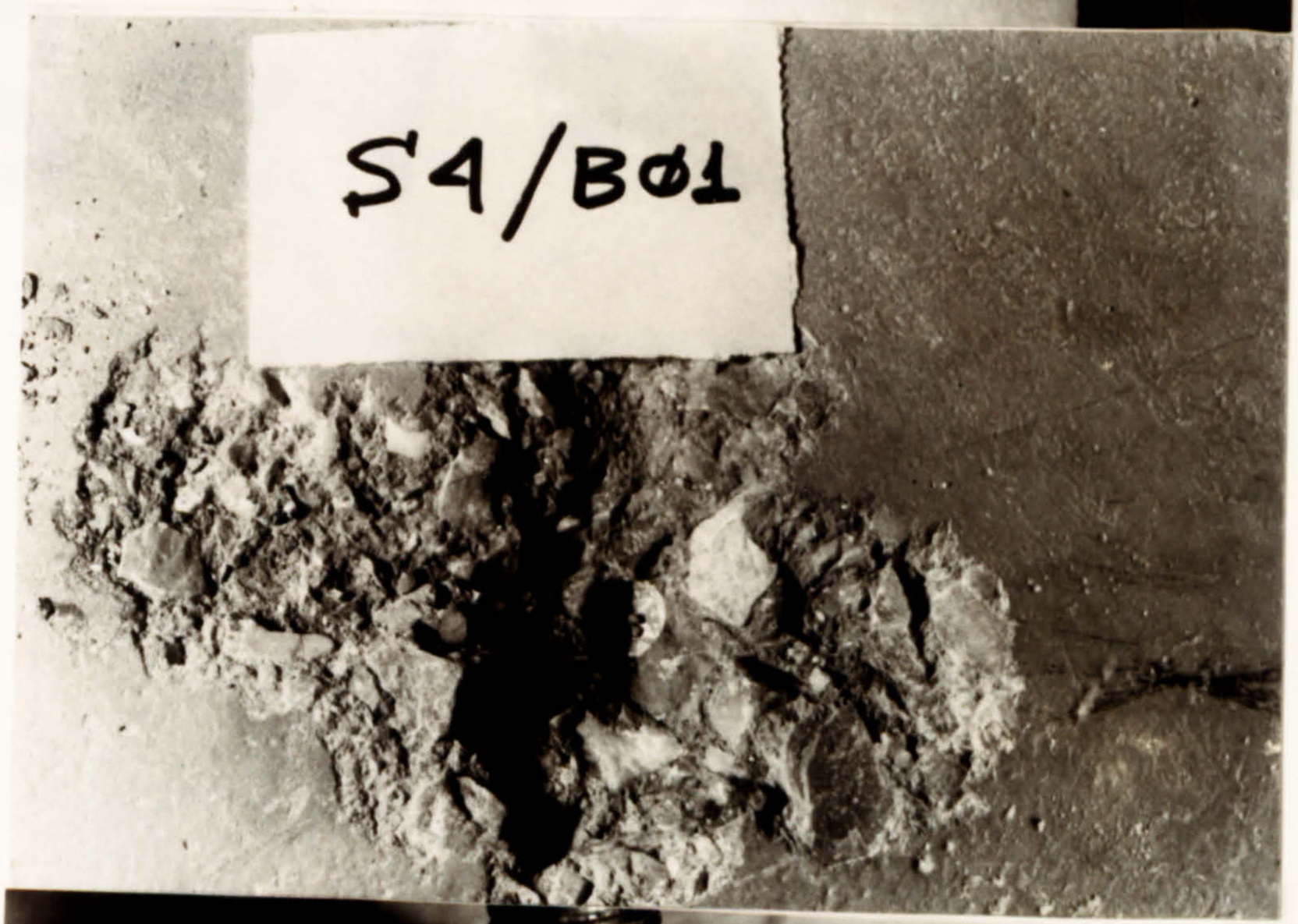

38.2

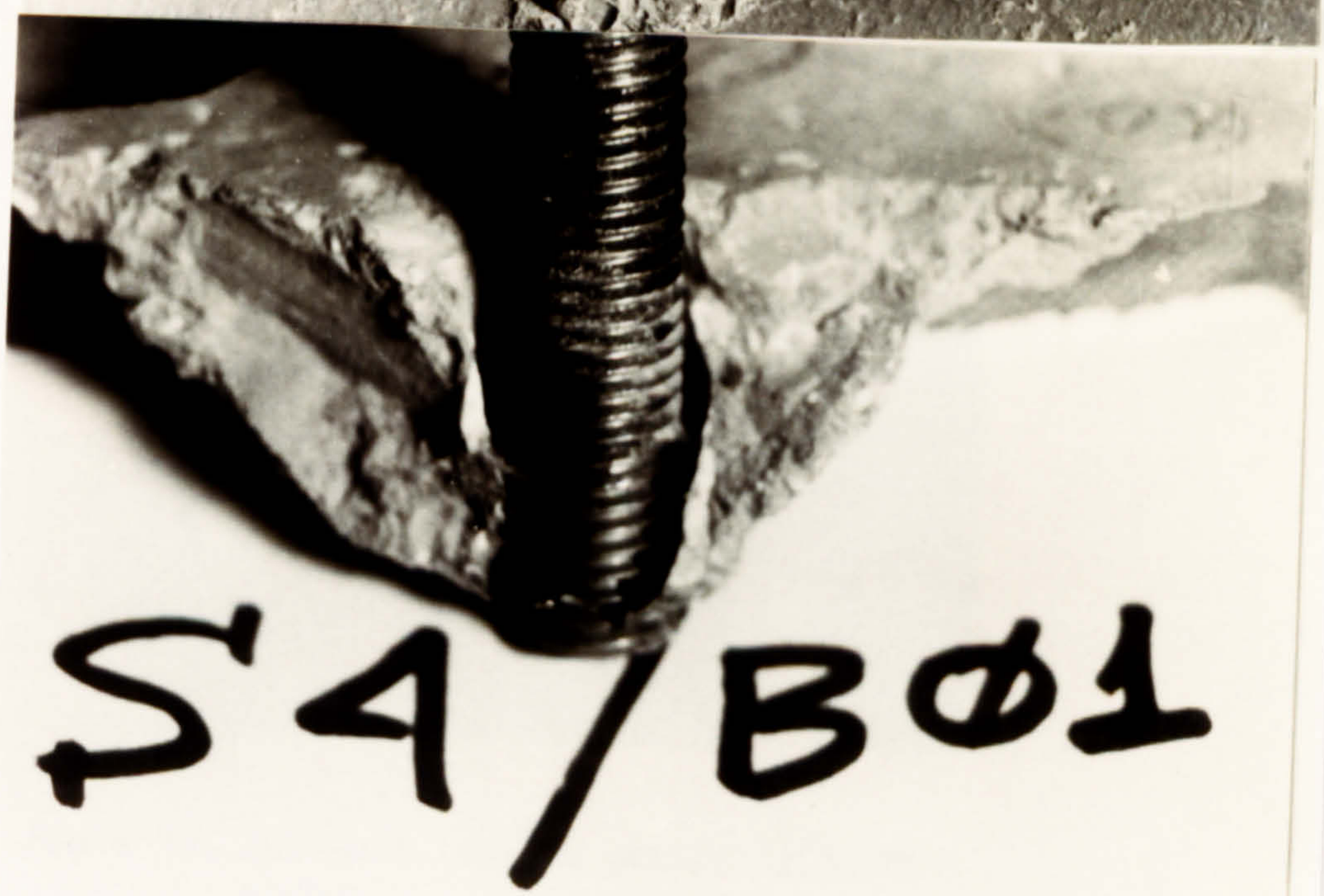

38.3

Plate 38. Pull-out test of partially bonded anchor.

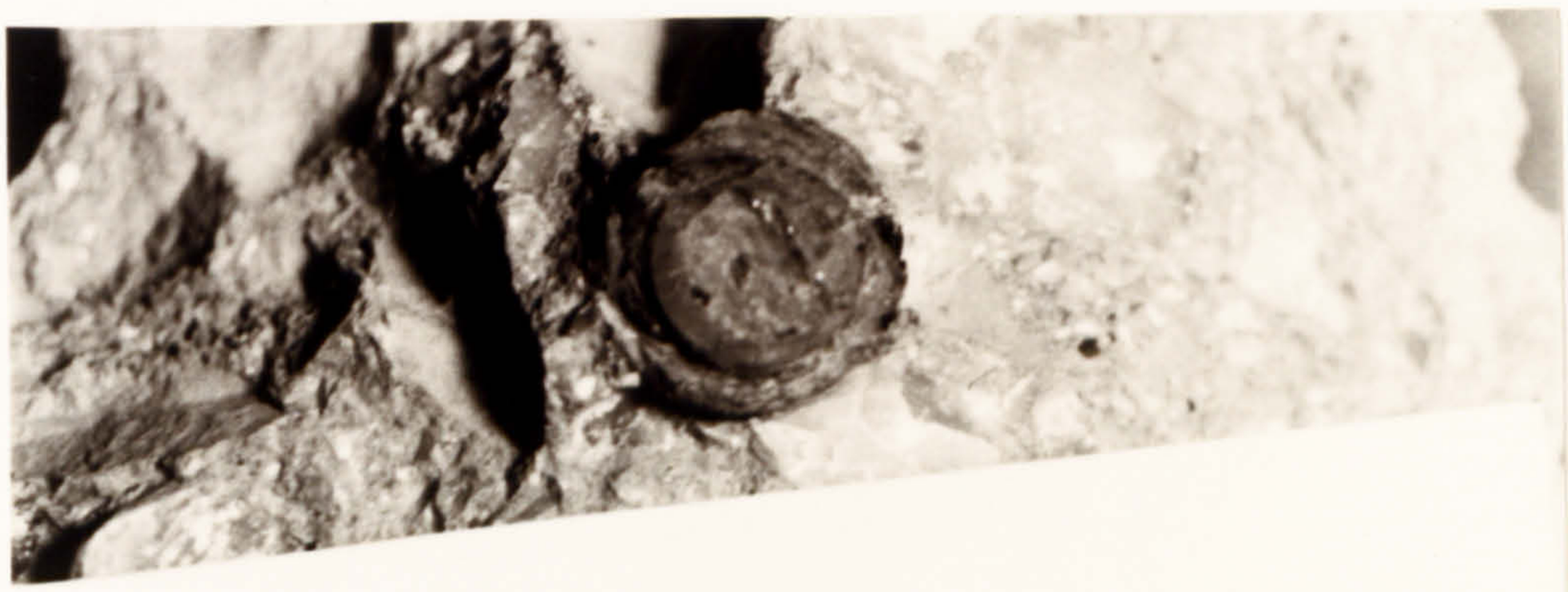

39.1 S4/B03

39.2

Plate 39. Pull-out test of partially bonded anchor.

Plate 40. Pull-out test of partially bonded anchor.

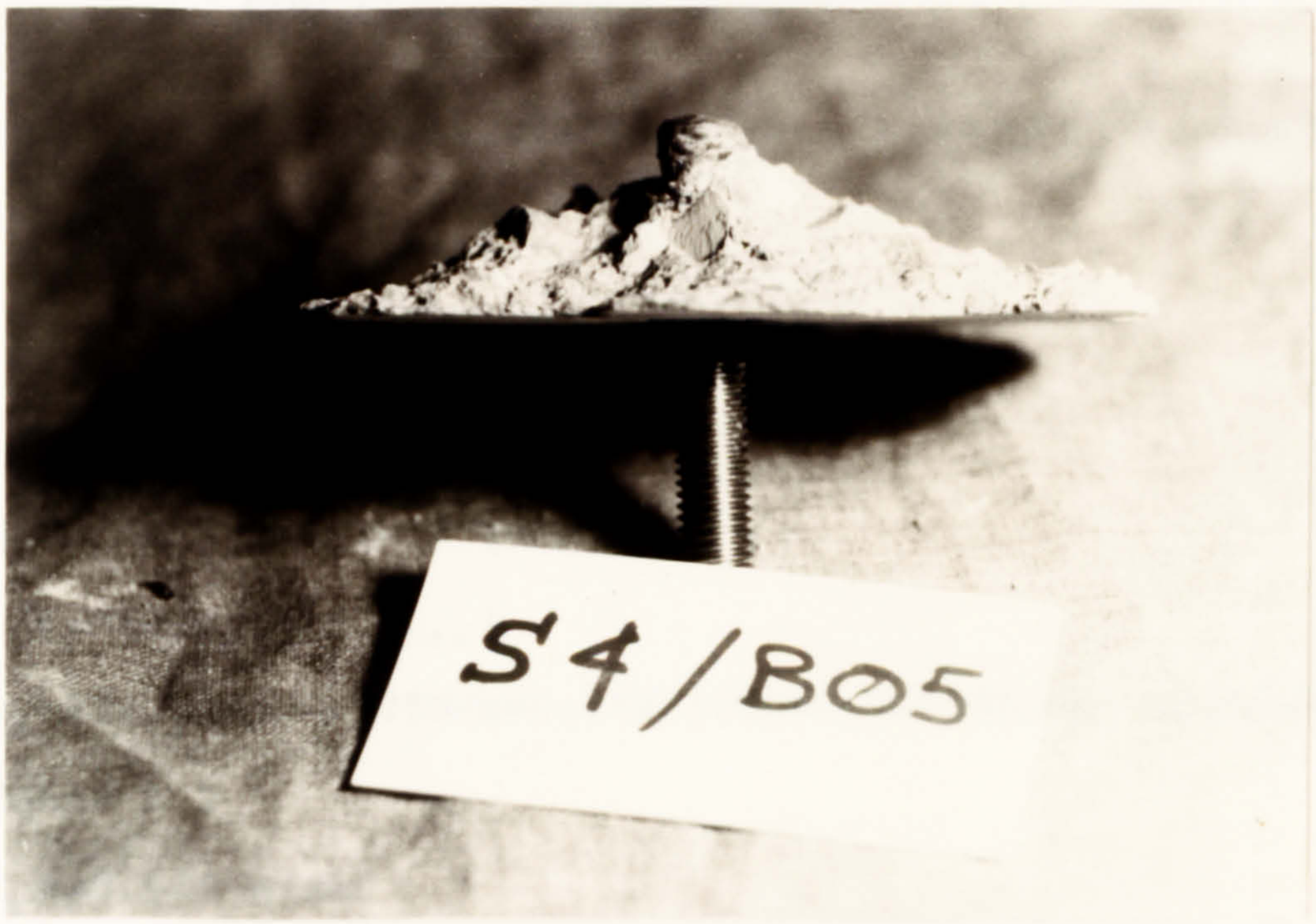

41.1

41.2

Plate 41. Pull-out test of partially bonded anchor.

APPENDIX A: CALCULATION OF ULTIMATE STRENGTH OF DIFFERENT CONCRETE - RESIN JOINTS

A.1 Ultimate tensile strength of a concrete - resin butt joint

$$\sigma_f = \frac{1+r^2/2h^2}{\sqrt{(1+(3r^2/h^2)}}\sqrt{(2E_a Q_s)}$$

$Q_s = W_a/h$, for thin joint.

$1/E_a = (1/E_c)+(1/E_{res})$

$W_a = 178.mN/m = 0.178N/m = 0.178/1000 = 0.00018N/mm$, according to Table 3.2

$E_c = 30,000\ N/mm^2$

$E_r = 3,000\ N/mm^2$

$1/E_a = (1/30,000)+(1/3,000) = 0.00037$

$E_a = 2,727\ N/mm^2$

For r=10mm, h=1mm

$$\frac{1+r^2/2h^2}{\sqrt{(1+(3r^2/2h^2))}} = \frac{1+(10)^2/2(1)^2}{\sqrt{(1+(3(10)^2/2(1.0)^2)}} = \frac{1+100/2}{\sqrt{[1+(3(100/2))]}}$$

$$= \frac{51}{\sqrt{(151)}} = 4.15$$

$Q_s = 0.00018Nmm/1.0mm = 0.00018N/mm^2$

$\beta.\sigma_f = 4.15\sqrt{(2(2727)(0.00018))} = 9.19N/mm^2$

and for $\varepsilon = 0.02$

$\beta = 1+(8/\pi)(r/h)(\varepsilon/(1+\varepsilon)^2) =$

$= 1+[(8/3.14)(10/1)(0.02/(1+0.02)^2)] = 1.489$

or

$\sigma_f = 6.17\ N/mm^2$

A.2 Ultimate shear strength of a concrete-resin single lap joint

$D_a = D_{res} = E_{res}/2(1+\nu_r) = 3{,}000/2(1+0.3) = 1154\ N/mm^2$

$E_2 = E_c = 30{,}000\ N/mm^2$, $2c = 60mm$, $t_2 = 60mm$, $t_a = 2mm$

$$\delta^2 = \frac{2(c)^2 D_a}{E_2 t_2 t_a} = \frac{2(30)^2(1154)}{(30{,}000)(60)(2)} = 0.5770$$

$$\varepsilon^2 = \frac{E_1 t_1 + E_2 t_2}{2E_1 t_1} = \frac{2E_1 t_1}{2E_1 t_1} = 1.0$$

$\delta = \sqrt{(0.5770)} = 0.76 \qquad \varepsilon = 1.0$

$\sinh(2\varepsilon\delta) = 2.176$

$\cosh(2\varepsilon\delta) = 2.395$

$\beta = (0.76/1.0)[(2(1)^2 - 1 + \cosh(2\varepsilon\delta)]/\sinh(2\varepsilon\delta)] =$

$= 0.76[(1+2.395)/2.176] = 1.186$

for $\alpha = 0.005$ mm:

$\tau_f = (1/1.186)\sqrt{[E_a W_a/\pi(1+\nu_a)\alpha]} =$

$= 0{,}843\sqrt{[(3{,}000 N/mm^2)(0.18 mN/m)]/\pi(1+0.3)(0.005)mm} =$

$= 0.843\sqrt{(28.07)} = (0.843)(5.30) N/mm^2 = 4.46\ N/mm^2$

In general:

$$\tau_f = (1/1.186)\ \frac{\sqrt{(E_a)(W_a)}}{(\pi(1+\nu_a))}\ \frac{1}{\sqrt{(\alpha)}} = 0.843\sqrt{(0.140/\sqrt{(\alpha)}} =$$

$$= 0.316/\sqrt{(\alpha)}$$

and thus:

$\alpha = 0.01$	mm	$\tau_f = 3.16\ N/mm^2$
$\alpha = 0.1$	mm	$\tau_f = 1.0\ N/mm^2$
$\alpha = 0.5$	mm	$\tau_f = 0.45\ N/mm^2$
$\alpha = 1.0$	mm	$\tau_f = 0.32\ N/mm^2$
$\alpha = 2.0$	mm	$\tau_f = 0.22\ N/mm^2$
$\alpha = 3.0$	mm	$\tau_f = 0.18\ N/mm^2$
$\alpha = 4.0$	mm	$\tau_f = 0.16\ N/mm^2$

A.3 Strength of a concrete-resin double shear joint

$\xi = E_2/E_1 = 30{,}000/3{,}000 = 10$, D = 40mm

$$\varphi_{12} = 1 + (E_2/2)\left(\frac{1+\nu_1}{E_1} - \frac{1+\nu_2}{E_2}\right) = 1 + (30{,}000/2)\left(\frac{1+0.3}{3{,}000} - \frac{1+0.3}{30{,}000}\right)$$

$$= 1 + 15.000(0.00043 - 0.00004) = 6.85$$

$$\rho_{12} = (\xi+1)/(\varphi_{12}+1) = (10+1)/(6.85+1) = 1.40$$

$$(2\rho_{12}-1)/\rho_{12}^2 = (2(1.4)-1)/(1.4)^2 = 0.92$$

$$G = (K^2/2)[(1/E_1) + (1/E_2)[(2\rho_{12}-1)/(\rho_{12}^2)]$$

$$= (K^2/2)(1/3{,}000 + 1/30{,}000)(0.92) =$$

$$= K^2[0.5(0.00033 + 0.000033)]0.92 = (0.00017)K^2$$

for G = 0.000180 N/mm² (See A.1):

$$K_{II}^2 = K^2 = 0.000180/0.00017 = 1.124$$

$$K = 1.06$$

$$Q = Q_h\sqrt{(E_a/E_s)}$$

$$Q_h \approx (\alpha/D)[0.0325 + 14.63(\alpha/D) - 46.07(\alpha/D)^2 + 61.03(\alpha/D)^3]$$

$$Q = Q_h(\sqrt{(E_a/E_s)})$$

$$\tau_f = \frac{K_{II}}{Q\sqrt{a}} = \frac{1.06}{Q\sqrt{a}}$$, according to Eq. (3.26)

a [mm]	a/D	constant	14.63(a/D)	-46.07(a/D)²	61.03(a/D)³	Q_h	$Q=Q_h\sqrt{(E_a/E_s)}$	$Q\sqrt{a}$	τ_f (MPa)
0.5	0.0125	0.0325	0.182	-0.007	0.000	0.207	0.065	0.046	23.04
1.0	0.0250	0.0325	0.365	-0.029	0.001	0.369	0.117	0.117	9.05
2.0	0.0500	0.0325	0.731	-0.115	0.001	0.649	1.205	0.220	4.82
3.0	0.0750	0.0325	1.097	-0.259	0.026	0.896	0.283	0.490	2.16
4.0	0.1000	0.0325	1.463	-0.460	0.061	1.096	0.346	0.692	1.53
5.0	0.1250	0.0325	1.823	-0.719	0.119	1.255	0.397	0.887	1.20

A.4 Calculation of stress and strain of each component, according to theoretical analysis (Chapter 5) at P=10 kN

$d = 12$ mm $\quad E_r = 3{,}000$ N/mm^2 $\quad A_{s,max} = 113$ mm^2

$t = 2$ mm $\quad E_c = 30{,}000$ N/mm^2 $\quad A_{s,min} = 75.39$ mm^2

$l = 100$ mm $\quad E_s = 210{,}000$ N/mm^2 $\quad A_{sm} = 93.26$ mm^2

$$Ga = \frac{E_r}{2(1+\nu)} = 1154 \text{ N/mm}^2 \qquad A_c = (600)(600) = 360{,}000 \text{ mm}^2$$

$$A_r = \pi/4(16^2 - 12^2) = 95.2 \text{ mm}^2$$

$A_{snetto} = 65$ mm^2, see Appendix C

$$\lambda_s = (E_s)\ A_s = (210{,}000 \text{ N/mm}^2)(65 \text{ mm}^2) = (1.37)10^7 \text{ N}$$
$$\lambda_c = (E_c)\ A_c = (30{,}000 \text{ N/mm}^2)(360{,}000 \text{ mm}^2) = (1.08)10^{10} \text{ N}$$
$$\lambda_r = (E_r)\ A_r = (3{,}000 \text{ N/mm}^2)(95.2 \text{ mm}^2) = (2.86)10^5 \text{ N}$$

Fig. 7.93. Test 4.03: $\delta = (70.15)P^{0.966} = 70.15(\tau.\pi.d_o.10)^{0.966} =$

$$= 70.15 \frac{[(3.14)(16)(.10)]^{0.966}}{1000} \tau^{0.966} =$$

$$= 36.07\ \tau^{0.966}$$

δ [μm], τ [N/mm^2]

$$a = (36/1000)\text{mm} \ .\ 1(\text{N/mm}^2) = 0.036 \text{ mm}^3/\text{N}$$

$$\mu = \alpha(1+\frac{d_o}{d}) + \frac{t}{G_a} = 0.036(1+(16/12)) + \frac{2}{1154} = 0.086 \text{ mm}^3/\text{N}$$

$$\rho_o = a\frac{d}{d_0} + \frac{t}{Ga} = 0.036(16/12)+(2/1154) = 0.051 \ [\frac{\text{N}}{\text{mm}^3}]$$

$$\varkappa = \sqrt{(\frac{\pi d_o}{\mu}(\frac{1}{\lambda_s} + \frac{1}{\lambda_c})} = \sqrt{(\frac{(3.14)16}{0.086}(\frac{1}{(1.37)10^7} + \frac{1}{(1.08)10^{10}}))} = \sqrt{(\frac{42.64}{10^6})}$$

$$= (6.53)10^{-3}[\frac{1}{\text{mm}}]$$

$$\varkappa l = [(6.53)10^{-3}](100) = 6.53 \quad 10^{-1} = 0.653$$

$$\sinh(\varkappa l) = 0.709, \quad \cosh(\varkappa l) = 1.22$$

A.4.1. STEP 1 - Interfacial shear stress τ

$$\tau = \frac{\varkappa P}{\pi d_o [\sinh(\varkappa l)]} [\cosh(\varkappa z)] = \frac{((6.53)10^{-3})[\cosh(\varkappa z)]}{(3.14)(16)(0.709)} =$$

$$= ((1.84)10^{-4})[\cosh(\varkappa z)]$$

$$\tau_o [\frac{N}{mm^2}] = (1.84\ 10^{-4})P\ [N]$$

$$\tau_1 = (\tau_o)\cosh(\varkappa z) = (1.22)\tau_o$$

A.4.2. STEP 2 - Steel force

$$P_s = \frac{P}{\sinh(\varkappa l)} \sinh(\varkappa z) = P \frac{P\sinh((0.00653)z)}{\sinh(0.653)}$$

A.4.3. STEP 3 - Resin strain

$$\varepsilon_o = P[-\frac{\rho_o \varkappa^2}{\pi d_o} + \frac{1}{E_s A_s}] = P[-\frac{0.051((6.53)10^{-3})^2}{(3.14)16} + \frac{1}{(1.37)10^7}]$$

$$= P[(-0.043)10^{-6} + (0.736)10^{-7}] =$$

$$= P[(0.300)10^{-7}]\ ,\ P\ [N]$$

or

$$\varepsilon_o\ [\mu\varepsilon] = [(0.300)10^{-1}]P,\ P[N]$$

for P = 10 KN = 10.000 N

$$\varepsilon_o = [(0.300)10^{-1}].10^4 = 300\ \mu\varepsilon$$

A.4.4. Distributions of stresses and strains at P=10 kN

A.4.4.1. τ_{cr} distribution for P=10 kN

$\tau=\tau_0(\cosh((0.00653)z))$

z	cosh(kz)	τ(N/mm²)
100	1.22	2.24
90	1.2009	2.21
80	1.1577	2.13
70	1.1200	2.06
60	1.0877	2.00
50	1.0606	1.95
40	1.0387	1.91
30	1.0217	1.88
20	1.0096	1.86
10	1.0024	1.84
0	1.0000	1.84

ε_s distribution for P=10kN

$\varepsilon_s=\varepsilon_{so}(\sinh(kz)/0.709)$, $\varepsilon_{so}=771\ \mu\varepsilon$

$\varepsilon_{so}=[10.000\ /\ A_{snetto}\cdot E_s]$

z	ε_s
100	771
90	685
80	600
70	520
60	440
50	364
40	285
30	216
20	143
10	71
0	0

ε_r distribution for P=10 kN

$$\varepsilon_r=\varepsilon_0\left(1-\frac{\sinh(kz)}{\sinh(kl)}\right)=\varepsilon_0\left(1-\frac{\sinh(0.0065z)}{0.709}\right)$$

z	sinh(0.0065)z)/0.709	ε_r (με)
100	1.0	0
90	0.974	8
80	0.854	44
70	0.738	84
60	0.623	113
50	0.512	146
40	0.411	177
30	0.307	208
20	0.204	238
10	0.007	398
0	0	300

A.4.5. Steel displacement at P=10 kN

$$W_s = W_o + \frac{P}{E_s A_s}\,\frac{1}{\varkappa}\,\frac{\cosh(kl) - 1}{\sinh(\varkappa l)} = W_o + \frac{P}{E_s A_s}\,\frac{1}{\varkappa}\,\frac{(1.22-1)}{0.709} =$$

$$= W_o + \left[\frac{(771.10^{-6})}{0.709}\,\frac{1\ (0.22)}{6.53\ 10^{-3}}\ [\mathrm{mm}]\right] =$$

$$= W_o + \left[\frac{0.771}{0.709}\ \frac{0.22}{6.53}\right]\ [\mathrm{mm}] =$$

$$= W_o + 0.037\ [\mathrm{mm}]$$

$$W_{o,1} = \int_0^l \varepsilon_r\ d_z = \int_0^l \varepsilon_o\ \frac{(1-\sinh(\varkappa z))d_z}{\sinh(\varkappa l)} =$$

$$=(\varepsilon_o)l - \frac{\varepsilon_o}{\sinh(\varkappa l)}\int_0^l \sinh(\varkappa z)\ d_z = (\varepsilon_o)l - \frac{\varepsilon_o}{\sinh(\varkappa l)}\left[\frac{1}{\varkappa}\cosh(\varkappa z)\right]_0^l =$$

$$= (\varepsilon_o)l - \frac{\varepsilon_o}{\sinh(\varkappa l)}\left[\frac{1}{\varkappa}[\cosh(\varkappa l)-1]\right] =$$

$$= 300.10^{-6}\left[100 - \left[\frac{1(1.22-1)}{6.53.10^{-3}}\ \frac{1}{0.709}\right]\right. = 0.027\ \mathrm{mm}$$

$$W_{o,2} = \left(a\,\frac{d_o}{d} + \frac{t}{G_a}\right)\tau = \left(0.036\,\frac{d_o}{d} + \frac{2}{1154}\right)2.24 = 0.193\ \mathrm{mm}$$

$$W_s = 0.037 + 0.027 + 0.193 = 0.257\ \mathrm{mm}$$

A.4.6. STEP 4 - concrete strains

A.4.6.1. Contribution of shear forces

It is assummed that P can be simulated by three equal shear forces along the anchor axis. T=P/3

Thus, according to Eq.(5.51)-(5.54) the stresses due to one only of these forces, are:

$$\sigma_x = \frac{P/3}{8\pi(1-\nu)} [\sigma_{o\,T\,x}] = \frac{(10,000/3)}{(8).(3.14)(1-0.20)} [\sigma_o] = 165.85\ [\sigma_{o\,x}]$$

$$\sigma_y = \frac{P/3}{8\pi(1-\nu)} [\sigma_{o\,T\,y}] = 165.85\ [\sigma_{o\,y}]$$

$$\sigma_z = \frac{P/3}{8\pi(1-\nu)} [\sigma_{o\,T\,z}] = 165.85\ [\sigma_{o\,z}]$$

$$\tau_{x\,y} = \frac{P/3}{8\pi(1-\nu)} [\tau_{o\,T\,z}] = [(165.85)]\ [\tau_{o\,x\,y}]$$

A.4.6.2. Contribution of radial pressure

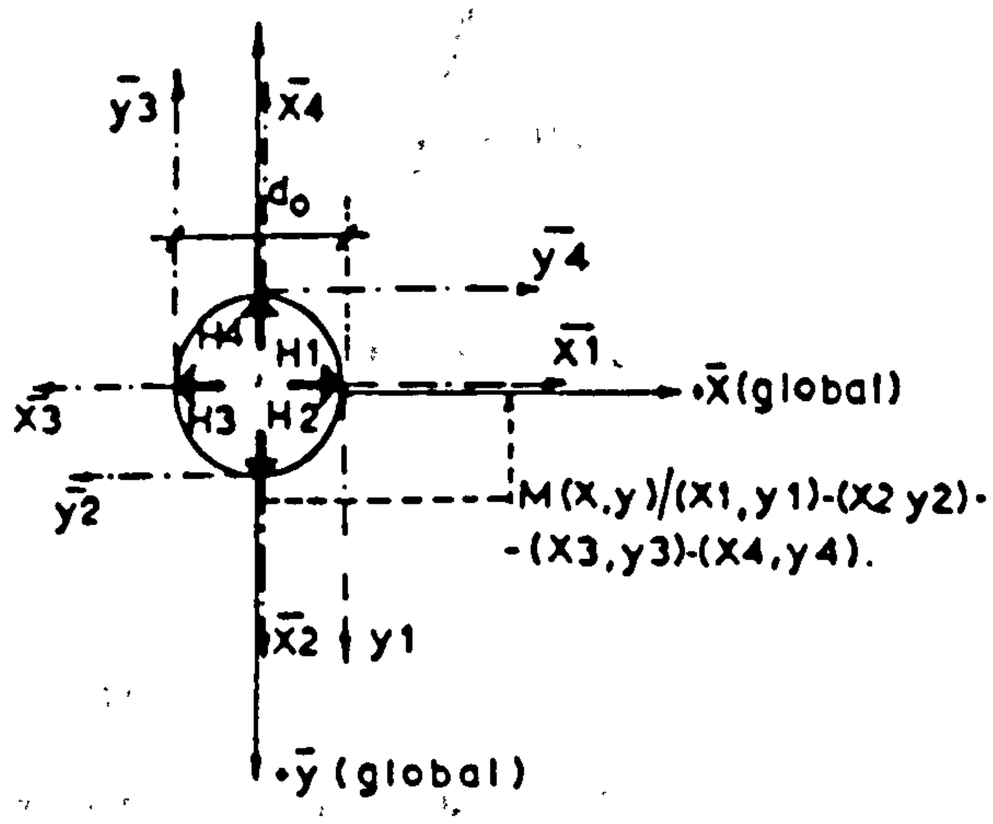

Fig. A

x_4
x_4 =-8 mm y_4 =+18 mm
z=0,15,35,55,75,95 mm
$\sigma_{M,x4,P4} = -\sigma_{M,x,P4}$
$\sigma_{M,y4,P4} = \sigma_{M,x,P4}$

$x=x_1$	x_2	x_3
x=18 mm y=0 mm	x_2 =-8 mm y_2 =-18 mm	x_3 =-26 mm y_3 =0 mm
z=0,15,35,55,75,95	z=0,15,35,55,75,95	z=0,15,35,55,75,95mm
$\sigma_{Mx1P1} = \sigma_{M,x,P1}$	$\sigma_{M,x2,P2} = -\sigma_{M,y,P2}$	$\sigma_{M,x3,P3} = -\sigma_{M,x,P3}$
$\sigma_{My1P1} = \sigma_{M,y,P1}$	$\sigma_{M,y2,P2} = +\sigma_{M,x,P2}$	$\sigma_{M,y3,P3} = -\sigma_{M,y,P3}$

$$\sigma_{M,x,P1+P2+P3+P4} = \sigma_{M,x1,P1} - \sigma_{M,y2,P2} - \sigma_{M,x3,P3} + \sigma_{M,y4,P4}$$

$$\sigma_{M,y,P1+P2+P3+P4} = \sigma_{M,y1,P1} + \sigma_{M,x2,P2} - \sigma_{M,y3,P3} - \sigma_{M,x4,P4}$$

A.4.6.3 . Calculation of values of lateral forces

(See distribution of interfacial shear stress τ_{cr})

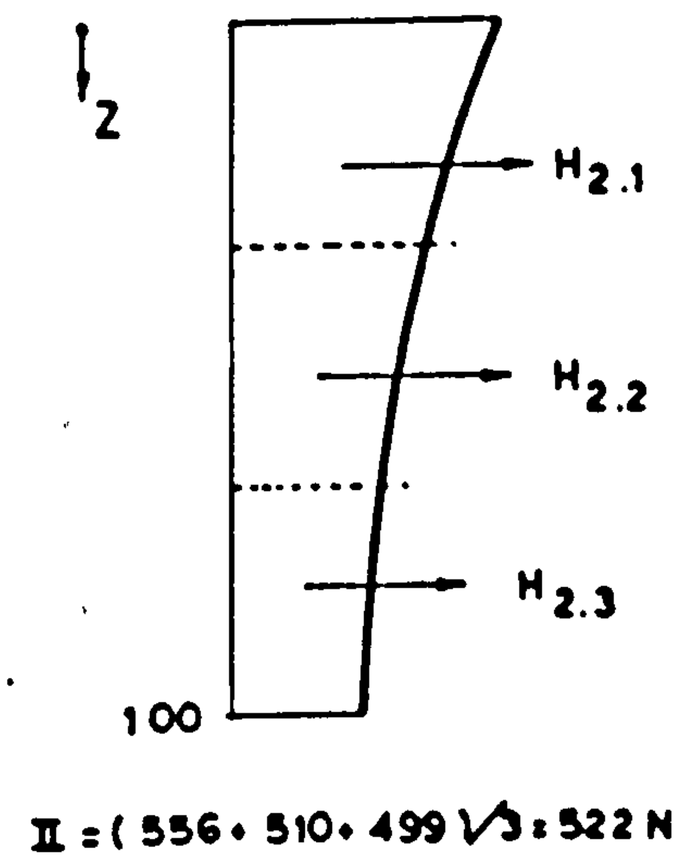

Fig. A. 2

$$H_1 = [(0.57.\tau_{cr} + 0.10)]\ l\ \pi\ d$$

$$H_{1,z1} = 1/4\ [(0.57\ \frac{2.24 + 2.06}{2} + 0.10]\ 33\ (3.14) =$$

$$= (1/4)(2.226) = 556\ N$$

$$H_{2,z2} = 510\ N$$

$$H_{3,z3} = 499\ N$$

For sake of simplicity the assumption is made that $H_1 = H_2 = H_3 = H = 500$ N.

Thus, according to Eq.(5.58)-(5.61), the stresses due to the action of one only of these forces, are:

$$\sigma_x = \frac{H}{8\pi(1-\nu)}\ [\sigma_{oHx}] = \frac{H}{8\pi(1-\nu)}\ \sigma_{x0}$$

$$\sigma_y = \frac{H}{8\pi(1-\nu)}\ [\sigma_{oHy}] = \frac{H}{8\pi(1-\nu)}\ \sigma_{y0}$$

$$\sigma_z = \frac{H}{8\pi(1-\nu)}\ [\sigma_{oHz}] = \frac{H}{8\pi(1-\nu)}\ \sigma_{z0}$$

$$\tau_{yz} = \frac{H}{8\pi(1-\nu)}\ [\tau_{oHyz}] =$$

$$= \frac{H}{8\pi(1-\nu)}\ \tau_{yz0}$$

$$\tau_{xy} = \frac{H}{8\pi(1-\nu)}\ [\tau_{oHxz}] =$$

$$= \frac{H}{8\pi(1-\nu)} \tau_{xy0}$$

and

$$\frac{H}{8\pi(1-\nu)} = \frac{500}{8(3.14)(1-0.20)} = 24.89 \text{ N}$$

and:

$$\varepsilon_{x,y,z}[\mu\varepsilon] = \frac{\sigma}{E} 10^6 = \frac{\sigma[N/mm^2]}{30,000 \ [N/mm^2]} 10^6 = (33.3)\sigma[N/mm^2]$$

A.4.6.4. Mindlin solution for interfacial shear forces

$T_1+T_2+T_3$, Fig 5.4.a, (S_A)

X	Y	Z	v	k	C_α	$Z-C_\alpha$	$R_{1\alpha}$	$R_{2\alpha}$	$Z+C_\alpha$	$\sigma_{\alpha x}$	$\sigma_{\alpha y}$	$\sigma_{\alpha z}$	$\tau_{\alpha yz}$	$\tau_{\alpha zx}$
18	0	0	.20	165.85	16.50	-16.50	24.42	24.42	16.50	1.91E-1	-1.07E+0	0.00E+0	0.00E+0	0.00E+0
18	0	15	.20	165.85	16.50	-1.50	18.06	36.28	31.50	-1.66E-1	-1.97E-1	-4.61E-1	-3.03E-2	-3.03E-2
18	0	35	.20	165.85	16.50	18.50	25.81	54.56	51.50	-2.12E-1	8.60E-2	-7.15E-1	-2.74E-2	-2.74E-2
18	0	55	.20	165.85	16.50	38.50	42.50	73.73	71.50	-8.32E-3	4.89E-2	-4.56E-1	-9.61E-3	-9.61E-3
18	0	75	.20	165.85	16.50	58.50	61.21	93.25	91.50	1.18E-2	2.76E-2	-2.70E-1	-3.92E-3	-3.92E-3
18	0	95	.20	165.85	16.50	78.50	80.54	112.94	111.50	1.15E-2	1.75E-2	-1.74E-1	-1.94E-3	-1.94E-3

X	Y	Z	v	k	C_β	$Z-C_\beta$	$R_{1\beta}$	$R_{2\beta}$	$Z+C_\beta$	$\sigma_{\beta x}$	$\sigma_{\beta y}$	$\sigma_{\beta z}$	$\tau_{\beta yz}$	$\tau_{\beta zx}$
18	0	0	.20	165.85	49.50	-49.50	52.67	52.67	49.50	-2.67E-1	-3.40E-1	0.00E+0	0.00E+0	0.00E+0
18	0	15	.20	165.85	49.50	-34.50	38.91	66.96	64.50	-1.09E-1	-1.71E-1	9.10E-2	-9.60E-3	-9.60E-3
18	0	35	.20	165.85	49.50	-14.50	23.11	86.40	84.50	1.96E-1	-1.55E-1	1.97E-1	-2.54E-2	-2.54E-2
18	0	55	.20	165.85	49.50	5.50	18.82	106.04	104.50	-3.11E-1	6.73E-2	-2.25E-1	-2.23E-2	-2.23E-2
18	0	75	.20	165.85	49.50	25.50	31.21	125.79	124.50	-6.31E-2	7.71E-2	-4.41E-1	-1.48E-2	-1.48E-2
18	0	95	.20	165.85	49.50	45.50	48.93	145.62	144.50	8.82E-3	3.58E-2	-2.65E-1	-4.95E-3	-4.95E-3

X	Y	Z	v	k	C_γ	$Z-C_\gamma$	$R_{1\gamma}$	$R_{2\gamma}$	$Z+C_\gamma$	$\sigma_{\gamma x}$	$\sigma_{\gamma y}$	$\sigma_{\gamma z}$	$\tau_{\gamma yz}$	$\tau_{\gamma zx}$
18	0	0	.20	165.85	84	-84	85.91	85.91	84	-1.25E-1	-1.36E-1	0.00E+0	0.00E+0	0.00E+0
18	0	15	.20	165.85	84	-69	71.31	100.62	99	-7.52E-2	-8.25E-2	2.34E-2	-1.68E-3	-1.68E-3
18	0	35	.20	165.85	84	-49	52.20	120.35	119	-4.42E-2	-6.41E-2	1.12E-1	-4.16E-3	-4.16E-3
18	0	55	.20	165.85	84	-29	34.13	140.16	139	1.23E-2	-8.80E-2	2.74E-1	-1.19E-2	-1.19E-2
18	0	75	.20	165.85	84	-9	20.12	160.02	159	3.21E-1	-1.18E-1	1.71E-1	-2.47E-2	-2.47E-2
18	0	95	.20	165.85	84	11	21.10	179.90	179	-3.13E-1	1.12E-1	-3.14E-1	-2.52E-2	-2.52E-2

σ_x	σ_y	σ_z	τ_{yz}	τ_{zx}
-2.00E-1	-1.54E+0	0.00E+0	0.00E+0	0.00E+0
-3.50E-1	-4.51E-1	-3.46E-1	-4.16E-2	-4.16E-2
-6.07E-2	-1.33E-1	-4.06E-1	-5.69E-2	-5.69E-2
-3.07E-1	2.82E-2	-4.07E-1	-4.38E-2	-4.38E-2
2.69E-1	-1.37E-2	-5.40E-1	-4.34E-2	-4.34E-2
-2.93E-1	1.65E-1	-7.54E-1	-3.21E-2	-3.21E-2

A.4.6.5. Mindlin solution for lateral pressure

A.4.6.5.1. Forces $(H_{1.1})+(H_{1.2})+(H_{1.3})$, Fig. 5.4.a $(S_{B.1})$

X_1	Y_1	Z_1	v	k	C_α	Z_1-C_α	$R_{1\alpha}$	$R_{2\alpha}$	Z_1+C_α	$\sigma_{\alpha X1}$	$\sigma_{\alpha Y1}$	$\sigma_{\alpha Z1}$	$\tau_{\alpha Y1Z1}$	$\tau_{\alpha Z1X1}$
18	0	0	.20	24.89	16.50	-16.50	24.42	24.42	16.50	-1.06E-1	7.18E-2	1.34E-19	0.00E+0	3.38E-2
18	0	15	.20	24.89	16.50	-1.50	18.06	36.28	31.50	-2.86E-1	5.11E-2	5.66E-2	0.00E+0	8.37E-3
18	0	35	.20	24.89	16.50	18.50	25.81	54.56	51.50	-5.86E-2	1.65E-2	-2.37E-2	0.00E+0	-6.57E-2
18	0	55	.20	24.89	16.50	38.50	42.50	73.73	71.50	-8.30E-3	3.89E-3	-1.20E-2	0.00E+0	-2.03E-2
18	0	75	.20	24.89	16.50	58.50	61.21	93.25	91.50	-2.31E-3	1.39E-3	-5.30E-3	0.00E+0	-9.11E-3
18	0	95	.20	24.89	16.50	78.50	80.54	112.94	111.50	-9.09E-4	6.52E-4	-2.80E-3	0.00E+0	-5.16E-3

X_1	Y_1	Z_1	v	k	C_β	Z_1-C_β	$R_{1\beta}$	$R_{2\beta}$	Z_1+C_β	$\sigma_{\beta X1}$	$\sigma_{\beta Y1}$	$\sigma_{\beta Z1}$	$\tau_{\beta Y1Z1}$	$\tau_{\beta Z1X1}$
18	0	0	.20	24.89	49.50	-49.50	52.67	52.67	49.50	4.63E-3	1.08E-2	-4.48E-20	0.00E+0	1.01E-2
18	0	15	.20	24.89	49.50	-34.50	38.91	66.96	64.50	-9.88E-3	6.86E-3	-7.81E-3	0.00E+0	1.49E-2
18	0	35	.20	24.89	49.50	-14.50	23.11	86.40	84.50	-8.90E-2	2.23E-2	-1.85E-2	0.00E+0	6.69E-2
18	0	55	.20	24.89	49.50	5.50	18.82	106.04	104.50	-2.25E-1	4.05E-2	2.42E-2	0.00E+0	-7.17E-2
18	0	75	.20	24.89	49.50	25.50	31.21	125.79	124.50	-2.40E-2	8.92E-3	-2.02E-2	0.00E+0	-3.57E-2
18	0	95	.20	24.89	49.50	45.50	48.93	145.62	144.50	-4.15E-3	2.34E-3	-7.43E-3	0.00E+0	-1.15E-2

X_1	Y_1	Z_1	v	k	C_γ	Z_1-C_γ	$R_{1\gamma}$	$R_{2\gamma}$	Z_1+C_γ	$\sigma_{\gamma X1}$	$\sigma_{\gamma Y1}$	$\sigma_{\gamma Z1}$	$\tau_{\gamma Y1Z1}$	$\tau_{\gamma Z1X1}$
18	0	0	.20	24.89	84	-84	85.91	85.91	84	1.67E-3	2.63E-3	1.43E-19	0.00E+0	3.96E-3
18	0	15	.20	24.89	84	-69	71.31	100.62	99	-6.58E-4	1.65E-3	-1.07E-3	0.00E+0	2.97E-3
18	0	35	.20	24.89	84	-49	52.20	120.35	119	-3.25E-3	2.22E-3	-5.33E-3	0.00E+0	6.63E-3
18	0	55	.20	24.89	84	-29	34.13	140.16	139	-1.64E-2	6.90E-3	-1.70E-2	0.00E+0	2.45E-2
18	0	75	.20	24.89	84	-9	20.12	160.02	159	-1.65E-1	3.30E-2	4.05E-4	0.00E+0	8.11E-2
18	0	95	.20	24.89	84	11	21.10	179.90	179	-1.33E-1	2.87E-2	-1.01E-2	0.00E+0	-8.23E-2

σ_{x1}	σ_{y1}	σ_{z1}	τ_{y1z1}	τ_{z1x1}
-9.95E-2	8.52E-2	2.33E-19	0.00E+0	4.79E-2
-2.97E-1	5.96E-2	4.77E-2	0.00E+0	2.63E-2
-1.51E-1	4.11E-2	-4.75E-2	0.00E+0	7.78E-3
-2.50E-1	5.13E-2	-4.73E-3	0.00E+0	-6.76E-2
-1.91E-1	4.34E-2	-2.51E-2	0.00E+0	3.63E-2
-1.38E-1	3.17E-2	-2.03E-2	0.00E+0	-9.90E-2

A.4.6.5.2. Forces $(H_{2.1})+(H_{2.2})+(H_{2.3})$, $(S_{B.2})$

X_2	Y_2	Z_2	v	k	Ca	Z_2-Ca	R_1a	R_2a	Z_2+Ca	σ_{aX2}	σ_{aY2}	σ_{aZ2}	τ_{aY2Z2}	τ_{aZ2X2}
-8	-18	0	.20	24.89	16.50	-16.50	25.70	25.70	16.50	4.53E-5	2.04E-2	-1.99E-20	0.00E+0	2.90E-2
-8	-18	15	.20	24.89	16.50	-1.50	19.75	37.15	31.50	3.40E-2	4.66E-2	-1.92E-2	6.42E-3	-1.03E-2
-8	-18	35	.20	24.89	16.50	18.50	27.02	55.14	51.50	1.08E-2	6.96E-3	7.95E-3	-1.37E-2	-3.05E-2
-8	-18	55	.20	24.89	16.50	38.50	43.25	74.16	71.50	2.43E-3	-3.49E-4	4.90E-3	-2.83E-3	-1.41E-2
-8	-18	75	.20	24.89	16.50	58.50	61.73	93.60	91.50	8.16E-4	-3.76E-4	2.27E-3	-7.80E-4	-7.48E-3
-8	-18	95	.20	24.89	16.50	78.50	80.93	113.23	111.50	3.47E-4	-2.24E-4	1.22E-3	-2.95E-4	-4.55E-3

X_2	Y_2	Z_2	v	k	C_β	Z_2-C_β	$R_{1\beta}$	$R_{2\beta}$	Z_2+C_β	$\sigma_{\beta X2}$	$\sigma_{\beta Y2}$	$\sigma_{\beta Z2}$	$\tau_{\beta Y2Z2}$	$\tau_{\beta Z2X2}$
-8	-18	0	.20	24.89	49.50	-49.50	53.28	53.28	49.50	-2.96E-3	-3.29E-3	-1.99E-20	3.58E-21	9.78E-3
-8	-18	15	.20	24.89	49.50	-34.50	39.73	67.44	64.50	2.45E-3	-9.07E-4	2.94E-3	3.92E-3	6.51E-3
-8	-18	35	.20	24.89	49.50	-14.50	24.46	86.77	84.50	1.31E-2	1.37E-2	5.07E-3	1.80E-2	1.87E-2
-8	-18	55	.20	24.89	49.50	5.50	20.45	106.34	104.50	2.50E-2	4.00E-2	-9.40E-3	-1.65E-2	-2.01E-2
-8	-18	75	.20	24.89	49.50	25.50	32.22	126.05	124.50	4.89E-3	1.96E-3	7.40E-3	-7.87E-3	-1.72E-2
-8	-18	95	.20	24.89	49.50	45.50	49.58	145.84	144.50	1.24E-3	-3.56E-4	3.06E-3	-1.62E-3	-8.05E-3

X_2	Y_2	Z_2	v	k	C_γ	Z_2-C_γ	$R_{1\gamma}$	$R_{2\gamma}$	Z_2+C_γ	$\sigma_{\gamma X2}$	$\sigma_{\gamma Y2}$	$\sigma_{\gamma Z2}$	$\tau_{\gamma Y2Z2}$	$\tau_{\gamma Z2X2}$
-8	-18	0	.20	24.89	84	-84	86.28	86.28	84	-8.19E-4	-1.03E-3	5.38E-20	1.79E-21	3.91E-3
-8	-18	15	.20	24.89	84	-69	71.76	100.94	99	1.94E-4	-6.06E-4	4.53E-4	3.96E-4	2.19E-3
-8	-18	35	.20	24.89	84	-49	52.81	120.62	119	1.01E-3	-4.85E-4	2.20E-3	1.32E-3	3.92E-3
-8	-18	55	.20	24.89	84	-29	35.06	140.39	139	3.62E-3	8.19E-4	6.42E-3	5.91E-3	1.11E-2
-8	-18	75	.20	24.89	84	-9	21.66	160.22	159	1.99E-2	2.88E-2	-1.78E-3	2.03E-2	2.09E-2
-8	-18	95	.20	24.89	84	11	22.56	180.08	179	1.70E-2	2.27E-2	1.85E-3	-2.02E-2	-2.44E-2

σ_{x2}	σ_{y2}	σ_{z2}	τ_{y2z2}	τ_{z2x2}
-3.74E-3	1.61E-2	1.39E-20	5.38E-21	4.27E-2
3.66E-2	4.51E-2	-1.58E-2	1.07E-2	-1.55E-3
2.49E-2	2.02E-2	1.52E-2	5.56E-3	-7.87E-3
3.11E-2	4.05E-2	1.91E-3	-1.34E-2	-2.31E-2
2.56E-2	3.04E-2	7.89E-3	1.17E-2	-3.84E-3
1.86E-2	2.21E-2	6.14E-3	-2.21E-2	-3.71E-2

A.4.6.5.3. Forces $(H_{3.1})+(H_{3.2})+(H_{3.3})$, $(S_{B.3})$

X_3	Y_3	Z_3	v	k	C_α	Z_3-C_α	$R_{1\alpha}$	$R_{2\alpha}$	Z_3+C_α	$\sigma_{\alpha X3}$	$\sigma_{\alpha Y3}$	$\sigma_{\alpha Z3}$	$\tau_{\alpha Y3Z3}$	$\tau_{\alpha Z3X3}$
-26	0	0	.20	24.89	16.50	-16.50	30.79	30.79	16.50	1.18E-1	-3.98E-2	0.00E+0	0.00E+0	1.69E-2
-26	0	15	.20	24.89	16.50	-1.50	26.04	40.84	31.50	1.47E-1	-2.74E-2	-2.37E-2	0.00E+0	-3.55E-3
-26	0	35	.20	24.89	16.50	18.50	31.91	57.69	51.50	5.72E-2	-1.31E-2	9.15E-3	0.00E+0	-4.54E-2
-26	0	55	.20	24.89	16.50	38.50	46.46	76.08	71.50	1.21E-2	-4.40E-3	1.13E-2	0.00E+0	-2.03E-2
-26	0	75	.20	24.89	16.50	58.50	64.02	95.12	91.50	3.56E-3	-1.78E-3	6.30E-3	0.00E+0	-9.63E-3
-26	0	95	.20	24.89	16.50	78.50	82.69	114.49	111.50	1.40E-3	-8.79E-4	3.63E-3	0.00E+0	-5.44E-3

X_3	Y_3	Z_3	v	k	C_β	Z_3-C_β	$R_{1\beta}$	$R_{2\beta}$	Z_3+C_β	$\sigma_{\beta X3}$	$\sigma_{\beta Y3}$	$\sigma_{\beta Z3}$	$\tau_{\beta Y3Z3}$	$\tau_{\beta Z3X3}$
-26	0	0	.20	24.89	49.50	-49.50	55.91	55.91	49.50	-1.28E-3	-1.21E-2	0.00E+0	0.00E+0	8.46E-3
-26	0	15	.20	24.89	49.50	-34.50	43.20	69.54	64.50	1.42E-2	-7.64E-3	4.58E-3	0.00E+0	1.56E-2
-26	0	35	.20	24.89	49.50	-14.50	29.77	88.41	84.50	7.23E-2	-1.54E-2	-3.06E-4	0.00E+0	3.63E-2
-26	0	55	.20	24.89	49.50	5.50	26.58	107.69	104.50	1.21E-1	-2.09E-2	-1.77E-2	0.00E+0	-2.81E-2
-26	0	75	.20	24.89	49.50	25.50	36.42	127.19	124.50	2.92E-2	-8.15E-3	1.11E-2	0.00E+0	-3.01E-2
-26	0	95	.20	24.89	49.50	45.50	52.40	146.82	144.50	6.44E-3	-2.76E-3	7.22E-3	0.00E+0	-1.22E-2

X_3	Y_3	Z_3	v	k	C_γ	Z_3-C_γ	$R_{1\gamma}$	$R_{2\gamma}$	Z_3+C_γ	$\sigma_{\gamma X3}$	$\sigma_{\gamma Y3}$	$\sigma_{\gamma Z3}$	$\tau_{\gamma Y3Z3}$	$\tau_{\gamma Z3X3}$
-26	0	0	.20	24.89	84	-84	87.93	87.93	84	-1.76E-3	-3.43E-3	6.47E-21	0.00E+0	3.69E-3
-26	0	15	.20	24.89	84	-69	73.74	102.36	99	1.18E-3	-2.18E-3	1.16E-3	0.00E+0	3.48E-3
-26	0	35	.20	24.89	84	-49	55.47	121.81	119	5.09E-3	-2.72E-3	5.15E-3	0.00E+0	7.59E-3
-26	0	55	.20	24.89	84	-29	38.95	141.41	139	2.16E-2	-6.77E-3	1.07E-2	0.00E+0	2.22E-2
-26	0	75	.20	24.89	84	-9	27.51	161.11	159	1.02E-1	-1.87E-2	-9.22E-3	0.00E+0	3.40E-2
-26	0	95	.20	24.89	84	11	28.23	180.88	179	9.07E-2	-1.73E-2	-4.49E-3	0.00E+0	-3.94E-2

σ_{X3}	σ_{Y3}	σ_{Z3}	τ_{Y3Z3}	τ_{Z3X3}
1.15E-1	-5.53E-2	6.47E-21	0.00E+0	2.90E-2
1.62E-1	-3.72E-2	-1.80E-2	0.00E+0	1.55E-2
1.35E-1	-3.13E-2	1.40E-2	0.00E+0	-1.51E-3
1.54E-1	-3.21E-2	4.37E-3	0.00E+0	-2.62E-2
1.35E-1	-2.87E-2	8.14E-3	0.00E+0	-5.77E-3
9.85E-2	-2.10E-2	6.36E-3	0.00E+0	-5.70E-2

A.4.6.5.4. Forces $(H_{4.1})+(H_{4.2})+(H_{4.3})$, $(S_{B.4})$

X_4	Y_4	Z_4	v	k	C_α	Z_4-C_α	$R_{1\alpha}$	$R_{2\alpha}$	Z_4+C_α	$\sigma_{\alpha X4}$	$\sigma_{\alpha Y4}$	$\sigma_{\alpha Z4}$	$\tau_{\alpha Y4Z4}$	$\tau_{\alpha Z4X4}$
-8	18	0	.20	24.89	16.50	-16.50	25.70	25.70	16.50	4.53E-5	2.04E-2	-1.99E-20	0.00E+0	2.90E-2
-8	18	15	.20	24.89	16.50	-1.50	19.75	37.15	31.50	3.40E-2	4.66E-2	-1.92E-2	-6.42E-3	-1.03E-2
-8	18	35	.20	24.89	16.50	18.50	27.02	55.14	51.50	1.08E-2	6.96E-3	7.95E-3	1.37E-2	-3.05E-2
-8	18	55	.20	24.89	16.50	38.50	43.25	74.16	71.50	2.43E-3	-3.49E-4	4.90E-3	2.83E-3	-1.41E-2
-8	18	75	.20	24.89	16.50	58.50	61.73	93.60	91.50	8.16E-4	-3.76E-4	2.27E-3	7.80E-4	-7.48E-3
-8	18	95	.20	24.89	16.50	78.50	80.93	113.23	111.50	3.47E-4	-2.24E-4	1.22E-3	2.95E-4	-4.55E-3

X_4	Y_4	Z_4	v	k	C_β	Z_4-C_β	$R_{1\beta}$	$R_{2\beta}$	Z_4+C_β	$\sigma_{\beta X4}$	$\sigma_{\beta Y4}$	$\sigma_{\beta Z4}$	$\tau_{\beta Y4Z4}$	$\tau_{\beta Z4X4}$
-8	18	0	.20	24.89	49.50	-49.50	53.28	53.28	49.50	-2.96E-3	-3.29E-3	-1.99E-20	-3.58E-21	9.78E-3
-8	18	15	.20	24.89	49.50	-34.50	39.73	67.44	64.50	2.45E-3	-9.07E-4	2.94E-3	-3.92E-3	6.51E-3
-8	18	35	.20	24.89	49.50	-14.50	24.46	86.77	84.50	1.31E-2	1.37E-2	5.07E-3	-1.80E-2	1.87E-2
-8	18	55	.20	24.89	49.50	5.50	20.45	106.34	104.50	2.50E-2	4.00E-2	-9.40E-3	1.65E-2	-2.01E-2
-8	18	75	.20	24.89	49.50	25.50	32.22	126.05	124.50	4.89E-3	1.96E-3	7.40E-3	7.87E-3	-1.72E-2
-8	18	95	.20	24.89	49.50	45.50	49.58	145.84	144.50	1.24E-3	-3.56E-4	3.06E-3	1.62E-3	-8.05E-3

X_4	Y_4	Z_4	v	k	C_γ	Z_4-C_γ	$R_{1\gamma}$	$R_{2\gamma}$	Z_4+C_γ	$\sigma_{\gamma X4}$	$\sigma_{\gamma Y4}$	$\sigma_{\gamma Z4}$	$\tau_{\gamma Y4Z4}$	$\tau_{\gamma Z4X4}$
-8	18	0	.20	24.89	84	-84	86.28	86.28	84	-8.19E-4	-1.03E-3	5.38E-20	-1.79E-21	3.91E-3
-8	18	15	.20	24.89	84	-69	71.76	100.94	99	1.94E-4	-6.06E-4	4.53E-4	-3.96E-4	2.19E-3
-8	18	35	.20	24.89	84	-49	52.81	120.62	119	1.01E-3	-4.85E-4	2.20E-3	-1.32E-3	3.92E-3
-8	18	55	.20	24.89	84	-29	35.06	140.39	139	3.62E-3	8.19E-4	6.42E-3	-5.91E-3	1.11E-2
-8	18	75	.20	24.89	84	-9	21.66	160.22	159	1.99E-2	2.88E-2	-1.78E-3	-2.03E-2	2.09E-2
-8	18	95	.20	24.89	84	11	22.56	180.08	179	1.70E-2	2.27E-2	1.85E-3	2.02E-2	-2.44E-2

σ_{X4}	σ_{Y4}	σ_{Z4}	τ_{Y4Z4}	τ_{Z4X4}
-3.74E-3	1.61E-2	1.39E-20	-5.38E-21	4.27E-2
3.66E-2	4.51E-2	-1.58E-2	-1.07E-2	-1.55E-3
2.49E-2	2.02E-2	1.52E-2	-5.56E-3	-7.87E-3
3.11E-2	4.05E-2	1.91E-3	1.34E-2	-2.31E-2
2.56E-2	3.04E-2	7.89E-3	-1.17E-2	-3.84E-3
1.86E-2	2.21E-2	6.14E-3	2.21E-2	-3.71E-2

A.4.6.5.5. Stresses due to $(S_{B1})+(S_{B2})+(S_{B3})$

σ_x	σ_y	σ_z	τ_{yz}	τ_{zx}
-2.15E-1	1.41E-1	2.67E-19	0.00E+0	1.62E-1
-4.59E-1	9.68E-2	-1.82E-3	0.00E+0	3.87E-2
-2.85E-1	7.24E-2	-3.11E-3	0.00E+0	-9.46E-3
-4.05E-1	8.34E-2	3.45E-3	0.00E+0	-1.40E-1
-3.26E-1	7.20E-2	-1.16E-3	0.00E+0	2.29E-2
-2.37E-1	5.26E-2	-1.65E-3	0.00E+0	-2.30E-1

A.4.6.5.6. Overall concrete stresses and strains, $(S_A)+(S_{B.1})+(S_{B.2})+(S_{B.3})$

σ_x	σ_y	σ_z	τ_{yz}	τ_{zx}	σ_{11}	σ_{22}	$\theta°$	V	ε_{xx}	ε_{yy}	ε_{zz}
-1.44E-2	1.68E+0	2.67E-19	0.00E+0	1.62E-1	1.55E-1	-1.70E-1	4.E+2	33.30	-4,79E-1	5,60E+1	8,90E-18
-1.09E-1	5.48E-1	3.44E-1	4.16E-2	8.03E-2	3.58E-1	-1.23E-1	1.E+2	33.30	-3,64E+0	1,82E+1	1,15E+1
-2.25E-1	2.05E-1	4.03E-1	5.69E-2	4.74E-2	4.07E-1	-2.28E-1	4.E+1	33.30	-7,48E+0	6,83E+0	1,34E+1
-9.80E-2	5.52E-2	4.10E-1	4.38E-2	-9.62E-2	4.28E-1	-1.16E-1	-102	33.30	-3,26E+0	1,84E+0	1,37E+1
-5.96E-1	8.57E-2	5.39E-1	4.34E-2	6.63E-2	5.43E-1	-6.00E-1	3.E+1	33.30	-1,98E+1	2,85E+0	1,79E+1
5.62E-2	-1.12E-1	7.52E-1	3.21E-2	-1.98E-1	8.05E-1	3.80E-3	-146	33.30	1,87E+0	-3,74E+0	2,50E+1

A.4.6.7. Calculation of the first crack load

$$\sigma_{11} = 0.805 \text{ N/mm}^2$$

$$\varepsilon_{11} = (0.805/30{,}000)10^6 = 26.8\ \mu\varepsilon$$

$$P_{cr} = 10(100/26.8) = 37.3 \text{ kN}$$

APPENDIX B: MINIMUM DIMENSIONS OF PULL-OUT SPECIMENS ACCORDING TO BS 5080 PART 1-1974 AND ASTM 488.81

B.S. 5080

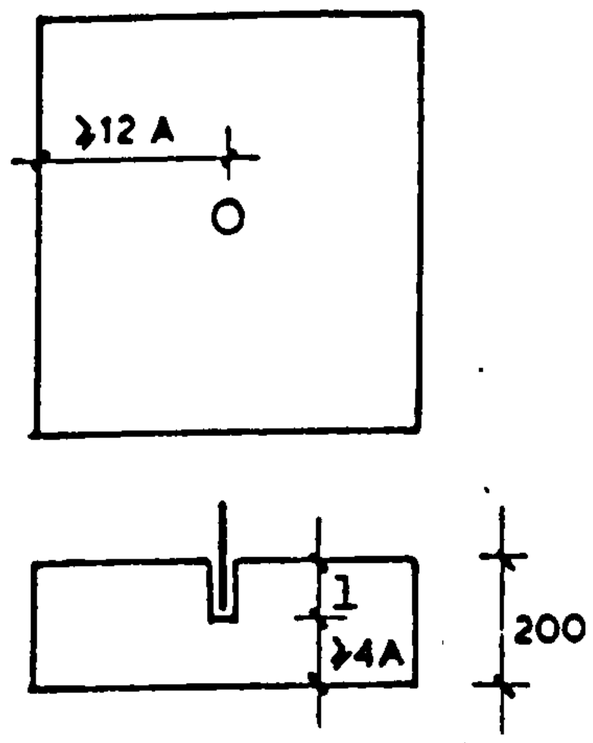

B 1

- Characteristic dimension of fixing:

$$A = \max[d, \frac{1}{4}\text{(embedment length)}]$$

- Dimensions of specimens for:

$d=8,\ l=7d=56,\ A=\max[8,\frac{56}{4}]=14.0\text{mm}$

$d=8,\ l=10d=80,\ A=\max[8,\frac{80}{4}]=20\text{mm}$

$d=10,\ l=7d=70,\ A=\max[10,\frac{70}{4}]=17.5\text{mm}$

$d=12, l=8.3d=100,\ A=\max[10,\frac{100}{4}]=25\text{mm}$

ASTM E 488

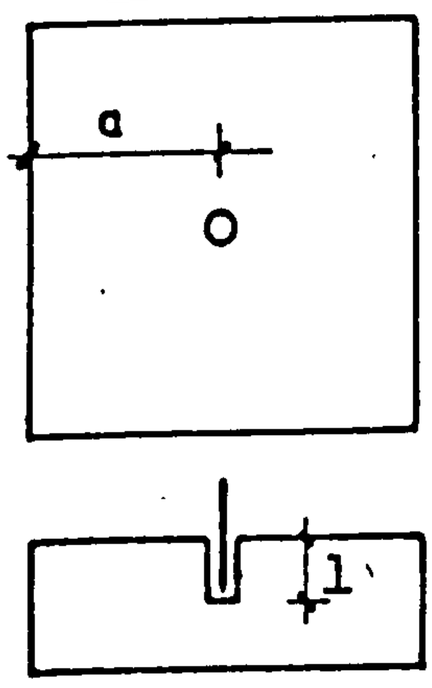

Half dimension of specimen:>= 12A = 12x25= 300 mm

$D = l_{max} + 4A = 100\text{ mm} + 4(25) = 200\text{ mm}$

ASTM. E488.81

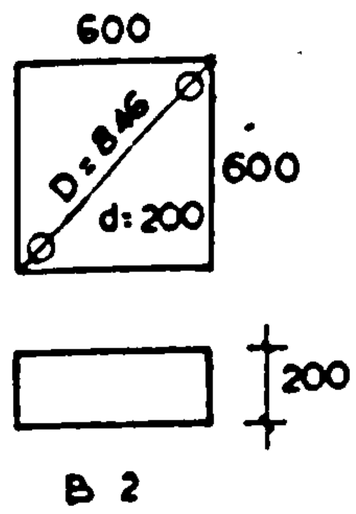

B 2

$\alpha > 41$

$d=8,\ l=7d=56 \rightarrow \alpha=4(56)=224\text{mm}$

$d=8,\ l=10d=80 \rightarrow \alpha=4(80)=320\text{mm}$

$d=10,\ l=7d=70 \rightarrow \alpha=4(70)=280\text{mm}$

$d=12,\ l=(8.3)d=100 \rightarrow \alpha=4(100)=400\text{mm}$

$D_o = 423$ mm

Where D_o: half of the diagonal of a square of 600mm side (diagonal length: 846mm)

APPENDIX C : FINITE ELEMENT ELASTIC PARAMETRIC ANALYSIS

C.1. Data

d_{max} = 12.0 mm , $A_{s\ max}$ = 113.0 mm^2

d_{min} = 9.8 mm , $A_{s\ min}$ = 75.39 mm^2

$d_{aver.}$ = 10.9 mm , $A_{s\ aver.}$ = 93.26 mm^2

The drill was bored with 5 mm bit, however, due to the lack of fixing during boring it is assumed that the bore had a 6mm diameter

$$A_{s\,netto} = 93.26 - \pi(6)^2/4 = 65.0\ mm^2$$

An axial hole was provided to the steel simulation in order to match the real cross section above.

For a thread like the one used, according to DIN 202: $y=60^0$, Fig 1.7.

Hence,

$$p_i = p_v \tan 30^o = 0.577\ p_v$$

the combined concrete resin shrinkage and steel lateral contraction effect was taken into account by means of the proposal of Laldji and Young /56/.

$$\sigma_i = (E_s.\varepsilon - \nu_s \sigma_s + 2m\sigma_o)/K, \text{ Eq. (5.57)}$$

where:

$$m = E_s/E_g = 210000/30000 = 7$$

$$K = (1-\nu_s)+m(1+\nu_g) = (1-0.29)+7(1+0.20) = 9.11$$

ν_g ,E_g :Poisson's ratio and modulus of elasticity of resin

ν_s ,E_s :Poisson's ratio and modulus of elasticity of steel

σ_o :The lateral pressure possibly applied at the other surface of concrete specimen.

σ_s :The steel tensile stress, which for the Laldji and Young set up was a local tensile stress (at the bonding section of the steel to grout). Therefore, here, in order to simulate specimen 3.01 the mean value of steel stress along the 100 mm anchor length is taken:

$$\sigma_s=(1/2)(10000/A_{s\,netto})=(1/2)(10000/65)= 76.9\ N/mm^2$$

ε:The concrete shrinkage rate which for the mix used for specimen 3.01 under the real curing and storage conditions can be calculated as follows (Technische Hochschule Muenchen - Lehrstuhl fuer Massivbau. Einfluss von Kriechen und Schwiden des Betons auf die Schnittgroessen und Spannungen. Muenchen 1966):

$$\varepsilon = \varepsilon_{s\,o}\ C_2\ C_5\ C_{4,t}$$

$$d_w =[(600x600)/(4x600) = 150\ mm\ ,\ C_5=0.90$$

$$w/c= 0.48,\ C=385\ kg/m^2\ \rightarrow\ C_2=1.1$$

$$\varepsilon_{s\,o}= 34.10^{-5}$$

$$t= 28\ days\ \rightarrow\ t\sqrt{(10/d_b)} = 22.86,\quad C_{4,t}=0.31$$

therefore,

$$\varepsilon = (34.10^{-5})(0.90)(1.1)(0.31) = 11.10^{-5}$$

and

$$\sigma_1= (2.1x10^5\ x\ 11.10^{-5}-0.29x76.9)/9.11= 0.10$$

The proposal of Laldji and Young could be applied omiting the resin shrinkage because its effect is negligible, as it is shown below:

$$\varepsilon_r = 6.10^{-4} \;,\; t_r = 2mm \;\cdot\; \Delta\varepsilon_r = 1(6.10^{-4}) = 6.10^{-4}\ mm$$

$$\varepsilon_c = 11.10^{-5} \;,\; t_c = 600mm \;\cdot\; \Delta\varepsilon_c = 300(11.10^{-5}) = 3300.10^{-5}\ mm$$

$$= 330.10^{-4}\ mm$$

Thus,

$$p_i = 0.577\ p_v + 0.10 = 0.577\ \tau + 0.10$$

where:

τ : the mean value of the shear stress across the concrete-resin interface.

C.2. Correction of the values of the resin strain ε_r derived from the idealized geometry in order to take into account the slip elements.

Stiffness of the slip elements at the bottom. Eq.(6.8)

$$E_2 A_2 = btl/2a_t = (A_{bott})l/2a_t \quad \text{.....(C.1)}$$

or

$$(E_2 A_2)/l = A_{bott}/2a_t \quad \text{.....(C.2)}$$

For

$a_{t1}=2a$: $(E_{2\cdot 1} A_{2\cdot 1})/l = A_{bott}/4a$, $\varepsilon_{r1}=134\mu\varepsilon$, model I

$a_{t2}=a$: $(E_{2\cdot 2} A_{2\cdot 2})/l = A_{bott}/2a$, $\varepsilon_{r2}=246\mu\varepsilon$, model I.1

which implies that

$$(\varepsilon_{r1}/\varepsilon_{r2}) \approx (E_{2.1} A_{2.1})/(E_{2.2} A_{2.2}) \quad \text{.....(C.3)}$$

and because for constant a_t, according to Eq.(C.2):

$$(E_{2.1} A_{2.1})/(E_{2.2} A_{2.2}) = (A_{bot1}/A_{bot2}) \quad \text{.....(C.4)}$$

$$(\varepsilon_{r1}/\varepsilon_{r2}) = (A_{bottom1}/A_{bottom2}) \quad \text{.....(C.5)}$$

Calculations of correction coefficients are in page C.12.

C.3. Calculation of the first crack load

Section y=18 mm; x=0

z	s_{yz} (N/mm²)	s_{yy} (N/mm²)	s_{zz} (N/mm²)	$\frac{s_{yy}+s_{zz}}{z}$	$\Delta=\frac{s_{yy}-s_{zz}}{z}$	$\sqrt{(\Delta^2+s^2_{yz})}$	s_{11}	s_{22}
5	- 1.56	- 0.45	0.07	- 0.19	- 0.26	1.58	1.39	-1.77
15	- 1.87	- 0.12	0.22	+ 0.05	- 0.77	1.88	1.93	-1.83
25	- 1.87	- 0.24	0.27	+ 0.01	- 0.26	1.89	1.90	-1.88
35	- 1.84	- 0.31	0.26	+ 0.02	- 0.28	1.86	1.88	-1.88
45	- 1.82	- 0.34	0.26	+ 0.04	- 0.30	1.84	1.88	-1.80
55	- 1.77	- 0.36	0.27	+ 0.04	- 0.31	1.80	1.84	-1.76
65	- 1.80	- 0.37	0.31	+ 0.03	- 0.34	1.83	1.86	-1.80
75	- 1.70	- 0.39	0.38	0	- 0.39	1.74	1.74	-1.74
85	- 1.79	- 0.36	0.54	+ 0.09	- 0.45	1.85	1.94	-1.86
95	- 1.34	- 0.12	0.66	+ 0.27	- 0.47	1.42	1.69	-1.25

Max. principal tensile stress : s_{11} = 1.94 N/mm²

$$\varepsilon_{11} = (1.94/30{,}000)10^6 = 64.6\ \mu\varepsilon$$

First crack load: P_{cr} = 10(100/64.6) = 15.5 kN

Text cut off in original

C.4. Some of the results of the finite element analysis

Model I Standard: l=100mm, d=12mm, t=2mm.

	Steel		Resin				Resin-concrete interface			Concrete x = 0 , y = 18 mm								Concrete x=0,y=18mm			
	Elements 21-30		Elements 121-130				Elements 161-170			Elements 241-250								Elements 241-250			
	Z=1t	$(\varepsilon_{zz})10^{-7}$	Z=1t	Pi	Z+Pi	$(\varepsilon_{zz})10^{-5}$	Z=1t	Pi	Z+Pi	Z=1t	Pi	Z+Pi	$(\varepsilon_{yy})10^{-6}$	Z=1t	Pi	Z+Pi	$(\varepsilon_{zz})10^{-6}$	Z=1t	Pi	Z+Pi	$(\varepsilon_{xx})10^{-6}$
z(mm)	S_{zz}		S_{zz}	S_{zz}	S_{zz}		S_{yz}	S_{yz}	S_{yz}	S_{yy}	S_{yy}	S_{yy}		S_{zz}	S_{zz}	S_{zz}		S_{xx}	S_{xx}	S_{xx}	
5	16600	7904.762	15.62	-0.1503	15.47	7.032=70με	-155.513	-0.419	-155.932	-7.567	-37.42	-44.987	-15.0	8.40	-1.098	7.302	2.434	52.53	12.08	64.61	21.54
15	13190	6280.96	28.48	0.02162	28.502	12.96=129.6με	-187.55	0.184	-187.366	25.66	-37.93	-12.27	-4.09	24.30	-3.028	21.272	7.10	16.31	10.41	26.72	8.907
25	12750	6071.43	42.83	0.042	42.872	19.49=194.9με	-187.275	-0.177	-187.452	13.91	-38.17	-24.26	-8.087	31.25	-4.205	27.045	9.015	9.923	10.66	20.583	6.861
35	10150	4833.34	41.49	0.0403	41.5303	18.88=188.8με	-183.84	-0.0425	-183.90	7.293	-38.22	-30.927	-10.309	30.39	-4.618	25.772	8.60	7.483	10.64	18.123	6.041
45	9161	4362.4	33.33	0.02746	33.36	15.163=151.63με	-182.463	-0.0645	-183.53	4.528	-38.28	-33.752	-11.251	30.45	-4.931	25.519	8.5064	6.374	10.58	16.954	5.6514
55	7052	3358.10	33.61	-0.0014	33.61	15.28=152.8με	-177.65	-0.079	-177.73	2.712	-38.37	-35.658	-11.886	32.77	-5.281	27.489	9.163	6.097	10.52	16.617	5.539
65	5789	2756.67	23.76	-0.0415	23.72	10.782=107.82με	-180.263	-0.0812	-180.344	1.597	-38.39	-36.793	-12.265	36.11	-5.528	30.582	10.19	5.884	10.48	16.364	5.455
75	3919	1866.2	28.37	-0.10	28.27	12.85=128.5με	-169.813	-0.0832	-169.90	0.00914	-38.99	-38.981	-12.994	44.63	-6.234	38.396	12.8	6.054	10.23	16.284	5.428
85	2533	1206.2	27.90	-0.1851	27.715	12.60=126.0με	-178.48	-0.75	-179.23	4.769	-40.56	-35.791	-11.93	59.15	-4.518	54.632	18.21	6.279	9.683	15.962	5.321
95	755.9	359.96	29.60	-0.12	29.48	13.4=134με	-137.335	2.474	-134.861	17.83	-30.14	-12.31	-4.104	67.96	-1.785	66.175	22.06	3.903	7.406	11.309	3.77
	$\varepsilon_{zz}=S_{zz}/E_s$ $E_s=(2.1).10^7$ [t/m^2]		$\varepsilon_{zz}= S_{zz(Z+Pi)}/Er$ $E_r = (2.2)10^5$ [t/m^2]				The S_{yz} values are multiplied by a correction factor 22/16 = 1.375 in order to take into account the idealized geometry due to the slip elements.			$\varepsilon_{yy} = S_{yy(Z+Pi)}/Ec$ $\varepsilon_{zz} = S_{zz(Z+Pi)}/Ec$ $E_c = (3)10^6$ [t/m^2]								$\varepsilon_{xx} = \frac{S_{xx}}{Ec}$ $E_c = (3)10^6$ [t/m^2]			
Remark: All stresses are given in t/m^2 and all forces in t.																					

Model I.1 Stiffness of tensile slip elements at the bottom the same as that of shear slip elements (α_t=a)

	Steel		Resin				Resin-concrete interface			Concrete x = 0 , y = 18 mm								Concrete x=0 y=18mm			
	Elements 21-30		Elements 121-130				Elements 161-170			Elements 241-250								Elements 242-250			
	Z=10 KN=1t		Z=1t	Pi	Z+Pi	$(\varepsilon_{zz})10^{-5}$	Z=1t	Pi	Z+Pi	Z=1t	Pi	Z+Pi	$(\varepsilon_{yy})10^{-6}$	Z=1t	Pi	Z+Pi	$(\varepsilon_{zz})10^{-6}$	Z=1t	Pi	Z+Pi	$(\varepsilon_{xx})10^{-6}$
z(mm)	S_{zz}	$(\varepsilon_{zz})10^{-7}$	S_{zz}	S_{zz}	S_{zz}		S_{yz}	S_{yz}	S_{yz}	S_{yy}	S_{yy}	S_{yy}		S_{zz}	S_{zz}	S_{zz}		S_{xx}	S_{xx}	S_{xx}	
5	16600	7904.77	15.61	-0.15	15.46	7.028	-154.825	-0.417	-155.242	-7.505	-37.21	-44.715	-14.905	8.364	-1.092	7.272	2.424	52.33	12.01	64.34	21.447
15	13200	6285.72	28.58	0.022	28.602	13.0	-186.725	0.183	-186.542	25.58	-37.71	-12.13	-4.044	24.20	-3.011	21.189	7.063	16.25	10.35	26.60	8.967
25	12770	6080.96	42.99	0.042	43.032	19.56	-186.45	-0.176	-186.626	13.88	-37.95	-24.07	-8.024	31.12	4.181	26.939	8.98	7.887	10.60	20.487	5.829
35	10170	4842.86	41.86	0.04	41.90	19.0455	183.013	-0.0427	-183.0557	7.288	-38.0	-30.712	-10.24	30.27	-4.592	25.678	8.56	7.45	10.58	18.03	6.01
45	9191	4376.67	34.01	0.0273	34.0373	15.4715	-181.64	-0.0647	-181.705	4.547	-38.06	-33.513	-11.171	30.33	-4.904	25.426	8.476	6.343	10.52	16.863	5.621
55	7091	3376.67	35.13	-0.0014	35.1286	15.968	-176.825	-0.0784	-176.904	4.747	-38.19	-35.402	-11.801	32.59	5.291	27.339	9.113	6.05	10.46	16.51	5.504
65	5830	2776.20	26.45	-0.0414	26.4086	12.004	-179.025	-0.08113	-179.107	1.679	-38.11	-36.491	-12.164	35.92	-5.496	30.424	10.142	5.835	10.42	16.255	5.419
75	3970	1800.50	34.69	-0.10	34.59	15.723	-168.85	-0.0825	-168.933	0.24	-38.77	-38.53	-12.844	44.14	-8.754	35.386	11.80	5.975	10.17	16.145	5.382
85	2577	1227.15	41.01	-0.184	40.826	18.558	-175.45	-0.744	-176.194	0.476	-40.33	-39.854	13.285	58.03	-8.591	49.439	16.48	6.178	9.628	15.806	5.269
95	807.0	384.29	54.40	-0.121	54.279	24.673	-72.30	2.462	-69.838	16.95	-29.97	-13.02	-4.34	66.48	-6.338	60.142	20.05	3.837	7.364	11.201	3.734

$\varepsilon_{zz} = S_{zz}/Es$

$Es=(2.1)10^7$ [t/m^2]

$\varepsilon_{zz} = S_{zz(Z+Pi)}/Er$

$Er = (2.2)10^5$ [t/m^2]

All Syz values are multiplied by a correction factor of 22/16 = 1.375 in order to take into account the idealized geometry due to slip element

$\varepsilon_{yy} = S_{yy(Z+Pi)}/Ec$

$\varepsilon_{zz} = S_{zz(Z+Pi)}/Ec$

$Ec = (3)10^6$ [t/m^2]

$E_{xx} = \frac{S_{xx}}{Ec}$

$Ec = (3)10^6$ [t/m^2]

Remark: all stresses are given in t/m^2 and all forces in t.

Model II. Model with thicker resin shell (t=4mm)

	Steel		Resin								Resin-concrete interface			Concrete x = 0 , y = 18 mm								Concrete x=0, y=18 mm			
	Elements 21-30		Elements 121-130 & 1505-1514								Elements 201-210			Elements 241-250								Elements 241-250			
	Z = 1t		Z=1t		Pi		Z+Pi				Z=1t	Pi	Z+Pi	Z=1t	Pi	Z+Pi		Z=1t	Pi	Z+Pi		Z=1t	Pi	Z+Pi	
z(mm)	Szz	(εzz)10-7	Szz		Szz		Szz		(εzz)10-5 *		Syz	Syz	Syz	Syy	Syy	Syy	(εyy)10-6	Szz	Szz	Szz	(εzz)10^{-6}	Sxx	Sxx	Sxx	(εxx)10^{-6}
5	16640	7923.81	37.0	-15.91	-0 014	-0.11	36.986	-16.02	16.812	7.30	-94.913	-0.426	-95.339	-16 64	-36.59	-53.23	-17.743	9.881	-1.324	8.557	2.853	48.63	9.937	58.567	19.53
15	13310	6338.10	60 78	-22.58	-0.032	0.024	60.75	-2.234	27.62	1.016	-133.38	$-4.316*10^{-4}$	-133.38	19.49	-37.07	-17.58	-5.86	28.45	-3.497	24.953	8.32	15.31	8.285	23.60	7.865
25	12960	6171.43	32.8	55.17	0.016	0.0153	32.81	55.19	14.93	25.1	-129.65	-0.092	-129.742	9.808	-37.16	-27.352	-9.12	31.61	-4.645	26.965	8.99	9.785	8.556	18.341	6.114
35	10440	4971.43	63.68	49.89	0.0091	0.0152	63.69	49.91	28.95	22.7	-128.505	-0.100	-128.605	5.931	-37.18	-31.25	-10.42	29.81	-4.993	24.817	8.273	7.359	8.544	15.903	5.301
45	9530	4538.10	71.66	65.8	$-0.25*10^{-4}$	0.0087	71.66	65.81	32.573	29.913	-123.942	-0.094	-124.036	4.554	-37.22	-32.666	-10.89	30.58	-5.287	25.30	8.431	6.227	8.485	14.712	4.904
55	7470	3557.143	99.89	89.64	-0 018	-0.0093	99.872	89.631	45 4	40.74	-119.327	-0.0666	-119.40	4.049	-37.30	-33.251	-11.09	31.76	-5.813	26.147	8.716	5.575	8.419	13.994	4.665
65	6260	2980.953	144.8	130.5	-0 039	-0.036	144.761	130.461	65.8	59.3	-111.41	-0.21	-111.62	4.019	-37.31	-33.30	-11.10	33.33	-5.851	27.48	9.16	5.032	8.356	13.388	4.463
75	4357	2074.762	202.0	217.5	-0.07	-0.044	201.93	217.456	91.79	98.85	-102.87	0.088	-102.782	5.825	-37.60	-31.775	-10.60	35.51	-6.567	28.943	9.65	4.897	8.144	13.041	4.347
85	2894	1378.10	426.2	272.3	-0.105	-0.092	426.1	272.211	193.68	123.731	-85.8	-1.4222	-87.23	4.021	-39.45	-35.43	-11.81	29.17	-5.820	23.35	7.784	3.799	7.481	11.28	3.76
95	846 4	403.05	446.7	653.2	-0.079	-0.176	446.62	653.121	203.01	296.88	-81.874	5.104	-76.77	-0.4742	-28.93	-29.404	-9.8014	27.04	-1.795	25.245	8.415	-1.067	5.962	4.895	1.632

$\varepsilon_{zz}=S_{zz}/Es$

$Es=(2.1)10^7 [t/m^2]$

$\varepsilon_{zz}= S_{zz(Z+Pi)}/Er$

$Er = (2.2)10^5 [t/m^2]$

*:All above values must be multiplied by a Correction factor of (1/2.37) due to idealized geometry, in order to take into account the slip elements, Appendix C_2

The S_{yz} values are multiplied by a corrective factor: 26/20 = 1.30, in order to take into account the idealized geometry due to the slip elements.

$\varepsilon_{yy} = S_{yy(Z+Pi)}/Ec$

$\varepsilon_{zz} = S_{zz(Z+Pi)}/Ec$

$Ec = (3)10^6 [t/m^2]$

$\varepsilon_{xx} = \frac{S_{xx}}{Ec}$

$Ec=(3)10^6 [t/m^2]$

Remark: All stresses are given in t/m^2 and all forces in t.

Model III. Small diameter (d=8mm)

	Steel		Resin								Resin-concrete interface			Concrete x=0 , y=18 mm								Concrete x=0 ,y=18 mm			
	Elements 11-20		Elements 1431-1440 & 1521-1530								Elements 1561-1570			Elements 241-250								Elements 241-250			
	Z=lt		Z=lt		Pi		Z+Pi				Z=lt	Pi	Z+Pi	Z=lt	Pi	Z+Pi		Z=lt	Pi	Z+Pi		Z=lt	Pi	Z+Pi	
z(mm)	S_{zz}	$(\epsilon_{zz})10^{-7}$	S_{zz}		S_{zz}		S_{zz}		$(\epsilon_{zz})10^{-5}$ **		S_{yz}	S_{yz}	S_{yz}	S_{yy}	S_{yy}	S_{yy}	$\epsilon_{yy}10^{-6}$	S_{zz}	S_{zz}	S_{zz}	$\epsilon_{zz}10^{-6}$	S_{xx}	S_{xx}	S_{xx}	$\epsilon_{xx}10^{-6}$
5	26120	12438.1	35.59	25.91	-0.078	-0.2	35.512	25.71	16.142	11.69=116.9	-195.6	-0.5838	-196.184	4.877	-25.06	-20.188	-6.73	6.85	-0.506	6.344	2.115	47.14	9.076	56.216	18.74
15	21920	10438.1	69.34	8.60	-0.041	0.08	69.3	8.68	31.5	3.95=39.5	-239.25	0.207	-239.043	28.89	-25.38	3.51	1.17	21.19	-1.662	19.528	6.51	14.33	7.913	22.243	7.415
25	20600	9809.542	64.53	102.2	0.065	-0.027	64.6	102.173	29.37	46.44=464.4	-227.25	-0.288	-227.538	16.16	-25.68	-9.52	-3.173	28.88	-2.408	26.472	8.824	8.434	8.087	16.521	5.507
35	16930	8061.905	79.41	38.09	0.0134	-0.055	79.43	38.035	36.11	17.29=173	-231.15	0.126	-231.024	8.831	-25.76	-16.929	-5.643	30.27	-2.776	27.494	9.17	6.632	8.064	14.696	4.90
45	15320	7295.24	93.80	108	-0.0453	0.034	93.76	108.04	42.616	49.107=491.0	-213.0	-0.348	-213.348	5.745	-25.80	-20.055	-6.685	30.30	-3.0	27.3	9.1	5.524	8.035	13.56	4.52
55	12050	5738.1	101.6	73.86	-0.0353	0.027	101.6	73.9	46.17	33.6=336.0	-223.35	0.448	-222.902	4.744	-25.87	-21.126	-7.042	33.08	-3.257	29.823	9.941	5.227	7.994	13.221	4.407
65	10220	4866.7	199.8	195.4	-0.048	-0.048	199.8	195.4	90.8	88.8=888	-185.7	-0.963	-186.663	4.67	-25.91	-21.24	-7.08	35.06	-3.448	31.612	10.54	4.635	7.97	12.605	4.202
75	7079	3370.96	299.2	271.1	0.0192	0.055	299.01	271.16	135.98	123.26=1232	-207.75	1.5255	-206.225	6.73	-26.43	-19.7	-6.57	37.35	-3.758	33.592	11.20	4.20	7.834	12.034	4.012
85	4918	2341.905	687.7	637.5	0.1671	-0.22	687.87	637.28	312.7	289.7=2897	-99.93	-3.6645	-103.60	5.083	-27.39	-22.307	-7.436	34.77	-2.434	32.336	10.78	3.557	7.463	11.02	3.674
95	1417	674.762	1324	1207	-0.24	0.203	1323.16	1207.2	601.71	548.73=5487	-125.925	7.818	-118.107	-1.60	-20.47	-22.07	-7.36	34.33	-0.811	33.52	11.18	1.999	5.718	7.717	2.573

$\epsilon_{zz} = S_{zz}/Es$
$Es = (2.1)10^7$ $[t/m^2]$

$\epsilon_{zz} = S_{zz(Z+Pi)}/Er$

$Er = (2.2)10^5$ $[t/m^2]$

**:All above values must be multiplied by a correction factor of (1/3.5) due to idealized geometry, in order to take into account the slip elements, Appendix C_2

The S_{yz} values are multiplied by a correction factor of: 18/12 = 1.50 in order to take into account the idealized geometry due to slip elements.

$\epsilon_{yy} = S_{yy(Z+Pi)}/Ec$

$\epsilon_{zz} = S_{zz(Z+Pi)}/Ec$

$Ec = (3)10^6$ $[t/m^2]$

$\epsilon_{xx} = \frac{S_{xx}}{Ec}$

$Ec = (3)10^6$ $[t/m^2]$

Remark: All stresses are given in t/m^2 and all forces in t.

Model IV Fully developed crack starting at a point (0.20)l deep and 39° inclined to vertical axis (standard: 100m, d=12mm, t=2mm)

	Steel		Resin				Resin-concrete interface			Concrete x = 0, y = 18 mm								Concrete x=0 y=18 mm			
	Elements 21-30		Elements 121-130				Elements 163-170			Elements 242-250								Elements 242-250			
	Z=lt		Z=lt	Pi	Z+Pi		Z=lt	Pi	Z+Pi	Z=lt	Pi	Z+Pi		Z=lt	Pi	Z+Pi		Z=lt	Pi	Z+Pi	
z(mm)	S_{zz}	$(\varepsilon_{zz})10^{-7}$	S_{zz}	S_{zz}	S_{zz}	$(\varepsilon_{zz})10^{-5}$	S_{yz}	S_{yz}	S_{yz}	S_{yy}	S_{yy}	S_{yy}	$(\varepsilon_{yy})10^{-6}$	S_{zz}	S_{zz}	S_{zz}	$(\varepsilon_{zz})10^{-6}$	S_{xx}	S_{xx}	S_{xx}	$(\varepsilon_{xx})10^{-6}$
5	16780	7990.48	366.6	0.057	366.657	166.67	-	-	-	-	-	-	-	-	-	-	-	-	-	-	-
15	13690	6519.05	408.7	-0.0055	408.70	185.77	-	-	-	-39.18	-11.16	-50.34	-16.78	-80.47	-9.417	-89.887	-29.97	7.127	0.6969	71.97	23.99
25	13460	6409.53	568.3	-0.2081	568.10	258.23	-391.19	-4.4964	-395.65	-25.70	-47.47	-73.17	-24.39	-49.49	-8.69	-58.18	-19.40	3.336	9.646	12.982	4.33
35	10940	5209.53	303.3	-0.1032	303.20	137.82	-187.4125	-0.2871	-187.70	45.03	-54.33	-9.30	-3.10	22.09	-7.844	14.246	4.79	7.592	13.95	21.542	7.181
45	9906	4717.15	151.3	-0.1173	151.19	68.72	-236.5	0.6189	-235.8811	9175	-53.57	-44.395	-14.80	41.24	-8.712	32.528	10.843	6.187	14.22	20.407	6.803
55	7701	3667.15	94.49	-0.1109	94.38	42.90	-189.89	-0.3146	-190.205	4.073	-53.32	-49.247	-16.416	32.82	-8.572	24.248	8.09	4.799	14.36	19.159	6.3864
65	6302	3000.96	50.48	-0.0255	50.3545	22.89	-206.8	0.14	-206.66	3.16	-53.21	-50.08	-16.70	40.58	-8.555	32.025	10.675	6.070	14.37	20.44	6.814
75	4297	2046.19	43.37	-0.1876	43.1824	19.63	-184.25	-0.1568	-184.407	0.01334	-54.0	-53.99	-18.00	46.88	-9.244	37.636	12.55	5.795	14.08	19.875	6.625
85	2759	1313.81	35.46	-0.2837	35.1663	15.985	-198.1375	-0.9441	-199.082	5.526	-56.16	-50.634	-16.878	63.89	-6.717	57.173	19.06	6.541	13.34	19.881	6.627
95	836.6	398.381	33.93	-0.1782	33.7518	15.342	-149.875	3.4265	-146.45	19.56	-41.73	-22.17	-7.39	72.81	-2.803	70.007	23.336	3.859	10.21	14.069	4.69
	$\varepsilon_{zz} = S_{zz}/E_s$ $Es=(2.1)10^7 [t/m^2]$		$\varepsilon_{zz} = S_{zz(Z+Pi)}/Er$ $Er = (2.2)10^5 [t/m^2]$				All S_{yz} values are multiplied by a correction factor of 22/16=1.375, in order to take into account the idealized geometry due to slip elements			$\varepsilon_{yy} = S_{yy(Z+Pi)}/Ec$ $\varepsilon_{zz} = S_{zz(Z+Pi)}/Ec$ $Ec = (3)10^6 [t/m^2]$								$\varepsilon_{xx} = \frac{S_{xx}}{Ec}$ $Ec = (3)10^6 [t/m^2]$			
Remark: all stresses are given in t/m^2 and all forces in t.																					

Model V Stabilized crack

	Steel		Resin				Resin-concrete interface			Concrete $x = 0$, $y = 18$ mm								Concrete x=0, y=18 mm			
	Elements 21-30		Elements 121-130				Elements 164-170, 1501-1541			Elements 241-250								Elements 241-250			
	Z=1t		Z=1t	Pi	Z+Pi		Z=1t	Pi	Z+Pi	Z=1t	Pi	Z+Pi		Z=1t	Pi	Z+Pi		Z=1t	Pi	Z+Pi	
z(mm)	S_{zz}	$(\varepsilon_{zz})10^{-7}$	S_{zz}	S_{zz}	S_{zz}	$(\varepsilon_{zz})10^{-5}$	S_{yz}	S_{yz}	S_{yz}	S_{yy}	S_{yy}	S_{yy}	$(\varepsilon_{yy})10^{-6}$	S_{zz}	S_{zz}	S_{zz}	$(\varepsilon_{zz})10^{-6}$	S_{xx}	S_{xx}	S_{xx}	$(\varepsilon_{xx})10^{-6}$
5	16600	7904.8	17.35	-0.43	16.92	7.70	-197.32	3.55	-193.77	-20.92	-39.70	-60.62	-20.207	-10.73	-2.773	-13.503	-4.50	43.90	9.43	53.33	17.777
15	13190	6280.96	29.51	-0.068	29.442	13.39	-226.6	-6.6715	-233.30	33.80	-49.71	-15.91	-5.304	45.25	-5.535	39.715	13.24	16.66	9.568	26.228	8.743
25	12760	6076.20	45.27	-0.0862	45.184	20.54	-197.175	8.30	-188.90	4.664	-47.98	-43.316	-14.44	54.14	-7.53	46.61	15.54	14.08	9.239	23.319	7.773
35	10160	4838.10	44.09	0.0468	44.14	20.063	-194.84	-6.325	-201.165	-7.0	-42.40	-49.4	-16.47	12.17	-3.30	8.87	5.16	-0.50	11.26	10.76	3.59
45	9167	4365.24	35.30	0.099	35.4	16.10	-170.8	3.0	-167.8	20.70	-44.87	-24.17	-8.057	41.96	-7.748	34.212	11.404	9.265	11.98	21.245	7.082
55	7058	3360.96	34.74	0.0876	34.83	15.83	-185.22	-1.677	-186.9	0.4308	-42.41	-41.98	-14.00	33.67	-5.219	28.451	9.484	5.013	12.19	17.203	5.74
65	5794	2752.05	24.22	-0.0354	24.19	11.0	-167.5	0.68	-166.82	2.245	-43.92	-41.675	-13.90	38.30	-6.117	32.183	10.73	6.290	11.89	18.18	6.06
75	3922	1867.62	28.68	-0.086	28.60	13.0	-180.2	-1.26	-181.46	-0.1663	-44.18	-45.35	-15.12	44.92	-7.04	37.88	12.63	5.936	11.63	17.566	5.86
85	2535	1207.143	28.02	-0.2062	27.814	12.643	-136.703	3.006	-133.70	4.839	-46.08	-41.241	-13.75	59.95	-5.0	54.95	18.317	6.405	11.02	17.425	5.809
95	756.6	360.30	29.67	-0.1306	29.54	13.43	-188.52	8.57	-179.95	17.81	-34.23	-16.42	-5.474	68.16	-2.012	66.148	22.05	3.889	8.412	12.361	4.10

$\varepsilon_{zz} = S_{zz}/Es$

$Es = (2.1).10^7 [t/m^2]$

$\varepsilon_{zz} = S_{zz(Z+Pi)}/Er$

$Er = (2.2)10^5 [t/m^2]$

All S_{yz} values are multiplied by a correction factor of 22/16 = 1.375, in order to take into account the idealized geometry due to slip elements.

$\varepsilon_{yy} = S_{yy(Z+Pi)}/Ec$

$\varepsilon_{zz} = S_{zz(Z+Pi)}/Ec$

$Ec = (3).10^6 [t/m^2]$

$\varepsilon_{xx} = \dfrac{S_{xx}}{Ec}$

$Ec = (3)10^6 [t/m^2]$

Remark: All stresses are given in t/m^2 and all forces in t.

d = 12/Std

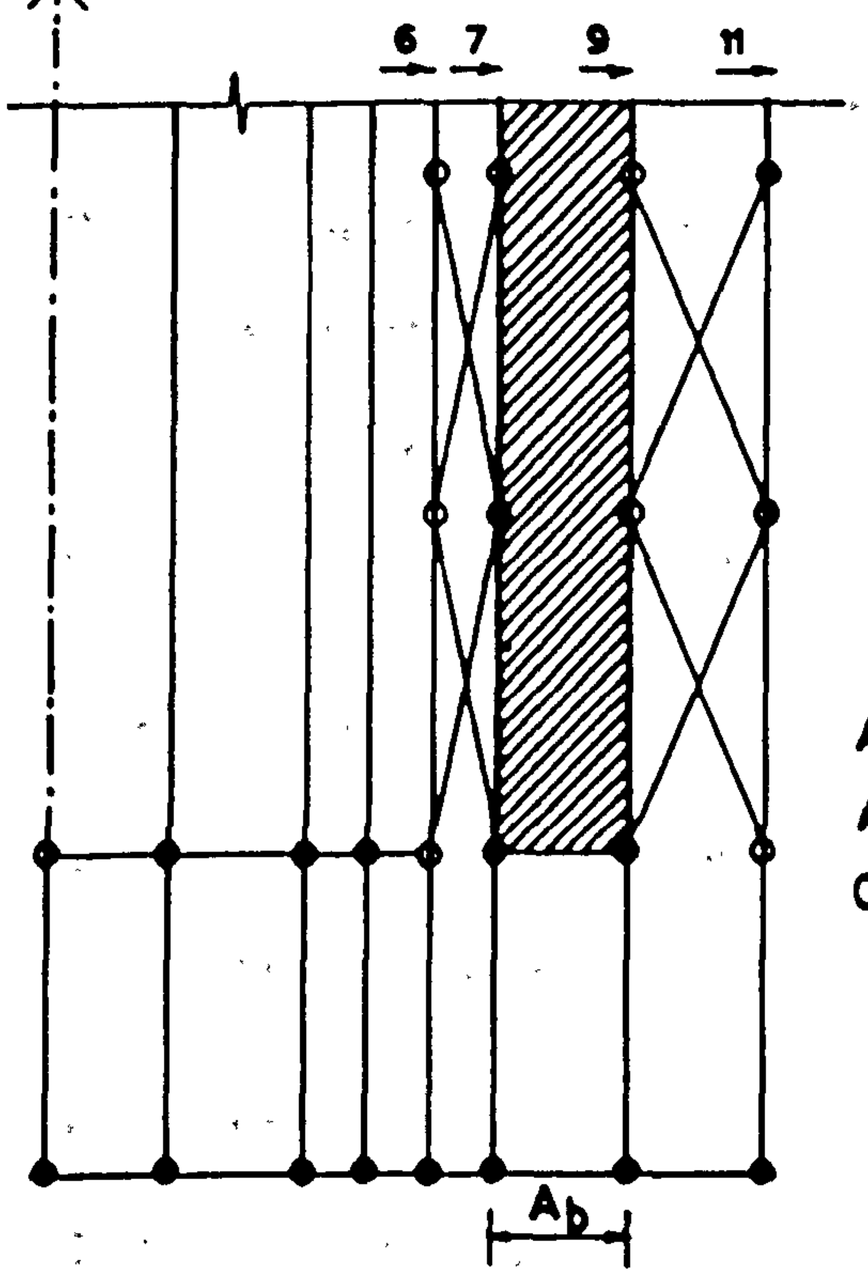

$A_{norm.} = \pi \cdot 14.2 = 87.9\ mm^2$

$A_b = \pi \cdot 14.2 = 87.9\ mm^2$

Correct. factor: 1.0

d = 8 mm

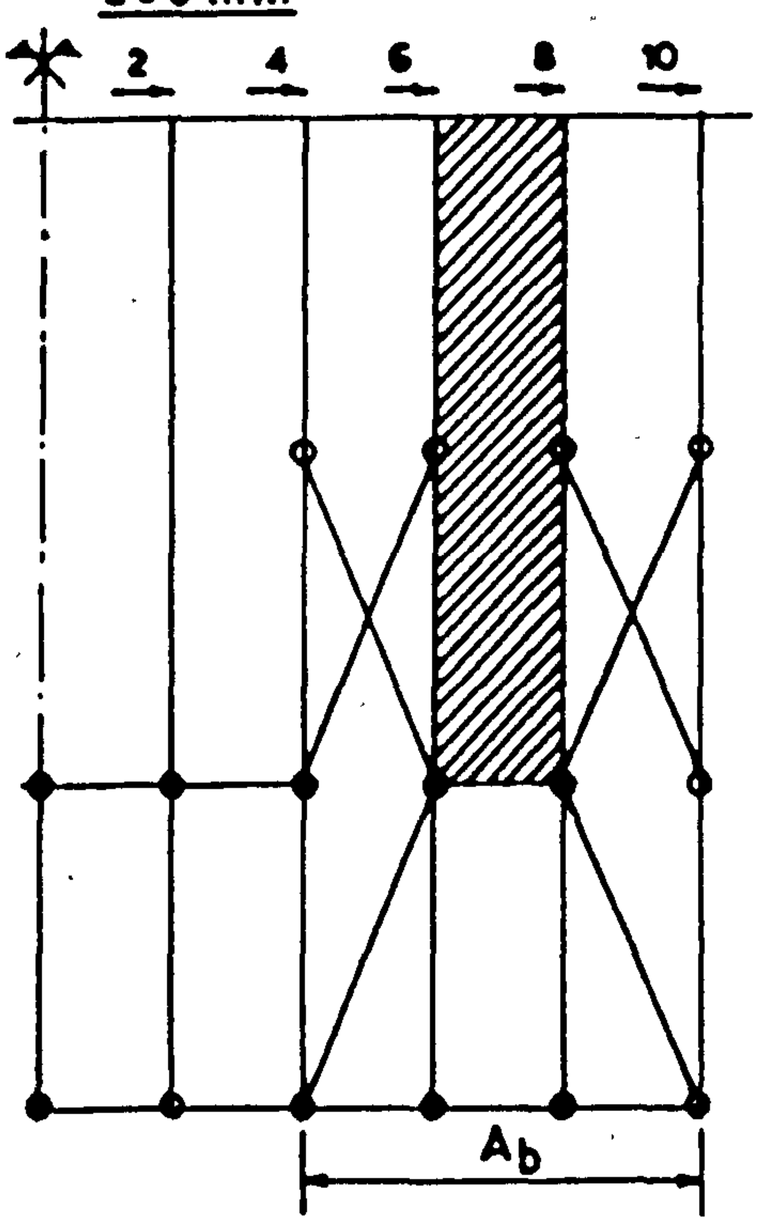

$A_b norm = \pi \cdot 12.2 = 75.36$

$A_b = \pi \cdot (\frac{20^2}{4} - \frac{8^2}{4} = \pi(100-16) = 263.76$

Corr. fact. = 263.76/75.36 = 3.50

t = 6 mm

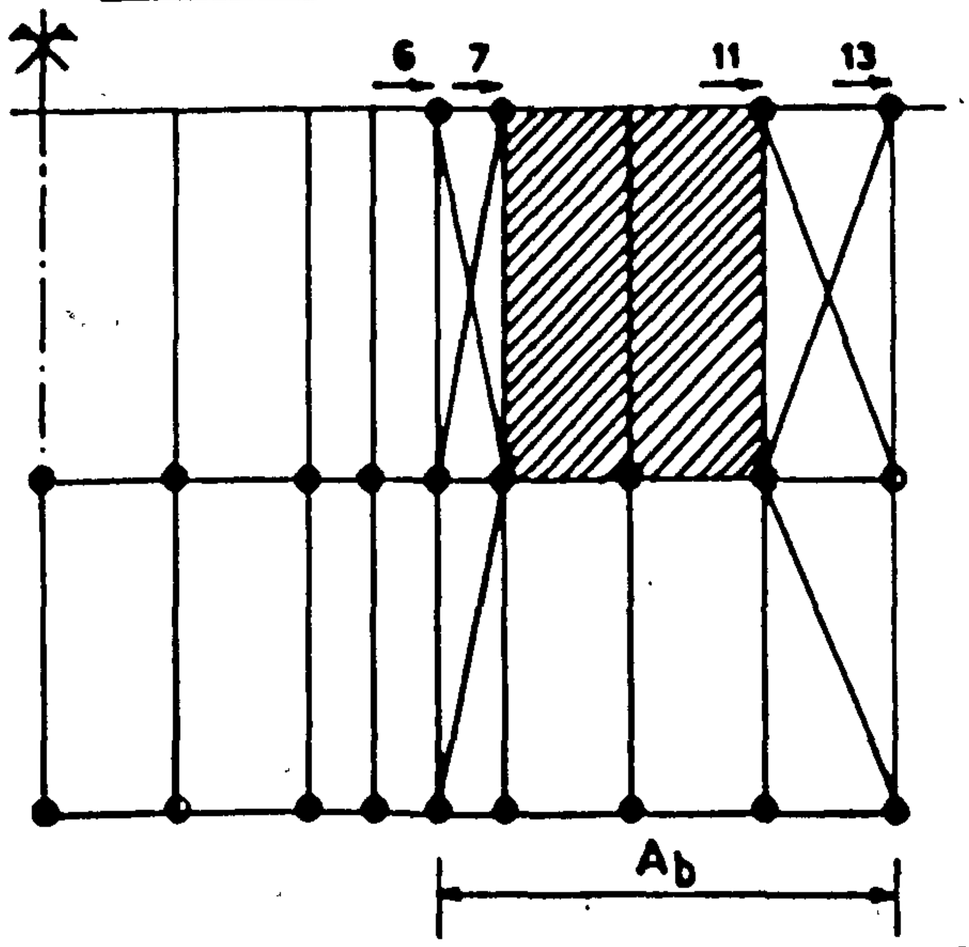

$A_{norm.} = \pi \cdot 14.4 = 175.8$

$A_b = \pi (\frac{26^2}{4} - \frac{12^2}{4}) = 417.6$

Corr. factor: 417.6/175.8 = 2.37

APPENDIX D: CHARACTERISTICS OF THE MATERIALS USED

D.1. Superplasticizers

CONPLAST 211

Water-reducing concrete admixture

Manufacturer: FOSROC Ltd

DESCRIPTION

CONPLAST 211 is based on selected stabilised, sugar-reduced lignosulphonates.

PROPERTIES

Calcium chloride content: Nil

Specific gravity; 1.19 at 200 C.

Air entrainment: Less than 1.5% additional air is entrained.

Effect of CONPLAST 211 on workability and strength

Test	Cement content kg/m^3	CONPLAST 211 per 50 kg cement litres	W/C	Slump mm	Compressive strength 7 days N/mm^2	Compressive strength 28 days N/mm^2	Density 28 days kg/m^3
Control	297	None	0.62	50	25.0	37.0	2395
Workability increased	297	0.14	0.62	100	26.0	38.0	2392
Strength increased	297	0.14	0.55	50	33.5	45.5	2413
Cement saved (30kg/m^3)	267	0.14	0.62	50	25.0	37.5	2395

CONPLAST 430

Super plasticising, water reducing, strength accelerating admixture

Manufacturer: FOSROC Ltd

DESCRIPTION

CONPLAST 430 is a synthetic plasticiser derived from sulphonated naphthalene.

PROPERTIES

Calcium chloride content:Nil

Specific gravity: 1.20 at 200 C

Air entrainment: Less than 1% additional air is entrained.

Effect of CONPLAST 430 on workability

OP cement 350kg/m^3
Zone 3 sand 650kg/m^3
20-5mm gravel 1175kg/m^3

CONPLAST 430		Slump	Flow table	Compressive strength N/mm^2			
dosage level litres/50kgs of Cement	Total w/c ratio	BS 1881 mm	spread DIN 1048 cms	1 Day	7 days	28 Days	Density kg/m^3
Nil (control)	0.60	70	-	17.0	39.0	50.0	2415
0.25	0.60	120	45 cms	16.5	37.5	46.5	2405
0.40	0.60	190	51 cms	15.5	38.5	47.5	2410
0.50	0.60	collapse	57 cms	14.0	36.5	48.0	2415

Effect of CONPLAST 430 on compressive strength

OP cement 330kg/m^3
Zone 3 sand 540kg/m^3
20-5mm gravel 1,280kg/m^3

CONPLAST 430					Compressive strength N/mm^2 (% of control)			
dosage level litres/50kgs of Cement	Total w/c ratio	Slump mm	Water reduction %	Air content %	1 Day	7 days	28 Days	Density kg/m3
Nil (control)	0.59	45	-	2.4	20	43	50	2415
0.70	0.49	45	17	2.9	28 (140)	53 (123)	60 (120)	2440
0.85	0.46	45	23	3.1	33 (165)	58 (135)	64 (128)	2450
1.00	0.44	45	26	3.2	35 (175)	64 (149)	70 (140)	2470

D.2. EPOXY RESINS

CONCRESIVE 1380

Formulator: Adhesive Engineering Co.

CONCRESIVE 1380 is a two - component, solventless, low - viscosity liquid adhesive for pressure injection grouting of cracked concrete.

DESCRIPTION

Form	: Two-component, low-viscosity liquid.	
Epoxide equivalent:	Part A	148 -164
	Part B	490 - 540
Mix Ratio	: 2 parts "A" to 1 part "B" by volume	
Viscosity at 25°C (cPs):	Part A - 640. Part B - 190. mixed - 352	
Typical Density [g/l]	: Part A - 1167, Part B - 991, Mixed - 1114.	

TYPICAL PROPERITES OF CURED MATERIAL AT 25' C

Tensile Strength	63.6 N/mm^2
Elongation at Break	2.5 %
Flexural Strength	83.4 N/mm^2
Compressive Yield Strength	115.6 N/mm^2
Flexural Modulus	4578 N/mm^2
Compressive Modulus (ASTM D)	1586 N/mm^2
Heat Deflection Temperature	57°C.

DURAL LV - DURAL GEL

Formulator: DURAL INTERNATIONAL CO.

DURAL LV is a low viscosity pressure grout and adhesive for

pressure injection into very fine cracks.

DURAL GEL is a non-sag, high modulus adhesive and mortar binder for vertical and overhead repairs of structural concrete.

PROPERTIES at 75 °F	DURAL LV	DURAL GEL	DURALCRYL
MIXING RATIO (Pt.A:Pt.B)	2:1	2:1	
MIXED VISCOSITY, cps	150-250	Gel	
POT LIFE, mins	30	45-65	12
TACK FREE (thin film), hrs	5	5	
INITIAL CURE, hrs	6	6	0.6
TENSILE STRENGTH, MPa	28.0	28.0	13.0
TENSILE ELONGATION, %	1-5	1-5	
TENSILE MODULUS, MPa	2340	1750	7000
COMPRESSIVE STRENGTH, MPa	56.0	56.0	87.5
COMPRESSIVE MODULUS, MPa	2340	1750	

D.3. PMMA Grout

DURALCRYL

Low shrinkage Polymer Comcrete based on methacrylate reactive resin for concrete repairs.

Formulator: DURAL INTERN. Co

DURALCRYL is a non-tacky, solvent-free, 2-component methacrylate based mortar with high compressive and flexural strength. It has a very low linear shrinkage, see above table.

D.4. Non shrink cementitious grout

CONBEXTRA HF

Non-shrink cementitious grout

Manufacturer: FOSROC Ltd

DESCRIPTION

CONBEXTRA HF is suplied as a ready to use dry powder requiring only the adition of water to produce a non-shrik grout.

The material is a blend of Portland cements, pre-graded

fillers and aditives which impart controlled expansion in both the plastic and hardened states.

TYPICAL PROPERTIES

Compressive strength:
Tested in accordance with BS 1881:
Part 116 and curing cubes under restraint.

Variation with consistency at 20°C

Age (days)	Compressive strength N/mm² Trowellable	Plastic	Flowable	Fluid
1	30	24	20	14
7	60	50	44	34
14	70	60	56	46
28	76	66	64	58
180	90	84	82	70

Flexural strength: Tested in accordance with BS for flowable consistency at 200C.

Age (days)	Flexural strength N/mm²
1	2.5
7	8
14	9.5
28	10
180	11

Variation with temperature at flowable consisten

Age (days)	Compressive strength N/mm2 5°C	20°C	35°C
1	4	20	30
7	30	44	46
14	50	56	56
28	64	64	60
180	84	82	70

Pressure to restrain plastic expansion: Approximately 0.004 N/mm²

Coefficient of thermal expansion: 11 x 10^{-6} per °C

Thermal conductivity: 1.5/m°C

Young's modulus: 29kN/mm2

Ultimate anchorage bond stress: Exceeds CP 100, Part1, 1972, Table 22 requirements for 40N/mm² concrete at 24 hours.

Fresh wet density: The fresh wet density will vary between 2100 kg/m³ and 2300 kg/m³ dependent on consistency.

Expansion characteristics: An expansion of 1-4% when measured to ASTM C827 overcomes plastic settlement in the unset material. Longer term expansion in the hardened state is designed to comply with the requirements of CRD 621-82A to compensate for drying shrinkage.

APPENDIX E: CALIBRATION OF TESTING EQUIPMENT

E.1. Pressure Tranducer (incorporated in the Testing machine TONIPACT 3000)

The calibration was made by means of proving ring. The results are shown below. The readings of the load cell were taken by the data acquisition and recording system described in section 7.8.7.

Table E.1 Calibration test of load cell

T.L. True load (prooving ring) (KN)	Readings of system with load cell	Differences of load cell readings (LCi)-(LCi-1)	Differenc. in true loads (TLi)-(TLi-1)	Local factor (TLi-TLi-1)/(LCi-LCi-1) -	Main factor (TLi-TLi-1)/(LCi-LCo) -
0.00	4090				
3.18	4111	21	3.18	0.151	0.151
5.20	4125	14	2.02	0.144	0.149
7.20	4139	14	2.00	0.143	0.147
10.20	4159	20	3.00	0.150	0.147
12.20	4172	13	2.00	0.153	0.148
14.13	4185	13	1.93	0.149	0.148
16.10	4199	14	1.97	0.141	0.148
18.22	4213	14	2.12	0.151	0.148
20.07	4225	12	1.85	0.154	0.148

From above table can be seen that there is a difference in the value of calibration test between the level of 0 - approximately 7.00 kN and the higher levels of load. This might be related to the greater errors, which the machine exhibits at load levels up to approximately 5.00 kN as is given by the manufacturer. (This error in the levels 0-5.00 kN is up to 2%).

E.2. Strain gauges

All the gauges used had the same resistance, 120 ± 0.3 Ohms and gauge factors varying from 2.02-2.10. The response of every channel of the system was taken before and after adding the shunt resistance to the strain gauge. This response then was related to the equivalent strain of the gauge:

$$\varepsilon = \frac{1}{F} \frac{R_{gauge}}{R_{gauge}+R_{ad.}}$$

where F=gauge factor = 2.06

which for R=120, R_{ad} = 98700, F=2.06 gives

$\varepsilon=(589.4).10^{-6}$

Table E.2. Calibration of analogue to digital converter and amplifier

Channel	Before adding the shunt resistance (a)	After adding the shunt resistance (b)	Diff. (a)-(b)	Str.gauge calibration coefficient
01	4413	3456	957	0.615×10^{-6}
	4938	3987	951	0.619 "
02	4155	3165	990	0.595 "
03	4100	3107	993	0.594 "
04	4373	3387	986	0.598 "
05	4150	3190	960	0.613 "
06	4750	3760	990	0.595 "
	4428	3436	992	0.594 "
07	5877	4907	970	0.607 "
08	4005	3020	985	0.598 "
09	4020	3070	950	0.620 "
10	5156	4172	984	0.599 "
11	4519	3532	987	0.597 "
	3986	3011	940	0.626 "
12	4236	3256	947	0.622 "
	4438	3448	990	0.595 "
13	4100	3117	983	0.600 "
14	(Load cell)			
15	4925	3905	1020	0.577 "
16	4820	3840	980	0.601 "
17	4805	3823	982	0.600 "

E.3. The slip measurement device

The displacement transducer was calibrated by using a dial gauge. The calibration measurements are shown in the Table E.3 below:

Table E.3. Calibration of the displacement transducer

Readings DT of the system with Displ.Trans.	Real displacement (Taken from dial, gauge).	Differences of Displ.Trans. indications [(TDi)-(TDi-1)]	Calibration coefficient
4678			
4512	0.250	166	
4334	0.250	" 178	
4146	0.250	" 188	$f = \frac{2.50}{1658} = 0.00150$
3960	0.250	" 186	
3770	0.250	" 190	
3585	0.250	" 185	
3390	0.250	" 195	$= 1.5(10^{-3})$ mm/digit
3225	0.250	" 165	
3030	0.250	" 195	
2840	0.250	" 190	
	2.50	1658	

E.4. The load cell for resin tensile tests

The load cell for the resin tensile tests was calibrated by means of a proving ring with known characteristic curve P=P(f). The calculated calibration factor was 1 digit = $(8.16)10^{-3}$ kN.

APPENDIX F: CALCULATION OF DISPLACEMENT OF THE CENTRE OF THE CONCRETE SPECIMENS UNDER CONCENTRATED LOAD.

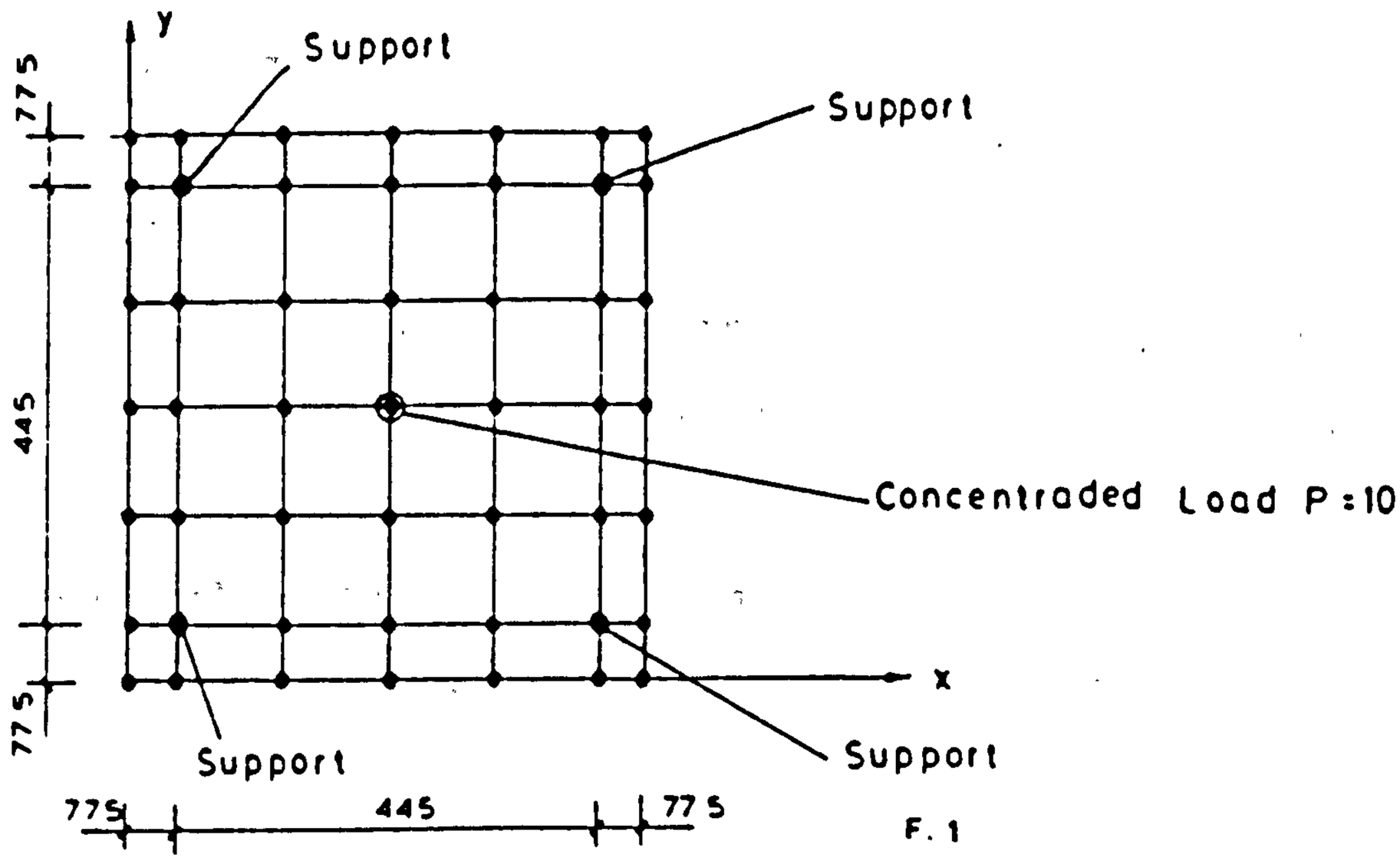

F.1

$$P = 10.0 \text{ kN}, \quad f_{25} = 0.2676 \times 10^{-5} \text{ m}$$

$$= 0.2676 \times 10^{-2} \text{ mm} \approx 0.003 \text{ mm}$$

APPENDIX G: AUGMENTATION FACTOR OF LATERAL SURFACE OF A THREADED BAR IN RELATION TO THAT OF PLAIN CYLINDER

Lateral Surface

AB,BC,CD,D,E

$$A_{ABB1A1} = \pi((12+10.05)/2)^2\sqrt{(1.50^2+((12-10.05)/2)^2} =$$

$$= (3.14)(11.025)(\sqrt{(2.25+0.950)}) = 61.92 \text{ mm}^2$$

Lateral surface with 12.0 mm diameter:

$$f_{cyl} = (3.14)(12.0)(1.50) = 56.5 \text{ mm}^2$$

$$\omega = \frac{61.92}{56.5} = 1.096$$

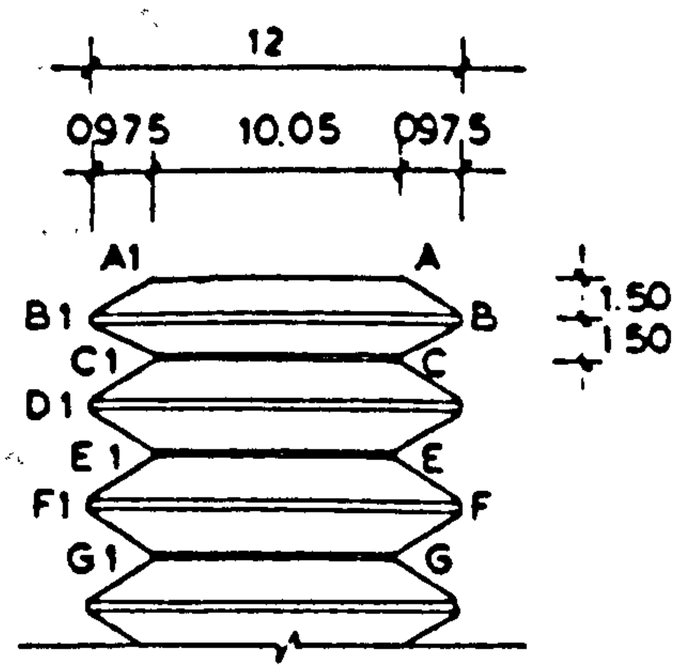

Fig. G 1

APPENDIX H: CALCULATIONS FOR NORMALIZATION WITH RESPECT TO CONCRETE STRENGTH OF DIFFERENT TEST RESULTS.

H.1 : Effect of embedment length

3.01: l= 8.3d

f_{cc}=19.56 MPa
δ_{10}=267 µm
δ_{20}=599 µm
δ_{30}=940 µm
$\delta_{10}\sqrt{f_{cc}}$=1180
$\delta_{20}\sqrt{f_{cc}}$=2647
$\delta_{30}\sqrt{f_{cc}}$=4154

$(\delta_{10in1})\sqrt{f_{cc}}$=1180

$(\delta_{20in1})\sqrt{f_{cc}}$=2647

$P_u/\sqrt{f_u}$=7.54

3.03 l= 5d.1

f_{cc}=21.29
δ_{10}=148 µm
δ_{20}=687 µm
δ_{30}= -
$\delta_{10}\sqrt{f_{cc}}$=683
$\delta_{20}\sqrt{f_{cc}}$=3170
$(\delta_{10in1})\sqrt{f_{cc}}$ = 683

$$\lambda_{20}=(1-\frac{21.29-19.56}{90.65})=0.981$$

$$(\delta_{20in1})\sqrt{f_{cc}}=\frac{3170}{0.981}=3230$$

P_u=20.10
$P_u/\sqrt{f_u}$=20.10/(√21.29)=4.36

3.02 /l=7.0d

f_{cc}=20.38 MPa
δ_{10}=397 µm
δ_{20}=668 µm
-
$\delta_{10}\sqrt{f_{cc}}$=1792
$\delta_{20}\sqrt{f_{cc}}$=3015
δ_{10}=1792

$$\lambda_{20}=(1-(\frac{20.38-19.80}{90.65}))=09910$$

$$(\delta_{20in1})\sqrt{f_{cc}}=\frac{3015}{0991}=3042$$

$P_u/\sqrt{f_u}$=28.90/√20.38=6.40

3.13 /l=(7.5)d

f_{cc}=37.9 MPa
δ_{10}=268 µm
δ_{20}=265 µm
δ_{30}=334 µm
$\delta_{10}\sqrt{f_{cc}}$=1650
-
δ_{10}=1650

$$\lambda_{20}=1-(\frac{37.9-19.56}{90.65})=0.796$$

$(\delta_{20in1})\sqrt{f_{cc}}$=1631/0796=2048

H.2. Effect of the diameter of anchor

Test 3.01 (d=12)

$\delta_{10}\sqrt{f_{cc}}$=1180
$\delta_{20}\sqrt{f_{cc}}$=2647

Test 3.06 (d=10)

$\delta_{10}\sqrt{f_{cc}}$=299√23.11=1437
$\delta_{20}\sqrt{f_{cc}}$=480√23.11=2307

Test 3.01 (d=12)

$\delta_{30}\sqrt{f_{cc}}=4.154$

$Pu/\sqrt{f_{cc}}=33.3/\sqrt{19.56}=7.54$

$(\delta_{10in1})\sqrt{f_{cc}}=1180$

$(\delta_{20in1})\sqrt{f_{cc}}=2647$

Test 3.06 (d=10)

$Pu/\sqrt{f_{cc}}=\frac{27.7}{\sqrt{23.11}}=5.76$

$\lambda_{10}=1$

$\lambda_{20}=1-\left(\frac{23.11-19.56}{90.05}\right)=1.04$

$(\delta_{20in1})\sqrt{f_{cc}}=2307/1.04=2401$

Test 3.07 (d=8)

$\delta_{10}\sqrt{f_{cc}}=920\sqrt{29.48}=4995$

$\delta_{20}\sqrt{f_{cc}}=1620\sqrt{29.41}=8795$

$\lambda_{10}=1$

$\lambda_{20}=1-\left(\frac{29.48-19.56}{90.65}\right)=08906$

$(\delta_{20in1})\sqrt{f_{cc}}=8795/08906=9875$

Test 2.07 (d=16)

$\delta_{10}\sqrt{f_{cc}}=8.0\sqrt{31.0}=445$

$\delta_{20}\sqrt{f_{cc}}=240\sqrt{31.0}=1336$

$\delta_{30}\sqrt{f_{cc}}=490\sqrt{31.0}=2728$

$\lambda_{10}=1$

$\lambda_{20}=1-\left(\frac{31.0-19.56}{90.65}\right)=08737$

$\lambda_{20}=1-\left(\frac{31.0-19.56}{70}\right)=08366$

$(\delta_{20in1})\sqrt{f_{cc}}=1336/08737=1529$

$(\delta_{30in1})\sqrt{f_{cc}}=2728/08366=3260$

correction due to shorter embedment length.

$\lambda_{10,1}=0.65$

$\lambda_{20,1}=0.76$

$(\delta_{20in11})\sqrt{f_{cc}}=(1529)(076)=1162$

$(\delta_{30in11})\sqrt{f_{cc}}=(3260)(076)=2478$

$\frac{Pu}{\sqrt{f_{cc}}}=\frac{53.0}{\sqrt{31.0}}\frac{1}{0859}=11.16$

$(\delta_{10in11})\sqrt{f_{cc}}=445(0.65)=289$

H.3. Effect of the thickness of the resin

Test 3.01 (t=2 mm)

$Pu/\sqrt{f_{cc}}=7.54$

$\delta_{10}\sqrt{f_{cc}}=1180$

$\delta_{20}\sqrt{f_{cc}}=2647$

$\delta_{30}\sqrt{f_{cc}}=4154$

$(\delta_{10in1})\sqrt{f_{cc}}=1180$

$(\delta_{20in1})\sqrt{f_{cc}}=2647$

Test 3.08 (t=4 mm)

$Pu/\sqrt{f_{cc}}=53.4/\sqrt{28.76}=9.96$

$\delta_{10}\sqrt{f_{cc}}=144\sqrt{28.76}=771$

$\delta_{20}\sqrt{f_{cc}}=260\sqrt{28.76}=1392$

$\delta_{30}\sqrt{f_{cc}}=518\sqrt{28.76}=2773$

$\delta_{40}\sqrt{f_{cc}}=1240\sqrt{28.76}=6638$

$\lambda_{10,1}=1$

$\lambda_{20,1}=1-(28.76-19.56)/90.65=$
$=08985$

$\lambda_{30,1}=1-(28.76-19.56)/70=$
$=0869$

Test 3.08 (t=4 mm)
$\delta_{20,in1}$=1392/08985=1549
$\delta_{30,in1}$=2773/0869=3191
$\delta_{40,in1}$=6638/0869=7638
provided $\lambda_{40in1}=\lambda_{30in1}$

Test 3.33 9t=8 mm)
$Pu/\sqrt{f_{cc}}$=46.7/√27.61=8.89
$\delta_{10}\sqrt{f_{cc}}$=41√27.61=215
$\delta_{20}\sqrt{f_{cc}}$=43√27.61=226
$\delta_{30}\sqrt{f_{cc}}$=488√27.61=2564
$\delta_{40}\sqrt{f_{cc}}$=113√27.61=5937
$\lambda_{10,1}$=1

$\lambda_{20,1}$=1-(27.61-19.56)/90.65
=0911

$\lambda_{30,1}$=1-(27.61-19.56)/70=
=0885
$(\delta_{20in1})\sqrt{f_{cc}}$=226/0911=248
$(\delta_{30in1})\sqrt{f_{cc}}$=2564/0885=2897
$(\delta_{40in1})\sqrt{f_{cc}}$=5937/0885=6708

Test 3.34 (t=10 mm)
$Pu/\sqrt{f_{cc}}$=48.2/√26.55=9.35
$\delta_{10}\sqrt{f_{cc}}$=542√26.55=2792
$\delta_{20}\sqrt{f_{cc}}$=870√26.55=4482
$\delta_{30}\sqrt{f_{cc}}$=1040√26.55=5358
$\delta_{40}\sqrt{f_{cc}}$=1220√26.55=6286
$\lambda_{10,1}$=1

$\lambda_{20,1}$=1-(26.55-19.56)/
/90.65=0922

$\lambda_{30,1}$=1-(26.55-19.56)/70=
=0990
$(\delta_{20in1})\sqrt{f_{cc}}$=4482/0922=4856
$(\delta_{30in1})\sqrt{f_{cc}}$=5358/0900=5953
$(\delta_{40in1})\sqrt{f_{cc}}$=6286/0900=6984

Test 3.26
$Pu/\sqrt{f_{cc}}$=18.0/√20.02=4.02
$\delta_{10}\sqrt{f_{cc}}$=385√20.02=1723

Test 3.27
$Pu/\sqrt{f_{cc}}$=36.2/√20.61=7.97
$\delta_{10}\sqrt{f_{cc}}$=205√20.61=931
$\delta_{20}\sqrt{f_{cc}}$=447√20.61=2029
$\delta_{30}\sqrt{f_{cc}}$=744√20.61=3378
$\lambda_{20,1}$=1-(20.61-19.56)/90.65=
=0988
$\lambda_{30,1}$=1-(20.61-19.76)/70.0=
=0985
$(\delta_{20in1})\sqrt{f_{cc}}$=2029/0988=2054
$(\delta_{30in1})\sqrt{f_{cc}}$=3378/0955=3429

H.4. Effect of the type of anchor

Test 3.01 (0) Threaded bar
$Pu/\sqrt{f_{cc}}$=7.54
$\delta_{10}\sqrt{f_{cc}}$=1180
$\delta_{20}\sqrt{f_{cc}}$=2647
$\delta_{30}\sqrt{f_{cc}}$=4154

$(\delta_{10in1})\sqrt{f_{cc}}$=1180

$(\delta_{20in1})\sqrt{f_{cc}}$=2647

Test 3.05 Ribbed bar
$Pu/\sqrt{f_{cc}}$=38.1/√23.2=7.91
$\delta_{10}\sqrt{f_{cc}}$=145√23.2=698
$\delta_{20}\sqrt{f_{cc}}$=193√23.2=927
$\delta_{30}\sqrt{f_{cc}}$=772√23.1=3718
If the correction factors for concrete strength can also be applied to ribbed bars:
$\lambda_{20,1}$=1-(23.2-19.50)/90.65=
=09598
$\lambda_{30,1}$=1-(23.2-19.50)/70=09480
$(\delta_{20in1})\sqrt{f_{cc}}$=927/09598=957
$(\delta_{30in1})\sqrt{f_{cc}}$=3718/0948=3922

Test 3.04 Plain bar
$Pu/\sqrt{f_{cc}}$=225/√26.39=4.38
$\delta_{10}\sqrt{f_{cc}}$=202√26.39=1038
$\delta_{20}\sqrt{f_{cc}}$=359√26.39=1844

Test 3.24 Ribbed bar
$Pu/\sqrt{f_{cc}}$=40.7√24.89=8.15

Test 3.04 Plain bar
Under the above assumption on the correction factor due to concrete strength:
$\lambda_{20,1}$=1-(26.39-19.56)/90.65=
=09247
$(\delta_{20in1})\sqrt{f_{cc}}$=1994

H.5. Effect of the type of resin

Test 3.01 - C1380-(I+C+R)
$Pu/\sqrt{f_{cc}}$=7.54
$(\delta_{10in1})\sqrt{f_{cc}}$=1180
$(\delta_{20in1})\sqrt{f_{cc}}$=2647
$(\delta_{30in1})\sqrt{f_{cc}}$=4154

Test 3.09 -LV-(I+C+R)
$Pu/\sqrt{f_{cc}}$=34.9/√31.67=6.20
$(\delta_{10})\sqrt{f_{cc}}$=165√31.67=926
$(\delta_{20}\sqrt{f_{cc}})$=418√31.67=2352
$\delta_{30}\sqrt{f_{cc}}$=558√31.67=3140
$\lambda_{20,1}$=1-(31.67-19.56)/90.65=
=0.866
$\lambda_{30,1}$=1-(31.67-19.57)/70=
=0.8270
$(\delta_{20in1})\sqrt{f_{cc}}$=2352/0.866=2716
$(\delta_{30in1})\sqrt{f_{cc}}$=3140/0827=3799

Test 3.23-LV-Splitting
$Pu/\sqrt{f_{cc}}$=45.0/√18.97=10.33
$(\delta_{10})\sqrt{f_{cc}}$=312√18.97=1358
$(\delta_{20})\sqrt{f_{cc}}$=589√18.97=2565
$(\delta_{30})\sqrt{f_{cc}}$=1060√18.97=4616

Test 3.10-GEL-I
$Pu/\sqrt{f_{cc}}$=30.2/√25.30=6.00
$(\delta_{10})\sqrt{f_{cc}}$=361√25.30=1816
$(\delta_{20})\sqrt{f_{cc}}$=921√25.30=4632
$(\delta_{30})\sqrt{f_{cc}}$=2350√25.30=11820
$\lambda_{20,1}$=1-(25.30-19.56)/90.65=
=09367
$\lambda_{30,1}$=1-(25.30-19.56)/70=0918
$(\delta_{20in1})\sqrt{f_{cc}}$=4632/09367=5085
$(\delta_{30in1})\sqrt{f_{cc}}$=11820/0918=
=12876

Test 3.29 -LV-(I+C+R)
$Pu/\sqrt{f_{cc}}$=45.3/√24.25=9.12
$(\delta_{10,2,1})\sqrt{f_{cc}}$=202√24.25=994
$(\delta_{20})\sqrt{f_{cc}}$=493√24.25=2428
$(\delta_{30})\sqrt{f_{cc}}$=682√24.25=3358
$\lambda_{20,1}$=0.948, $\lambda_{30,1}$=0933
$(\delta_{20in1})\sqrt{f_{cc}}$=2428/0948=2602

$(\delta_{30,2,1})\sqrt{f_{cc}}$=3358/0933=3599

Test (2.06) LV/l=12d-(I+C+R)
$Pu/\sqrt{f_{cc}}$=41.3/√26.0=8.10
$(\delta_{10,2,1})\sqrt{f_{cc}}$=100√26.0=510
$\delta_{20}\sqrt{f_{cc}}$=390√26.0=1989
$\delta_{30}\sqrt{f_{cc}}$=1040√26.0=5303
Because l=12d>8.3d
λ_1=1.00 Sect.7.12.4

$$\lambda_{20,1}=1-\frac{(26.0-19.56)}{90.65}=093$$

$\lambda_{30,1}$=1-(26.0-19.560/70=0909
$(\delta_{20in1})\sqrt{f_{cc}}$=1989/0.93=2139
$(\delta_{30in1})\sqrt{f_{cc}}$=5303/0.909=
=5839

H.6. Effect of the size of specimen

Test 3.01
$Pu/\sqrt{f_{cc}}$= 7.54
$\delta_{10}\sqrt{f_{cc}}$=1180
$\delta_{20}\sqrt{f_{cc}}$=2647
$\delta_{30}\sqrt{f_{cc}}$=4154

Test 3.26-(300)(300) spec
$Pu/\sqrt{f_{cc}}$=18.0/√20.02=4.02
$\delta_{10}\sqrt{f_{cc}}$=385√20.02=1723

Test 3.27 -(300)(300)spec.-t=4
t=4

$Pu/\sqrt{f_{cc}}=36.2/\sqrt{20.61}=7.97$
$\delta_{10}\sqrt{f_{cc}}=205\sqrt{20.61}=931$
$\delta_{20}\sqrt{f_{cc}}=497\sqrt{20.61}=2029$
$\delta_{30}\sqrt{f_{cc}}=744\sqrt{20.61}=3378$
$\lambda_{20,1}=1-(20.61-19.56)/90.65=$
$=09884$
$\lambda_{30,1}=1-(20.61-19.56)/70=$
$=0.985$
$(\delta_{20in1})\sqrt{f_{cc}}=2029/09884=$
$=2053$
$(\delta_{30in1})\sqrt{f_{cc}}=3429$

Test 3.08 Spec.with normalized values (see above)
$Pu/\sqrt{f_{cc}}=9.96$
$\delta_{10}\sqrt{f_{cc}}=771$
$(\delta_{20in1})\sqrt{f_{cc}}=1549$
$(\delta_{30in1})\sqrt{f_{cc}}=3191$
$(\delta_{40in1})\sqrt{f_{cc}}=7638$

H.7. Influence of the reinforcement

Test 3.01

$Pu/\sqrt{f_{cc}}=7.54$
$(\delta_{10in1})\sqrt{f_{cc}}=1180$
$(\delta_{20in1})\sqrt{f_{cc}}=2647$
$(\delta_{30in1})\sqrt{f_{cc}}=4154$

Test 3.20 $\mu_x=\mu_y=1\%,\mu_z=0.7\%$/
/splitting
$Pu/\sqrt{f_{cc}}=42.09/\sqrt{26.7}=8.15$
$\delta_{10}\sqrt{f_{cc}}=533\sqrt{26.7}=2754$
$\delta_{20}\sqrt{f_{cc}}=1140\sqrt{26.7}=5891$
$\delta_{30}\sqrt{f_{cc}}=1620\sqrt{26.7}=8370$
$\lambda_{20,2,1}=1-(26.7-19.56)/90.65=$
$=09212$
$\lambda_{30,2,1}=1-(26.7-19.56)/70=$
$=0898$
$(\delta_{20in1})\sqrt{f_{cc}}=5891/09212=$
$=6395$
$(\delta_{30in1})\sqrt{f_{cc}}=5370/0898=9321$

Test 3.21/ $\mu x=\mu_y$ 2%
$Pu/\sqrt{f_{cc}}=32.6/\sqrt{29.93}=7.13$
$\delta_{10}\sqrt{f_{cc}}=169\sqrt{20.93}=773$
$\delta_{20}\sqrt{f_{cc}}=292\sqrt{20.93}=1006$
$\delta_{30}\sqrt{f_{cc}}=576\sqrt{20.93}=2635$
$\lambda_{20,2,1}=1-(20.93-19.56)90.65=$
$=0985$
$\lambda_{30,1}=0.980$

$(\delta_{20in1})\sqrt{f_{cc}}=1006/0.985=1021$

$(\delta_{30in1})\sqrt{f_{cc}}=2635/0.98=2689$

Test 3.12 - splitting
$Pu/\sqrt{f_{cc}}=39.7/\sqrt{21.93}=8.48$
$\delta_{10}\sqrt{f_{cc}}=861\sqrt{4.93}=4032$
$\delta_{20}\sqrt{f_{cc}}=16.10\sqrt{21.93}=7540$
$\delta_{30}\sqrt{f_{cc}}=2150\sqrt{21.93}=10068$
$\lambda_{20,2,1}=1-(21.93-19.56)/$
$/90.65=0974$
$\lambda_{30,1}=1-(21.93-19.56)/$
$/90.65=0966$
$(\delta_{20in1})\sqrt{f_{cc}}=7540/0974=$
$=7741$
$(\delta_{30in1})\sqrt{f_{cc}}=10068/0966=$
$=10462$

test 3.23 -Splitting-LV
$Pu/\sqrt{f_{cc}}=10.33$
$\delta_{10}\sqrt{f_{cc}}=1358$
$\delta_{20}\sqrt{f_{cc}}=2565$
$\delta_{30}\sqrt{f_{cc}}=4616$

H.8. Effect of the method of drilling, the injection of resin and the $Pu/\sqrt{f_{cc}}$ eccentricity of the anchor

Test 3.01 t=2

$Pu/\sqrt{f_{cc}}=7.54$
$(\delta_{10in1})\sqrt{f_{cc}}=1180$
$(\delta_{20in1})\sqrt{f_{cc}}=2647$
$(\delta_{30in1})\sqrt{f_{cc}}=4154$

Test 3.11-Eccentrically placed anchor /t=4

$Pu/\sqrt{f_{cc}}=34.5/\sqrt{8.48}=6.47$
$\delta_{10}\sqrt{f_{cc}}=139\sqrt{28.48}=742$
$\delta_{20}\sqrt{f_{cc}}=506\sqrt{28.48}=2700$
$\delta_{30}\sqrt{f_{cc}}=531\sqrt{28.48}=2833$
$\lambda_{20,1}=0902, \lambda_{30,1}=0873$
$(\delta_{20in1})\sqrt{f_{cc}}=2700/0902=2993$
$(\delta_{30in1})\sqrt{f_{cc}}=2833/0873=3245$

Test 3.15-Inject./t=2 mm

$Pu/\sqrt{f_{cc}}=46.3/\sqrt{21.48}=9.99$
$\delta_{10}\sqrt{f_{cc}}=14.9\sqrt{21.48}=691$
$\delta_{20}\sqrt{f_{cc}}=398\sqrt{21.48}=1854$
$\delta_{30}\sqrt{f_{cc}}=672\sqrt{21.48}=3114$
$\lambda_{20,1}=0979, \lambda_{30,1}=0973$
$(\delta_{20in1})\sqrt{f_{cc}}=1845/0979=1885$
$(\delta_{30in1})\sqrt{f_{cc}}=3114/0973=3200$

Test 3.25-Diam.Dril. /t=4

$Pu/\sqrt{f_{cc}}=47.3/\sqrt{22.25}=10.03$
$\delta_{10}\sqrt{f_{cc}}=656\sqrt{22.25}=3094$
$\delta_{20}\sqrt{f_{cc}}=916\sqrt{22.25}=4321$
$\delta_{30}\sqrt{f_{cc}}=1370\sqrt{22.25}=6462$
$\lambda_{20,1}=0970, \lambda_{30,1}=0962$
$(\delta_{20in1})\sqrt{f_{cc}}=4321/0970=4455$
$(\delta_{30in1})\sqrt{f_{cc}}=6462/0962=6177$
$(\delta_{40in1})\sqrt{f_{cc}}=9892/0962=$
$=10283$

test 3.08/t=4 mm

Normalized values see above
$Pu/\sqrt{f_{cc}}=9.96$
$\delta_{10}\sqrt{f_{cc}}=771$
$(\delta_{20in1})\sqrt{f_{cc}}=1549$
$(\delta_{30in1})\sqrt{f_{cc}}=3191$
$(\delta_{40in1})\sqrt{f_{cc}}=7638$

APPENDIX I: CORRECTION OF VALUES OBTAINED FROM TEST 4.01

I.1. ANCHOR 4.01 (LONGER BONDED LENGTH)

$l_{fact.} = 13$ mm

$l_i = 10$ mm

The relationship of $\delta_{10in1}\sqrt{f_{cc}}$, $\delta_{20in1}\sqrt{f_{cc}}$, $\delta_{30in1}\sqrt{f_{cc}}$ is nearly linear with inclination as in Fig 7.111. Therefore:

$$K = \frac{(\delta_{10in1}\sqrt{f_{cc}})_{l=13}}{(\delta_{10in1}\sqrt{f_{cc}})_{l=10}} = \frac{(\delta_{10in1}\sqrt{f_{cc}})_{l=(8.3)d}}{(\delta_{10in1}\sqrt{f_{cc}})_{l=((8.3)d/1.3)=(6.38)d}} =$$

$$= \frac{1180}{1800} = 0.65$$

Thus the converted values of 4.01 are (τ_{ac}=P/(3.14)(16)(10))

P [KN]	δ(μm)	τ(N/mm²)
1.5	34	2.99
3.0	132	5.97
4.5	336	8.95
6.01	508	11.94
7.5	671	14.93
9.0	812	17.91
10.2	1208	20.90

I.2. Anchor 4.03 (eccentrically placed)

By taking Fig. 7.118 into consideration

$$K = \frac{(\delta_{a\,in1}\sqrt{f_{cc}})\text{eccentric}}{(\delta_{a\,in1}\sqrt{f_{cc}})\text{symmetric}}$$, for any load level a.

Thus,

Test 3.11

P	$\tau_{a,c}$*	K
10	1.99	742/771=0.96
20	3.98	2993/1549=1.93
30	5.97	3245/3191=1.017

*average vlaues along the embedment length

Test 4.03

$\tau_{a,c}$	K**
τ=1.5	K=0.96
τ=3.0	K=1.45
τ=4.5	K=1.70
τ=6.0	K=1.017

**values calculated from the curve obtained from test 3.11 below

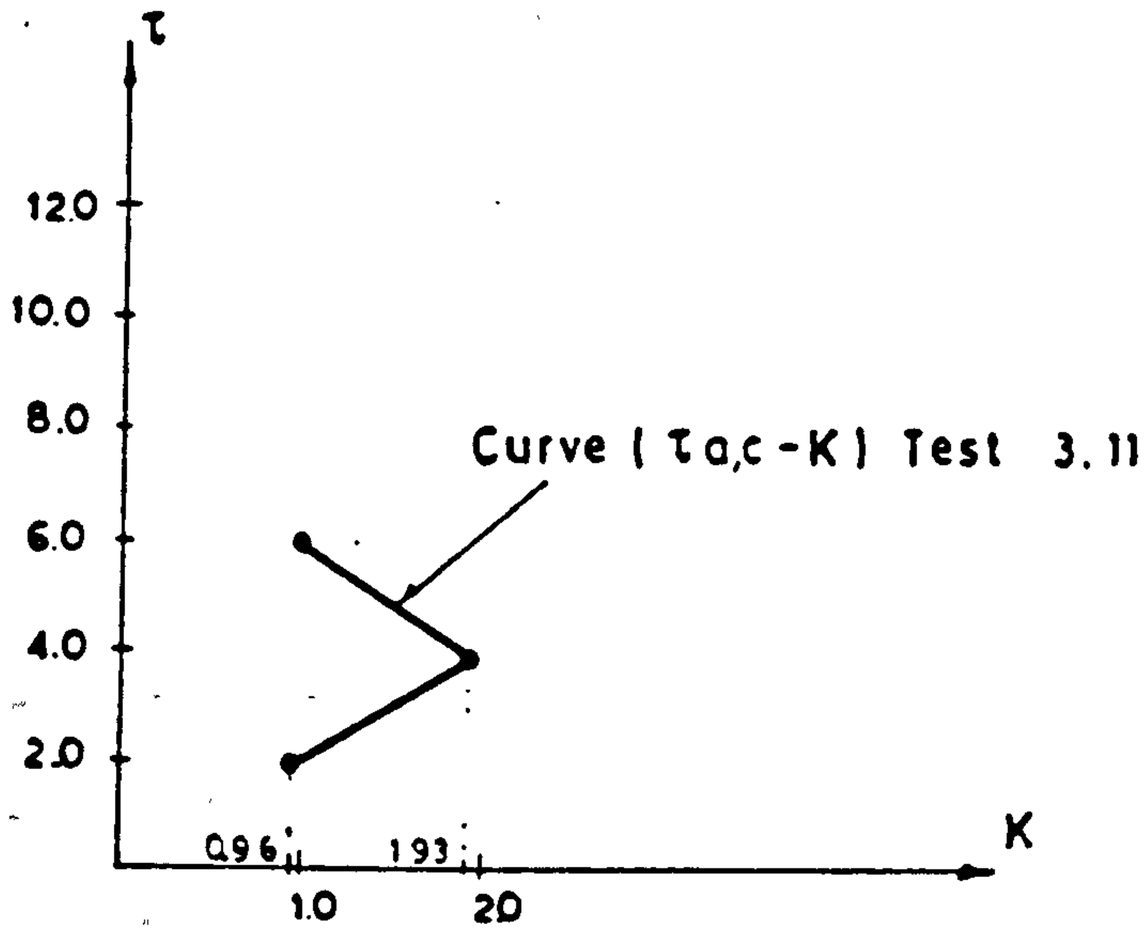

Fig. I.1

APPENDIX J: CALCULATED DESIGN EXAMPLE OF A PARTICULAR ADHESIVE ANCHOR

Anchoring system

- f_{cc}=30 N/mm² (=4500 p_{si})
- f'_c= 3 N/mm²
- resin C1380 (low viscosity, E=2200 N/mm²)
- unreinforced concrete
- percussive drilling
- pouring of resin
- d =14 mm
- d_0=18 mm
- t = 2 mm
- high hield reinforcing bar

Calculation of the ultimate pull-out load

a. According to ACI 355

E = 120 mm, cone radius

$P_{ult} = \pi E^2(2/f'_{t\cdot 3}) =$

$= \pi(120^2)[(2/3)f'_c] = (3.14)(144)(10^2)(2) =$

$= 90.432$ p. = 41.00 kN

Especially for bonding anchors, Section 11.1.2

$P_{ult} = \pi(d_o)(l)(9) = \pi(18)(120)(9) = 61.04$ N

b. According to ACI 349

$P_{ult} = A(4\Phi(\sqrt{f'_c}) =$

$= \pi(4.72)^2(4)(0.65)(\sqrt{4500}) =$

= 8,184 pounds = 37.16 kN

c. According to P.C.I.

$P_{ult} = \pi dl(8.0) = \pi(18)(120)(8.0\ N/mm^2) = 54.3$ kN

d. According to this thesis

$P_u = (P_{uo})(\mu_2)(\mu_3)(\mu_4)(\mu_5)(\mu_6)(\mu_9)(\mu_{10}) =$

$(37.0)(1.0)(1.2)(1.0)(1.08)(1.0)(1.0)(1.0)=49.0$ kN

where:

P_{uo} :the fundamental value of the ultimate pull-out load for an anchor with 12 mm diameter

$\mu_1 - \mu_{10}$:coefficients to take the effect of the different parameters on the $(P_u/\sqrt{f_{cc}})$ values, Section 11.5

for a d=12 , $P_u/\sqrt{f_u}=6.9$ (mean value obtained from Fig 7.168)

$P_{uo}=(6.9)(\sqrt{30})=37.8$ kN

Effect of the embedment length

l/d= 120/14 = 8.6

$\mu_2 = [(P_u/\sqrt{f_{cc}})_{l/d=8.3}] / [(P_u/\sqrt{f_{cc}})_{l/d=8.6}] = 1.0$

Effect of the anchor diameter

$\mu_3=1.2$, Fig 7.112

Effect of resin thickness

t/d= 2/14 = 0.1429

$\mu_4 = [(P_u/\sqrt{f_{cc}})_{t/d=0.166}]/[(P_u/\sqrt{f_{cc}})_{t/d=0.149}] =$

$= 1.0$, Fig 7.113

Effect of the type of anchor

$\mu_5 = 1.08$..... Fig 7.114

Effect of the type of resin

$\mu_6 = 1.0$..... Fig 7.115

Effect of the method of insertion of resin

$\mu_9 = 1.0$ ..... Fig 7.118

Effect of the drilling method

$\mu_{10} = 1.0$ ..... Fig 7.118

$$\delta_i = \delta_{io}\left[(\lambda_{e1})(\lambda_{e2})(\lambda_{e3})(\lambda_{e4})(\lambda_{e5})(\lambda_{e6}) \quad (\lambda_{e8})(\lambda_{e9})(\lambda_{e10})\right]$$

Suppose the service load is 20 kN. Then, the displacement under P=20 kN must be calculated.

$\delta_{20}\sqrt{f_{cc}}$ = 2647 ..... Fig 7.109

λ_{20} = (1-(30.0-19.56)/90.65) = 0.8848

$(\delta_{20,0})$ = (2647)(0.8848) = 2342 μm

The corresponding coefficients λ_{e1}-λ_{e10} in order to take the effect of the same variables on $\delta_i\sqrt{f_{cc}}$ values are:

λ_{e2} : l/d = 8.6 -> λ_1 = 0.94

λ_{e3} : d/d = 14/12 = 1.17 -> λ_2 = 1.03

λ_{e4} : t/d = 2/14 = 0.143 -> λ_4 = 1.05

λ_{e5} : ribbed bar, λ_5 = 0.36

λ_{e6} : low viscisity resin, E_r = 2200 N/mm², λ_6 = 1.0

λ_{e9} : resin poured, λ_9 = 1.0

λ_{e10}: percussive drilling, λ_{10} = 1.0

Thus, $\delta_{20}\sqrt{f_{cc}}$ = (2342)(0.94)(1.03)(1.05)(0.36)(1.0)(1.0)(1.0) = 857 μm

or

δ_{20} = (857/√30) = 156 μm = 0.16 mm